

**Production and Application of Monoclonal  
Antibodies Suitable for the Specific Detection  
of *Listeria monocytogenes***

**A thesis submitted for the degree of Ph.D.**

**By**

**Stephen Hearty B.Sc. (Hons),**

**July 2005.**

**Based on research carried out at**

**School of Biotechnology,**

**Dublin City University,**

**Dublin 9,**

**Ireland.**

**Under the supervision of Professor Richard O’Kennedy.**



## Acknowledgements

Firstly, I would like to say a sincere “thank you” to Professor Richard O’Kennedy for his support and guidance, much appreciated (and often needed) counsel and his boundless and infectious enthusiasm for research.

To the lab group, past and present, thanks for all the help, especially ‘Lenny’ an exceptional scientist and valued colleague.

I would also, especially like to acknowledge my family for their constant encouragement and unwavering support. In order of appearance: Mam and Dad, my sister Lisa, Chloe and also my uncle Ciarán, who sadly passed away during the course of this research.

*Glann go bee, Glann go deo*





## **Table of contents:**

<b>Declaration</b>	<b>iii</b>
<b>Acknowledgements</b>	<b>iv</b>
<b>Table of contents</b>	<b>v</b>
<b>Abbreviations</b>	<b>xiv</b>
<b>Units</b>	<b>xxii</b>
<b>Publications and Presentations</b>	<b>xxiii</b>
<b>Abstract</b>	<b>xxvii</b>

## ***Chapter 1: Introduction*** **1**

1.1	<i>Listeria monocytogenes</i> : discovery and history	2
1.2	Bacteriology and biochemistry of <i>Listeria</i>	3
1.3	Listeriosis: pathophysiology and incidence	5
1.4	Infection	9
1.4.1	Virulence factors involved in adhesion and invasion	9
1.4.1.1	Internalins	9
1.4.1.2	<i>Listeria</i> adhesion protein (LAP) or p104	17
1.4.1.3	Amidase (Ami)	17
1.4.2	Virulence factors involved in intra- and inter-cellular survival and proliferation	18
1.4.2.1	p60	18
1.4.2.2	ActA	18
1.4.2.3	Listeriolysin O	20
1.4.2.4	Phospholipases	21
1.4.3	Genome organisation and genetic determinants of virulence	23
1.4.3.1	Central virulence gene cluster	23
1.4.3.2	<i>inl</i> virulence gene cluster	25
1.4.3.3	Virulence gene regulation: the PfA regulon	26
1.5	Epidemiology	28
1.6	Biodiversity of clinically important strains	32
1.7	Legislation	33
1.8	Current detection methods	38
1.9	Rapid methods	40



<b>Chapter 2:</b>	<b>Materials and Methods</b>	44
2.1	Equipment	45
2.2	Consumable items	48
2.3	Reagents and media	49
2.3.1	Standard solutions	53
2.3.2	Denaturing SDS-PAGE	53
2.3.3	Non-denaturing PAGE	56
2.3.4	Western blot analysis	59
2.3.5	Bicinchoninic (BCA) assay for estimation of protein concentration	60
2.3.6	SEM and AFM image analysis solutions	61
2.4	Antigen isolation and preparation	62
2.4.1	Preparation of bacterial stocks	62
2.4.2	Preparation of InlB extract	62
2.4.3	Preparation of protein-enriched supernatant	62
2.4.4	Preparation of formalin-inactivated <i>L. monocytogenes</i> cells	63
2.4.5	Extraction of <i>Listeria</i> surface proteins	63
2.4	Animal experiments	64
2.5.1	Licencing for animal usage	64
2.5.2	Immunisation protocol for mice for the production of monoclonal antibodies to <i>L. monocytogenes</i>	64
2.5.3	Monoclonal antibody production by ascitic growth	65
2.6	Antibody purification	66
2.6.1	Ammonium sulphate precipitation	66
2.6.2	Concentration of tissue culture supernatant	66
2.6.3	ProteinA/G affinity-purification of immunoglobulin	66
2.6.4	Desalting of affinity-purified IgG fractions	67
2.7	Mammalian cell culture	68
2.7.1	Preparation of mammalian cell culture media	68
2.7.2	Recovery of frozen cells	68
2.7.3	Cell counts and viability testing	68
2.7.4	Growth of suspension cell lines	69
2.7.5	Storage of cell lines	69
2.7.6	Mycoplasma screening	69
2.7.6.1	Cell culture of NRK cells	69
2.7.6.2	Screening for mycoplasma contamination	69



2.7.7	Hybridoma production and isolation	70
2.7.7.1	Somatic cell fusion	70
2.7.7.2	Screening for specific monoclonal antibody production	71
2.7.7.3	Cloning of hybridomas secreting <i>Listeria</i> -specific antibodies	71
2.8	Solid phase immunoassays	73
2.8.1	ELISA's for estimation of antibody levels in hybridoma supernatants	73
2.8.2	Isotyping of monoclonal antibodies	73
2.8.3	Determination of antibody working dilution	73
2.8.4	Inhibition ELISA	74
2.9	Molecular biology	75
2.9.1	Standard solutions	75
2.9.2	Isolation of <i>L. monocytogenes</i> genomic DNA	78
2.9.3	Sequence-specific primer design	79
2.9.4	Agarose gel electrophoresis	79
2.9.5	Preparation of high efficiency competent bacterial cells	80
2.9.6	Polymerase chain reaction	80
2.9.7	PCR product ligation into pCR2.1 plasmid (blunt-ended)	81
2.9.8	Transformation of pCR2.1- <i>inlA</i> plasmid into bacterial cells	82
2.9.8.1	Restriction analysis of 'white colonies' (pCR2.1- <i>InlA</i> transformants) from X-gal agar plates	82
2.9.8.2	Restriction digestion of pCR2.1- <i>InlA</i> constructs	83
2.9.9	Restriction digestion of <i>inlA</i> PCR product (directional)	83
2.9.10	PCR product ligation into pQE60 plasmid (directional)	84
2.9.11	Transformation of pQE60- <i>inlA</i> plasmid into bacterial cells	84
2.9.12	PCR product purification (Gel clean-up)	84
2.9.13	PCR product purification (ethanol precipitation)	85
2.9.14	Plasmid purification	86
2.9.15	Protein expression and time course analysis	87
2.9.16	Purification of recombinant His-tagged protein by immobilised metal affinity chromatography (IMAC)	87
2.9.17	Identification of recombinant protein by Western blotting	87
2.10	Biacore studies	88
2.10.1	Pre-concentration studies	88
2.10.2	Immobilisation of monoclonal antibody	88
2.10.3	Preparation of an IgG2a control surface	89



2.10.4	<i>L. monocytogenes</i> -specific, direct-cell-binding assay	89
2.10.5	Binding analysis using the NTA chip	89
2.10.6	Measurement of steady-state affinity	89
2.11	HPLC analyses	91
2.11.1	Analysis of affinity-purified antibody fractions	91
2.11.2	Standard curve for estimation of molecular weight (Mr)	91
2.11.3	Analysis of IMAC-purified recombinant proteins	92
2.12	SEM and AFM image analysis	93
2.12.1	Sample preparation	93
2.12.1.1	Fixing	93
2.12.1.2	Post-fixing	93
2.12.1.3	Drying	93
2.12.2	Sample preparation	93
2.12.2.1	SEM analysis	93
2.12.2.2	AFM analysis	93
 <b>Chapter 3: Production and Characterisation of Monoclonal Antibodies to <i>Listeria monocytogenes</i></b>		 94
3.1	Introduction	95
3.1.1	The Immune system	95
3.1.1.1	The humoral immune response	96
3.1.1.2	Antibody structure	97
3.1.1.3	<i>L. monocytogenes</i> and the immune response	105
3.1.1.4	Antibody diversity	108
3.1.2	Monoclonal antibody production	112
3.1.2.1	Production of monoclonal antibodies following <i>in vivo</i> immunisation	112
3.1.2.2	Screening of hybridoma progeny	115
3.1.2.3	Cloning of hybridoma cells	116
3.2	Results and discussion	118
3.2.1	Production of a panel of monoclonal antibodies to <i>L. monocytogenes</i> -derived supernatant proteins	118
3.2.1.1	Precipitation of <i>L. monocytogenes</i> supernatant proteins	118
3.2.1.2	Titration of LLO-specific antibody against <i>L. monocytogenes</i> supernatant proteins	118





3.2.1.3	Estimation of total protein concentration in TCA-precipitated supernatant proteins	119
3.2.1.4	Immunisation with <i>L. monocytogenes</i> supernatant proteins	119
3.2.1.5	Hybridoma production using lymphocytes primed with <i>L. monocytogenes</i> supernatant proteins	120
3.2.1.6	Affinity-purification of monoclonal antibody G94F8 (mAbG94F8)	127
3.2.2	Characterisation of mAbG94F8	128
3.2.2.1	Determination of mAbG94F8 isotype	128
3.2.2.2	Demonstration of solution-phase inhibition ELISA with <i>L. monocytogenes</i> -derived supernatant proteins	129
3.2.2.3	Confirmation of p60-specificity of mAbG94F8	129
3.2.2.4	Cross-reactivity analysis of mAbG94F8	133
3.2.3	Production of a panel of monoclonal antibodies to InlB	135
3.2.3.1	Preparation of <i>L. monocytogenes</i> -derived InlB-enriched extract	135
3.2.3.2	Estimation of total protein concentration in the Tris-HCl extract	135
3.2.3.3	Immunisation with <i>L. monocytogenes</i> -derived InlB-enriched extract	135
3.2.3.4	Hybridoma production using lymphocytes primed with <i>L. monocytogenes</i> -derived InlB-enriched extract	136
3.2.4	Characterisation of anti-InlB monoclonal antibody (mAbG54D4)	140
3.2.4.1	Determination of mAbG54D4 antibody isotype	140
3.2.4.2	Immunoreactivity of mAbG54D4 towards Tris-HCl extract	141
3.2.4.3	Solution-phase immunoreactivity of mAbG54D4-inhibition ELISA	142
3.2.4.4	Determination of cell-binding potential of mAbG54D4	143
3.2.5	Production of monoclonal antibodies to whole-cell <i>L. monocytogenes</i>	149
3.2.5.1	Preparation of formalin-inactivated <i>L. monocytogenes</i> cells	149
3.2.5.2	Immunisation with formalin-inactivated <i>L. monocytogenes</i> cells	149



3.2.6	Characterisation of mAb2B3 monoclonal antibody	152
3.2.6.1	Determination of mAb2B3 isotype	152
3.2.6.2	Affinity-purification of mAb2B3	153
3.2.6.3	Determination of integrity and degree of purification of mAb2B3	153
3.2.6.4	Observations on the nature of the specific mAb2B3-cell binding interaction	156
3.2.6.5	Cross-reactivity of apathogenic <i>Listeria</i> spp. with mAb2B3	158
3.2.6.6	Elucidation of the mAb2B3-reactive listerial protein	158
3.2.7	Optimisation of ELISA for detection of <i>L. monocytogenes</i> cells using mAb2B3	161
3.2.7.1	Checkerboard ELISA for determination of optimal loading ratios of cell coating and optimal antibody dilution for mAb2B3 monoclonal antibody	161
3.2.7.2	Inhibition ELISA evaluation	164
3.3	Summary and conclusions	169

#### **Chapter 4: Cloning, Heterologous Expression and Purification of Recombinant InlA Protein** 172

4.1	Introduction	173
4.1.1	Expression vectors	173
4.1.2	Expression hosts	175
4.1.3	Cloning strategies	176
4.1.4	High-fidelity PCR	179
4.2	Results and discussion	180
4.2.1	Extraction of genomic DNA	180
4.2.2	Cloning of full-length <i>inlA</i> gene into pCR2.1 (TA cloning)	181
4.2.3	Cloning of full-length <i>inlA</i> gene into pQE60	186
4.2.3.1	Time course experiments to determine the full-length rInlA expression levels	191
4.2.3.2	Sequencing of the cloned full-length <i>inlA</i> gene sequence	195
4.2.4	Cloning of 'truncated' <i>inlA</i> gene into pQE60	199



4.2.4.1	Determination of rInlA protein expression	208
4.2.4.2	Sequencing of the cloned truncated <i>inlA</i> gene sequence	211
4.2.4.3	Time course experiments to optimise rInlA expression in <i>Pfu9</i>	213
4.2.4.4	Determination of the optimum IPTG concentration for induction	214
4.2.5	Purification of the <i>inlA</i> gene product by IMAC	217
4.2.5.1	Optimisation of IMAC purification process	218
4.3	Summary and conclusions	227
<b>Chapter 5: Biosensor-Based Detection of <i>L. monocytogenes</i></b>		230
5.1	Introduction	231
5.1.1	Definition of biosensors	231
5.1.2	History of surface plasmon resonance sensing	231
5.1.3	Theory of surface plasmon resonance biosensing	232
5.2	Results and discussion	239
5.2.1	Direct detection of <i>L. monocytogenes</i> cells using surface plasmon resonance	239
5.2.1.1	Pre-concentration of mAb2B3 monoclonal antibody onto the CM5 sensor chip surface	239
5.2.1.2	Pre-concentration of IgG2a control antibody onto the CM5 sensor chip surface	239
5.2.1.3	Immobilisation of mAb2B3 onto CM5 sensor chip	242
5.2.1.4	Assessment of specific cell-binding potential of mAb2B3-CM5 sensor surface	243
5.2.1.5	SEM and AFM image analysis of mAb2B3-captured <i>L. monocytogenes</i> cells on mAb2B3-immobilised sensor chip surface	245
5.2.1.6	Immobilisation of mAb2B3 onto C1 sensor surface	246
5.2.1.7	Assessment of specific cell-binding potential of mAb2B3-C1 sensor surface	246
5.2.1.8	Critical explanation of factors contributing to <i>L. monocytogenes</i> cell capture	248
5.2.1.9	Development of a model SPR-based, cell-binding assay for direct detection of <i>L. monocytogenes</i>	252



5.2.1.10	Assessment of signal amplification using a sandwich-assay approach	253
5.2.1.11	Assessment of non-specific binding of non- <i>L. monocytogenes</i> cells to mAb2B3-CM5 sensor chip surface	255
5.2.1.12	Assessment of non-specific binding of heat-inactivated <i>L. monocytogenes</i> cells to mAb2B3-CM5 sensor chip surface	256
5.2.1.13	Construction of a calibration curve for estimation of <i>L. monocytogenes</i> cell concentration	258
5.2.2	Biacore-based characterisation of the mAb2B3-InlA interaction	263
5.2.2.1	Characterisation of the mAb2B3-rInlA interaction using a covalently-immobilised rInlA-CM5 surface	263
5.2.2.1.1	Pre-concentration of rInlA onto the CM5 sensor chip surface	263
5.2.2.1.2	Preparation of rInlA-CM5 sensor chip surface	263
5.2.2.1.3	Equilibrium steady-state affinity of mAb2B3 for amine-coupled rInlA	266
5.2.2.2	Analysis of the mAb2B3-InlA interaction using NTA chip technology	269
5.2.2.2.1	Optimisation of the NTA-linked rInlA surface operating conditions	269
5.2.2.2.2	Non-specific binding profile of NTA chip surface	270
5.2.2.3	Characterisation of the mAb2B3-rInlA interaction using an anti-His-tag antibody ligand-capture approach	276
5.2.2.3.1	Pre-concentration of anti-His-tag antibody onto the CM5 sensor chip surface	276
5.2.2.3.2	Immobilisation of anti-His-tag antibody onto the CM5 sensor chip surface	277
5.2.2.3.3	Steady-state affinity of mAb2B3 on Nova-His-captured rInlA surface	281
5.2.2.4	Non-denaturing PAGE analysis of IMAC-purified rInlA	284





5.2.2.5	HPLC analysis of IMAC-purified rInIA	284
5.2.3	Characterisation of the mAbG94F8-p60 interaction using Biacore	288
5.2.3.1	Confirmation of p60 specificity of mAbG94F8 using Biacore	288
5.3.2.1.1	Preparation of rLLO-CM5 sensor chip surface	288
5.2.3.1.2	Assessment of mAbG94F8 binding to immobilised rLLO	289
5.2.3.2	Preparation of mAbG94F8-CM5 sensor chip surface	290
5.2.3.3	Assessment of p60 protein binding to immobilised mAbG94F8	292
5.2.3.4	Immobilisation of rp60 onto the CM5 sensor chip surface	293
5.2.3.5	Preliminary assessment of binding to the rp60-CM5 sensor chip surface	294
5.2.3.6	The effect of salt concentration on binding to the rp60-CM5 surface	297
5.2.3.7	Immobilisation of rp60 onto the B1 sensor chip surface	298
5.2.3.8	Optimisation of binding to the rp60-B1 sensor chip surface	299
5.3	Summary and conclusions	301
<b>Chapter 6: Overall Summary and Conclusions</b>		304
6.1	Overall summary and conclusions	305
<b>Chapter 7: References</b>		309



## Abbreviations

Ab	antibody
AB	actin-binding domain
Abs	absorbance
ActA	actin A (Actin Assembly protein)
AD	alcohol dehydrogenase
AFM	atomic force microscopy
Ag	antigen
AID	activation-induced-deaminase
ALOA	'Agar Listeria according to Ottavani and Agosta'
Ami	amidase
AMP	adenosine monophosphate
Amp <sup>(r)</sup>	ampicilin <sup>(resistance)</sup>
AOAC	Association of Official Analytical Chemists
AP	alkaline phosphatase
APC	antigen-presenting cell
API	Analytical Profile Index
Arp2/3 complex	stable assembly of seven protein subunits that always include actin-related protein 2 (Arp2) and actin-related protein 3 (Arp3)
ATCC	American Type Culture Collection
Aut	<i>L. monocytogenes</i> -specific autolysin
BCA	bicinchoninic acid
B-cells	Bursa-equivalent-derived small lymphocyte cells
BCIP/NBT	5-bromo-4-chloro-3'-indolylphosphate/nitro blue tetrazolium chloride
β-A	β-Amylase
BHI	brain heart infusion media
BIA	biomolecular/biospecific interaction analysis
BSA	bovine serum albumin
BSH	bile salt hydrolase
BSI	British Standards Institute
CA	carbonic anhydrase
Cam <sup>(r)</sup>	chloramphenicol <sup>(resistance)</sup>
cAMP	3', 5'-cyclic AMP
CAMP	Christie, Atkins, Munch-Petersen
Cap	cap domain



CC	cytochrome C
CDC	Centre for Disease Control and Prevention (US)
cDNA	complementary DNA
CDR	complementarity determining region
CDTX	cholesterol-dependent, pore-forming toxin
CEA	chicken egg albumin (ovalbumin)
cfu	colony forming unit
C <sub>H</sub>	constant region of heavy chain
CHR	cofilin homology region
C <sub>L</sub>	constant region of light chain
CM	carboxymethyl(ated) / cell membrane
c-Met	cell surface protein-tyrosine kinase receptor ligand for hepatocyte growth factor/scatter factor (HGF-SF)
CNRL	Centre National de référence des Listérias (Switzerland)
conc (c)	concentration
CRP/CAP	cAMP receptor protein
CV	coefficient of variation
CW	cell wall
d	diameter
3-D	3-dimensional
DC	dendritic cell
dH <sub>2</sub> O	distilled H <sub>2</sub> O
DMEM	Dulbecco's modification of Eagles' medium
DMSO	dimethylsulfoxide
DNA	deoxyribonucleic acid
dNTP	deoxynucleotidyl triphosphates
dTNB	5,5'-dithio-bis(2-nitrobenzoic acid)
dTT	dithiothreitol
ε	dielectric constant
EDC	N-ethyl-N'-(dimethylamio)propyl carbodiimide
EDTA	ethylenediaminetetra-acetic acid
EF-hand	calcium binding motif composed of two helices (E and F) joined by a loop
ELISA	enzyme-linked immunosorbent assay
EU	European Union
Fab	antigen-binding region of an antibody
FAO	Food and Agriculture Organisation



Fas	fatty acid synthase
FasL	fatty acid synthase ligand (Fas receptor)
Fc	fragment crystallisable (constant region of antibody)
FCA	Freunds's Complete adjuvant
FCS	foetal calf serum
FDA	Food and Drug Administration (US)
FIA	flow injection analysis
Fnr	fumerate-nitrate reduction protein
FOPH	Federal Office for Public Health (Switzerland)
Fv	fragment variable (variable binding region of an antibody)
gC1q-R	receptor of the globular part of the complement component, C1q
gDNA	genominc DNA
GW repeat	repeating units of glycine and tryptophan amino acids
HAT	hypoxanthine aminopterin thymidine
HBMEC	human brain microvascular endothelial cells
HBS	hepes buffered saline
(h)Ecad	(human) E-cadherin
HGF-SF	hepatocyte growth factor and scatter factor
HGPRT	hypoxanthine-guanine phosphoribosyl transferase
His	histidine
6xHis	hexahistidine
HIV	human immunodeficiency virus
HPLC	high performance liquid chromatography
Hpt	hexose phosphate transport
HRP	horseradish peroxidase
Hsp60	heat shock protein 60
HT	hypoxanthine thymidine
IFR	Institute for Food Research (UK)
Iap	invasion associated protein
IgG	immunoglobulin class G
IL	interleukin
ILO	ivanolysin O
IMAC	immobilized metal affinity chromatography
IMS	immunomagnetic separation
INF- $\gamma$	interferon gamma





InI	internalin (series of <i>L. monocytogenes</i> surface proteins)
InIA	internalin A
InIB	internalin B
InIC	internalin C
InIC2	internalin C2
InIE	internalin E
InIF	internalin F
InIG	internalin G
InIH	internalin H
iNOS	nitric oxide synthase
i.p	intra-peritoneal
IPTG	isopropylthiogalactoside
IR	inter-repeat
Irp	internalin-related protein
ISO	International Organisation for Standardisation
K <sub>A</sub>	association (affinity) constant (units = M <sup>-1</sup> )
Kan <sup>(r)</sup>	kanamycin <sup>(resistance)</sup>
K <sub>D</sub>	dissociation constant (units = M)
K <sub>SPR</sub>	SPR wave propagation vector
KLH	keyhole limpet haemocyanin
λ	wavelength
lac O	lac operator/operon
LAP	<i>Listeria</i> adhesion protein
LB	Lauria-Bertani
LCAM	liver cell adhesion molecule
LCMV	lymphocytic choriomeningitis virus
ldh	lactate dehydrogenase gene
LEB	<i>Listeria</i> enrichment base
LED	light emitting diode
LFIA	lateral flow immunoassay
LIP-1/LIP-2	<i>Listeria</i> pathogenicity island 1/ <i>Listeria</i> pathogenicity island 2
LLO	listeriolysin O
LLOQ	lower limit of quantitation
Log	logarithmic
LPTTG	consensus Gram-positive cell-wall anchor sequence (leucine, praline, threonine, threonine and glycine)



LPXTG	consensus Gram-positive cell-wall anchor sequence (leucine, praline, threonine, X and glycine), where X represents 'any' amino acid
LRR	Leucine rich repeat
LTA	lipoteichoic acid
mAb	monoclonal antibody
MAP kinase	mitogen-activated protein kinase
MCS	multiple cloning site
<i>m</i> -Dpm	<i>meso</i> -diaminopimelic acid
(m)Ecad	(murine) E-cadherin
(M)ena	(mammalian) enabled protein
2-ME	2-mecaptoethanol / $\beta$ -mercaptoethanol
MET	c-met proto-oncogene / c-Met tyrosine kinase
MHC	major histocompatibility complex
Mpl	metalloprotease
Mr	molecular weight
mRNA	messenger RNA (ribonucleic acid)
<i>n</i>	refractive index
n	valence
NCIMB	National Collection of Food Industrial and Marine Bacteria
NCTC	National Collection of Type Cultures
NF- $\kappa$ B	nuclear factor $\kappa$ B
NHS	N-hydroxysuccinimide
NK	natural killer
NRK	normal rat kidney
NTA	nitrilotriacetic acid
OD	optical density
ORF	open reading frame
PAGE	polyacrylamide gel electrophoresis
PBS	phosphate buffer saline
PBS/T	PBS containing 0.05 % (v/v) Tween 20
PBS/TM	PBS containing 0.05 % (v/v) Tween 20 and 1 % (w/v) milk protein
PC-PLC	phosphatidylcholine-specific phospholipase C
PCR	polymerase chain reaction
PDA	photodiode array



PDB	Protein Data Bank
PEG	polyethylene glycol
PEST sequence	protein region that is rich in proline (P), glutamic acid (E), aspartic acid (D), serine (S) and threonine (T)
PFO	perfringolysin O
( <i>Pfu</i> ) polymerase	( <i>Pseudomonas furiosis</i> ) DNA polymerase
pH	log of the hydrogen ion concentration
PHLS	Public Health Laboratory Service (UK)
pI	isoelectric point
PI 3-K	phosphatidylinositol/phosphoinositide 3-kinase
PI-PLC	phosphatidylinositol-specific phospholipase C
Plc A	phospholipase C A
Plc B	phospholipase C B
pNPP	<i>para</i> -nitrophenol phosphate
p-polarised	plane polarised
Pr	profilin
PrfA	positive regulatory factor A
PRR	Proline rich region
Prs	phosphoribosyl-pyrophosphate synthase
PSD	paddle-style dipstick
P T5	phage T5
P T7	phage T7
RE	relative error
Req	equilibrium binding response
R <sub>f</sub>	relative mobility
rInlA	recombinant InlA
rInlB	recombinant InlB
rLLO	recombinant LLO
R <sub>max</sub>	maximum binding response
RNI	reactive nitrogen intermediate
ROI	reactive oxygen intermediate
rp60	recombinant p60
rRNA	ribosomal RNA (ribonucleic acid)
R.T.	room temperature
RTE	ready-to-eat
RT-PCR	reverse transcriptase PCR
RU(s)	response unit(s)



Scar	suppressor of G-protein-coupled receptor (cAR) proteins
scFv	single chain Fv
SD	standard deviation
SDS	sodium dodecyl sulphate
SEC	size exclusion chromatography
SEM	scanning electron microscopy
Sig	signal sequence
SLO	streptolysin O
SOD	superoxide dismutase
SPR	surface plasmon resonance
SrtA	sortase A
TAE	Tris-acetate-EDTA
( <i>Taq</i> ) polymerase	( <i>Thermus aquaticus</i> ) DNA polymerase
TBS	Tris-buffered saline
TBS/T	TBS containing 0.05 % (v/v) Tween 20
TBS/TM	TBS containing 0.05 % (v/v) Tween 20 and 1 % (w/v) milk protein
T <sub>C</sub>	cytotoxic T-cells
TCA	trichloroacetic acid
T-cells	thymus-derived small lymphocyte cells
TEMED	N,N,N',N'-tetramethyl-ethylenediamine
Tet <sup>(r)</sup>	tetracycline <sup>(resistance)</sup>
T <sub>H</sub>	helper T-cells
THG	thyroglobulin
θ <sub>c</sub>	critical angle
θ <sub>SPR</sub>	SPR angle
TIR	total internal reflection
T <sub>m</sub>	melting temperature
TMB	3,3',5,5'-tetramethylbenzidine
TNF-α	tumour necrosis factor alpha
Tr	retention time
Tris-base	Tris (hydroxymethyl)-amino-methane
Tris-HCL	Tris hydrochloride
T <sub>s</sub>	suppressor T-cells
upH <sub>2</sub> O	ultra-pure H <sub>2</sub> O
USDA	United States Department of Agriculture
UV	ultraviolet





VASP	vasodilator-stimulated phosphoprotein
ve	elution volume
V <sub>H</sub>	variable region of heavy chain
V <sub>L</sub>	variable region of light chain
vo	void volume
WASp	Wiskott-Aldrich syndrome protein
WHO	World Health Organisation
X-Gal	5-bromo-4-chloro-3-indolyl-β-D-galactoside
χ <sup>2</sup>	Chi <sup>2</sup> ('goodness of fit')



## Units

μg	microgram
(k)bp	(kilo)base pair
(m)bp	(mega)base pair
(k)Da	(kilo)Daltons
μl	microlitre
μM	micromoles
°C	degrees Celcius
cm	centimeter(s)
g	gram(s)
h	hour(s)
HU	haemolytic unit(s)
Hz	Hertz
kg	kilogram
l	litre
m	metre
M	molar
mAU	milliabsorbance units
Mbp	mega base pair
mg	milligram
min	minute
ml	millilitre
mm	millimeters
mol	molar
mM	millimolar
nM	nanomolar
nm	nanometre
pg	picogram
rpm	revolutions per minute
RU	response units
s	seconds
%	percent(age)
v/v	volume per unit volume
(k)V	(kilo)volt/volt(s)/volt(age)
w/v	weight per unit volume



## Publications

O'Kennedy, R., Carolan, N., **Hearty, S.**, Finlay, W., Dillon, P. and Daly, S. (2005). "Applications and future developments of sensors in relation to post harvest analysis of fruit, vegetables and other crops." *Stewart Postharvest Review*, (In preparation).

Lacy, A., Dunne, L., Fitzpatrick, B., Daly, S., Keating, G., Baxter, A., **Hearty, S.** and O'Kennedy, R. (2005). "A review of rapid analysis of coumarins using surface plasmon resonance." *J. AOAC Int.* (Submitted).

**Hearty, S.**, Leonard, P. and O'Kennedy, R. (2005). "Production, characterisation and potential application of a novel monoclonal antibody for detection of virulent *Listeria monocytogenes*." *J. Microbiol. Meth.* (Submitted)

Leonard, P., **Hearty, S.**, Quinn, J. and O'Kennedy, R. (2005). "Sensitive Detection of *Listeria monocytogenes* Using Fully Engineered Recombinant scFv Antibody Fragments." 92nd Annual Meeting of the International Association for Food Protection Book of Abstracts, page 168.

Leonard, P., **Hearty, S.**, Wyatt, G., Quinn, J. and O'Kennedy, R., (2005). Development of a surface plasmon resonance-based immunoassay for *Listeria monocytogenes*. *J. Food Protect.*, 68(4), 728-735.

Leonard, P., O'Kennedy, R., **Hearty, S.**, Clyne, M., Brennan, J., Fanning, L., Dillon, M. and Porter, A. (2004). "Exploiting monoclonal and recombinant antibodies for the development of SPR-based sensor arrays for bacteria, drugs and tumour markers." 11<sup>th</sup> International Conference on Human Antibodies and Hybridomas, Alexander Hotel, Dublin, 6<sup>th</sup>-8<sup>th</sup> October 2004, Book of abstracts, 13(1-2), 31.

Leonard, P., **Hearty, S.**, Quinn, J. and O'Kennedy, R. (2004). "A generic approach for the detection of whole *Listeria monocytogenes* cells in contaminated samples using surface plasmon resonance." *Biosens. Bioelectron.*, 19(10), 1331-1335.

Leonard, P., **Hearty, S.**, Brennan, J., Dunne, L., Quinn, J., Chakraborty, T., and O'Kennedy, R. (2002). "Advances in biosensors for the detection of pathogens in food and water." *Enzyme Microb. Tech.*, 32(1), 3-13.



**Hearty, S., Leonard, P., Quinn, J.Q. and O’Kennedy, R. (2002).** “Background to new rapid technology in detection of pathogens, part II: Biosensor-based detection methods.” Book of abstracts, *New methods for the detection of Listeria monocytogenes. Inco Coperinicus project PL 979012*, May 2002.

Leonard, P., **Hearty, S.**, Quinn, J.G., and O’Kennedy, R. (2001). “A pathogenic life cycle of *Listeria monocytogenes*.” *INCO COPERINICUS News*, **3**, 1-2.

Fitzpatrick, J., Fanning, L., **Hearty, S.**, Leonard, P., Manning, B.M., Quinn, J.G., and O’Kennedy, R. (2000). “Applications and recent developments in the use of antibodies for analysis.” *Anal. Letts.*, **33(13)**, 2563-2609

### ***Presentations***

Leonard, P., **Hearty, S.**, Dillon, P., Killard, A. and O’Kennedy, R. (2005). “Biacore as a tool for antibody-based protein and drug analysis.” *Developments in Protein Interaction Analysis (DiPIA)*, Philadelphia, USA, 28<sup>th</sup>-31<sup>th</sup> August 2005.

Leonard, P., **Hearty, S.**, Dillon, P., Killard, A. and O’Kennedy, R. (2005). “Sensitive detection of *Listeria monocytogenes* using fully engineered recombinant scFv antibody fragments.” *International Association for Food Protection (IAFP), 92<sup>nd</sup> annual meeting*, Baltimore MA, USA, 14<sup>th</sup>-17<sup>th</sup> August 2005.

O’Kennedy, R., Leonard, P., **Hearty, S.**, Brennan, J., Dunne, L., Darmaninsheehan, A., Stapleton, S., Tully, E., Quinn, J.G. and Chakraborty, T. (2004). “Advances in biosensors for detection of pathogens in food and water.” *Rapid Methods Europe 2004*, Noordwijk aan Zee, Netherlands, 25<sup>th</sup>-26<sup>th</sup> March 2004.

**Hearty, S.**, Leonard, P. and O’Kennedy, R. (2003). “Direct detection of the pathogen *Listeria monocytogenes* using surface plasmon resonance.” *Biacore user day*, Stevenage, UK, 2<sup>nd</sup> October, 2003.

Leonard, P., **Hearty, S.** and O’Kennedy, R. (2003). “Development of an immunoassay to detect *Listeria monocytogenes* using a scFv antibody selected against purified recombinant Internalin B protein.” *VIIth International Conference on Agri-Food Antibodies*, Uppsala, Sweden, 10<sup>th</sup>-13<sup>th</sup> September 2003.





**Hearty, S.** and O’Kennedy, R. (2003). “Monoclonal antibody production- an overview.” *Antibody production workshop*, Dublin City University, 12<sup>th</sup> February 2003.

**Hearty, S.** (2002). “Targeting *Listeria monocytogene*: an antibody-based approach.” *Ph.D. Transfer meeting*, Dublin City University, September 2002.

**Hearty, S.** and O’Kennedy, R. (2002). “Targeting *Listeria monocytogenes*.” *Predoctoral series, The Biochemical Society- Irish Area Section, Cellular Stress Response and Cancer Colloquium*, NUI Galway 4<sup>th</sup> July 2002.

**Hearty, S.** (2002). “Monoclonal Antibodies- a technical perspective”. *The National Centre for Sensor Research (NCSR) cluster seminar*, Dublin City University, Dublin, 23<sup>rd</sup> May 2002.

**Hearty, S.** (2001). “SPR-based approaches to detecting pathogens.” *Institute for Medical Microbiology and Virology*, Justus Liebig University, Geissen, Germany, 21<sup>st</sup> June 2001.

Leonard, P., **Hearty, S.**, Quinn, J.G., and O’Kennedy, R. (2001). *Listeria monocytogenes*: antibody characterisation, biosensing developments and recombinant studies. *Inco Coperinicus PL 979012 project meeting*, Zivkov, Czech Republic, 10<sup>th</sup>-11<sup>th</sup> May 2001

**Hearty, S.** (2001). “Drug discovery in the biotech age.” *BPP Publishing*, Dublin, 12<sup>th</sup> April 2001.

**Hearty, S.**, Leonard, P., Quinn, J.G., and O’Kennedy, R. (2000). “Antibodies to *Listeria*: cross-reactivity studies and biosensor applications.” *Inco Coperinicus PL 979012 project meeting*, Slovak Technical University, Bratislava, Slovak Republic, 23<sup>rd</sup>-24<sup>th</sup> November 2000.

**Hearty, S.** (2000). “New and emerging pathogens.” *CTYI guest lecture*, Dublin City University, Dublin, 23<sup>rd</sup> June 2000.

Leonard, P., **Hearty, S.**, Quinn, J.G., and O’Kennedy, R. (2000). “Characterisation of anti-*Listeria monocytogenes* polyclonal antibodies by ELISA and BIAcore.” *Inco Coperinicus PL 979012 project meeting*, Dublin City University, Dublin, 25<sup>th</sup>-26<sup>th</sup> May 2000.



Fitzpatrick, J., Fanning, L., **Hearty, S.**, Leonard, P., Lacy, A., Daly, S., Dillon, P., Manning, B.M., Quinn, J.G. and O’Kennedy, R. (1999). “Antibodies- guided missiles in pursuit of food contaminants and illegal drugs.” *Science and Enterprise- The Best of Irish*, Royal Dublin Society, 5<sup>th</sup> November, 1999.



## Abstract

The principal objective of this research concerned the production, characterisation and application of antibodies for the specific detection of *Listeria monocytogenes*.

Monoclonal antibodies were generated against various *L. monocytogenes*-derived antigens. Initially, a panel of antibodies was produced against a 60 kDa extracellular protein isolated from exponentially growing *L. monocytogenes* culture supernatants. Subsequently, the *L. monocytogenes*-specific surface pathogenicity protein, Internalin B (InlB), was biochemically isolated and used to generate InlB-specific monoclonal antibodies. The specific reactivity of these antibodies was demonstrated using purified recombinant InlB (rInlB) and p60 (rp60) proteins, respectively. However, the anti-p60 antibody was cross-reactive with certain non-pathogenic members of the *Listeria* genus and the anti-InlB monoclonal antibody was not capable of efficiently binding InlB on the *L. monocytogenes* cell surface.

Thus, a third panel of monoclonal antibodies was generated using intact, formalin-inactivated *L. monocytogenes* cells as the immunogen. From this panel, a promising antibody was selected and shown to demonstrate improved specificity for the *L. monocytogenes* species. This antibody was further examined in order to demonstrate its potential application in traditional immunoassay and SPR-based biosensor formats.

The *L. monocytogenes inlA* gene was cloned into a compatible expression vector and recombinant InlA protein (rInlA) was heterologously expressed in *Escherichia coli*. This was then used to confirm that the antibody was indeed specific for the *L. monocytogenes* pathogenicity marker, InlA. The results indicated that the anti-InlA monoclonal antibody produced was capable of specifically binding to intact *L. monocytogenes* cells and therefore, it was concluded that it could potentially be employed to facilitate more rapid, reliable and specific detection of *L. monocytogenes* cells.



***Chapter 1***  
***Introduction***





### 1.1 *Listeria monocytogenes: discovery and history*

The original identification and description of *Listeria monocytogenes* is accredited to E.G.D. Murray, R.A Webb and M.B.R. Swann. While working in the pathology laboratories at Cambridge University in May 1924 Murray and co-workers undertook to investigate the cause of an outbreak of severe septicemic illness occurring in their laboratory rabbit population (Murray *et al.*, 1926). *Post-mortem* examination revealed localised hepatic lesions and systemic monocytosis. A small Gram-positive rod-shaped bacterium, (ATCC 4428, ATCC 15313 and NCTC 10357), was isolated from the infected rabbits and this was concluded to be the etiological agent. As a result of the monocytotic effect of the disease, the infected hosts were observed to compensate for this by initiating a rapid and significant up-regulation in their *monocyte generating* activity, thus, the bacterium was named *Bacterium monocytogenes*. One year later, in Johannesburg, a similar bacterium was isolated from wild gerbils displaying septicemic illness, by J.H Pirie. The bacterium was named *Listerella hepatolytica*, reflecting the pathogens necrotic effect on the liver. It soon became apparent that the organism isolated in both the rabbit and gerbil outbreaks was one and the same. This prompted Pirie to re-name the bacterium *Listerella monocytogenes*. However, the name *Listerella* had previously been used to classify a metazoan that was frequently isolated from both human and animal hosts suffering from “Listerellosis” and, thus, in 1940 the genus *Listerella* was re-classified as *Listeria* and the species *Listerella monocytogenes* was re-named *Listeria monocytogenes* (Pirie, 1940).

Although only identified in 1926, the first recorded culture of what we now know as *L. monocytogenes*, was actually documented in a soldier suffering from meningitis in France at the end of World War I (Dumont and Cotoni, 1921; Seeliger, 1988; McLaughlin, 1997). In fact, records suggest a very similar disease to listeriosis was recorded in 1891 (Gray and Killinger, 1966). The first reported cases of human listeriosis occurred in Denmark, three years after Murray’s identification of the causal bacterium (Nyfelt, 1929).

*L. monocytogenes* is one of six species within the genus *Listeria*. The remainder comprise *L. innocua*, *L. ivanovii*, *L. welshimeri*, *L. grayi* and *L. seeligeri* (Seeliger and Jones, 1986). The genus classification has been subject to regular revision and updating. For instance, in the early 1970’s a new species, *L. murrayi*, was putatively added to the genus (Stuart and Welshimer, 1974). However, it was subsequently designated a subspecies of *L. grayi* (Rocourt *et al.*, 1992). In addition, when *L. ivanovii* was first isolated in 1955, from congenitally infected lambs, it was classified as *L. monocytogenes* serotype 5 (Ivanov, 1962). It is now considered to comprise two divergent subspecies, *L. ivanovii* subsp. *ivanovii* and *L. ivanovii*



subsp. *londiensis* (Boerlin *et al.*, 1992). These are differentiated on the basis of the latter strains inability to ferment ribose.

Although it was earlier classified within the family *Corynebacteriaceae*, 16S rRNA sequencing has confirmed the genus *Listeria* to be taxonomically situated in the *Clostridium* sub-branch, along with *Staphylococcus*, *Streptococcus*, *Lactobacillus* and *Brochothrix* (Collins *et al.*, 1991; Sallen *et al.*, 1996). The latter of these is phylogenetically closest to *Listeria* (Seeliger and Jones, 1986). Indeed this phylogenetic position of *Listeria* is consistent with its low G+C content (Allerberger *et al.*, 2002).

## **1.2 Bacteriology and biochemistry of *Listeria***

*Listeria* are Gram-positive, regular short rods ranging in size from 0.4 - 0.5  $\mu\text{m}$  in diameter and 0.5 - 2  $\mu\text{m}$  in length (Seeliger and Jones, 1986). They generally exhibit motility between 20 and 28 °C by means of one to five peritrichous flagella and this can be demonstrated by performing a hanging drop experiment at room temperature or by inoculating semi-solid 'motility agar' containing 0.2 – 0.4 % agar (Allerberger, 2002). They are both aerobic and facultatively aerobic (Seeliger and Jones, 1986) and when grown in motility agar, disseminate and demonstrate localised increased growth just below the agar surface. It appears that in this zone of reduced oxygen tension, *Listeria* shows a better development than under either aerobic or strictly anaerobic conditions (Allerberger, 2002). The optimal growth temperature is between 30 and 37 °C although growth can occur temperatures between 1 and 45 °C, at pH 6 – 9 and in the presence of up to 10 % (w/v) salt (Seeliger and Jones, 1986).

All members of the genus *Listeria* are catalase positive. However, only *L. monocytogenes*, *L. ivanovii* and *L. seeligeri* are haemolytic. The CAMP (Christie, Atkins, Munch-Petersen) test (Schuchat *et al.*, 1991a) is commonly employed to assess haemolytic patterns in *Listeria*. It uses a  $\beta$ -haemolysin-producing *Staphylococcus aureus*, and a *Rhodococcus equi* strain streaked in one direction on a sheep blood agar plate and test cultures of *Listeria* spp. streaked at right angles to (but not touching), the *S. aureus* and *R. equi* lines. Haemolysis of *L. monocytogenes* (and to a lesser extent *L. seeligeri*) is enhanced in the vicinity of the *S. aureus* streak and *L. ivanovii* haemolysis is enhanced in the vicinity of *R. equi* (Allerberger, 2002). Problems have been described in the interpretation of haemolytic reactions (McLaughlin, 1997), particularly when using the CAMP test (Schuchat *et al.*, 1991b; Vázquez-Boland *et al.*, 1992; McKellar, 1994; Fernandez-Garayzabal *et al.*, 1996). These problems have been



attributed to the occasional synergistic haemolytic activity between *L. monocytogenes* and *R. equi* (Bille *et al.*, 1999; Allerberger, 2002). In addition to the characteristic haemolytic patterns, each species' ability or inability to ferment selected sugars has formed the basis for biochemical identification to the species level using the 'Analytical Profile Index', or API test (bioMérieux, France). The fermentation patterns exhibited by each species are outlined in Table 1.1. However, despite its widespread use, occasional discrepant results have been reported with the API test (Bille, 1992).

**Table 1.1: Biochemical differentiation across the genus *Listeria*. (Adapted from Seeliger and Jones, 1986; Allerberger, 2002).**

	<i>L. monocytogenes</i>	<i>L. innocua</i>	<i>L. welshimeri</i>	<i>L. seeligeri</i>	<i>L. ivanovii</i> <sup>*1</sup>	<i>L. grayi</i>
<b>Haemolysis</b>	+	-	-	+	+	-
<b>L-rhamnose</b>	+	V	V	-	-	-
<b>D-xylose</b>	-	-	+	+	+	-
<b><math>\alpha</math>-methyl-D-mannoside</b>	+	+	+	-	-	+
<b>D-mannitol</b>	-	-	-	-	-	+
<b>CAMP test (<i>S. aureus</i>)</b>	+	-	-	+	-	-
<b>CAMP test (<i>R. equi</i>)</b>	-	-	-	-	+	-

+: positive

-: negative

V: variable

\*1: Ribose fermenting

The *L. monocytogenes* species is further sub-classified by serotyping with antisera derived from immunised rabbits (Seeliger and Höhne, 1979). This discriminates on the basis of reactivity patterns towards defined somatic (O) and flagellar (H) antigens. There are thirteen serotypes in total: 1/2a, 1/2b, 1/2c, 3a, 3b, 3c, 4a, 4ab, 4b, 4c, 4d, 4e and 7 (Table 1.2). The serogroups 1/2 and 3 are subdivided into serovars according to their H-antigen profile, while the serogroup 4 serovars all contain similar H-antigen profiles and are, thus, divided into



serovars according to their O-antigen profile (Schönberg *et al.*, 1996). Unfortunately, certain serotyping antigens are also present in *L. innocua*, *L. seeligeri* and *L. welshimeri*. This significantly compromises the discriminatory power of serotyping, by preventing species-level identification. Nonetheless, serotyping serves a useful purpose for confirming the genus diagnosis of *Listeria* and for allowing first-level subtyping for epidemiological purposes (Allerberger, 2002).

**Table 1.2:** Serotyping of *L. monocytogenes* according to O and H antigens. (Adapted from Seeliger and Höhne, 1979 and Allerberger 2003).

Serotype	O-Antigens													H-Antigens			
	I	II	III	IV	V	VI	VII	VIII	IX	X	XI	XII	XIII	A	B	C	D
1/2a	•	•	(•)											•	•		
1/2b	•	•	(•)											•	•	•	
1/2c	•	•	(•)												•		•
3a		•	(•)	•										•	•		
3b		•	(•)	•								(•)	(•)	•	•	•	
3c		•	(•)	•								(•)	(•)		•	•	
4a			(•)	(•)			•		•					•	•	•	
4ab			(•)		•	•	•		•	•				•	•	•	
4b			(•)		•	•								•	•	•	
4c			(•)		•		•							•	•	•	
4d			(•)		(•)	•		•						•	•	•	
4e			(•)		•	•		(•)	(•)					•	•	•	
7			(•)									•	•	•	•	•	

The brackets, '( )' indicate variable interpretation of reactivity.

### 1.3 *Listeriosis: pathophysiology and incidence*

*Listeria monocytogenes* is ubiquitous in the natural environment and is frequently isolated from both domestic (Duggan and Phillips, 1998), and food processing (Blackman and Frank, 1996; Gravani, 1999; Senczek *et al.*, 2000; Silva, *et al.*, 2003) environments. The associated potential for significant contamination is exacerbated by virtue of the organism's ability to tolerate high salt concentrations (Marth, 1993; Esvan *et al.*, 2000), acidic media (Dykes and





Moorhead, 2000; Scott Merrel and Camili, 2002), modified atmosphere packaging (Beuchat and Brackett, 1990), in addition to its capacity to multiply at refrigeration temperatures (Walker *et al.*, 1990).

In 2000, the Centres for Disease Control (CDC) reported that all of all the foodborne pathogens tracked by the CDC, *L. monocytogenes* had the second highest case fatality rate (21 %) and the highest hospitalisation rate (90.5 %) (Anon., 2003a).

In fact, because listeriosis so often results in medical intervention, the CDC postulate that its 'Foodborne Active Surveillance Network' (FoodNet) misses only half of all listeriosis cases, compared with 97 % in the case of other pathogens (Mead *et al.*, 1999). Thus, when the data in Table 1.3 is considered, pathogens such as *Campylobacter* spp. and *Salmonella* spp. may account for as many as 50 times the number of *Listeria* infections, yet the latter still accounts for one third of the total deaths due to foodborne pathogens. It has even been suggested that salmonellae may account for 500 times as many cases of foodborne illness, annually, with an associated fatality rate of just 0.04 % (Mead *et al.*, 1999; Doyle, 2001). A similar scenario is depicted in the UK and Denmark, where, despite the incidence of listeriosis between 1995 and 1999 remaining quite low, at 1.7-2.4 cases per million head of population (Smeardon *et al.*, 2001), and 6-7 per million head of population (Slutsker and Schuchat, 1999), respectively, mortality rates were consistently above 20 %. A recent review of selected cases from around the world puts the mean incidence of non-pregnancy associated listeriosis at 0.1-1.1 per one hundred thousand head of population with an associated mortality of 36 %. While, for pregnancy-associated listeriosis, incidence is estimated to be 0.6-4.1 per ten thousand births, with an associated mortality of 33 % (Siegman-Igra *et al.*, 2001). This emphasises the alarming clinical severity of the pathophysiological effects of listeriosis.



**Table 1.3: Incidence of foodborne pathogens in USA, 2000 (Anon., 2003b).**

Pathogen	Infections (Cases per 1x10 <sup>6</sup> population)
<i>Vibrio</i>	2.1
<i>Listeria</i>	3.4
<i>Yersinia</i>	4.4
<i>E. coli O157:H7</i>	21
<i>Shigella</i>	79
<i>Salmonella</i>	144
<i>Campylobacter</i>	157
Total pathogens	411.6

Infection with *L. monocytogenes* can be categorised as invasive or non-invasive (Figure 1.1). Cases can be further defined as either non-pregnancy-associated, which refers to all cases in patients aged over one month and un-associated with pregnancy, or pregnancy-associated (Duggan and Phillips, 1998). The principal transmission route for infection with *L. monocytogenes* is the consumption of contaminated food (McLaughlin, 1996; Schlech, 2000). In a healthy population, consumption of foods contaminated with *L. monocytogenes* may cause self-limiting gastrointestinal symptoms that include fever, nausea, vomiting and diarrhoea (DiMaio, 2000). Gastrointestinal symptoms are observed in approximately one third of documented cases of listeriosis (Donnelly, 2001). It is likely, however, that a significant proportion of sporadic cases of gastrointestinal illness due to *L. monocytogenes* infection go unreported and, are thus, unaccounted for in the epidemiological statistics. The oral bacterial load required to cause infection has been estimated to be greater than  $1 \times 10^4$  cells (DiMaio, 2000). The relatively short median incubation time (typically 18-20 hours) between consumption of contaminated food and noticeable gastrointestinal symptoms in healthy, immunocompetent individuals suggests that the etiologic dose is significantly higher than this conservative estimate. Available epidemiological data have indicated levels ranging from  $10^6$  cells/g of food, to  $10^{11}$  cells/ml of milk (Azadian *et al.*, 1989; Juntilla and Brander, 1989; Dalton *et al.*, 1997) may be necessary, which is in agreement with experimental and risk assessment estimates (Golnazarian *et al.*, 1989; Farber and Peterkin, 1991; Buchanan *et al.*, 1997; Notermans *et al.*, 1998; Haas *et al.*, 1999; Lindqvist and Westöö, 2000, Anon WHO/FAO, 2002). It would appear from recent outbreaks that gastrointestinal symptoms might, in fact, represent the principal pathophysiological manifestation of listeriosis (Salamina *et al.*, 1996; Miettinen *et al.*, 1999; Aureli *et al.*, 2000). This is acknowledged by



calls for *L. monocytogenes* infection to be specifically investigated in patients presenting with acute gastroenteritis and diarrhoea (Jensen, 1994; Lorber, 1997).

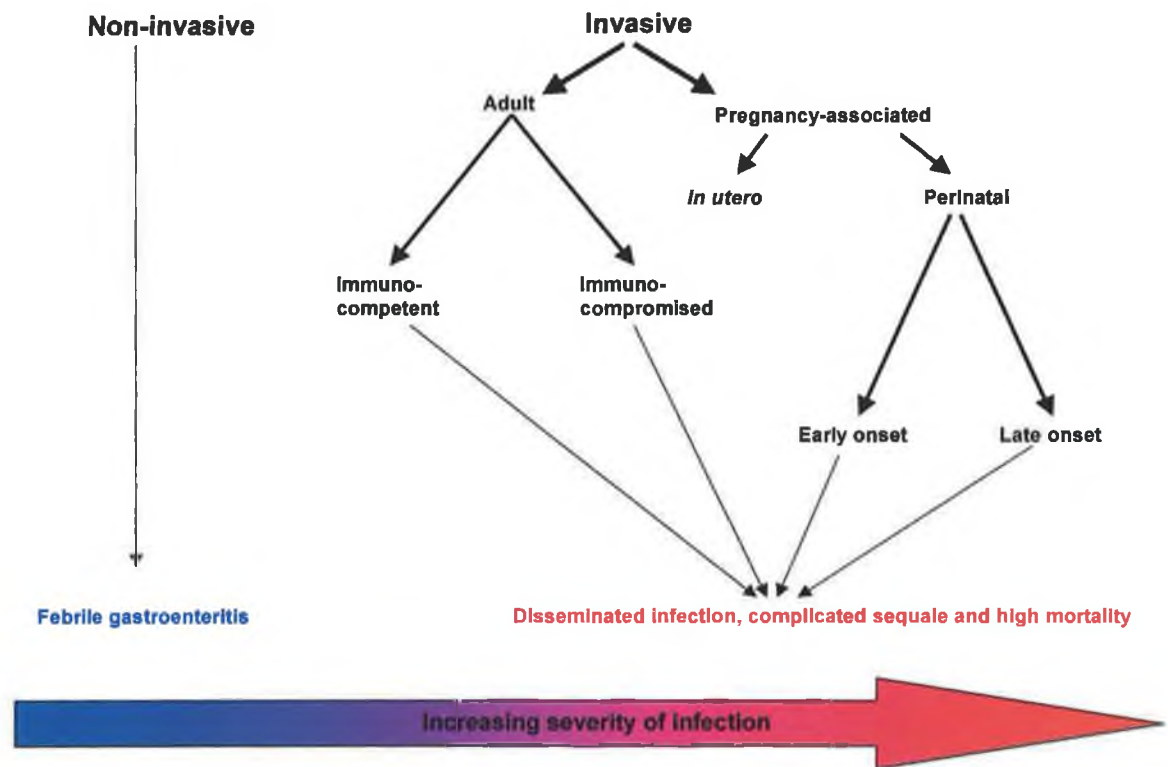


**Figure 1.1:** Classification of listeriosis in humans. The disease can be classified as 'non-invasive', which normally results in self-limiting gastrointestinal symptoms, with no significant side-effects. Alternatively, 'invasive' listeriosis is a more debilitating disease, which normally manifests in susceptible members of the population with predispositions to infection, such as the immunocompromised and new born infants.



## **1.4 Infection**

The precise locus of bacterial infection has long been debated. Undisputed however, is the fact that during an acute infection, multiple tissues are infected. This has also been demonstrated *in vitro* (Cossart and Mengaud, 1989). Further *in vitro*-mediated cellular assays have elucidated a complex cascade of host-pathogen interactions that culminate in direct cell-to-cell dissemination (Cossart and Lecuit, 1998). Initial exposure to the pathogen generally occurs in the gastrointestinal tract following ingestion of contaminated food (Schuchat *et al.*, 1991a). The infection cascade begins when the pathogen becomes internalised by host phagocytic cells (macrophage). *L. monocytogenes* can also induce its own uptake by cells that are not normally phagocytic (non-professional phagocytes). These include epithelial cells and hepatocytes. Pron and co-workers (1998) have identified a preferential site of early multiplication in the phagocytes underlying the Peyer's patches, using a novel rat model. Generally, invading cells are cleared rapidly via the lymph system and blood stream to the liver. Cells that succeed in evading the Kupffer cells are internalised by the parenchymal cells (hepatocytes) where rapid intracellular replication ensues (Rogers *et al.*, 1996; Gregory *et al.*, 1997).

### **1.4.1 Virulence factors involved in adhesion and invasion**

#### **1.4.1.1 Internalins**

Phagocytic internalisation of *L. monocytogenes* occurs similar to the 'zipper' mechanism exhibited by *Yersinia* species (Cossart and Lecuit, 1998; Frischknecht and Way, 2001). This involves the stimulated development of pathogen-accomodating protrusions in the host cell membrane, adjacent to the invading bacteria. It is distinct from the 'trigger' type pinocytosis exhibited during *Salmonella* and *Shigella* pathogenesis (Finlay and Ruschkowski, 1991; Swanson and Baer, 1995). The principle route of infection by *L. monocytogenes* is via the gastrointestinal tract and, more specifically, the gut wall epithelium. The ligands involved in the internalisation process have been suitably termed 'internalins'. *Listeria monocytogenes* employs two surface bound internalins, internalin A (InlA) and internalin B (InlB), to promote its internalisation by non-phagocytic mammalian cells (Gaillard *et al.*, 1991; Lingnau *et al.*, 1995). InlA (also referred to, generically, as 'internalin') is essential for entry into cultured human epithelial (Caco-2) cells (Dramsai *et al.*, 1993), whereas the 630 amino acid InlB protein has been shown to promote bacterial internalisation in several cultured cell types including, hepatocytes (Dramsai *et al.*, 1995; Gregory *et al.*, 1997) and endothelial cells (Greiffenberg *et al.*, 1998; Parida *et al.*, 1998).





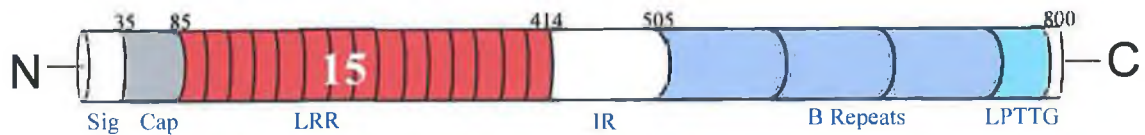
The primary structure of the internalin molecules is conserved within *L. monocytogenes* and is characterised by two repeat regions separated by an inter-repeat (IR) region (Figure 1.2). InlA is the most 'typical' example of the complete internalin modular structure. It is 800 amino acids in length (Gaillard *et al.*, 1991), and is the largest member of the internalin family. The N-terminal positively charged signal sequence is followed by a series of 15 highly conserved leucine-rich repeats (LRRs). These LRR domains are a pervading feature throughout the internalin family of proteins (Kajava, 1998) and normally indicate virulence association. The 'B' repeat region follows a short IR sequence and consists of 3 successive repeats, the first two consist of 70 amino acids, the third consists of 49 amino acids, that lack the periodicity of non-polar (leucine/isoleucine) residues evident in the LRR region.

The anchor structure of cell wall-bound InlA has been compared to a wide range of Gram-positive surface-displayed proteins (Navarre and Schneewind, 1999). The most comprehensively studied of such proteins are those expressed by *Staphylococcus aureus*. These are characterised by a C-terminal LPXTG motif (where X represents any amino acid) that is linked to the pentaglycine cross-bridge via the threonine (T) residue, following cleavage the T-G bond with the transpeptidase enzyme sortase (Ton-That *et al.*, 1999). InlA of *L. monocytogenes* produces threonine hydroxamate when treated with the strong nucleophile, hydroxylamine, indicating a similar T-G bond cleavage (Dhar *et al.*, 2000). This transpeptidase activity covalently links the InlA protein to the *meso*-diaminopimelic acid (*m*-Dpm) cross-bridge present in the cell wall of *L. monocytogenes* (Figure 1.4). The gene encoding the sortase responsible for InlA anchoring has been identified as *srtA* (Bierne *et al.*, 2002; Cabanes *et al.*, 2002).

The InlB protein is only loosely tethered to the cell membrane through a series of C-terminal GW repeats that associate with lipoteichoic acids (Figure 1.4) at the peptidoglycan-cell membrane interface (Braun *et al.*, 1997; Jonquières *et al.*, 1999; Cabanes *et al.*, 2002). Unlike InlA, InlB is generally not very accessible at the cell wall surface (Jonquières *et al.*, 1999) but significant amounts can be released into growth media (Cossart, 2001). It has also been shown that free InlB in the media can reattach to the cell membrane via the GW repeat region without any loss in functionality (Braun *et al.*, 1997).



## Inl A



## Inl B

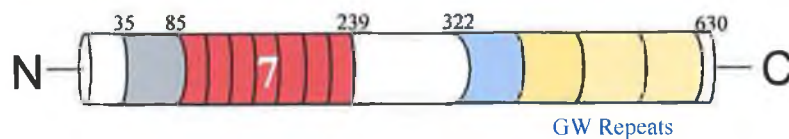


**Figure 1.2:** Primary 'domain' structure of the *InlA* and *InlB* proteins. The key difference to note is that *InlC* lacks the cell wall anchoring motif (LPTTG) present in *InlA* and all the other classified internalins

The key structural and functional aspects of internalin-mediated adhesion to host cells have been recently reviewed (Cabanès *et al.*, 2002; Cossart *et al.*, 2003; Schubert and Heinz 2003). A central clue to identifying the functional region of internalin is the conserved nature of the LRR hydrophobic repeats (Figure 1.3). Such sequences are often associated with functional domains. The fact that they are highly conserved within the species suggests that they have probably been retained as a result of functional selective pressure. It has been demonstrated that the combined LRR, IR and cap regions are necessary and sufficient to promote entry into human epithelial cells (Lecuit *et al.*, 1997), while the LRR domain of *InlB*, alone, is sufficient to promote entry into parenchymal cells (Braun, 1998; Braun, 1999). The crystal structure of the LRR domain from *InlB* was successfully resolved by Marino and co-workers (1999), and it revealed each tandem repeat to adopt an oval structure, consisting of a  $\beta$ -strand on one side and an antiparallel  $3_{10}$ -helix on the opposite side, connected by short loops (Marino *et al.*, 2000; Schubert *et al.*, 2001). Similar structural arrangements were first reported in the pectate lyase enzyme produced by the plant pathogen *Erwinia chrysanthemi* (Yoder *et al.*, 1993; Heffron *et al.*, 1998; Herron *et al.*, 2000). It is probable that the LRR domain structure is conserved throughout the internalin family. More recently, the crystal structure of the entire *InlB* protein has been elucidated (Schubert *et al.*, 2001). It demonstrates that *InlB* is



composed of three clustered domains; an N-terminal cap domain (amino acids 63-79), a central LRR domain (amino acids 80-240) and a C-terminal domain (amino acids 241-321 and 263-343). The cap domain consists of three  $\alpha$ -helices and one anti-parallel, two-stranded  $\beta$ -sheet that resembles a truncated EF-hand motif, similar to those identified in calmodulin and related calcium-binding proteins (Babu *et al.*, 1988; Flaherty *et al.*, 1993).

The LRR domain is typified by a  $\beta$ -strand-loop-antiparallel helix that exhibits an overall 'bent' shape with distinct concave and convex faces. The IR domain represents the most conserved region within the internalin family (Schubert *et al.*, 2001). The domain structure is dominated by an imperfect, four-stranded antiparallel  $\beta$ -sheet, linked to the LRR  $\beta$ -strand that contributes structural similarity to single immunoglobulin-like domains. This 'Ig-like' structure fused to a second domain is unique and distinct from the multiply linked Ig domains common in antibodies and cell surface receptor molecules (Harpaz and Chothia, 1994).

E-cadherin was identified as the InlA receptor through a series of affinity chromatography experiments with extracted surface proteins from cultured epithelial cells (Mengaud, 1996). Attempts to demonstrate InlA-mediated epithelial invasion *in vivo* using mouse or rat models proved impossible. The reason for this became evident when it was discovered that a single amino acid in the human E-cadherin (hEcad) molecule was responsible for host specificity towards the *Listeria monocytogenes* pathogen (Lecuit *et al.*, 1999). A single proline residue at position 16 was essential to facilitate InlA 'docking'. However, the mouse model was flawed because mouse E-cadherin (mEcad) contains a glutamic acid residue instead of proline at position 16. This was proven by demonstrating that a Pro→Glu substitution in hEcad prevented InlA binding and, conversely, that a Glu→Pro substitution conferred InlA specificity in mEcad. Using these findings, a hEcad overexpressing transgenic mouse has recently been applied to the development of a murine model of orally acquired listeriosis (Lecuit *et al.*, 2001).

The first of at least two InlB receptors, gC1q-R, was also identified through affinity chromatographic experiments (Braun *et al.*, 2000). The crystal structure of gC1q-R (Jiang *et al.*, 1999) does not reveal properties typical of transmembrane or glycosylphosphatidylinositol-anchored proteins and, thus, implies the likely involvement of an ancillary transmembrane protein to mediate membrane-to-cytosol signalling. The second confirmed InlB receptor is the hepatocyte growth factor and scatter factor (HGF-SF) receptor (Shen *et al.*, 2000). This protein had previously been characterised as a disulphide-linked heterodimer consisting of a 45 kDa  $\alpha$ -, and 145 kDa  $\beta$ -subunit (Birchmeir and Gerardi, 1998;

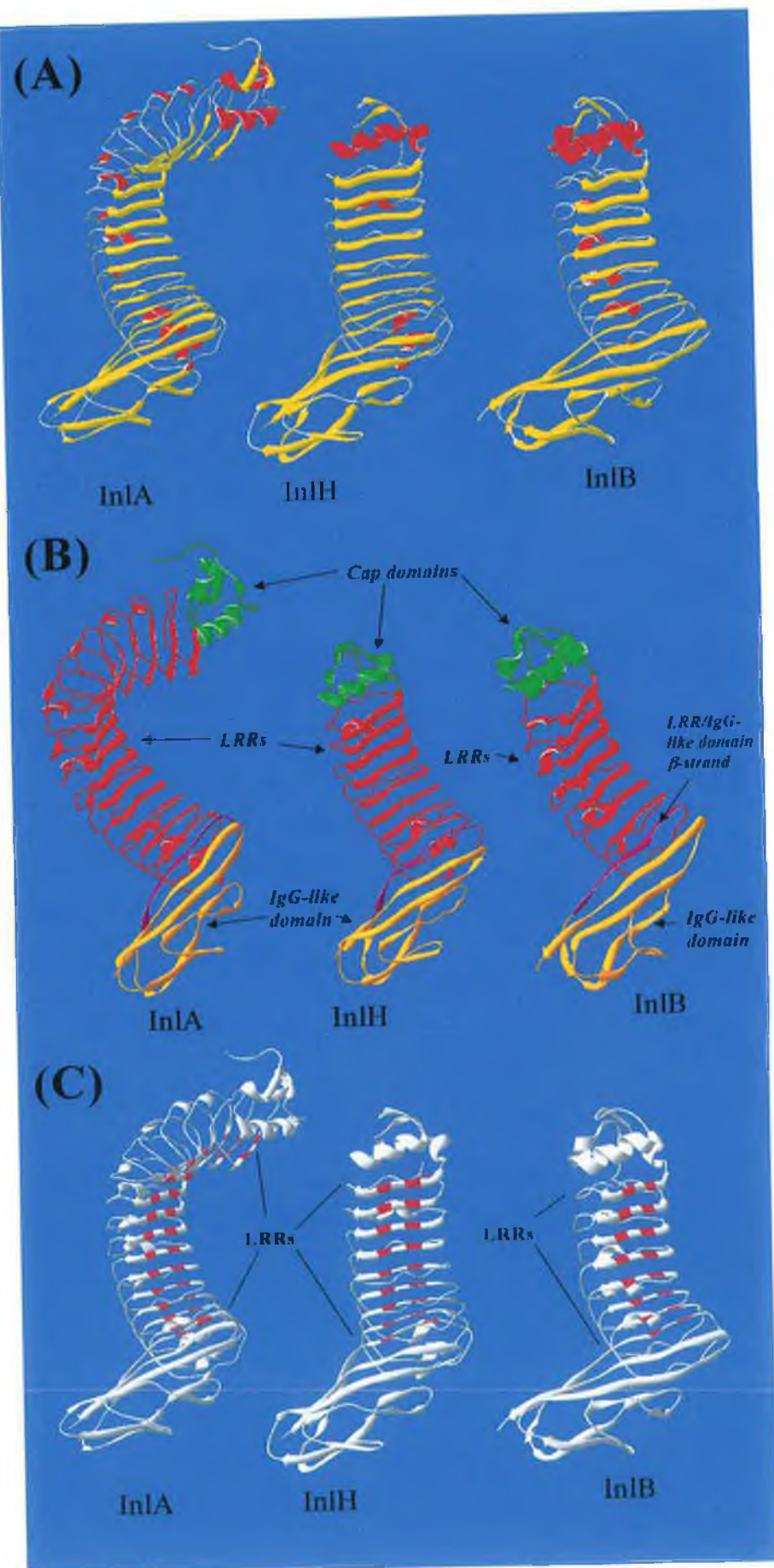


Trusolino *et al.*, 1998). The latter contains a transmembrane component and a cytoplasmic domain possessing both tyrosine kinase activity and a tyrosine-rich, autophosphorylation site. The receptor has also been referred to as the c-met proto-oncogene, c-Met tyrosine kinase and simply, MET (Birchmeir and Gerardi, 1998; Trusolino *et al.*, 1998). Evidence to support its role as an InlB receptor includes the observed InlB-induced tyrosine phosphorylation of the adaptor proteins Gab1, Cbl and Shc, linked with concomitant activation of p85-p110, mammalian phosphoinositide 3-kinase (PI 3-K) (Ireton *et al.*, 1999). Activation of p85-p110 has been highlighted as an essential mediator of bacterial uptake by mammalian cells (Ireton *et al.*, 1996; Ireton *et al.*, 1998). In addition, InlB, in common with HGF, activates multiple signalling cascades that are not directly involved in the invasion process (Bierne and Cossart, 2002). An overview of the receptor-ligand interactions and primary signalling events is provided in Figure 1.4.

Identification of the principal InlB receptor molecules may shed light on how the surface-bound InlA from the invading bacteria gains access to hEcad that is predominantly located at the basolateral surface, and junction regions of gut epithelial cells. The ubiquitous distribution of c-Met on mammalian cell surfaces and more convincingly, its tendency to congregate with hEcad (Kamei *et al.*, 1999) suggest that free InlB may leach into the epithelial junctions and, upon interacting with c-Met, cause 'scattering' (Kamei *et al.*, 1999; Mansell *et al.*, 2000) of adjacent cells with concomitant exposure of hEcad receptors.









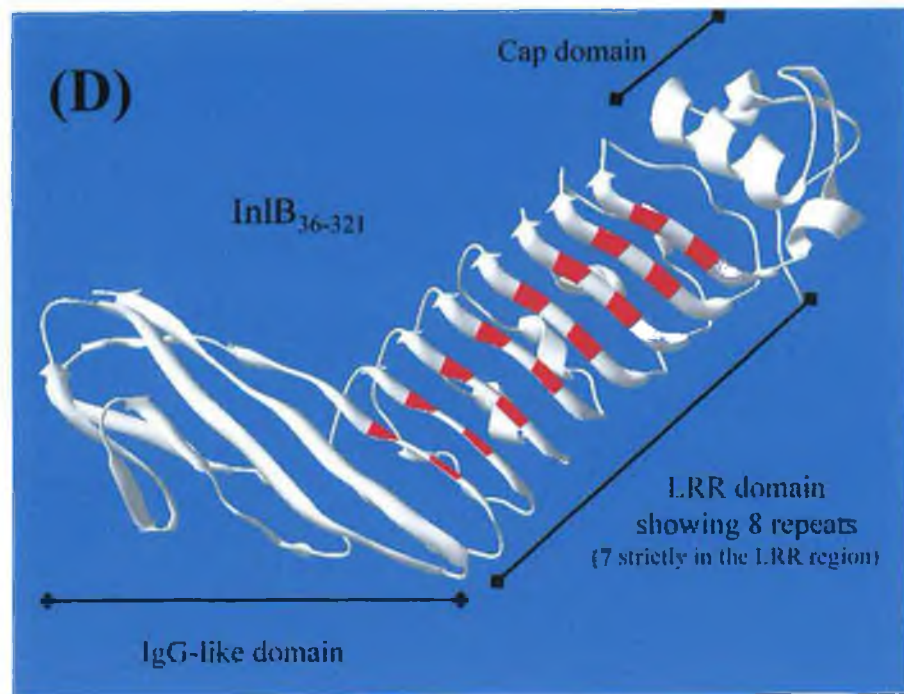


**Figure 1.3:** 3-D ribbon structures of InlA<sub>36-496</sub> (PDB code 1O6T), InlH<sub>36-343</sub> (PDB code 1H6U) and InlB<sub>36-321</sub> (1H6T) viewed using Swiss-PDB viewer. Panel A shows the 3D structures of InlA, InlH and InlB in a view towards the concave surface of the leucine-rich repeat (LRR) region.  $\alpha$ -helices are coloured in red, loops in solid grey and  $\beta$  strands as yellow arrows pointing in a N-terminus to C-terminus direction. Panel B shows the structures presented in panel A coloured according domain structure. The area coloured in green represents the cap domain, the LRR region is coloured in red and the 'IgG-like' domain coloured in orange. The final  $\beta$  strand (coloured purple) of the LRR region is simultaneously the first strand of the 'IgG-like' domain. Panel C shows the structures coloured in grey with the leucine rich repeats coloured in red. Generally LRRs are 20-29 residues long and contain a conserved 11-residue segment with the consensus sequence LXXLXLXXXXL, where X can be any amino acid and leucine (L) can also be substituted with valine (V), isoleucine (I) or phenylalanine (F) (Kobe and Kajava, 2001). In *Listeria*, the internalin family of LRR proteins have varying numbers of repeats of 22 amino acid residues. In the diagram only the two repeat residues (i.e. LXXLXLXXXXL) present on the  $\beta$ -strands are coloured in red. InlA has 15 tandemly arranged leucine-rich repeats, InlH has 8 repeats and InlB has 7 repeats. Panel D shows an enlarged view of the InlB structure shown in C with the leucine-rich repeat residues coloured in red. The last  $\beta$ -strand of the LRR region simultaneously forms the first strand of the IgG-like domain, as shown in panel B. The InlB structure presented, can be classified as having 7 or 8 repeats, depending on the classification of the LRR region (i.e. inclusion of the last  $\beta$ -strand).



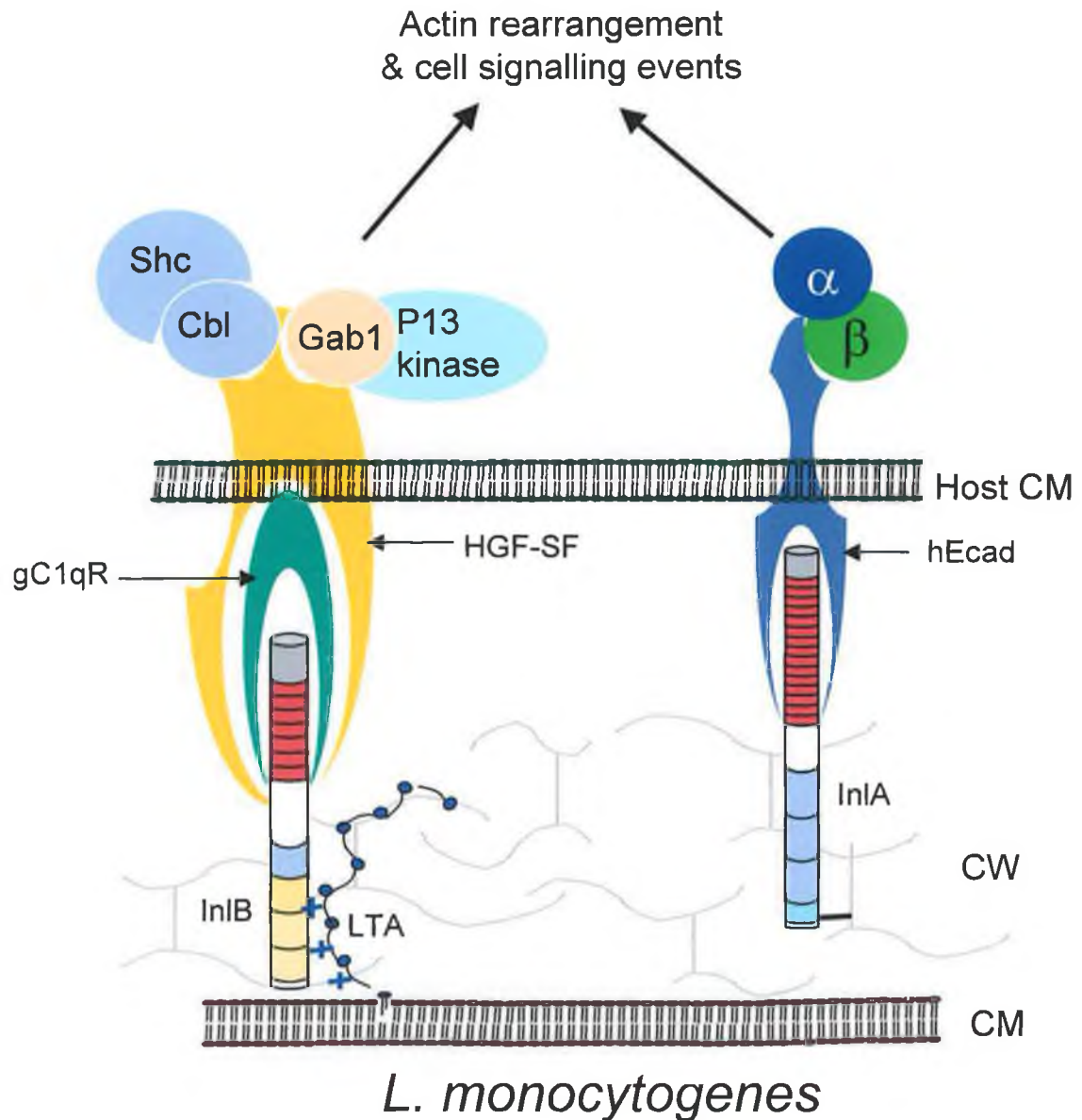


**Figure 1.4:** Schematic overview of *L. monocytogenes*-mediated host cell interaction. InlB, which is loosely tethered to lipoteichoic acid (LTA), is thought to induce tyrosine phosphorylation of Gab1, Cbl and Shc, following binding to gC1qR and HGF-SF. These mammalian adaptor molecules are thus primed to associate with the p85 subunit of P13-kinase and mediate cytoskeletal rearrangements. InlA is covalently linked to cell wall peptidoglycan and its N-terminal LRR domain binds to hEcad. Subsequently, the cytoplasmic domain of the InlA-activated hEcad interacts directly with  $\beta$ -catenin, which in turn associates with  $\alpha$ -catenin to mediate actin rearrangement (Galán et al., 2000). The full complement of signalling events in the invasion cascade has yet to be confirmed.



Such synergies within the internalin family may indeed be more widespread than at first appreciated. By studying the effect on internalisation into epithelial-like Caco-2 and the human microvascular endothelial (HBMEC) cell lines of various *inl* deletion mutants, Bergmann *et al.*, (2002) have shown that InlA in particular acts in concert with one or several other internalins to function efficiently during invasion. More specifically, it has been demonstrated that deletion of the *inlGHE* cluster results in enhanced expression of bicistronic *inlA* and *inlB* but not *inlC*. Whereas InlB alone is necessary and sufficient to promote host cell invasion in HBMEC (Greiffenberg *et al.*, 1998), InlA requires the cooperative intervention of InlC and InlGHE or InlB to mediate invasion of Caco-2 cells, as had been previously suggested (Lingnau, *et al.*, 1995). Enhanced InlB-mediated invasiveness of HBMEC has been demonstrated for *inlGHE*-deficient cells and even more so for *inlGH*- / *inlC*-deficient cells (Bergman *et al.*, 2002). InlA-induced phagocytosis has conversely been shown to demonstrate an absolute requirement for coexpression of InlB, or InlC, or both InlC plus *inlGHE* (Bergman *et al.*, 2002).

These results suggest that InlA-mediated phagocytosis intrinsically relies upon coexpression of soluble InlC protein and a favourable host cell disposition induced by either InlB or *inlGHE* proteins, which are possibly competing for the same host cell receptors.

#### **1.4.1.2 *Listeria* adhesion protein (LAP) or p104**

The role of a 104 kDa listerial surface protein (p104) in adhesion of *Listeria monocytogenes* to human intestinal cells was demonstrated by Pandrillally and co-workers (1999). The specific eukaryotic receptor ligand remained unclear until quite recently. Through a sequence Western blot ligand overlay assays, the receptor for p104, or *Listeria* adhesion protein (LAP) was putatively identified as a 58 kDa protein, 'heat shock protein 60' (Hsp60) and this was subsequently confirmed by immunoaffinity chromatography (Wampler *et al.*, 2004).

#### **1.4.1.3 *Amidase* (Ami)**

*L. monocytogenes* serovar 1/2a EGD produces a 917 amino acid (102 kDa) autolytic amidase (Ami) that is targeted to the bacterial cell surface via a dedicated C-terminal GW-repeat domain, and it accounts for 66 % of the total lytic enzyme activity (McLaughlan and Foster, 1998). In addition to this confirmed role as a peptidoglycan hydrolase, the GW-repeat region has been implicated in adhesion of *L. monocytogenes* to mammalian cells (Milohanic *et al.*, 2001). It appears that the GW repeat region is the key determinant of Ami-mediated adhesion. The *L. monocytogenes* serotype 4b-derived Ami (Ami 4b), which, is only 770 amino acids in





length, contains an identical N-terminal region to that of Ami 1/2a. However, it contains only six GW repeats, in comparison to Ami 1/2a's eight, and this correlates with a reduced ability of Ami 4b to bind Hep-G2 human hepatocytic cells (Milohanic *et al.*, 2004).

#### **1.4.2 Virulence factors involved in intra- and inter-cellular spreading**

##### **1.4.2.1 p60**

The p60 protein, encoded by the invasion-associated protein (*iap*) gene (Kuhn and Goebel, 1989; Köhler *et al.*, 1990) present in both culture supernatant (Kuhn and Goebel, 1989), and localised at the cell surface (Ruhland *et al.*, 1993). Analysis of serum from listeriosis patients indicates that p60 is a potent B-cell stimulator (Gentshev *et al.*, 1992). The protein comprises 484 amino acids and is characterised by a central sequence of Thr-Asn repeats (Köhler *et al.*, 1990; Bubert *et al.*, 1992). The C-terminal region possesses a murein hydrolase activity that mediates efficient septum formation during cell proliferation (Wuenschel *et al.*, 1993). Further evidence for this hydrolase activity stems from the fact that spontaneously occurring 'rough' phenotypes that are made up of long filamentous colonies with attenuated virulence in fibroblast cells, have been shown to be deficient in p60 expression (Kuhn and Goebel, 1989). *L. monocytogenes* cells that are deficient in p60 also exhibit an uneven distribution of ActA protein with a concomitant reduction in actin tail formation and, thus, reduced intercellular invasiveness (Pilgrim *et al.*, 2003). The full and exact role of p60 in listerial virulence is unclear. However, it is possible that it essentially functions as a dedicated cell wall hydrolase, with a significant, yet principally indirect contribution to strain virulence.

##### **1.4.2.2 ActA**

Once the bacterium has escaped from the phagosome into the cytoplasm, it adopts an intricate system of directional propulsion mediated by actin polymerisation (Figure 1.5). The actin assembly (*actA*) gene product has been highlighted as an essential factor for actin accumulation, since *actA*<sup>-</sup> genotypes fail to harness actin filaments and thus, grow as localised microcolonies in host cells (Domann *et al.*, 1992; Kocks *et al.*, 1992). This 90 kDa protein exhibits a C-terminal hydrophobic anchor region indicating membrane bound localisation. In fact it adopts an inversely proportional polar distribution (Kocks *et al.*, 1993) at the bacterial surface, serving as a focal point for an actin tail formation. Studies conducted with truncated ActA derivatives have demonstrated that there are two further distinct functional regions (Pistor *et al.*, 1995; Niebuhr *et al.*, 1997). The first is a central (amino acids 234-395) region of proline rich repeats (PRR), that sequesters actin filaments from the cytoskeleton by



interfacing with the focal adhesion molecule, vasodilator-stimulated phosphoprotein (VASP) (Holt and Koffer, 2001) and mammalian 'enabled' (Mena) protein. It has recently been demonstrated that binding of profilin (Pr), complexed to actin protein, to the PRR domain, plays a crucial role in mediating intracellular actin-based motility (Grenklo *et al.*, 2003).

The second functionally important domain is a highly positively charged N-terminal region that is required for actin filament nucleation. This region activates host cell Arp2/3 complex concomitantly stimulating actin polymerisation and has been shown to be essential for actin-based motility of *L. monocytogenes* (May *et al.*, 1999). In mammalian cells, the Arp2/3 complex interacts with the C-terminal regions of the Wiskott-Aldrich syndrome (WASP/Scar) family proteins to mediate rearrangement of the cytoskeleton. (Machesky and Insall, 1998; Machesky *et al.*, 1999). The N-terminal ActA region functionally mimics WASP/Scar activation of the Arp2/3 complex (Frischknecht and Way, 2001). The acidic region (amino acids 33-46) of ActA increases the efficiency of Arp2/3-mediated actin nucleation *in vitro* and enhances the rate and frequency of motility *in vivo*, whereas the 60-101 amino acid actin-monomer-binding region is not a prerequisite for *in vivo* actin-based motility. Conversely, the highly basic cofilin-homologous stretch of the N-terminal ActA sequence (amino acids 146-150) is essential for both Arp2/3 activation and actin-based *in vivo* motility (Pistor *et al.*, 2000; Skoble *et al.*, 2000). Although ActA is a major surface-exposed virulence protein, it is only presented by either MHC class I or class II molecules when administered in soluble form, and CD8<sup>+</sup> cells so elicited, do not confer *in vivo* anti-listerial protection (Darji *et al.*, 1998).

In addition to its documented role in cytosolic motility, a possible role for ActA in the primary adhesion and invasion processes has been suggested (Alvarez-Domínguez *et al.*, 1997; Suárez *et al.*, 2001), following confirmation that expression of ActA in *L. innocua* was sufficient to promote entry into epithelial cells (Suárez *et al.*, 2001).



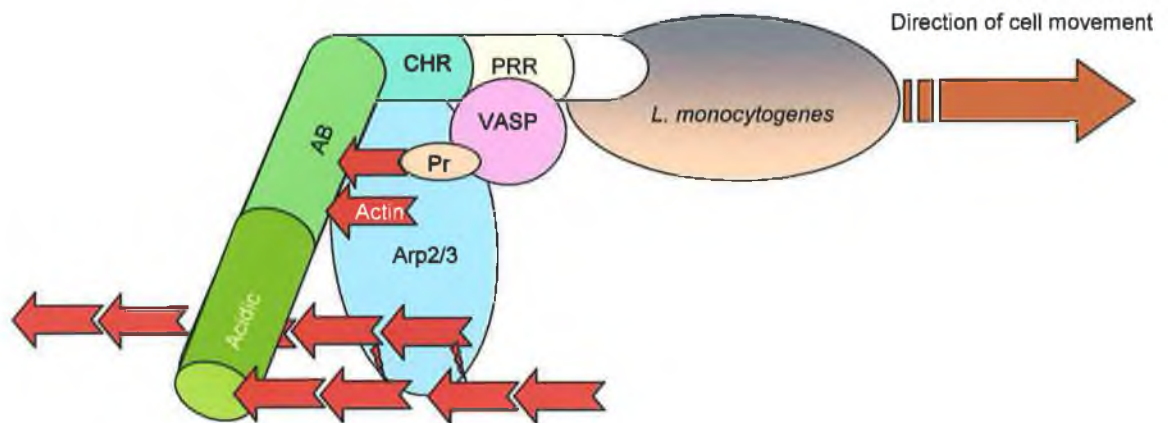


**Figure 1.5:** Mechanics of actin-based motility. The ActA protein contains the following domains: PRR, proline-rich region; CHR, cofilin homology region; AB, actin-binding domain, preceding an acidic N-terminal sequence. Other molecules involved in cytoskeletal actin rearrangement include the VASP, vasodilator-stimulated phosphoprotein and Pr, profilin. The AB region serves as the principle site of actin nucleation. After nucleation, the Arp2/3 complex, having been activated by its interaction with the acidic N-terminal and CHR domains, dissociates from ActA and cross-links actin polymers during tail formation. The red arrows represent actin and indicate the direction of the actin 'tail' formation.

#### 1.4.2.3 Listeriolysin O

The production of a soluble  $\beta$ -haemolytic protein by *L. monocytogenes* was first demonstrated in 1941 (Harvey and Farber, 1941). Much effort was invested in the isolation and characterisation of the native haemolysin (Girard *et al.*, 1963; Jenkins *et al.*, 1964; Siddique *et al.*, 1974; Darji *et al.*, 1995a). The haemolysin was identified as listeriolysin O (LLO), a 58-60 kDa, sulphhydryl-activated member of the cholesterol-dependent, pore-forming toxins (CDTX), which, also include streptolysin O (SLO) (Geoffroy *et al.*, 1987) and perfringolysin O (PFO) (Rossjohn *et al.*, 1997). A related haemolysin protein has also been identified in *L. ivanovii* (ivanolysin O or ILO) and the non-pathogenic species, *L. seeligeri* (seeligerilysin O) (Geoffroy *et al.*, 1989; Vázquez-Boland *et al.*, 1989; Leimeister-Wächter *et al.*, 1992). Unlike SLO and PFO, LLO possesses a PEST-like sequence (Decatur and Portnoy, 2000) and a low optimal pH for activity ( $\sim 5.5$ -6.0) (Beauregard *et al.*, 1997; Dramsi and Cossart, 2002). The latter of which has been putatively attributed to the presence of a specific leucine residue at



position 461 in the nascent sequence (Glomski *et al.*, 2002). Both of these features restrict the activity of LLO to the cytolytic vacuolar compartments and, thus, underline the principle role of LLO in escape from primary and secondary vacuoles without compromising the host cell membrane integrity.

Recent findings suggest that LLO may play a broader role in the overall virulence of *L. monocytogenes*. Stimulation of the mitogen-activated protein (MAP) kinase cascade, by LLO, has been clearly demonstrated (Tang *et al.*, 1994; Tang *et al.*, 1996; Weiglein *et al.*, 1997). In addition, treatment with LLO has been demonstrated to induce apoptosis in dendritic cells (Guzman *et al.*, 1996; Carrero *et al.*, 2004), expression of cell adhesion molecules on infected cells (Krüll *et al.*, 1997; Kayal *et al.*, 1999), nuclear factor  $\kappa$ B (NF- $\kappa$ B) induction (Kayal *et al.*, 2002), mucin exocytosis in intestinal cells (Coconnier *et al.*, 1998; Lie' vin-Le Moal *et al.*, 2002), cytokine induction in macrophage (Kuhn *et al.*, 1994; Kuhn *et al.*, 1995; Nishibori *et al.*, 1996; Kohda *et al.*, 2002), and degranulation/leukotriene formation in neutrophils (Sibeliuss *et al.*, 1999). Many of these responses are  $\text{Ca}^{2+}$ -dependent (Dussurget *et al.*, 2004) and this is not surprising given that free LLO binds to cholesterol-rich membranes, oligomerises and forms arc-shaped  $\text{Ca}^{2+}$ -permeable pores, leading to a concomitant intracellular  $\text{Ca}^{2+}$  flux (Repp *et al.*, 2002). This intracellular  $\text{Ca}^{2+}$ -flux has been directly implicated in listerial invasion of epithelial cells (Dramsi *et al.*, 2003). Furthermore, LLO associates with lipid rafts (Coconnier *et al.*, 2000) and the resultant raft clustering has been postulated to induce tyrosine phosphorylation in LLO-treated cells (Gekara and Weiss, 2004).

#### **1.4.2.4 Phospholipases**

Pathogenic *Listeria* spp. produce three different enzymes with phospholipase C (PLC) activity that are involved in virulence. Two, PlcA and PlcB, are present in *L. monocytogenes* and *L. ivanovii*, while the third, SmcL is specific to *L. ivanovii* (Vázquez-Boland *et al.*, 2001a).

PlcA is a 33 kDa phosphatidylinositol-specific PLC (PI-PLC) enzyme (Leimeister-Wächter *et al.*, 1991; Mengaud *et al.*, 1991a; Notermans *et al.*, 1991; Goldfine and Knob, 1992). Its role in mediating escape from the primary host vacuole is disputed (Schwan *et al.*, 1994), although it is suggested that the PlcA may act in concert with PlcB to affect phagosomal escape (Smith *et al.*, 1995).

PlcB is a 29 kDa phosphatidylcholine-specific PLC (PC-PLC) enzyme (Geoffroy *et al.*, 1991), yet it has a much broader substrate range than its name suggests. It is secreted as a 33 kDa proenzyme that becomes activated by a zinc metalloprotease that is encoded by the *mpl* gene,





which is proximally located in the PlcA/B-encoding lecithinase operon (Domann *et al.*, 1991; Mengaud *et al.*, 1991b; Poyart *et al.*, 1993; Broer *et al.*, 1998; Coffey *et al.*, 2000). It has been demonstrated that PC-PLC does indeed play an intimate and essential role in mediating escape from the primary vacuole (Marquis *et al.*, 1995; Grundling *et al.*, 2003) and, in addition, it has been implicated in cell-to-cell dissemination during cerebral infections (Schluter *et al.*, 1998).

Both PI-PLC and PC-PLC act synergistically with each other, and with LLO to mediate phagosomal escape (Geoffroy *et al.*, 1991; Camilli *et al.*, 1993). In particular, PI-PLC, in the presence of LLO, induces phosphatidylinositol hydrolysis in macrophage cells (Sibeliu *et al.*, 1996; Goldfine *et al.*, 2000), leading to mobilisation of protein kinase C and concomitant intracellular  $\text{Ca}^{2+}$  elevation that affects listerial internalisation and phagosomal breaching (Wadsworth and Goldfine, 2002).

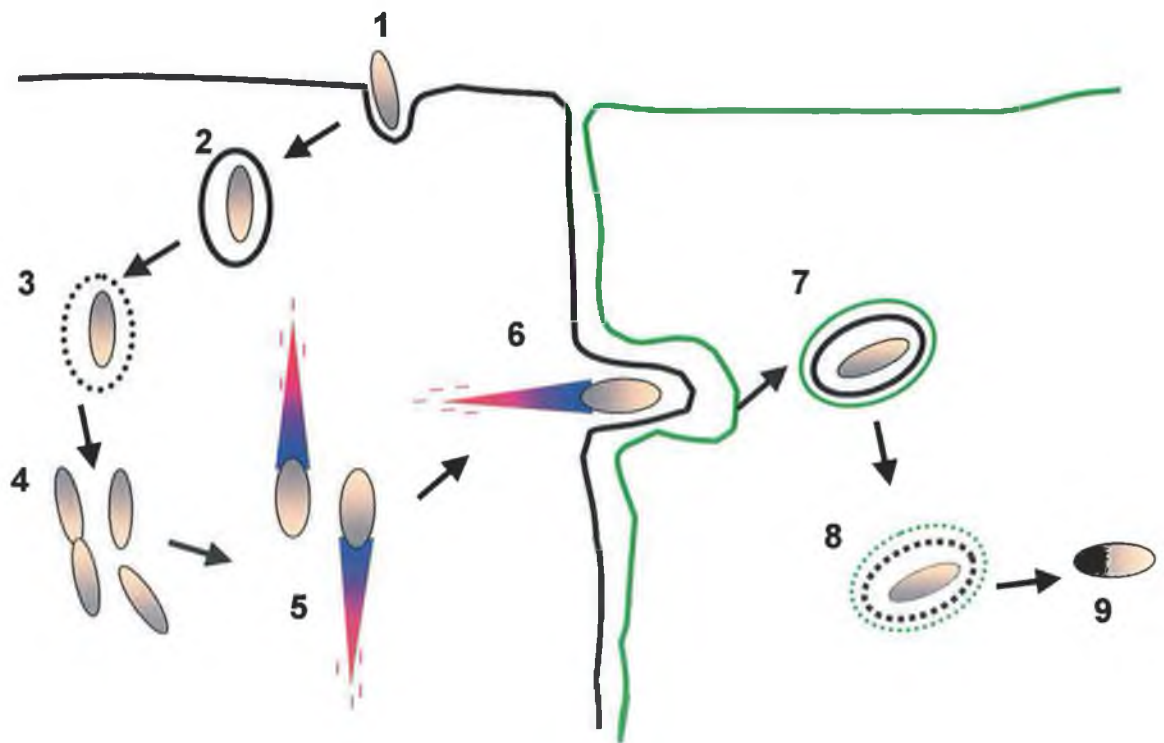


**Figure 1.6:** Schematic overview of host cell invasion and cellular spreading of *L. monocytogenes*. (1), host cell 'docking' and internalisation by phagocytosis; (2), temporary localisation within the phagocytic vacuole (phagosome); (3), enzymatic degradation of vacuolar membrane (mediated by LLO); (4), replication and multiplication within the cytosol;



(5), actin-based motility. The 'comet'-like tails provide a platform to propel the bacteria through the cytosol. Polymerised actin is represented by the red region of the tails; (6), intercellular spreading; (7), temporary localisation within the secondary (double-membrane) phagocytic vacuole; (8), enzymatic degradation of secondary vacuolar membranes (mediated by LLO and PC-PLC); (9), successful completion of one round of cell-to-cell dissemination and starting point for subsequent rounds. (Adapted from Vázquez-Boland *et al.*, 2001a, 2001b).

### 1.4.3 Genome organisation and genetic determinants of virulence

Comparative analysis of the genomes of *L. monocytogenes*, strain EGD-e (serovar 1/2a) and the closely related pathogenic species, *L. innocua*, strain CLIP11262 (serovar 6a), revealed that *L. monocytogenes* contained a 2.94 Mbp chromosome with a high G+C ratio (39 %), while *L. innocua* contained a comparably large, 3.01 Mbp chromosome with an equally high G+C ratio (37 %) (Glaser *et al.*, 2001; Buchrieser *et al.*, 2003).

Surprisingly, a perfect conservation of order and relative orientation of orthologous genes was observed in both species, showing a high degree of stability in genome organisation, with no evidence of significant inversion events or shifting of large genome segments (Buchrieser *et al.*, 2003). In addition to the 3.01 Mbp chromosome, *L. innocua* also harboured an 81.9 kbp plasmid, conferring heavy metal resistance (Glaser *et al.*, 2001). However, similar plasmids have been previously observed in *L. monocytogenes* (Poyart-Salermont *et al.*, 1990; Lebrun *et al.*, 1994). Current opinion holds that, in addition to a high percentage of transcriptional regulator genes, the preponderance of surface and secreted protein-encoding genes in the *L. monocytogenes* genome (which is not reciprocated in the *L. innocua* genome) directly reflects the pathogenicity potential of *L. monocytogenes*. In particular, its capacity to co-ordinate gene expression to maximise environmental persistence and to efficiently colonise many different cell types in the host (Dussurget *et al.*, 2004).

#### 1.4.3.1 Central virulence gene cluster

The genes encoding several of the key virulence factors are housed in a 9 kbp chromosomal region, referred to as 'Listeria pathogenicity island 1' (LIP-1) (Vázquez-Boland *et al.*, 2001a, 2001b; Kreft *et al.*, 2002). The physical organisation of the pathogenicity cassette is depicted in Figure 1.7 and it is clearly demonstrated that LIP-1 is absent from the genome of non-pathogenic *Listeria* spp., with the exception of *L. seeligeri* (Kreft *et al.*, 2002; Chakraborty *et*



*al.*, 2000; Vázquez-Boland *et al.*, 2001b). Phylogenetic analysis indicates that the most parsimonious evolutionary scenario is, that the virulence gene cluster was originally present in the common ancestor of *L. monocytogenes*, *L. innocua*, *L. seeligeri*, and *L. welshimeri*, and that the pathogenic capability has been lost in two separate events represented by *L. innocua* and *L. welshimeri* (Schmid *et al.*, 2005).

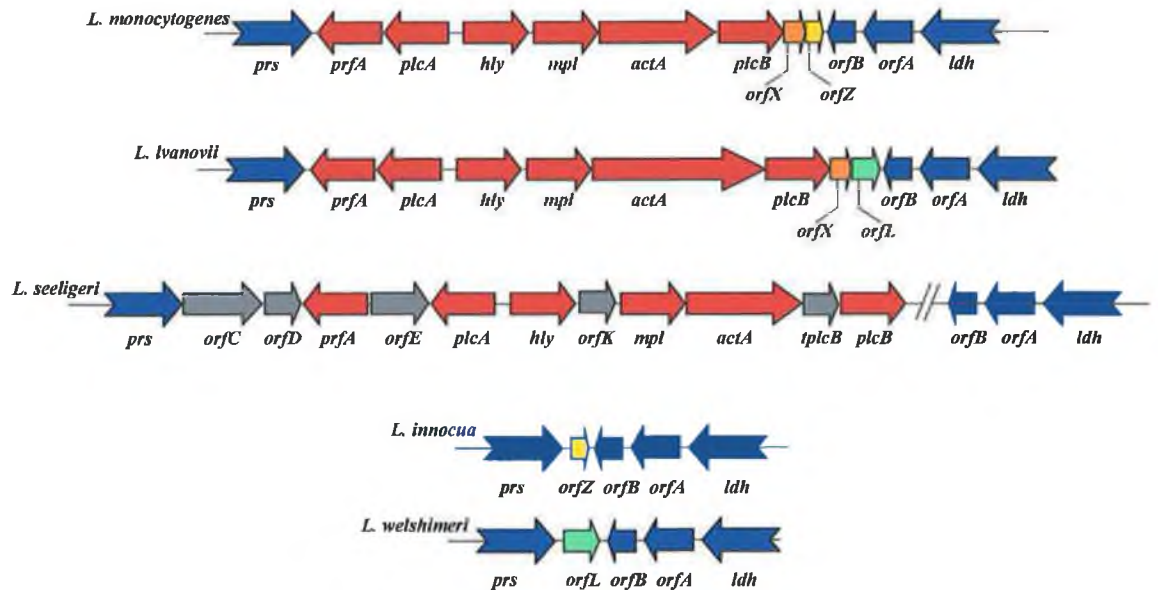


**Figure 1.7:** Physical map of the listerial central virulence gene cluster (LIP-1). Genes belonging to LIP-1 are indicated in red. These virulence determinants are housed between the genes encoding the housekeeping enzymes phosphoribosyl-pyrophosphate synthase (*prs*) and lactate dehydrogenase (*ldh*). All *Listeria* spp. harbour two small open reading frames, *orfB* and *orfA*, in the *plcB*-*ldh* intergenic region, and it is thus, likely, that this represents the original site of LIP-1 insertion. *L. monocytogenes* contains two small ORFs, *orfX* (orange) and *orfZ* (yellow), which indicate the putative deletion point of LIP-1 in *L. innocua*. *L. ivanovii* harbours a *L. monocytogenes*-homologous *orfX* gene and an *orfL* gene in place of *orfZ*, and this indicates the possible site of LIP-1 deletion in *L. welshimeri*. The *L. seeligeri* genome contains the full complement of LIP-1 virulence genes and multiple additional ORFs (grey). These include *tplcB*, a truncated variant of *plcB*, and *orfE*, which is situated between the *prfA* and *plcA*. It is this latter ORF that effectively prevents faithful regulation of virulence gene transcription and renders *L. seeligeri* non-pathogenic. The difference in size between the *actA* genes of *L. monocytogenes* and *L. innocua*, which is pronounced at the amino acid level (Kreft *et al.*, 1995; Gouin *et al.*, 1995), suggest a bifurcated divergent evolution of the genus.



#### 1.4.3.2 *inl* virulence gene clusters

The genes that encode the various proteins of the internalin family are not part of the central virulence gene cluster. Instead, as Figure 1.8 shows, they are found as clusters of two or more 'islets', each orientated in the same direction (Buchrieser *et al.*, 2003; Doumith *et al.*, 2004). The largest internalin island is LIP-2, a chromosomal locus specific to *L. ivanovii*, which contains ten *inl* genes (Vázquez-Boland *et al.*, 2001a, 2001b).

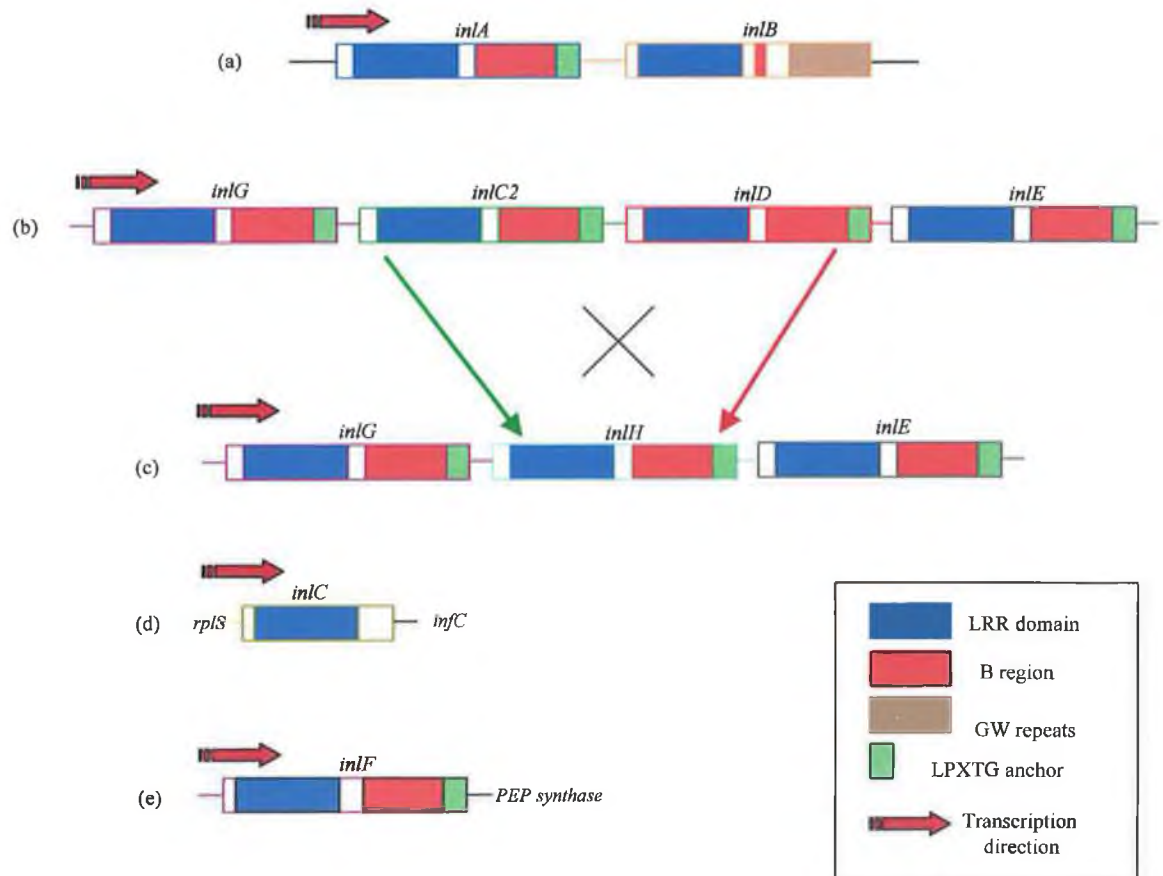


**Figure 1.8:** The internalin gene cluster that is encoded by the *L. monocytogenes* chromosome. (Adapted from Vázquez-Boland *et al.*, 2001a, 2001b). These genes are essential for the primary invasion of host cells by pathogenic strains of this species. The internalin-encoding genes are arranged into a multi-gene cluster that is specific for the genus *Listeria* and contains sequences that confer cell tropism and pathogenicity upon *L. monocytogenes*. The *inlAB* operon was the first to be identified, by demonstrating decreased ability of various transposon mutants to invade Caco2 cells in vitro (Gaillard *et al.*, 1991). Additional internalin genes identified, include *inlG*, *inlC2*, *inlD* and *inlE* (Dramsai *et al.*, 1997; Rafflelsbauer *et al.*, 1998), all of which possess a cell wall anchoring (LPXTG-encoding) C-terminal sequence. Even within the serovar 1/2a of the strain EGD, this cluster demonstrates





a degree of heterogeneity with the *inlC2D* recombinant gene product (*inlH*) being preferentially expressed in divergent isolates. The *inlA* gene arose through recombination of the N-terminal encoding region of *inlC2* and the C-terminal encoding region of *inlD*. *inlF* and *inlC* are both housed on individual loci and *inlC* is unique among the internalins in that it does not encode a bona-fide cell wall- or cell membrane- anchoring sequence.

#### 1.4.3.3 Virulence gene regulation: the PrfA regulon

The majority of the listerial virulence genes, including the entire LIP-1 cassette, are coordinately regulated by a transcriptional activator protein. This was originally identified as a 27 kDa protein that positively regulated the expression of listeriolysin O, and was, thus, called the 'positive regulatory factor of the listeriolysin (*hlyA*, formerly *lisA*) gene, or PrfA (Leimeister-Wächter *et al.*, 1990). The PrfA protein is a structural analogue of the cyclic AMP receptor protein (Crp/Fnr) family of transcriptional activators (Mengaud *et al.*, 1991c; Lampidis *et al.*, 1994).

All PrfA-regulated genes possess a 14 bp palindromic sequence in the -41 region (upstream of the transcriptional start site), termed the 'PrfA box' (Dickneite *et al.*, 1998), and PrfA-mediated transcription requires binding of PrfA protein to this palindromic sequence. There is a hierarchy in the 'quality' of PrfA boxes, which ranges from sequences exhibiting perfect dyad symmetry (e.g. *plcA/hly*), to those with 1 bp (e.g. *mpl/actA/inlC*) or 2 bp (e.g. *inlA*) substitutions (Lalic-Mülthaler *et al.*, 2001). Thus, expression of the *plcA/hly* gene sequences, is much more tightly controlled by PrfA, than the *inlA* gene (Sheehan *et al.*, 1995; Brehm *et al.*, 1996; Williams *et al.*, 2000).

PrfA controls virulence gene expression using two distinct mechanisms. The first involves the 'de-inhibition' of translation of *prfA* mRNA in response to elevation of temperature to 37 °C. This brought about by a sequence of untranslated mRNA that immediately precedes *prfA* and acts as a thermosensor, masking the ribosomal binding site at temperatures below 37 °C (Johansson *et al.*, 2002).

The second involves a PrfA-dependent bicistronic *plcA-prfA* transcript that creates a positive feedback loop, by which PrfA induces its own synthesis (Ermolaeva *et al.*, 2004). The insertional disruption of this autoregulatory circuit leads to a total loss of virulence, even if the *prfA* gene and its promoters remain intact (Mengaud *et al.*, 1991; Camilli *et al.*, 1993; Freitag *et al.*, 1993), showing that it is essential for the normal function of the PrfA regulon (Ermolaeva *et al.*, 2004).



It has been demonstrated that simply increasing the temperature to 37 °C alone, is insufficient to mediate virulence, because PrfA-dependent genes are expressed weakly *in vitro* when cultured in rich media at this temperature (Ripio *et al.*, 1996; Ripio *et al.*, 1997a). This is in contrast to the highly elevated levels of PrfA-dependent proteins, expressed intracellularly, following escape from the phagosomal vacuole (Freitag and Jacobs, 1999; Moors *et al.*, 1999; Shetron-Rama *et al.*, 2002). Thus, it is presumed that chemical signals, present in the intracellular environment, somehow intervene, to upregulate PrfA activity. The requirement for an exogenous chemical signalling pathway is further suggested by the observation that, adding activated charcoal to nutrient-rich brain heart infusion (BHI) broth cultures, significantly increased the expression of PrfA-dependent genes (Ripio *et al.*, 1996; Ripio *et al.*, 1997a; Ripio *et al.*, 1997b; Ermolaeva *et al.*, 2004).

This 'charcoal effect' was easily reversed by the addition of cellobiose or other readily fermentable sugar (Ripio *et al.*, 1997b; Brehm *et al.*, 1999). However, although cellobiose reduces the level of PrfA-dependent gene expression, the level of PrfA protein, itself, is not affected (Milenbachs *et al.*, 1997; Renzoni *et al.*, 1999). It would, thus, appear reasonable to conclude that efficient expression of PrfA-dependent genes is more influenced by PrfA functionality or activity (Vega *et al.*, 2004), rather than concentration alone. Recent findings suggest that the charcoal effect may arise following the sequestration of a diffusible autorepressor substance that is specifically released by *L. monocytogenes* during exponential growth, and which, affects directly or indirectly, the activity of PrfA (Ermolaeva *et al.*, 2004). Two genetic loci, *gcr* and *csr*, both unlinked by general transduction to LIP-1, have been shown to be required for cellobiose-mediated repression of the PrfA regulon, thus, suggesting the existence of two, semi-independent pathways for cellobiose-mediated repression (Milenbachs Lukowiak *et al.*, 2004).

The quintessential role of PrfA in listerial virulence is underlined by the particular disposition of *L. seeligeri*. Although *L. seeligeri* possesses the full complement of LIP-1 virulence genes (Gouin *et al.*, 1994), they are not expressed correctly. This is due to the presence of a divergently transcribed *oprN* reading frame E (*orf E*), inserted between the *plcA* and *prfA* gene sequences, which prevents the positive autoregulatory loop, necessary for efficient PrfA-dependent virulence gene expression (Karunasagar *et al.*, 1997; Vázquez-Boland *et al.*, 2001b).



### 1.5 Epidemiology

Careful assessment of the epidemiological profiles (Table 1.4), indicate that most illness are associated with serovars 4b and 1/2a (Jacquet *et al.*, 2004). It is clear that serovar 4b is most frequently isolated in outbreaks (Farber and Peterkin, 1991). A study of 1363 listeriosis cases undertaken by McLaughlin (1990) indicated that serotype 4b was responsible for 64 % of the cases, while serovar 1/2a was responsible for only 15 %. A more comprehensive profiling of 24 outbreaks (3338 cases) reported in the literature since 1966, by McLaughlin (1997), highlighted that 58 % of the total outbreaks and 40 % of the total cases were attributable to serotype 4b. This trend was mirrored by the epidemiology of human listeriosis in Sweden between 1976 and 1985, that, showed serotype 4b to responsible for 70 % of cases (Ericsson *et al.*, 1996). These observations lend significant weight to the notion that there is a significant degree of heterogeneity in the virulence, or pathogenic potential of *Listeria* strains (Wiedman *et al.*, 1997), the genetic basis of which has also been investigated (Nelson *et al.*, 1994).



**Table 1.4: Worldwide reported outbreaks of listeriosis (1979-2002) with implicated foods and available statistics. Compiled and adapted from Anon., USDA, 2003; Donnelly, 2001 and McLaughlin *et al.*, 2004).**

Date	Country	Implicated food	Cases				Deaths (% mortality)	Sero-var	Original reference
			Total cases	Immuno-compromised/ predisposed	Pregnancy-associated	Non-pregnancy-associated			
1978-79	Australia	Raw veg.	12	nd	nd	nd	0	nd	Le Souëf and Walters, 1981
1979	USA	Salad veg. *a1	23	*a2	nd	nd	(15%)	4b	Ho <i>et al.</i> , 1986
1980	New Zealand	Fish	22	10	22	0	7 (32%)	1/2a	Lennon <i>et al.</i> , 1984
1981	UK	Misc. dairy products	11	nd	nd	nd	5 (45.5%)	1/2a	Ryser, 1999
1981	Canada	Coleslaw	41	0	34	7	(41%)	4b	Schlech <i>et al.</i> , 1983
1983-87	Switzerland	Soft cheese	122	nd	65	nd	31 (25.4%)	4b	Bille, 1990; Bula <i>et al.</i> , 1995
1983	USA	Pasteurised whole milk and 2 % milk	49	42	7	42	14 (29%)	4b	Fleming <i>et al.</i> , 1985
1985	USA	Mexican-style cheese	142	93	48	49	30 (33%)	4b	Linnan <i>et al.</i> , 1988
1986	Austria	Unpast. milk, organic veg.	28	nd	24	nd	5 (17.9)	nd	Allerberger and Guggenbichler, 1989
1986-87	USA	Ice cream, salami, brie cheese	36	nd	4	32	16 (44.4%)	4b, 1/2b, 1/2a	Schwartz <i>et al.</i> , 1989
1986-87	USA	Raw eggs	2	nd	nd	nd	nd	4b	Schwartz <i>et al.</i> , 1988
1987	USA	Butter	11	nd	nd	nd	nd	nd	Ryser <i>et al.</i> , 1999
1987-89	UK	Pâté	355* <sup>b</sup>	nd	185	129	94 (26.5%)	4b	McLaughlin <i>et al.</i> , 1991
1989-90	Denmark	Semi-soft (blue) cheese	23	nd	nd	nd	nd	4b	Jensen <i>et al.</i> , 1994
1989	Finland	Salted mushrooms	1	nd	nd	nd	0	4b	Juntilla and Brander, 1989
1989	USA	Shrimp	2	nd	nd	nd	0* <sup>c</sup>	4b	Riedo <i>et al.</i> , 1994
1990	Australia	Pâté	11	nd	11	nd	6 (54.5%)	1/2a	Paul <i>et al.</i> , 1994; Ryser <i>et al.</i> , 1999





**Table 1.4: ...continued**

1991	Australia	Smoked mussels	4	0	0	4	0	1/2a	Mitchel, 1991; Misrahi <i>et al.</i> , 1991; Paul <i>et al.</i> , 1994
1992	New Zealand	Smoked mussels	4	2	2	2	1	1/2a	Brett <i>et al.</i> , 1998
1993	France	Pork tongue	280	nd	93	nd	63 (22.5%)	4b	Jacquet <i>et al.</i> , 1995
1993	France	Pork rillettes	38	nd	31	7	11 (28.9 %)	4b	Goulet <i>et al.</i> , 1998
1993	Italy	Rice salad	39	nd	nd	nd	0	1/2b	Salamina <i>et al.</i> , 1996
1994	USA	Chocolate milk	45	1	1	44	0	1/2b	Dalton <i>et al.</i> , 1997
1994-95	Sweden	Rainbow trout	9	nd	3	6	2 (22.2%)	4b	Ericsson <i>et al.</i> , 1997
1995	France	Soft cheese	33	5	11	17	4	4b	Goulet <i>et al.</i> , 1995
1996	Canada	Crab meat	2	0	0	2	0	1/2a	McLaughlin <i>et al.</i> , 2004
1997	Italy	Sweet corn	1566	nd	0	1566	0	4b	Aureli <i>et al.</i> , 1997
1997	France	Pon l'Eveque cheese	14	nd	nd	nd	nd	4b	Ryser, 1999
1997	Denmark	nd	3	nd	nd	nd	0	4	Heitmann <i>et al.</i> , 1997
1998-99	Finland	Rainbow trout	5	nd	0	5	0	1/2a	Meittinen <i>et al.</i> , 1999
1998-99	Finland	Butter	25	24	0	25	6	3a	Lyytikäinen <i>et al.</i> , 2000
1998-1999	USA	Hot dog/deli meats	101* <sup>d1</sup>	nd	nd	nd	21* <sup>d2</sup> (21 %)	4b	Anon., 1999
1999	England	Cheese/cheese salad sandwich	2	2	0	2	1	4b	McLaughlin <i>et al.</i> , 2004
1999-2000	France	Pork rillettes	10	6	3	7	2	4b	de Valk <i>et al.</i> , 2001
1999	England	Cheese/cheese salad sandwich	2	2	0	2	1	4b	McLaughlin <i>et al.</i> , 2004
1999-2000	France	Pork rillettes	10	6	3	7	2	4b	de Valk <i>et al.</i> , 2001
1999-2000	France	Jellied pork tongue	32	11	9	23	10	4b	de Valk <i>et al.</i> , 2001
1999-2000	France	Pork tongue in aspic	26	nd	nd	nd	7	nd	Dorozynski <i>et al.</i> , 2000
2000	New Zealand	Cold meats	7	nd	nd	nd	0	Unspecified 1/2 serovar	Sim <i>et al.</i> , 2002
2000	New Zealand	Cold meats	21	nd	nd	nd	0	Unspecified 1/2 serovar	Sim <i>et al.</i> , 2002
2000	USA	Turkey meat	29* <sup>c</sup>	nd	8	21	7	nd	Anon., CDC 2000b
2000-01	USA	Mexican-style soft cheese	12	1	10	2	5	nd	Anon., CDC 2001
2001	USA	Sliced turkey	16	nd	nd	nd	0	1/2a	Frye <i>et al.</i> , 2002
2002	USA	Sliced turkey	63* <sup>f</sup>	30	11	7	10* <sup>B</sup>	nd	Current Class Actions, 2002. ( <a href="http://www.kbmoll.com/class">www.kbmoll.com/class</a> ) Anon., CDC 2002b



<sup>\*a1</sup>, Hospital food implicated.; <sup>\*a2</sup>, 50 % of patients were immunosuppressed owing to cancer, chemotherapy or steroid treatment. 60 % reported use of antacids or cimetidine (inhibitors of gastric acid).

<sup>\*b</sup>, Information not available to classify 41 patients.

<sup>\*c</sup>, 1 foetal demise confirmed.

<sup>\*d1</sup>, Spread over 22 states.; <sup>\*d2</sup>, Included 15 adult deaths and 6 miscarriages.

<sup>\*e</sup>, Spread over 10 states.

<sup>\*f</sup>, Spread over 8 north-eastern states.

<sup>\*g</sup>, Including 3 miscarriages or stillbirths.

It is clear from examination of frequently implicated foods, that serotype 1/2a is more frequently isolated from food and food-processing areas than serotype 4b. In fact recent studies would indicate that serotype 1/2a is becoming the single most frequent cause of listerial contamination of food (da Silva *et al.*, 2001; Pak *et al.*, 2002; Wagner and Allerberger, 2002). It is also significantly more frequently isolated from infected ruminants (Low *et al.*, 1993). Whether this can be taken as evidence that serotype 4b exhibits a genuinely more potent tropism towards human hosts, as suggested by Kathariou (2002), is debatable. The ability of 1/2a serovars to particularly thrive in silage may be responsible for its apparent prevalence in ruminants and both dairy and vegetable produce. Moreover, oral inoculation of pregnant mice with serovars 1/2a and 4b failed to reveal any discernable difference in infectivity (Lammerding *et al.*, 1994).

Recent trends indicate that serovar 1/2 strains are becoming increasingly prevalent in human isolates (Gerner-Smidt *et al.*, 1995; McLaughlin and Newton, 1995; Loncarevic *et al.*, 1998). For instance, the situation in Sweden has changed significantly since 1985. For the period 1986-1999, 45 % of human isolates belonged to serovar 4b while 44 % belonged to serovar 1/2a (Unnerstad, 2001). The proportion of serotype 4b strains isolated in human cases has decreased markedly, with an estimated 30 % prevalence in 1999-98 falling to 10 % in 2000 (Unnerstad, 2001), while 1/2a prevalence continues to increase.

The prevalence in livestock is conservatively estimated to be between 1 and 10 % and a typical report from Germany in 1997 where a 49,324 livestock sample population was tested, *L. monocytogenes* was detected in 4 % of test animals (Anon, 1999 E.C. Vet. Comm.). Low-level exposure to *L. monocytogenes* generally only leads to symptomatic listeriosis in susceptible hosts with suppressed immune responses or other predilection to disseminated infection. It has been indicated that the prevalence of asymptomatic carriage within the human



population can range from less than 1 % to as much as 21 % (Kampelmacher and Van Noorle Jansen, 1980; Gledel, 1987; Farber and Peterkin, 1991; Hof, 2001; Anon., FSIS/USDA. 2003b). As with attempts to establish a minimum infective dose, it is undetermined as to how faecal carriage relates to length of incubation or manifestation of symptomatic, invasive listeriosis (Anon., FSIS/USDA. 2003b). Although described as 'asymptomatic', such a high circulating prevalence of *L. monocytogenes* in the human population cannot be disregarded as a source of contamination. It is now apparent that *L. monocytogenes* can rapidly colonise inert food-processing surfaces such as stainless steel (Herald and Zottola, 1988; Arizcun *et al.*, 1997; Wong, 1998) and become almost endemic, leading to widespread endemic contamination of various food types (Jay, 1996; Pak *et al.*, 2002; Silva *et al.*, 2003; Aguado *et al.*, 2004). Endemic colonisation with *L. monocytogenes* has been confirmed in both dairy plants (Unnerstad *et al.*, 1996), and fish-processing plants (Loncarevic *et al.*, 1996). It is also noteworthy that in a recent study conducted by Okutani and co-workers (2004), in Japan, the prevalence of *L. monocytogenes* in foods was found to be comparable to that found in both the USA and Europe. However, the mean incidence of listeriosis was substantially lower. This re-affirms the notion that the incidence of listeriosis in the population may not be solely proportional to the degree of prevalence in food material. It is likely that it is a cumulative function of contamination level, food type, serotype virulence/diversity and the health status of the population and associated predispositions to infection.

## **1.6 Biodiversity of clinically important strains**

It has been suggested that food-related environmental factors (such as presence of bacteriocins) may offer an explanation as to why 1/2a predominates in food isolates. More, specifically, the demonstrated capacity of serotype 1/2a to survive prolonged cold storage may lead to more efficient isolation of this strain from foods, while the ability of serotype 4b strains to proliferate after post-cold storage heat treatment, may lead to more concentrated contamination levels and, thus, increased likelihood of infection (Buncic *et al.*, 2001).

Comparison of the 1/2a and 4b genomic sequences has thus far failed to provide a conclusive answer to the apparent strain diversity. A 1/2a-specific operon that encodes the rhamnose biosynthetic pathway, associated with teichoic acid biosynthesis, in addition to operons for five glycosyl transferases and an adenine-specific DNA methyl transferase, may confer a competitive advantage to 1/2a in environmental niches (Nelson *et al.*, 2004). In addition, a gene encoding a bile salt hydrolase (BSH) enzyme has been identified in the *L. monocytogenes* 4b genome, which confers increased bile resistance (Dussurget *et al.*, 2002).



More recently, the *L. monocytogenes*-specific 'aut' gene, which encodes a GW-anchored autolysin (Auto), has been shown to be necessary, but not sufficient for invasion of epithelial and fibroblastic cell lines by certain *L. monocytogenes* strains (Cabanès *et al.*, 2004). Curiously, the *aut* gene is absent from the *L. monocytogenes* 4b genome (Cabanès *et al.*, 2004). Correspondingly, at least three *L. monocytogenes* serovar 4b-specific surface protein-encoding genes have been putatively identified in 4b (Doumith *et al.*, 2004), and these may confer increased virulence. In addition, the production of truncated InlA protein (Jonquières *et al.*, 1998) has recently been cited as a major impairment to the cellular invasion mechanism of *Listeria monocytogenes* (Olier *et al.*, 2003). Furthermore, a close analysis of clinically isolated strains has revealed that variant strains, producing truncated InlA proteins tend to be of the 1/2 (specifically a and b) serovars (Jacquet *et al.*, 2004).

Following successful internalisation, hexose phosphate transport system (Hpt) is used by *L. monocytogenes* to obtain nutrients from the host cell cytosol, in particular, glucose-1-phosphate, which is abundant in the cytosolic compartment (Chico-Calero *et al.*, 2002). The significance of Hpt is underlined by the fact that *hpt*<sup>-</sup> *L. monocytogenes* mutants are avirulent in the mouse model (Taylor *et al.*, 2002). Moreover, *hpt*<sup>+</sup> *L. innocua* demonstrate increased adherence to Hep-2 cells, although this has not been linked to a concomitant increase in overall internalisation efficiency in the same *L. innocua* mutant (Slaghuis *et al.*, 2004). The evidence would suggest that Hpt is a vital virulence determinant for intracellular survival and proliferation of *L. monocytogenes*.

## 1.7 Legislation

The epidemiological profile of listeriosis has highlighted the need for increased clinical vigilance as well as improved monitoring, screening and control of the food preparation environment.

The USA were the forerunners in terms of addressing clinical surveillance, with the CDC, USDA and FDA co-establishing the Foodborne Disease Active Surveillance Network (FoodNet) in the mid 1990's. This incorporated PulseNet, a national network of Public Health laboratories that fingerprint foodborne pathogens, such as *L. monocytogenes*, using pulsed-field gel electrophoresis (Donnelly, 2001). The situation in Europe was, until recently, less harmonised, with each member state responsible for defining case criteria and collecting notifiable case data. Listeriosis is reported to be a mandatory notifiable disease in Finland, Italy, Sweden, Denmark and Norway. While, in Spain, reporting is based on the





microbiological information system operated within hospital laboratories (SIM) (Anon, 2001). Switzerland, in addition to reporting cases to the Federal Office for Public Health (FOPH), has established the dedicated Centre National de référence des Listérias (CNRL, Institute of Microbiology, CHUV, Lausanne), while the sentinel surveillance network, operated in France, is comprehensively reviewed elsewhere (Leclerc *et al.*, 2002). In eight countries infections in children under one year old are notified, while, the position in Sweden is that mother and child/foetus is regarded as one case and in Germany, a new act notifies co-natal infections and cases of meningitis from all sixteen Federal Länder (Anon, 2001). Case definitions are less defined in all other member states. Based on EU Decision 2119/98/EC (Community Network for the Epidemiological Surveillance and Control of Communicable Diseases) the various national reference laboratories have agreed to co-operate in a multi-lateral surveillance network approach.

In light of the high mortality associated with listeriosis, the USDA/FDA/FSIS have adopted a 'zero-tolerance' approach, that, stipulates *L. monocytogenes* should not be present in 25g of any given food sample (Shank *et al.*, 1996). Italy also enforces a 'zero-tolerance' approach, while other EU member states such as Germany, Netherlands and France have a tolerable level of 100 or 1000 *L. monocytogenes*/g at the point of consumption (ANON, 1999 Vet measures). These discrepancies in acceptable limits have significant economic implications, since food that has been processed in a country with a high tolerance level cannot be marketed in a country where more stringent cut-off levels are in place.

It has been suggested that complete absence of *L. monocytogenes* from all food may be unnecessary and unattainable (FAO/WHO working group, 1988). The UK PHLS has suggested that a cut-off level of 100 *L. monocytogenes* cells/g food may be more appropriate (McLaughlin, 1996). Fifteen trade associations in the USA have recently issued a request to the FDA to revise the acceptable levels of *L. monocytogenes* in certain foods that do not support growth of the bacteria, to 100 CFU/g. The FDA has provided the opportunity for public comment on the petition, to be submitted by the 9<sup>th</sup> August 2004 (<http://www.foodlineweb.co.uk/FoodWeb/>). The epidemiological trends outlined in Section 1.5, indicate that while such levels may be acceptable in healthy members of the population, even levels as low as 100 CFU/g could potentially cause symptoms in pre-disposed individuals. Several countries, including Canada (Farber and Hartwig, 1996), Germany, (Bartelt *et al.*, 1999) and Denmark (Nørrung *et al.*, 1999) have proposed a differential ranking of foods with respect to acceptable levels of *L. monocytogenes* contamination. These are based on each food group's propensity to support growth of *L. monocytogenes*, whether or not



the food is to be heated prior to consumption, the anticipated storage/shelf-life and likely consumer profile.

**Table 1.5: Prevalence of *L. monocytogenes* in food samples in Europe, (2001).**

<b>Food</b>	<b>Prevalence (%)</b>
Beef and veal	0.6-15.4
Pork	0-40.6
Other meat	0-22.2
Minced meat	11.9-18.3
Meat products	0-10.2
Poultry meat	2.6-16.7
Poultry meat products	0-7.6
Milk	0-2.2
Milk products	0-4.4
Fish products	0-13.5
Vegetables	0-12.5
Other ready-to-eat (RTE) food	0-16.7

Recently, the European Commission has followed the US FDA in adopting a ‘zero tolerance’ attitude towards *L. monocytogenes* in ‘ready-to-eat’ foods in its proposed draft guidelines on the application of general principles of food hygiene to the management of *L. monocytogenes* in foods (Anon., 2004), although, current European Community legislation only provides for microbiological standards with regard to *Listeria* in provisions for soft cheeses, pasteurised milk and other selected dairy produce under the EU Council Directive 92/46/EEC (Table 1.7). Unfortunately, manufacturer-undertaken end-product testing is still not compulsory in the US or Europe, rather, this is conducted by the relevant regulatory authority. Manufacturers have incorporated the general principles of food hygiene and, in particular, the Hazard Analysis Critical Control Point (HACCP)-concept as described in the Food Hygiene Directive 93/43/EEC. As a consequence, the fall in numbers of reported cases has demonstrated the efficacy of both veterinary inspection procedures and corrective measures based on HACCP (Goulet *et al.*, 2001; Meyer-Broseta, *et al.*, 2002). However, HACCP is not a ‘final solution’ to the problem of *Listeria* in food. It is particularly difficult to generalise control points, with regard to *L. monocytogenes* contamination in food, due to the bacterium’s ubiquitous



presence, robustness and ability to multiply at refrigeration temperatures. To this effect, in a 1999 Federal Register notice, the USDA advised manufacturers of ready-to-eat (RTE) meat and poultry products of the need to reassess HACCP plans to ensure that they adequately address *L. monocytogenes*. This is in addition to, suggestions from the USDA for the incorporation of finished product testing as a verification tool (Donnelly, 2001). Failure to detect *L. monocytogenes* in food prior to product release can result in product recalls. The cost incurred with such recalls is frequently, significant, in both financial terms, and in relation to consumer confidence and allegiance. In 2002, 27.4 million pounds of turkey produce were recalled under the Wampler Foods brand of Pilgrims Pride corp., making it the largest meat recall in the history of the United States ([www.belluckfox.com/listeria.html](http://www.belluckfox.com/listeria.html)). This resulted in several fatalities and a subsequent nationwide class-action lawsuit filed by Kenneth B. Moll and Associates ([www.kbmoll.com/class](http://www.kbmoll.com/class)) in November 2002. This highlighted the inefficiency in relying on manufacturer-implemented HACCP. In fact, several judicial commentators have referred to this strategy as “yanking the referees from the football field” and equivalent to a “have a cup of coffee and pray” attitude ([www.belluckfox.com](http://www.belluckfox.com)). In Europe, the Rapid Alert System for Food and Feed (RASFF) has been established under Article 8 of Directive 92/59/EEC, to provide a procedure to inform the member states of when a product represents a serious risk for the health and safety of consumers ([http://europa.eu.int/comm/food/fs/sfp/ras\\_index](http://europa.eu.int/comm/food/fs/sfp/ras_index)). On 21<sup>st</sup> February 2002, RASFF received a new legal base (Regulation (EC) No. 178/2002) to extend the system to include all food and feed products finally destined for human consumption. ‘Alert’ notifications relate to products which are on the market and which present a risk to the consumer, while, ‘Information’ notifications relate to products presenting a risk to the consumer for which it can be assumed that they have not yet reached the market or for which the risk is limited. Data for the year ending 2002 indicated that *Listeria* were responsible for 17 % of microbiological reasons for alert notifications and 13 % of information notifications ([http://europa.eu.int/comm/food/fs/sfp/ras\\_report2002](http://europa.eu.int/comm/food/fs/sfp/ras_report2002)). Thus, it is clearly apparent that both the food industry and the consumer would benefit from an efficient means of rapidly screening end produce for the presence of *L. monocytogenes*.



**Table 1.6: Reported cases of listeriosis in Europe, (1996-2001).**

Country	Listeriosis cases					
	1996	1997	1998	1999	2000	2001
Belgium	77	40	60	64	48	57
Denmark	39	33	41	44	39	38
Finland	29	53	46	46	18	28
France	-	243	238	275	261	187
Germany	32	27	41	31	33	213 <sup>*/</sup>
Greece	-	-	1	1	2	3
Ireland	-	7	4	-	7	7
Italy	32	64	45	17	13	31
Portugal	-	-	0	-	-	-
Spain	21	19	16	32	35	57
Sweden	28	18	32	27	46	67
Holland	22	22	23	12	19	16
Scotland	11	6	13	7	11	15
Northern Ireland	2	4	6	1	4	5
England/Wales	116	118	91	108	100	136
Norway	-	-	-	19	18	18

<sup>\*/</sup> New classification of cases beginning 1<sup>st</sup> January 2001.





**Table 1.7:** Current microbiological criteria for foodstuffs in European Community legislation, with reference to *L. monocytogenes*.

Food category	Limit	Sampling	
		N	c
Cheeses made from raw milk and thermized milk (Directive 92/46/EEC, SI 9/1996)	Absence in 1g (hard cheeses) or in 25g (other)	5	0
Soft cheese (made from heat-treated milk) (Directive 92/46/EEC, SI 9/1996)	Absence in 25g	5	0
Fresh cheese (Directive 92/46/EEC, SI 9/1996)	Absence in 25g	5	0
Other cheeses than those mentioned above (Directive 92/46/EEC, SI 9/1996)	Absence in 1g (hard cheeses) or in 25g (other)	5	0
Powdered milk and milk-based products (Directive 92/46/EEC, SI 9/1996)	Absence in 1g	5	0
Frozen milk-based products (Directive 92/46/EEC, SI 9/1996)	Absence in 1g	5	0
Liquid milk-based products (Directive 92/46/EEC, SI 9/1996)	Absence in 1g	5	0
Butter (Directive 92/46/EEC, SI 9/1996)	Absence in 1g	5	0

*N*: The number of units making up the sample.

*c*: The number of sample units where the *L. monocytogenes* cell count can be above the defined limit.

## 1.8 Current detection methods

Originally, the ability of *L. monocytogenes* to grow at low temperatures was taken advantage of for isolation of the bacterium from clinical samples in a process termed 'cold-enrichment' (Gray *et al.*, 1948; Gray and Killinger, 1966). It was not uncommon for this process to require up to eight weeks (Hayes *et al.*, 1991) of continuous, repeated sub-inoculation and incubation from the original sample (stored at 4 °C), before *L. monocytogenes* was successfully isolated



and identified as blue colonies using oblique trans-illumination or 'Henry-light' illumination (Henry, 1933). Cold-enrichment is no longer seen as necessary (Grif *et al.*, 2001).

Contemporary and traditional methods of detection, specifically pertaining to food samples, rely exclusively on the use of specific growth media to isolate and enumerate viable bacterial cells from food samples, followed by serological and biochemical confirmatory tests (e.g. ISO 10 560:1999; ISO 11 290:1996), as validated by Scotter *et al.*, (2001a) and Scotter *et al.*, (2001b). It is often necessary to resuscitate contaminating *L. monocytogenes* cells that may have been partially inactivated, by a primary enrichment phase. As the numbers of *Listeria monocytogenes* present in food, especially in dairy products, are usually low, attempts to directly isolate *Listeria monocytogenes* frequently fail (Doyle and Schoeni, 1987). The primary enrichment broth is, thus, supplemented with the selective components- one volume of LiCl and half volumes of both acriflavine and nalidixic acid (half Fraser broth)- and incubated with the relevant food sample at 30 °C for 24 hrs. Secondary enrichment is conducted in broth containing a full complement of the selective agents (Fraser broth) at 35 °C or 37 °C for 48 hrs. Samples from both the primary and secondary enrichment cultures are streaked onto the selective agar media, PALCAM (polymyxin-acriflavine-LiCl-ceftazidime-aesculin-mannitol) or Oxford agar. Both these media presumptively identify *Listeria* spp. by revealing Esculinase ( $\beta$ -glucosidase) activity. After incubation at 30 °C for 24 hrs the Oxford agar plates are examined for the presence of typical small *Listeria* spp. colonies. After a further 24 hrs the *Listeria* colonies adopt a distinctly darker shade with a greenish halo and concave colony centres. The PALCAM agar is incubated at 30 °C for 48 hrs under microaerobic conditions and *Listeria* spp. colonies appear grey-green with concave centres that are black in colour. It has been reported that PALCAM agar is more selective than Oxford agar (Gunasinghe *et al.*, 1994). Suspect colonies are transferred to blood agar plates and incubated at 35 °C or 37 °C for 18 hrs. At this stage results are still presumptive and have to be further confirmed using a selection of the biochemical tests outlined in Section 1.2.

The diagnostic problems associated with such 'horizontal' detection methods have been recently reviewed (Beumer and Hazeleger, 2003; Leclercq, 2004). The outstanding limitation is the 'sample-to-result' time that takes a minimum of six full days. Another major concern is the inability to detect *L. monocytogenes* in the presence of other, non-pathogenic *Listeria* spp., such as *L. innocua*, that frequently appears as a co-contaminant and exhibits a competitive growth advantage over *L. monocytogenes* in enrichment media (Rijpens and Herman, 2004; Cocolin *et al.*, 2002; Cornu *et al.*, 2002; Beumer *et al.*, 1996; Curiale and Lewis, 1994; MacDonald and Sutherland, 1994;), possibly due to production, by *L. innocua* of anti-*L. monocytogenes* bacteriocin-like inhibitors (Yokoyama *et al.*, 1998). These have



prompted the investigation of alternative enrichment media with faster and more reliable discriminatory selectivity. Two such media are Rapid'L.mono (Bio-Rad) and 'Agar Listeria according to Ottaviani and Agosti' or ALOA ( Vlaemynck *et al.*, 2000). These discriminate on the basis of phosphatidylinositol-specific phospholipase C activity in *Listeria* spp.. Both media have recently been compared with the recommended PALCAM and Oxford media (Leclercq, 2004). Despite improving the degree of successful discrimination of *Listeria* spp. when used instead of or with the recommended media, neither was effective in reducing the selective enrichment period.

### **1.9 Rapid methods**

Most commercially available tests (Table 1.8) for the rapid detection of *Listeria* spp. from food samples in selective enrichment broths are immunoassay-based (Allerberger, 2002). In addition to traditional ELISA-based immunoassays, paddle style dipstick (PSD) and lateral flow immunoassay (LFIA) formats, as described by Aldus and co-workers (2003) and Capps and co-workers (2004), for detection of verotoxigenic *E. coli*, have been gaining prominence as rapid and easy-to-use commercial platforms. At present, many of the antibodies employed in commercial kits are broadly reactive and only allow detection of *Listeria* to the genus level.

Similarly, antibodies that favourably react with *Listeria* spp. are frequently reported in the literature (Bhunja, 1997). However, most are of limited potential for the specific immunodetection of *L. monocytogenes*. Several reportedly react with numerous *Listeria* genus members (Butman *et al.*, 1988; Mattingly *et al.*, 1988; Siragusa and Johnson, 1990; Torensma *et al.*, 1993; Loiseau *et al.*, 1995), while others react with *L. monocytogenes* in addition to non-pathogenic *L. innocua* (Bhunja *et al.*, 1991; Bubert *et al.*, 1994; Kathariou *et al.*, 1994, Sølve *et al.*, 2000). Inability to differentiate between live and dead cells is also a pervading limitation (Siragusa and Johnson, 1990; Butman *et al.*, 1998). Kathariou and co-workers, (1994) successfully generated antibodies capable of reliably discriminating live from dead *L. monocytogenes* serotype 4b cells, yet they failed to recognise other *L. monocytogenes* serovars, including the 1/2 (a, b and c) varieties which consistently predominate in food isolates (Boerlin and Piffaretti, 1991; Rocourt, 1994; da Silva *et al.*, 2001; Pak *et al.*, 2002; Okutani *et al.*, 2004).



**Table 1.8: Table of commercially available antibody-based tests for *Listeria*.**

Test	Format	Supplier
<b>Assurance <i>Listeria</i> EIA*<sup>1</sup></b> Used to identify <i>Listeria</i> spp. including <i>L. monocytogenes</i>	Enzyme immunoassay	BioControl Systems, Inc. <a href="http://www.biocontrolsys.com">www.biocontrolsys.com</a>
<b>VIP for <i>Listeria</i>*<sup>1</sup></b> Used to identify <i>Listeria</i> spp. including <i>L. monocytogenes</i>	Visual immunoprecipitate	BioControl System, Inc <a href="http://www.biocontrolsys.com">www.biocontrolsys.com</a>
<b>Transia Plate</b> Used to identify <i>L. monocytogenes</i>	Sandwich-type enzyme immunoassay	Diffchamb <a href="http://www.diffchamb.com">www.diffchamb.com</a>
<b>Dynabeads anti-<i>Listeria</i></b> Used to identify <i>L. monocytogenes</i>	IMS	Dynal, Inc. <a href="http://www.dynal.no/">www.dynal.no/</a>
<b>EIA Foss <i>Listeria</i></b>	Combination of ELISA and IMS	Foss N. America, Inc. <a href="http://www.Fossnorthamerica.com">www.Fossnorthamerica.com</a>
<b><i>Listeria</i> Rapid Test*<sup>1</sup></b> Used to identify <i>Listeria</i> spp. including <i>L. monocytogenes</i>	EIA	Oxoid, Inc.
<b><i>Listeria</i>-Tek<sup>TM</sup>*<sup>1</sup></b>	ELISA	Organon Teknika Corp.
<b>ListerTest<sup>TM</sup>*<sup>1</sup></b>	IMS	Vicam, L.P. <a href="http://www.vicam.com">www.vicam.com</a>
<b>MICRO-ID <i>Listeria</i>*<sup>1</sup></b> Used to identify <i>Listeria</i> spp.	Latex agglutination	Remel, Inc. <a href="http://www.remelinc.com">www.remelinc.com</a>
<b>Reveal<sup>®</sup> for <i>Listeria</i>*<sup>1</sup></b> Used to identify <i>Listeria</i> spp	Sandwich ELISA	Neogen Corporation <a href="http://www.neogen.com">www.neogen.com</a>
<b>VIDAS LMO</b> Used to identify <i>L. monocytogenes</i>	Enzyme-linked fluorescent assay	(Sewell <i>et al.</i> , 2003) BioMerieux Inc. <a href="http://www.biomerieux.com">www.biomerieux.com</a>
<b>Singlepath<sup>®</sup> GLISA <i>Listeria</i></b> Used to identify <i>Listeria</i> spp	(LFIA)Gold-labelled Immunosorbent assay	Merck, Inc. <a href="http://www.merck.com">www.merck.com</a>
<b>RapidChek<sup>®</sup> for <i>Listeria</i>*<sup>1</sup></b> Used to identify <i>Listeria</i> spp	LFIA	Strategic Diagnostics <a href="http://www.sdix.com">www.sdix.com</a>
<b>Unique<sup>®</sup> <i>Listeria</i>*<sup>1</sup></b>	PSD	TECRA International <a href="http://www.sdix.com">www.sdix.com</a>

\*<sup>1</sup> :AOAC Approved ([www.aoac.org](http://www.aoac.org)).





Thus, there is still a major requirement for antibodies that are capable of reliably and specifically detecting live *L. monocytogenes* cells for the development of immunoassays suitable for routine analysis.

Molecular methods, in particular the polymerase chain reaction (PCR), have gained increasing favour for detection of pathogens, such as *L. monocytogenes* in food samples (Wernars *et al.*, 1991; Fluit *et al.*, 1993; Makino *et al.*, 1995; Manzano *et al.*, 1997; Scheu, *et al.*, 1999; Olsen *et al.*, 2000; Norton, 2002). PCR has provided the basis for many assays developed for the detection of *L. monocytogenes* in recent years with the listeriolysin O (*hlyA*) (Deneer and Boychuk, 1991; Golsteyn Thomas, 1991; Norton and Batt, 1999), the p60 (*iap*) (Bubert *et al.*, 1997a; Bubert *et al.*, 1997b; Hein *et al.*, 2001; Schmid *et al.*, 2003), the Actin A (*ActA*) (Longhi *et al.*, 2003) and the internalin (*inlAB*) (Almeida and Almeida, 2000; Ingianni *et al.*, 2001; Pangallo *et al.*, 2001; Kaclíková, *et al.*, 2003; Jung *et al.*, 2003) genes being frequent targets. As with immunoassays, there are several commercial test kits that incorporate this strategy for more rapid, sensitive and reliable detection of *L. monocytogenes*. These include the BAX<sup>®</sup> Screening System (Qualicon, USA) (Norton *et al.*, 2000; Hofman and Wiedmann, 2001) and the Probelia<sup>®</sup> *Listeria monocytogenes* (Sanofi Diagnostic Pasteur) microplate method. The latter system employs a peroxidase-labelled probe to detect *L. monocytogenes*-specific amplicons.

Complications with PCR-based approaches are common. The presence of inhibitory substances such as organic and phenol compounds, glycogen fats and Ca<sup>2+</sup> ions in food samples (Rossen *et al.*, 1992; Wilson, 1997) can effect performance. To combat this, various extensive DNA extraction procedures have been described (Lantz *et al.*, 1994; Makino *et al.*, 1995), but these are often cumbersome and time consuming and involve hazardous reagents such as phenol-chloroform, and present a significant risk of losing target DNA in each purification step (Garrec *et al.*, 2003). With the developments in production of *Listeria*-specific antibodies, immunomagnetic separation (IMS) and immunocapture centrifugation (ICC) has been reported to offer a more reliable method of isolating and enriching (*L. monocytogenes*) cells from food complex food matrices (Uyttendale *et al.*, 2000; Hudson *et al.*, 2001; Hsieh and Tsen, 2001; Kaclíková, *et al.*, 2001). However, perhaps the single most significant limitation associated with direct PCR-based detection, is the inability of the process to discriminate dead from live cells. An inherent problem with such methods is, that they cannot effectively discriminate viable from dead cells. The only practical way of addressing this inherent limitation is by incorporating a lengthy enrichment step to, hopefully, 'dilute out' the dead cell population. This concomitantly negates the perceived improvement in sensitivity over the antibody-based approach. Alternatively, targeting mRNA by RT-PCR



would undoubtedly abrogate false positives arising from dead cells. However, the expression of many *Listeria*-specific genes, such as *inlA*, is principally synchronised at the transcriptional level. Thus, levels of mRNA, even in moderately large populations, may be quite low. It is highly likely that reliable detection of InlA-encoding mRNA would necessitate extended enrichment at 37 °C to achieve appropriate levels of exponentially growing cells. Thus, apparent improvements in sensitivity attributed to PCR-based detection of *L. monocytogenes* must retain the caveat of acknowledgement of the need for an associated enrichment step. The necessity of enrichment was clearly demonstrated in a recent comprehensive analysis of multiple factors affecting the sensitivity of a PCR-based method for detecting *L. monocytogenes* in food samples, conducted by Aznar and Alarcón (2003).

At present, the traditional horizontal isolation method is still the 'gold-standard' (Allerberger, 2002) for detection and identification of *L. monocytogenes*. With the increasing epidemiological significance of *L. monocytogenes*, in terms of public health concerns and the associated implications for food-processing industries, the need for more rapid, user friendly and discriminatory tests for *L. monocytogenes* has never been greater. The major objective of this work was to produce a monoclonal antibody suitable for reliable detection of *L. monocytogenes* and also to demonstrate its potential for application in 'real-time' identification of *L. monocytogenes* from enriched cultures.



***Chapter 2***  
***Materials and Methods***



## 2.1 *Equipment*

**Table 2.1:** *Equipment model used and suppliers.*

<b>Class</b>	<b>Model</b>	<b>Source</b>
<b>AFM instrument</b>	Nano-R™ AFM instrument	Pacific Nanotechnology, 3350 Scott Blvd., Suite 29, Santa Clara, CA 95054, USA.
	AFM Image Analysis software	
<b>Biacore™</b>	Biacore™ 1000	Biacore AB, Church Farm, Eyeworth, Bedfordshire, SG1 2HH, UK.
	Biacore™ 3000	
<b>Blood tube rotator</b>	SB1 Blood tube rotator	Stuart Scientific, Holmthorpe Industrial Estate, Redhill, Surrey, UK
<b>Centrifuges</b>	Heraeus Christ Labofuge 6000	Heraeus Instruments Inc., 111a Corporate Boulevard, South Plainfield, New Jersey, 07080, USA.
	Biofuge A Microcentrifuge	
	Beckman J2-21 centrifuge	Beckman-Coulter Inc., 4300N Harbour Boulevard, Fullerton, CA 92834-3100, USA.
<b>CO<sub>2</sub> Tissue culture incubators</b>	EG 115 IR	Heraeus Instruments Inc., 111a Corporate Boulevard, South Plainfield, New Jersey, 07080, USA.
	Thermoforma series II 3110 series	
<b>Evaporation unit</b>	Pierce Evaporation Unit	Pierce, 3747 North Meridian Road, PO box 117, Rockford, IL 61105, USA.
<b>HPLC apparatus</b>	System Beckman Gold Software	Beckman-Coulter Inc., 4300N Harbour Boulevard, Fullerton, CA 92834-3100, USA.





	Varian Star 9030 pump, 9012 UV detector, Fluorescence detector, AI-200 autosampler	J.V.A. Analytical Ltd., Long Mile Rd., Dublin 12, Ireland.
	Phenomenex 3000 SEC column	Phenomenex (UK), Queens Ave., Huddersfield Ind. Est., Macclesfield, Cheshire SK10 2BN, UK.
<b>Laminar flow units</b>	Holten 2448K laminar air flow unit	Holten Laminar A/S, Gydevang 17, DK 3450 Allerod, Denmark.
	FASTER BH2000	Biosciences, 3 Charlemont Tce., Crofton Rd., Dun Laoghaire, Dublin, Ireland.
<b>Microplate reader</b>	Titertek Multiscan plate reader	Medical Supply Company, Damastown, Mulhuddart, Dublin 15, Ireland.
<b>Microscope</b>	Nikon Diaphot inverted microscope	Nikon Corporation, 2-3 Marunouchi 3-chome, Chiyoda-ku, Tokyo, Japan.
<b>Millipore filtration apparatus</b>	Millipore Filtration Device (250 ml reservoir)	Millipore, 290 Concord Road, Billerica, MA 01821, USA.
<b>Orbital incubator</b>	Gallenkamp orbital incubator (100X400.XX1.C)	Sanyo Gallenkamp PLC., Monarch Way, Belton Park, Loughborough, Leicestershire LE11 5XG, UK.
<b>pH meter</b>	3015 pH meter	Jenway Ltd., Gransmore Green, Felsted Dunmow, Essex CM6 3LB, UK.
<b>Protein electrophoresis apparatus</b>	Atto dual minislabs system AE-6450	Atto Corp., 2-3 Hongo 7-Chrome, Bunkyo-Kui, Tokyo 113, Japan.
<b>Rocker platform</b>	Stuart Platform Shaker STR6	Lennox, P.O. Box 212A, John F. Kennedy Drive, Naas Rd., Dublin 12, Ireland.



---

<b>UV gel analyser</b>	UVP ImageStore 7500 gel documentation system	Ultra Violet Products Ltd.
<b>UV Spectrophotometer</b>	UV-160A	Shimadzu Corp., 1 Nishinokyo-Kuwabaracho, Nakagyo-ku, Kyoto 604, Japan.
<b>Ultrafiltration cell</b>	Stirred Cell 8400	Amicon Inc., Beverly, Massachusetts 01915, USA.
<b>PCR machine</b>	Biometra T gradient Uno II Thermocycler	Anachem Ltd., Anachem House, Charles St., Luton, Bedfordshire, UK.
<b>Waterbath</b>	RM6 Lauda waterbath	AGB Ltd., Dublin Industrial Estate, Dublin 11, Ireland.
<b>SEM instrument</b>	Hitachi S 300N SEM	Hitachi Corp. Ltd., 6-6 Marunouchi 1-chome, Chiyoda-ku, Tokyo 100-8280, Japan.
	SEM Image Analysis software	Oxford Instruments, Microanalysis Group, Halifax Road, High Wycombe, Bucks HP12 3SE, UK.

---



## 2.2 Consumable items

**Table 2.2: Consumables used and suppliers**

Class	Item	Source
<b>Disposables</b>	Eppendorf tubes, PCR tubes and pipette tips	Sarstedt Ltd., Sinnatstown, Drinagh, Wexford, Ireland.
	Sterile universals	Medical Supply Company, Damastown, Mulhuddart, Dublin 15, Ireland.
	Nunc Maxisorp™ plates (439454) <sup>*a</sup> Tissue culture plastic-ware	Nunc, Kamstrup, DK, Roskilde, Denmark.
	Nitrocellulose membrane	Schleicher and Schuell Bioscience GmbH, Hahnestrass3, D-37586, Dassel, Germany.
<b>Filters</b>	Acrodisc® 0.2 µm syringe filters Nanosep™ ultrafiltration membranes Omega™ 1.0, 10.0 and 50 kDa polyethersulfone membrane filters	PALL Corp., Newquay, Cornwall, UK. (c/o VWR International Ltd., Rath Business Park, Ashbourne Co. Meath, Ireland.)
	Durapore® 0.2 and 0.45 µm membrane filters (HVLP4700)	Millipore, 290 Concord Road, Billerica, MA 01821, USA. (c/o AGB Scientific Ltd., Dublin Industrial Estate, Dublin 11, Ireland.)
<b>Sensor chips</b>	Sensor chip CM5 (BR-1000-14) <sup>*b</sup>	Biacore AB, Church Farm, Eyeworth, Bedfordshire, SG1 2HH, UK.
	Sensor chip C1 (BR-1005-40) <sup>*b</sup>	
	Sensor chip CM4 (BR-1005-39) <sup>*b</sup>	
	Sensor chip NTA (BR-1004-07) <sup>*b</sup>	

( ): Catalogue code.

<sup>\*a</sup> : Certified grade.

<sup>\*b</sup> : Research grade.



## 2.3 Reagents and chemicals

All chemicals were reagent grade and were purchased through **Sigma-Aldrich Co.** (Poole, Dorset, England) except as noted below.

**Table 2.3: Reagents and chemicals used:**

<b>Class</b>	<b>Chemical</b>	<b>Supplier</b>
<b>Biochemistry</b>	Alkaline phosphatase-labelled secondary antibodies: Caprine anti-mouse IgG and IgM (222-CK-6GM) Caprine anti-mouse IgG2a (222-AB-6G4Z)	AMS Biotechnonogy (Europe), 185 A and B Milton Park, Abingdon, Oxon, OX14 4SR, UK.
	BSA-free anti His-tag monoclonal antibody (70796-3)	Novagen Inc., 441 Charmany Dr., Madison, WI 53719, USA.
	Phosphate buffered Saline tablets (BR0014)	Oxoid, Basingstoke, Hampshire, UK.
	Pre-stained molecular weight markers BlueRanger <sup>®</sup> (26681) BCA protein assay kit (23225)	Pierce, 3747 North Meridian Road, PO box 117, Rockford, IL 61105, USA.
	Amine coupling kit (BR-100-50)	Biacore AB, Church Farm, Eyeworth, Bedfordshire, SG1 2HH, UK.
	Osmium tetroxide (75633)	Fluka Chemie AG, Industriestrasse 25, 9471, Buchs, Switzerland.
<b>Genetics</b>	PCR Primers	MWG-Biotech Ltd., Milton Keynes MK12 5RD, UK.
	Restriction enzymes and compatible buffers	New England Biolabs, 32 Tozer Rd., Beverly, MA 01915-5599, USA.





---

	Wizard® Plus SV Mini-prep kit ( <i>A1330</i> ) <i>Pfu</i> DNA polymerase ( <i>M7741</i> )	Promega Corporation, 2800 Woods Hollow Rd., Madison, WI 53711- 5399, USA.
	Perfectprep® gel cleanup kit ( <i>0032 007.740</i> )	Eppendorf AG, 22331, Hamburg, Germany.
	Ni-NTA Superflow resin ( <i>30430</i> ) pQE-60 plasmid	Qiagen Ltd., Qiagen House, Fleming Way, Crawley, West Sussex RH10 9AX, UK.
<b>Microbiology</b>	Bacteriological media: Brain heart infusion broth (BHI) ( <i>CM225</i> ) <i>Listeria</i> enrichment broth base (LEB) ( <i>CM863</i> ) Yeast extract ( <i>L0021</i> ) Tryptone ( <i>L0042</i> ) Agar technical (Agar No. 3) ( <i>L0013</i> )	Oxoid, Basingstoke, Hampshire, UK.
<b>Tissue culture</b>	Briclone	Archport Ireland Ltd., Dublin City University, Glasnevin, Dublin 9, Ireland.
	Fetal calf serum ( <i>10270-106</i> ) L-glutamine (200mM) (100x) ( <i>25030-024</i> ) Non-essential amino acids (100x) ( <i>11140-035</i> ) Sodium pyruvate (100 mM) ( <i>11360-039</i> )	Gibco BRL, Trident House, Renfrew Rd., Paisley PA4 9RF, Scotland, UK.

---



**Table 2.4: Bacterial cultures used:**

Genus	Species	Strain	Source
<b>Listeria spp.</b>	<i>L. monocytogenes</i> 1/2a	NCTC 4886	IFR
	<i>L. monocytogenes</i> 1/2c	NCTC 5348	IFR
	<i>L. monocytogenes</i> 4a	NCTC 5214	IFR
	<i>L. monocytogenes</i> 4b	NCTC 4885	IFR
	<i>L. innnocua</i> 6a	NCTC 11288	IFR
	<i>L. innnocua</i> 6b	NCTC 11289	IFR
	<i>L. ivanovii</i> (PA) <sup>*a</sup>	NCTC 11846	PA Lab, Dublin
	<i>L. ivanovii</i> (PHLS) <sup>*b</sup>	PHLS isolate	IFR
	<i>L. welshimeri</i>	NCTC 11857	IFR
	<i>L. seeligeri</i>	ATCC 35967	IFR
	<i>L. monocytogenes</i> (1/2a)	-	IFR <sup>*c</sup>
	EGDpERL3 50-1prfA <sub>EGD</sub>		
<b>Non-Listeria spp.</b>	<i>Escherichia coli</i>	NCIMB 9485	DCU
	<i>Enterobacter aerogenes</i>	NCIMB 10102	DCU
	<i>Enterococcus faecilis</i>	NCIMB 775	DCU
	<i>Bacillus subtilis</i>	NCIMB 1650	DCU
	<i>Bacillus cereus</i>	NCIMB 3329	DCU
<b>Expression hosts</b>	<i>Escherichia coli</i>	XL10-Gold®	Stratagene
	<i>Escherichia coli</i>	INV αF'	Invitrogen

NCTC: National Collection of Type Cultures, Central Public Health Laboratory, 61 Colindale Avenue, London NW9 5HT, UK.

ATCC: American Type Culture Collection, Manassas, Virginia, USA.

NCIMB: National Collection of Food, Industrial and Marine Bacteria Ltd., 23 St. Machar Drive, Aberdeen AB24 3RY Scotland, UK.

Stratagene: North Torrey Pines Rd., La Jolla, Ca. USA.

Invitrogen: 9704-CH-Groningen, Netherlands.

<sup>\*a</sup>: Provided by the Vincent Young and Rachel Hewitt at the Public Analyst (PA) Laboratory, Sir Patrick Duns Hospital, Dublin 2, Ireland.

<sup>\*b</sup>: Serotype unconfirmed. Provided by Gary Wyatt at the Institute for Food Research (IFR), Norwich Research Park, Colney, Norwich NR4 7UA, UK. Originally sourced from the UK Public Health Laboratory Service (PHLS).



<sup>\*c</sup>: Provided by Gary Wyatt at the IFR. Originally sourced from Prof. Trinad Chakraborty, Institute for Medical Microbiology and Virology, Giessen, Germany (Lingnau et al., 1995). This recombinant strain produces elevated PrfA protein levels. The origins of the pERL3 50-1 construct have been outlined elsewhere (Chakraborty et al., 1992; Domann et al., 1992).



### **2.3.1     *Standard solutions***

#### ***Phosphate buffered saline (PBS)***

One tablet was dissolved per 100 ml of distilled water according to the manufacturer's instructions. When dissolved, the tablets prepare Dulbecco's A PBS which contains 10 mM phosphate buffer and 0.15 M NaCl, pH 7.2-7.4.

#### ***Wash buffer (PBS/T)***

PBS containing 0.05 % (v/v) Tween-20 (*Sigma, P-7949*).

#### ***Diluent buffer (PBS/TM)***

PBS containing 0.05 % (v/v) Tween-20. This was supplemented with dry skimmed milk powder (Marvel) was at 1 % (w/v) when used for dilution of secondary, enzyme-labelled antibodies.

#### ***Hepes buffered saline (HBS)***

Hepes buffered saline (Biacore running buffer) containing 50 mM NaCl, 10 mM HEPES (*Sigma, H-3375*), 3.4 mM EDTA and 0.05 % (v/v) Tween-20 was prepared by dissolving 8.77 g of NaCl, 2.56 g of HEPES, 1.27 g of EDTA. and 500 µl of Tween 20 in 800ml of distilled water. The pH of the solution was then adjusted to pH 7.4 by addition of 2 M NaOH. The final volume was then made up to 1000 ml in a volumetric flask. The solution was filtered through 0.2 µm filter and degassed prior to use.

#### ***Trichloroacetic acid (TCA)***

A 100 % (w/v) stock solution of TCA (*Sigma T-9159*) was prepared by adding 454 ml dH<sub>2</sub>O to 1 Kg of C<sub>2</sub>HCl<sub>3</sub>O<sub>2</sub> and bringing the resulting solution up to a final volume of 1000 ml with dH<sub>2</sub>O. The solution was stored at 4 °C.

*(Warning: Due to the highly corrosive nature of TCA, the solid was never weighed out, instead the water was always added to the original, freshly opened bottle of TCA.)*

### **2.3.2     *Denaturing SDS-PAGE***

#### ***Denaturing polyacrylamide gel electrophoresis (PAGE)***

Polyacrylamide gel electrophoresis was carried out using the discontinuous system, in the presence of sodium dodecyl sulphate (SDS), as described by Laemmli (1970). 12.5 % (w/v)





resolving and 5 % (w/v) stacking gels were routinely used and prepared from the following stock solutions as outlined in Table 2.5.

**Stock Solutions**

(A) 30 % (w/v) acrylamide (*Sigma, A3553*) containing 0.8 % (w/v) N, N'-methylene bis-acrylamide (*Sigma, M-7179*).

(B) 1.5 M Tris-base, pH 8.8, containing 0.4 % (w/v) SDS (*Sigma, L4509*).

(C) 0.5 M Tris-base, pH 6.8, containing 0.4 % (w/v) SDS.

(D) 10 % (w/v) ammonium persulphate.

**Table 2.5:** The quantities of stock solutions required for the preparation of two standard sized resolving and stacking gels used for polyacrylamide gel electrophoresis.

<b>Solution</b>	<b>Resolving Gel (12.5 %)</b>	<b>Stacking Gel (5 %)</b>
Acrylamide (A)	8.34 ml	1.66 ml
Distilled Water	6.6 ml	5.75ml
Resolving Gel Buffer (B <sup>1</sup> )	5.0 ml	-----
Stacking Gel Buffer (C <sup>1</sup> )	-----	2.5 ml
Ammonium Persulphate (D)	100µl	60 µl
TEMED	15 µl	15 µl

Samples were mixed 6:1 with 6x sample buffer and boiled for 5 minutes before loading onto the gel. Electrophoresis was conducted in electrophoresis buffer, pH 8.3 at 12.5 mA for the stacking gels and 15 mA for the resolving gel, using an ATTO vertical mini electrophoresis system, until the tracking dye reached the bottom of the gel.



### ***Staining of gels with Coomassie brilliant blue***

Gels were stained with Coomassie staining solution for visualisation of protein bands. Gels were stained for 1 hr in 0.2 % (w/v) Coomassie brilliant blue dye in methanol:acetic acid:distilled water (3:1:6). Gels were destained overnight in methanol:acetic acid:distilled water (3:1:6).

### ***Coomassie blue stain solution***

Coomassie Blue R-250 ( <i>Sigma, B-7920</i> )	1.250 g
Methanol	227 ml
dH <sub>2</sub> O	227 ml
Glacial acetic acid	46 ml

The components were dissolved, mixed thoroughly, filtered through Whatman paper grade number 1, and stored at room temperature (R.T.) in a dark bottle.

### ***Destain solution***

Methanol	300 ml
Glacial acetic acid	100 ml
dH <sub>2</sub> O	600 ml

The above components were mixed, thoroughly, and stored at R.T.

### ***5x Electrophoresis buffer***

Tris-base	15.15 g
Glycine	72.00 g
SDS	5.00 g

The components were dissolved in 1L of dH<sub>2</sub>O, and stored at R.T.

### ***6x Sample buffer (S<sup>d</sup>)***

1.2 M Tris-base (pH 6.8)	10.0 ml
2-ME (2-Mercaptoethanol)	66.0 µl
Bromophenol blue	0.06 g
Glycerol (99.99 % purity)	5.00 ml
SDS	2.40 g

The components were mixed in this order, brought to 20 ml with dH<sub>2</sub>O and stored at – 20 °C.



#### ***Acrylamide stock solution (A)***

Acrylamide	30.00 g
Methylene bisacrylamide	0.80 g

The components were dissolved in 100 ml dH<sub>2</sub>O, and stored in the dark at 4 °C.

#### ***4x Resolving gel buffer (B<sup>1</sup>)***

3.0 M Tris-base (pH 8.8)	50.0 ml
10 % (w/v) SDS	4.0 ml
dH <sub>2</sub> O	46.0 ml

The components were thoroughly mixed together, and stored at 4 °C.

#### ***4x Stacking gel buffer (C<sup>1</sup>)***

1.0 M Tris-base (pH 6.8)	50.0 ml
10 % (w/v) SDS	4.0 ml
dH <sub>2</sub> O	46.0 ml

The components were thoroughly mixed together, and stored at 4 °C.

#### ***Ammonium persulphate solution (D)***

Ammonium persulphate	0.10 g
dH <sub>2</sub> O	1.00 ml

The components were mixed thoroughly and stored at -20 °C.

### **2.3.3 Non-denaturing-PAGE**

#### ***Non-denaturing polyacrylamide gel electrophoresis (PAGE)***

The procedure was similar to that followed for denaturing SDS PAGE with several key differences. Samples and reagents were kept free from SDS and 2-mercaptoethanol, at all times. A 4 % (w/v) stacking gel was routinely used. Resolving gels containing varying acrylamide concentrations were employed with each sample been analysed over at least four different concentrations (7, 8, 9 and 10 % (w/v) acrylamide). Stock solutions used, and gel formulations are outlined in Table 2.6.



### **Stock Solutions**

(A) 30 % (w/v) acrylamide containing 0.8 % (w/v) methylene bis-acrylamide.

(B') 1.5 M Tris-base, pH 8.8.

(C') 0.5 M Tris-base, pH 6.8.

(D) 10 % (w/v) ammonium persulphate.

**Table 2.6:** The quantities of stock solutions required for the preparation of two standard sized resolving and stacking gels used for polyacrylamide gel electrophoresis.

<b>Solution</b>	<b>Stacking Gel (4 %)</b>	<b>Resolving Gel (7 %)</b>	<b>Resolving Gel (8 %)</b>	<b>Resolving Gel (9 %)</b>	<b>Resolving Gel (10 %)</b>
Acrylamide (A)	1.33 ml	4.67 ml	5.33 ml	6.00 ml	6.66 ml
Distilled Water	6.17 ml	10.33 ml	9.66 ml	9.00 ml	8.34 ml
Resolving Gel Buffer (B <sup>2</sup> )	-----	5.00 ml	5.00 ml	5.00 ml	5.00 ml
Stacking Gel Buffer (C <sup>2</sup> )	2.50 ml	-----	-----	-----	-----
Ammonium Persulphate (D)	50 µl	50 µl	50 µl	50 µl	50 µl
TEMED	10 µl	10 µl	10 µl	10 µl	10 µl

### **6x Sample buffer (S<sup>2</sup>)**

1.0 M Tris-base (pH 6.8) 3.0 ml

Bromophenol blue 0.06 g

Glycerol (99.99 % purity) 5.00 ml

The components were mixed in this order, then adjusted to 10 ml with dH<sub>2</sub>O and stored at -20 °C.

### **4x Resolving gel buffer (B<sup>2</sup>)**

3.0 M Tris-base (pH 8.8) 50.0 ml

dH<sub>2</sub>O 50.0 ml





The components were thoroughly mixed together, and stored at 4 °C.

**4x Stacking gel buffer (C<sup>2</sup>)**

1.0 M Tris-base (pH 6.8)	50.0 ml
dH <sub>2</sub> O	50.0 ml

The components were thoroughly mixed together, and stored at 4 °C.

Samples were mixed 6:1 with 6x sample buffer on ice and loaded immediately onto the gel. Molecular weight markers (Table 2.7) were added to dedicated, individual wells. Electrophoresis was conducted in electrophoresis buffer, pH 8.3 at 12.5 mA for the stacking gels and 15 mA for the resolving gel, using an ATTO vertical mini electrophoresis system, until the tracking dye reached a defined height above the bottom of the gel. The gel was then stained with Commassie blue. Relative mobility ( $R_f$ ) of the standard and sample proteins was calculated according to the following relationship:

$$R_f = \frac{\text{distance of protein migration}}{\text{distance of tracking dye migration}} \quad (\text{Equation 2.1})$$

100[log ( $R_f \times 100$ )] values for each protein were plotted against the respective resolving gel concentration (% (w/v) acrylamide). The resulting negative slope values were plotted against the known molecular weights of the standards. The unknown molecular weights were estimated from this standard curve.

**Table 2.7:** Molecular weight standards used in non-denaturing SDS PAGE.

Standard	Mr (kDa)	Source	Catalogue code
Urease, Jack Bean	272.0 (trimer)	Sigma	U-7752
	545.0 (hexamer)		
Bovine serum albumin (BSA)	66.0 (monomer)	Sigma	A-8654
	132.0 (trimer)		
Chicken egg albumin (CEA)	45.0	Sigma	A-8529
Carbonic anhydrase (CA)	29.0	Sigma	C-5024



### **2.3.4 Western blot analysis**

#### ***Western blotting***

Proteins were transferred from acrylamide gels to nitrocellulose using a BioRad wet blotter for 90 minutes at 72 V, in electrophoresis buffer containing 20 % (v/v) methanol. The membrane was blocked with Tris buffered saline (TBS) containing 5 % (w/v) milk marvel powder overnight at 4 °C. Primary antibody (hybridoma supernatant at 1/5 or purified IgG at 1/2000 in TBS/TM) was then added to the membrane and incubated for 1.5 hours at room temperature. The membrane was then washed three times in TBS/T, for 15 minutes each time and alkaline phosphatase-labelled detection antibody (anti-mouse) diluted in TBS/TM was incubated for 1 hr with the membrane. The blot was developed following three 10 minute washings in TBS/T and two further washes in TBS using 5-bromo-4-chloro-3'-indoly]phosphate/nitro blue tetrazolium chloride (BCIP/NBT) substrate reagent. Colour development was stopped by addition of TBS containing 0.5 M EDTA followed by extensive washing with distilled water. Alternatively, when horseradish peroxidase- (HRP)-labeled secondary antibodies were employed, 3,3',5,5'-tetramethylbenzidine (TMB) was used as the substrate.

#### ***Tris-buffered saline (TBS)***

10 mM Tris-HCl, pH 8.0, containing 150 mM NaCl was prepared by dissolving 1.57 g of Tris-HCl and 8.77 g of NaCl in 800 ml of distilled water. The pH of the solution was then adjusted to pH 8.0 by the addition of 1M NaOH. The final volume was then made up to 1000 ml in a volumetric flask.

#### ***Wash buffer (TBS/T)***

TBS containing 0.05 % (v/v) Tween-20.

#### ***Diluent buffer (TBS/TM)***

TBS containing 0.05 % (v/v) Tween-20 and 1 % (w/v) dry skimmed milk powder.

#### ***Transfer buffer***

25 mM Tris-Base (pH approximately 8.3-8.6, unadjusted), 192 mM glycine and 0.1 % (w/v) SDS. A 5x stock was prepared by dissolving 15.15 g of Tris-base, 72 g of glycine and 5 g of SDS in 1000 ml of distilled water. The stock solution was stored at R.T. and a 1x working dilution prepared by adding 100 ml to 200 ml methanol and 200 ml distilled water and mixing thoroughly.



### ***2.3.5 Bicinchoninic (BCA) assay for estimation of protein concentration***

BCA reagents were supplied as components of the BCA protein assay kit. Reagent 'A' contained an optimised formulation of sodium carbonate, sodium bicarbonate, bicinchoninic acid and sodium tartrate in a 0.1 M NaOH solution. Reagent 'B' consisted of an aqueous solution of 4 % (w/v) cupric sulphate. Standard solutions containing BSA at concentrations of 0, 25, 125, 250, 500, 750, 1000, 1500 and 2000 µg/ml were prepared in the same buffer as the sample being analysed (this normally consisted of PBS). 25 µl of each standard was pipetted in triplicate into microplate wells. This was repeated for each test sample. The BCA working reagent was prepared by mixing reagents 'A' and 'B' in the ratio 50:1. A 200 µl aliquot of working reagent was added to each well and the plate was then covered and incubated at 37 °C for 30 minutes. Absorbance values were read at 590 nm. The blank (0 µg/ml) absorbance value was subtracted and a standard curve of net absorbance at 590 nm versus concentration (µg/ml) was constructed and then used to estimate the concentration of each test sample. This technique was frequently used to estimate the total protein concentration in samples prior to PAGE analysis, particularly when dealing with crude or impure samples.



### **2.3.6 SEM and AFM image analysis solutions**

All buffers used in fixing, washing and post-fixing samples for image analysis were prepared using ultra-pure water ( $\text{upH}_2\text{O}$ ). All solutions were prepared in a fume hood.

#### ***Cacodylate buffer***

A stock solution of 200 mM sodium cacodylate trihydrate ( $\text{C}_2\text{H}_6\text{AsO}_2\text{Na} \cdot 3\text{H}_2\text{O}$ ) (*Sigma, C0250*) was prepared with the pH adjusted to pH 7.4 with 200 mM HCl. A 100 mM working solution was prepared by diluting the stock solution 1:1 with  $\text{upH}_2\text{O}$  or fixing solution as required. (*Warning: This reagent contains arsenic and all relevant precautions should be taken when handling.*).

#### ***Glutaraldehyde fixing solution***

A 25 % (v/v) aqueous stock solution of glutaraldehyde (*Sigma G-4004*) was purchased and stored in a sealed, spillage-secure container at  $-20\text{ }^\circ\text{C}$ . Immediately prior to use, the stock solution was diluted 1:10 with cacodylate buffer. (*Warning: This is a volatile and toxic cross-linking agent and should be handled with the appropriate safety precautions.*).

#### ***Osmium tetroxide post fixing solution***

A 1 % (w/v) aqueous stock solution of Osmium tetroxide ( $\text{OsO}_4$ ) was purchased and stored in a sealed, spillage-secure container at  $4\text{ }^\circ\text{C}$ . Immediately prior to use, the stock solution was diluted 1:1 with cacodylate buffer. (*Warning: This is a volatile and toxic cross-linking agent and should be handled with the appropriate safety precautions.*).





## **2.4 Antigen isolation and preparation**

The *L. monocytogenes* EGD pERL3 50-1 *prfA*<sub>EGD</sub> strain contains multiple copies of the *prfA* gene and has been confirmed to produce elevated levels of virulence-associated proteins in *L. monocytogenes*, such as InlA and, in particular, PrfA-regulated virulence proteins, such as InlB (Lingnau *et al.*, 1995). It was thus, used to ensure maximum yield of pathogenicity-associated proteins during antigen isolation experiments.

### **2.4.1 Preparation of bacterial stocks**

Isolated colonies from freshly streaked BHI agar plates were picked cultured overnight at 37 °C and 200 rpm in BHI broth. A 1 ml sample was then sub-cultured into fresh BHI broth (50 mls) and grown to late exponential phase at 37 °C and 200 rpm. Sterile glycerol (12.5 mls) was then added to each 50 ml culture to give a final glycerol concentration of 20 % (v/v). The cells were then dispensed into 2 ml cryovials in 1.2 ml volumes and stored at -80 °C.

### **2.4.2 Preparation of InlB extract**

One 1.2 ml aliquot of *L. monocytogenes* EGD pERL3 50-1 *prfA*<sub>EGD</sub>, prepared as above (Section 2.4.1) was thawed and inoculated into 50 mls of BHI containing 5 µg/ml erythromycin (*Sigma*, E-5389). The culture was incubated overnight for 12 hours at 37 °C and 200 rpm. The overnight culture was diluted 1/50 with fresh BHI media that had been pre-filtered with a 10 kDa cut-off membrane and then incubated at 37 °C at 120 rpm. When an O.D.<sub>600nm</sub> value of between 0.8 and 1.0 was reached the cells were removed by centrifugation at 4000 rpm for 20 minutes at 4 °C. The supernatant was decanted and the cell pellet was washed three times in 0.5 % (v/v) of the original culture volume sterile-filtered PBS. The pellet was re-suspended in 0.5 % (v/v) the original culture volume of 1 M Tris-HCl, pH 7.5 and incubated on ice for one hour, as previously described by Müller *et al.*, 1998a. The cells were then pelleted by centrifugation at 10000 rpm for 10 minutes at 4 °C. The supernatant (InlB-enriched extract) was dialysed extensively against PBS, concentrated using PEG and finally dispensed into eppendorf tubes and stored at -20 °C.

### **2.4.3 Preparation of protein-enriched supernatant**

An exponential phase culture of *L. monocytogenes* EGD pERL3 50-1 *prfA*<sub>EGD</sub> was prepared as above (Section 2.4.2). When an O.D.<sub>600nm</sub> value of between 0.8 and 1.0 was reached, cells were pelleted by centrifugation at 6000 rpm for 20 minutes at 4 °C. The resultant supernatant was decanted and filtered through a 0.2 µm filter to remove residual cells or particulate matter. The supernatant proteins were then precipitated by dropwise addition trichloroacetic



acid (TCA) to a final concentration of 10 % (v/v) and left stirring gently overnight at 4 °C. The precipitated proteins were pelleted by centrifugation at 6000 rpm for 30 minutes at 4 °C, resuspended in PBS (at a volume equivalent to 0.5 % of the original culture volume), dialysed extensively against PBS and concentrated using PEG before being dispensed into eppendorf tubes and stored at -20°C.

#### **2.4.4 Preparation of formalin-inactivated *L. monocytogenes* cells**

An exponential phase culture of *L. monocytogenes* EGD pERL3 50-1 *prfA*<sub>EGD</sub> was prepared as above (Section 2.4.2). Exponential phase cells were pelleted by centrifugation at 8000 rpm and 4 °C for 15 minutes. The cell pellet was carefully resuspended in a 10 % (v/v) formalin solution (i.e. 3.7 % (v/v) formaldehyde in sterile-filtered PBS) and incubated in a sterile universal at 37 °C for 1 hr at 110 rpm. The cell suspension was then centrifuged at 4000 rpm and 4 °C for 25 minutes. The formalin-containing supernatant fraction was carefully decanted and the remaining cell pellet was washed three times in sterile-filtered PBS. The final washed pellet was resuspended in 5 ml sterile filtered PBS, dispensed into eppendorff tubes at appropriate volumes and stored at -20 °C until required.

#### **2.4.5 Extraction of *Listeria* surface proteins**

A 1 ml cell suspension was aseptically sub-cultured from an overnight BHI broth culture into a fresh 50 mls BHI or *Listeria* enrichment broth (LEB), as required. When exponential growth was achieved, the cells were pelleted by centrifugation at 6000 rpm for 15 minutes at 4 °C. The cell pellet was washed three times in 0.5 % of the original culture volume (i.e. 250 µl) PBS. The washed cells were then resuspended in 250 µl of a 2 % (w/v) SDS solution in PBS and incubated for 45 minutes at 37 °C and 200 rpm. The solubilised protein fraction was isolated following centrifugation of the mixture at 6000 rpm and 4 °C for 15 minutes. The extracted proteins in the SDS solution were either applied directly to an SDS PAGE gel analysis or desalted and stored at -20 °C until required.



## 2.5 *Animal experiments*

### 2.5.1 *Licencing for animal usage*

All procedures involving the use of animals were approved and licensed by the Department of Health, and every precaution was taken to ensure the minimum distress to the animals.

### 2.5.2 *Immunisation protocol for mice for the production of monoclonal antibodies to *L. monocytogenes**

Balb/C mice of aged 5-8 weeks were used for the production of monoclonal antibodies to *L. monocytogenes* whole cells or *L. monocytogenes*-derived proteins, using the immunisation schedule described below:

- Day 1:** A 1 mg/ml solution of antigen (if using *L. monocytogenes*-derived proteins) or  $2 \times 10^9$  cells (if using *L. monocytogenes* whole cells) was prepared in PBS and mixed with an equal volume of Freund's Complete Adjuvant (FCA) (*Sigma, F-5581*). This solution was then vortexed to form an emulsion and 150-200  $\mu$ l of the emulsion used to immunise mice by intraperitoneal (i.p.) injection.
- Day 21:** Mice were re-immunised intraperitoneally, with a similar dose of the immunogen (as above) in Freund's Incomplete Adjuvant (FICA) (*Sigma, F-5506*) in the case of *L. monocytogenes*-derived proteins, or, PBS in the case of whole cells.
- Day 28:** Mice were bled from the tail vein, and the specific antibody titre determined.
- Post-Day 28:** Mice were boosted intraperitoneally, with a similar mix of antigen and FICA or PBS as per day 21.
- Post-Day 28:** The above immunisation and blood sampling sequence was continued until a satisfactory antibody titre was recorded. Once the antibody titre was sufficiently high, the mouse was immunised intravenously (i.v.) with respective antigen in PBS, 24 hr prior to conducting the fusion. In cases where the immunogen consisted of complete cells, this final boost was administered via the i.p. route. Finally, the mouse was sacrificed by cervical dislocation and the spleen (or other specified lymph node) was removed and used for subsequent somatic cell fusion procedures.

*Note: This represents a generic outline of the typical immunization regime employed. The exact protocol varied for each given antigen is outlined in detail in the corresponding relevant sections of chapter three.*



### **2.5.3    *Monoclonal antibody production by ascitic growth***

Ascitic fluid (also called ascites) is an intra-peritoneal fluid extracted from mice that have developed a peritoneal tumour. For antibody production, the tumour is induced by injecting hybridoma cells into the peritoneal cavity of mice of the same genetic background as the hybridoma.

Balb/C mice of the same genetic background as the hybridomas were given an intra-peritoneal injection of 0.5 ml of pristane (2,6,10,14-tetramethylpentadecane) (Sigma, P-1403). This solution acts as an immuno-adjuvostimulant/irritant to the mice, which respond by secreting nutrients and recruiting monocytes and lymphoid cells into the peritoneum, thus creating a rich environment for hybridoma growth. Approximately 7-10 days later,  $2-3 \times 10^7$  hybridoma cells were injected intra-peritoneally. Tumour growth was evident after 1-2 weeks and the mice were sacrificed. The ascitic fluid was then drained under sterile conditions by insertion of a needle into the peritoneal cavity.





## **2.6     *Antibody purification***

### **2.6.1     *Ammonium sulphate precipitation***

The ammonium sulphate precipitation was carried out according to the method of Hudson and Hay (1980). Approximately 1 ml of ascites fluid was diluted 1:2 with PBS and saturated ammonium sulphate was then added to bring the final concentration to 45 % (v/v). This mixture was then stirred at room temperature for 30 minutes, and the resulting precipitate centrifuged at 3000 rpm for 20 minutes at 4 °C. The precipitate was then resuspended in a volume of PBS, equal to that of the original volume of ascites. Saturated ammonium sulphate was then added to a final concentration to 40 % (v/v) and the mixture centrifuged at 3000 rpm for 20 minutes. The pelleted precipitate was then resuspended, in a volume of PBS equal to twice the original volume of ascites. The resuspended precipitate was then dialysed overnight against PBS with 0.02 % (w/v) sodium azide at 4 °C.

### **2.6.2     *Concentration of tissue culture supernatant***

Up to 300 ml of spent supernatant from the relevant hybridoma cell line was collected over a period of several days. Sodium azide was added to a final concentration of 0.02 % (w/v) to the supernatants and it was then stored at 4 °C until required. The supernatant was concentrated 15-fold to a final volume of 20 ml, using a stirred ultrafiltration cell with a 76 mm Omega™ ultrafiltration membrane, with a molecular weight cut-off of 10 kilodaltons (kDa), and the concentrate stored at 4 °C, until required.

### **2.6.3     *Protein A/G affinity-purification of immunoglobulin***

Concentrated supernatant from cultured hybridoma cells was stored at 4 °C prior to affinity purification. A 1 ml suspension of immobilised protein A (immobilised on Sepharose 4B, stored in sterile-filtered PBS containing 20 % (v/v) ethanol) was equilibrated in a column with 20 ml of sterile-filtered PBS. Up to 10 ml of concentrated hybridoma supernatant was passed through the column and the eluant collected and passed through the column a second time. At least 25 mls of wash buffer was passed through the column and, subsequently, the retained protein was eluted with 0.1 M glycine-HCl buffer (pH 2.5). Fractions of eluate collected in eppendorf tubes containing 150 µl of neutralization buffer (2 M Tris-HCl, pH 8.5). This served to rapidly neutralize the highly acidic environment of the elution buffer, thereby, preventing denaturation of the eluted IgG fraction. The absorbance of each fraction was measured, at 280 nm. Those fractions containing significant protein were pooled, desalted on PD10™ size exclusion columns against PBS and stored at -20 °C until required for further use. All purification and desalting procedures were conducted at 4 °C.



#### **2.6.4 Desalting of affinity-purified IgG fractions**

A PD10™ column (*Amersham Pharmacia Biotech*) containing an 8.3 ml bed volume of Sephadex G25 was equilibrated with 25 mls of running buffer (PBS). Up to 2.5 ml of the affinity-purified IgG fraction was then loaded onto the column. When the sample meniscus reached the top of the gel, fresh running buffer was added and the IgG protein components were eluted in approximately 2.5-3.5 ml of PBS.



## **2.7 Mammalian Cell Culture**

All mammalian cell cultures were manipulated aseptically and grown in a humidified (5 % (v/v) CO<sub>2</sub>) atmosphere, at 37 °C.

### **2.7.1 Preparation of mammalian cell culture media:**

All cell lines were routinely grown in DMEM (Dulbecco's modification of Eagle's medium) (*Sigma, D-5671*) supplemented with 10 % (v/v) foetal calf serum (FCS), 2 mM L-glutamine, and 25 µg/ml gentamycin sulphate (*Sigma G-1522*).

DMEM lacking foetal calf serum was prepared for use during somatic cell fusion procedures. Additionally, HAT (Hypoxanthine, Aminopterin and Thymidine) medium was prepared, which consisted of DMEM supplemented with 1 mM sodium pyruvate, non-essential amino acids (NEAA, 1 %, v/v), 100 µM hypoxanthine, 400 nM aminopterin, and 16 µM thymidine. This particular culture medium allowed for the selective growth of hybridoma cells post-fusion in the presence of Sp2/0 cells, which are unable to proliferate in HAT medium because they lack the requisite enzyme systems (Section 3.1.2.). DMEM supplemented with 1 mM sodium pyruvate, non-essential amino acids (1 % (v/v)), 100 µM hypoxanthine and 16 µM thymidine was also prepared (referred to as HT medium). All media were stored at 4 °C.

### **2.7.2 Recovery of frozen cells**

Cells were recovered from liquid nitrogen by rapidly thawing at 37 °C, and transferring to a sterile universal containing DMEM. The cells were then centrifuged at 2000 rpm for 10 minutes, resuspended in fresh culture medium, transferred to a tissue culture flask and incubated at 37 °C in a humidified 5 % CO<sub>2</sub> incubator. Prior to incubation, a 100 µl sample of the resuspended pellet was tested for cell viability using Trypan blue (Section 2.7.3.). Only cells with > 90 % viability on recovery from frozen stocks were cultured further.

### **2.7.3 Cell counts and viability testing**

All cell counts were made using an improved Neubauer Counting Chamber. Viable cell counts were obtained by mixing 50 µl of cell suspension with 10 µl of a commercial isotonic Trypan blue solution (0.25 %, (w/v)) (*Sigma, T-8154*). The viable cell count was carried out within 5 minutes of the addition of Trypan blue. A sample of this mixture was then used to perform the cell and viability count. Viable cells excluded the dye and remained white, while dead cells were stained blue. Cells were visualised under phase contrast on an inverted



microscope at 40x magnification. At all times cells were pelleted by centrifugation at 2000 rpm for 5 minutes unless otherwise stated.

#### **2.7.4 *Growth of suspension cell lines***

The Sp2/0 (ATCC CRL 1581) myeloma cell line was routinely cultured in DMEM. The cells were subcultured, using a split ratio of 1:4, at approximately 70 % confluency. For subculturing, the cells were flushed off the surface of the flask using a Pasteur pipette, collected and centrifuged at 2000 rpm. The pellet was then resuspended in 4 ml of fresh culture medium. Finally, 1 ml of the resuspended pellet was transferred to T-75 flasks containing 14 ml of fresh, pre-warmed DMEM.

#### **2.7.5 *Storage of cell lines***

Cells were harvested from the surface of a confluent T-75 flask by flushing the surface of the flask with a Pasteur pipette, and pelleted by centrifugation at 2000 rpm. Pellets were resuspended in 3 ml of an 8 % (v/v) solution of DMSO (Dimethyl sulphoxide) in FCS, and dispensed into 3 cryovials. A freezing-tray was used to gradually cool the cells, over a 3.0 hr. period, in the vapour-phase of liquid nitrogen. They were then immersed in the liquid-phase for long-term storage. Alternatively, cells were placed in isopropanol baths at -80 °C for 12 hours before being placed in liquid nitrogen for long-term storage.

#### **2.7.6 *Mycoplasma screening***

Cell lines were screened for mycoplasma contamination in conjunction with the National Cell and Tissue Culture Centre (NCTCC), Dublin City University.

##### **2.7.6.1 *Cell culture of NRK cells***

Adherent NRK (normal rat kidney) cells were cultured in DMEM. When cells had reached 70 % confluency, the medium was poured off, and the flask rinsed three times with 10ml of sterile PBS. A 3 ml of trypsinising solution (0.025 % (v/v) and 0.02 % EDTA (v/v)) was added to the flask, which was replaced back in the incubator until all of the cells had detached. Next, 5 ml of fresh DMEM was added to this cell suspension, which was then centrifuged at 2000 rpm and the pellet resuspended in the required volume of fresh DMEM.

##### **2.7.6.2 *Screening for Mycoplasma contamination***

NRK cells were cultured for at least 3 passages prior to mycoplasma screening in antibiotic-free medium. Hoechst stain was used for visualisation of the mycoplasma. Mouse myeloma cell lines used for somatic cell fusion procedures, and various hybridoma cell lines were





grown in antibiotic-free media for 2 weeks prior to screening for mycoplasma, to ensure any intracellular antibiotic was removed. Cells were then seeded at a low density and allowed to proliferate for 3 days to 70 % confluence, the conditioned medium was then removed and stored for subsequent screening at  $-20^{\circ}\text{C}$ .

NRK (Normal Rat Kidney) cells were prepared to a final cell density of  $2 \times 10^3$  cells/ml in a modified version of DMEM containing 5 % (v/v) FCS and 1 % (v/v) L-glutamine, and 1 ml of cell suspension was then added onto sterile coverslips in petri-dishes. The cells were then incubated at  $37^{\circ}\text{C}$  overnight. The following day, 0.5 ml of conditioned medium was removed from the test samples and added to the NRK cells growing on the coverslips. The petri dishes were then incubated for a further 3-4 days at  $37^{\circ}\text{C}$ .

The medium from each petri-dish was then removed and the coverslips were washed twice with sterile PBS, and once with PBS/Carnoy's fixative (cold). A 2 ml aliquot of Carnoy's fixative (glacial acetic acid: methanol, 1:3, (v/v)) was then added to each coverslip and allowed to fix for 10 minutes. The samples were then allowed to air-dry overnight.

A 2 ml aliquot of the DNA-intercalating dye Hoechst 33258 (working stock 50 ng/ml) was then added to each sample. The samples were then allowed to stain for 10 minutes in low-light. After 10 minutes, the stain was very carefully removed and each coverslip washed with  $3 \times 2$  ml of sterile distilled water. The washed coverslips were then mounted onto slides, and with the aid of a drop of mounting medium observed under the microscope using the 100x objective lens on a fluorescent microscope. Uncontaminated cells show strong fluorescence in the nuclei only, whereas mycoplasma contaminated cells are detected by cytoplasmic staining of the mycoplasmic DNA.

### **2.7.7 *Hybridoma production and isolation***

Hybridoma production was performed according to the original method of Kohler and Milstein, (1975), with amendments.

#### **2.7.7.1 *Somatic cell fusion***

Sp2/O cells were grown for at least two weeks, prior to fusion. Cells were not grown above 50 % confluency, and were subcultured at a split ratio of 1:2 the day before fusion. On the day of the fusion, the medium was poured off the Sp2/O cells, and fresh DMEM lacking FCS was added. Cells were resuspended and counted.



Lymphocytes, from an immunised mouse were harvested (from the spleen or relevant lymph nodes), resuspended in DMEM lacking FCS, and counted. The splenocytes and Sp2/O cells were mixed to give a cell ratio of 5-10 lymphocytes per Sp2/O cell. This cell mixture was pelleted by centrifugation at 1250 rpm and washed 4 times with 5 mls of fresh DMEM lacking FCS.

All of the supernatant, from the final wash, was removed, except for 50-100 µl (simply pouring of the supernatant sufficed). The cells were resuspended by tapping the outside of the centrifuge tube. The cell suspension was placed in an ice-water bath, and 1.5 ml of 50 % (v/v) PEG (polyethylene glycol, molecular weight 1540 Da) that had been previously chilled on ice was added to the cell suspension over a 1 minute period with constant mixing. Mixing was continued for another 1.5 minutes. The centrifuge tube was removed from the ice-water bath, and clasped tightly, while 20 mls of pre-warmed (to 37 °C) DMEM, lacking FCS was then added at a constant rate with the aid of a 1 ml Gilson pipette over a 5 minute interval with continual, slow, swirling of the centrifuge tube. The resulting suspension was placed at 37 °C in a water bath for 15-20 minutes. The suspension was centrifuged, at 1000 rpm for 10 minutes, and the cells resuspended at a cell density of  $1.2 \times 10^6$  cells/ml, in HAT medium supplemented with 5 % (v/v) Briclone. The suspension was plated, in 96 well plates, at 0.1 ml per well, and incubated for 7 days. On day 7, 75 µl of fresh HAT medium supplemented with 5 % (v/v) Briclone was added to each well. Wells were then fed as required. Media was supplemented with HAT until at least day 14 after the fusion.

#### ***2.7.7.2 Screening for specific monoclonal antibody production***

105 µl of 'spent' hybridoma supernatant was removed from the masterplate wells, and replaced with 105 µl fresh DMEM supplemented with 5 % (v/v) Briclone. The 'spent' hybridoma medium was then screened for specific antibody production by conventional ELISA, as described in Section 2.8.1. Positive wells from the initial screening were then transferred to 24-well plates, and subsequently to 6-well plates for cloning.

#### ***2.7.7.3 Cloning of hybridomas secreting Listeria-specific antibodies***

Cells from wells, which tested positive in the ELISA, were expanded in HAT medium, from 96-well plates, to 24-well plates, 6-well plates and finally to T25 flasks. Cells were cloned, by limiting dilution, when they had reached 50 % confluency at the T25 stage. Briefly, cells were resuspended, and diluted to a concentration of 66 cells/ml in HT supplemented with 5 % (v/v) Briclone. From this stock cell-suspension, dilutions of 1/2, 1/10 and 1/20 were prepared



in HT media. These were then seeded at 150  $\mu$ l/well in separate 96-well plates to give well densities of 5, 1 and 0.5 cells/well, approximately. After 7 days, the plates were examined microscopically and wells containing single colonies were noted. On days 10-12 screening for positive wells proceeded, using ELISA (as described in Section 2.8.1), with neat medium from the well, as the test sample. Only cells that demonstrated specific and competitive binding were expanded further.

Positive wells were expanded, as already described, and recloned once at 1 cell/well, and once at 0.5 cell/well. The second time, cells were cloned in DMEM containing 10 % (v/v) FCS, NEAA (1 %, (v/v)), and 1 mM sodium pyruvate, rather than in HT medium. Positive wells at this stage were considered, to be monoclonal.



## **2.8      *Solid phase immunoassays***

### **2.8.1      *ELISA's for estimation of antibody levels in hybridoma supernatants***

From a freshly prepared suspension of *L. monocytogenes* whole cells in PBS ( $1 \times 10^9$  cells/ml), or *Listeria*-derived proteins at an optimized concentration, 100  $\mu$ l aliquots of a solution, were added to all of the wells of a Nunc Maxisorp™ plate and incubated at 37 °C for 1 hour. Wells were washed with 3 x 200  $\mu$ l of PBS, and 200  $\mu$ l of a 5 % (w/v) solution of dry skimmed milk in PBS was added to each well, and incubated for 1 hr at 37 °C. Wells were then washed out with 5 x 200  $\mu$ l of PBS/T. A 100  $\mu$ l sample of neat hybridoma supernatant or purified monoclonal antibody, diluted in PBS/T was added to the wells of the plate. Samples were incubated for 1 hr at 37 °C on a rocking platform. Wells were washed with 4 x 200  $\mu$ l PBS/T and 1 x 200  $\mu$ l PBS before 100  $\mu$ l of secondary antibody (alkaline phosphatase-labeled goat anti-mouse antibody), diluted 1/2000 in PBS/TM, was added to each well and incubated for 1 hr at 37°C. Wells were washed with 4 x 200  $\mu$ l of PBS/T and 1 x 200  $\mu$ l of PBS before adding 100  $\mu$ l of SigmaFast™ para-nitrophenyl phosphate (pNPP) substrate (*Sigma*, N2770) substrate to all wells. The substrate was left to develop, in the dark at 37 °C for 30 minutes. Absorbance readings were read at 405 nm using a Titertek plate reader.

### **2.8.2      *Isotyping of monoclonal antibodies***

ELISA plates were coated and blocked as described in Section 2.8.1. A 100  $\mu$ l sample of culture supernatant from positive hybridomas, following cloning by limiting dilution, was then added to each well of the coated plate. Alkaline phosphatase-labeled goat anti-mouse immunoglobulin subtypes were then added to the wells and the ELISA developed as described in Section 2.8.1. The wells that elicited a positive response to a single subtype (i.e. absorbance at 405nm greater than the normal background +3 SD's) were taken to indicate the monoclonal antibody isotype.

### **2.8.3      *Determination of antibody working dilution***

ELISA plates were coated and blocked as described in Section 2.8.1. Ten serial dilutions of purified monoclonal were then prepared in PBS/T, beginning dilutions at 1/100. A 100  $\mu$ l sample of monoclonal antibody at each dilution was then added to the wells of the plate in triplicate, and the plate incubated at 37 °C for 1 hour.

Wells were then washed with 4 x 200  $\mu$ l of PBS/T and 1 x 200  $\mu$ l of PBS, before 100 $\mu$ l of the appropriate secondary antibody (i.e. alkaline phosphatase-labeled goat anti-mouse IgG2a





antibody), prepared in PBS/TM, was added to each well. The plate was then incubated at 37 °C for 1 hr on a rocking platform. Wells were then washed 4 x 200 µl of PBS/T and 1 x 200 µl of PBS before 100µl of substrate (pNPP) was added per well. The absorbance was measured after a 30 minute incubation at 37 °C, using a Titertek plate reader at 405 nm. The optimal dilution of purified antibody was determined in this manner as the dilution closest to the mid-point of the linear portion of the sigmoidal curve obtained.

#### **2.8.4 Inhibition ELISA**

Nunc Maxisorp™ plates were coated and blocked as previously described. Serial dilutions of the appropriate test cells (or alternative test antigen) were prepared in PBS/T and 100 µl aliquots of each were then placed in individual 500 µl microcentrifuge tubes. A similar volume of purified monoclonal antibody, diluted 1/2000 in PBS/T (determined by checkerboard titration), was then added to each tube. The sample tubes were incubated at 37 °C for 1 hr on a rocking platform. At 10 minute intervals, the tubes were inverted to ensure homogenous mixing. Samples were then transferred to the coated and blocked microwells in 100 µl aliquots and incubated for a further 1 hr at 37 °C on a rocking platform. Wells were then washed as before and 100 µl aliquots of a 1/2000 dilution of alkaline phosphatase-labeled goat anti-mouse IgG2a secondary antibody in PBS/TM was added to the each well and the plate incubated as before. Following washing, pNPP substrate was added to the wells. After a 30 minute incubation at 37 °C, the absorbance values were measured at 405 nm using a Titertek plate reader. Absorbance values at each antigen concentration (A) were then divided by the absorbance measured in the presence of zero antigen ( $A_0$ ) to give normalised absorbance readings. A plot of the normalised absorbance reading versus cell concentration (cell/ml) was used to construct the calibration curve.



## 2.9 Molecular biology

### 2.9.1 Standard Solutions

#### *Tris-acetic acid-EDTA buffer (TAE)*

A 50x stock solution of TAE buffer was prepared by dissolving 242 g Tris-HCl in 700 ml upH<sub>2</sub>O. When the salt had dissolved, 57.1 ml of glacial acetic acid and 100 ml of 0.5 M EDTA. pH 8.0 were added and the final volume brought to 1000 ml with upH<sub>2</sub>O. Agarose gel electrophoresis was conducted in 1X TAE buffer, prepared in upH<sub>2</sub>O.

#### *TES-1 buffer*

Tris-HCl (pH 8.0)	10 mM
EDTA (disodium salt)	1 mM

#### *TES-1 buffer*

Tris-HCl (pH 8.0)	10 mM
EDTA (disodium salt)	1 mM
NaCl	50 mM

#### *TES-2 buffer*

Tris-HCl (pH 7.4)	10 mM
EDTA (disodium salt)	3.5 mM
NaCl	400 mM

#### *Kirby mix*

Phenol	100 ml
Chloroform	100 ml
Isoamylalcohol	4.0 ml
8-hydroxy quinolone	0.8 g

#### *GES reagent*

Guanidium thiocyanate	5.0 M
EDTA (disodium salt)	100 mM
Sarkosyl reagent	0.5 % (v/v)



<i><b>TB buffer</b></i>	<i><b>g/L</b></i>
Pipes (10mM)	3.02
MnCl <sub>2</sub> (55 mM)	10.89
CaCl <sub>2</sub> (15 mM)	2.21
KCl (250 mM)	18.64

All components except the MnCl<sub>2</sub> were mixed until dissolved in upH<sub>2</sub>O and the pH then adjusted to 6.7 with KOH solution. The MnCl<sub>2</sub> was then added and the solution sterile filtered through a 0.2 µm filter and stored at 4 °C.

***SOB media***

Tryptone	20.0 g
Yeast extract	5.0 g
NaCl	0.5 g
KCl	2.5 mM
MgCl <sub>2</sub>	20.0 mM

All solutes were dissolved fully in 965 ml sterile upH<sub>2</sub>O. This was followed by the addition of 10 ml of KCl solution (250 mM) and the pH adjusted to 7.0 with 5 M NaOH. The media was the sterilized by autoclaving. Just before use, 5 ml of sterile 2 M MgCl<sub>2</sub> solution and 20 ml of 1 M MgSO<sub>4</sub> solution that had been sterilized separately (sterile-filtered) were added to the base media.

***Super optimal catabolites (SOC) media***

Tryptone	20.0 g
Yeast extract	5.0 g
NaCl	0.5 g
KCl	2.5 mM
MgCl <sub>2</sub>	20.0 mM
Glucose	20.0 mM

All solutes were dissolved fully in 950 ml sterile upH<sub>2</sub>O. This was followed by the addition of 10 mls of KCl solution (250 mM) and the pH adjusted to 7.0 with 5 M NaOH. The media was then sterilized by autoclaving. Just before use, 5 ml of sterile 2 M MgCl<sub>2</sub> solution and 20 ml of 1 M MgSO<sub>4</sub> solution that had been sterilized separately (sterile-filtered) were added to the base media. Finally, 20 ml of 1 M glucose (sterile-filtered) was added.



<b><i>Lauria–Bertani broth (LBB)</i></b>	<b><i>g/L</i></b>
Tryptone	10.0
Yeast extract	5.0
NaCl	5.0

The pH was adjusted to 7.0 prior to autoclaving with 2 M NaOH.

<b><i>Lauria –Bertani agar (LBA)</i></b>	<b><i>g/L</i></b>
Tryptone	10.0
Yeast extract	5.0
NaCl	5.0
Agar	15.0

The pH was adjusted to 7.0 prior to autoclaving with 2 M NaOH.

<b><i>2xty broth</i></b>	<b><i>g/L</i></b>
Tryptone	16.0
Yeast extract	10.0
NaCl	5.0

<b><i>2xty agar</i></b>	<b><i>g/L</i></b>
Tryptone	16.0
Yeast extract	10.0
NaCl	5.0
Agar	15.0

***IPTG (Isopropylthiogalactoside)*** 40 mM

This was prepared by dissolving 238 mgs of IPTG in 10 ml upH<sub>2</sub>O. This stock solution was sterile-filtered (0.2 µm cut-off) and stored in 1 ml aliquots at –20 °C.

***X-gal*** mg/L  
40.0

The stock solution was prepared in dimethylformamide (DMF) and stored at –20 °C in a light-proof glass bottle. To incorporate into previously prepared agar plates, 40 µl of the stock X-gal solution was spread evenly over the agar surface and left to dry for approximately 15 minutes at room temperature while protected from light. Agar plates were treated with X-gal according to demand. They were used immediately and never stored for extended time periods.





***dNTP mix***

dATP	10 mM
dCTP	10 mM
dGTP	10 mM
dTTP	10 mM

***Pfu 10x reaction buffer***

Tris-HCl (pH 8.8)	200 mM
KCl	100 mM
(NH <sub>4</sub> ) <sub>2</sub> SO <sub>4</sub>	100 mM
MgSO <sub>4</sub>	20 mM
Nuclease-free BSA	1 mg/ml
Triton <sup>®</sup> X-100	1 % (v/v)

**2.9.2 Isolation of *L. monocytogenes* genomic DNA**

A 15 ml cell suspension from a 50 ml overnight culture of *L.monocytogenes* serotype 1/2a in BHI broth was aseptically transferred into a sterile universal. The cell suspension was centrifuged at 4000 rpm for 10 minutes at 4 °C. The supernatant was discarded and the remaining pellet was washed twice with 1.5 ml volumes of TES buffer and once with 1.5 mls of TE buffer to remove extraneous contaminating salts. The pellet was then resuspended in 500 µl of lysozyme (50 mg/ml prepared fresh in TE buffer) in a 1.9 ml eppendorf tube and incubated at 30 °C for 1 hr in a water-bath. At 10 minute intervals, during the incubation period, the tube was inverted by hand to ensure even mixing. After the 1 hr incubation, 500 µl of GES reagent was added to the suspension and the contents were then vortexed for 10 minutes. 500 µl ice-cold of 7.5 M sodium acetate was added to give a final concentration of 2.5 M and the suspension was placed on ice for 10 minutes. The contents of the eppendorf were then split into two 750 µl aliquots for ease of manageability, and dispensed into fresh eppendorf tubes. The remainder of the extraction protocol was carried out in duplicate, using both 750 µl crude extracts. 500 µl of Kirby reagent was mixed with the 750 µls of extract. After centrifugation at 13000 rpm for 4 minutes at room temperature, the aqueous phase was removed using a pipette and retained. The solvent phase and cellular debris were discarded. A further 500 µl of Kirby reagent was added to the retained fraction and, after centrifugation at 13000 rpm for 4 minutes, the aqueous phase was again retained. Approximately 500-700 µl of a chloroform:isopropyl alcohol (24:1) mixture was added to the retained fraction and the resulting solution was centrifuged at 13000 rpm for 4 minutes at room temperature to partition the aqueous and solvent phases. Once again, the aqueous phase was retained and the DNA



content was precipitated by the dropwise addition of an equal volume of isopropyl alcohol. The DNA strands were harvested by briefly centrifuging the sample at 13000 rpm. The small resultant pellet was washed with twice with 200 µl volumes of 70 % (v/v) ethanol and left to air dry for 5-10 minutes at room temperature or dried rapidly using a commercial evaporator. The final pellet was resuspended in 150-200 µl TE buffer and stored at 4 °C. The presence of genomic DNA was verified by subjecting the sample to agarose gel electrophoresis.

### 2.9.3 Sequence-specific primer design

Primers were designed (Table 2.8) for compatible ligation into the QIAexpress® type ATG construct pQE60 (QIAGEN). The *inlA* gene specific primers were designed in accordance with the sequence determined for *L. monocytogenes* strain EGD, seovar 1/2a (accession number AJ012346). The sequence coding for the signal peptides were omitted. The multi-cloning region of the pQE60 vector contains an *NcoI* site at the N' end of the sequence and a *BamHI* site at the C' end. Therefore, forward primers were designed to include the *NcoI* binding site sequence and the reverse primers were designed to contain the *BamHI* sequence. Forward primers were designed using the same bases found in the starter sequence of the required protein and reverse primers were designed using the complementary bases from the 3' to 5' end of the sequences. The approximate T<sub>m</sub> values (i.e. the temperature at which 50% of the oligonucleotide and its complement are in duplex) were estimated using the 'Wallace method' according to  $T_m = 2 \times (A + T) + 4 \times (G + C)$ . A more precise estimation of T<sub>m</sub> values was provided by the data accompanying the synthesized primers from the manufacturer (MWG Biotech), based on the formula  $T_m = 69.3 + (0.41 \times GC\%)-(650 / \text{length})$ .

**Table 2.8:** Primers used for the specific amplification of the *inlA* gene sequence.

Primer Name	Sequence
InlAR II	5' <u>GGATCC</u> -TTT-ACT-AGC-ACG-TGC-TTT-TTT-AGT-AAG-AGC 3'
TAF II-A	5' <u>CCATGG</u> -GA-AAG-ACG-GTC-TTA-GGA-AAA-AC 3' ↑ <i>NcoI</i> ↑
TAF II-B	5' <u>CATG-CCATGG</u> -GA-AAG-ACG-GTC-TTA-GGA-AAA-AC 3' ↑ <i>NcoI</i> ↑
TAB I	5' <u>CGC-GGATCC</u> -TGA-TTC-TTT-TGA-ATT-ATA-AGG 3' ↑ <i>BamHI</i> ↑

### 2.9.4 Agarose gel electrophoresis

DNA samples were analysed by horizontal electrophoresis in agarose gels containing 0.5 µg/ml ethidium bromide. A 1 % (w/v) gel was prepared by adding 0.5 g electrophoresis grade agarose to 50 ml TAE buffer and boiling the mixture in a microwave oven. Ethidium bromide



was added to the solubilised agarose to yield a final concentration of 0.5 µg/ml. When the solution had cooled sufficiently it was poured onto the horizontal gel platform, the well comb was inserted and the gel left to set at room temperature. Once set, the gel was placed in the electrophoresis unit filled with TAE buffer and the comb removed. A tracker dye was added to samples (1 µl dye + 5 µl sample) to increase visibility during loading of the samples. The samples were resolved by applying a direct current of appropriate voltage and the results were visualized on a UV transilluminator and photographed using a UV image analyzer. A 0.7 % (w/v) gel was used when samples run in agarose were required to be excised and purified.

### 2.9.5 *Preparation of high efficiency competent bacterial cells*

High efficiency competent cells were prepared as previously described by Inoue *et al.* (1990). Cells from a frozen stock of *E. coli* XL10<sup>®</sup> Gold were streaked on an LB agar plate containing tetracycline (10 µg/ml) and incubated at 37 °C overnight. Approximately 10-12 large colonies were removed from the plate and inoculated into 250 ml of SOB medium in a 2 L baffled flask. The culture was grown at 18 °C with vigorous shaking (200-250 rpm) until an OD<sub>600nm</sub> of 0.6 was reached. The flask was then removed and placed on ice for 10 minutes before being transferred to two 250 ml centrifuge tubes and centrifuged at 4000 rpm for 5 minutes at 4°C in a Beckman J2-21 centrifuge. The two resulting pellets were pooled and resuspended in 80 ml of ice-cold TB buffer, incubated on an ice-bath for 15 minutes and then centrifuged as before. The cell pellet was gently resuspended in 20 ml of ice-cold TB buffer and DMSO was then added slowly and with continual gentle swirling to a final concentration of 7 % (v/v). After incubation in an ice bath for a further 10 minutes the cell suspension was dispensed in 1 ml aliquots into sterile cryovials. The competent cells were then flash frozen in liquid nitrogen and stored at -80 °C.

### 2.9.6 *Polymerase chain reaction (PCR)*

Polymerase chain reaction (PCR) was used to amplify specific DNA sequences derived from *L. monocytogenes* gDNA. A standard PCR reaction was set up as follows:

	<u>1x</u>
(A) 10mM dTNP mix (200 µM end concentration)	1.0 µl
10x PCR buffer	5.0 µl
Primers (0.5 nM/µl) (total of 1 µl)	0.5 µl (each)
Template DNA	1.0 µl
Sterile molecular grade upH <sub>2</sub> O	39.5 µl
<i>Taq</i> polymerase (2.5 units final concentration)	2.5 µl
Reaction volume	50 µl



	<u>1x</u>
(B) 10mM dTNP mix (200 $\mu$ M end concentration)	1.0 $\mu$ l
10x <i>Pfu</i> buffer (containing 20 mM MgSO <sub>4</sub> )	5.0 $\mu$ l
Primers (0.5 nM/ $\mu$ l) (total of 1 $\mu$ l)	0.5 $\mu$ l (each)
Template DNA	1.5 $\mu$ l
Sterile molecular grade H <sub>2</sub> O	41.0 $\mu$ l
Hot start	
<i>Pfu</i> DNA polymerase (1.5 units final concentration)	0.5 $\mu$ l
<i>Reaction volume</i>	50 $\mu$ l

The optimum annealing temperature for primer sets was estimated by conducting a 'gradient PCR' reaction over a range of temperatures differing by between 1 and 2 °C. The temperature which gave the 'cleanest' and most specific band was chosen as the annealing temperature for a given primer set. Only 1.5 units *Pfu* DNA polymerase per 50  $\mu$ l reaction mix was used, yet this was deemed sufficient due to the high stringency, faithful binding exhibited by *Pfu* polymerase and its greater heat resistance. It was held on ice until after the addition of dNTPs so as to avoid degradation of the primers via the intrinsic 3'  $\rightarrow$  5' exonuclease activity. *Pfu* DNA Polymerase exhibits a lower extension rate (0.5 kb/minute) than that of *Taq* DNA Polymerase, so a 5 minute extension time was employed for the 2.1 kb *inlA* gene sequence being amplified. *Pfu*-catalysed amplification was used where high fidelity PCR product was essential, as in the case of primary gene sequence amplification from gDNA. For routine PCR reactions used to check for the presence of inserts in plasmid constructs, *Taq* polymerase was adequate.

#### **2.9.7 PCR product ligation into pCR 2.1 plasmid (blunt-ended)**

The ligation reaction was set up as follows:

upH <sub>2</sub> O (molecular grade)	4 $\mu$ l
10X ligation buffer	1 $\mu$ l
pCR 2.1 vector (~25 ng/ $\mu$ l)	2 $\mu$ l
*Fresh PCR product	2 $\mu$ l
T4 DNA Ligase	1 $\mu$ l
<i>Total volume</i>	10 $\mu$ l





The ligation reaction was incubated at 14 °C overnight and then used immediately for transformation. It was acceptable to store the ligated construct at -20 °C for an extended period of several months.

*\*Only fresh PCR product was used so as to reduce the risk of the single stranded 3' poly-A overhangs degrading.*

### **2.9.8 Transformation of pCR2.1-inlA plasmid into bacterial cells**

The vial containing the fresh ligation reaction was centrifuged briefly and placed on ice. An aliquot of competent cells (*E. coli* XL10-Gold®) was removed from storage at -80°C and allowed to thaw at room temperature. A 200 µl aliquot of the cell suspension was transferred to a sterile, pre-chilled 15 ml polypropylene tube and placed immediately on ice. A 2 µl volume of the fresh ligation reaction was then pipetted directly into the tube and the tube swirled briefly and gently before being incubated on ice for 30 minutes. The remaining ligation mixture was stored at -20 °C. Each Vial was heat shocked for exactly 30 seconds in a 42 °C water bath (without agitation) and transferred back to ice. 250 µl of SOC medium (LB broth was also acceptable) at room temperature was added to the tube. The tube was then shaken horizontally at 37 °C for 1 hr at 225 rpm in an orbital incubator. After 1 hour, 50-100 µl from each transformation tube was spread on separate, labelled LB agar plates coated with X-Gal and containing 10 µg/ml tetracycline, 50 µg/ml of kanamycin and 100 µg/ml ampicillin. The plates were then inverted and incubated at 37 °C for 18-24 hours before being placed at 4 °C for 2-3 hours to allow for full colour development.

#### **2.9.8.1 Restriction Analysis of 'white colonies' (pCR2.1-inlA transformants) from X-gal agar plates**

A restriction digest was carried out at 37 °C for 1 hour, on plasmids derived from individual, isolated white colonies as follows:

REact® 3 buffer (10x)	1.0 µl
Plasmid DNA	3.0 µl
upH <sub>2</sub> O (molecular grade)	5.0 µl
<i>Eco</i> RI	1.0 µl
<i>Total volume</i>	10.0 µl



Each digest was run in a 1.0 % (w/v) agarose gel and examined for the presence of a band corresponding to the desired *inlA* insert.

#### 2.9.8.2 Restriction digestion of pCR2.1-*inlA* constructs

Plasmids confirmed to contain the *inlA* insert were digested as follows:

REact® 3 buffer (10x)	3.0 µl
Plasmid DNA	20.0 µl
upH <sub>2</sub> O (molecular grade)	3.0 µl
BamH I	3.0 µl
<i>Nco</i> I	3.0 µl
<i>Total volume</i>	50.0 µl

Each digest was run on a 0.7 % (w/v) agarose gel and the restricted *inlA* insert cut from the gel using a clean sharp scalpel and placed in sterile 1.5 ml centrifuge tubes for further purification, if necessary.

#### 2.9.9 Restriction digestion of *inlA* PCR product (directional)

Fresh *Pfu*-amplified *inlA* PCR product was purified from 50 µl of fresh PCR reaction mixture. This was achieved by isolation and purification of the PCR product from a 0.7 % (w/v) agarose gel (Section 2.9.12), or ethanol precipitation (Section 2.9.13). The principle objective was to separate the PCR product from PCR reaction components that might adversely affect restriction enzyme activity and, thus, ethanol precipitation was favoured because it was quicker and less harsh, thereby reducing the potential for degradation of the PCR amplicon and concomitantly yielding a greater product recovery.

Purified <i>inlA</i> amplicon	20.0 µl
REact® 3 buffer	3.0 µl
<i>Nco</i> I	3.0 µl
<i>Bam</i> HI	3.0 µl
H <sub>2</sub> O (molecular grade)	1.0 µl
<i>Total volume</i>	50.0 µl

The restricted *inlA* amplicon was recovered by ethanol precipitation (Section 2.9.12).



### 2.9.10 PCR product ligation into pQE60 plasmid (directional)

The ligation reaction was set up as follows:

upH <sub>2</sub> O (molecular grade)	1.5 µl
10X ligation buffer	1.0 µl
pQE60 vector ( <i>Bam</i> HI/ <i>Nco</i> I digested)	1.5 µl
<i>inlA</i> insert ( <i>Bam</i> HI/ <i>Nco</i> I digested)	5.0 µl
T4 DNA Ligase	1.0 µl
Total volume	10.0 µl

The ligation reaction was incubated at 15.5 °C overnight and then used immediately for transformation. It was acceptable to store the ligated construct at -20 °C for an extended period of several months.

### 2.9.11 Transformation of pQE60-*inlA* plasmid into bacterial cells

An aliquot of competent cells (*E. coli* XL10-Gold<sup>®</sup>)\*<sup>a</sup> was removed from storage at -80°C and allowed to thaw at room temperature. 200 µl of the cell suspension was transferred to a sterile, pre-chilled 15 ml polypropylene tube and placed immediately on ice. 2 µl of the fresh, *Bam*HI/*Nco*I-digested *inlA* insert was added to the 200 µl competent cell suspension. The remainder of the procedure was as previously described (Section 2.9.7). However, LB agar selection plates were not treated with X-gal and 25 µg/ml chloramphenicol was used in place of 50 µg/ml of kanamycin, in addition to 10 µg/ml tetracycline and 100 µg/ml ampicillin.

\*<sup>a</sup> XL10-Gold genotype: TET<sup>R</sup>  $\Delta$ (*mcrA*) 183  $\Delta$ (*mcrCdSMR-mrr*) 173 *endA1 supE44 thi-1 recA1 gyrA96 relA1 lac* Hte [F' *proAB lacI<sup>f</sup>*Z $\Delta$ M15 Tn10 (TetR) Amy Cam<sup>R\*</sup>].

*Chloramphenicol resistant (Cam<sup>R</sup>) at  $\leq 40$  µg/ml, Chloramphenicol sensitive (Cam<sup>S</sup>) at  $\geq 100$  µg/ml. The genes indicated in italics signify mutant alleles carried by the bacterium. The genes *The F'* episome genes indicate the wild-type alleles.*

### 2.9.12 PCR product purification (Gel clean-up)

DNA was purified from the agarose gel using an Eppendorf Perfectprep<sup>®</sup> Gel Cleanup PCR kits outlined below:

The DNA band of interest was located in a 0.7 % (w/v) agarose gel and excised using a clean, sterile scalpel blade. The agarose slice was transferred to a sterile 1.5 ml eppendorf tube and weighed. Up to 400 mg agarose could be processed in a single 1.5 ml eppendorf tube. Three



volumes of binding buffer (containing guanidium thiocyanate) were added for every one hundred volumes of gel (1 mg gel was taken as equivalent to 1  $\mu$ l of volume). The tube was incubated at 50 °C until the agarose melted (5-10 minutes). When the gel had completely dissolved, one volume of isopropanol (equal to the original gel volume) was added and mixed by inverting several times. The suspension was then placed in a spin column housed in a 2 ml collection tube. Up to 800  $\mu$ l of sample could be added to the spin column. The spin column/collection tube assembly was centrifuged at 7500 rpm for 1 minute and the resultant flow-through discarded. Next, 750  $\mu$ L wash buffer (1 part concentrated wash buffer : 4 parts 100 % ethanol) was added to the spin column and the assembly centrifuged at 7500 rpm for 1 minute. The flow-through was again discarded and the empty spin column rehoused in the same collection tube before being centrifuged at 7500 rpm for a further 1 minute to remove residual wash buffer. The spin column was placed in a fresh, sterile 1.5 ml eppendorf tube and 30  $\mu$ l of molecular grade water or TE buffer was added carefully. The column was centrifuged at 10,000 rpm for 1 minute and the purified DNA was eluted into a final volume of 30  $\mu$ l. Purified DNA was stored in the tube at 4 °C for up to 24 hr or at -20 °C for long-term storage (several months).

#### **2.9.13 PCR product purification (ethanol precipitation)**

DNA was purified directly from the PCR reaction mixture by precipitation as follows. Typically, 40  $\mu$ l of PCR reaction mixture was diluted to a final volume of 400  $\mu$ l with molecular grade upw. An equal volume of Kirby mix (400  $\mu$ l) was added and the solution mixed by inverting. The contents were then centrifuged for 5 minutes at 13,000 rpm and 4 °C. The aqueous (upper) layer was removed to a fresh, sterile 1.5 ml eppendorf tube carefully avoiding disruption of and carry-over from the interlayer and organic phase. An equal volume of molecular grade chloroform was added to the aqueous retentate. The contents were mixed and centrifuged as before. The aqueous layer was again removed to a fresh eppendorf tube and 1/10 the volume of 3 M sodium acetate (to a final concentration of 0.3 M) was added. Next, 2.5 volumes of 100 % (v/v) ethanol were added, the contents mixed by inverting and incubated at -20 °C for at least 1 hr. The precipitated DNA was harvested by centrifuging for 20 minutes at 13000rpm and 4 °C. The supernatant was decanted and 200  $\mu$ l cold 70 % (v/v) ethanol added to the remaining pellet (without mixing) to wash out any residual salts. The contents were then centrifuged at 13000 rpm for 10 minutes at 4 °C and the supernatant was again carefully decanted and any residual liquid removed by brief and gentle vacuum evaporation. The pellet was then resuspended in TE buffer or molecular grade upw and stored on ice for immediate use or at -20 °C for long-term storage.





#### **2.9.14 Plasmid purification**

A Promega Wizard® Plus SV Minipreps DNA Purification System was used to purify plasmid DNA as follows:

A 5-10 ml overnight bacterial culture was centrifuged for 5 minutes at 4000 rpm, the supernatant decanted and tubes blotted dry on a paper towel. A 250 µl aliquot of cell resuspension solution (50 mM Tris-HCl, pH 7.5, 10 mM EDTA and 10 µg/ml RNase A) was added and the cell pellet completely resuspended by repeat pipetting. The mixture was transferred to sterile 1.5 ml microcentrifuge tube(s), 250 µl of cell lysis solution (0.2 M NaOH and 1% (w/v) SDS) added and mixed by inverting the tube 4 times. 10 µl of alkaline protease solution was then added and the suspension mixed by inverting the tube 4 times. This helped to inactivate endonucleases and other undesirable proteins released during the lysis of the bacterial cells that could adversely affect the quality of the isolated DNA). After 5 minutes incubation at room temperature 350 µl of Wizard® Plus SV neutralisation solution (pH 4.2 buffer containing 4.09 M guanidine hydrochloride, 0.759 M potassium acetate and 2.12 M glacial acetic acid) was added and immediately mixed by inverting the tube 4 times. The bacterial lysate was then centrifuged at 14000 rpm for 10 minutes at room temperature. The cleared lysate was transferred (~ 850 µl) to the prepared spin column using a sterile pipette. The cleared fraction was centrifuged at 14000 rpm for 1 minute at room temperature after which the spin column was removed from the collection tube and the flow through discarded. 750 µl of column wash solution (162.8 mM potassium acetate, 22.6 mM Tris-HCl, pH 7.5 and 0.109 mM EDTA), previously diluted with ethanol to 95% (v/v) final concentration, was then added to the reinserted spin column. Wash solution was flushed through the spin column by centrifuging at 14000 rpm for 1 minute at room temperature. The flow-through was again discarded from the collection tube and the wash procedure repeated using 250 µl of column wash solution. In order to remove any residual wash solution the decanted spin column was centrifuged at 14000 rpm for a further 2 minutes at room temperature. Subsequently the spin column was transferred to a fresh, sterile 1.5 ml eppendorf, taking care not to transfer any residual column wash solution with the spin column. The plasmid DNA was finally eluted by addition of 65-100 µl of sterile ultra pure water to the spin column and centrifuging the supernatant at 14000 rpm for 1 minute at room temperature. After eluting the plasmid DNA, the spin column was discarded and DNA stored in the tube at 4 °C for up to 24 h or -20 °C for long-term storage (several months).



#### ***2.9.15 Protein expression and time course analysis***

Approximately 5 mls of LB broth containing 100 µg/ml ampicillin, 10 µg/ml tetracycline 25 µg/ml chloramphenicol and 1 % (v/v) glucose was inoculated with 100 µl of stock transformant and grown overnight at 37 °C. A 5 ml volume of this culture was then used to inoculate 50 mls LB broth containing 100 µg/ml ampicillin, 10 µg/ml tetracycline and 25 µg/ml chloramphenicol and 1 % (v/v) glucose was incubated at 37 °C until an OD<sub>600 nm</sub> of 0.6 was reached. At this point a 1 ml sample was taken and placed at -20 °C until needed. The culture was induced with IPTG to a final concentration of 1 mM and a 1 ml sample taken every hour. Each 1 ml sample was centrifuged at 14000 rpm for 5 minutes, at 4 °C, and the supernatant discarded. The pellet was resuspended in 200 µl of appropriate buffer, PBS for native extract and lysis buffer (8 M urea, 10 mM Tris-HCl, 100 mM NaH<sub>2</sub>PO<sub>4</sub>, pH 8.0) for denatured extract. The samples were then sonicated for 45 seconds at an amplitude of 40, using a microtip Vibra Cell™ sonicator, and the cell debris removed by centrifugation at 14,000 rpm for 5 minutes. The supernatant was mixed with SDS-PAGE sample buffer and SDS-PAGE analysis carried out as described in Section 2.3.2.

#### ***2.9.16 Purification of recombinant His-tagged protein by immobilised metal affinity chromatography (IMAC)***

A 1 ml aliquot of Ni<sup>2+</sup>-NTA agarose resin (QIAGEN) was added to a 20 ml universal tube and equilibrated with 20 ml of running buffer (PBS/T with 1% (v/v) Tween-20, 500 mM NaCl and 10 mM β-mercaptoethanol). The solution was centrifuged at 4000 rpm for 10 minutes and the supernatant (running buffer) removed. 2-3 ml of sonicated cytoplasmic extracts containing His-tagged recombinant protein were added to the pellet (Ni<sup>2+</sup>-NTA resin) and mixed for 1-2 hours at room temperature on a rocking platform. The mixture was then centrifuged at 4000 rpm for 10 minutes and the supernatant (unbound material) removed. The pellet (resin with bound protein) was washed 3 times with 20 ml of running buffer as before. The proteins were eluted with 2-3 ml of sodium acetate buffer, pH 4.5, and neutralised with 2 M Tris buffer, pH 8.8. Purified proteins were stored at -20 °C. This represents a generic protocol for IMAC purification. Optimisation for purification of the protein of specific interest is discussed in detail in chapter 4 (Section 4.4.6).

#### ***2.9.17 Identification of recombinant protein by Western blotting***

Purified proteins were analysed by SDS-PAGE and Western blotting, as described in Sections 2.3.2 and 2.3.4. Purified recombinant protein bands were detected with a commercial mouse anti-His tag monoclonal antibody or with a specifically generated anti-InlA murine monoclonal antibody.



## **2.10    *Biacore studies***

Analyses were carried out on a Biacore 3000™ instrument using the CM5 sensor chip. The running buffer for all Biacore experiments was HBS buffer, pH 7.4, containing 10 mM HEPES, 150 mM NaCl, 3.4 mM EDTA, and 0.05% (v/v) Tween 20. Running buffer was freshly prepared, filtered (pore size of 0.22 µm) and degassed using a vacuum filtration apparatus (Millipore sintered glass filtration unit) before use. All data points were collected at a frequency of 1 Hz.

### **2.10.1    *Pre-concentration studies*\*<sup>a</sup>**

Proteins were diluted in sterile-filtered 10 mM sodium acetate buffers that had been adjusted with 10% (v/v) acetic acid to pH values 4.0, 4.2, 4.4, 4.6, 4.8 and 5.0. 10 µl of protein at each respective pH was sequentially passed over an un-activated carboxymethylated dextran sensor chip surface at a flow rate of 10 µl/min. The pH that afforded the greatest degree of pre-concentration, reflected by the highest response unit (RU) value, was chosen as the carrier buffer for immobilisation. TES buffer was used when optimising pre-concentration of nucleic acid probes.

### **2.10.2    *Immobilisation of monoclonal antibody*\*<sup>a</sup>**

The carboxymethylated dextran matrix on the sensor chip was activated by mixing equal volumes of 100 mM NHS (N-hydroxysuccinimide) and 400 mM EDC (N-ethyl-N-(dimethylaminopropyl) carbodiimide hydrochloride), and injecting the mixture over the sensor chip surface for 10 minutes at a flowrate of 5 µl/minute. The purified monoclonal antibody was diluted in 10 mM sodium acetate, pH 4.0, at a concentration of 100 µg/ml. This solution was then injected over the activated chip surface for 24 minutes at 5 µl/minute. Unreacted NHS groups were capped and loose, non-covalently attached proteins were removed by injection of 1 M ethanolamine hydrochloride, pH 8.5, for 11 min. Loosely bound material was further removed using a 30 second pulse of 5 mM NaOH and 5 mM HCl, respectively.

*\*<sup>a</sup>: These methods represent generic template protocols, and where specific modifications or amendments have been made, they are clearly cited and justified within the relevant results and discussion sections in chapter 4.*



### **2.10.3 Preparation of IgG2a control surface**

A standard, purified murine IgG2a antibody (Sigma, M9144) was immobilised on the flowcell immediately downstream of the test flowcell at a similar level to the immobilised test surface (anti-InlA or anti-His-tag).

### **2.10.4 *L. monocytogenes*-specific, direct-cell-binding assay**

All bacterial cells tested were prepared from cultures that had been grown in LEB broth at 37 °C and 200 rpm. Cells were harvested, washed twice in PBS buffer and adjusted to the desired cell concentration in PBS (estimated from a standard curve of OD<sub>550nm</sub> versus cell concentration). Cells were passed over the sensor surface at 1 µl/min and surface regeneration was mediated by a 45 second pulse of 5 mM NaOH.

### **2.10.5 Binding analysis using the NTA chip**

The NTA chip surface was activated by passing 20 µl of a 500 µM solution of NiCl<sub>2</sub> across the surface at a flow rate of 20 µl/min. The His-tagged ligand (recombinant InlA protein) was then passed across the activated surface at 20 µl/min, until the desired immobilisation level was achieved. The complementary analyte (anti-InlA monoclonal antibody) was the injected and the binding interaction monitored and noted. The surface was regenerated by injecting 20 µl of a 400 µM solution of EDTA.

### **2.10.6 Measurement of steady-state affinity**

Approximately 10500 RUs of anti-His antibody was immobilised onto a CM5 chip surface. To ensure an optimally active anti-His surface it was important that the antibody was pure and free from BSA or other stabilising proteins as amine coupling is non-specific and could lead to more favourable attachment of the undesired protein component. IMAC-purified recombinant InlA (rInlA) protein in HBS buffer was passed over the anti-His surface at 5 µl/min for 2 minutes generating an approximate response of 470 RUs. The His-tag capture approach ensured that the rInlA protein was in an accessible orientation for mAb2B3 binding. 200 µl of serial doubling dilutions of mAb2B3, ranging from  $3.3 \times 10^{-6}$  to  $1.29 \times 10^{-8}$  M, were individually passed over the rInlA surface. To conserve antibody, samples of mAb2B3 were passed over the rInlA surface at a reduced flow rate of 2 µl/min. After the 40 min exposure equilibrium was approached and the equilibrium response (Req) was noted. Regeneration was achieved by stripping the rInlA from the anti-His surface with two 30 second pulses of freshly prepared 5 mM NaOH. All sensorgrams were reference subtracted from a murine IgG-immobilised reference surface. To remove systematic anomalies a blank run consisting of HBS that contained no mAb2B3 was subtracted from each of the test sensorgrams. Results were plotted





as Req versus mAb2B3 concentration and the data analysed using the BIAevaluation™ steady state affinity model for bivalent analytes.



## 2.11 HPLC analyses

All buffers used throughout high performance liquid chromatography analyses were degassed and sterile filtered with a 0.2  $\mu\text{m}$  cut-off membrane filter prior to being used. The column employed for size exclusion chromatography (SEC) was a Phenomenex 3000 SEC, packed column.

**Table 2.9:** *Molecular weight standards used in size exclusion chromatography.*

Standard	Mr (kDa)	Source	Catalogue code
Blue dextran	2000.0	Sigma	D-4772
$\beta$ -amylase ( $\beta$ -A)	200.0	Sigma	A-8781
Alcohol dehydrogenase (AD)	150.0	Sigma	A-8656
Bovine serum albumin (BSA)	66.0	Sigma	A-8531
Carbonic anhydrase (CA)	29.0	Sigma	C-7025
Cytochrome C (CC)	12.4	Sigma	C-7150
IgG2a	150.0	Sigma	M9144

### 2.11.1 Analysis of affinity-purified antibody fractions

The column equilibration and mobile phase buffer used was PBS. 50  $\mu\text{l}$  of affinity-purified monoclonal antibody in PBS buffer was injected onto the SEC column at a flow rate of 0.5  $\mu\text{l}/\text{min}$  and the protein content of the eluted fractions monitored spectrophotometrically at 280 nm. The resulting chromatogram ( $A_{280\text{nm}}$  versus retention time) was compared to that for a 50  $\mu\text{l}$  sample of commercial IgG2a standard, prepared in PBS buffer.

### 2.11.2 Standard curve for estimation of molecular weight (Mr)

The column equilibration and mobile phase buffer used was PBS. The void volume ( $v_0$ ) of the SEC column was estimated by calculating the column retention time for a 50  $\mu\text{l}$  sample of blue dextran at a concentration of 1 mg/ml and a flow rate of 1  $\mu\text{l}/\text{min}$ , again using UV detection at 280 nm. A standard curve was constructed using the standards ( $\beta$ -A), (AD), (BSA), (CA) and (CC). The retention times of each standard ( $v_e$ ), when applied individually to the column, were normalised with respect to the void volume ( $v_e/v_0$ ) and plotted against the  $\log_{10}$  value of the corresponding molecular weight, to generate a linear calibration curve.



### ***2.11.3 Analysis of IMAC-purified recombinant protein***

A 50  $\mu$ l sample of IMAC-purified recombinant His-tagged protein in PBS buffer was injected onto the SEC column at a flow rate of 1  $\mu$ l/min. The normalised retention time was used to estimate the  $M_r$  of the major components of the IMAC-purified sample from the standard curve as described in Section 2.11.2.



## **2.12 SEM and AFM image analysis**

### **2.12.1 Sample preparation**

#### **2.12.1.1 Fixing**

Bacterial cells that bound to specific antibody immobilized on the dextran matrix of a CM5 chip were fixed *in situ* according to the following. Briefly, the CM5 chip was undocked from the Biacore instrument having been exposed to a completed cycle of bacterial sample analysis. The chip was then immediately placed in a glass petri dish (sample surface facing upwards) containing 25 mls 2.5 % (v/v) glutaraldehyde in cacodylate buffer and left overnight at 4 °C.

#### **2.12.1.2 Post-fixing**

The chip was removed from the glutaraldehyde solution and washed (x2) in 40 mls fresh cacodylate buffer. The chip was then incubated in freshly prepared 1 % (w/v) osmium tetroxide in cacodylate buffer for 90 minutes at room temperature.

#### **2.12.1.3 Drying**

The chip was washed briefly in fresh cacodylate buffer before being exposed to a graded series of ethanol in ultra-pure water (25, 50, 75, 90 and 100 % (v/v)) for 10 minute periods at room temperature. After the final incubation in 100 % (v/v) ethanol, the dehydrated chip was removed from the PVC mounting and placed in a sealed dessicator for 8-10 hours, or overnight. Samples fixed in this fashion were suitable for both SEM and AFM imaging.

### **2.12.2 Sample analysis**

#### **2.12.2.1 SEM analysis**

The sample chip was mounted on the SEM stage and the sample chamber was then evacuated. The filament was saturated and then the electron gun was aligned, as appropriate. The voltage and working distance were set at 7.0 kV and 27.9 mm, respectively and images were collected via an incorporated secondary electron detector module.

#### **2.12.2.2 AFM analysis**

The sample chip was examined by 'contact mode' surface probing using a Nano-R™ AFM instrument. This experiment was kindly facilitated by the National Centre for Plasma Science and Technology (NCPST) in DCU.





***Chapter 3***  
***Production and Characterisation of***  
***Monoclonal Antibodies to L.***  
***monocytogenes***



### **3.1 Introduction**

#### **3.1.1 The immune system**

The term immunity is derived from the latin 'immunitas', (meaning freedom from) and in it's original usage referred to exemption from military service and payment of taxes (Weir, 1988). The current definition of immunity relates to the complex cascade of genetic and biochemical events that, in healthy mammals at least, reduces the individuals susceptibility to infection and attack by foreign bodies.

Innate immunity is best described as a 'general' or 'non-specific' defence mechanism. It represents the body's first line of defence against infection and includes anatomic barriers (skin and mucous membranes) and physiological barriers. The latter include the presence of the hydrolytic enzyme, lysozyme in tear secretions and the acidic environment of the stomach. In instances where the external innate immune barrier becomes breached, the internal innate immune system becomes activated. The predominant elements include the cells derived from the mononuclear phagocyte system, such as, macrophage that engulf and destroy foreign bodies. Neutrophils and especially natural killer (NK) cells are directed against host cells that have been infected with virus material and/or become malignant. The body's inflammatory response is a means of expediting the concentration of such cells around the areas of infected tissue.

Adaptive or acquired immunity is distinct from innate immunity by virtue of its extreme specificity and is sub-divided into humoral and cell-mediated immune responses (Figure 3.1). The foreign body that elicits an adaptive response is termed the 'immunogen', the specific molecules present on the immunogen that allow the adaptive immune system to distinguish between different immunogens are referred to as 'antigens'. The smallest defined region of a given antigen recognised by an antibody is termed the 'epitope'. Thus, an individual's adaptive status is a reflection of the diversity of antigens to which they have been exposed, and the frequency of such exposures. Since the efficiency of the adaptive response improves with each subsequent exposure to a given antigen, it is also a reflection of the frequency of exposure. The cells of the lymphatic system, termed lymphocytes mediate adaptive immunity. These include the antibody-producing B-cells (Bursa-equivalent-derived small lymphocyte) and T-cells (Thymus-derived small lymphocytes), the latter of which include helper ( $T_H$ ), cytotoxic ( $T_C$ ) and suppressor ( $T_S$ ) varieties. The approximate percentage of each type within the major lymphoid organs is outlined for a typical murine model in Table 3.1.



**Table 3.1:** Lymphocyte sub-populations of major murine lymphoid organs. (Adapted from Hudson and Hay, 1980).

Organ	% T-Cells	% B-Cells
Thymus	97	1
Lymph node	77	18
Spleen	35	38
Blood	70	24
Thoracic duct lymph	80	19

### 3.1.1.1 The humoral immune response

Far from being mutually exclusive events, the B and T-cell activation cascades are inextricably linked. A key co-ordinator of the adaptive immune response is the major histocompatibility complex (MHC) set of molecules. These glycoproteins, act as cell membrane appendages that display, or present antigen molecules for processing by the adaptive components. The two principal variants include; MHC I (present on most nucleated cells), and MHC II (only expressed by antigen-presenting cells). To elicit an immune response, a given immunogen must generally be of molecular weight greater than 5-6 kDa and exhibit a degree of complexity within its structure. Small molecules, such as certain drug and pesticide compounds, are often incapable of eliciting an immune response on their own by virtue of their size and are called 'haptens'. From a research point of view, such molecules can be altered, by conjugating to larger molecular weight carrier molecules (e.g. BSA, KLH or THG), which are easily appreciated by the immune system. Larger molecules, such as bacteria contain a multitude of surface antigens, which each in turn may contain many epitopes, rendering them easily identifiable as 'foreign', to the immune system. In fact, inactivated *Mycobacterium* and *Bordetella* spp. have been used as the principal constituent of adjuvant preparations (e.g. Freund's adjuvant). When immunogens are delivered suspended within such adjuvants, the inactivated bacterial content stimulates heightened macrophage activity localised around the area of immunisation.

Following phagocytosis and partial digestion of the foreign entity, the antigenic material is displayed on the surface of the macrophage or antigen-presenting cell (APC) via MHC II molecules. T<sub>H</sub> cells then bind to the MHC II molecules using T-cell receptor molecules that are present on the surface of T-cells. Like an antibody, each T-cell receptor is a heterodimer composed of  $\alpha$ - and  $\beta$ - chain domains that incorporate both variable and constant domains.



This initial binding event sets in place a sequence of events that revolve around the release of stimulatory molecules called cytokines. At this stage Interleukin-1 (IL-1) induces rapid proliferation and differentiation of T-cells, while release of IL-2 induces B-cell proliferation. Circulating B-cells can also take up, process and present antigens to  $T_H$  cells. Only one B-cell is reactive towards any given epitope, and this specificity is dictated by the nature of the antibody displayed on the surface of each B-cell. The B-cell/ $T_H$  cell interaction stimulates IL-4 receptor production on the B-cell surface and secretion of IL-4 itself by the activated  $T_H$  cell. Concomitant secretion of IL-5 by the B-cell itself culminates in differentiation of the B-cell into 'plasma' and 'memory' B-cell variants. Plasma B-cells are short-lived variants of the parent B-cell, which are characterised by heightened rough endoplasmic reticulum activity, conducive to rapid production and secretion of soluble antibody. Conversely, the memory B-cells are pervasive, circulating variants that display surface-bound antibody and are ready to respond rapidly during instances of re-exposure to antigen.

#### **3.1.1.2 Antibody structure**

At any given time the population of soluble antibodies in an individual's serum is wide and varied and is generally referred to as 'polyclonal'. It is this circulating pool of antibodies that directs humoral clearance of invading entities, such as bacterial cells.

Antibodies are a class of predominantly soluble, globular proteins with specific features that place them in the 'immunoglobulin' (Ig) family of folded protein structures. Immunoglobulin  $\gamma$  (IgG) is the predominant antibody component within polyclonal serum and it serves as a good generic representation of the key monomeric Ig structural features. These include two identical copies of a heavy (H) chain (approximately 50 kDa) and two identical copies of a light (L) chain (approximately 25 kDa), with each light chain being attached to a corresponding heavy chain by a disulphide bond. Both H chains are also covalently linked by disulphide bonds located proximal to the 'hinge' axis. The L chain is divided into two domains (1x variable ( $V_L$ ) and 1 x constant ( $C_L$ )) and the H chain into four domains (1x variable ( $V_H$ ) and 3 x constant ( $V_L$ )). Each domain consists of homologous units of approximately 110 amino acids arranged in antiparallel  $\beta$ -strands and stabilised by intra-strand hydrogen bonding and core hydrophobic localisation. Sequence analysis of the amino acid content of the  $V_L$  and  $V_H$  regions indicates that sequence variation is predominantly focused around three 'hypervariable' regions that contain residues and structures complementary to their respective antigens. They are referred to as 'complementarity determining regions' or CDR's. The remaining, more conserved region of the variable domains, are referred to as 'framework' regions.





## Humoral Immune response

## Cell-Mediated Immune response

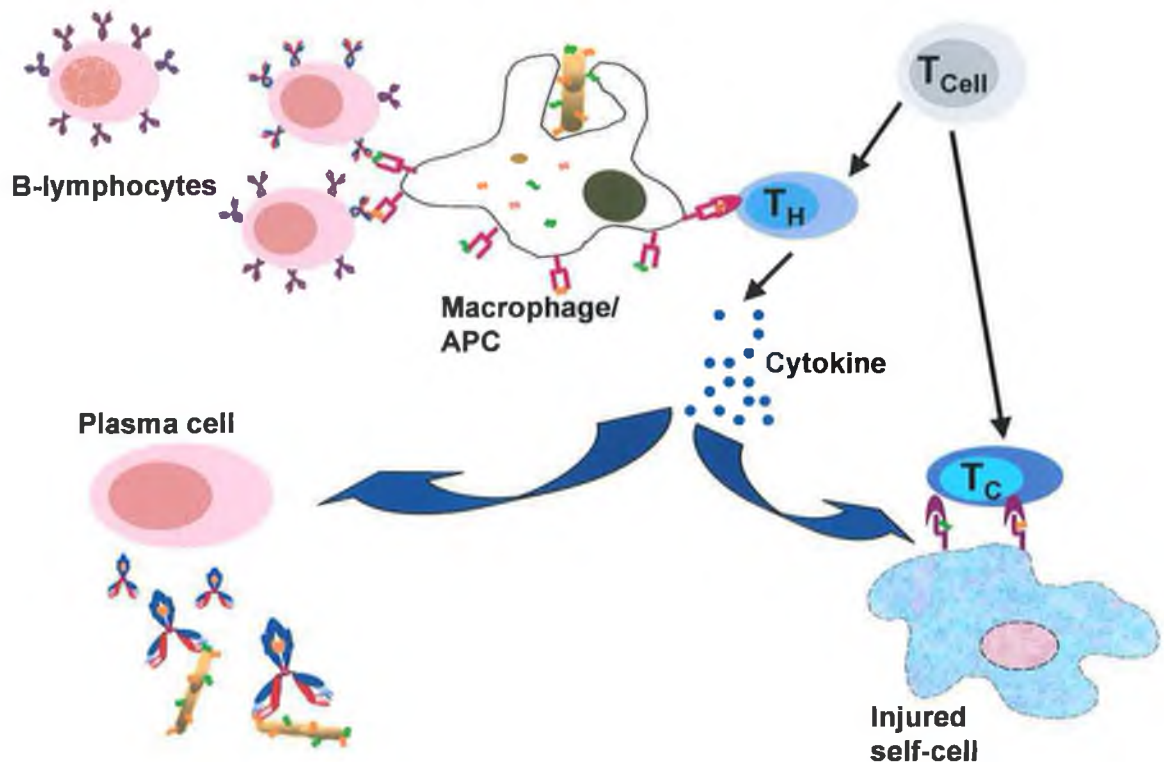


**Figure 3.1:** Outline of the immune response following exposure to an invading bacterium. The bacterial cell is identified as 'foreign' by circulating macrophage, which then phagocytoses the cell. The bacterial cell is then hydrolytically and oxidatively digested in the endosome compartment of the macrophage. Bacterial debris is translocated to the macrophage surface where it is displayed on MHC II molecules and these are recognised by complementary IgG-bearing B-lymphocytes or CD4<sup>+</sup>-restricted helper T cells. This begins the cascade of cytokine release, which direct CD8<sup>+</sup>-restricted cytotoxic T-cell activation and B-cell differentiation. CD8<sup>+</sup>-restricted cytotoxic T-cells can also directly degrade host cells that display antigens on their MHC I appendages signalling alterations within the cell due to viral infection or tumour growth. In addition, secreted bacterial proteins in the extra-cellular environment can directly stimulate circulating B-cells differentiation.



In the natural course of the humoral immune response, the primary objective in the development of an immunoassay targeting a given antigen, is to isolate an antibody with the requisite degree of specificity and affinity for reproducible analysis. Both of these attributes are controlled by the CDRs. At a structural level, each CDR folds into a 'canonical' loop formation (Chothia and Lesk, 1987). Each  $V_L$  and  $V_H$  domain contain three CDR loops (CDR1, CDR2 and CDR3) that juxtapose at the amino terminal of the associated domains. All CDRs can potentially make contact with the antigen, although, very seldom all at the same time for anti-hapten or anti-peptide antibodies (Muyldermans, *et al.*, 2001). The CDR3 region (of both  $V_L$  and  $V_H$  domains) exhibits the greatest sequence diversity and coincidentally, exerts the greatest influence on the antigen specificity. In addition, the size of the  $V_H$  CDR3 loop, in conjunction with the flexible association of the  $V_L$  and  $V_H$  domains at various angles and distances, generates a structural diversity of binding sites (Muyldermans, *et al.*, 2001). These can include cavities, grooves and planar sites that correspond to the size and type (hapten, peptide and protein, respectively) of the antigen (Webster *et al.*, 1994).

The structural analysis of the anti-HIV-1 IgG1 antibody, designated 'b12', (Protein Data Bank reference code: *1h7h.pdb*) and recently characterised by Saphire and co-workers, (2002), serves as a useful case study for highlighting the key structural facets relevant to antibody specificity, affinity and efficacy. Figures 3.2 to 3.5 demonstrate that antibody 'b12' represents the first intact human IgG with a full length hinge region for which all domains are ordered and visible in the electron density map and in essence offers a 'snapshot' within the wide spectrum of conformers that can be attained by the immunoglobulin molecule (Saphire *et al.*, 2002). In itself, this serves to dispel the common misconception that antibodies are rigid and symmetrical 'Y' shaped molecules. Moreover, the extreme asymmetry evident in the crystal structure suggests extraordinary interdomain flexibility (rotational, linear and planar) about the hinge regions that, until recently, was often overlooked in terms of assessing and characterising immunoglobulin structure-related function. The 'b12' antibody is a recombinant human antibody isolated from a phage display library, which had been developed from a long-term asymptomatic, HIV-1 infected individual (Burton *et al.*, 1994). Antibodies produced by recombinant means are generally capable of a much greater diversity in terms of antigen specificity and affinity. Whereas, during the humoral process of affinity maturation, an 'affinity ceiling' (Foote and Eisen, 1995) normally manifests at  $K_D$  values approaching  $10^{-10}$  M (Ohlin and Zouali, 2003), recombinant antibodies have been routinely isolated with affinities in excess of  $10^{-14}$  M. The IgG1 b12 antibody has been postulated to neutralise approximately 75% of primary HIV-1 isolates (Burton *et al.*, 1994) and has been highlighted as significant in the development of a HIV vaccine (Saphire *et al.*, 2001). The noteworthy feature of this particular antibody is its extremely prominent and extended CDR



H3 loop, which incorporates a 10-residue insertion (Figure 3.4). This is postulated to enable the loop to protrude into and thus, recognise the highly recessed CD4 binding site of the HIV-1 protein gp120 (Kwong *et al.*, 1998; Saphire *et al.*, 2001). IgG1 b12 thus emphasises the role of the CDR 3 loop in 'fine-tuning' the specificity of the hypervariable element of the Fv domains with respect to corresponding antigen, especially when the given antigen is of 'hapten-like' dimensions and/or embedded within non-antigenic recesses.

Although IgG1 is a useful example of generic immunoglobulin structure, it represents only one, among a suite of antibody molecules. They are divided into five classes (IgG, IgM, IgA, IgE and IgD) and each class is referred to as the 'isotype'. The light chain component of all antibodies is either of kappa ( $\kappa$ ) or lambda ( $\lambda$ ) designation. Whereas, IgG, IgE and IgD consist of one monomeric H<sub>2</sub>L<sub>2</sub> unit, IgA can be mono- di- or tri-meric and IgM exhibits a pentameric structure. Multivalent IgM is the first antibody secreted in response to primary exposure to antigen but normally accounts for only approximately 10 % of the polyclonal population in human serum. IgG is the predominant component and would normally represent in excess of 70 % of the polyclonal pool. In addition to valency, the classes can be distinguished based upon the number of C<sub>H</sub> domains. IgG, IgA and IgD molecules contain three C<sub>H</sub> domains, while both IgM and IgE contain four C<sub>H</sub> domains, the fourth compensating for the dedicated hinge domains present in the aforementioned IgG, IgA and IgD. The IgG class itself is further sub-divided into sub-classes that vary in their flexibility around the hinge region and their ability to trigger dedicated effector functions. The murine IgG subclasses consist of IgG1, IgG2a, IgG2b and IgG3, whereas, the human IgG subclasses comprise IgG1, IgG2, IgG3 and IgG4. The structures of the subclasses vary in their pattern of disulphide bonding (King, 1998). Human IgG1, IgG2a, IgG2b and IgG3 contain two, four, fifteen and two disulphide bonds, respectively, while murine IgG4 contains four disulphide bonds and the remaining subclasses contain three disulphide bonds each. Additionally, the position of the disulphide bond between the heavy and light chains varies from between the C<sub>L</sub> and C<sub>H</sub>1 region to between the C<sub>L</sub> and V<sub>H</sub>/C<sub>H</sub>1 interdomain region (King, 1998). The humoral immune response in humans is dominated by IgG1-mediated events. Attached to residue 297 of the C<sub>H</sub>2 domain of all IgG subclasses is an N-terminal linked oligosaccharide residue that controls the quaternary structure about the Fc region (Elgert, 1996). This is of paramount importance in directing the effector function of IgG. As a result, when producing human antibodies for therapeutic purposes by recombinant means, the type of expression system employed must be carefully assessed in terms of its ability to properly glycosylate the recombinant molecule in a compatible fashion (Parekh, *et al.*, 1989; Raju, 2000; Raju, 2003).



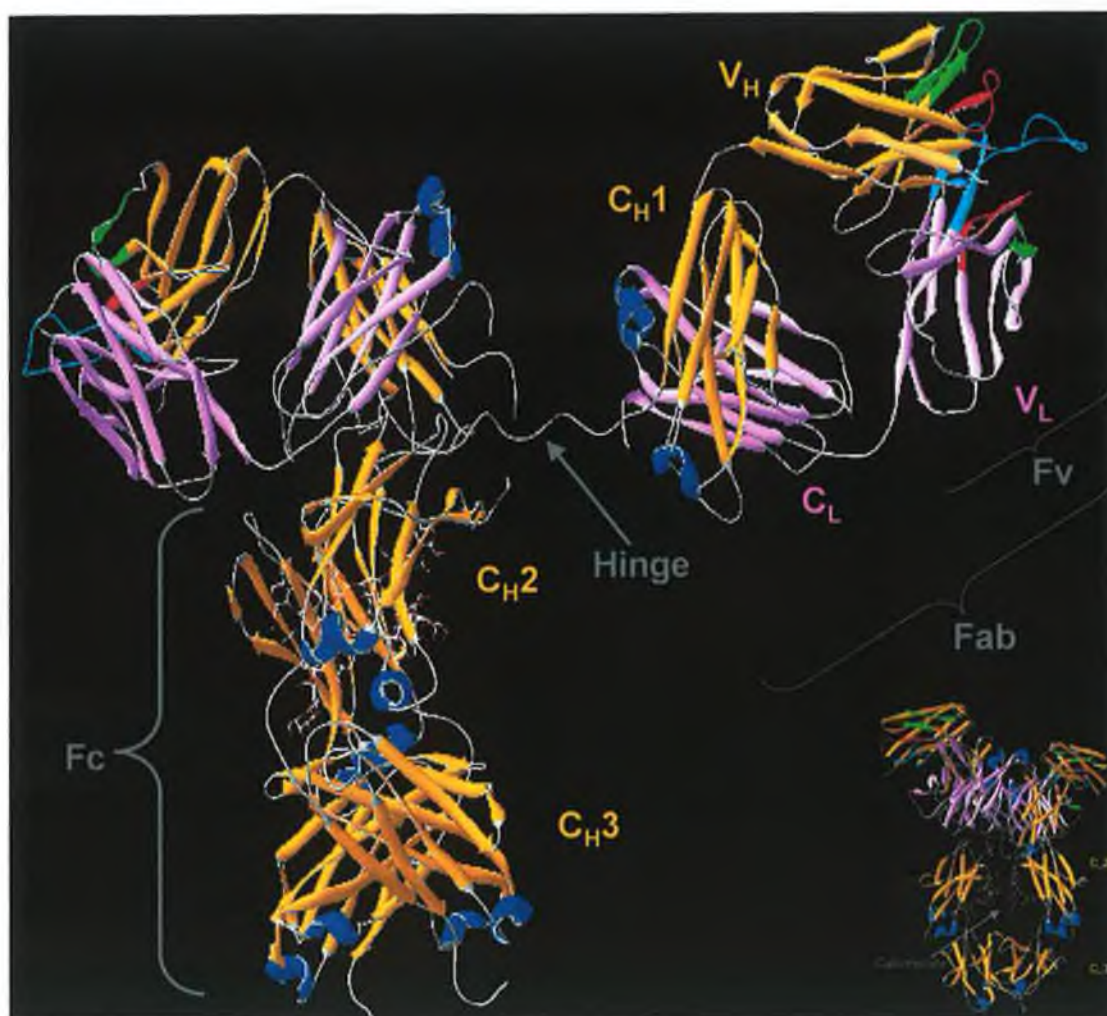


**Figure 3.2:** Structure of an IgG molecule. The generic immunoglobulin components are demonstrated in the ribbon structure which is based on the published sequence data for the IgG1 antibody 'b12' (PDB reference code: 1h7h.pdb). The molecule comprises two identical heavy chains that each consist of three constant heavy chain ( $C_H$ ) and one constant light ( $C_L$ ) domains. These are joined to two identical light chains, each of which consists of one constant light ( $C_L$ ) and one variable light ( $V_L$ ) region, by disulphide bonds and multiple non-covalent interactions. The structure can be broken down into four distinct segments as follows. The crystallisable fragment (Fc), that incorporates a carbohydrate element and dictates the isotype specificity and thus, effector function of the antibody. This is separated by a hinge region from the antigen-binding fragment (Fab). The antigen-binding specificity is determined by the variable fragment (Fv), more specifically, the hypervariable or complementarity determining region (CDR). Each  $V_H$  and  $V_L$  domain possesses three complementary CDR regions and these are indicated as prominent red, green and cyan loop structures, situated at the extreme N-terminus of the molecule. The bottom right-hand corner shows a side profile of the IgG molecule with its carbohydrate component visible in the Fc region.





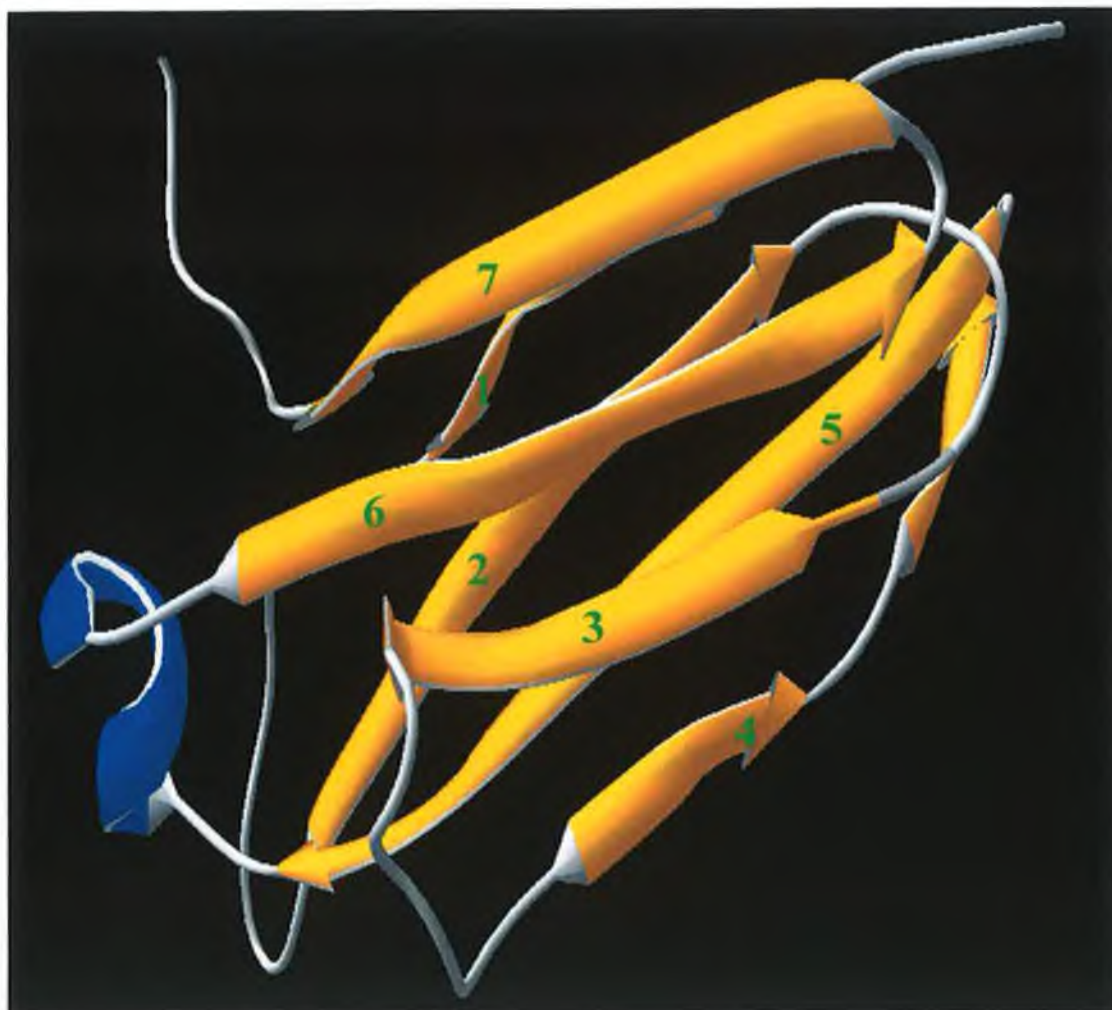


**Figure 3.3:** Structure of the immunoglobulin constant domain. A ribbon structure of the constant heavy domain of an IgG1 antibody (PDB reference code: 1h7h.pdb) is depicted with the  $\beta$  strands coloured yellow. The  $\beta$  strand arrows point from the N terminus to the C terminus and are numbered in green. All constant domains are built up from seven  $\beta$  strands arranged so that four strands form one  $\beta$  sheet and remaining three strands form a second sheet. The sheets are closely packed against each other and joined together by a disulphide bridge from  $\beta$  strand 6 in the three-strand sheet to  $\beta$  strand 2 in the four-strand sheet. Most of the invariant residues of the constant domain, including the disulphide bridge, are found in the sheets of the framework region. These invariant residues have two important functions. One is to form and stabilise the framework, or molecular scaffolding, by packing the  $\beta$  sheets through hydrophobic interactions to give a hydrophobic core between sheets. Their second function involves interactions between constant domains of different chains to form a complete immunoglobulin molecule.



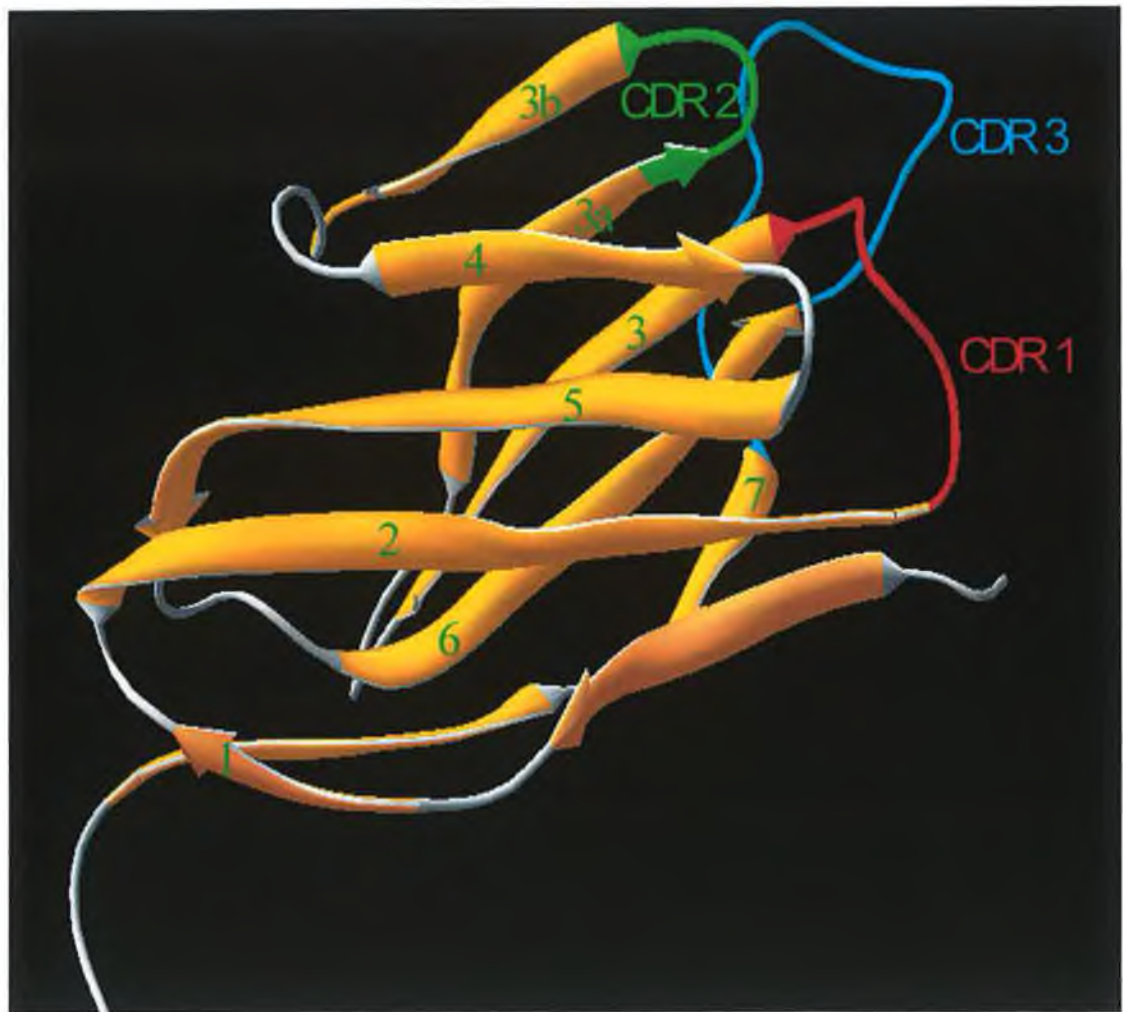


**Figure 3.4:** Structure of the immunoglobulin variable domain. The model demonstrates a ribbon structure of the variable heavy domain of an IgG1 antibody (PDB reference code: 1h7h.pdb). The overall structure of the variable domain is very similar to that of the constant domain but there are nine  $\beta$  strands instead of seven. The two additional  $\beta$  strands are inserted into the loop region that connects  $\beta$  strand 3 and 4 (labeled 3a and 3b). Functionally, this part of the polypeptide chain is important since it contains the hypervariable region CDR2. The two extra  $\beta$  strands provide the framework that positions CDR2 close to the other two hypervariable regions in the domain structure. The CDR1 and 3 loops are found between  $\beta$  strands 2 and 3, and 6 and 7, respectively.  $\beta$  strands are coloured in yellow, and the canonical CDR loop structures are highlighted individually. The  $\beta$  strand arrows point from the N terminus to the C terminus and are numbered in green.



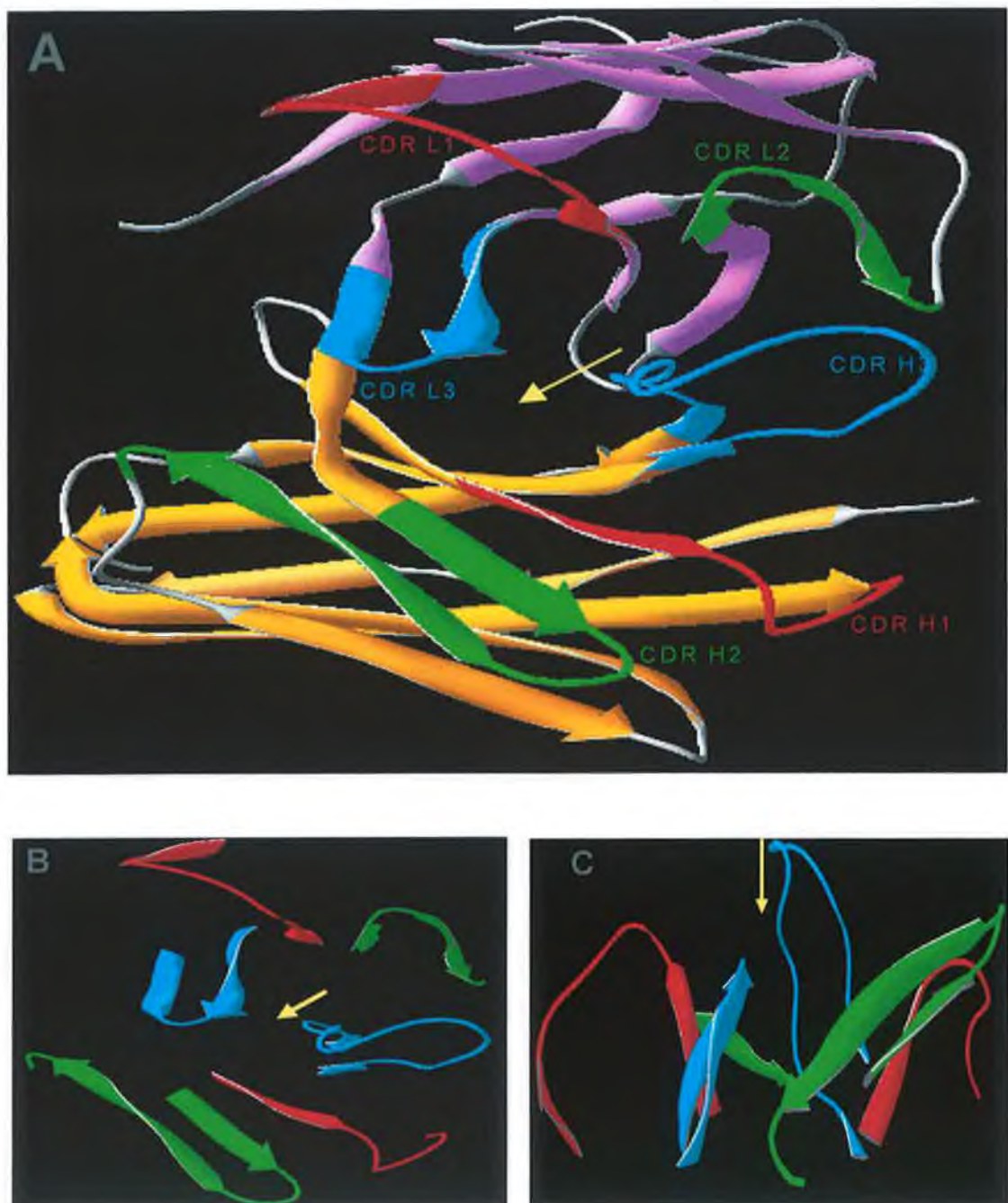


**Figure 3.5:** Overview of the CDR-binding 'cleft' using the published 'b12' crystal structure (Saphire et al., 2001; 2002; PDB reference code: 1h7h.pdb). The  $V_H$  and  $V_L$  scaffold domains are colored yellow and purple respectively. (A), Top-view of complete Fv domain with the CDR loops 1, 2 and 3 highlighted in red, green and cyan, respectively. (B), Top-view of CDR-binding cleft, with the Fv scaffold removed. (C), Side-view of CDR-binding cleft. This clearly demonstrates the prominent protrusion of the CDR H3 loop.





### 3.1.1.3 *L. monocytogenes* and the immune response

*L. monocytogenes* is an intracellular pathogen and as such, it circumvents the hosts extracellular humoral immune system. The principal immune response to listerial infection involves close interaction between the innate cellular and dedicated T-cell response (Unanue, 1997a). Invading *L. monocytogenes* cells are efficiently engulfed by macrophage cells through phagocytosis. In addition, *L. monocytogenes* can induce its own uptake by normally non-phagocytic cells (Schuchat *et al.*, 1991). *L. monocytogenes* cells that infect via the intestinal route, following oral exposure, are transported to the mesenteric lymph nodes, spleen and liver, while, reticulo-endothelial-infecting *L. monocytogenes* cells are sequestered by the liver-resident macrophage or Kupffer cells (Ebe *et al.*, 1999). Immediately following phagocytosis, the *L. monocytogenes* cells reside in phagosomes, where the majority, are efficiently killed by the combined oxidative effects of reactive oxygen intermediates (ROIs) and reactive nitrogen intermediates (RNIs) (Unanue, 1997b; Ohya *et al.*, 1998a; Ohya *et al.*, 1998b; Ouadrhiri *et al.*, 1999). The listericidal activity of the macrophage is amplified by increased secretion of cytokines such as interferon gamma (INF- $\gamma$ ) and tumour necrosis factor alpha (TNF- $\alpha$ ), that in turn, upregulate inducible nitric oxide synthase (iNOS) and intensify the oxidative process within the phagosome. *Listeria*-derived, degradation products are subsequently displayed on the macrophage MHC-II surface molecules and CD4<sup>+</sup>T<sub>H1</sub> cells are recruited and these control the perpetuation of the antigen-induced T-cell response. The efficacy of this, principally, innate response is not 100 % and it has been suggested that only a small percentage of *L. monocytogenes* cells need to survive the oxidative environment of the phagosome and reach the cytosol, to elicit infection (De Chastellier and Berche, 1994). In fact, *L. monocytogenes* cells can take advantage of their ability to survive within macrophage and the rapid recruitment of macrophage to infected endothelial cells, by using them to facilitate a "Trojan horse"-type (Drevets, 1999; Vázquez-Boland, 2001) delivery to endothelial epithelia (Drevets *et al.*, 1995; Greiffenberg *et al.*, 2000) and transfer across the blood brain barrier, leading to disseminated CNS infection. This also ensures the pathogen remains isolated from the humoral branch of the immune system.

It has been suggested that intracellular pathogens such as *L. monocytogenes* may be able to counteract the oxidative effect of ROI and RNI by producing the enzymes catalase and superoxide dismutase, or SOD (Haas and Goebel, 1992; Miller and Britigan, 1997). However, deletion of the genes encoding either the catalase (Leblond-Francillard *et al.*, 1989), or SOD (Brehm *et al.*, 1992) enzymes was not found to substantially reduce the proliferation capacity of *L. monocytogenes* in host cells.





Much more significant, and particular to *L. monocytogenes*, is its ability to escape from the phagosome into the cytosol of the host macrophage. This is principally mediated by secretion of listeriolysin O (LLO) (Portnoy *et al.*, 1988; Cossart *et al.*, 1989), in addition to phospholipase C (PI-PLC) and phosphatidylcholine-preferring phospholipase C (PC-PLC) (Cossart and Lecuit, 1998; Cossart *et al.*, 2003). LLO is a potent pore-forming cytolysin, that, exhibits optimal activity in the low pH environment of the phagosome (Dramsı and Cossart, 2002; Glomski *et al.*, 2002). It also possesses a PEST-like sequence (Decatur and Portnoy, 2000) that, targets LLO for phosphorylation in the mammalian cytosol and subsequent degradation. These features restrict the cytolytic activity of LLO to the host phagosome and prevent damage to the host cell. Having successfully escaped the hostile environment of the phagosome, *L. monocytogenes* proceeds to proliferate and differentiate within the cytosolic compartment. At this stage, the MHC-I-restricted CD8<sup>+</sup> T cell-mediated immune response (the classical, MHC-Ia and non-classical MHC-Ib responses) is initiated (Brunt *et al.*, 1990; Lara-Tejero and Pamer, 2004) resulting in activation of Tc cells and destruction of the infected cell. Although both macrophages and dendritic cells (DCs) are able to take up, process and present antigens *in vitro*, there is mounting evidence indicating that macrophages do not have the ability to prime naïve T cells to become Tc cells and that this function is carried out exclusively by DCs (Jung *et al.*, 2002; Lara-Tejero and Pamer, 2004). It was also commonly theorised that once primed to proliferate by the appropriate stimulus, CD8<sup>+</sup> T cells proceeded to proliferate and differentiate, independent of the priming antigen (Wong and Pamer, 2001). It has been shown, however, that effective antigen presentation leading to activation of naïve or memory CD8<sup>+</sup> T cells is limited to the first three days of infection, despite persistence of the bacterial cell and associated antigens for up to a week, following primary exposure (Wong and Pamer, 2003). The major conclusions drawn from these observations and related work (Badovinac *et al.*, 2002; Badovinac *et al.*, 2003) were, that the larger the T cell memory pool, the stronger the Tc response, leading to elimination of effective antigen presentation and thereby, limiting the recruitment of naïve T cells (Lara-Tejero and Pamer, 2004).

The non-classical MHC-Ib response, as demonstrated by the H2-M3-restricted CD8<sup>+</sup> T cell response to *L. monocytogenes* infection in mice (Lenz and Bevan, 1997), is distinct from the classical response in several respects. In infected mice, the H2-M3 molecule can present peptides with N-formylated amino termini that, are typical of prokaryote N-formylmethionine-initiated proteins, produced in the cytoplasm. H2-M3-restricted cells exhibit an activated phenotype in naïve animals and demonstrate a more rapid primary response. However, following a secondary challenge they demonstrate more limited expansion (Kerksiek *et al.*, 1999; Lara-Tejero and Pamer, 2004). Despite their inability to



proliferate, it is thought that a population of H2-M3-restricted memory cells is generated and that they are indistinguishable from MHC-Ia-restricted CD8<sup>+</sup> T cells, with respect to surface markers and longevity (Kerksiek *et al.*, 2003). It has also been shown that H2-M3-restricted CD8<sup>+</sup> T cells can be selected in the thymus on bone marrow-derived cells (Urdahl *et al.*, 2002) and it has been postulated that differences in thymic selection might account for the distinct behaviour H2-M3-restricted T cells during memory responses to *L. monocytogenes* infection (Lara-Tejero and Pamer, 2004).

The major CD8<sup>+</sup> T cell response in *L. monocytogenes*-infected cells is directed against LLO (Berche *et al.*, 1987; Bouwer *et al.*, 1992; Hitbold *et al.*, 1996). LLO has been demonstrated to be processed efficiently into peptides that are presented by MHC I molecules (Darji *et al.*, 1995; Villanueva *et al.*, 1995). A specific nine residue peptide subunit from LLO has been shown to be especially immunodominant and capable of conferring *L. monocytogenes* resistance when administered to naïve mice (Pamer *et al.*, 1991; Harty and Bevan, 1992). In addition to LLO, the *L. monocytogenes* p60 protein, a murein hydrolase enzyme that is needed for efficient cell division during cytoplasmic proliferation, is the next most potent elicitor of T cell response to *L. monocytogenes* infection (Harty and Pamer, 1995; Geignat *et al.*, 1999; Geignat *et al.*, 2001). Protective *L. monocytogenes*-specific T cell epitopes from LLO and p60 have been recombinantly expressed on the surface (Verma *et al.*, 1995; Spreng *et al.*, 2003) of *Salmonella* spp. and successfully used as live vaccines to confer T cell-mediated protection against murine listeriosis.

It is noteworthy that both these immunodominant proteins are secreted proteins. Indeed, it has been reported that somatic or cell-surface-localised antigens, are not able to generate a protective CD8<sup>+</sup> T cell response to *L. monocytogenes* (Shen *et al.*, 1998). This paradigm was elaborated upon in a series of experiments performed by Zenewicz and co-workers (2002). The authors investigated the degree of protection afforded against recombinant variants of *L. monocytogenes* expressing a heterologous epitope derived from lymphocytic choriomeningitis virus (LCMV) in somatic or secreted form, in mice that had been immunised with either the somatic or secreting variants or the LCMV virus alone. The recall response of LCMV-immune mice was similar in mice challenged with either the somatic or secreting variants, yet, significant CD8<sup>+</sup> T cell-mediated protection was only afforded against the variant expressing the secreted LCMV antigen, not the somatic form. These results indicated that the lack of protection against *L. monocytogenes*, expressing the somatic antigen, was not attributable to a lack of T cell memory response. Rather, since presentation of the somatic antigen was most likely limited to cross-presentation, and the fact that cells actively infected



with *L. monocytogenes* might not present the somatic form of the antigen, they therefore fail to be eliminated by the complementary CD8<sup>+</sup> T response (Lara-Tejero and Pamer, 2004).

*L. monocytogenes* has evolved a variety of mechanisms to combat the host T-cell responses. For instance, LLO has been implicated as a cause of down-regulation of the gene encoding MHC II antigen I-Ab and MHC I antigen, H-2K, in infected host cells (Schüller *et al.*, 1998). Furthermore, although there is no evidence to suggest that *L. monocytogenes* bacterial cells invade T cells (Merrick *et al.*, 1997), a potent, *L. monocytogenes*-specific counter-T cell response has recently been proposed by Zenewicz and co-workers, (2004). The FasL protein is a member of the tumour necrosis family and it is predominately expressed by activated T-cells, B cells, neutrophils and macrophage (Suda *et al.*, 1995; Hahne *et al.*, 1996; Liles *et al.*, 1996; Kiener *et al.*, 1997). When FasL binds to its receptor molecule (Fas), which is constitutively expressed on many cell types (Watanabe-Fukunaga *et al.*, 1992), it leads to apoptosis of the Fas-expressing cell (Suda and Nagata, 1994). Expression of FasL is normally only apparent in T-cells following activation and manifests in a biphasic process. Immediately following activation, pre-stored intracellular FasL is released to the surface by degranulation (Bossi and Griffiths, 1999) and this is followed by transcriptional activation of FasL synthesis, which is induced by NF- $\kappa$ B (Kasibhatla *et al.*, 1999). It was shown that both LLO alone, as well as PC-PLC acting in synergy with LLO, were capable and sufficient to induce early FasL expression on T cell surfaces (Zenewicz *et al.*, 2004). This is probably a result of LLOs ability to increase calcium permeability in mammalian membranes (Repp *et al.*, 2002) and alter intracellular calcium homeostasis and calcium flux, a condition which has previously been confirmed to induce degranulation in T cells (Glass *et al.*, 1996). Thus, it is proposed that upregulation of FasL on T cells by *L. monocytogenes* may allow the pathogen to exploit Fas-FasL-mediated apoptosis and associated cytokine production to modulate the host immune response and influence the course of infection (Zenewicz *et al.*, 2004).

#### **3.1.1.4 Antibody diversity**

The complete collection of antibody specificities available within an individual is known as the 'antibody repertoire' and is estimated to consist of up to 10<sup>11</sup> uniquely distinct antibodies in the human (Janeway and Travers, 1997). The study of human monoclonal antibodies to different infectious agents shows that the antibody response is generated to a relatively small number of target surface proteins and carbohydrates expressing an array of epitopes (Ohlin and Zouali, 2003). Given the huge variety of potentially infectious foreign bodies an individual is exposed to throughout a lifetime it is not plausible to entertain the notion that a naïve pool of B-cells, producing a limited number of antibodies, with a degree of variation dependent on and proportional to the levels of germ-line genetic material dedicated to



antibody production, is sufficient to meet such a challenge. In 1983, Tonegwa demonstrated that the embryonic germline DNA encoding immunoglobulin expression actually consisted of a consecutive but non-sequential alignment of variable (V), joining (J) and constant (C) exons, separated by substantial, non-coding intron sequences. Heavy chains contain an additional diversity, (D) exon, between the J and C regions. The manner in which these principal V, J, D and C sequences assembled to form a composite coding sequence is the primary determinant of progeny antibody specificity. 'Combinatorial diversity' is the name given to the permutations that are generated by the recombination of gene segments selected from these sets (Collins *et al.*, 2003). Figure 3.6 gives an outline of the combinatorial events involved. It is as a direct consequence of the limited number of germline V exons that a relatively low number of different  $V_H/V_L$  combinations can be generated based on this diversity alone, in total, amounting to  $6 \times 10^6$  different sequences (Ohlin and Zouali, 2003).

The process of 'junctional diversity,' which, manifest at VD, DJ and VJ regions, accentuates the diversity of the composite sequences and thus, the repertoire potential. Junctional diversity arises as a result of palindromic (P) nucleotide additions (Feeney *et al.*, 1994) during RAG1 and RAG2 mediated (Oettinger *et al.*, 1990; McBlane *et al.*, 1995 and Sawchuk *et al.*, 1997) hairpin loop opening in the early stages of recombination. Random enzymatic N-terminal nucleotide addition by terminal deoxynucleotidyl transferase can occur at the light chain VJ, and especially the heavy chain VD and DJ junctions resulting in further generation of diversity (Benedict *et al.*, 2000), notably in the CDR 3 regions of both chains, which are the quintessential determinants of immunoglobulin specificity. In addition to nucleotide additions, exonuclease-catalysed removal of multiple nucleotides within the coding regions can significantly alter immunoglobulin specificity. However, this may not be an entirely random activity as it has been reported that the amount of nucleotide excision varies depending on the coding sequence (Feeney *et al.*, 1994), with 'pliable' AT rich regions potentially more prone to such events (Gauss and Lieber, 1996).

When considering infection with pathogens, especially intracellular pathogens such as *L. monocytogenes*, the 'neutralising' activity of immunoglobulins can be of paramount importance. This has recently been purported to account for antibody-mediated resistance to *L. monocytogenes* as a result of studies indicating neutralisation of the pathogen following *in vivo* administering of anti-listeriolysin O monoclonal antibody (Edelson and Unanue, 2001). Although not a typical example of the humoral immune response (in fact such neutralising activity has been attributed to a separate branch of intrinsic antibody-mediated immunity (Wentworth *et al.*, 2000; Wentworth Jr. *et al.*, 2002)) the efficiency of neutralisation is dependent on the antibody's intrinsic affinity and avidity towards the respective infectious





material. Whereas, combinatorial and junctional diversity could account for a suitably varied repertoire of B-cells capable of recognising one, or several epitopes on an invading bacteria, the likelihood that the affinity of the antibody would be sufficient to effect neutralisation, is less certain.

The process of somatic point (hyper)mutation adds a further element of diversity to the repertoire. A random mutation rate of approximately  $10^3$  mutations/base pair (Jacob *et al.*, 1993) with affinity-improving mutations preferentially retained (McHeyzer-Williams *et al.*, 2001), results in selection of 'affinity-matured' immunoglobulin. Although the mutations themselves are random, they are localised to certain regions of the composite 5' V regions of both the heavy and light chains, referred to as 'hot spots' (Dorner *et al.*, 1998; Rada and Milstein, 2001; Rogozin *et al.*, 2001 and Diaz and Casali, 2002). The process of affinity maturation occurs in the disseminated nodes of the lymphatic system. Co-localised within the nodes is a cytidine deaminase homologue termed 'activation-induced-deaminase' or AID (Lieber, 2000). Knockout mice, deficient in AID have been shown to be incapable of producing IgG, IgE and IgA (Muramatsu *et al.*, 2000). Furthermore, deficiency in this enzyme has been associated with ablation of somatic hypermutation, as occurs in sufferers of type 2 hyper-IgM syndrome (Muramatsu *et al.*, 2000; Revy *et al.*, 2000), as well as indicating a concomitant association with class switching. Recent studies (Rogozin *et al.*, 2001; Pavlov *et al.*, 2002) indicate that the error prone DNA polymerase, DNA polymerase  $\eta$  may be responsible for the preponderance of somatic mutations within the V region 'hot spots'. This polymerase exhibits an error rate one thousand times greater than the commonly associated replicative polymerases (Matsuda *et al.*, 2000).



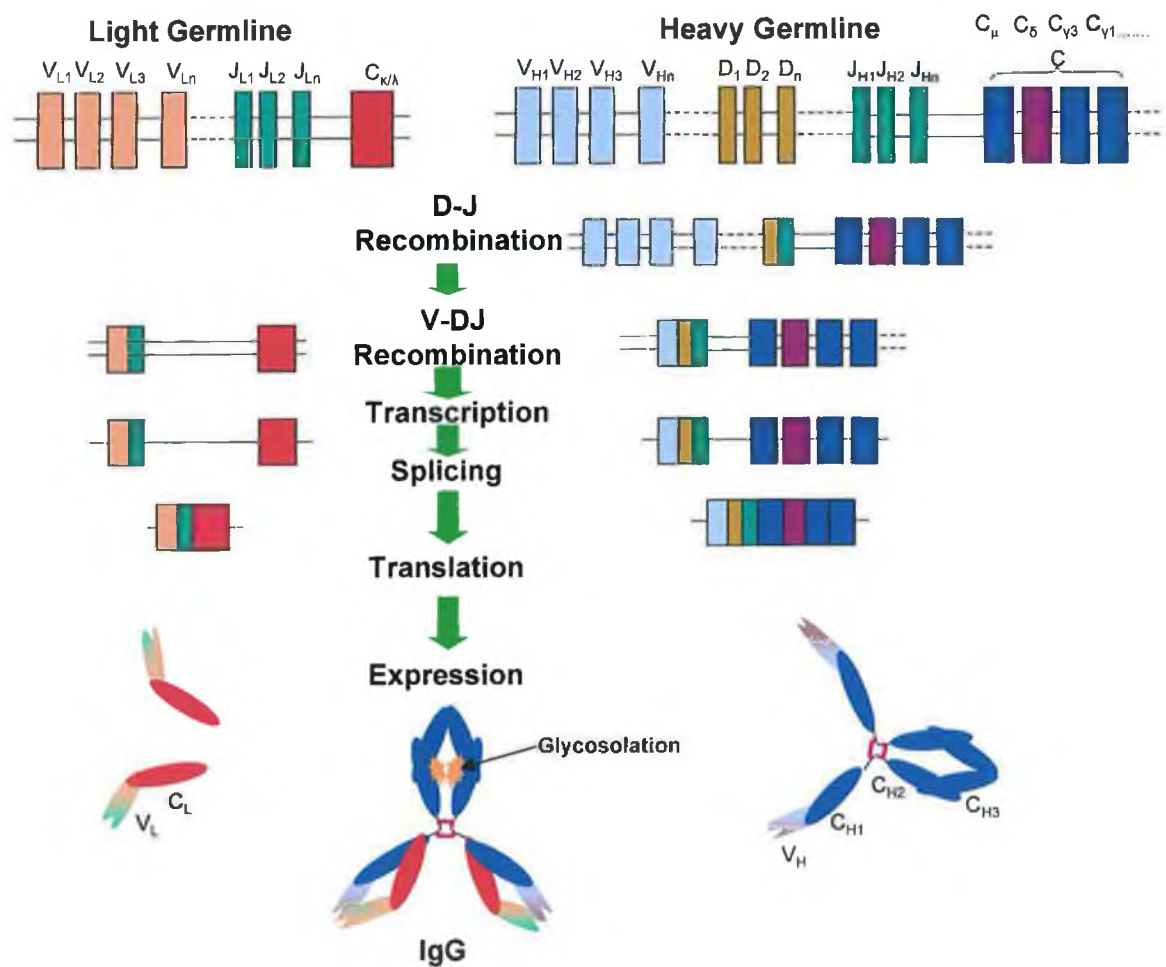


**Figure 3.6:** Generic overview of somatic recombination in humans. Light chain *V*-region genes are constructed from two germline DNA segments, a variable (*V*) and joining (*J*) that are joined to form a complete light-chain *V*-region gene. The *C* region is encoded on a separated gene locus and is joined to the variable region gene segment by splicing of the light-chain RNA to remove the *J* to *C* introns.  $\lambda$ -light chains comprise 29 *V<sub>L</sub>* segments and 4 pairs of functional *J<sub>L</sub>* and *C<sub>λ</sub>* segments.  $\kappa$ -light chains comprise 40 *V<sub>L</sub>* segments and 5 *J<sub>L</sub>* segments that are arranged in a cluster, preceding a single *C<sub>κ</sub>* segment. Heavy chain *V* regions are constructed from three gene segments as shown on the right hand side of the diagram. First, the diversity (*D*) and *J<sub>L</sub>* gene segments join, then the *V<sub>L</sub>* gene segment joins to the combined *DJ* sequence, forming a complete *V<sub>H</sub>* gene. The heavy chain *C*-region genes are each encoded by several exons (the exon encoding the hinge region is shaded olive/brown). The *C*-region exons are spliced to the *V*-domain sequence during processing of the heavy chain RNA transcript. The heavy chain gene locus comprises 51 functional *V<sub>H</sub>* gene segments and approximately 27 *D<sub>H</sub>* segments, preceding 6 *J<sub>H</sub>* segments. Light chain and heavy chain genes are translated into large polypeptide chains that associated to form the antibody molecule. The diagram present here was adapted from Janeway et al., (1999).



### **3.1.2 Monoclonal antibody production**

In 1900 the phrase “magic bullets” was used to emphasise the specific function of antibody molecules within the body’s immune system (Ehrlich, 1900; Little *et al.*, 2000). It was 75 years later before scientists gained the ability to successfully produce these highly specific molecules. This was facilitated by the publication of the Nobel Prize-winning method of somatic cell fusion between a myeloma (plasmacytoma) and an immune lymphoblast expressing a specific gene (Kohler and Milstein, 1975). Each individual resultant hybridoma (*hybrid-myeloma*) combines the immortality of the myeloma with the antibody production virtues of the lymphocyte, thus serving as a stable (*cloned*) source of *mono*-specific antibody.

The ability to routinely produce and maintain homogeneous populations of monoclonal antibodies with defined specificities and affinities has enhanced the biochemists armamentarium and significantly increased the potential for immunoassay and biosensor development and commercialisation. Monoclonal antibodies are finding ever-diversifying applications in areas such as environmental and food analysis, immunodiagnostics and clinical therapeutics (Fitzpatrick *et al.*, 2000).

#### **3.1.2.1 Production of monoclonal antibodies following *in vivo* immunisation**

The decision to produce a given monoclonal antibody should always begin with careful examination of the intended application of the resultant antibodies and assessment of the availability and purity of the antigen in question. Mice (BALB/c strain) are then immunised with the antigen of interest and boosted periodically over a period of weeks or months. Specific serum antibody levels or titres are measured (Kemeny *et al.*, 1992) from tail bleed samples. When the serum titre is deemed sufficient (usually  $\geq 1/50,000$ ) the animal is sacrificed and the lymphocytes are removed from the spleen (or alternatively, the lymph nodes) and used for the cell fusion procedure. The myeloma cells used as the fusion partner were originally derived from BALB/c lineage mice and were selected on the basis of their hypoxanthine-guanine phosphoribosyltransferase (HGPRT) deficiency. It is possible to select for cells deficient in HGPRT with the agent 6-azoguanine, which becomes toxic to cells expressing HGPRT. Two of the most commonly used myeloma cell lines include Sp2/0-Ag14 (Shulman *et al.*, 1978) and X63/Ag8.653 (Brown and Ling, 1988). Neither of these cell lines possess the inherent genetic capacity to produce immunoglobulin. Although, the original fusing agent, was UV-inactivated Sendai virus, this has now been supplanted by the chemical fusion agent, polyethylene glycol (PEG) (Zola and Brooks, 1995). This polywax causes membrane fusion between adjacent cells. Subsequent cell division facilitates chromosome



mixing between the fused parent cells. Fusion progeny consists of a heterogeneous population of unfused myelomas and lymphocytes, fused myeloma/myeloma, lymphocyte/lymphocyte and the desired myeloma/lymphocyte hybrids. Selective propagation of these desired hybridomas is based on the HAT (Hypoxanthine, Aminopterin and Thymidine) system, originally proposed by Littlefield (1964). Myeloma cells demonstrate excellent proliferation in favourable *in vitro* cell culture conditions. However, they lack the HGPRT enzyme and thus, when the *de novo* synthesis of purines and pyrimidines is blocked by the addition of HAT to the growth media, the compensatory salvage pathway cannot be induced and the cells cease to be able to synthesise DNA (Figure 3.7). Lymphocytes, although HGPRT<sup>+</sup> do not grow well in culture and naturally die off. Thus, in the presence of HAT only myeloma/lymphocyte hybrids will thrive.

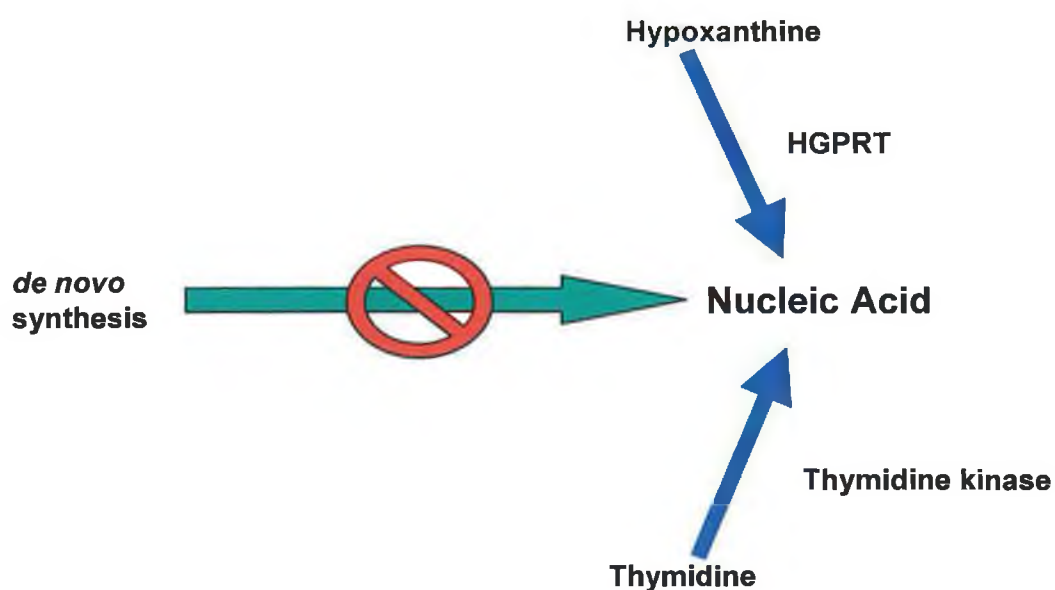


**Figure 3.7:** Aminopterin (HAT) is used to block *de novo* synthesis of purines. Hypoxanthine (HAT), a major source of purine precursors, will only be effectively incorporated into mature purines if HGPRT is present. Since aminopterin also prevents synthesis of thymidine (HAT), an exogenous source of thymidine must also be present.





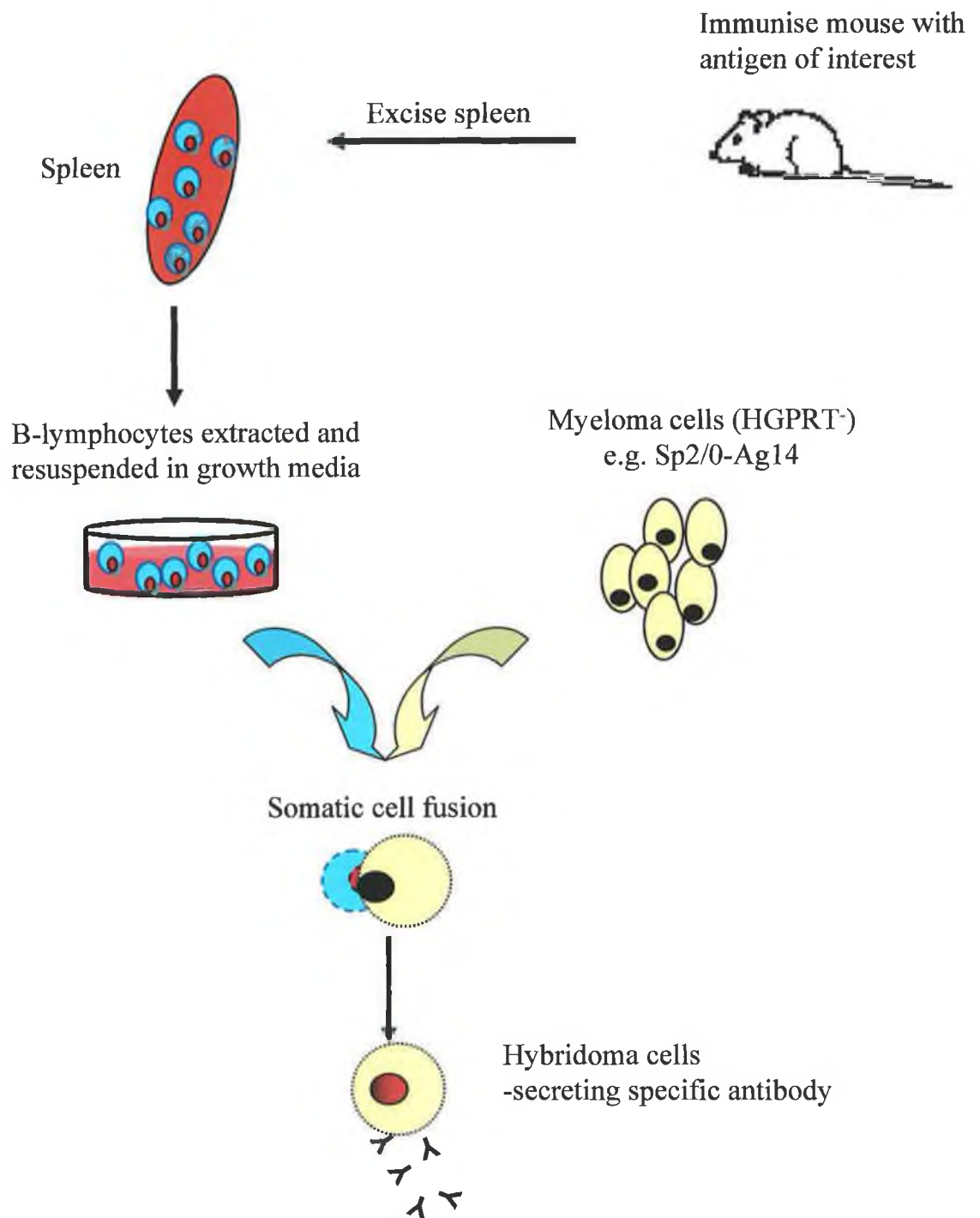


**Figure 3.8:** Overview of monoclonal antibody production by somatic cell fusion. B-lymphocytes are isolated from the excised spleen of a mouse that has been immunised with a defined antigen. These HGPRT<sup>+</sup> cells are somatically fused with a compatible, murine myeloma cell line using polyethylene glycol (PEG). The latter cells are HGPRT-deficient (HGPRT<sup>-</sup>), and thus, only proliferate in vitro, in the presence of HAT supplement, if successfully fused with a B-lymphocyte cell.



### ***3.1.2.2 Screening of hybridoma progeny***

The fusion progeny consist of wells containing multiple heterogenous populations of hybridomas. Each hybridoma within a given well population can contribute anywhere between 0 and 100 % of the secreted antibody content. It is imperative that wells containing hybridomas secreting antibodies exhibiting the desired traits for the intended application are confidently identified as early as possible. ELISA screening assays facilitate multiple screening of wells and are the method of choice in many cases. A direct ELISA format can be easily optimised and is particularly suitable for initial screening of a very large number of wells. This consists of coating the antigen of interest onto an ELISA plate, adding test supernatant (diluted in PBS-T to limit non-specific binding) followed by an anti-species detection antibody. The physical nature of the antigen also requires consideration. If for instance the antigen used is a pure and defined peptide sequence, each antigen thus presents a single epitope and the relationship between the corresponding specific antibody and peptide is a purely arithmetic one. Such peptides or other defined small molecules (e.g. elicit drugs or pesticides) can be simply adsorbed or linked via adaptor molecules to the surface of the ELISA plate (Danilova, 1994). In cases where more complex antigens are employed such as a bacterial cell, the scenario becomes more complicated. Surface adsorption of cells may actually distort the physical conformation of the cell and render epitope-bearing regions inaccessible to or 'masked' from the corresponding antibody. Covalently attaching the cells to the surface may exacerbate the problem by introducing undesirable chemical modification of the surface epitopes.

The adoption of a sandwich ELISA approach can help overcome some of these problems. This involves anchoring the cells to a polyclonal antibody that has been raised using the same antigen, in a non-murine (i.e. rabbit or goat) host. If, however, the cell only expresses a small number of the monoclonal-reactive epitopes, these may become 'swamped' by the polyclonal anchor layer. Once the number of hybridoma populations has been streamlined it is possible to employ a more informative screening assay. A competitive, or inhibition assay is favoured because the monoclonal antibodies and complex antigen are allowed to interact in the solution phase, where epitope accessibility is not compromised. This also more closely resembles the conditions of the intended final application. Further information regarding the identity of the specific antigenic protein can be gleaned by conducting a western blot analysis of the resolved protein components of the complex antigen with the selected monoclonal antibodies.



### 3.1.2.3 Cloning of hybridoma cells

Once a hybridoma population secreting the desired antibody has been identified, it is essential that the individual hybridoma be isolated from the heterogeneous mixture (Figure 3.9). The simplest method to implement, particularly where 96 well plates are being employed is that of, cloning by 'limiting dilution'. This entails seeding the mixed population of hybridomas over a range of dilutions calculated to maximise the chances of only one cell being distributed in a given well.

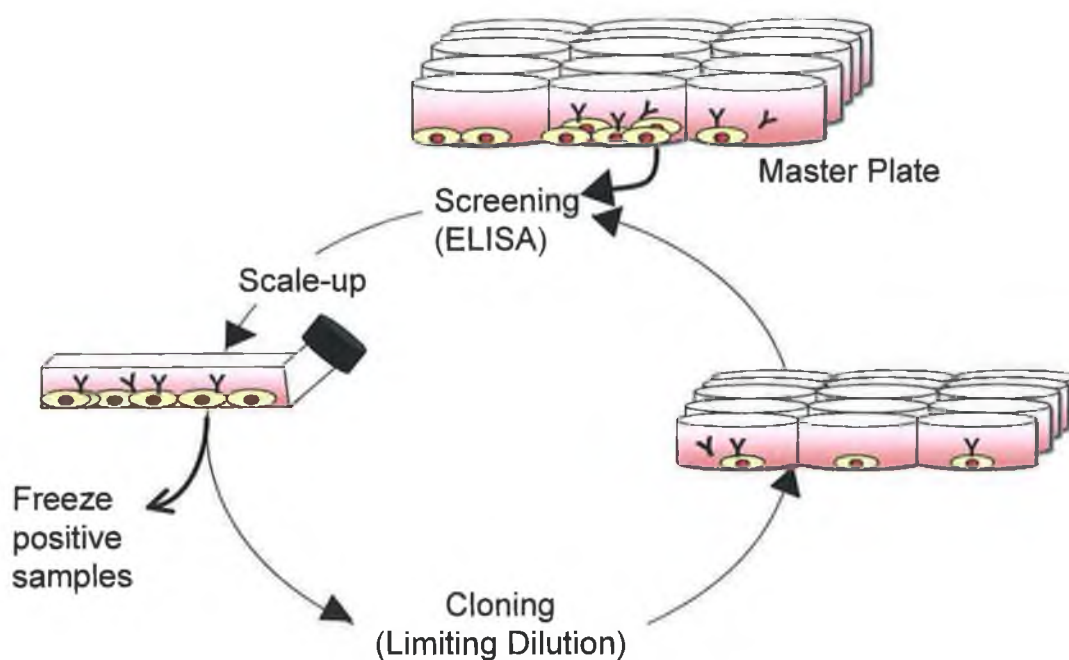


**Figure. 3.9:** Schematic overview of the stages involved in the identification and isolation of stable clones secreting desired antibody. Samples from positive hybridoma populations are frozen as soon as possible to serve as a 'back-up' stock. The original heterogeneous population of 'first-round' hybridomas is sub-cultured by limiting dilution to generate sub-populations. After several rounds of such cloning, the hybridoma populations within each well can be considered homogenous or monoclonal.

A mathematical approach indicates that were less than 63 % of the wells seeded with concentrations of  $\leq 1$  cell/well demonstrate cell growth, Poisson-distribution dictates that they most likely contain a single clone (Lefkovitz, 1979; Eshhar, 1985). The tendency of cells to clump, however, means that this mathematical explanation is not the most appropriate. To



ensure 'monoclonality' it is best to repeat the cloning procedure again for several rounds, after which the hybridoma can be statistically considered 'monoclonal' (Lietske and Unsicker, 1985). One of the main problems with seeding the cells at such low concentrations is the need to add feeder layers to increase the seeding efficiency. The use of conditioned growth media such as Briclone™ can obviate the need for such layers. Cloning in semi-solid agar is the principle alternative to limiting dilution. The medium allows the cells to easily divide and grow to produce a viable, defined colony, without permitting cells to break away and cause disperse colony development (McCullough and Spier, 1990). Isolated colonies can then be picked off with a pipette tip and transferred to fresh liquid media. A more direct approach to cloning is one that involves the use of a Peltier controlled pipette (Wewetzer and Seilheimer, 1995) to select a single colony and transfer it to the new well of a microtitre plate. This method increases confidence that only single hybridoma cells have been seeded and reduces the cloning period significantly in comparison to the traditional methods.

The strategies outlined above, allied with the methodologies detailed in sections 2.4-2.8 were exploited in an attempt to isolate stable hybridoma clones producing antibodies specific for various *L. monocytogenes*-specific pathogenicity markers. This approach was three-pronged insofar as three different antigen preparations were used in three distinct immunisation and screening/selection regimes. The first immunogen tested was a p60-enriched protein extract, crudely fractionated from the culture supernatant of exponential-phase *L. monocytogenes* cells. The second consisted of a crudely extracted, yet highly enriched wild-type InlB preparation, selectively isolated from the *L. monocytogenes* cell surface by a simple buffer extraction. The final and ultimately, most successful strategy employed formalin-inactivated whole *L. monocytogenes* cells as the primary immunogen.





## 3.2 Results and discussion

### 3.2.1 Production of a panel of monoclonal antibodies to *L. monocytogenes*-derived supernatant proteins:

#### 3.2.1.1 Precipitation of *L. monocytogenes* supernatant proteins

Supernatant from a 1 L culture of exponentially growing *L. monocytogenes* EGDpERL3 50-1 prfA<sub>EGD</sub> in BHI media that had been pre-filtered through a 10 kDa cut-off membrane filter, was collected. To remove any cell debris the supernatant was then filtered through a 0.2 µm syringe filter. The clarified supernatant was then concentrated twenty fold by ultrafiltration using a 10 kDa cut-off membrane filter. The major protein content in the concentrated supernatant was precipitated with 10 % (v/v) TCA, resuspended in PBS and dialysed extensively against PBS (Section 2.4.3). A sample of the precipitated protein fraction was resolved on a 12.5 % (w/v) SDS PAGE gel (Figure 3.10). Major bands were evident at the 30, 60 and the 66 kDa regions.

The 30 and 66 kDa proteins were most likely attributable to Internalin-related protein or 'Irp' (Lingnau *et al.*, 1996), and InlB, respectively. Both are under control of the PrfA regulator protein and thus, expected to be over-produced by this particular recombinant *L. monocytogenes* strain. The 60 kDa band was postulated to comprise principally of p60, which, although not subject to PrfA-induced over-expression, is a major extracellular protein transcribed from the *iap* gene. It is regulated at the post-transcriptional level (Köhler *et al.*, 1991) and although classically considered as a cell wall-localised protein, as much as 75 % of total expressed p60 has been reported to be present in the culture medium (Ruhland *et al.*, 1993). Listeriolysin O (Cossart *et al.*, 1989; Darji *et al.*, 1995), a 60 kDa, secreted protein, was also expected to contribute to the 60 kDa protein region on the gel. In wild-type *L. monocytogenes*, LLO is known to be produced at quite low concentrations, approximately 20 to 200 hemolytic units (HU)/ml in conventional broth culture (Geoffroy *et al.*, 1987). However, the LLO-encoding gene (*hly*) is transcriptionally regulated by PrfA and, therefore, was expected to be up-regulated in the recombinant strain employed here.

#### 3.2.1.2 Titration of LLO-specific antibody against *L. monocytogenes* supernatant proteins

Classically, antibody titre has been described as the lowest dilution of the sample that can be detected at a predetermined cut-off (Ciclitira *et al.*, 1986). Unlike using a reference curve, where values are recorded over a range of antibody/antigen dilution ratios, the titre is an end-



point measurement with a constant antibody/antigen ratio. This assumes that the coating antigen component of the assay is sufficiently in excess so that differences in affinity (particularly with polyclonal antisera) are minimised and the result is as close to the actual concentration as possible (Kemeny, 1991). It is important to emphasise that the titre end-point is not the least amount of antibody present, but the smallest quantity that can be reliably detected. Some researchers suggest taking 0.2 units above the background (Kemeny, 1992). However, this measurement would be subject to variable interpretation depending on parameters such as time and temperature of incubation and, therefore, cannot be used as generic criteria for comparative titration. For the purposes of this research, the titre was defined as the greatest antibody dilution that gave an absorbance value greater than or equal to 1.5 x the background response at the similar dilution of the control serum (in the case of polyclonal antisera) or diluent buffer (in the case of affinity-purified antibody).

LLO-specific polyclonal antiserum was kindly donated by Trinad Chakraborty and Ayub Darji (Institute for Medical Microbiology and Virology, Giessen, Germany). This was affinity purified as described in Section 2.6.3. When this affinity-purified polyclonal anti-LLO antibody was tested against various dilutions of the supernatant fraction, a titre of 1/25,600 was achieved (Figure 3.11). This indicated that there was indeed a significant amount of LLO present in the concentrated supernatant fraction.

#### **3.2.1.3 Estimation of total protein concentration in TCA-precipitated supernatant**

Total protein content in the TCA-precipitated fraction was estimated by conducting a BCA assay, as described in Section 2.3.5. BSA was employed as the protein standard since it is a globular protein of comparable molecular weight (66 kDa) to that of the principle protein of interest in the crude precipitate (60 kDa). A neat sample, in addition to a sample diluted 1 in 2 in PBS, were assayed and the resultant absorbance values were read from the standard curve (Figure 3.12), yielding an estimated total protein concentration of 853 µg/ml.

#### **3.2.1.4 Immunisation with *L. monocytogenes* supernatant proteins**

Three mice were immunised in the peritoneal cavity with TCA-precipitated protein from concentrated *L. monocytogenes* culture supernatant mixed 1:1 with Freund's complete adjuvant (FCA) at day 20, pre-fusion. Subsequent boosts were prepared in PBS at days 18, 14, 10, 6, 2 and 1, pre-fusion.



#### ***3.2.1.5 Hybridoma production using lymphocytes primed with *L. monocytogenes* supernatant proteins***

The spleens were removed from each of three immunised mice and the lymphocytes from within were harvested and pooled. Following the fusion procedure, hybridoma supernatants were screened approximately 9 days post fusion for specific antibody, as described in Sections 2.8.1 and 2.7.7.2. 'Positive' wells were scored on the basis of a positive result being greater than the control normal background reading plus 3 standard deviations (SDs), and scaled up to 48 well plates. A total of 30 wells were selected for scaling up to 24-well, 6-well and finally to tissue culture flasks. At this stage samples from each of the 30 preliminary positives were cloned out at 10 cells/well on 96 well plates. Samples were subjected to Western blot analysis. The majority demonstrated affinity towards an ~60 kDa protein band although some samples showed binding to multiple protein bands (Figure 3.13). An inhibition ELISA format (Section 2.7.7.2) was used in this second round of screening. The wells were coated with 100 µl of approximately 10 µg/ml total protein in PBS. Hybridoma supernatants were diluted 1/25 with PBS/T and 50 µl added to each well. The wells were then supplemented with 50 µl of supernatant protein at specified dilutions. The supernatant proteins were diluted to 200 µg/ml in PBS/T prior to preparing the serial dilutions. Thus, the 1/10 dilution corresponded to approximately 10 µg/ml.

Samples from 19 of the selected 30 clones demonstrated competitive binding to the free supernatant proteins and a typical profile is demonstrated in Figure 3.14. Following several rounds of cloning, hybridoma clone 'G94F8' was selected on the basis that it demonstrated stable secretion of antibody, competitive solution-phase binding to antigen and specific binding to a 60 kDa band, when used to probe the supernatant protein preparation in Western blot analysis (Figure 3.15).



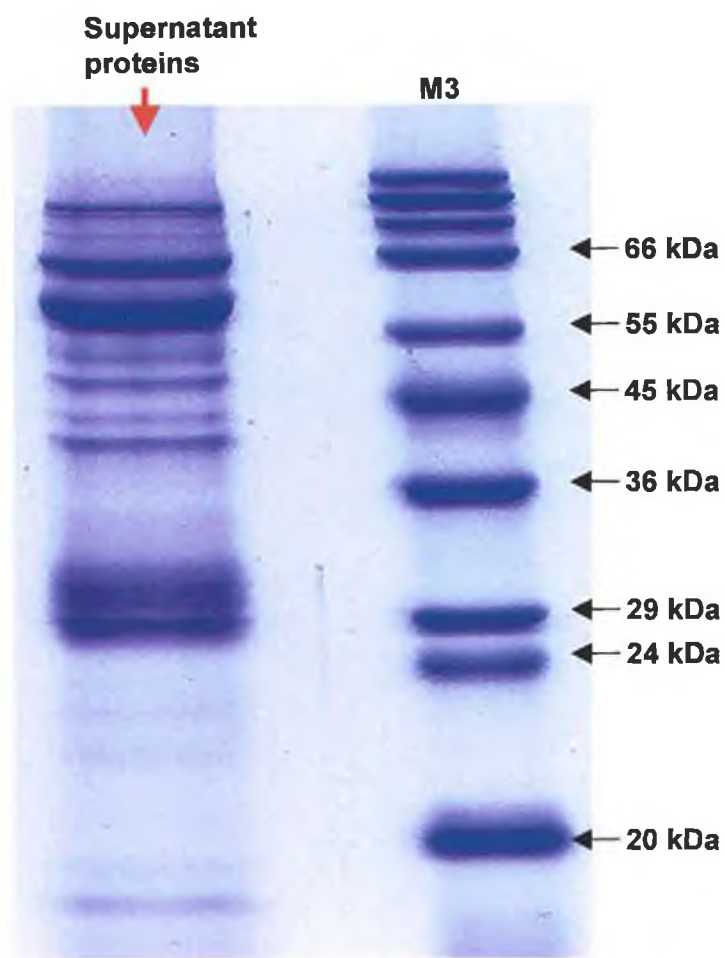


**Figure 3.10:** SDS PAGE analysis of TCA-precipitated concentrated culture supernatant derived from *L. monocytogenes* EGDpERL3 50-1 *prfA*<sub>EGD</sub>. A 12.5 % (w/v) acrylamide resolving gel was used and 20  $\mu$ l of neat sample was loaded onto the gel. Major protein bands were evident at the 30, 60 and 66 kDa region. 'M3' represents SigmaMarker™ (low range) molecular weight marker.





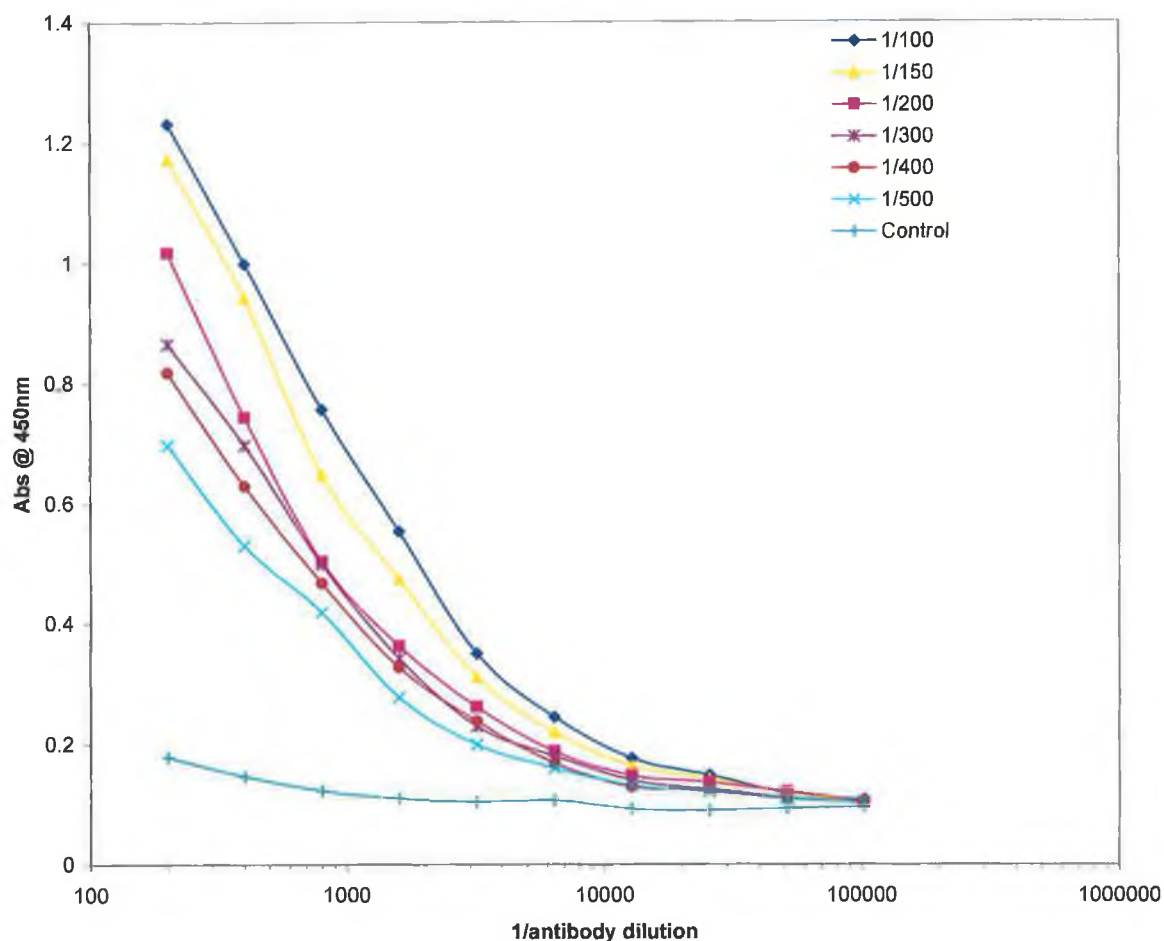


**Figure 3.11:** Estimation of listeriolysin O (LLO) content in TCA-precipitated *L. monocytogenes* supernatant. Protein G-purified polyclonal anti-LLO antibody was diluted in PBS/T and titrated against TCA-precipitated *L. monocytogenes* supernatant in a checkerboard fashion. Coating dilutions of TCA-precipitated supernatant proteins ranged from 1/100 to 1/500 in PBS. The negative control comprised of uncoated wells that had been blocked with 5 % (w/v) dried skimmed milk. The titre of the polyclonal antibody was estimated to be 1/25600, thus, indicating significant LLO content in the precipitate.



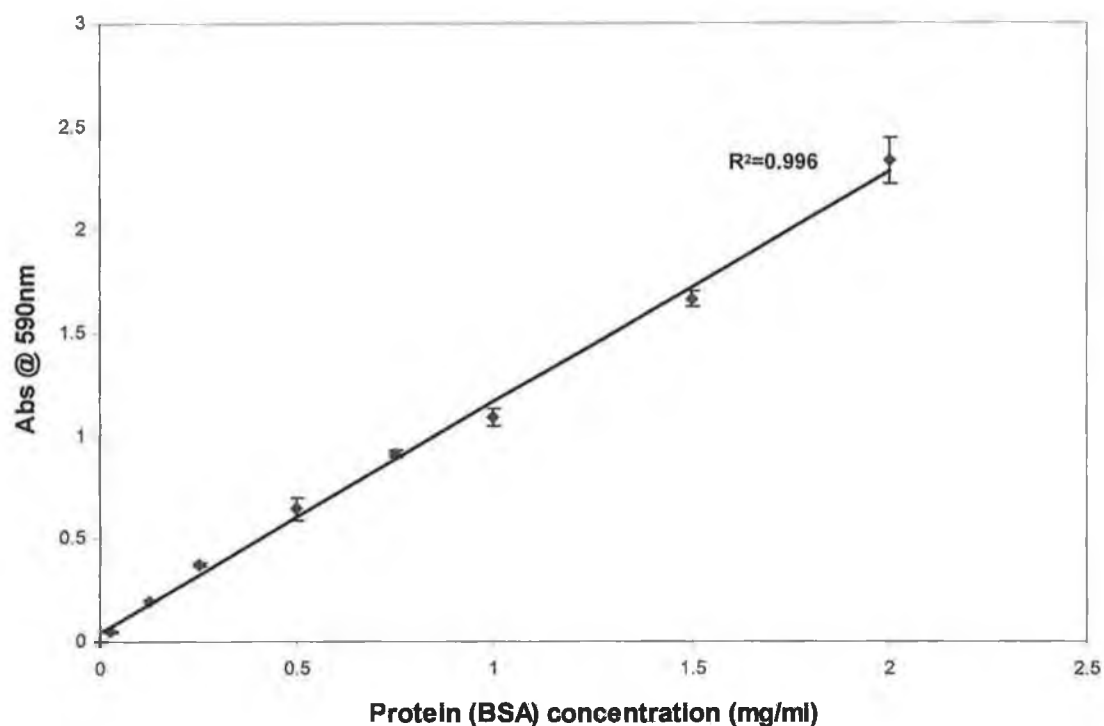


**Figure 3.12:** Standard curve for estimation of total protein concentration in TCA-precipitated fractions of *L. monocytogenes* supernatant. The assay was performed according to Section 2.3.4. The mean absorbance reading for the neat sample tested was 0.953, which, when extrapolated from the curve, corresponded to 0.812 mg/ml. The mean absorbance reading for the 1/2 diluted sample was 0.543, which, when extrapolated from the curve, corresponded to 0.894 mg/ml. The final estimate was taken as the mean of the two test determinants, 853 µg/ml.



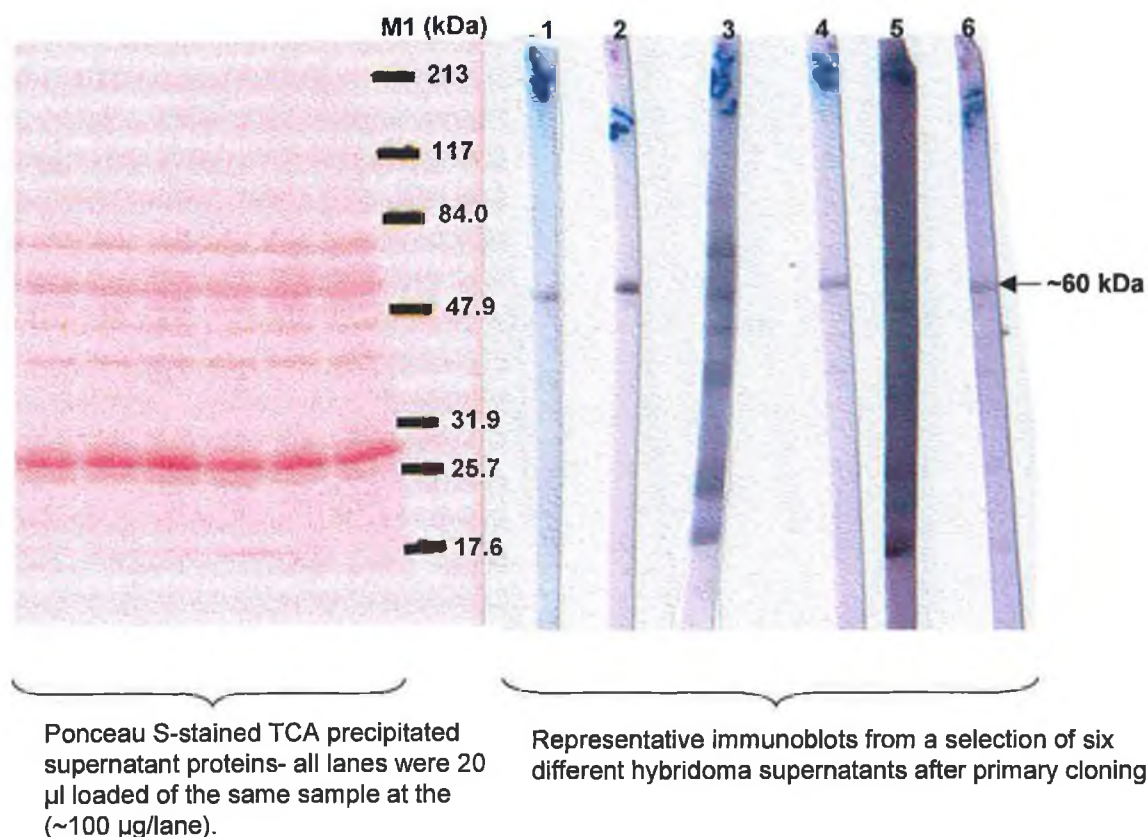


**Figure 3.13:** Western blot analysis of hybridoma supernatants after the first round of cloning by limiting dilution. The lane designated 'M3', contained SigmaMarker™ (wide range) molecular weight marker. A sample of TCA-precipitated protein from concentrated *L. monocytogenes* culture supernatant was resolved on a 12.5 % (w/v) SDS gel and the separated supernatant proteins were transferred to a nitrocellulose membrane. The membrane was then cut into strips to facilitate multiple sample screening. Most of the hybridoma supernatants tested reacted with a band in the ~60 kDa region. However, some demonstrated multiple-reactivity (e.g. immunoblots 3 and 5).



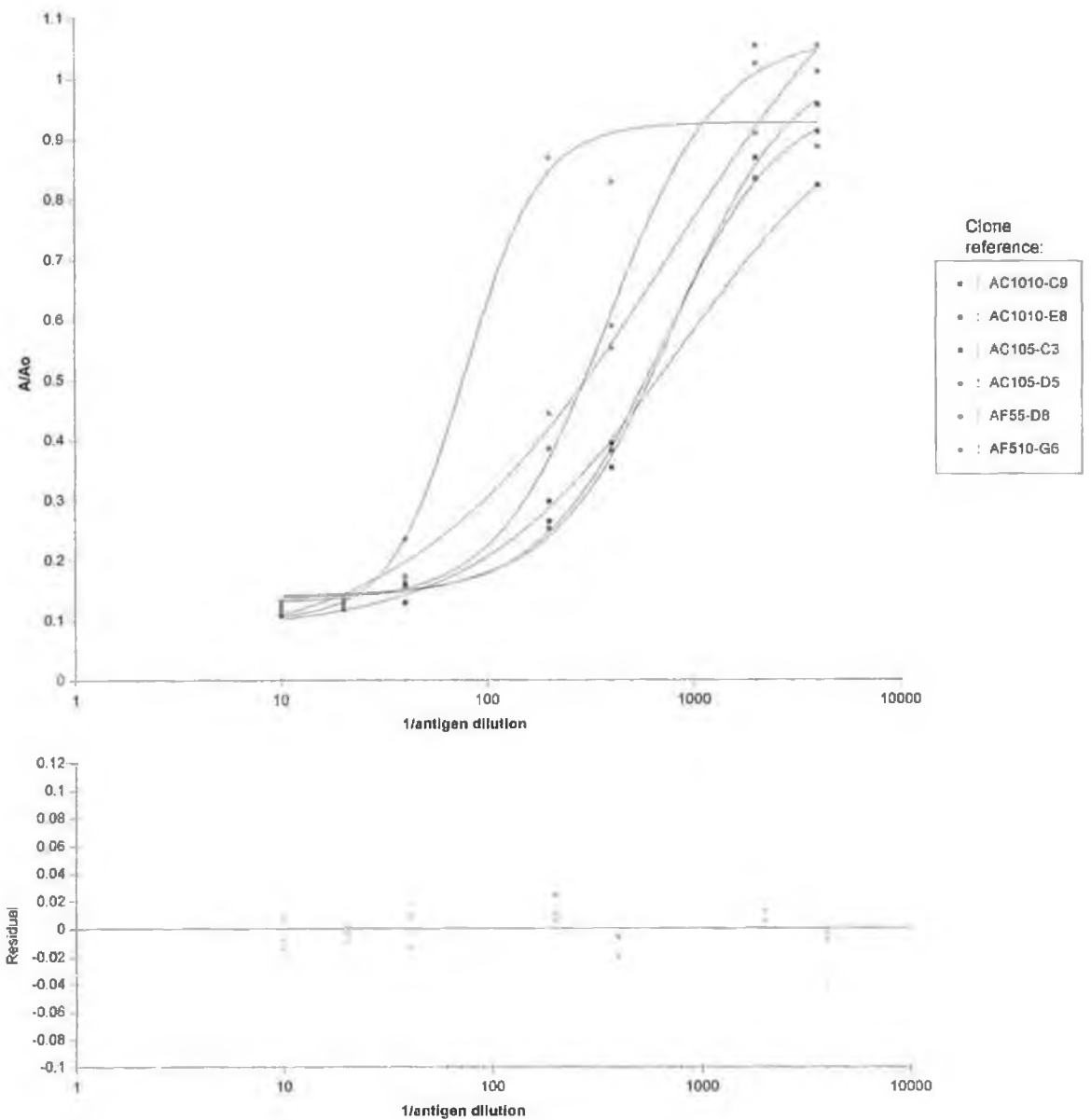


**Figure 3.14:** Typical results of solution phase inhibition ELISA for hybridoma supernatants from a selection of clones produced using lymphocytes primed with *L. monocytogenes* EGDpERL3 50-1 *prfA*<sub>EGD</sub>-derived supernatant proteins.





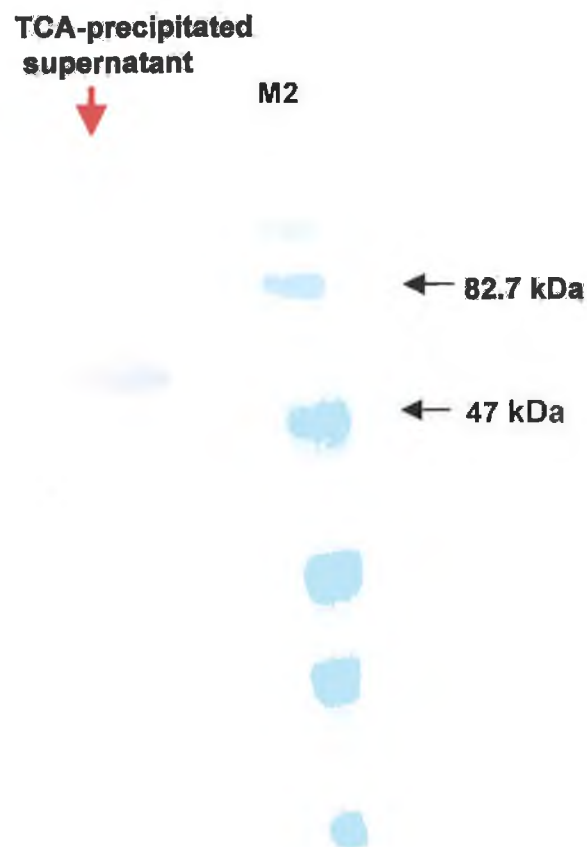


**Figure 3.15:** Western blot analysis of monoclonal antibody derived from hybridoma clone G94F8. The lane designated 'M2', contained BlueRanger® (prestained) molecular weight marker. A 20 µl sample of TCA-precipitated protein from concentrated *L. monocytogenes* culture supernatant was resolved in 12.5 % (w/v) SDS-PAGE gel and the separated protein bands were transferred to a nitrocellulose membrane. The hybridoma supernatant was used at a 1/1000 dilution in PBS/TM containing 1 % (w/v) dried skimmed milk. The purified antibody reacted with a single protein band at an approximate molecular weight of 60 kDa.



### 3.2.1.6 Affinity-purification of monoclonal antibody G94F8 (mAbG94F8)

Spent hybridoma supernatant was collected from hybridoma clone G94F8 cells that had been grown to exhaustion. The supernatant was concentrated ten fold by ultrafiltration, using a 10 kDa cut-off membrane filter. A 10 ml volume of concentrated supernatant was purified using a freshly prepared 1 ml Protein G column (Section 2.6.3). The elution profile for the purification process is demonstrated in Figure 3.16. Fractions 1-6 were pooled, desalted and resuspended in PBS buffer. The approximate concentration of purified IgG was estimated from the  $A_{280\text{nm}}$  value, assuming a molar extinction co-efficient of 1.4.

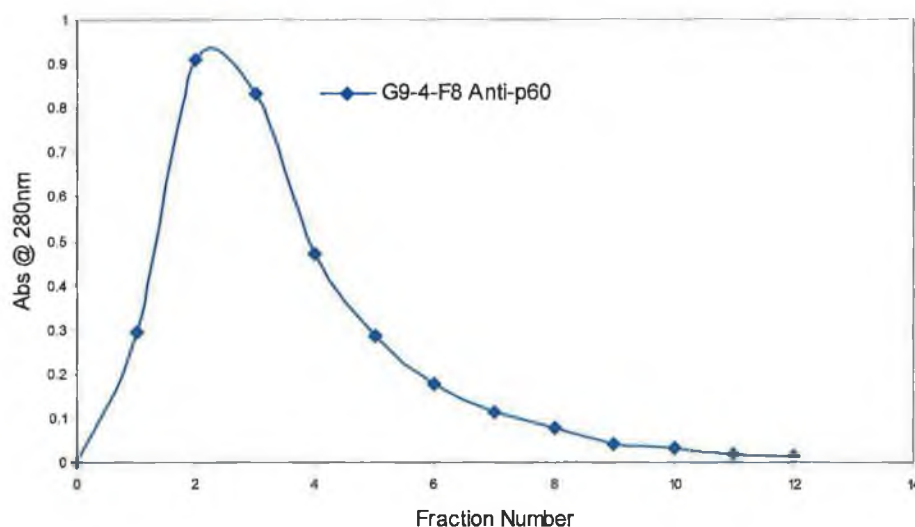


**Figure 3.16:** Typical elution profile for monoclonal G94F8 following purification on a 1 ml Protein G column. A total of 10 mls of concentrated hybridoma supernatant was applied to the column, which was then washed with 20 mls of wash buffer. Elution was performed using 0.1 M Glycine-HCl (pH 2.5) and 850  $\mu\text{l}$  fractions were collected in microcentrifuge tubes containing 150  $\mu\text{l}$  of 1 M Tris-HCl (pH 8.0) as a neutralisation buffer. Fractions 1-6 were found to contain the majority of the eluted antibody.



### 3.2.2 Characterisation of mAbG94F8

#### 3.2.2.1 Determination of mAbG94F8 isotype

The isotype of the affinity-purified mAbG94F8 was determined using ELISA, as described in Section 2.8.2. The results of the isotyping ELISA (Figure 3.17), clearly indicated that mAbG94F8 was an IgG1 type antibody, comprising kappa light chain domains.

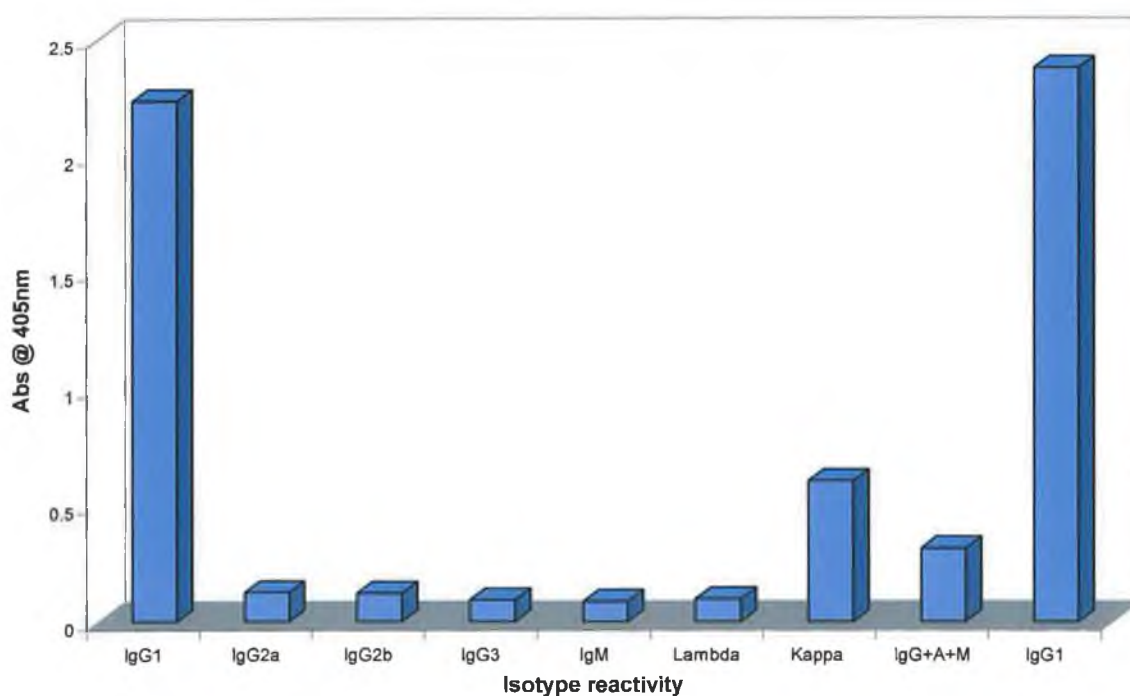


**Figure 3.17:** Isotype profile of affinity-purified monoclonal antibody (Clone G94F8). ELISA plates were coated with TCA-precipitated *L. monocytogenes* supernatant proteins at approximately 10 µg/ml. Monoclonal antibody G94F8 was used at a 1/500 dilution in PBS/T. The absorbance values indicated that the monoclonal antibody was composed of IgG1 heavy chains and kappa light chains.



### **3.2.2.2 Demonstration of solution-phase inhibition ELISA with *L. monocytogenes*-derived supernatant proteins**

ELISA plates were coated with approximately 10 µg/ml of *L. monocytogenes* EGDpERL3 50-1 prfA<sub>EGD</sub>-derived supernatant proteins in PBS. Supernatant proteins were also freshly prepared from a 50 ml culture of exponentially growing *L. monocytogenes* serotype 1/2a cells, as described in Section 2.8.4. In this instance the supernatant was not concentrated prior to precipitation with TCA. Serial dilutions of this freshly precipitated supernatant fraction were prepared in PBS/T and 50 µl of each dilution was added to the wells of the coated ELISA plate along with 50 µl of a 1/2000 dilution of affinity-purified mAbG94F8 in PBS/T. Inhibition of mAbG94F8 binding to the coated plate by the free *L. monocytogenes* 1/2a-derived supernatant proteins was clearly demonstrated (Figure 3.18).

### **3.2.2.3 Confirmation of p60-specificity of mAbG94F8**

It is almost impossible to distinguish between p60 and listeriolysin O (LLO) bands using standard SDS-PAGE resolution, as their comparable, approximate molecular weights of 58-60 kDa renders both electrophoretic mobilities identical. It was tempting to designate the reactive protein, LLO, especially since the *L. monocytogenes* strain from which the proteins were derived was the recombinant EGD pERL 3-50<sub>prfA</sub> variant, which harbours additional copies of the prfA gene. The anti-LLO polyclonal titration had confirmed there to be an appreciable LLO content in the supernatant protein fraction. Whereas expression of LLO from the *hlyA* gene is under direct transcriptional control of the PrfA protein, p60 expression from the invasion-associated protein (*iap*) gene, is independent of PrfA levels. The amount of LLO expressed in wild-type *L. monocytogenes* cells is quite low, especially when grown in rich media such as BHI, as already stated. Thus, the ability of mAbG94F8 to demonstrate solution-phase inhibition by wild-type supernatant proteins (Figure 3.18), further suggested that the protein being recognised was indeed, p60.

p60 has been shown to elicit the strongest B- and T- cell responses following exposure to *Listeria* spp. (Gentshev *et al.*, 1992; Geignat *et al.*, 1999; Kolb-Mäurer *et al.*, 2001) and although all the results thus far indicated that mAbG94F8 was specific for p60, a source of pure p60 protein was required in order to confirm the specificity. This was provided as a recombinantly-expressed *L. monocytogenes* p60 protein (rp60), by Paul Leonard (DCU, Ireland). The recombinant version comprised the complete mature *L. monocytogenes* p60 amino acid sequence fused to a C-terminal hexahistidine tag and was heterologously expressed in *E. coli*. The protein was provided in PBS buffer, following purification by immobilised metal affinity chromatography (IMAC) via the hexahistidine tag.





A neat sample (20  $\mu$ l) was resolved on a 12.5 % (w/v) acrylamide gel using SDS PAGE, to confirm that it exhibited the correct molecular weight (60 kDa) and also to assess the degree of purity. Figure 3.19(A) demonstrates that the major band corresponded to the expected molecular weight of p60 (i.e. 60 kDa) and only a small amount of lower molecular weight impurities were evident. These were attributed to inefficiencies in the IMAC purification process.

A 1/20 dilution of the rp60 protein was also prepared in PBS buffer. Following SDS PAGE, this diluted sample was transferred to a nitrocellulose membrane and subjected to Western blot analysis using the affinity-purified mAbG94F8 antibody. After substrate addition, a specific band was evident at 60 kDa, thus, strongly corroborating the postulated p60-specificity of mAbG94F8 (Figure 3.19-right). It was not possible however, to perform a comparative experiment confirming non-specificity for LLO due the unavailability of a suitably pure source of LLO. This problem was addressed later, in chapter 5 (Section 5.2.3.1.2).



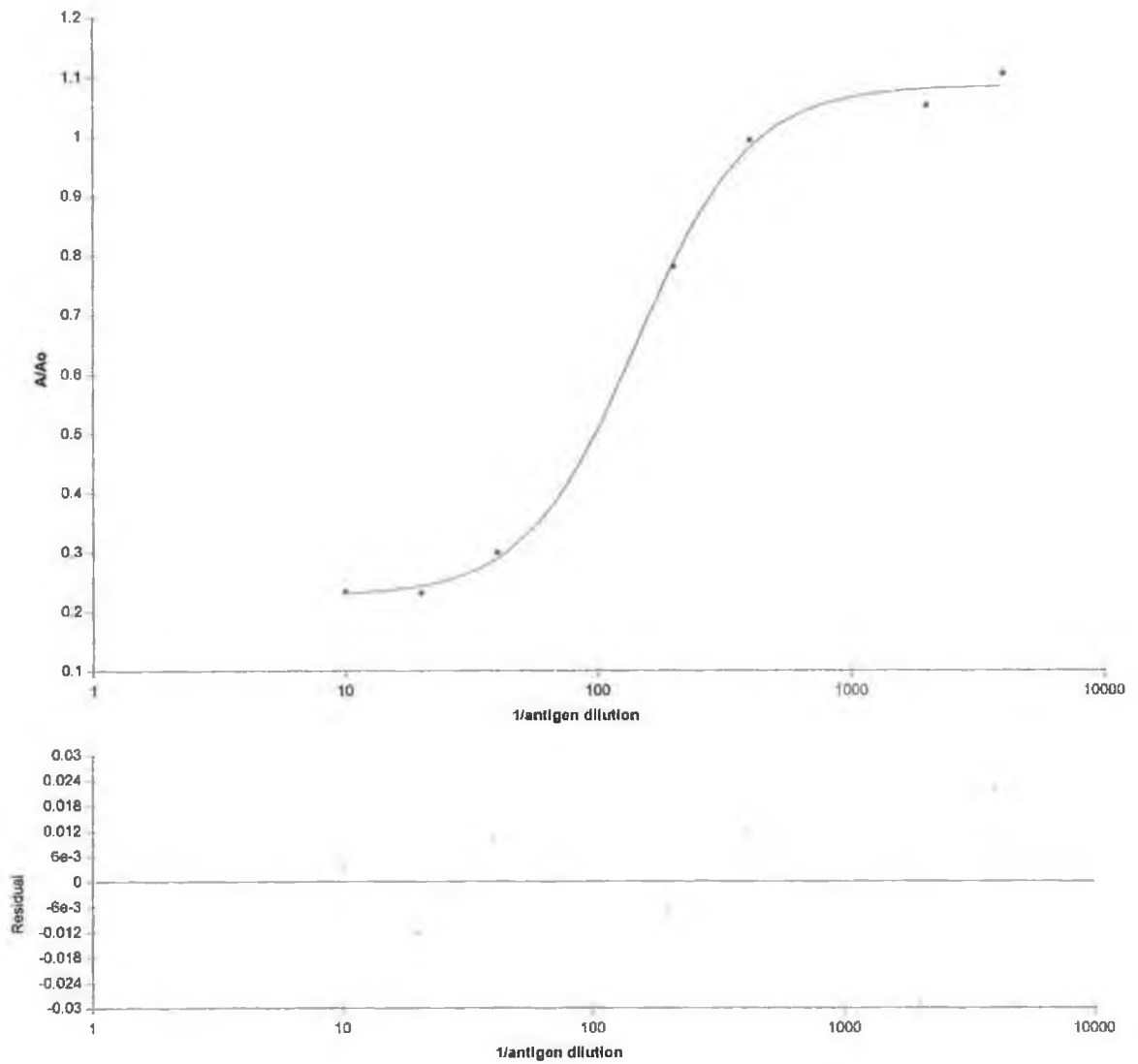


**Figure 3.18:** Inhibition ELISA using affinity-purified mAbG94F8 antibody. The competing antigen was TCA-precipitated *L. monocytogenes* serotype 1/2a-derived supernatant proteins. The supernatant proteins were diluted to 200  $\mu\text{g/ml}$  in PBS/T prior to preparing the serial dilutions. Thus, the 1/10 dilution corresponded to approximately 10  $\mu\text{g/ml}$ .



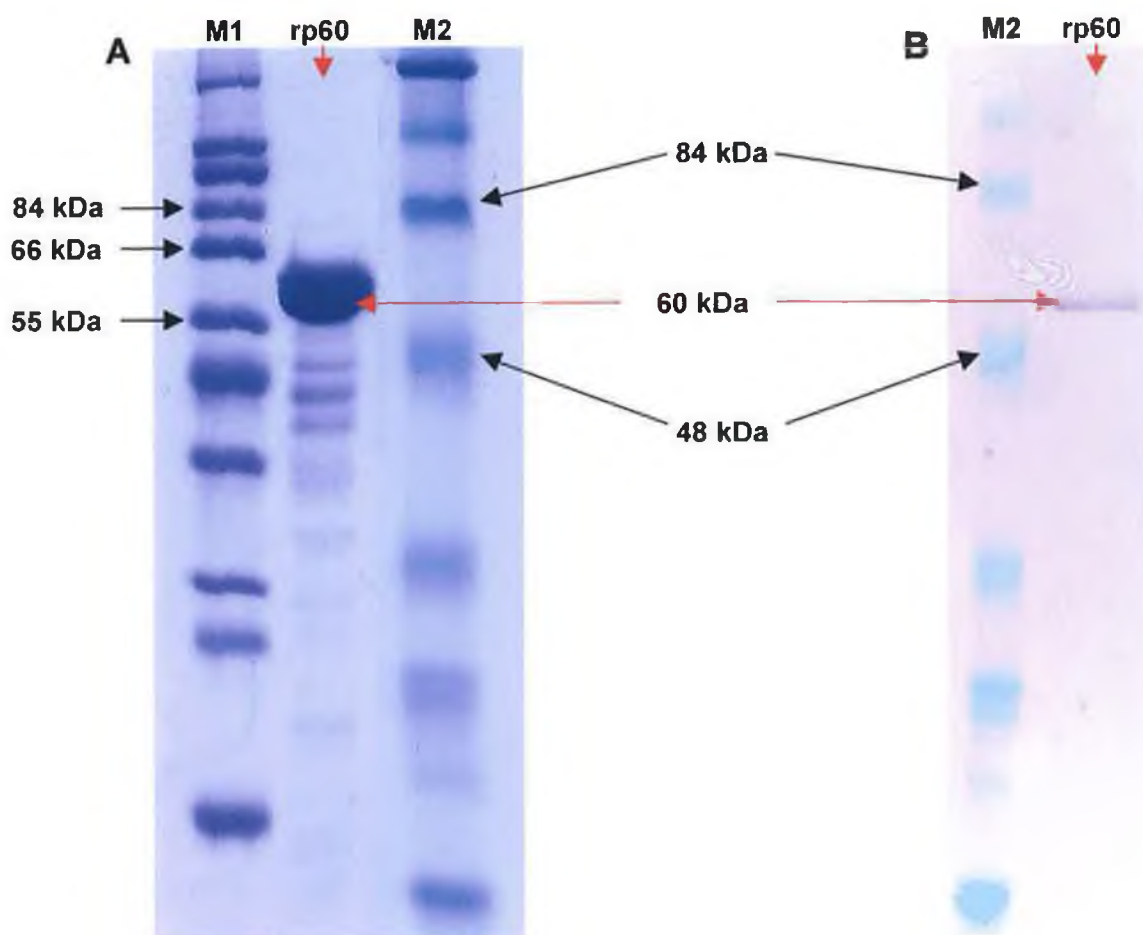


**Figure 3.19:** Immunoreactivity of mAbG94F8 towards recombinant p60 protein (rP60). The gel on the left, (A), represents 20  $\mu$ l of neat, IMAC purified rp60 in PBS resolved on a 12.5 % (w/v) SDS PAGE gel. 'M1' and 'M2' refer to SigmaWide™ (wide range) and BlueRanger® (prestained) molecular weight markers, respectively. There is one principal band apparent at approximately 60 kDa. There are also several lower molecular weight contaminating bands. It was not confirmed whether these were degradation products of the rp60 protein, or distinct impurities. The membrane on the right, (B), corresponds to a 1/50 dilution of the rp60 protein following Western blotting with mAbG94F8 used as the immunoprobng antibody at a 1/1000 dilution in PBS/TM containing 1 % (w/v) dried skimmed milk.



#### 3.2.2.4 Cross-reactivity analysis of mAbG94F8

Although the inhibition ELISA (Section 3.2.2.2), and rp60 investigations (Section 3.2.2.3) strongly suggested that mAbG94F8 recognised a *L. monocytogenes* p60 epitope, p60 homologous proteins have been reported to be present throughout the *Listeria* genus (Bubert *et al.*, 1992a; Bubert *et al.*, 1992b). It was, thus, necessary to investigate the degree of cross-reactivity and whether in fact, mAbG94F8 was specific for *L. monocytogenes*-derived p60 protein.

Supernatant protein fractions were prepared from 50 ml cultures of exponentially growing *Listeria* spp. and representative non-*Listeria* spp. The supernatant protein preparations from each test strain were then subjected to Western blot analysis using affinity-purified mAbG94F8 at a 1/2000 dilution in PBS/T (Figure 3.20). Specific binding was apparent at the expected 60 kDa position for all of the *L. monocytogenes* strains tested (*L. monocytogenes* 1/2a, 1/2c, 4a and 4b). However, mAbG94F8 also appeared to recognise 60 kDa bands in both *L. innocua* strains tested (*L. innocua* PA and PHLS) and the *L. ivanovii* PA strain. In addition, mAbG94F8 reacted with a band slightly greater than 60 kDa in *L. ivanovii* PHLS. The fact that p60 has been shown to demonstrate heterogeneous molecular weights among *Listeria* spp. (Bubert, *et al.*, 1992a) could explain why the reactive band appeared slightly greater than 60 kDa.

No apparent cross-reactivity was observed for any of the other strains examined. The status of *L. ivanovii* as a pathogen of considerable veterinary concern meant that cross-reactivity with this species could, perhaps, be tolerated and even incorporated into the development of a test for pathogenic *Listeria* spp. (i.e. *L. monocytogenes* and *L. ivanovii*). *Listeria* genus-specific immunoassays that target the p60 protein have been previously described (Bubert *et al.*, 1994; Wieckowska-Szakiel, *et al.*, 2002) and commercial assays using this strategy have also been developed (Axelsson and Sorin, 1998). However, as the stated objective was to isolate a monoclonal antibody for detecting *L. monocytogenes* of food origin, from enriched cultures, cross-reactivity with *L. innocua* was seen as a major limitation of mAbG94F8. Cross-reactivity with *L. innocua* was particularly undesirable, given that this species is often found as a co-contaminant in food and demonstrates a competitive advantage over *L. monocytogenes* in enrichment broths, thereby indicating a potential propensity for false-positive results if this anti-p60 monoclonal antibody were used for detection purposes.





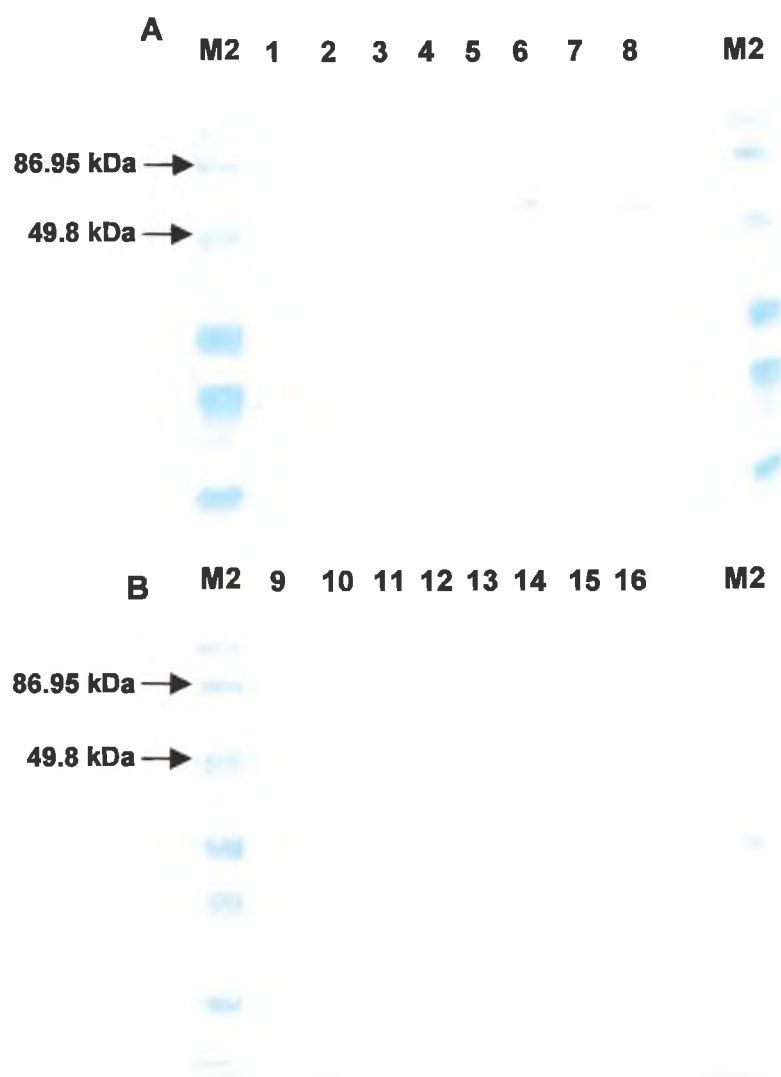


**Figure 3.20:** Western blot analysis of mAbG94F8 cross-reactivity. The top membrane (A) represents supernatant proteins derived from: (1), *L. monocytogenes* 1/2a; (2), *L. monocytogenes* 1/2c; (3), *L. monocytogenes* 4a; (4), *L. monocytogenes* 4b; (5), *L. innocua* PA; (6), *L. innocua* PHLS; (7), *L. ivanovii* PA and (8), *L. ivanovii* PHLS. The bottom membrane (B) represents supernatant proteins derived from: (9), *L. welshimeri*; (10), *L. seeligeri*; (11), *E. coli*; (12), *B. subtilis*; (13), *B. cereus*; (14), *S. faecilis*; (15), *E. aerogenes* and (16), BHI broth precipitate (negative control). Since neither *L. innocua* nor *L. ivanovii* produce LLO, the binding of mAbG94F8 evidenced here was further confirmation that p60 was the protein being recognised by mAbG94F8. The lanes designated 'M2', contained BlueRanger® (prestained) molecular weight marker.



### **3.2.3 Production of a panel of monoclonal antibodies to InlB**

#### **3.2.3.1 Preparation of *L. monocytogenes*-derived InlB-enriched extract**

InlB was extracted from the surface of PBS-washed *L. monocytogenes* EGDpERL3 50-1 *prfA*<sub>EGD</sub> cells by incubating the cells with 1 M Tris-HCl on ice for 1 hour (Section 2.4.2). This method has been shown to provide superior quantitative extraction of InlB, which possesses a very high isoelectric point of 10.1 (Müller *et al.*, 1998a). It is hypothesised that the high ionic strength of the Tris-HCl extractant interferes with the amino-carboxylate salt bridges anchoring InlB to the cell surface and this mediates the release of InlB. The extract was dialysed extensively against PBS.

A 20 µl sample of the dialysed extract was analysed by SDS PAGE (Figure 3.21) to confirm the efficacy of the extraction process and to assess the approximate degree of purity. The major protein band was evident at 66 kDa, which, corresponded to the molecular weight of InlB.

#### **3.2.3.2 Estimation of total protein concentration in the Tris-HCl extract**

Total protein content in the InlB-enriched, Tris-HCl extract was estimated by conducting a BCA assay, as described in Sections 2.3.5 and 3.2.1.3. BSA was again employed as the protein standard since it is a globular protein of identical molecular weight (66 kDa) to that of the principle protein of interest in the extract, InlB. A neat sample, in addition to a sample diluted 1 in 2 in PBS, were assayed and the resultant absorbance values were read from the standard curve of net absorbance at 590 nm versus protein (BSA) concentration (mg/ml), as in Section 3.2.1.3. The estimated total protein concentration was calculated to be 720 µg/ml.

#### **3.2.3.3 Immunisation with *L. monocytogenes*-derived InlB-enriched extract**

Balb/C mice were immunised via the peritoneal cavity with InlB-enriched, Tris-HCl extract of *L. monocytogenes* EGDpERL3 50-1 *prfA*<sub>EGD</sub> cells, mixed 1:1 with Freund's Complete adjuvant (FCA). Subsequent boosts were prepared in Freund's Incomplete adjuvant (FICA) and administered by i.p. injection over a period of 6-8 months. When the specific serum titre was deemed sufficiently high (Figure 3.22), the mice were primed for fusion. This consisted of administering booster i.p injections prepared in PBS on days 5 and 3 before fusion. The final boost was administered in pre-warmed (37 °C) PBS on day 1 before fusion, intravenously, via the tail vein.



#### **3.2.3.4 Hybridoma production using lymphocytes primed with *L. monocytogenes*-derived InlB-enriched extract**

On the day of the fusion (day 0), the spleen was removed from one primed mouse and the lymphocytes from within were harvested. Following the fusion procedure, hybridoma supernatants were screened approximately 9 days post fusion for specific antibody as described in Sections 2.7.7.2 and 2.8.1. In excess of 85 % of the wells tested demonstrated 'positive' reactivity towards the plates coated with InlB. 'Positive' wells were initially scored on the basis of a positive result being greater than the control normal background reading + 3 standard deviations. Due to such a high percentage of 'positives' a higher nominal cut-off value of 0.5 absorbance units at 405 nm was employed. In addition, wells that exhibited a low number of defined colonies were preferentially selected above those which contained a visibly higher proportion of multiple, defined colonies. The selected well populations were scaled up to 24 well plates. An inhibition ELISA format (Section 2.8.1) was used in this second and all subsequent rounds of screening and a typical profile for a selection of isolated clones is demonstrated in Figure 3.23. Following several rounds of cloning, hybridoma clone 'G54D4' was selected on the basis that it demonstrated stable secretion of antibody and competitive solution-phase binding to the InlB-enriched, Tris-HCl extract.



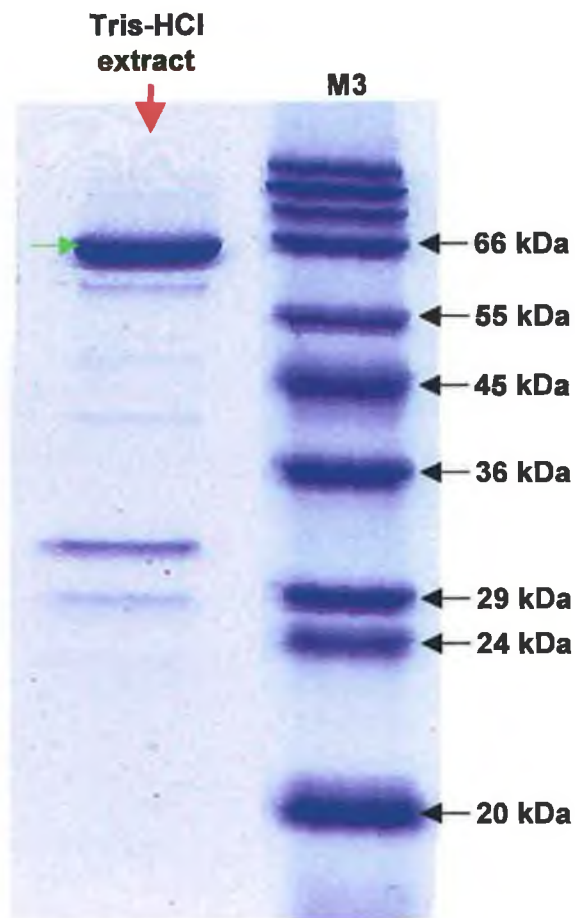


**Figure 3.21:** SDS-PAGE analysis of the *InlB*-enriched, Tris-HCl-extracted *L. monocytogenes* EGDpERL3 50-1 *prfA*<sub>EGD</sub> surface proteins, resolved on a 12.5% (w/v) acrylamide gel. Lane 'M3', contained SigmaWide™ (low range) molecular weight marker. The 66 kDa band was very prominent and assumed to principally comprise of *InlB*. Only a small number of significantly less pronounced contaminating bands were evident. Overall, the analysis demonstrates the efficiency of the crude extraction procedure.





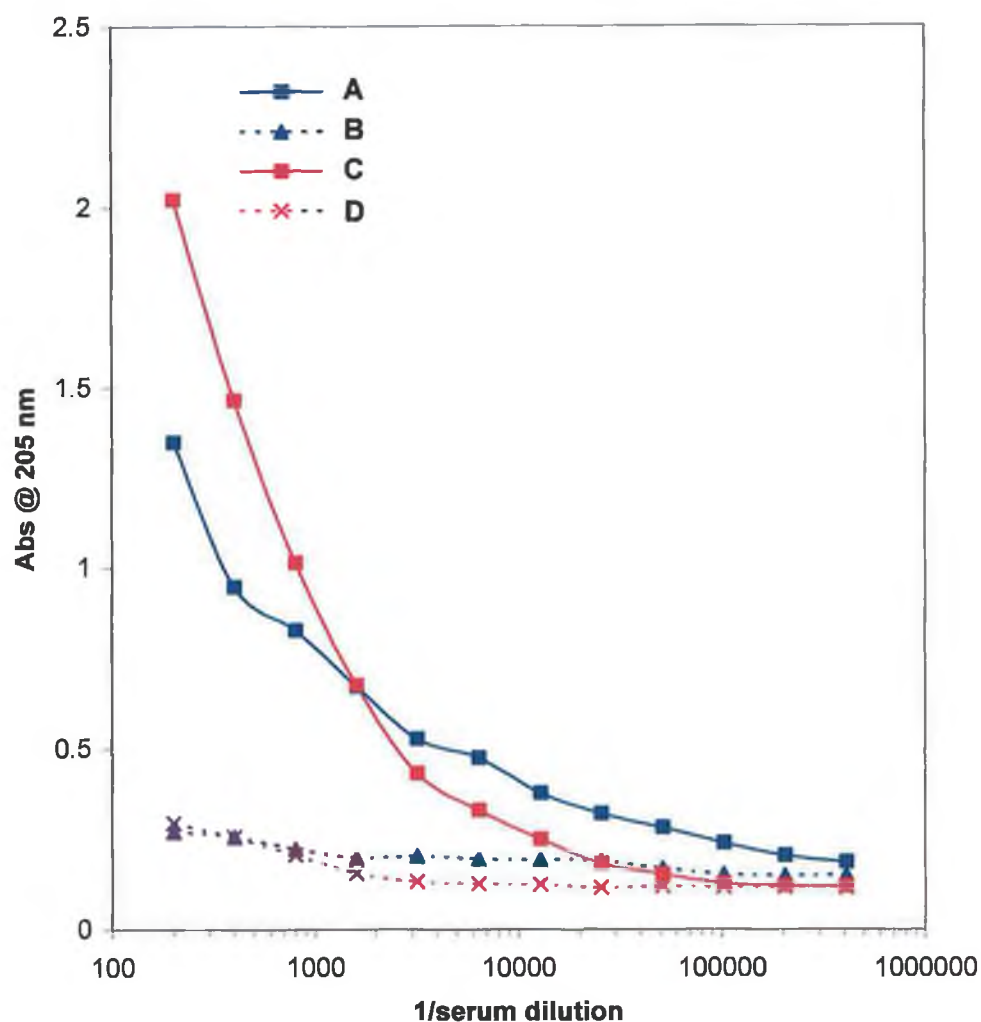


**Figure 3.22:** Specific serum antibody titre from mouse that had been immunised with InlB-enriched Tris-HCl extract. 'A' and 'B' represent a serum sample taken from the immunised mouse and a control serum taken from a naïve, non-immunised mouse, respectively. Both were screened against InlB-enriched Tris-HCl extract at a coating concentration of 10 µg/ml. The same serum samples were also screened against heat-killed *L. monocytogenes* 1/2a cells at  $1 \times 10^9$  cells/well (C and D). The specific titre obtained was 1/102,400 when screened against InlB-enriched Tris-HCl extract and 1/51,200, when screened against heat-killed *L. monocytogenes* 1/2a cells. This was deemed sufficiently high to proceed with the fusion process.



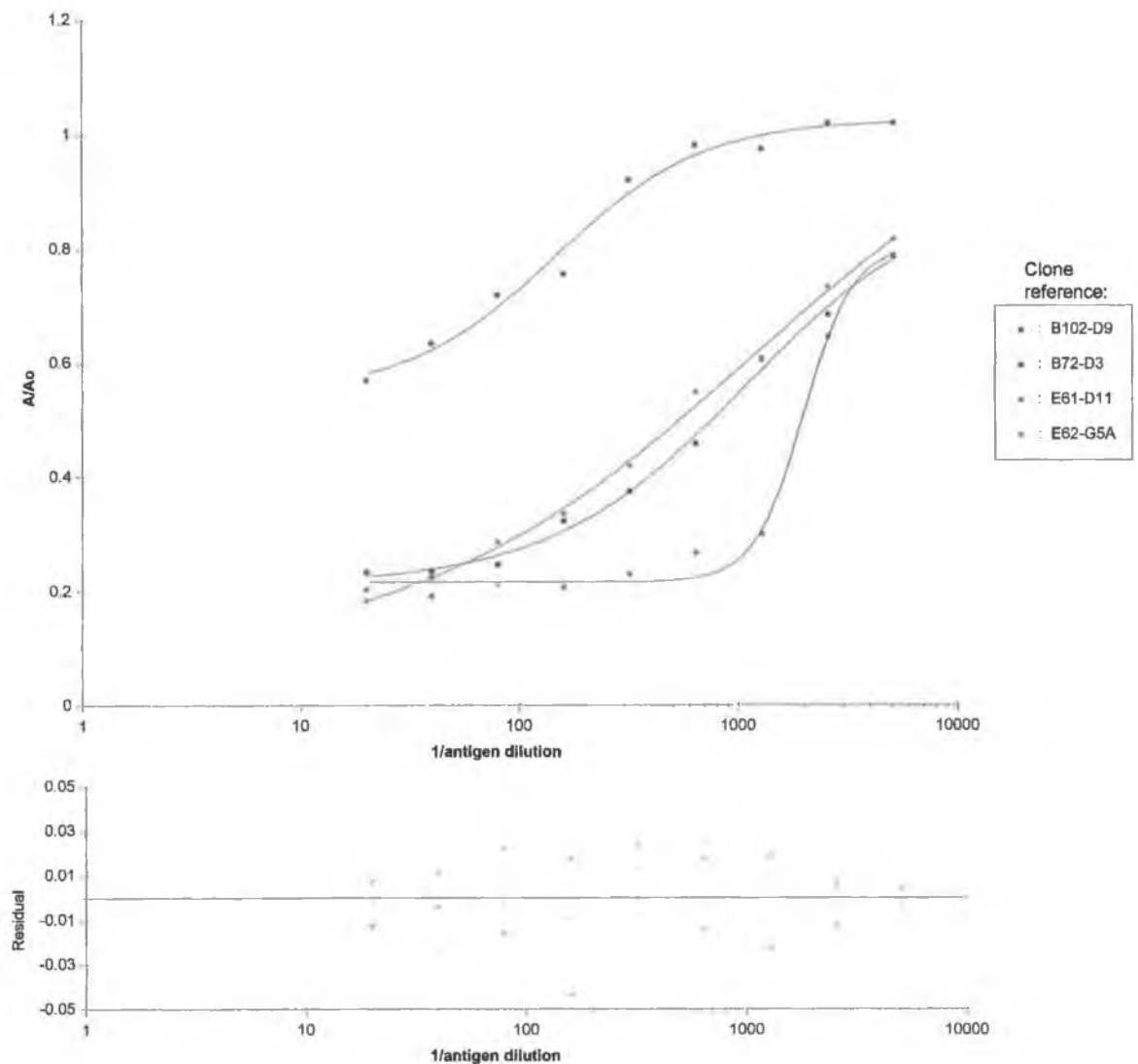


**Figure 3.23:** Typical results of solution phase inhibition ELISA for hybridoma supernatants from a selection of clones produced using lymphocytes primed with *L. monocytogenes*-derived InlB-enriched Tris-HCl extract. The wells were coated with 100  $\mu$ l of approximately 10  $\mu$ g/ml total protein in PBS. Hybridoma supernatants were diluted 1/100 with PBS/T and 50  $\mu$ l added to each well. The wells were then supplemented with 50  $\mu$ l of Tris-HCl extract at specified dilutions. The supernatant proteins were diluted to 200  $\mu$ g/ml in PBS/T prior to preparing the serial dilutions.



### 3.2.4 Characterisation of anti-InlB monoclonal antibody (mAbG54D4)

#### 3.2.4.1 Determination of mAbG54D4 antibody isotype

The isotype of the anti-InlB antibody secreted in hybridoma G54D4 supernatant was determined by ELISA, as described in Section 2.8.2. The results of the isotyping ELISA (Figure 3.24), clearly indicated that mAbG54D4 was an IgG1 type antibody, comprising kappa light chain domains. Although the hybridoma had been fully cloned out by limiting dilution, the background values across the isotype range tested were slightly higher than expected, particularly for isotypes IgG2a and IgG2b. This was attributed to the fact that the monoclonal had not been purified prior to testing and thus the hybridoma supernatant contained heterogenous proteins such as BSA at appreciable concentrations.

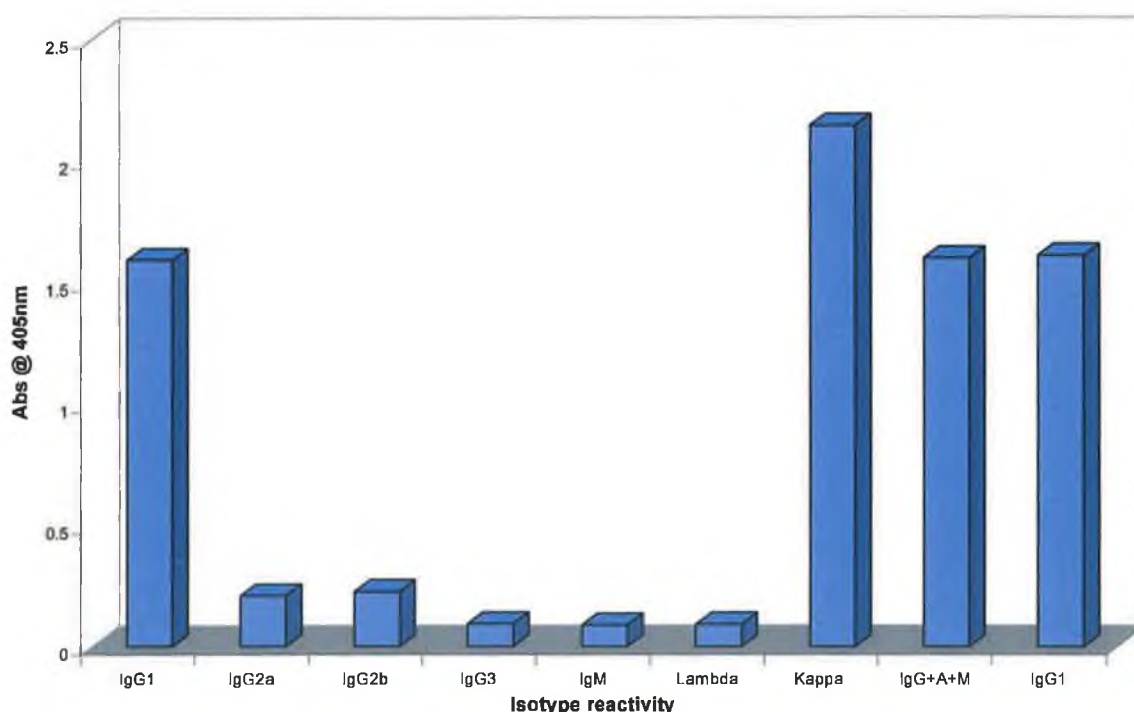


**Figure 3.24:** Isotype profile of anti-InlB monoclonal antibody in hybridoma supernatant from clone G54D4. ELISA plates were coated with InlB-enriched, Tris-HCl extract at a coating concentration of approximately 10 µg/ml. G54D4 hybridoma supernatant was employed at a 1/10 dilution in PBS/T. The absorbance values indicated that the monoclonal antibody was composed of IgG1 heavy chains and kappa light chains.



#### 3.2.4.2 Immunoreactivity of mAbG54D4 towards Tris-HCl extract

A 20  $\mu$ l sample of *L. monocytogenes* EGDpERL3 50-1 prfA<sub>EGD</sub>-derived, InlB-enriched, Tris-HCl extract was resolved on a 12.5 % (v/v) acrylamide gel (Sections 2.3.2 and 3.2.3.1) and transferred to a nitrocellulose membrane (Section 2.3.4). The membrane was blocked with 5 % (w/v) milk in PBS/T and then probed with a 1/10 dilution of fresh mAbG54D4 hybridoma supernatant in PBS/TM containing 1 % (w/v) milk (Figure 3.25). The mAbG54D4 supernatant was shown to react with a single ~66 kDa band, that was assumed to represent the InlB fraction in the Tris-HCl extract.

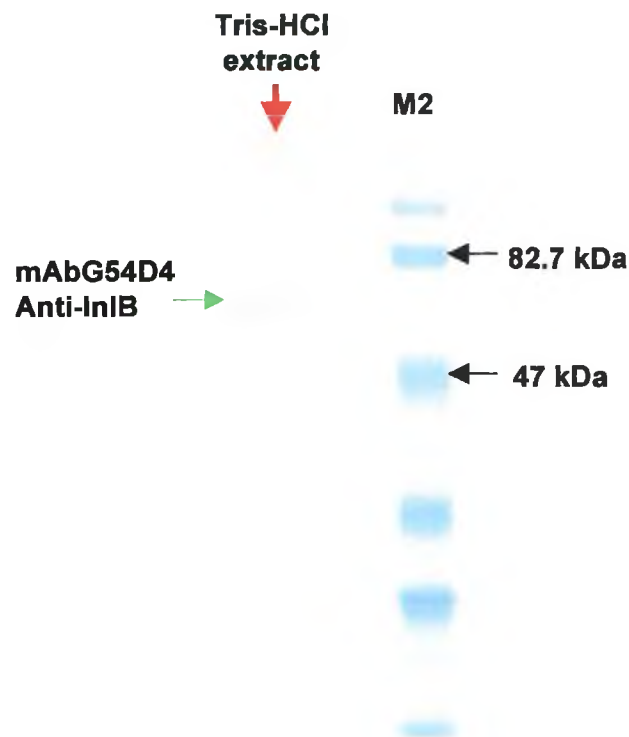


**Figure 3.25:** Western blot analysis of InlB-enriched, Tris-HCl-extracted *L. monocytogenes* EGDpERL3 50-1 prfA<sub>EGD</sub> surface proteins with mAbG54D4. A specific band was obtained at ~66 kDa, corresponding to the molecular weight InlB. The lane on the right, designated 'M2' contained BlueRanger® (prestained) molecular weight markers.





### 3.2.4.3 Solution-phase immunoreactivity of mAbG54D4- inhibition ELISA

In order to ensure that the solution-phase binding capacity of mAbG54D4 had not been compromised during the cloning-out process, an inhibition ELISA was performed (Section 2.8.4). The ELISA plate was coated with approximately 10 µg/ml of *L. monocytogenes* EGDpERL3 50-1 prfA<sub>EGD</sub>-derived, InlB-enriched, Tris-HCl extract. A dilution series of Tris-HCl extract was prepared in PBS/T, from an initial stock solution at a concentration of approximately 200 µg/ml total protein and 50 µl from each of the dilutions were added to the ELISA wells. Next, 50 µl of fresh mAbG54D4 hybridoma supernatant (diluted 1/250 in PBS/T) was added to each of the wells. Thus, the 1/100 dilution of extract corresponded to approximately 1 µg/ml, the 1/1000 dilution corresponded to approximately 0.1 µg/ml, etc. In addition, to assess solution phase binding to cell bound InlB, a similar inhibition series was set up using live *L. monocytogenes* cells and mAbG54D4 hybridoma supernatant at the same dilution. In order for the test to simulate a real detection scenario, wild type *L. monocytogenes* serotype 1/2a (expressing normal, wild type levels of InlB) was used instead of the recombinant *L. monocytogenes* EGDpERL3 50-1 prfA<sub>EGD</sub> strain. Live *L. monocytogenes* 1/2a cells were prepared in PBS/T at a starting stock concentration of approximately  $5 \times 10^{11}$  cells/ml and thus, the 1/100 dilution corresponded to approximately  $2.5 \times 10^{10}$  cells/ml, the 1/1000 dilution corresponded to approximately  $2.5 \times 10^9$  cells/ml, etc

The findings (Figure 3.26) indicated that mAbG54D4 demonstrated solution-phase binding to InlB-enriched, Tris-HCl extract, with inhibition apparent at levels in excess of 270 ng/ml of extract. No apparent inhibition was achieved with *L. monocytogenes* cells. However, as a caveat, these observations must be qualified by acknowledging that the inhibition assay had not been optimised in terms of antigen coating concentration or antibody working dilution prior to the analysis. It is expected that the assay sensitivity for the InlB-enriched Tris-HCl extract could be improved following judicious parameter optimisation. Nonetheless, it would appear, from the inability of very high concentrations of *L. monocytogenes* cells to elicit inhibition, that a comparable improvement in sensitivity, with respect to detection of cells, could not be achieved.



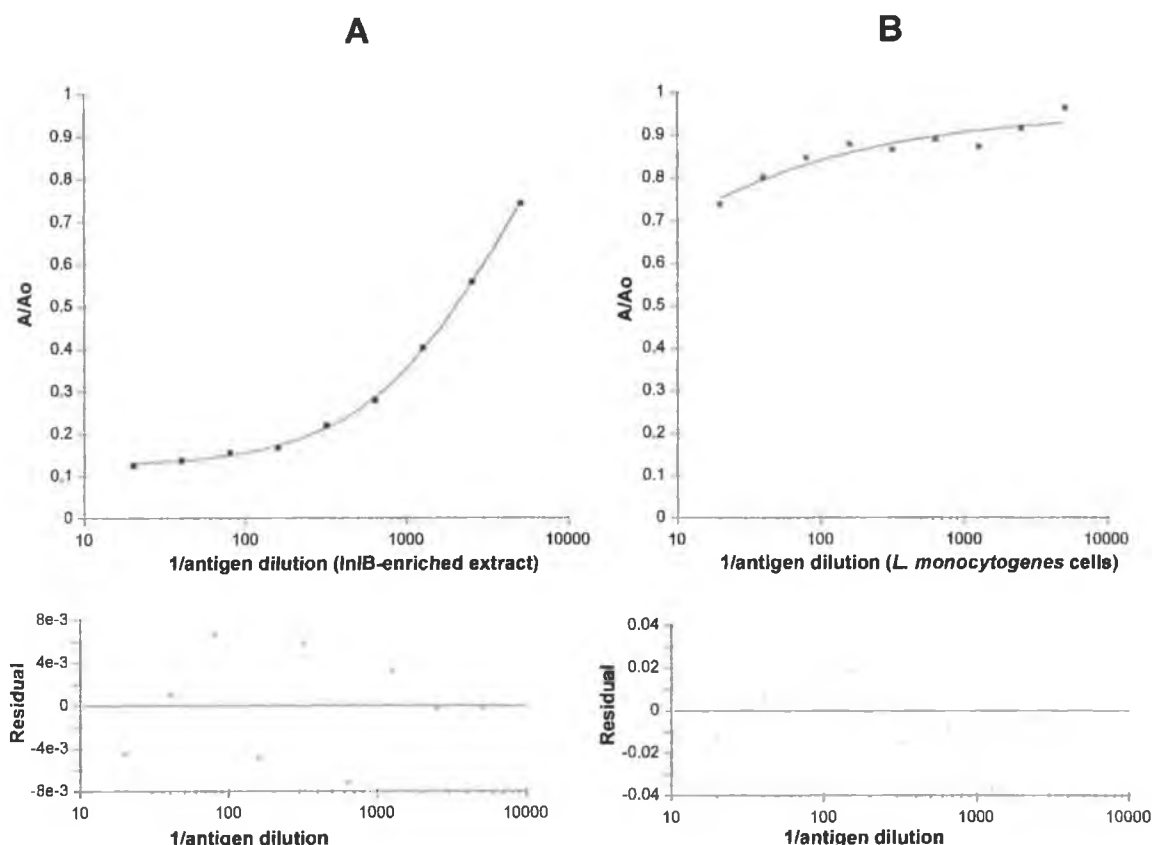


**Figure 3.26:** Inhibition ELISA using mAbG54D4 hybridoma supernatant at a 1/1000 dilution in PBS/T (effective dilution, 1/2000) against free InlB-enriched, Tris-HCl extract (A) and *L. monocytogenes* cells (B). The range of inhibition with respect to the Tris-HCl extract was between 2.5  $\mu\text{g/ml}$  and 270  $\text{ng/ml}$ . In fact, the lower limit may have been substantially less than 270  $\text{ng/ml}$ , however, since the assay did not reach a curve saturation point it was not possible to extrapolate an exact cut-off. Unfortunately, the presence of cells did not appear to induce any significant level of competitive inhibition of mAbG54D4 to the immobilised Tris-HCl extract across the range of concentrations tested.

#### 3.2.4.4 Determination of cell-binding potential mAbG54D4

The apparent inability of mAbG54D4 to bind *L. monocytogenes*-bound InlB protein, as indicated by the results in Section 3.2.4.3, was seen as a major limitation to the application of mAbG54D4 in an assay for the detection of *L. monocytogenes* cells. Given, that the serum sample from the immunised mouse used in the fusion, had demonstrated a significant titre against both the InlB-enriched, Tris-HCl extract (1/102400) as well as *L. monocytogenes* EGDpERL3 50-1 prfA<sub>EGD</sub> cells (1/51200), this problem had not been anticipated. However, given the polyclonal nature of the serum and the heterogenous protein impurities evident in



the crude Tris-HCl extract (Figure 3.21) it was entirely possible that the cell binding antibody component of in the serum, was specific for one of these unidentified proteins and that this was the reason for the discrepancy between the polyclonal mouse serum and the selected, anti-InlB monoclonal antibody, in terms of their cell binding capacity. This may be seen to reflect an inherent flaw and short-sightedness in the screening and selection process. It is acknowledged that screening against whole cells may have revealed a more appropriate antibody, capable of reliably binding the *L. monocytogenes* via the cell-bound form of InlB. However, in regard to this issue, it is pertinent to note that the aim of this particular strategy was to exploit the specific expression of InlB by *L. monocytogenes* spp. as a cell surface-localised protein, by efficiently targeting this particular protein to produce a correspondingly, *L. monocytogenes*-specific monoclonal antibody.

The cells used in the serum titration were *L. monocytogenes* EGDpERL3 50-1 prfA<sub>EGD</sub> that had been heat-killed by inactivation at 80 °C for 25 minutes, whereas, the cells used in the inhibition assay (Section 3.2.4.3) were live, wild-type *L. monocytogenes* 1/2a cells. In order to assess the effect of heat killing process and over-expression of InlB by *L. monocytogenes* cells, on the capacity of mAbG54D4 to bind cells, a simple, direct ELISA was performed (Section 2.8.1). Individual sets of microplate wells were coated with samples of heat-killed and live, wild-type and recombinant, *L. monocytogenes* cells. The test wells were then incubated with 100 µl of mAbG54D4 hybridoma supernatant diluted 1/2 in PBS/T. Although the overall absorbance response values were low, there did appear to be a slightly higher propensity for binding to the recombinant strain (Figure 3.27). This was hardly surprising given that it was capable of expressing significantly higher levels of InlB protein. More significant, was the fact that mAbG54D4 also exhibited an apparent predilection for cells that had been heat-killed. This suggested that the cell wall morphology may have been preventing the antibody binding to InlB and that the heat-killing process altered the morphology sufficiently to render the epitope-bearing region recognised by mAbG54D4 more accessible.



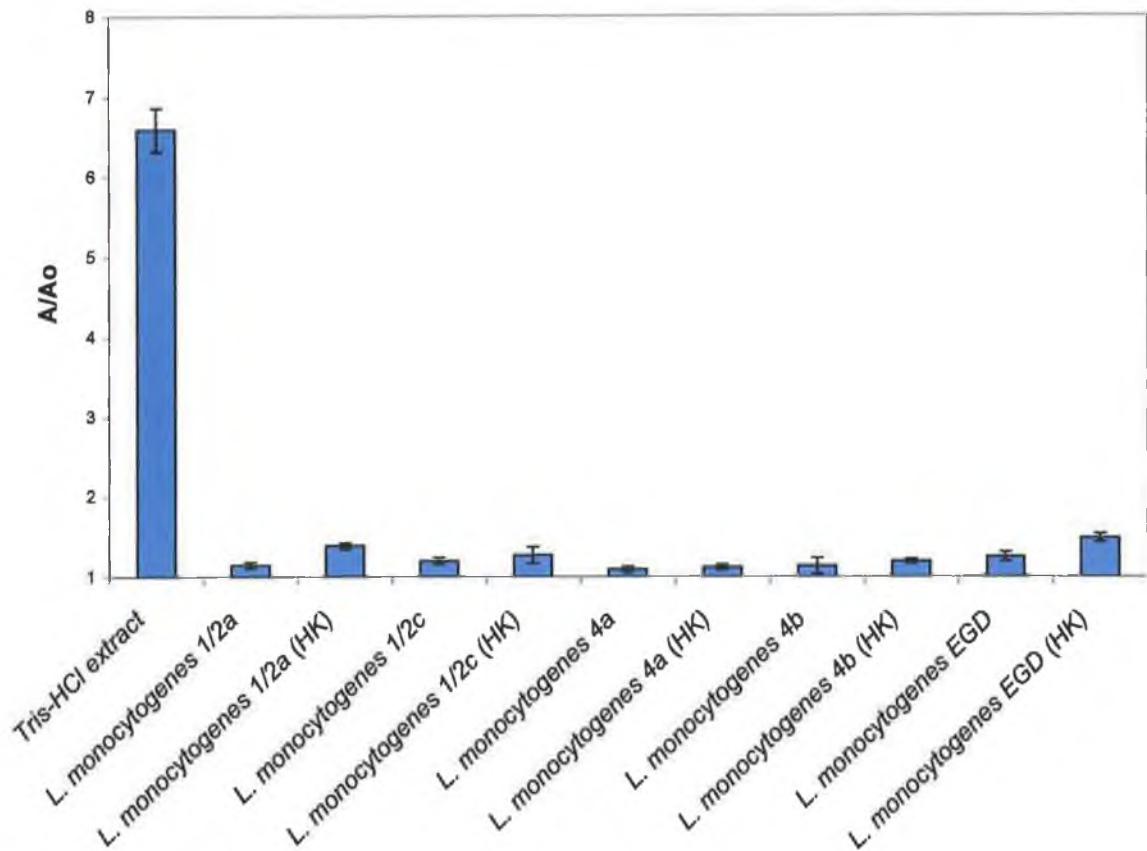


**Figure 3.27:** Direct cell ELISA for determination of mAbG54D4 cell binding capacity ( $n=3$ ). Wells were coated with approximately  $1 \times 10^{11}$  cells/ml. 'HK' denotes heat-killed cells and 'L. monocytogenes EGD' refers to *L. monocytogenes* EGDpERL3 50-1 *prfA*<sub>EGD</sub>. The G54D4 hybridoma supernatant was used at a 1/2 dilution in PBS/T and an additional set of wells were coated with InlB-enriched, Tris-HCl extract (approximately 20  $\mu\text{g/ml}$ ) to act as a positive control. Despite the high cell coating concentration and minimally diluted supernatant, only very weak binding to cells was evident. The strongest response was for the *L. monocytogenes* 1/2a and EGD strains. In both strains there was a slight increase in apparent response between the native and heat-killed cells.





The crystal structure of the major domain components of the InlB protein has been published (Marino *et al.*, 1999). The mature protein consists of four distinct domains (as outlined in Figure 3.28). A recombinant version of the complete InlB protein (1), as well as, several truncated variants, were kindly provided by Paul Leonard and Liz Tully (DCU, Ireland). The truncated versions comprised of the mature InlB protein minus (2), the GW repeat anchor region; (3) the GW repeat anchor region and the B repeat region and (4) the GW repeat anchor region, the B repeat region and the IgG-like domain.

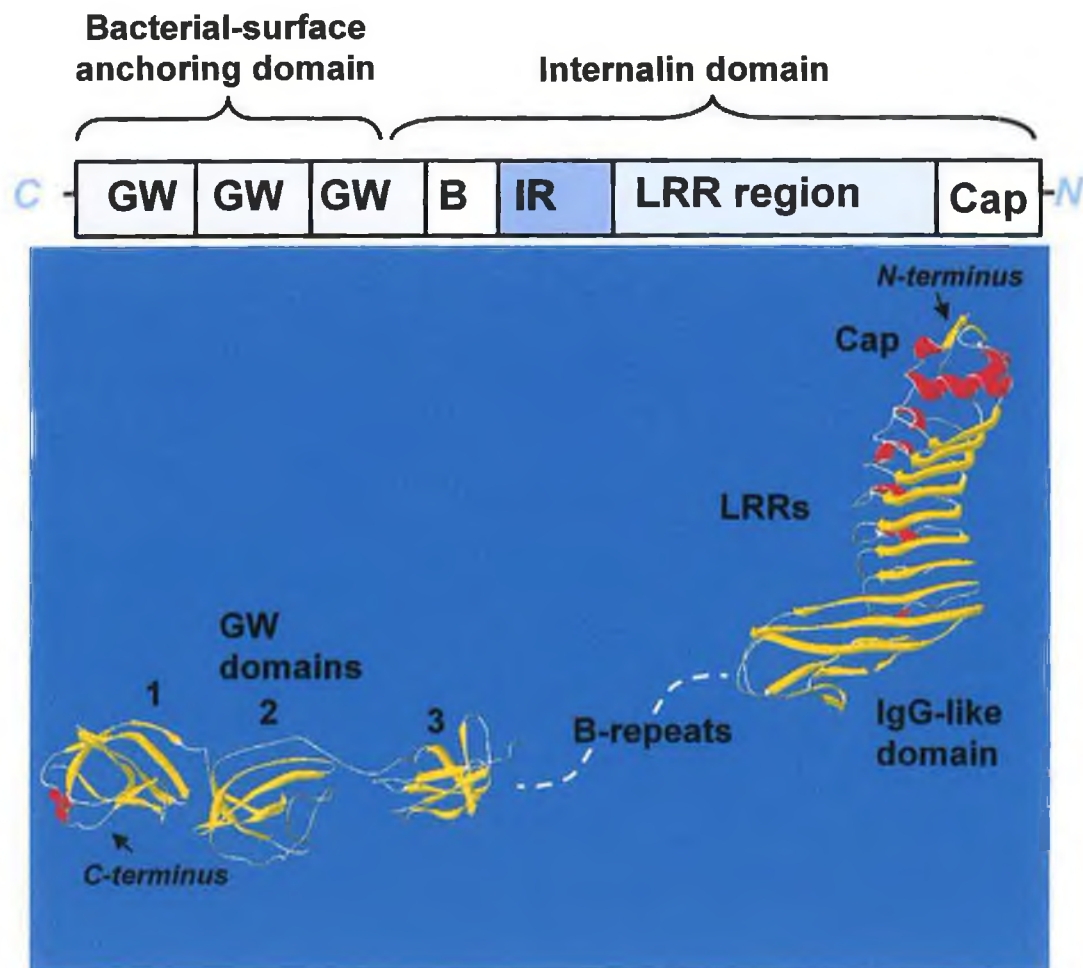


**Figure 3.28:** Outline of the tertiary domain structure of mature InlB protein from available crystallographic data (PDB reference code: 1M9S, adapted from Marino *et al.*, 1999; Cossart *et al.*, 2003), viewed using the Swiss-PDB viewer program. There are four distinct domains; a cap region, leucine rich repeats (LRRs), an IgG-like domain, also known as an inter-repeat (IR) region, and a B-repeat region. The amino terminal part encompassing the LRR is the most exposed region of cell-bound InlB. The protein is anchored to the cell surface via its carboxy-terminal GW repeat domains.



The complete recombinant InlB protein was provided in PBS buffer and had been purified by IMAC. The recombinant variants were provided as crude cell lysates in urea-based denaturing buffer 'B'. Samples of each recombinant protein were resolved on a 12.5 % acrylamide gel (Figure 3.29a) and then transferred to a nitrocellulose membrane and probed with mAbG54D4 hybridoma supernatant (Figure 3.29b). The results indicated that the antibody was specific for the N-terminal, LRR domain. This domain is the most exposed domain of *L. monocytogenes* surface-bound InlB and thus, suggested that mAbG54D4 should be capable of binding to cells. Moreover, since the antibody was capable of binding to the recombinant LRR domain, following crude cell lysis in a urea-based denaturing buffer and denaturing SDS PAGE, it appeared that the epitope being recognised was not conformation-dependent.

On the basis of these results it seemed surprising that mAbG54D4 was not capable of binding live cells. Some success has also been reported when polyclonal anti-InlB antibodies were employed in a sandwich immunoassay for the detection of *L. monocytogenes* cells (Gary Wyatt, personal communication). However, problems have been encountered by others (Trinad Chakraborty, personal communication) and it has been proposed that the manner in which InlB is associated with the cell surface can render it inaccessible to antibodies (Jonquères *et al.*, 1999).



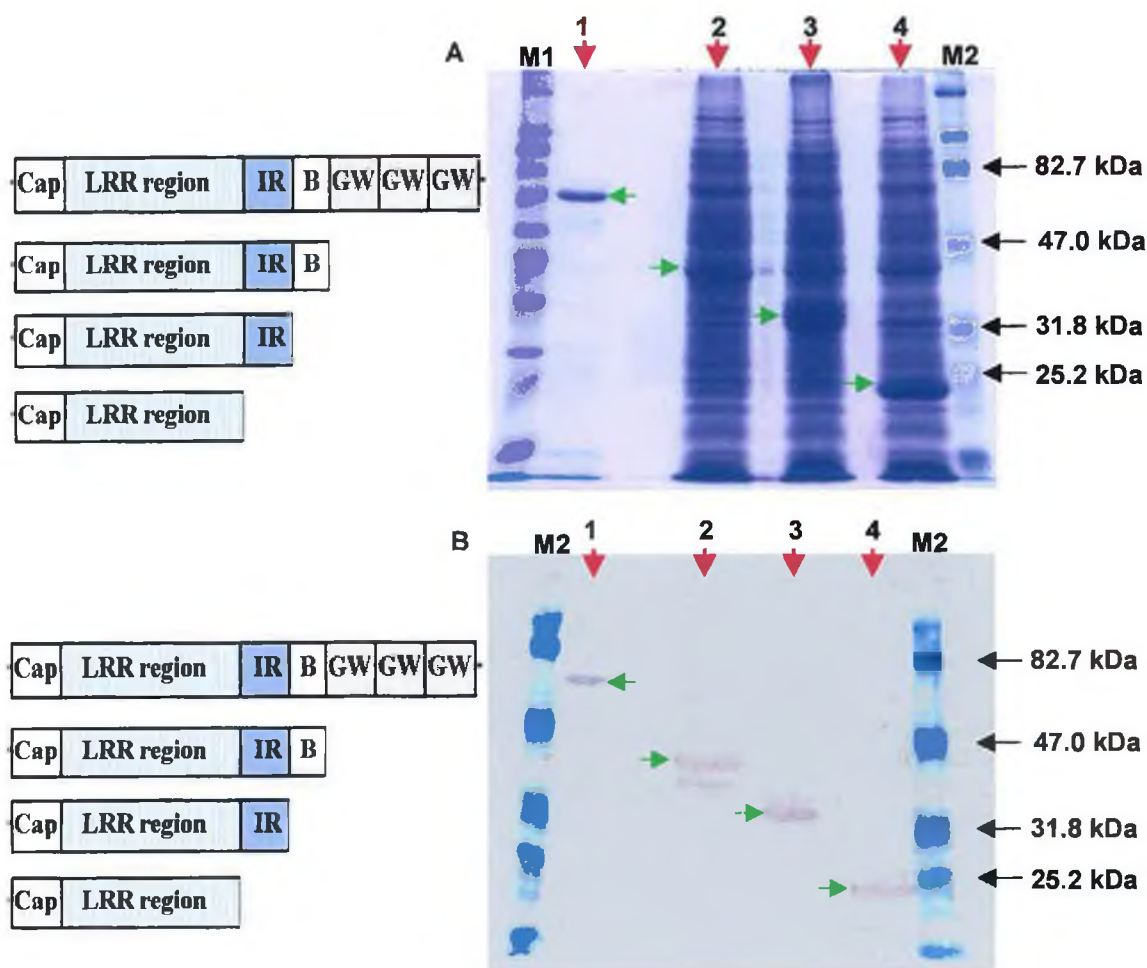


**Figure 3.29:** Immunoreactivity of mAbG54D4 towards complete and truncated versions of recombinant InlB proteins. Samples of each of the proteins (20  $\mu$ l) were resolved on a 12.5 % (w/v) SDS PAGE gel (A). 'M1' and 'M2' refer to SigmaWide™ (wide range) and BlueRanger® (prestained) molecular weight markers, respectively. The complete InlB protein had been provided in purified form and thus, generated a single band (1). The truncated versions comprised of the mature InlB protein minus; the GW repeat anchor region (2), the GW repeat anchor region and the B repeat region (3), and the combined GW repeat anchor region, B repeat region and IgG-like domain (4). These were provided in crude cell lysates and thus, contained multiple heterogenous, *E. coli*-derived proteins. The bands corresponding to the InlB proteins are indicated with the green arrows. The resolved samples were then subjected to Western blot analysis using G54D4 hybridoma supernatant at a 1/1000 dilution in PBS/TM containing 1 % (w/v) dried skimmed milk (B). The binding profile suggested that the epitope being recognised by mAbG54D4 was contained within the N-terminal LRR domain of InlB, which was the smallest fragment tested (lane 4).



### **3.2.5      *Production of monoclonal antibodies to whole-cell *L. monocytogenes****

#### **3.2.5.1    *Preparation of formalin-inactivated *L. monocytogenes* cells***

Previous unpublished results had indicated that polyclonal antibodies raised against *L. monocytogenes*, that had been heat-inactivated, were not suitable for detection of the live bacteria. This was thought to be due to the fact that many of the surface proteins had become excessively denatured during the inactivation process. Heat inactivation was not considered an option since favourable detection of heat-killed cells over healthy cells was contrary to the envisaged diagnostic application and would likely render false positive results an inherent problem with any resulting assay. It was thus decided inactivate the cells using a formalin solution in PBS (Section 2.4.4) before immunising mice in order to present a more stable surface protein topography.

#### **3.2.5.2    *Immunisation with formalin-inactivated *L. monocytogenes* cells***

Three mice were immunised via the peritoneal cavity with approximately  $1 \times 10^7$  formalin-inactivated *L. monocytogenes* serotype 1/2a cells prepared 1:1 with PBS and Freund's Complete adjuvant (FCA). Subsequent boosts were prepared in PBS and administered by i.p. injection over a period of 6-8 months. When the specific serum titre (Figure 3.30) was deemed sufficiently high, the mice were primed for fusion. This consisted of administering booster i.p injections prepared in PBS on days 5 and 3 before fusion. The final boost was administered in PBS on day 1 before fusion, via the i.p route. It was not possible to administer the final booster intravenously because the complex cellular suspension could quite conceivably have led to toxic shock or even pulmonary embolism.

On the day of the fusion (day 0), the spleen was removed from one primed mouse and the lymphocytes from within were harvested. Following the fusion procedure, hybridoma supernatants were screened approximately 9 days post fusion for specific antibody as described in Sections 2.8.1 and 2.7.7.2. The initial 600 hybridoma containing wells were screened using a comparative, negative screening direct ELISA format, where one set of wells was coated with *L. monocytogenes* serotype 1/2a cells in PBS ( $1 \times 10^8$  cells/well) and a separate set of wells was coated with a combination of *L. welshimeri*, *L. seeligeri* and *L. innocua* cells ( $3 \times 10^8$  cumulative cells/well), prepared under the same conditions. From this preliminary screening, 39 clones were identified that demonstrated favourable binding to *L. monocytogenes*. Following scale-up, the hybridoma populations were re-screened. A proportion of the 39 clones tested exhibited substantial cross-reactivity (Figure 3.31). However, a significant percentage also continued to demonstrate an enhanced response to *L. monocytogenes* cells.





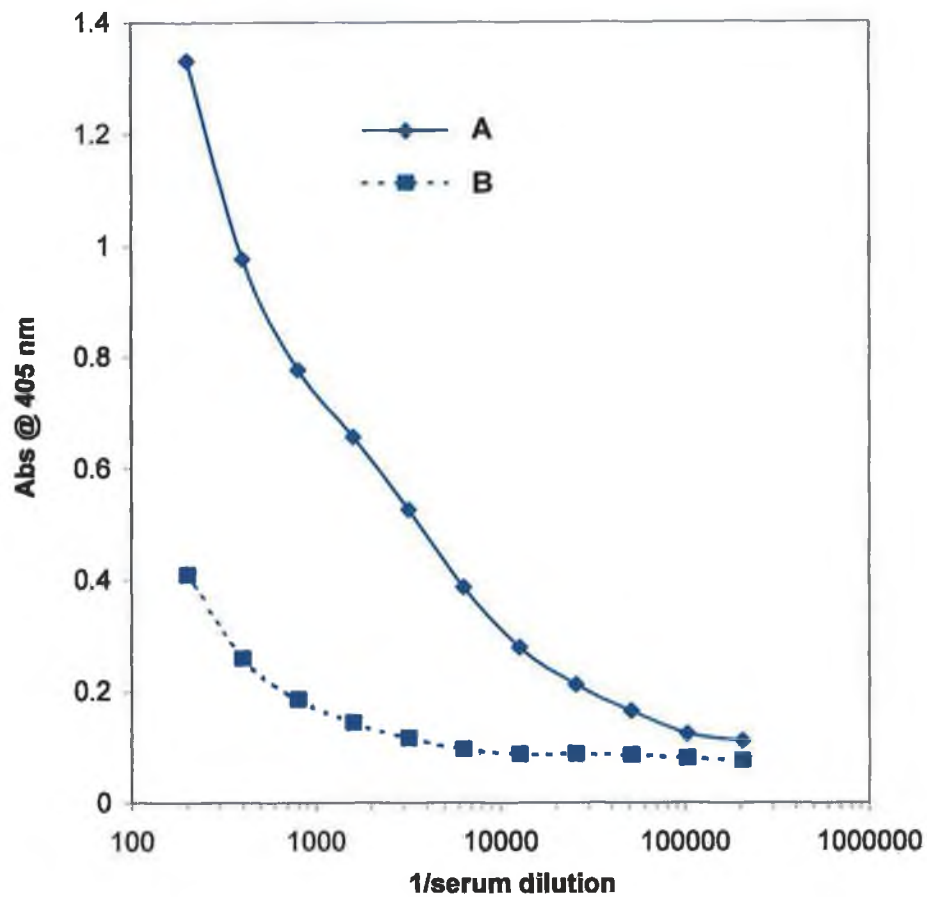


*Figure 3.30: Specific serum antibody titre from a mouse that had been immunised with formalin-inactivated *L. monocytogenes* 1/2a whole cells. The same cells were used as the coating antigen in the ELISA at a concentration of approximately  $1 \times 10^9$  cells/ml. 'A' corresponds to the serum from the immunised mouse, while 'B' refers to a control serum taken from a naïve, un-immunised mouse. The specific titre was estimated to be 1/100,000.*



In particular, clone no. 39 was found to simultaneously generate the greatest response against *L. monocytogenes* 1/2a cells and the lowest response to the heterogenous population of non-pathogenic strains. It was also demonstrated to bind *L. monocytogenes* cells in a solution phase inhibition ELISA. This clone was further isolated and stabilised by limiting dilution and was designated 'mAb2B3'.

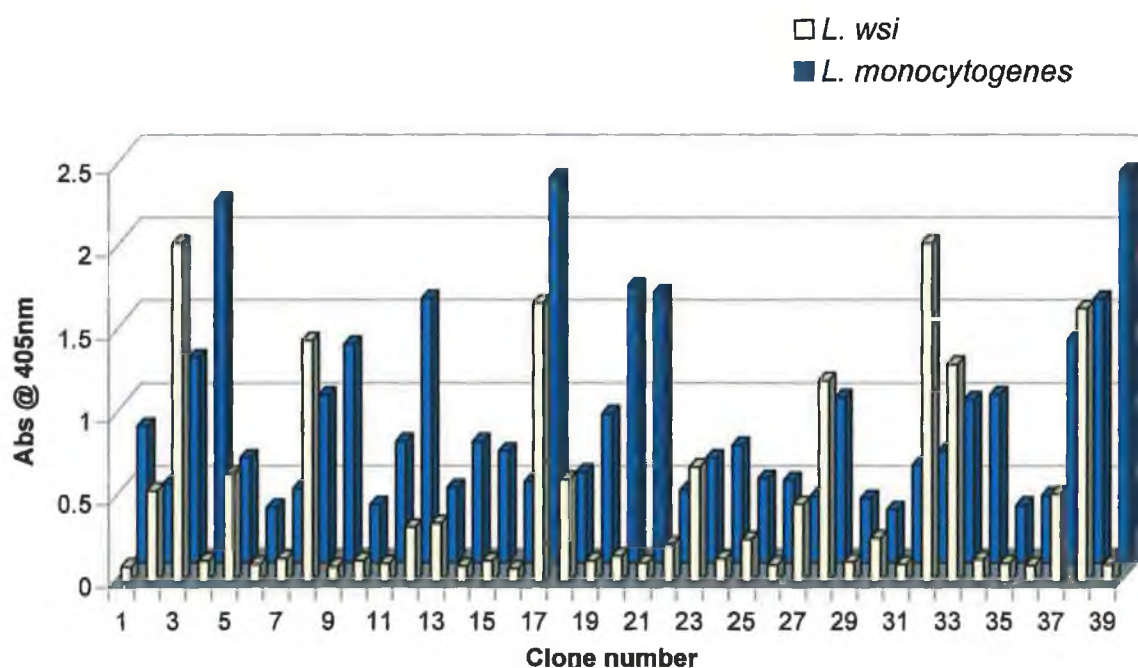


**Figure 3.31:** Screening of supernatants from preliminary selected hybridoma populations. The light bars in the chart foreground represent the supernatant activity towards the heterogeneous population of non-pathogenic *L. welshimeri*, *L. seeligeri* and *L. innocua* ('*L. wsi*'), while the shaded bars in the chart background represent the supernatant activity towards *L. monocytogenes* serotype 1/2a cells.



### 3.2.6 Characterisation of mAb2B3 monoclonal antibody

#### 3.2.6.1 Determination of mAb2B3 isotype

The isotype of the antibody secreted by hybridoma clone '2B3' was carried out using ELISA, as described in Section 2.8.2. The results of the isotyping ELISA (Figure 3.32), clearly indicated that mAb2B3 was an IgG2a type antibody, comprising kappa light chain domains.

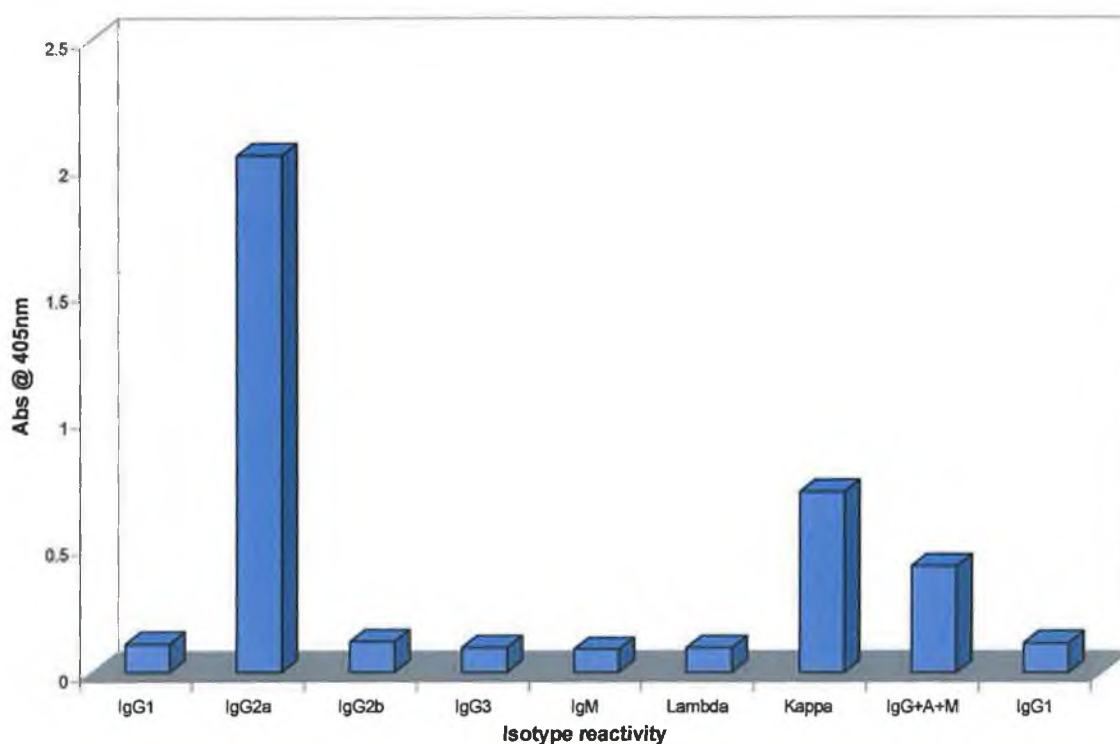


**Figure 3.32:** Isotype profile of monoclonal antibody mAb2B3. ELISA plates were coated with live, PBS-washed *L. monocytogenes* serotype 1/2a cells at  $1 \times 10^8$  cells/well. mAb2B3 hybridoma supernatant was employed at a 1/10 dilution in PBS/TM containing 1 % (w/v) dried skimmed milk. The absorbance values indicated that the monoclonal antibody was composed of IgG2a heavy chains and kappa light chains.



### **3.2.6.2 Affinity-purification of mAb2B3**

Spent hybridoma supernatant was collected from hybridoma clone 2B3 cells that had been grown to exhaustion. The supernatant was concentrated ten fold by ultrafiltration, using a 10 kDa cut-off membrane filter. A 10 ml volume of concentrated supernatant was purified using a freshly prepared 1 ml Protein A column (Section 2.6.3). Protein A was chosen because is known to bind murine IgG2a strongly but not BSA/bovine IgG and thus, prevents co-purification of such proteins from the culture supernatant. The approximate concentration of purified IgG was estimated from the  $A_{280\text{nm}}$  value, assuming a molar extinction co-efficient of 1.4 and was calculated to be 620  $\mu\text{g/ml}$ . The protein-containing eluant fractions were pooled, desalted and resuspended in PBS buffer.

### **3.2.6.3 Determination of integrity and degree of purification of mAb2B3**

The purity and integrity of the protein A-affinity purified mAb2B3 monoclonal antibody was confirmed by SEC HPLC (Section 2.11.1) and combined SDS PAGE and Western blot analysis. For the SEC HPLC analysis (Figure 3.33), the purified antibody exhibited a single peak with an identical retention time to that of the standard IgG2a antibody (15 minutes). This corresponded to approximately 155 kDa by reference to a standard curve of globular proteins of known molecular weight.

The purity and integrity of the purified monoclonal antibody was further confirmed by subjecting neat samples of both the purified mAb2B3 antibody and the concentrated unpurified mAb2B3 hybridoma supernatant, to SDS PAGE analysis on a 12.5 % (w/v) acrylamide resolving gel. The resulting electrophoretic profiles were compared with that of the standard IgG2a (Figure 3.34, top). The concentrated supernatant yielded multiple bands reflecting a heterogeneous protein population contained within. In addition, there was a dominant protein band at 66 kDa and this was attributed to the foetal-bovine BSA content in the growth media composition (Section 2.7.1). It was also possible to discern strong bands at approximately 50 kDa and 25 kDa, which corresponded to the IgG heavy and light chain fragments, respectively. The affinity-purified mAb2B3 antibody yielded just heavy and light chain bands, which corresponded exactly with the protein bands yielded by the IgG2a standard. The immunoreactivity (with regard to goat-anti mouse-IgG2a antibody) of the three antibody test samples was confirmed by subsequent Western blot analysis (Figure 3.35, bottom).





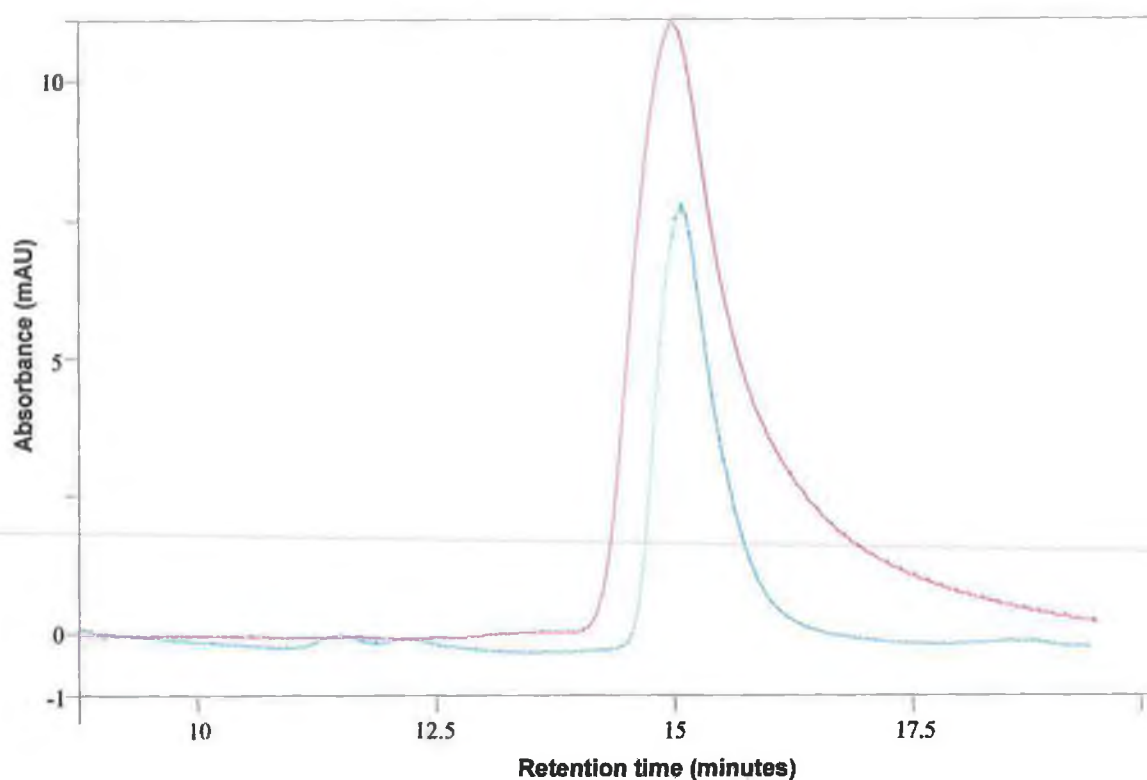


**Figure 3.33:** SEC HPLC profiles of a commercial standard (1 mg/ml in PBS) murine IgG2a antibody (pink), and a neat sample of protein A-purified mAb2B3 in PBS (blue), performed as described in Section 2.11.1. A Phenomenex 3000 SEC column was used with PBS mobile phase at a flow rate of 0.5 ml/min and monitored by UV absorbance at 280 nm. The retention times for both the standard and test antibody correlate at a value of 15 minutes. The single peak evident at this retention time is indicative of sample purity.



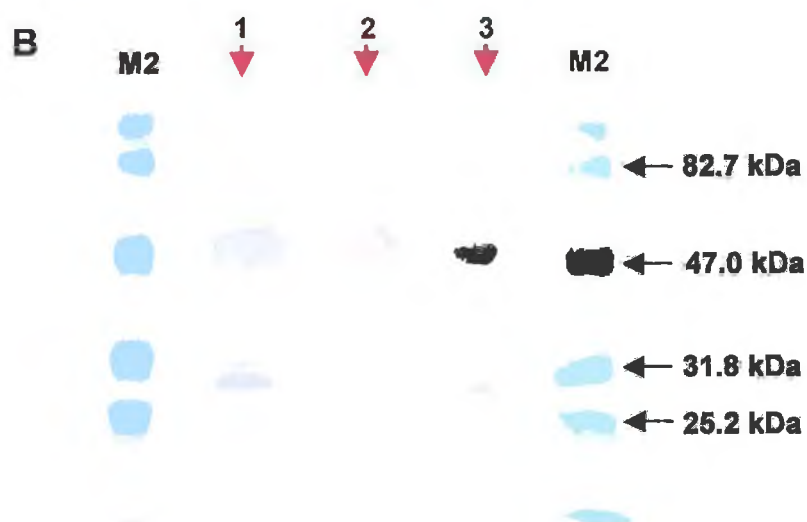
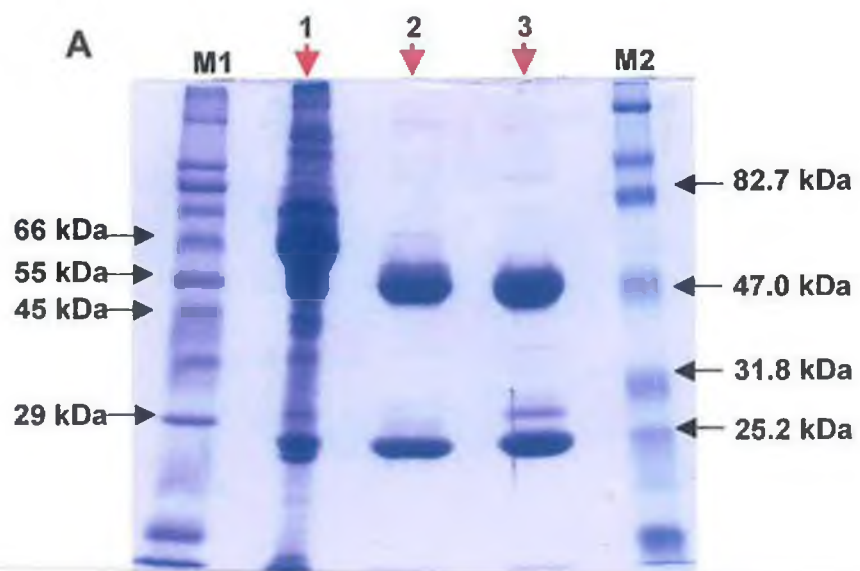


**Figure 3.34: Determination of antibody purity.** Gel (A) represents SDS PAGE analysis of (1), concentrated mAb2B3 hybridoma supernatant; (2), protein A-affinity purified mAb2B3 and (3), a commercial IgG2a standard in PBS. 'M1' and 'M2' refer to SigmaWide™ (wide range) and BlueRanger® (prestained) molecular weight markers, respectively. The heavy and light chain protein bands are clearly visible at 50 kDa and 25 kDa, respectively. The bottom image (B) represents the corresponding Western blot following immuno-probing with an AP-labelled, goat anti-mouse-IgG2a antibody.



#### 3.2.6.4 Observations on the nature of the specific mAb2B3-cell binding interaction

In order to glean further information regarding the exact nature of mAb2B3's ability to bind *L. monocytogenes* cells, a panel of pathogenic *Listeria* spp. were comparatively assessed following a selection of treatments. These treatments included growth in BHI, as opposed to LEB broth, the effect of solubilising the listerial cell wall proteins and the effect of heat inactivation. The test format employed throughout, for the determination of the extent of mAb2B3 binding to treated cells, was a direct ELISA (2.8.1 and 2.8.3), such as had been used for screening hybridoma supernatants. The absorbance values recorded ( $A$ ) were normalised against the background response ( $A_0$ ) according to  $A/A_0$  and the results were plotted in Figure 3.35.

It was apparent that the activity of mAb2B3 was most potent against *L. monocytogenes* serotype 1/2a cells and strongest when cells were prepared in LEB rather than BHI medium (Figure 3.35, 1). No activity towards *L. ivanovii* was detected in either media. The strong response to *L. monocytogenes* serotype 1/2a was undoubtedly due to the fact that this was also the serotype used for immunisation and hybridoma screening. However, the cells used for immunisation and screening had also been cultivated in BHI broth. The higher response to LEB-cultured serotype 1/2a cells suggested some degree of up-regulation of the epitope-bearing protein. The response to the *L. monocytogenes* 1/2c, 4a and 4b strains was, weaker, yet still significant. Interestingly, the serotype 4a strain was the only species that demonstrated a weaker response when cultured in LEB medium than BHI. More significantly, the response against the serotype 4b strain tested was substantially enhanced by growth in LEB medium. This is important given the frequent association of *L. monocytogenes* 4b strains with invasive listeriosis in humans. It has previously been reported that, although, there is a high degree of homogeneity between all strains of the same *L. monocytogenes* serovar, there are large differences between serovars of the 1/2 family and serotype 4b (Tabouret *et al.*, 1992). When the cell wall proteinaceous content was partially solubilised by treatment with detergent (Figure 3.35, 2) the activity was generally reduced, thus, reaffirming the cell-wall localisation of the reactive protein. Subjecting the cells to a temperature of 80 °C reduced the reactivity (Figure 3.35, 4 and 5). This was viewed as a significant advantage for the development of a *L. monocytogenes*-specific immunoassay since it could potentially abrogate false positive results arising from non-viable, heat-inactivated *L. monocytogenes* cells.



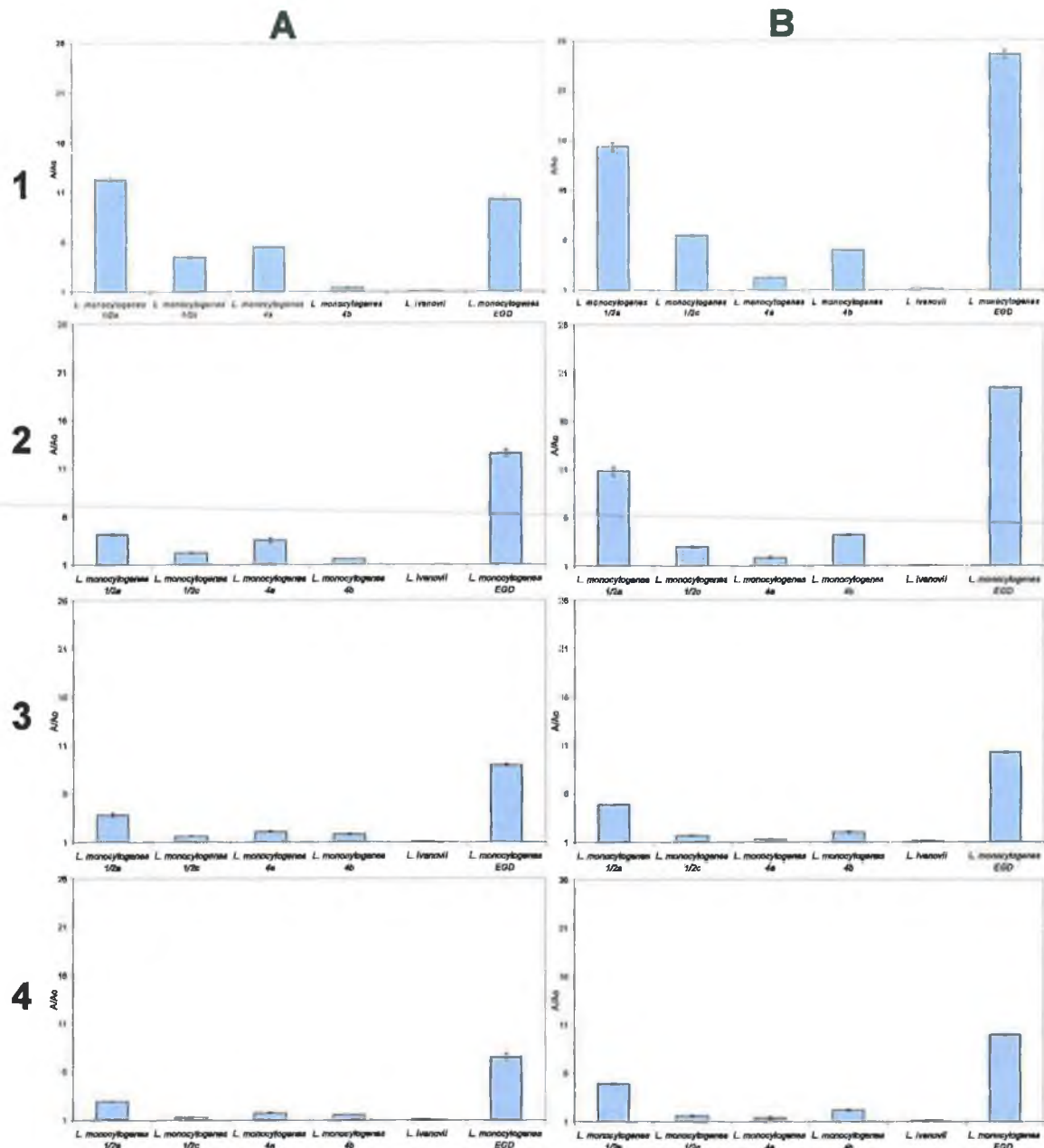


**Figure 3.35:** Reactivity profiles of purified mAb2B3 against representative pathogenic *Listeria* spp., grown in either BHI (panel A) or LEB (panel B), broth media. The data represents the mean of triplicate measurements. The top profile (1) represent ELISA wells coated with  $1 \times 10^8$  freshly prepared cells, washed and resuspended in PBS. Profile (2) represents the same cell samples after having been subjected to SDS-mediated surface protein extraction, washed and resuspended in PBS, while profiles (3) and (4) refer to the freshly prepared samples after being held at 80 °C for 15 and 20 minutes, respectively.





#### **3.2.6.5 Cross-reactivity of apathogenic *Listeria* spp. with mAb2B3**

Although both the immunisation and screening that led to the selection of mAb2B3 had been conducted using cells that had been cultivated in BHI medium, it was clear from the results outlined in Section 3.2.6.4, that mAb2B3 exhibited a greater binding capacity to *L. monocytogenes* 1/2a and 4b cells that had been cultured in LEB medium. This was interpreted to suggest an up-regulation of the reactive protein and/or a change in the surface topography of the cells. It was important to determine whether a similar effect was exhibited by non-*L. monocytogenes* strains. A selection of test bacteria were grown under identical conditions to those of the representative *L. monocytogenes* strains under investigation, in LEB broth. The subsequent binding of mAb2B3 to the various cell types was compared using a direct ELISA and the results are outlined in Figure 3.36. It was clearly evident that significant binding was only apparent in wells coated with the representative pathogenic *L. monocytogenes* strains. No significant cross-reactivity was observed in any of the non-*L. monocytogenes* strains tested.

#### **3.2.6.6 Elucidation of the mAb2B3-reactive listerial protein**

In order to putatively determine the key identifying parameters of the protein being recognised by mAb2B3 and to re-affirm degree of cross-reactivity determined in Section 3.2.6.5, a series of immunoblotting experiments were performed. Surface proteins were extracted from *L. monocytogenes* cells (Section 2.4.5) that had been grown in BHI and LEB media, in addition to a selection of apathogenic *Listeria* spp. that had been grown in LEB medium. The heterogenous surface protein profiles were visualised by SDS PAGE analysis (Figure 3.37a). These were then subjected to Western blot analysis, with the mAb2B3 antibody, and it was revealed that the antibody reacted only with extracts derived from *L. monocytogenes* spp. and specifically with an 80 kDa-localised protein (Figure 3.37b). When this estimated molecular weight was considered along with the demonstrated cell surface localisation of the protein and its apparent exclusivity to *L. monocytogenes* spp., the mAb2B3-reactive protein was tentatively theorised to be InlA. However, this was subject to further confirmation (Chapter 4). Although InlA is exclusive to *L. monocytogenes*, a significant number of internalin homologues have been identified within the *L. ivanovii* species (Engelbrecht, *et al.*, 1998a; Engelbrecht, *et al.*, 1998b) comprising the characteristic LRR domain (Kajava, 1988). In prokaryotes, this particular domain structure is usually restricted to virulence-associated appendages. Cell wall-anchored proteins are widespread in gram-positive bacteria (Navarre and Schneewind, 1999) and many share the common LPXTG motif and the similarly hydrophobic C-terminal domain present in InlA. However, since this region is buried within the cell wall and thus inaccessible, it was highly improbable that this region housed the reactive epitope for mAb2B3 and, correspondingly, was unlikely to mediate cross-reactivity.



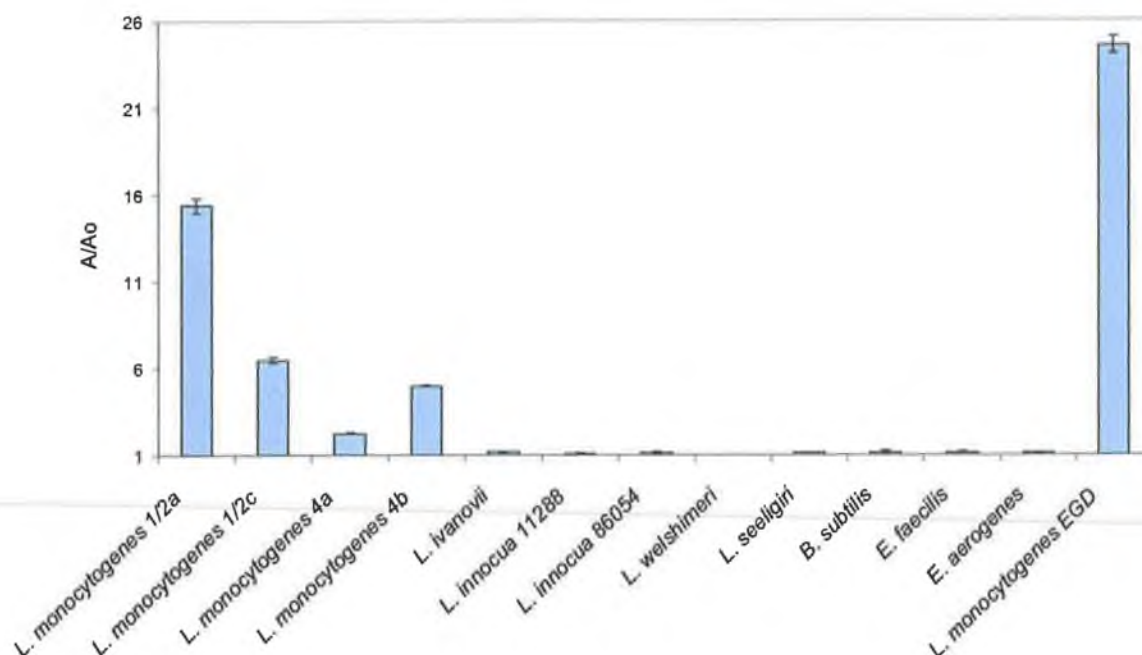


**Figure 3.36:** Cross-reactivity profiles of purified mAb2B3 against representative pathogenic and apathogenic *Listeria* spp., grown in LEB broth media. The data represents the mean of triplicate measurements. The concentration of each cell sample was adjusted in PBS to give a final coating concentration of  $1 \times 10^8$  cells/well.

It was not possible to infer a significant up-regulation or variance in the expression levels of the 80 kDa protein between the different *L. monocytogenes* serotypes tested, or between identical serotypes cultured in LEB as opposed to BHI, from the surface-extract profiles and corresponding immuno-blots with mAb2B3. It is more likely that the overall cellular morphology and surface topography is influenced by the type of growth medium used, with more accessible reactive epitope sites dominating in LEB-cultured cells. Furthermore, despite an obvious decrease in binding capacity of mAb2B3 to heat-inactivated cells (Section 3.2.6.4) this could not be entirely attributed to protein denaturation, since reactivity was observed following denaturing SDS-PAGE (Figure 3.39b). This adds further weight to the postulation that successful binding of mAb2B3 antibody to *L. monocytogenes* is dependent not only on expression of the specific 80 kDa protein, but also on the overall surface topography and accessibility of the epitope site.



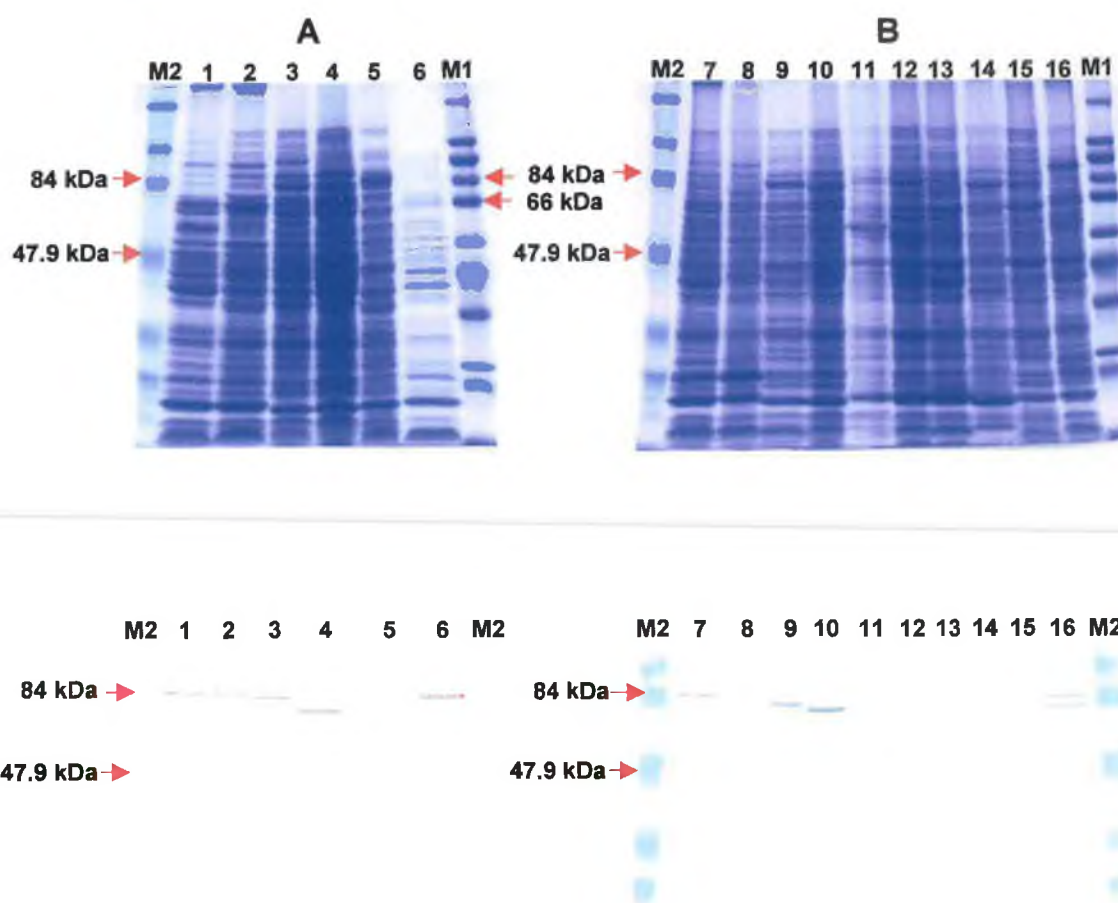


**Figure 3.37:** Determination of the specific immunoreactivity of mAb2B3. SDS-extracted protein fractions (~100-150 µg/ml) from various *Listeria* genus members grown under identical conditions in either BHI (A) or LEB (B) broth media, were resolved by SDS-PAGE (top) and then immunoprobed with mAb2B3 (bottom). 'M1' and 'M2' refer to SigmaWide™ (wide range) and BlueRanger® (prestained) molecular weight markers, respectively. Gel A represents; (1), *L. monocytogenes* 1/2a; (2), *L. monocytogenes* 1/2c; (3), *L. monocytogenes* 4a; (4), *L. monocytogenes* 4b; (5), *L. ivanovii* PA and (6), *L. monocytogenes* EGDpERL3 50-1 prfA<sub>EGD</sub>. Gel B represents; (7), *L. monocytogenes* 1/2a; (8), *L. monocytogenes* 1/2c; (9), *L. monocytogenes* 4a; (10), *L. monocytogenes* 4b; (11), *L. ivanovii* PA; (12), *L. innocua*; (13), *L. innocua*; (14), *L. welshimeri*; (15), *L. seeligeri* and (16), *L. monocytogenes* EGDpERL3 50-1 prfA<sub>EGD</sub>. The mAb2B3 antibody reacted with an ~80 kDa protein exclusively present in the *L. monocytogenes*-derived samples tested. No non-specific binding to extracts derived from the other genus members tested was observed.



### **3.2.7 Optimisation of ELISA for detection of *L. monocytogenes* cells using mAb2B3**

Having established that mAb2B3 was specific for an 80 kDa protein present on the surface of *L. monocytogenes* cells, it was decided to demonstrate the potential usefulness of this monoclonal antibody in an immunoassay for the direct detection of live *L. monocytogenes* cells.

#### **3.2.7.1 Checkerboard ELISA for determination of optimal loading ratios of cell coating and optimal antibody dilution for mAb2B3 monoclonal antibody**

It is likely, that, all reagents being equal and optimal, coating of antigen can play a very influential role in determining assay performance. The simplest approach to coating microtitre plates with antigen is to do so directly, by passive adsorption (Canterero *et al.*, 1980). The effectiveness of such an approach is dependent on how well the integrity of the adsorbed antigen is preserved (Pesce *et al.*, 1977; Butler *et al.*, 1992) and how firmly the antigen is bound (Rubin *et al.*, 1977; Salonen and Vaheri, 1979). Ideally, the antigen should retain its native conformation and accessibility of the reactive epitope should not be compromised. In general, at high concentrations of coating antigen there is a tendency of protein molecules to bind to each other due to saturation of available binding surface. These intra-molecular interactions are often weaker than those between the protein and the plastic surface and can, thus, result in dissociation of supposedly 'bound' protein during the assay (Kemeny, 1992). The acceptable range of protein concentrations at which there is no interference with binding to the plastic is called the 'zone of independent binding' (Canterero *et al.*, 1980; Kemeny, 1992). When coating with whole cells these considerations remain pertinent (Sedgwick and Czerkinsky, 1992). Often, cells, particularly mammalian cells are 'fixed' with a cross-linking reagent such as formaldehyde or glutaraldehyde. However, due to the non-discriminatory cross-linking activity mediated by these potent fixatives, epitope structure and/or accessibility could quite conceivably be impaired by this procedure.

In polyclonal antisera, raised against whole cells, this potential complication would most likely not arise. The heterogenous composition of such antisera would ensure that a significant proportion of the immunoglobulin content was capable of recognising its complementary component epitope on the surface of the fixed cells. The key advantage with using monoclonal antibodies, and in particular, the reason for the high discriminatory power of mAb2B3 with regard to *L. monocytogenes*, lies in the fact that it recognises a single





epitope. Thus, any deleterious effect on the cell surface, epitope-bearing protein, brought about by fixing, could totally abrogate the capacity of the monoclonal antibody to bind cells.

It may be argued that because mAb2B3 was produced from mice immunised with formalin-inactivated *L. monocytogenes* cells, it would be expected to be capable of recognising or even preferentially bind to similarly treated cells. However, the principal objective was to isolate a monoclonal antibody specific for live *L. monocytogenes* cells and this was reflected in the screening process and selection of mAb2B3, which had been performed using live *L. monocytogenes* 1/2a cells.

In an inhibition ELISA format, the degree of sensitivity in terms of detection limits (proportional to the slope of the curve), is a cumulative function of the antibody affinity and the antigen valency and results are interpreted at equilibrium between both free and immobilised antigen. Consequently, using too high a coating concentration of antigen will shift the binding equilibrium in favour of binding to the ELISA plate and cause reduced sensitivity to free antigen in solution. Similarly, utilising too high an antibody concentration, will require high concentrations of free antigen in solution to inhibit antibody binding to the ELISA plate, and will therefore result in decreased assay sensitivity.

In order to determine the optimal working dilution of the purified antibody and optimal cell coating concentration, a checkerboard ELISA was performed as described in Section 2.8.3. For the purposes of assay standardisation and reproducibility it is desirable to have a pure and readily available source of coating antigen. In the absence of such and being restricted to coating with whole cells, as was the case described herein, it may be argued that the recombinant *L. monocytogenes* EGDpERL3 50-1 prfA<sub>EGD</sub> strain would be the best choice for coating, due to its inherent, constitutive high level expression of prfA-regulated virulence proteins. However, the principal objective was to demonstrate the absolute, generic application of mAb2B3 for detection of live *L. monocytogenes* cells. Thus, wild type *L. monocytogenes* serotype 1/2a was employed as the coating and solution-phase antigen. The checkerboard results were plotted (Figure 3.38) and these indicated that the optimal coating concentration of *L. monocytogenes* cells was approximately  $1 \times 10^9$  cells/ml. The optimal mAb2B3 antibody dilution, which gave the greatest change in absorbance per change in antibody dilution, was determined to be 1/10,000.



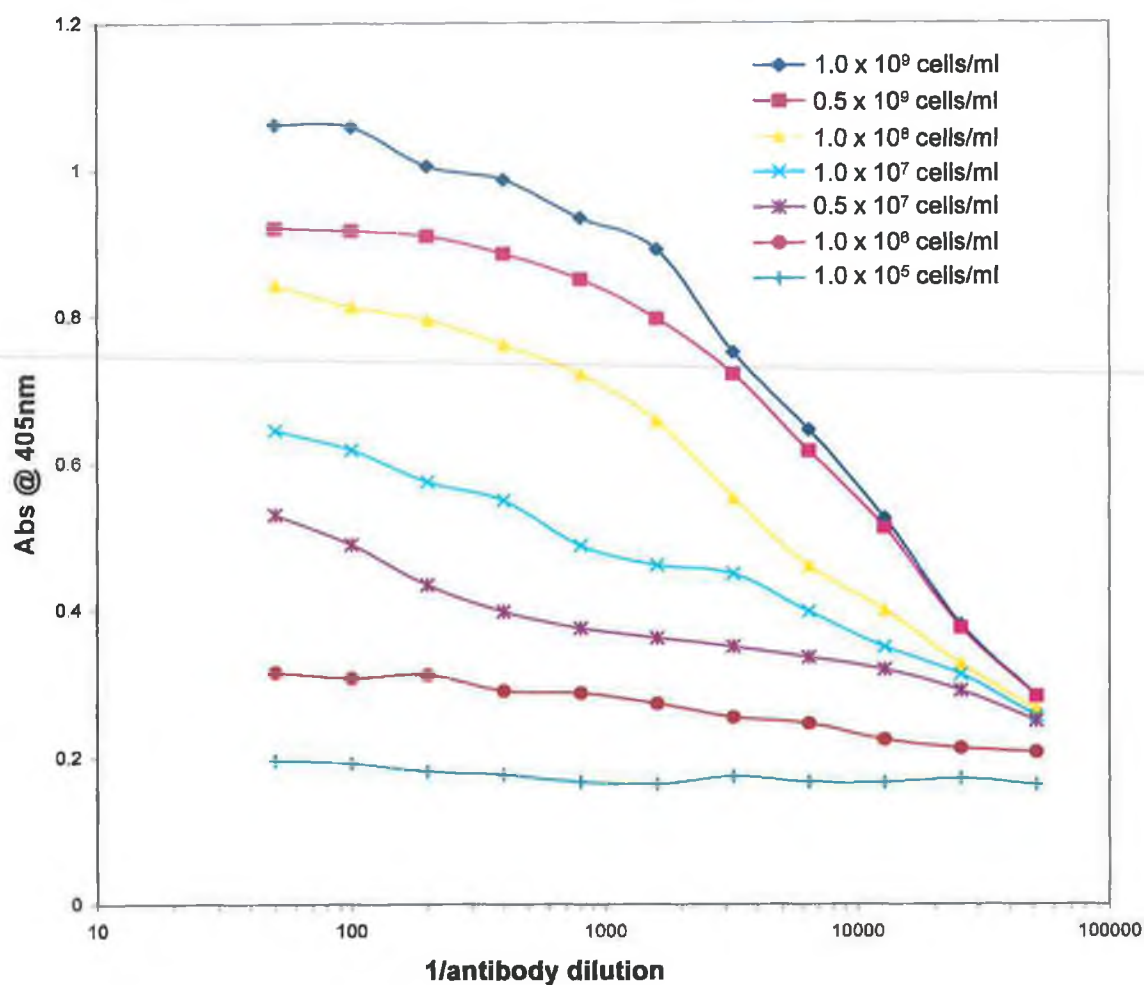


**Figure 3.38:** Checkerboard ELISA for determination of optimal *L. monocytogenes* cell coating concentration and mAb2B3 antibody working dilution for the development of an inhibition immunoassay for detection of live *L. monocytogenes* cells. The absorbance values were read at 405 nm after 15 minutes exposure to substrate at 37 °C.



### 3.2.7.2 Inhibition ELISA evaluation

Protein A-affinity-purified mAb2B3 monoclonal antibody was employed in an inhibition ELISA format for the detection of free *L. monocytogenes* cells in solution as described in Section 2.8.4.

Typically, immunoassay response curves are inherently non-linear and adopt a sigmoidal bell shape on semi-log plots (Findlay *et al.*, 2000). Such assays are most effectively modelled using a four-parameter equation, of the form:

$$R = R_{HI} - \frac{R_{HI} - R_{LO}}{1 + \left( \frac{Conc}{A_1} \right)^{A_2}} \quad \text{(Equation 3.1)}$$

Where	$R_{HI}$	=	Response at infinite concentration
	$R_{LO}$	=	Response at zero concentration
	$Conc$	=	Analyte concentration (M or cells/ml)
	$A_1$	=	Fitting constant
and	$A_2$	=	Fitting constant

The four-parameter (4-parameter) equation above was fitted to the data sets for each immunoassay run, using BIAevaluation 3.1 software™. When used as a calibration curve, the 4-parameter fitting facilitated the estimation of sample test concentrations from the resultant plot. It was thus possible to estimate the degree of precision of analytical measurement at different standard concentration points relative to the fitted 4-parameter plot. This was reported as the % relative error (% RE) between the standard 'input' concentration and the estimated 'output' concentration generated from the curve.

Alternatives to the 4-parameter equation include the log-logit and linear models. Although the log-logit function fits many immunoassays quite effectively it is not suitable when a significant degree of asymmetry is present such as can often occur when using polyclonal antibodies at very low working dilutions or when labelled antigen exhibits heterogeneity with respect to unlabelled antigen (Raggatt, 1992). Both the log-logit and, in particular, the linear modelling of the straight-line portion of the sigmoidal curve, frequently render the asymptote regions of the data plot unreliable and unusable. The 4-parameter equation however, confidently fits the asymptote region thereby greatly extending the working range of the immunoassay calibration curve at both ends of the concentration range employed.



The intermediate precision and repeatability was calculated by conducting the assay over three consecutive days. Each day, two assay runs were performed and sample cell concentrations were measured in triplicate. This was sufficient to satisfy the validation criteria outlined by Findlay *et al.*, (2000). The absorbance values (A) for each data point were then divided by the measured absorbance in the presence of zero cells ( $A_0$ ) to yield normalised response values ( $A/A_0$ ). A calibration curve of the mean normalised absorbance values was plotted against the standard cell concentrations (cells/ml) on a logarithmic x-axis (Figure 3.40). The normalised mean values for the standard cell concentrations were entered as 'input' values into the fitted equation and the resulting mean, back-calculated 'output' values were then used to calculate the coefficient of variation for the inter-assay performance (Table 3.2). The differences between the actual or 'input' concentrations and the 'output' cell concentrations extrapolated from the curve were used to calculate the % recovery and the associated % relative error (% RE).

$$\chi^2 = \frac{\sum_{i=1}^n (r_f - r_x)^2}{n - p} \quad (\text{Equation 3.2})$$

It was possible to estimate the 'goodness-of-fit' of the 4-parameter equation by measuring the  $\chi^2$  ( $\chi^2$ ) value. This is a standard statistical parameter that facilitates a numerical interpretation of the 'goodness-of-fit' and was calculated according to the following equation:

Where	$r_f$	=	The fitted value at a given mean data point
	$r_x$	=	The experimental value at the same point
	$n$	=	Total number of data points
and	$p$	=	The number of fitted parameters

The  $\chi^2$  value obtained for the fit in Figure 3.39 was very low ( $2.56 \times 10^{-4}$ ) and thus, reflected an acceptable fitting. However, using the  $\chi^2$  value alone, as a measure goodness-of-fit is can be unreliable, since the presence of even a few points that deviate wildly from the fitted curve can markedly affect the absolute value. A more meaningful and robust estimate of the goodness-of-fit was obtained by plotting the 'residual' values. When plotted against the nominal cell concentration values, the residual plots reflect the difference between the experimental and fitted data. These can also be expressed as relative residual values, which reflect the absolute residuals as a fraction of the experimental value.





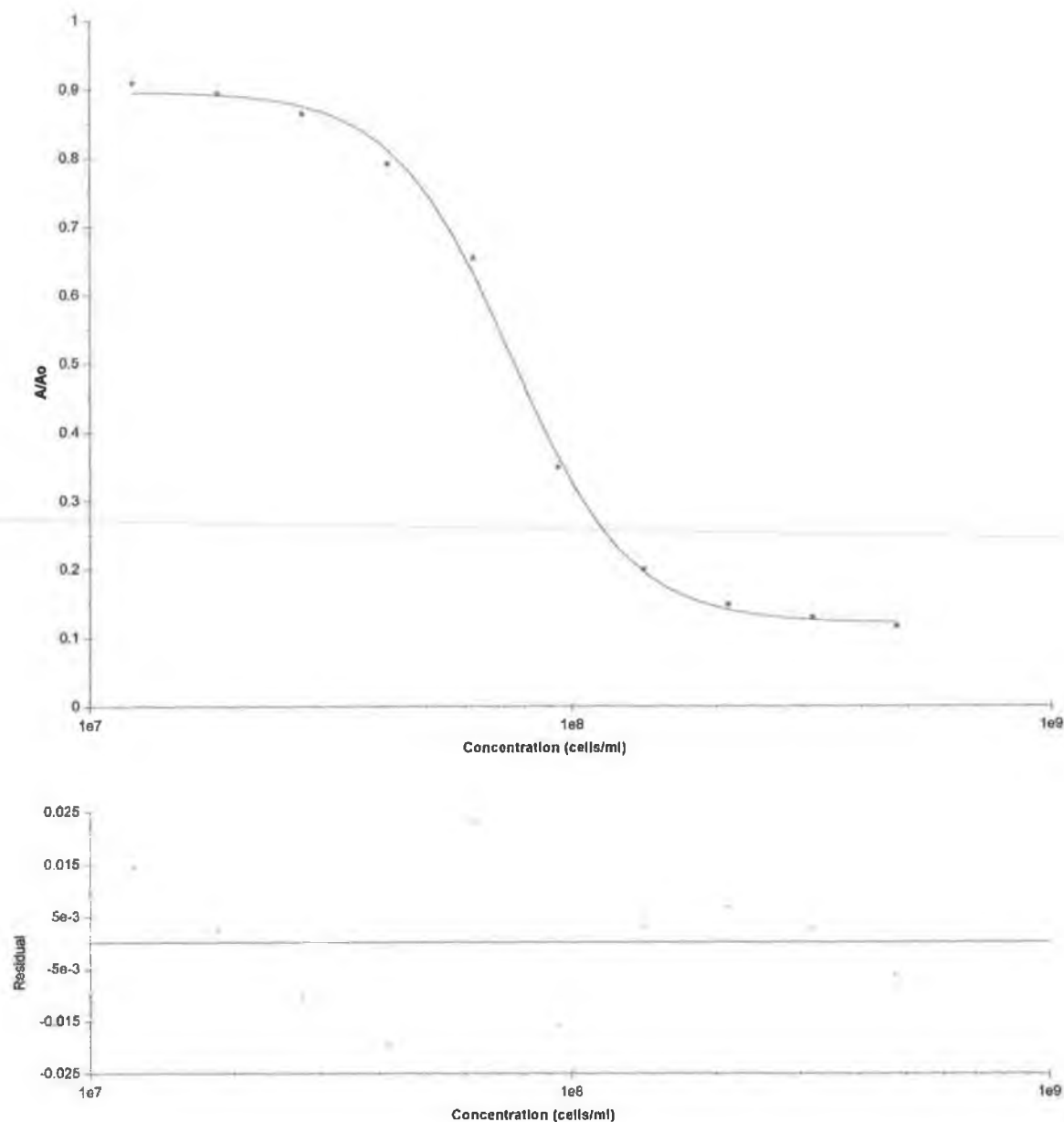


**Figure 3.39:** Inter-assay calibration curve for estimation of *L. monocytogenes* cell concentration in PBS. Data is the result of three replicate measurements from six independent assay runs and the curve was fitted using a four-parameter equation. A residual plot for the calibration curve is included to provide a visual illustration of the 'goodness of fit' of the 4-parameter model.



**Table 3.2:** Inter-assay reproducibility determinants for detection of *L. monocytogenes* cells in PBS.

Mean (actual) cell concentration	Back calculated cell concentration	CV (%)	Recovery (%)
$1.23 \times 10^7$	Low	2.25	-
$1.85 \times 10^7$	$1.55 \times 10^7$	2.50	83.63
$2.77 \times 10^7$	$3.10 \times 10^7$	3.00	111.77
$4.16 \times 10^7$	$4.45 \times 10^7$	2.71	106.87
$6.24 \times 10^7$	$6.01 \times 10^7$	6.76	96.23
$9.36 \times 10^7$	$9.62 \times 10^7$	11.33	102.78
$1.41 \times 10^8$	$1.39 \times 10^8$	7.75	98.72
$2.11 \times 10^8$	$1.40 \times 10^8$	10.22	91.69
$3.16 \times 10^8$	$2.81 \times 10^8$	7.84	88.78
$4.74 \times 10^8$	High	8.86	-

(-): denotes that data could not be extrapolated from the standard curve.

The lower limit of quantitation (LLOQ) was estimated to be  $1.85 \times 10^7$  cells/ml, with inter-assay reproducibility within the set 20 % acceptance limit recommended by Findlay *et al.*, (2000). Although similar, inhibition type assays have been reported in the literature for detection of bacterial cells (Eriksson *et al.*, 1995, Leornard *et al.*, 2004), this format may not be the most appropriate for direct cell detection. The bulky dimensions of the bacterial cells may interfere with free antibody binding to the immobilised cells. This would be expected to compress the working range of assay and may explain why the dynamic range of this particular assay appeared slightly constricted. The sensitivity and working range could perhaps be improved by adopting an alternative format. A possible candidate may be a sandwich immunoassay that incorporates a sequential capture and signal generating labelled-antibody binding event. A polyclonal genus-specific antibody could potentially fill the role of either the signal-generating antibody component, as has previously been demonstrated by Gavalchin and co-workers (1991). Alternatively, the polyclonal genus-specific antibody could be used as the capture-antibody component, with subsequent binding of species-specific, fluorescently-labelled monoclonal antibody, such as described by Sewell and co-workers (2003). The incorporation of such broadly reactive antibodies could conceivably impinge on the specificity of the assay.



Overall, considering that the initial cell contamination level is going to be substantially augmented by an incorporated enrichment incubation step, and the fact that unlike other *L. monocytogenes* virulence proteins, InlA expression is not down-regulated by growth in nutrient-rich media at 37 °C (Bohne *et al.*, 1996; Bubert *et al.*, 1999), a slight improvement in sensitivity is not essential and definitely not warranted at the expense of assay specificity. Alternatively, it has also been shown that a monoclonal antibody can be used as both the capture and signal generating components of a sandwich immunoassay for detection of *L. monocytogenes* and *L. innocua* (Sølvé *et al.*, 2000). This is a facet of sandwich immunoassays that is restricted to the detection of large, multi-epitope bearing analytes, such as cells. The high copy number and wide distribution of accessible InlA on the surface of *L. monocytogenes* make this protein a particularly suitable target for future development of such an assay. Moreover, expression of most listerial virulence-associated (and consequently, pathogenicity marker) genes closely correlates with that of *prfA*, and appreciable amounts of the nascent proteins are only achieved when growth conditions mimic those of the intracellular environment, such as was experimentally achieved by addition activated charcoal to growth media (Ripio *et al.*, 1996; Ermolaeva *et al.*, 2004). InlA expression, on the other hand, is not subject to this 'charcoal-effect' and, thus, sample enrichment can proceed in rich media and at 37 °C, resulting in more rapid attainment of detectable levels of *L. monocytogenes* cells without fear of compromising the key antigen expression level.



### 3.3 Summary and conclusions

The principal objective of this chapter was to isolate a monoclonal antibody that was specific for the pathogenic *Listeria* species, *L. monocytogenes*. Three strategies for isolation of a suitable monoclonal antibody were explored.

A panel of monoclonal antibodies was initially produced against a concentrated preparation of *L. monocytogenes* culture supernatant proteins. The *L. monocytogenes* strain used was the recombinant strain (*L. monocytogenes* EGDpERL3 50-1 prfA<sub>EGD</sub>), which had been provided, supplemented with multiple copies of the *prfA*, virulence regulator gene. It was reasoned that this would lead to increased virulence protein expression and thus, improve the chances of B-cells being stimulated against a virulence-, and therefore, pathogen-associated protein when mice were immunised. An IgG1- $\kappa$  antibody was isolated (mAbG94F8) that reacted specifically with a 60 kDa protein present in the supernatant of *L. monocytogenes* EGDpERL3 50-1 prfA<sub>EGD</sub>. The supernatant fraction was shown to contain a significant level of the LLO protein, attributed to the heightened PrfA expression and since this protein was known to have an approximate molecular weight of 60 kDa, an initial assumption was made that was the protein recognised by mAbG94F8. However, when the antibody was tested against supernatant proteins from panel of representative bacterial species that included non-pathogenic *Listeria* spp. and non-*Listeria* spp., the antibody was found to cross-react with a 60 kDa protein produced by *L. innocua* and *L. ivanovii*. Although *L. ivanovii* was known to produce a homologous cytolysin similar to listeriolysin, termed ivanolysin, *L. innocua* does not produce an equivalent protein. This indicated that the protein being recognised was not LLO and more likely to be p60, which is an immunodominant, prfA-independent and constitutively expressed protein. This was confirmed by demonstrating immunoreactivity towards a purified recombinant *L. monocytogenes* p60 protein. Although p60 homologous proteins are shared throughout the *Listeria* genus, nonetheless, the antibody was discriminatory up to point, insofar as it appeared to recognise all the pathogenic *Listeria* spp. tested, in addition to only one non-pathogenic *Listeria* spp. (*L. innocua*). Since *Listeria*-positive food samples usually contain low numbers (~10 %) of *L. monocytogenes* and high numbers (~90 %) of, typically, *L. innocua* spp. (Bhunja, 1997), a situation that is exacerbated by *L. innocua*'s competitive advantage over *L. monocytogenes* in enrichment media (Cornu *et al.*, 2002; Beumer *et al.*, 1996; Curiale and Lewis, 1994; MacDonald and Sutherland, 1994; Yokoyama *et al.*, 1998), this antibody may be of diagnostic use in an indicative-type test where indication of potential listerial (i.e *Listeria* genus) contamination is the main criteria. However, it was deemed unsuitable for the stated objective of reliable and specific detection of *L. monocytogenes*.





A second monoclonal antibody was produced, against the protein InlB. Unlike p60 there are no reported InlB-homologous proteins expressed by non-pathogenic *Listeria* spp. and it was felt that the strategy of targeting InlB would overcome the undesirable species cross-reactivity apparent with the anti-p60 antibody. Also, whereas p60 is predominantly secreted into the culture supernatant, InlB is localised to the *L. monocytogenes* cell envelope and thus, it was postulated that antibodies to this protein would facilitate direct cell detection. As transcription of the InlB-encoding gene was highly dependent on prfA regulation, the PrfA-over-expressing recombinant *L. monocytogenes* strain was again used as the antigen source, which was reliably extracted from the cell surface using 1 M Tris-HCl. An IgG1- $\kappa$  antibody (mAbG54D4) was isolated that was capable of recognising *L. monocytogenes*-extracted InlB in solution. However, it failed to significantly react with intact, viable *L. monocytogenes* cells. Subsequent analysis of the activity of the anti-InlB monoclonal antibody towards selected, domain-truncated recombinant InlB proteins confirmed that the antibody was specific for the LRR domain, which is known to be simultaneously the region of greatest heterogeneity and specificity to *L. monocytogenes* and more importantly, the most surface exposed region of the protein. Thus, the inability of the antibody to react with cell bound InlB was interpreted to indicate a potentially unfavourable *L. monocytogenes* cell surface morphology that rendered the epitope inaccessible and concomitantly rendered the protein an unreliable target for specific detection of *L. monocytogenes* cells.

The final strategy that was investigated for isolation of a *L. monocytogenes*-specific monoclonal antibody was based on a 'shotgun' immunisation approach. This entailed immunising mice with formalin-inactivated *L. monocytogenes* 1/2a cells. Although this was anticipated to stimulate a humoral response to a multitude of proteins, reflecting the diverse and heterogeneous *L. monocytogenes* cell surface protein topology, it was also felt that as the intact cell immunogen would most appropriately simulate the envisaged diagnostic target morphology of the antibody being sought. This placed greater significance on the antibody screening process, which had to be more rigorous and discriminatory. A negative screening approach was employed, whereby hybridoma clones were selected from the preliminary population pool and all subsequent rounds of cloning, on the basis of demonstrated significant binding to *L. monocytogenes* cells and failure to bind a heterogeneous selection of non-pathogenic *Listeria* spp. Using this method, an IgG2a- $\kappa$  isotype (mAb2B3) antibody was identified that demonstrated favourable binding to *L. monocytogenes*. The selected antibody was affinity-purified and subsequently, extensively characterised in terms of its ability to specifically bind *L. monocytogenes* cells. It was concluded that the antibody reacted most potently with *L. monocytogenes* serotype 1/2a cells and was strongest following cultivation of cells in basic LEB, rather than BHI broth. In addition, it was demonstrated that the antibody



binding capacity was significantly reduced in *L. monocytogenes* cells that had been subjected to heat inactivation. This was regarded as highly desirable characteristic since it could potentially safeguard against false-positive detection of dead cells in the envisaged application of this antibody in a food-industry setting.

The propensity for cross-reactivity was initially assessed in a simple, direct ELISA format. The antibody failed to react with any of the non-*L. monocytogenes* species investigated. These observations were mirrored by the results of Western blot analyses of detergent-extracted surface proteins from the panel of test species. No reactivity was observed in any of the extracts derived from non-*L. monocytogenes* strains. A single dominant mAb2B3-immunoreactive band was in the extracts derived from the five *L. monocytogenes* strains tested. The molecular weight of the reactive protein was estimated to be ~80 kDa and in view of this, in addition to its cell surface location and apparent exclusivity to *L. monocytogenes*, it was putatively identified as InlA.

As a final component of this chapter, the potential use of mAb2B3 in an inhibition immunoassay for routine detection/enumeration of *L. monocytogenes* cells from enriched cultures was demonstrated by performing an inter-assay-repeatability study over several consecutive days. The LLOQ was estimated to be approximately  $1.85 \times 10^7$  cells/ml. It is acknowledged, though, that this type of assay may not be the most appropriate for detection of cells and several avenues of improvement in terms of sensitivity are proposed. Moreover, an improved sensitivity in terms of reliable quantitation is perhaps not a prerequisite, especially given the current state of affairs with regard to acceptable limits of this *Listeria* in food. What is desired is an effectively 'presence or absence' test capable of specifically identifying *L. monocytogenes* in enriched cultures.

Overall, when the performance of this antibody was compared with published anti-*Listeria* antibodies and available immunoassay-based detection systems for *L. monocytogenes*, it was concluded that mAb2B3 demonstrates significant advantages and potential for further development with regard to the specific detection of *L. monocytogenes*.



## ***Chapter 4***

---

### ***Cloning, Heterologous Expression and Purification of Recombinant InlA Protein***



## 4.1 Introduction

The monoclonal antibody 'mAb2B3', selected in Chapter 3, had been shown to specifically bind to a surface-localised protein in *L. monocytogenes*. In addition, the antigen was confirmed to be approximately 80 kDa in size (Section 3.2.6.6). On this evidence, the antigen was tentatively postulated to be InlA. However, in order to substantiate this presumption, it was necessary to clearly demonstrate specific binding of mAb2B3 to highly purified InlA protein.

The InlA protein is typical of many Gram-positive bacterial cell wall proteins insofar as it is tethered to the peptidoglycan scaffolding via a dedicated covalent link. While it is possible to differentially fractionate secreted internalin proteins and isolate those that are localised to the cell surface by loose, non-covalent interactions (e.g. InlB), no method exists for purification of native InlA from *L. monocytogenes* cells. It was possible to design primer sequences to mediate PCR-based amplification of the *inlA* gene sequence encoding the mature protein, using the recently completed *L. monocytogenes* genotype (Glaser *et al.*, 2001). This gene can then be introduced, using a suitable expression vector, into an unrelated Gram-negative host cell (e.g. *E. coli*) that facilitates heterologous translation from the *inlA* gene into a soluble, recombinant form of the protein. A key attribute of this recombinant approach is the relative ease by which various fusion tags can be selectively incorporated into the recombinant protein for the purposes of downstream purification or detection of expression constructs. Furthermore, heterologous expression completely obviates the need to culture large volumes of pathogenic cells in order to crudely extract even a small amount of the desired protein.

The principal objective of this chapter was to selectively clone the *inlA* gene of interest into a suitable expression vector and optimise its expression and purification from a compatible expression host. Once purified, it was anticipated that the recombinant InlA protein (rInlA) would be used to confirm the putatively designated specificity of mAb2B3 for InlA.

### 4.1.1 Expression vectors

The majority of expression vectors are based on either, or a combination of two promoter systems (Sutton and Richardson, 1998). The component criteria of a 'good' promoter include high potency and a capacity to reach expression levels in excess of 10-30% of the total cellular protein content. This potency should be easily repressible so as to minimise basal





transcription, particularly in the case of toxic proteins and also be amenable to controllable induction (Hannig and Makrides, 1998). The T7 promoter system employs a promoter that is recognised by the RNA polymerase from bacteriophage T7 (P T7). This promoter is not recognised by *E. coli* RNA polymerase and, thus, facilitates cloning and propagation of sequences encoding toxic proteins by abrogating basal transcription. Induction can only be achieved by supplying the T7 RNA polymerase gene on a second compatible plasmid, a phage or on the chromosome of a specialised *E. coli* host strain (Sutton and Richardson, 1998).

The *lac* operon promoter system is the most widely used bacterial expression system. Classically, the *lac* operon in *E. coli* encodes proteins that facilitate the uptake and metabolism  $\beta$ -galactosides. Negative regulation is brought about by binding of the lac repressor protein to the *lac* operator (positioned between the promoter and the coding regions), a specific sequence of DNA to which the lac repressor binds, greatly decreasing the frequency of successful transcription elongation events by the RNA polymerase (Novy and Morris, 2001). IPTG (an allolactose analogue) is a gratuitous inducer of the *lac* operon (Singleton, 1995), insofar as it competes strongly with the *lac* operator for binding to the lac repressor, yet is itself not metabolised in the process and can, thus, be used to induce expression.

Positive regulation is stimulated by the presence of 3', 5'-cyclic adenosine monophosphate (cAMP) and the cyclic AMP receptor protein, called CRP or CAP. The CAP/cAMP complex binds just upstream of the *lac* promoter and directly stimulates transcription by RNA polymerase. However, cAMP levels are strongly influenced by the carbon source present in the medium. In the presence of glucose, (an easily metabolised monosaccharide), cAMP levels are low, so transcription from the *lac* promoter is low, a phenomenon known as the 'glucose effect' or 'catabolite repression' (Novy and Morris, 2001). Thus, complete induction of the *lac* operon system only occurs in the presence of both inducer and elevated cAMP levels. The lac repressor protein can be encoded upstream from the promoter region, or, as is the case of the pQE60 vector, the lac repressor protein can be encoded on a separate plasmid.

QIAGEN<sup>TM</sup> pQE<sup>®</sup> vectors contain an optimised promoter-operator element consisting of the coliphage T5 promoter (recognised by *E. coli* RNA polymerase) and two *lac* operator sequences that increase lac repressor binding and ensure efficient repression of the powerful T5 promoter. Each vector also contains a synthetic ribosomal binding site for high translation rates, a hexahistidine, or, 6xHis tag (5' or 3' to the multiple cloning site) for convenient detection and purification, strong transcriptional terminators to prevent read-through transcription and ensure stability of the expression product, a  $\beta$ -lactamase gene (*bla*)



conferring resistance to ampicillin and a Col E1 origin of replication (QIAGEN Ltd., 2000). Regulation of expression from the pQE60 vector (Figure 4.1) can be controlled by the addition of glucose (catabolite repression) and by co-expressing the plasmid in cells containing the pREP4 plasmid, a low copy number plasmid that expresses the lac repressor protein encoded by the *lacI<sup>r</sup>* gene (QIAGEN Ltd., 2000). *E. coli* strains that harbour the *lacI<sup>r</sup>* mutation, such as XL1 Blue, TG1 and XL10-Gold®-Gold, produce enough lac repressor to efficiently block transcription, and are ideal for storing and propagating pQE plasmids (QIAGEN Ltd, 2000).

pQE60 in particular, facilitates expression of functional proteins with a C-terminal 6xHis tag. The number of His-tagged recombinant protein constructs listed in the Protein Data Bank ([www.rcsb.org/pdb](http://www.rcsb.org/pdb)) is continually growing. It is acknowledged that proteins with a His-tag may vary slightly with regard to their mosaicity and diffraction pattern when compared to the native protein (Hakanson *et al.*, 2000). In principle, it cannot be excluded that the affinity tag may interfere with the protein activity (Wu and Filutowicz, 1999), although the relatively small size and charge of the polyhistidine tag normally ensure that protein activity is rarely affected (Terpe, 2003).

#### **4.1.2 Expression hosts**

In *E. coli*, successful transcription requires the presence of a promoter region, recognised by RNA polymerase, situated immediately upstream of the gene of interest. Comparison of many promoters has led to the formulation of a consensus sequence that consists of the -35 region (5'-TTGACA-) and the -10 region, or 'Pribnow' box (5'-TATAAT-), the transcription start point being assigned the +1 position (Old and Primrose, 1989). Effective translation depends on the mRNA transcript possessing a dedicated ribosome-binding site. Shine and Dalgarno, (1975) were the first to postulate that in addition to a translational start codon (AUG or GUG), a recognisable ribosome binding site required a sequence of bases complementary to the 3' end of 16s ribosomal RNA. The accepted consensus sequence is 5'-TAAGGAG-3' (Karlin and Mrazek, 2000), with the central 5'-AGGA-3' representing the most highly conserved region (Kibler and Hampson, 2002). Traditionally it has been shown that ligated DNA molecules transform at a significantly lower efficiency than supercoiled molecules, and large plasmids less efficiently than small plasmids. *E. coli* XL10-Gold are preferred for accommodating large expression constructs, by virtue of the fact that they possess the Hte phenotype, that increases transformation efficiency (Jerpseth *et al.*, 1997). This was particularly pertinent, given the large size of the *inlA* gene to be cloned.



#### 4.1.3 Cloning strategies

TA cloning using the pCR2.1<sup>®</sup> vector (Figure 4.2) does not allow directional cloning of PCR products, a fact that can result in the desired genes being present in the wrong orientation or in the wrong reading frame. The pCR2.1 vector is supplied as a linearised plasmid with 3' -T overhangs flanking the multiple cloning site (MCS), that conveniently and universally accommodate PCR products that have complementary 3' -A overhangs. This latter feature is a pervading characteristic of PCR products that have been amplified using *TAQ* polymerase. This process is commonly referred to as 'blunt-end', or, 'non-directional' cloning. The *lacZα* gene sequence encodes the first 146 amino acids of β-galactosidase. If self-ligation or reannealing of the pCR2.1 plasmid occurs, transcription can proceed through *lacZα* and the *lacZα* protein is expressed. Complementation *in trans* with the Ω fragment leads to active β-galactosidase in host bacterial cells bearing such plasmids. These are easily identified by their ability to cleave X-gal and thus, produce blue-colored colonies on X-gal supplemented agar media.

The housing of the MCS within the *lacZα* gene sequence means that transformants harbouring pCR2.1 with a ligated insert have a redundant *lacZα* gene and are easily identified as white colonies. This is referred to as 'blue-white' screening.

The 'non-directionality' of the ligation process is not a problem since the principal function of TA cloning is to provide a universal and rapid, one-step cloning strategy for the direct insertion of unmodified PCR product into the pCR2.1 vector. This vector thus acts as a 'utility' vector providing a stable and reproducible source of the sequence of interest in a framework-construct that facilitates gene modification and manipulation. Most restriction enzymes require additional DNA flanking the restriction site in order to sufficiently digest DNA. Cloning of the *inlA* gene sequences into a TA cloning vector also provides the additional DNA needed for the efficient digestion of the PCR products. Technically, the pCR 2.1 vector can mediate protein gene expression in host bacterial cells that do not possess the *lacI<sup>f</sup>* genotype, by virtue of the *lac* promoter. However, in order to ensure that the gene of interest is in the correct reading frame and ligated in the correct 5' → 3' orientation it is necessary to directionally clone the *inlA* gene into the purposely selected or designed expression vector (e.g. pQE60). This concomitantly ensures that the corresponding protein of interest is subject to controllable (or inducible) expression and fused to a suitable tag for expression signalling and purification purposes.



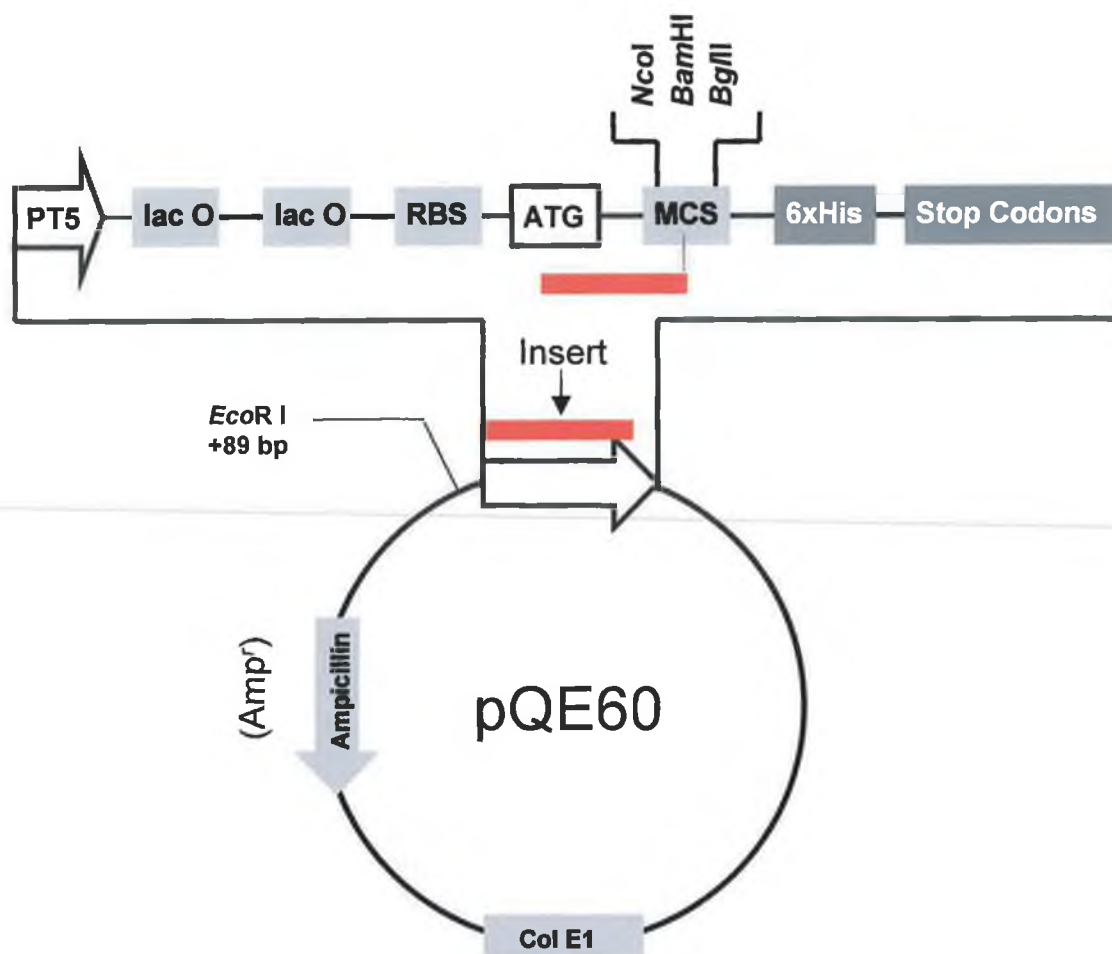


**Figure 4.1:** Vector map of the Qiagen 3.4 kbp pQE60 plasmid and its principal components. PT5 refers to the phage T5 promoter, which is followed by a dual lac operator (lac O) sequence to increase the probability of lac repressor binding and concomitant repression of the strong PT5 promoter. The ATG universal start codon is coupled within the NcoI restriction sequence, which is followed by a BamH I restriction site within the multiple cloning site (MCS). A hexahistidine sequence (6xHis) is located at the 3' end of the coding sequence, which translates to a C-terminal tag. Translational stop codons are located immediately downstream of the 6xHis sequence in all reading frames to facilitate convenient preparation of expression constructs. The Col E1 origin of replication and ampicillin-resistance gene (*Amp<sup>r</sup>*), permit propagation and selection of *E.coli* cells, respectively, which have been transformed with a pQE60-based plasmid construct.





<sup>*lacZα* ATG</sup>  
 CAG GAA ACA GCT ATG AC C ATG ATT ACG CCA AGC TTG GTA CCG AGC TCG GAT CCA CTA  
 GTC CTT TGT CGA TAC TG G TAC TAA TGC GGT TCG AAC CAT GGC TCG AGC CTA GGT GAT

<sup>*Bam*H I</sup>  
 CAG GAA ACA GCT ATG AC C ATG ATT ACG CCA AGC TTG GTA CCG AGC TCG GAT CCA CTA  
 GTC CTT TGT CGA TAC TG G TAC TAA TGC GGT TCG AAC CAT GGC TCG AGC CTA GGT GAT

<sup>*Eco*R I</sup>  
 GTA ACG GCC GCC AGT GTG CTG G AA TTC GGC TT **PCR product** AA GCC G AA TTC TGC  
 CAT TGC CGG CGG TCA CAC GAC C TT AAG CCG AA TT CGG C TT AAG ACG

AGA TAT CCA TCA CAC TGG CGG CCG CTC GAG CAT GCA TCT AGA GGG CCC AAT TCG CCC  
 TCT ATA GGT AGT GTG ACC GCC GGC GAG CTC GTA CGT AGA TCT CCC GGG TTA AGC GGG

TAT AGT GAG TCG TAT TAC AAT TCA CTG GCC GTC GTT TTA CAA CGT GAC TGG GAA AAC  
 ATA TCA CTC AGC ATA ATG TTA AGT GAC CGG CAG CAA AAT GTT GCA CTG ACC CTT TTG

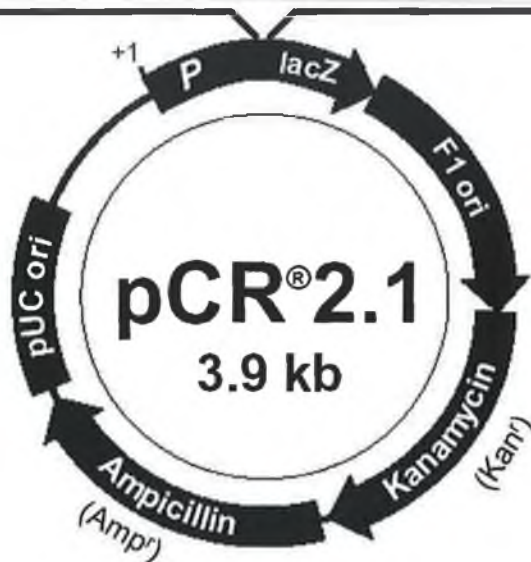


**Figure 4.2:** Vector map of the Invitrogen pCR2.1 plasmid. Key features include the *lacZα* gene (position 1-545) that also incorporates the MCS site (234-355) and facilitates 'blue-white' screening. *Eco*RI sites are located at +283 and +299 bps providing convenient restriction sites for 'insert' excision and analysis. The ampicillin-resistance (*Amp<sup>r</sup>*) and kanamycin-resistance (*Kan<sup>r</sup>*) open reading frames (ORF) confer resistance to ampicillin and kanamycin and, in conjunction with the pUC origin of replication, facilitate propagation and selective plasmid retention in *E. coli* cells.



#### 4.1.4 High fidelity PCR

'*Pfu*' DNA polymerase is a thermostable enzyme of approximately 92 kDa isolated from *Pyrococcus furiosus* (Fiala and Stetter, 1986). It catalyses the DNA-dependent polymerisation of nucleotides into duplex DNA in the 5'→3' direction. More significantly, it exhibits 3'→5' exonuclease (or 'proofreading') activity. This means that base mismatches that can occur (albeit infrequently) during polymerisation, are rectified by the proofreading element (Lundberg *et al.*, 1991). *Pfu* DNA Polymerase, unlike *Taq* DNA Polymerase, lacks terminal transferase activity and generates blunt-ended PCR products, lacking terminal -'A' overhangs. Sequences amplified in this fashion are not amenable to TA cloning. The replication fidelities of *Pfu* and a number of commercial DNA polymerases have been compared using a PCR-based forward mutation assay (Cline *et al.*, 1996). The error rates of a *Taq/Pfu* DNA polymerase mixture and a Klenow fragment/*Taq/Pfu* DNA polymerase mixture were found to be less than the error rate of *Taq* DNA polymerase, but approximately 3-4-fold higher than the error rate of *Pfu* DNA polymerase. Confidence in the PCR fidelity is especially relevant when the gene sequence being cloned is large (> 2 kbp), such as is the case with *inlA*.

The above technologies were cumulatively exploited for the efficient cloning, heterologous expression and purification of a recombinant version of the *L. monocytogenes* InlA protein.



## 4.2 Results and discussion

### 4.2.1 Extraction of genomic DNA

Initial attempts to extract genomic DNA (gDNA) from *L. monocytogenes* using Proteinase K and lysozyme treatment were unsuccessful. This was probably due to the high peptidoglycan content and robust nature of the cell wall, which is typical of Gram-positive bacteria. Genomic DNA was successfully extracted from a fresh culture of *L. monocytogenes* 1/2a cells, using guanidium thiocyanate, in a modification of the method recommended by Pitcher and co-workers, (1989) and as outlined in Section 2.9.2. The quality of the extracted gDNA was checked by running a sample on a 1 % agarose gel (Figure 4.3).

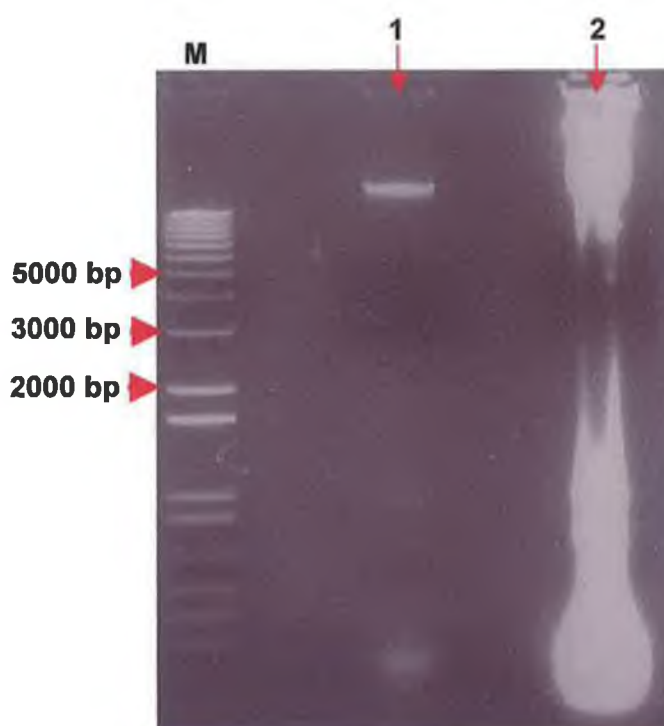


**Fig 4.3:** Electrophoretic profile of extracted *L. monocytogenes* genomic DNA (gDNA). The lane on the extreme right (2) represents a neat, undiluted sample of freshly isolated gDNA. The concentration of nucleic acids was very high, so high in fact that a large portion actually remained in the reservoir. A sample diluted 1/20 was run in the central lane (1) and resulted in a high molecular weight band, typical of gDNA. The lane on the left, labelled 'M' consisted of a graduated molecular weight marker (1 kbp ladder) for band size approximation.



#### 4.2.2 Cloning of full-length *inlA* gene into pCR2.1 (TA cloning)

The primer sequences TAFII-A and InlARII (Section 2.9.3) were designed to amplify the complete *inlA* protein gene minus the signal and precursor peptide sequence, beginning from the *L. monocytogenes* 1/2a *inlA* native translational start codon, 'ATG'. The primers were also synthesised with terminal ends designed to incorporate dedicated *Nco*I and *Bam*HI restriction sequences at the respective 5' and 3' termini of the amplified *inlA* gene. A 500 µl TAQ-PCR master reaction mixture was set up according to the component ratios outlined in Section 2.9.6. The mixture was split into individual 50 µl reaction volumes in PCR tubes that were then subjected to temperature gradient PCR over the range 59 °C - 69.0 °C. The results are depicted in Figure 4.4. The optimum temperature was taken as 65 °C. Although all the temperatures tested gave suitably defined, single bands at the desired molecular weight (2.4 kb), the temperature at the higher end of the scale was selected to maximise primer fidelity and reduce the propensity for non-specific annealing.

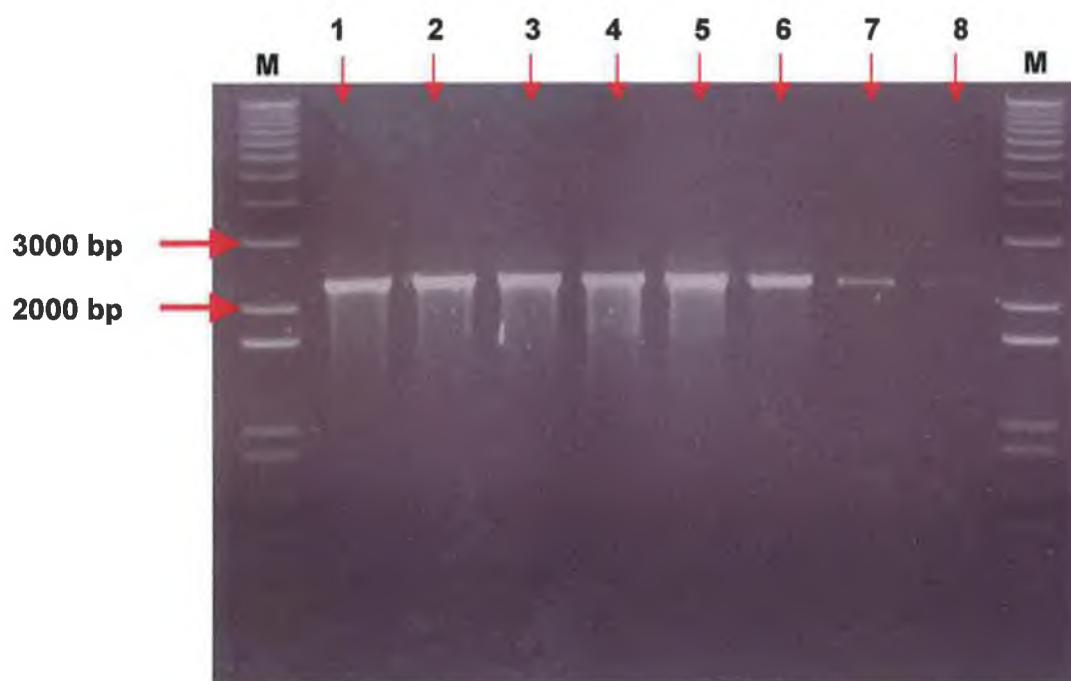


**Figure 4.4:** Temperature gradient analysis for optimisation of TAFII/InlARII-primed TAQ-PCR amplification of the *inlA* gene. The lanes 1-8 represent PCR products obtained following annealing at 59.0, 59.9, 61.5, 63.2, 64.8, 66.5, 68.0 and 69.0 °C. The outer lanes, designated 'M', contain molecular weight markers.





A 2 µl sample of freshly amplified *TAQ* PCR reaction mixture was 'blunt-end' ligated into linearised pCR2.1 vector at 14 °C, overnight, as described in Section 2.9.7. The freshly ligated pCR2.1- *inlA* construct was then transformed (Section 2.9.7) into One Shot® *E. coli* INVαF' cells that were supplied in ultra-competent status as part of the TA cloning kit supplied by Invitrogen Ltd. Plates containing transformed cells were screened following overnight incubation at 37 °C and subsequent cooling at 4 °C for 2 hours. A total of 10 isolated white colonies and one blue, control colony were picked and sub-cultured into fresh LB broth for overnight propagation at 37 °C. When the overnight cultures were examined, growth was only evident in the control sample. This suggested that expression of the recombinant InlA (rInlA) product was toxic to the host *E. coli* INVαF' cells. In order to overcome this problem, the transformation process was repeated using *E. coli* XL10-Gold® cells. Unlike *E. coli* INVαF' cells, the *E. coli* XL10-Gold® cell genotype included the *lacI<sup>d</sup>* gene, encoding the lac repressor protein. This meant that expression of the rInlA protein from the pCR2.1- *inlA* construct could only proceed following induction with IPTG. Basal leakage of the rInlA protein was further inhibited by adding 1 % (w/v) glucose to the broth media, thereby abrogating rInlA-induced cellular toxicity. Hence, following blue-white screening, all selected colonies were successfully cultured in LB broth. Plasmid preparations were subsequently conducted on all the cultured transformants (Section 2.9.14) and each sample was then analysed by agarose gel electrophoresis (Figure 4.5). The results indicated that nine out of the ten selected clones contained an insert. The presence of the *inlA* sequence was further confirmed by subjecting each of the samples to PCR using the *inlA*-specific primers (Figure 4.6).

Two representative samples that were deemed positive, based on the PCR analysis, were subjected to restriction analysis in order to confirm the presence of the desired 2.2 kb *inlA* gene insert. Plasmid samples from clones 7 and 8 (XG7 and XG8) were digested with *EcoRI* enzyme (Section 2.9.8.1). In addition, a plasmid sample from clone 4 (XG4) was also digested with *EcoRI* to serve as a control. Figure 4.7 demonstrates that the presence of the *inlA* insert was confirmed in both XG6 and XG8.



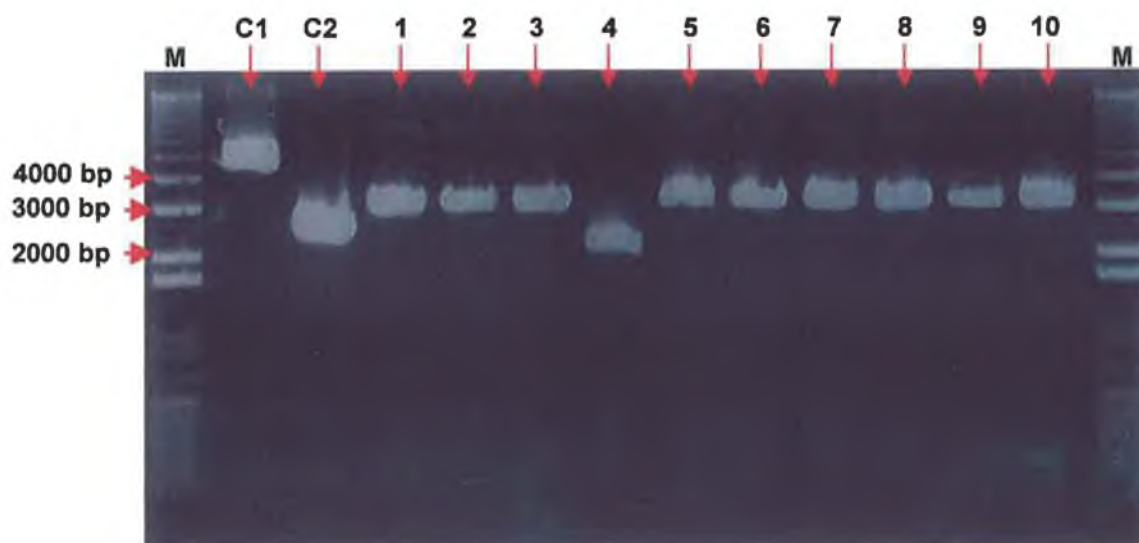


**Figure 4.5:** Plasmid preparations from *E. coli* XL10-Gold cells following transformation with pCR2.1- *inlA* construct. The lanes were loaded with 5  $\mu$ l of each 'plasmid prep'. Lanes (C1 and C2) contained the control plasmid isolated from two individual 'blue' colonies. All of the plasmid samples, except for sample 4 (lane 4), derived from the selected 'white' colonies, yielded a single plasmid band of universally greater molecular weight than that of the control. These were predicted to contain the *inlA* gene insert. A possible reason for the unexpectedly high molecular weight of control sample plasmid (C1) was, that two linearised pCR2.1 plasmids had ligated together, producing an 'double-blue' genotype. If it was the case that sample 4 contained only re-annealed pCR2.1 plasmid, it would also be expected that the control sample C2 should appear as a band at the same molecular weight. The fact that the C2 plasmid appeared at a slightly higher molecular weight suggested that it contained a higher concentration of plasmid, arising from a higher cell yield. This is not surprising given that the total absence of the *inlA* gene insert would render the clone at a competitive advantage, in terms of growth rate, over those cells bearing the *inlA* gene insert (even if expression is minimised by the presence of *lacI<sup>f</sup>* and glucose). The outer lanes, designated 'M', contain molecular weight markers.



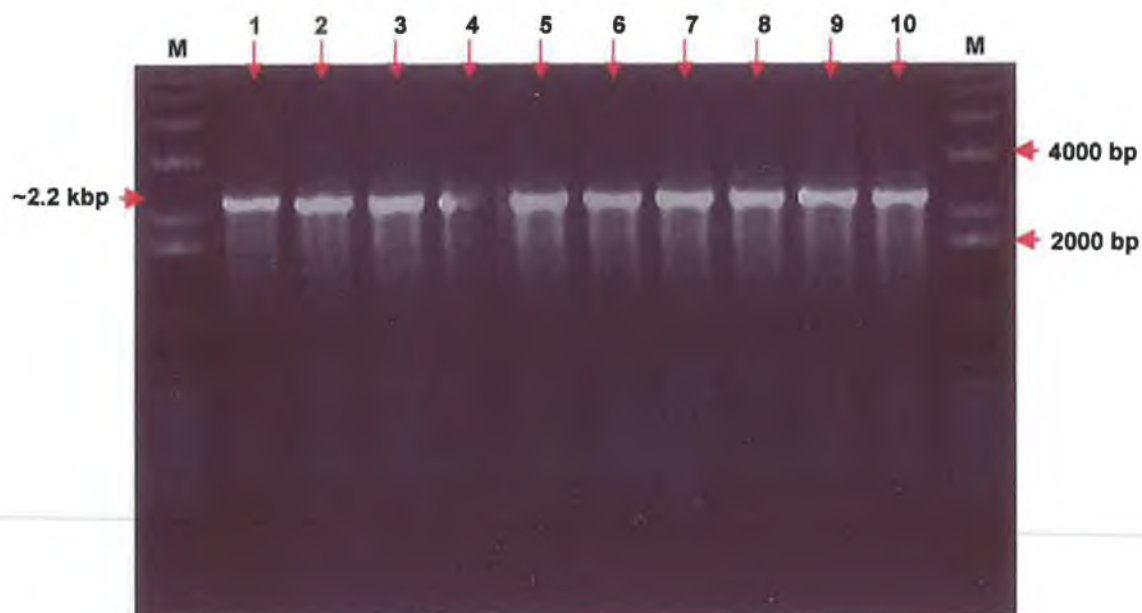


**Figure 4.6:** PCR analysis of plasmid preparations from *E. coli* XL10-Gold cells following transformation with pCR2.1-*inlA* construct. The results corresponded with the plasmid molecular weight analysis (Figure 4.5). Sample 4 was the only sample that failed to yield an *inlA* band following PCR amplification. The outer lanes, designated 'M', contain molecular weight markers. The appearance of a small amount of *inlA* PCR product in lane 4 was due to accidental sample run-over from lane 3 during loading.



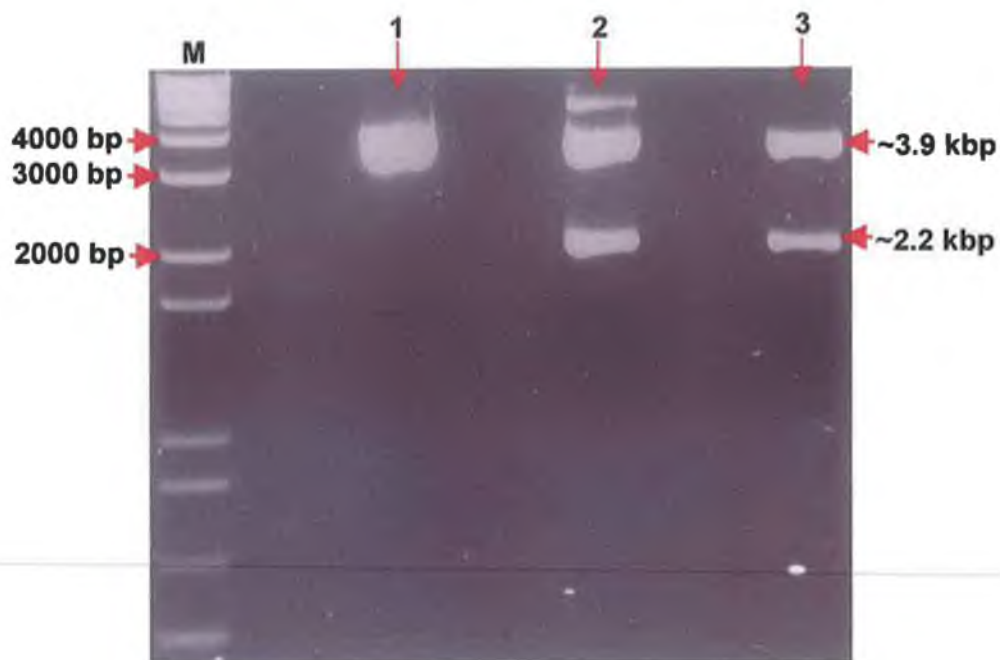


**Figure 4.7:** *EcoRI* restriction analysis of plasmids purified from selected pCR2.1-inlA transformants. The lane labelled 'M' represents the molecular weight marker. Lanes 1-3 correspond to clones 'XG4', 'XG7' and 'XG8', respectively. The XG7 and XG8-derived plasmids yielded a linearised pCR2.1 fragment at 3.9 kbp and an inlA insert band at ~2.2 kbp. The additional high molecular weight band in XG7 was due to incomplete plasmid digestion. The control plasmid, derived from XG4 yielded only a 3.9 kbp band corresponding to linearised pCR2.1.





#### 4.2.3 Cloning of full-length *inlA* gene into pQE60

It is pertinent to re-emphasise that the pCR2.1 plasmid was being employed as a 'utility vector' to allow rapid, high fidelity reproduction of the insert gene, not as an expression construct. The 'blunt-end' (non-directional) ligation associated with TA cloning did not favour one particular orientation of the insert over another. Thus, normally at this stage the positive PCR and *EcoRI* restriction analyses would be deemed sufficient information to proceed, pending confirmatory sequence analysis. The plasmid from XG8 was digested with *NcoI* and *BamHI* enzyme (Section 2.9.8.2) in preparation for directional ligation of the *inlA* gene into complimentary, restricted pQE60 expression plasmid (Figure 4.8). The pQE60 plasmid used was one that had been previously ligated with the *L. monocytogenes* p60 protein encoding gene or invasion associated protein (*iap*) gene, (kindly donated by Paul Leonard, DCU).

Following *BamHI/NcoI*-restriction, the 'donor' pQE60 plasmid yielded an upper 3.4 kbp band (corresponding to linearised pQE60) and a lower band (corresponding to the excised *iap* gene insert). The *BamHI/NcoI*-restricted XG8-derived pCR2.1-*inlA* plasmid yielded only two bands also. However, upon consultation with the relevant restriction map for plasmid pCR2.1 (Figure 4.9) it was concluded that the upper band actually consisted of two fragments. One of which was the desired 2.2 kbp *inlA* gene, yet it was 'contaminated' with a second, 2.275 kbp fragment that arose due to restriction of the plasmid at the *NcoI* site located at position +1877. This was an unfortunate coincidence that made excision of the *inlA* band and subsequent purification impossible. The lower band (~1.6 kbp) was due to restriction of the plasmid at the *BamHI* (+252) and *NcoI* (+1877) sites.

One possible way to overcome this problem was investigated. Plasmids from both XG7 and XG8 were preliminarily restricted with *BamHI* enzyme alone. It was clear from the results (Figure 4.10) that the XG8-derived plasmid contained the insert oriented with its 5' *BamHI* site proximal to that of the pCR2.1 *BamHI* (+252) site. Thus, *BamHI* restriction yielded a single, effectively linearised band corresponding to the combined molecular weights of both pCR2.1 and *inlA* (~ 6.1 kbp). Conversely, it was apparent that the XG7-derived plasmid harboured the *inlA* insert in the opposite orientation. *BamHI* restriction therefore, yielded two bands. In addition to providing a useful means of determining the insert orientation these results also suggested that it might be possible to isolate the band of interest (*inlA*) by conducting a stepwise digestion. However, this would also necessitate two separate digest incubations and two sequential purifications of the *inlA* band from the gel. *BamHI* and *NcoI*



digested termini had proved to be quite susceptible to degradation and thus, prolonged holding at elevated temperature associated with a double sequential digest and purification was not favoured. It would also be impossible to distinguish whether the secondary *NcoI* restriction had been successful, since the small amount of DNA removed would not be visible on the gel and its removal would have no discernable effect on the migration distance of the primary, *BamHI*-digested fragment. Conversely, by digesting the XG8-derived plasmid simultaneously, with a *BamHI/NcoI* cocktail, the presence of two bands was taken to indicate successful and complete restriction of the insert gene. The fact that this was contaminated with an equal amount of the residual pCR2.1 was not unduly worrying. This was because any re-annealing between the *inlA* and residual pCR2.1 sequence was expected to result in a product that would be constrained by having two identical terminal restriction sites (i.e. *BamHI* at both ends or *NcoI* at both ends). These would therefore, fail to ligate into *BamHI/NcoI*-digested pQE60.

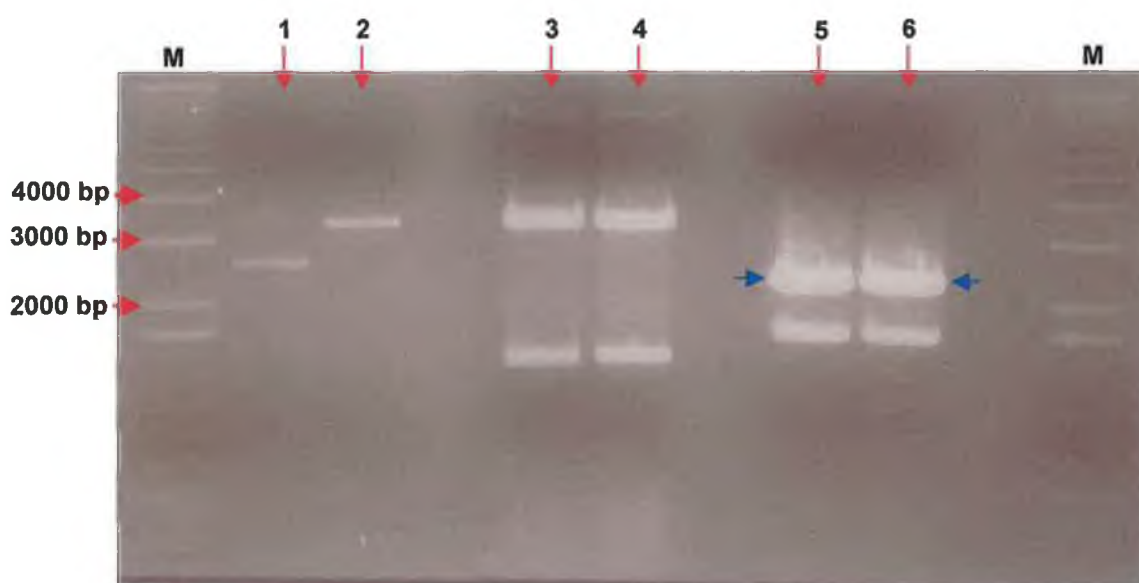


**Figure 4.8:** Lane (1) contained 5  $\mu$ l of undigested 'donor' pQE60 plasmid containing the *iap* gene insert; lane (2), 5  $\mu$ l of undigested XG8-derived pCR2.1-*inlA* plasmid; lanes (3) and (4), 20  $\mu$ l each of *BamHI/NcoI*-restricted 'donor' pQE60 and lanes (5) and (6), 20  $\mu$ l each of *BamHI/NcoI*-restricted XG8-derived pCR2.1-*InlA* plasmid. The ~2.2 kbp band in lanes 5 and 6 (indicated by blue arrows) appears twice as intense as the lower band because it contains twice the amount of DNA due to co-migration of the *inlA* insert gene and the residual pCR2.1 fragment. The outer lanes, designated 'M', represent molecular weight markers.



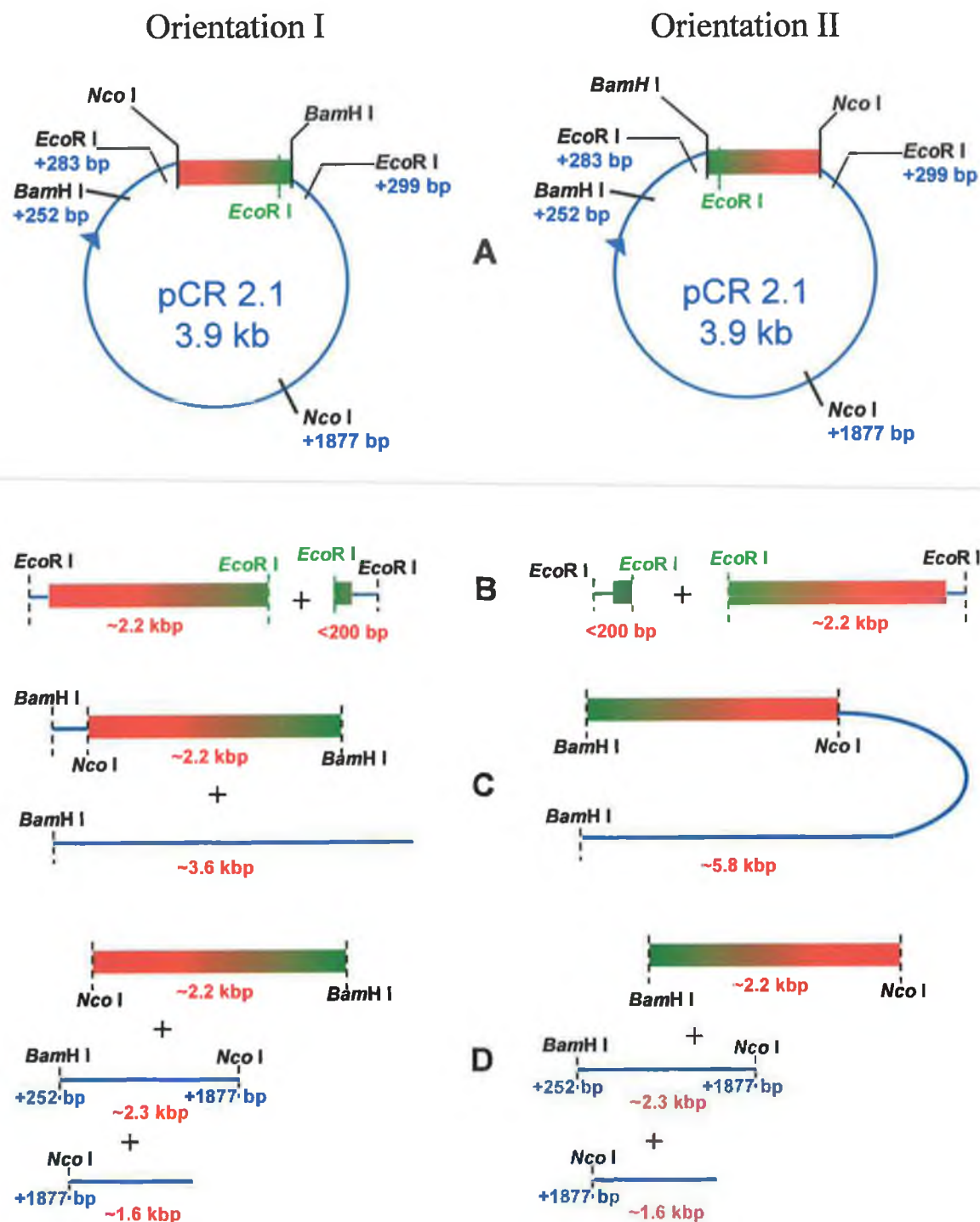


**Figure 4.9:** Restriction map for plasmid pCR2.1 with the *inLA* gene insert in both possible orientations, (A). The predicted products resulting from restriction with either *EcoRI*, (B), *BamHI*, (C), or a *BamHI/NcoI* cocktail, (D), are given along with their approximate molecular sizes.



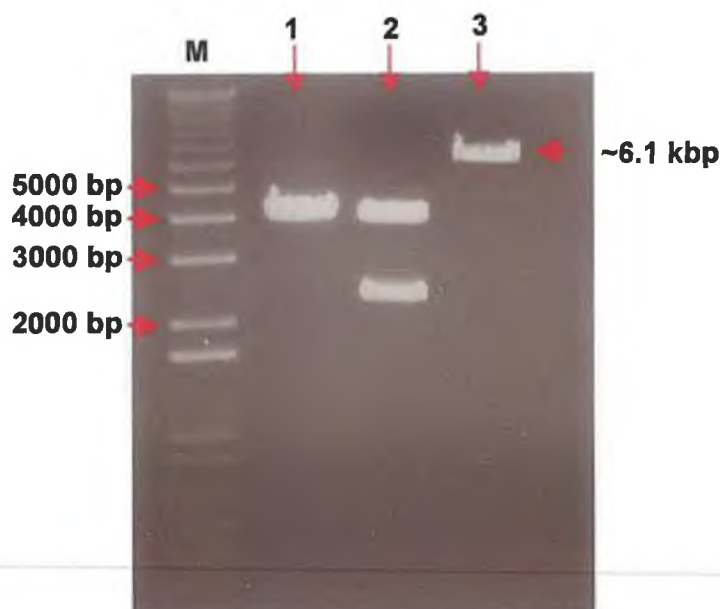


**Figure 4.10:** *Bam*HI analysis of *inlA* insert orientation in selected pCR2.1 plasmids. The lane labelled 'M' represents the molecular weight marker. Lanes 1-3 correspond to *Bam*HI-restricted plasmids, derived from clones 'XG4', 'XG7' and 'XG8', respectively. The *Bam*HI-restricted XG4 plasmid served as a control. It did not harbour the *inlA* gene insert and thus, generated a band at approximately 3.9 kbp. XG7-derived plasmid yielded two distinct bands, indicating a distal separation of the *Bam*HI sites. The XG8-derived plasmid generated only one apparent, high molecular weight band (~6.1 kbp), indicating proximal separation of the *Bam*HI sites.

The *Bam*HI/*Nco*I-excised *inlA* insert was ligated into compatibly restricted pQE60 expression plasmid (Section 2.9.10) and transformed into *E. coli* XL10-Gold®-Gold cells (Section 2.9.11). Following overnight incubation at 37 °C, a total of twenty isolated colonies were randomly selected and individually sub-cultured into fresh 5 ml volumes of LB broth. The selected clones were grown overnight at 37 °C and 200 rpm, reaching stationary growth phase. Plasmid isolation was performed on the resulting cell pellet and a sample of each plasmid prep' was then analysed by *Eco*RI restriction. Unlike the pCR 2.1 vector that has *Eco*RI restriction sites conveniently bracketing the MCS region, pQE60 only harbours one *Eco*RI restriction site, immediately preceeding the 5' insert region (Figure 4.1). However, the fact that the *inlA* gene insert also possesses a single *Eco*RI site located just upstream from its C-terminal encoding region, means that both the presence and orientation of the *inlA* gene in pQE60 can be confirmed by a one-step *Eco*RI restriction. Six out of the twenty samples





tested, demonstrated a 2.2 kbp *inlA* insert band (Figure 4.11). The parent clones were designated XGQ3, XGQ4, XGQ7, XGQ10, XGQ12 and XGQ19. The presence of the *inlA* sequence was further confirmed by *inlA* gene-specific PCR (Figure 4.12). Considering the fact that the *inlA* gene was exactly 50 % contaminated with a residual pCR 2.1 fragment of similar size, the results indicated a successful cloning efficiency of 60 %, using the TA strategy.

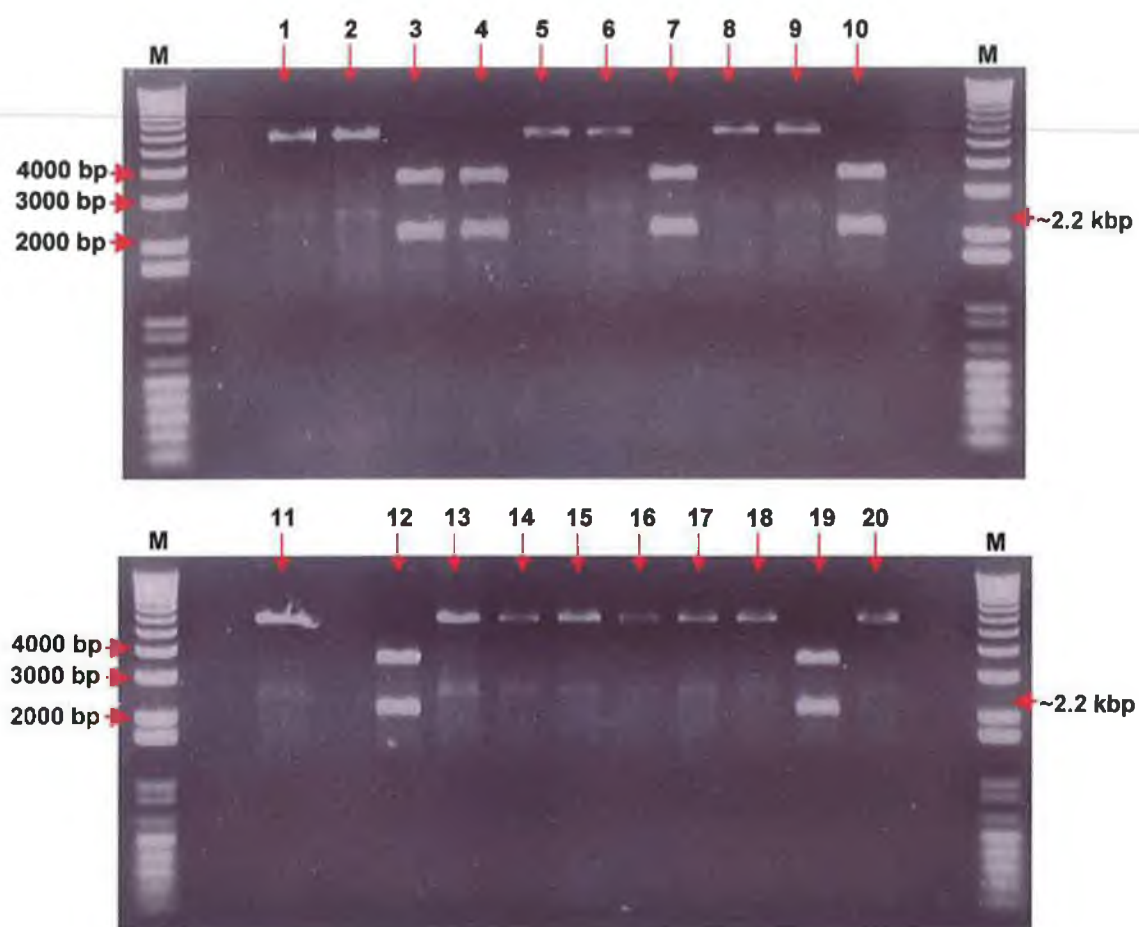


**Figure 4.11:** *EcoRI*-mediated restriction analysis of plasmids purified from twenty randomly selected *pQE60-inlA* transformed *E. coli* XL10-Gold® clones. Clones 3, 4, 7, 10, 12 and 19 harboured a 2.2 kbp insert and were putatively deemed positive for the *inlA* gene. The peripheral lanes, labelled 'M', represent the molecular weight marker.



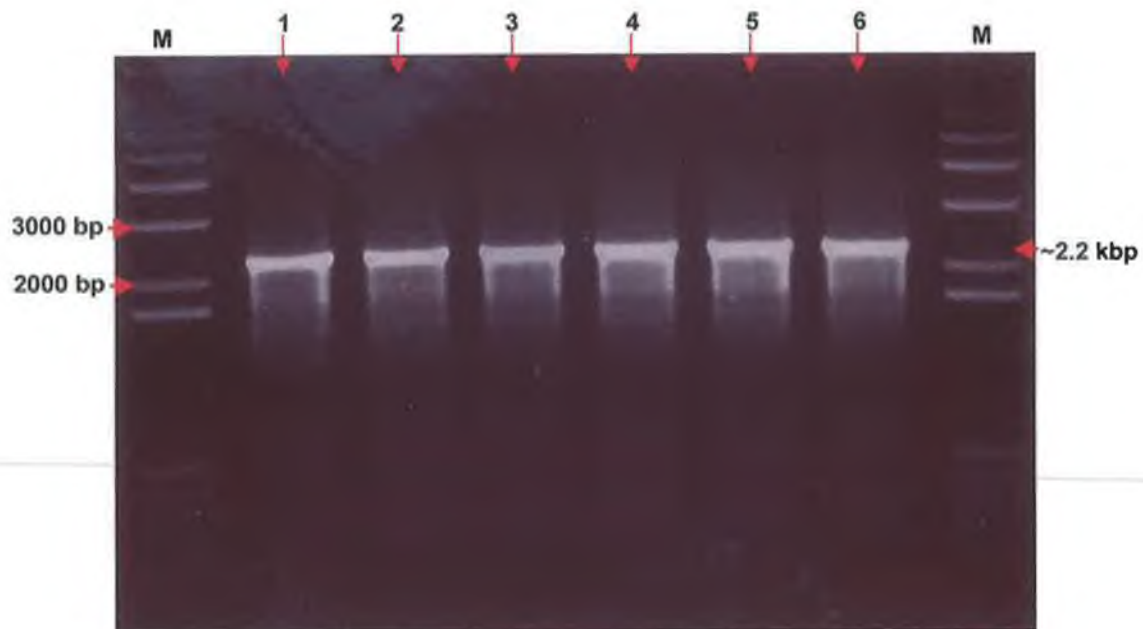


**Figure 4.12:** *inlA* gene-specific PCR of plasmids previously confirmed to harbour 2.2 kbp insert. The lanes 1-6 represent PCR products obtained following *inlA* gene-specific amplification of plasmids that had previously confirmed to contain a 2.2 kbp insert (Figure 4.9). The outer lanes, designated 'M', contain molecular weight markers. All six plasmids generated an *inlA* gene-specific band at 2.2 kbp, thus confirming the plasmid insert to be the *inlA* gene.

#### 4.2.3.1 Time course experiments to determine the full-length *rInlA* expression levels

The six selected *E. coli* XL10-Gold transformant cells harbouring the pQE60-*InlA* plasmid construct were induced with 1 mM IPTG and samples taken every hour. Due to the potential toxicity associated with the *InlA* recombinant protein, particularly at higher growth temperatures (37 °C), expressing cultures were evaluated at 30 °C. Time point cell samples were resuspended in lysis buffer (2x PBS) and sonicated. The resulting cytoplasmic extracts were analysed by SDS-PAGE as shown in Figure 4.13. No apparent expression of any up-regulated band in the 80 kDa region was discernable. When the corresponding Western blots were probed with an anti-His-tag monoclonal antibody (Section 2.9.17) no obvious band development was apparent. However, although not readily visible, when the blot was held up to a light source it was possible to barely discern a very faint band in the 80 kDa region of the latter stage lysates from clones XGQ3, XGQ4 and XGQ12. Each of these three clones were



then re-analysed. The clones were induced overnight (~10 hrs) and then lysed as before. In addition, a duplicate set of samples was lysed in a urea-based denaturing buffer. It was hoped that this buffer would combat aggregation or vesicle/membrane localisation of the rInlA. However, when the lysates were subjected to SDS PAGE analysis, there was still no visible up-regulation of a band corresponding to the expected rInlA molecular weight (Figure 4.14, top). The corresponding Western blot did, however, develop a slightly reactive band at ~80 kDa when probed with the anti-His-tag monoclonal antibody (Figure 4.14, bottom).

Despite repeated attempts, it proved impossible to improve the expression levels or even achieve reproducible expression levels with the three selected clones. In order to confirm that the *inlA* gene sequence had been faithfully cloned in terms of nucleotide content and was 'in-frame', XGQ8 was taken as a representative clone and its plasmid DNA was sequenced. The XGQ8-derived plasmid DNA, when translated, demonstrated 100 % homology with the native InlA protein (Figure 4.15). This confirmed that the problem was most probably post-translational and prompted a fundamental re-assessment of the InlA protein with respect to its amino acid content and associated physicochemical properties. It has been reported that recombinantly produced proteins with appreciable hydrophobic regions can have a toxic effect on host cells (as was also seen with this protein when expressed at even a basal level in permissive Inv $\alpha$ F' cells), due to association of the protein with, or incorporation into vital membrane structures (Qiagen, 2002). The fully translated InlA amino acid content was evaluated in terms of its hydrophobicity, using the hydropathic index and associated method outlined by Kyte and Doolittle, (1982). The region between amino acid 776 and the C-terminus was calculated to exhibit the most pronounced hydropathic characteristics (Figure 4.16). This corresponded exactly with the LPTTG-anchored cell wall domain and its preceding, cell membrane localised sequence. It was thus highly likely that this anchoring region, typical of Gram-positive cell wall proteins, was preventing efficient expression of the recombinant InlA protein in the Gram-negative *E.coli* expression host.



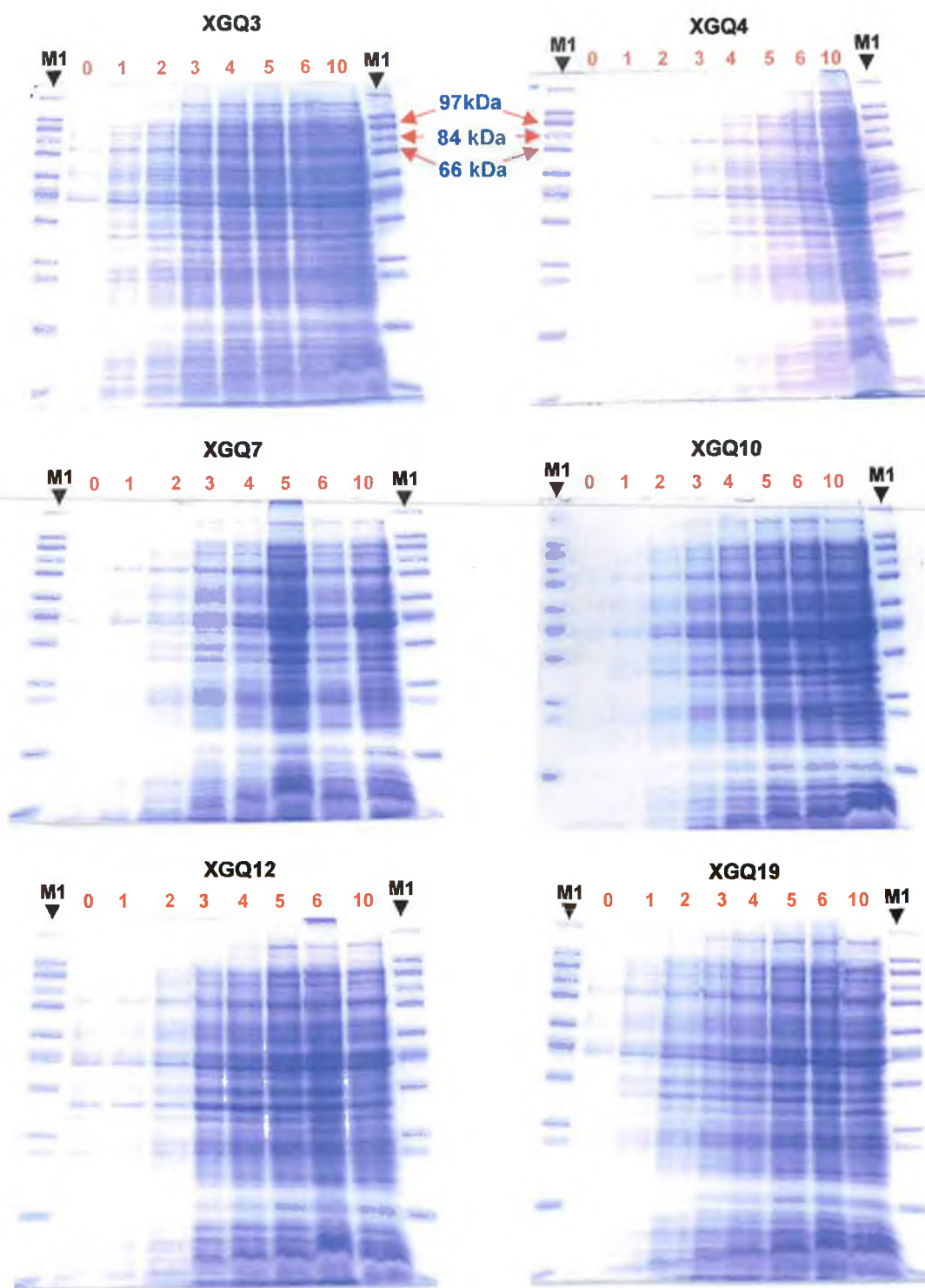


**Figure 4.13:** Time course analysis of selected transformants containing the pQE60-inlA expression construct. Lysates were prepared in non-denaturing buffer (2x PBS) from 1 ml samples taken at time  $T=0$  and six, hourly intervals, plus a  $T=10\text{hr}$  (overnight) sample, following induction at  $30^\circ\text{C}$  with mM IPTG. Time-point samples are indicated with red numerals. 'M1' indicates lanes containing SigmaWide™ molecular weight marker. There was no discernable up-regulated expression of rInlA protein in the anticipated 80 kDa region.





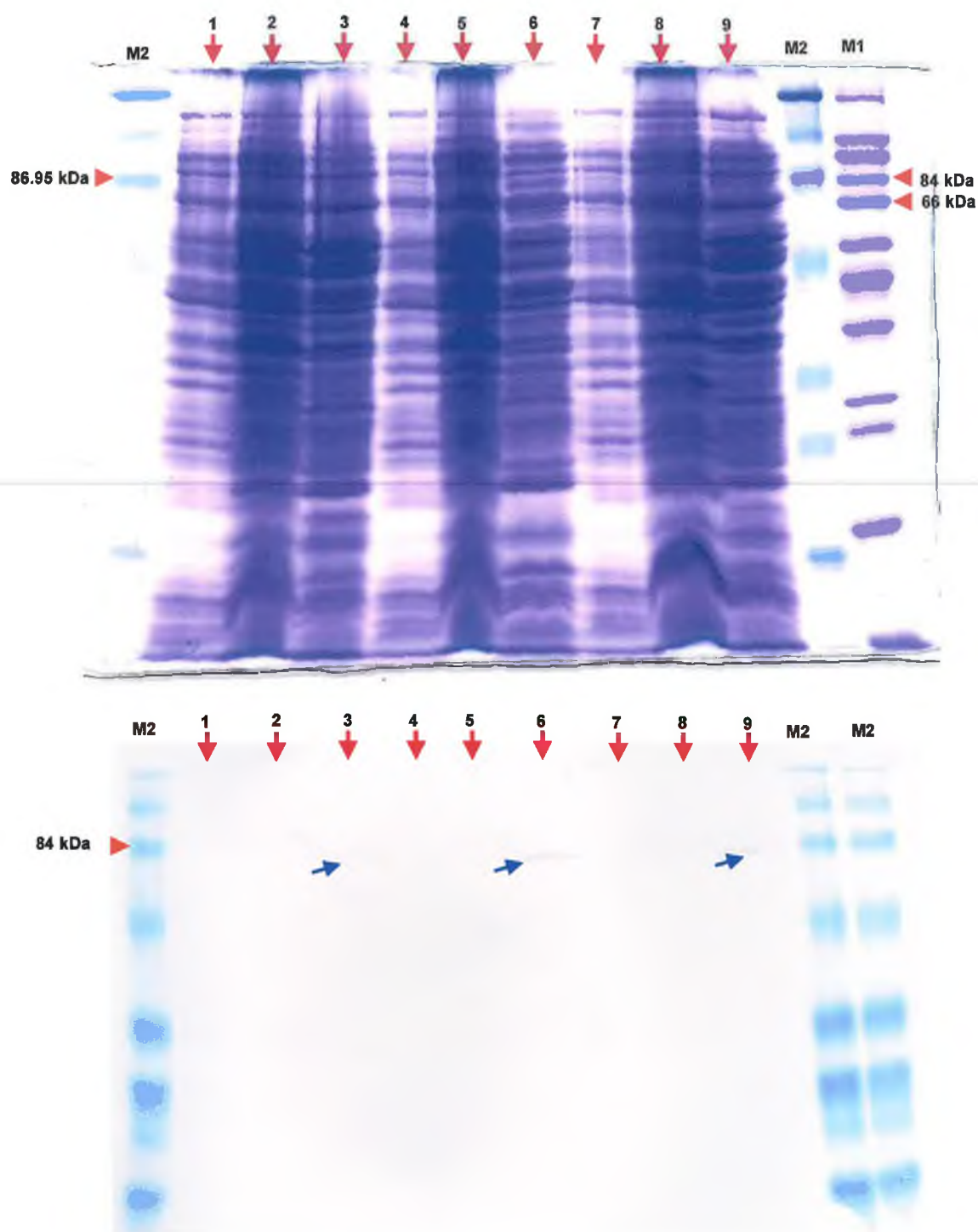


**Figure 4.14:** Comparison of expression levels following overnight induction when lysates are prepared in denaturing (urea-based) or non-denaturing (2x PBS) buffer. Lanes 1, 4 and 7 contain lysates in 2x PBS buffer prepared from pre-induction cultures of XGQ3, XGQ4 and XGQ12, respectively. Lanes 2, 5 and 8 contain samples from the same set of cultures following overnight induction at 30 °C with 1 mM IPTG, prepared in denaturing buffer. Lanes 3, 6 and 9 contain a similar sample from the overnight, induced cultures, but, prepared



in 2x PBS. Although the SDS PAGE gel (A) did not reveal any remarkable expression in the 80 kDa region, the corresponding Western blot (B) did develop a weak band (indicated by blue arrows) in this region when probed with anti-His-tag monoclonal antibody. This was only noticeable in samples that had been prepared in no-denaturing buffer. 'M1' and 'M2' refer to SigmaWide™ wide range and Pierce BlueRanger™ (prestained) molecular weight markers, respectively.

#### **4.2.3.2 Sequencing of the cloned full-length *inlA* gene sequence**

The results of the Western blot depicted in Figure 4.14, were inconclusive. The XG4 clone sample had demonstrated the strongest apparent band and thus a sample of plasmid DNA from this clone was sent to MWG-Biotech (UK) Ltd, for sequencing. Sequencing results, received as linear nucleotide sequences, were subsequently translated into amino acid sequences and aligned with the known amino acid sequence of each protein using the ClustalW multiple alignment program. Aligned sequences were imported into Genedoc, and examined (Figure 4.15). The cloned *inlA* gene sequence demonstrated 100 % homology with the corresponding, complete mature InlA protein-encoding sequence, provided by Genedoc (reference AJ012346).

The sequence homology suggested that the *inlA* gene was being faithfully translated and that the difficulties apparent in the apparent expression and detection of the recombinant InlA protein were related to intrinsic complications when expressed in the heterologous host species, *E. coli*. More specifically, it was felt that inherent regions of localised hydrophobicity, commonly associated cell wall proteins, might be prohibiting efficient soluble expression of the recombinant protein. The sequence data was subjected to a hydropathy profile analysis and a prominent C-terminal hydrophobic region was revealed (Figure 4.16). It was concluded that this represented the most probable cause of the weakly detectable expression levels.



```

      *      20      *      40      *      6
COMPLETE_I : MRKKRYVWLKSIILVILVFGSGVWINTSNGTNAQAATITQDTPINQIFTDALAEKME : 59
CLONED_In1 : -----MGE : 4
                                         KT

      0      *      80      *      100      *      1
COMPLETE_I : VLKKTNVTDIVSQTDLDQVTTLQADRLGIKSIDGVEYLNNLTQINFSSNNQLTDITPLKN : 118
CLONED_In1 : VLKKTNVTDIVSQTDLDQVTTLQADRLGIKSIDGVEYLNNLTQINFSSNNQLTDITPLKN : 63
              VLKKTNVTDIVSQTDLDQVTTLQADRLGIKSIDGVEYLNNLTQINFSSNNQLTDITPLKN

      20      *      140      *      160      *
COMPLETE_I : LTKLVDIILMNNNQIADITPLANLTNLTLGLTLFNNQITDIDPLKNLTNLNRLELSSNTIS : 177
CLONED_In1 : LTKLVDIILMNNNQIADITPLANLTNLTLGLTLFNNQITDIDPLKNLTNLNRLELSSNTIS : 122
              LTKLVDIILMNNNQIADITPLANLTNLTLGLTLFNNQITDIDPLKNLTNLNRLELSSNTIS

      180      *      200      *      220      *
COMPLETE_I : DISALSGLTSLQQLSFGNQVTDLKPLANLTTLERLDISSNKVSDISVLAKLTNLESLIA : 236
CLONED_In1 : DISALSGLTSLQQLSFGNQVTDLKPLANLTTLERLDISSNKVSDISVLAKLTNLESLIA : 181
              DISALSGLTSLQQLSFGNQVTDLKPLANLTTLERLDISSNKVSDISVLAKLTNLESLIA

      240      *      260      *      280      *
COMPLETE_I : TNNQISDITPLGILTNLDELSSLNGNQLKDIGTLASLTNLTDLDLANNQISNLAPLSGLT : 295
CLONED_In1 : TNNQISDITPLGILTNLDELSSLNGNQLKDIGTLASLTNLTDLDLANNQISNLAPLSGLT : 240
              TNNQISDITPLGILTNLDELSSLNGNQLKDIGTLASLTNLTDLDLANNQISNLAPLSGLT

      300      *      320      *      340      *
COMPLETE_I : KTELKLGANQISNISPLAGLTALTNLLENQLEDISPISNLKNLTLYLTLYFNNSIDI : 354
CLONED_In1 : KTELKLGANQISNISPLAGLTALTNLLENQLEDISPISNLKNLTLYLTLYFNNSIDI : 299
              KTELKLGANQISNISPLAGLTALTNLLENQLEDISPISNLKNLTLYLTLYFNNSIDI

      360      *      380      *      400      *
COMPLETE_I : SPVSSLTQLQLFFYNNKVSDVSSLANLTNINWLSAGHNQISDLTPLANLTRITQLGLN : 413
CLONED_In1 : SPVSSLTQLQLFFYNNKVSDVSSLANLTNINWLSAGHNQISDLTPLANLTRITQLGLN : 358
              SPVSSLTQLQLFFYNNKVSDVSSLANLTNINWLSAGHNQISDLTPLANLTRITQLGLN

      420      *      440      *      460      *
COMPLETE_I : DQAWTNAPVNYKANVSIPTVNTVGALIPATISDGGSYTEPDITWNLPSTNEVSYT : 472
CLONED_In1 : DQAWTNAPVNYKANVSIPTVNTVGALIPATISDGGSYTEPDITWNLPSTNEVSYT : 417
              DQAWTNAPVNYKANVSIPTVNTVGALIPATISDGGSYTEPDITWNLPSTNEVSYT

      480      *      500      *      520      *
COMPLETE_I : FSQPVTTIGKGTTFSGTVTQPLKAIFNVKHFVDGKETTKEVEAGNLLTEPAKPVKEGHT : 531
CLONED_In1 : FSQPVTTIGKGTTFSGTVTQPLKAIFNVKHFVDGKETTKEVEAGNLLTEPAKPVKEGHT : 476
              FSQPVTTIGKGTTFSGTVTQPLKAIFNVKHFVDGKETTKEVEAGNLLTEPAKPVKEGHT

      540      *      560      *      580      *
COMPLETE_I : FVGWFDAQTGGTKWNFSTDKMPTNDINLYAQFSINSYTATFDNDGVTTTSQTVDYQGLLQ : 590
CLONED_In1 : FVGWFDAQTGGTKWNFSTDKMPTNDINLYAQFSINSYTATFDNDGVTTTSQTVDYQGLLQ : 535
              FVGWFDAQTGGTKWNFSTDKMPTNDINLYAQFSINSYTATFDNDGVTTTSQTVDYQGLLQ

```



```

          600          *          620          *          640
COMPLETE_I : EPTAPTKEGYTFKQWYDAKTGGDKWDFATSKMPAKNITLYAQYSANSYTATFDVDGKST : 649
CLONED_Inl : EPTAPTKEGYTFKQWYDAKTGGDKWDFATSKMPAKNITLYAQYSANSYTATFDVDGKST : 594
          EPTAPTKEGYTFKQWYDAKTGGDKWDFATSKMPAKNITLYAQYSANSYTATFDVDGKST

          *          660          *          680          *          700
COMPLETE_I : TQAVDYQGLLKEPKAPTKEGYTFKQWYDEKTDGKKWDFATDKMPANDITLYAQFTKNPV : 708
CLONED_Inl : TQAVDYQGLLKEPKAPTKEGYTFKQWYDEKTDGKKWDFATDKMPANDITLYAQFTKNPV : 653
          TQAVDYQGLLKEPKAPTKEGYTFKQWYDEKTDGKKWDFATDKMPANDITLYAQFTKNPV

          *          720          *          740          *          760
COMPLETE_I : APPTTGGNTTPPTTNNGGNTTPPSANI PGSDTSNTSTGNSASTTSTMNAYDPYNSKEASL : 767
CLONED_Inl : APPTTGGNTTPPTTNNGGNTTPPSANI PGSDTSNTSTGNSASTTSTMNAYDPYNSKEASL : 712
          APPTTGGNTTPPTTNNGGNTTPPSANI PGSDTSNTSTGNSASTTSTMNAYDPYNSKEASL

          *          780          *          800
COMPLETE_I : PTTGDSDNALYLLGLLAVGTAMALTKKARASH----- : 800
CLONED_Inl : PTTGDSDNALYLLGLLAVGTAMALTKKARASHHHHHH : 751
          PTTGDSDNALYLLGLLAVGTAMALTKKARASK

```

**Figure 4.15:** Alignment of the cloned *inlA* gene sequence with the *inlA* gene sequence (accession number AJ012346), derived from Genebank. The nucleotide sequences were translated into their respective constituent amino acid sequences ([//ca.expasy.org/tools/dna.html](http://ca.expasy.org/tools/dna.html)) and aligned using the online ClustalW program ([www.ebi.ac.uk/clustalw](http://www.ebi.ac.uk/clustalw)). The aligned sequences were imported into Genedoc and manipulated using Genedoc software ([www.psc.edu/biomed/genedoc](http://www.psc.edu/biomed/genedoc)). Sequences highlighted in black demonstrated 100 % homology. It was apparent from these results that the cloned protein was 100 % homologous with the native amino acid sequence from amino acids 58-800. The only areas of non-homology were the six histidine residues that had been purposely added to the C-terminal of the cloned protein and the additional glycine (G) residue at position two of the cloned protein. This was incorporated during the cloning stage to ensure that the gene sequence was 'in-frame' when ligated into the pQE60 plasmid.





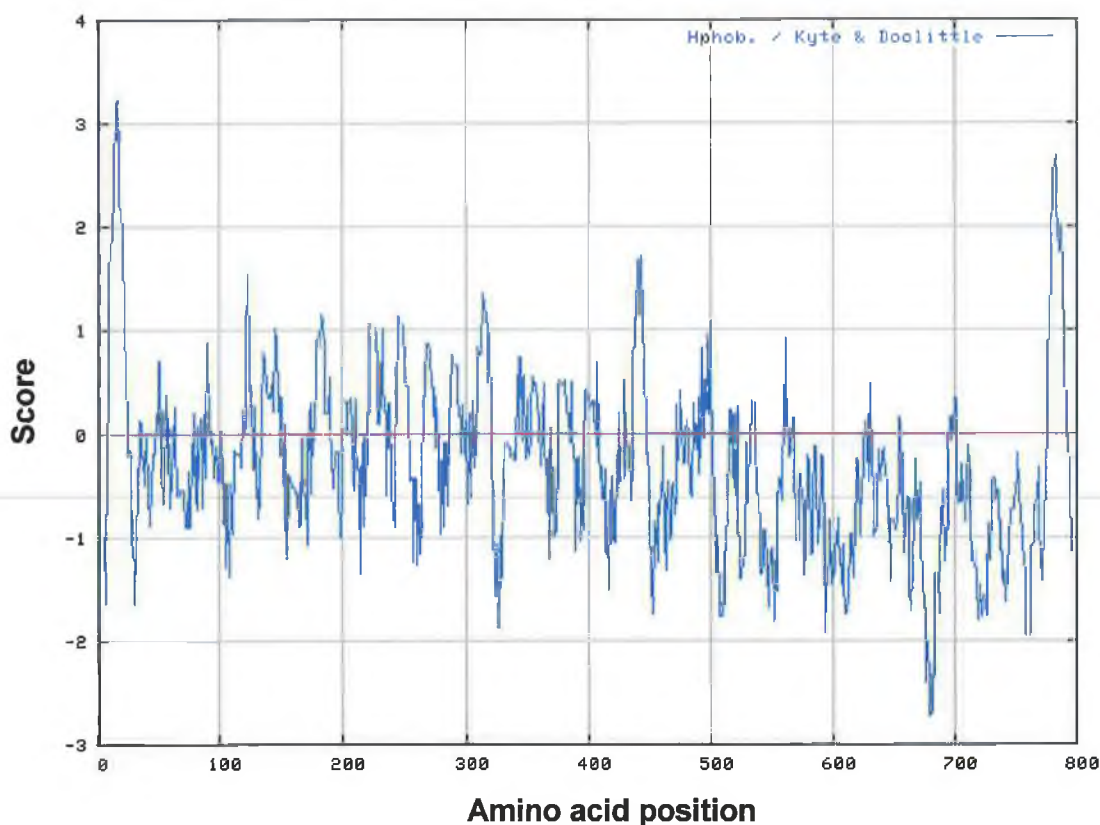


**Figure 4.16:** Hydropathy plot of the complete, 800 amino acid sequence of native InlA. The sequence corresponded to the accession number AJ012346. The plot was approximated by calculating the average hydropathy, over Sections (or 'windows') of nine amino acids in length, traversing the entire sequence using an unbiased, 'even linear weight variation model'. The average 'score' for each window was plotted against the amino acid position using online software (<http://ca.expasy.org/cgi-bin/protscale>). More hydrophobic regions were reflected by higher score values. The initial region, comprising the first 56 amino acids was highly hydrophobic. However, this represented the signal peptide region that had not been included in the cloned sequence. It is clear from the data that the region between amino acid 776 and the C-terminus is the most hydrophobic region of the cloned sequence.



#### 4.2.4 Cloning of 'truncated' *inlA* gene into pQE60

The problems encountered during the attempts to clone the full-length InlA protein (Sections 4.2.2 and 4.2.3), indicated that it may be necessary to remove the problematic hydrophobic anchor region. The anchor region is not exposed on the *L. monocytogenes* cell surface. Thus, it was not considered possible that the epitope recognised by mAb2B3 was contained in this region. In addition, because the anchor sequence of native InlA is buried in the cell wall of *L. monocytogenes*, it is unlikely to contribute to folding of the extracellular InlA domain. The anchor region was therefore, 'expendable' in terms of the overall experimental objective, which was to confirm the InlA-specificity of mAb2B3.

The primer sequences TAFII-B and TABI (Section 2.9.3) were designed to amplify the major extracellular, surface expressed domain of the InlA protein gene. This consisted of the complete protein sequence minus the 105 bp hydrophobic C-terminal anchor region. Both primers contained 'clamping' sequences flanking the restriction site to be incorporated. These clamps provided sufficient overhang DNA for efficient digestion of the flanked (*NcoI* and *BamHI*) restriction sites thus obviating the need for preliminary blunt end TA cloning.

Cloning of the truncated *inlA* gene sequence was attempted using both *Pfu*- and *Taq*- DNA polymerase in separate experiments. It was felt that, since the sequence being cloned was ~2.1 kb in length, use of a high annealing temperature, coupled with the proof reading capacity of *Pfu* should ensure a higher fidelity product.

The respective PCR reaction mixtures were set up as described in Section 2.9.6. The reaction program consisted of the following parameters:

Stage	Temperature (°C)	Time (s)
1 Primary denaturation	95	300
2 Denaturation	95	60
3 Annealing	66	30
4 Extension	72	300
5 Final extension	72	600
x 30 cycles		
6 Holding	4	(Indefinite)



While the *TAQ* enzyme was added to the reaction mixture prior to stage 1, the *Pfu* enzyme was held on ice and only added to its respective mixture after the primary denaturation stage. This was to ensure that none the component primers were degraded by promiscuous exonuclease activity. Reaction mixtures that demonstrated a high yield of the specifically desired 2.1 kbp *inlA* amplicon were subjected to purification by ethanol precipitation (Section 2.9.13). The purified PCR products were then digested with *Bam*HI and *Nco*I restriction enzymes. Only the *Pfu*-catalysed PCR resulted in successful amplification of the *inlA* gene when performed at the elevated annealing temperature (Figure 4.17). It was thus necessary to optimise the annealing temperature for the *TAQ* and corresponding TAFII/TABI primer set by performing a temperature gradient PCR (Figure 4.18). The optimal annealing temperature, when using *Taq* enzyme was 61 °C. Next, the *inlA* gene was amplified using both *Pfu* and *Taq* enzyme at their respective optimised annealing temperatures and the *inlA* amplicons were purified by ethanol precipitation. These were subsequently digested using an *Nco*I/*Bam*HI cocktail, and recovered by ethanol precipitation (Figure 4.19) in preparation for ligation into compatibly-restricted expression vector.



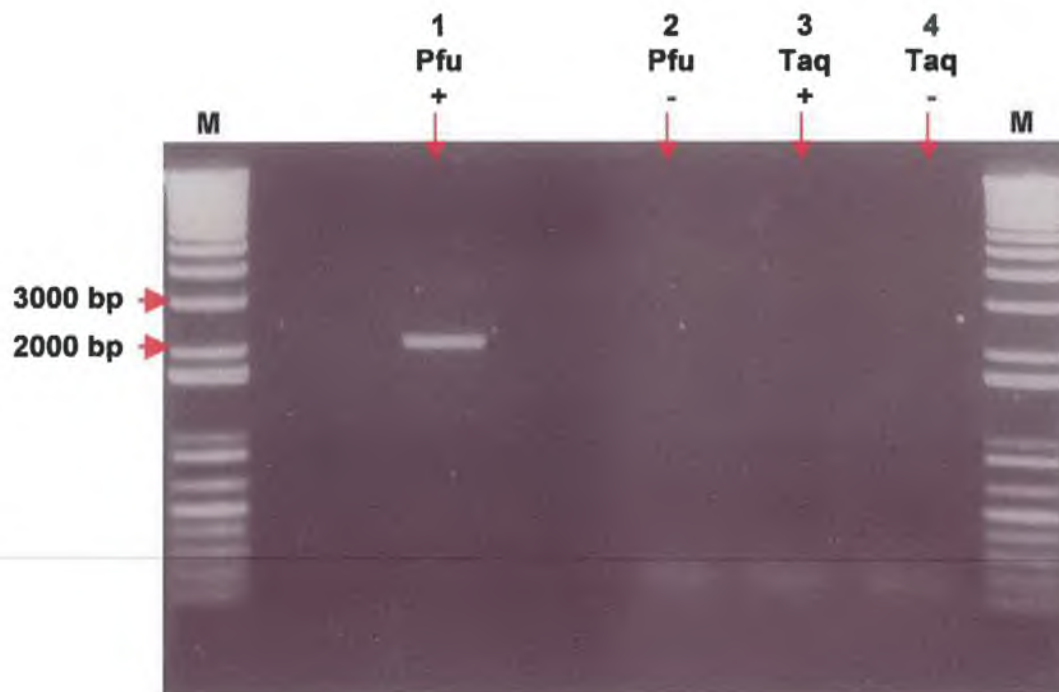


**Figure 4.17:** Comparison of high temperature annealing on the performance of Pfu and Taq DNA polymerase in conjunction with primers TAFII and TABI. The outer peripheral lanes consisted of graduated molecular weight markers. Lane 1, *inlA* 2.1 kbp sequence successfully amplified using Pfu enzyme. Lane 3, indicates unsuccessful amplification using Taq enzyme. Lanes 2 and 4 represent negative controls (i.e. no gDNA present) for the respective Pfu- and Taq-based reaction mixtures. The outer lanes, designated 'M', contain molecular weight markers.





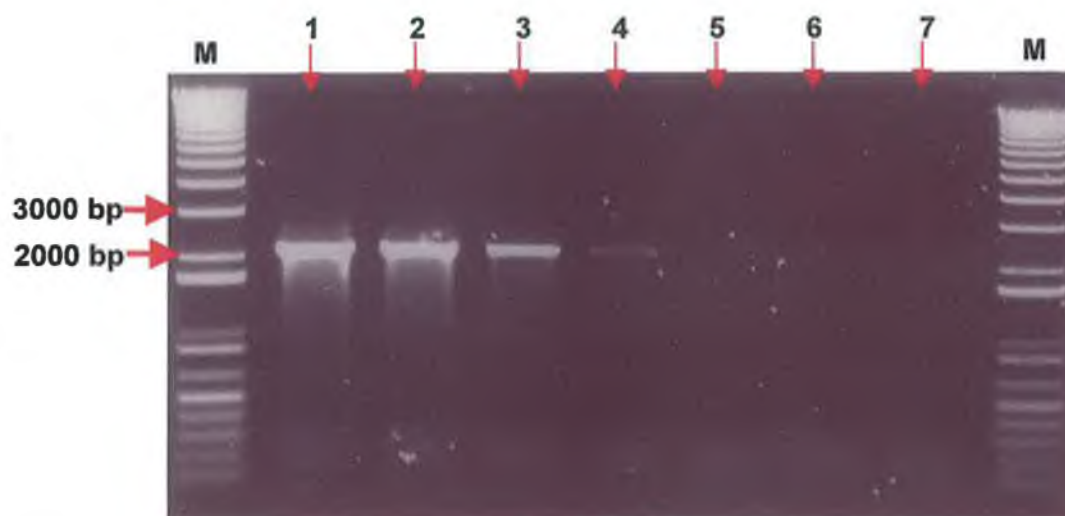


**Figure 4.18:** Gradient PCR profile for amplification of *inlA* gene sequence using Taq DNA polymerase. The lanes 1-6 represent PCR products obtained following annealing at 59.0, 59.9, 61.5, 63.2, 64.8, 66.5, 68.0 and 69.0 °C. Each lane contained 5  $\mu$ l of respective fresh PCR reaction product. In agreement with the results outlined in Figure 4.17, no amplification was apparent at the 66 °C annealing temperature. A faint product was evident at the 64 °C annealing temperature. However, significant yield of the desired 2.1 kbp product was only achieved at or below 62 °C. The optimal annealing temperature was concluded to be 61.0 °C. The peripheral lanes, designated 'M', contain molecular weight markers.



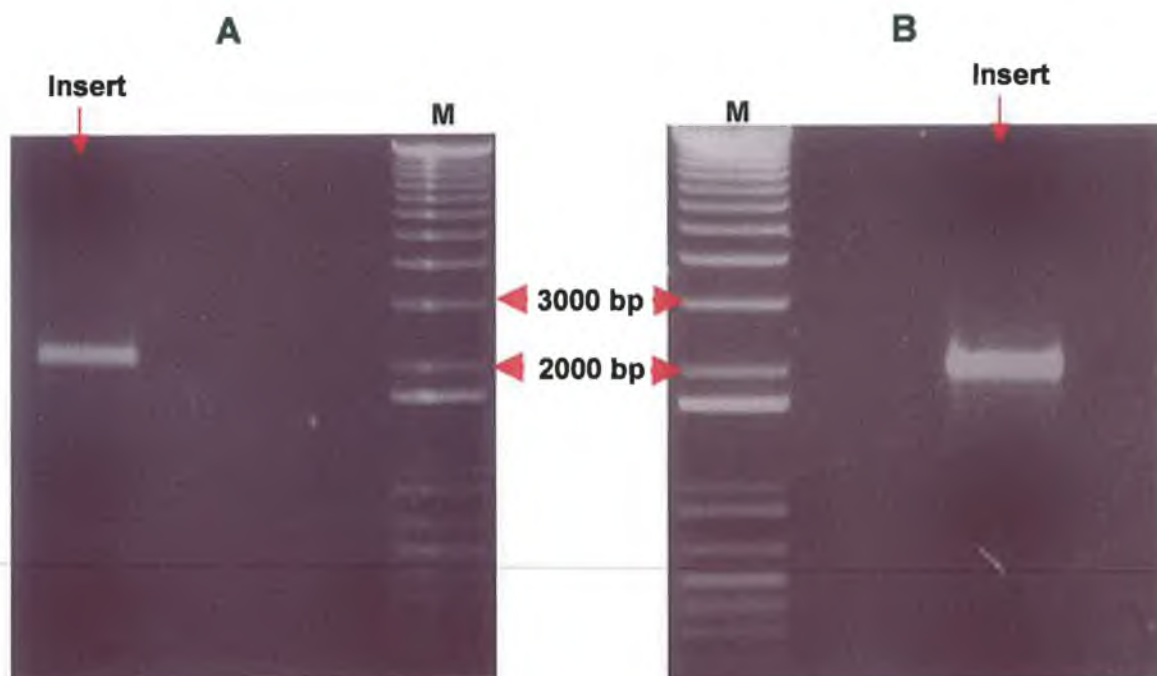


**Figure 4.19:** Digested *Pfu*- and *Taq*-generated *inlA* sequences, following purification by ethanol precipitation. Gel A represents 20  $\mu$ l of the *NcoI/BamHI*-digested *Pfu*-amplified *inlA* sequence. Gel B represents 20  $\mu$ l of the *NcoI/BamHI*-digested *Taq*-amplified *inlA* insert sequence. The inner peripheral lanes, labelled 'M', contained graduated DNA molecular size markers.

A duplicate ligation mixture was set up using *NcoI/BamHI*-digested *Pfu* and *Taq* amplicons, respectively. The composition of the ligation mixture was as follows:

Component	Volume ( $\mu$ l)
Insert (digested amplicon)	5
pQE60 vector ( <i>NcoI/BamHI</i> digested)	1.5
10x ligation buffer	1
H <sub>2</sub> O (molecular grade)	1.5
T <sub>4</sub> DNA ligase	1

The separate ligation mixtures were incubated in a heating block overnight (16-18 hrs) at 15.5 °C and then held on ice prior to transformation into competent *E. coli* XL10-Gold cells. Freshly transformed cells were spread onto LB agar plates and incubated overnight at 37 °C. Non-transformed XL10-Gold cells were spread onto a similar plate, as a control. On



inspection after overnight incubation, colonies were only evident on the plates that had been inoculated with transformed cells. Ten colonies derived from *Pfu*-amplified inserts and eight from *Taq*-amplified inserts were selected and inoculated into 10 ml volumes of LB broth in sterile universals. The tubes were incubated overnight at 30 °C and 220 rpm. The low temperature (30 °C rather than 37 °C) was employed to reduce the growth rate and safeguard against basal transcription and deleterious ‘leakage’ of the potentially toxic InlA protein. All of the colonies demonstrated significant growth (as determined by an increase in the OD<sub>600nm</sub> value) after overnight incubation. In order to ensure that the colonies contained the desired pQE60-*inlA* construct, a ‘plasmid prep’ was conducted on a portion of each culture (Section 2.9.14). The presence of the *inlA* sequence insert was verified by subjecting a sample of each purified plasmid to *TAQ*-mediated PCR with the *inlA* primer set TAFII and TABI. The correct size and orientation of the *inlA* insert was further confirmed by digesting a sample of individual purified plasmid with *EcoRI* and running it on an agarose gel. The results are outlined in Figures 4.20 and 4.21. In order to clarify the information that can be ascertained from the digest analysis, a schematic restriction map of the pQE60-*inlA* construct with the *inlA* insert in both the desired and incorrect orientation is provided (Figure 4.22).



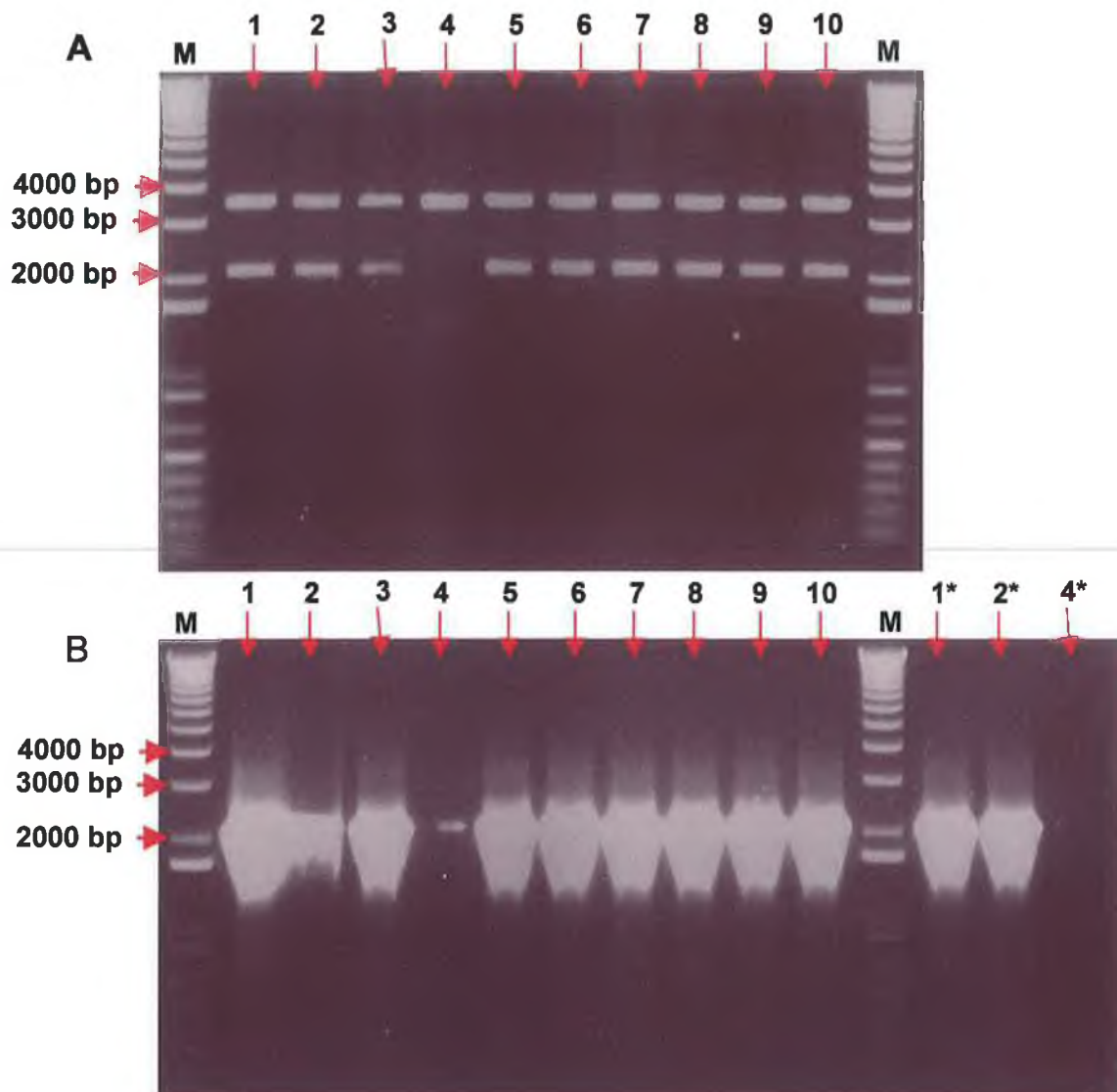


**Figure 4.20:** Analysis of plasmids bearing *Pfu*-amplified *inLA* inserts. The lane numbers correspond to the *Pfu* clone number, from which plasmids were isolated. Gel (A) depicts electrophoretic profile of *EcoRI*-digested plasmids. The lanes on the left and right extremes, designated 'M', contain a graduated DNA molecular weight marker. All of the samples exhibited a 3.4 kb band which represented linearised *pQE60* plasmid. Moreover, all except sample 4 exhibited a 2.1 kb band, characteristic of the correctly orientated *inLA* sequence insert. The fact that only a single band of similar molecular weight to the linearised plasmid band was evident in sample 4 suggested that this plasmid was more than likely a result of re-circularisation during the during the ligation stage. Gel (B) illustrates the *inLA* sequence-specific PCR products for plasmid samples 1 to 10. Samples 1, 2 and 4 were run in duplicate (denoted '\*') because cross over contamination during the loading process was suspected. The results agreed with those in the digest profile insofar as the 2.1 kb *inLA* sequence appeared to be present in all but sample 4.





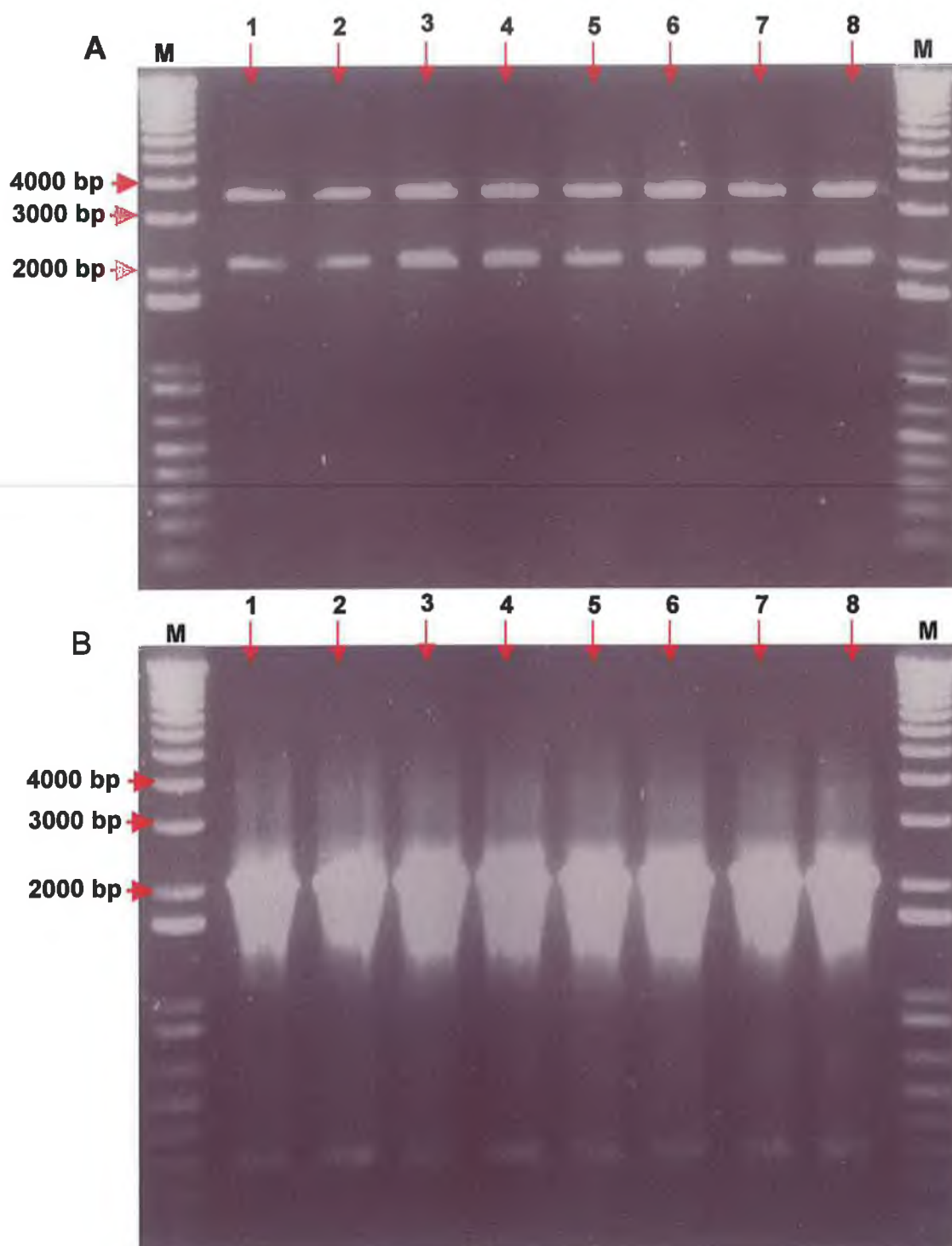


**Figure 4.21:** Analysis of selected plasmids bearing Taq-amplified *inIA* inserts. The lane numbers correspond to the Taq clone number, from which plasmids were isolated. The peripheral lanes, designated 'M', contain a graduated DNA molecular weight marker. Gel (A) demonstrates the electrophoretic profile of EcoRI-digested plasmids. Gel (B) represents *inIA* sequence-specific PCR products for plasmid samples 1 to 7. Both sets of results demonstrated a clear agreement and suggested the presence of the desired *inIA* sequence in all seven plasmids tested. They also indicated that the insert was correctly orientated.



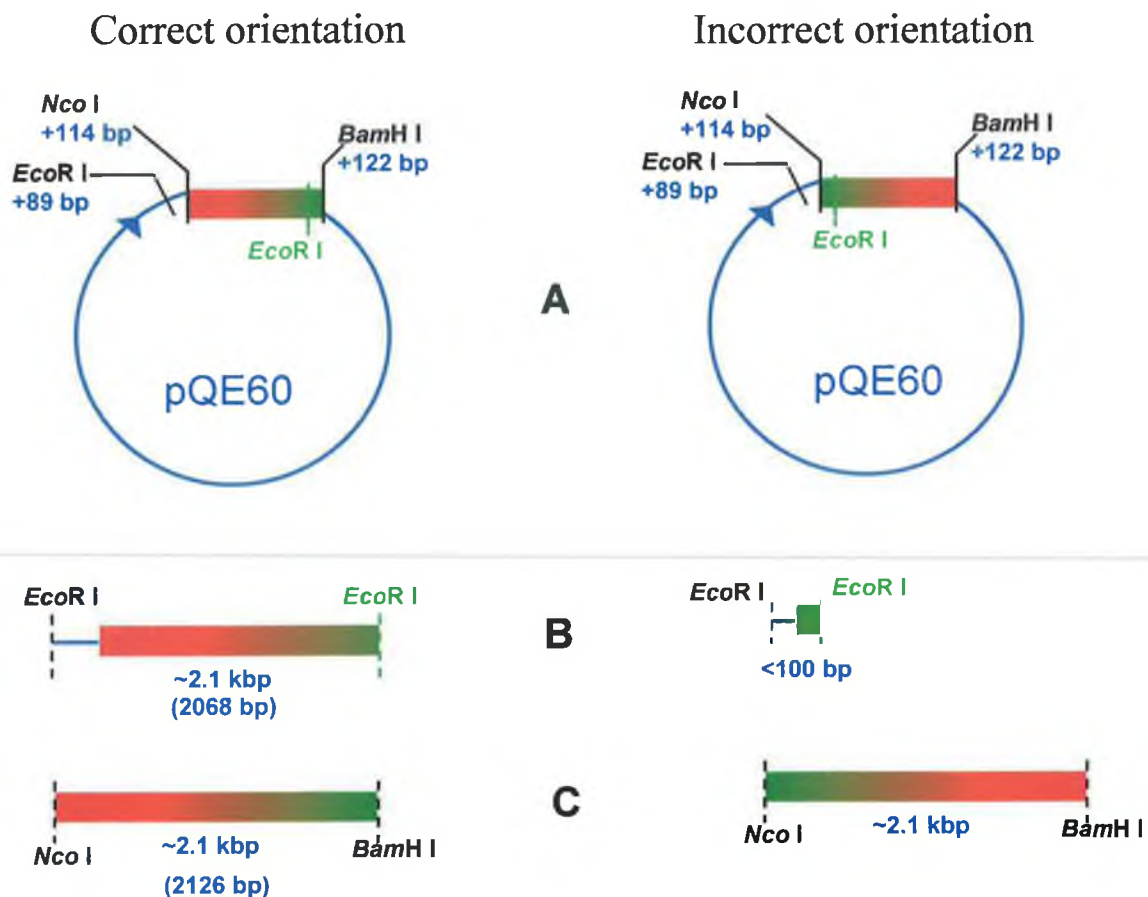


**Figure 4.22:** Possible restriction profile of the pQE60-*inlA* construct with the insert in both the desired, or, correct orientation for efficient transcription and the incorrect orientation. 'A' represents the 5.5 kbp constructs. A single *EcoRI* restriction site was located 59 bp upstream from the 3' terminal of the *inlA* sequence being cloned. The fact that the pQE60 plasmid itself had also, just one *EcoRI* restriction site, 25 bp upstream of the *NcoI* restriction site made it possible to deduce the orientation of the insert sequence by means of a simple *EcoRI* digest. 'B' demonstrates that when the insert is in the correct 5' → 3' orientation the pQE60 *EcoRI* and *inlA* *EcoRI* sites are furthest apart resulting in restriction products of ~2.1 kbp and 3.4 kbp. When the incorrect orientation prevails, the *EcoRI* sites are proximal to each other and yield a tiny 100 bp fragment. 'C' depicts the excised insert using an *NcoI*/*BamHI* restriction digest. This digest is independent of the orientation of the insert in the plasmid as both excised sequences are of similar molecular weights and would each be expected to appear as ~2.1 kbp bands, in addition to a linearised plasmid band of 3.4 kbp on an agarose gel.



#### 4.2.4.1 Determination of *rInlA* protein expression

Once the clones that contained the correctly orientated pQE60-*inlA* construct had been identified it was necessary to determine whether they were capable of expressing the recombinant protein in an active form. Nine selected *Pfu*-derived clones and eight selected *Taq*-derived clones were induced with 1 mM IPTG overnight (10 hrs) at 30 °C. 1 ml samples were then taken from each induced culture and sonicated in 2x PBS buffer. Samples were then subjected to SDS PAGE analysis and Western blotting using an anti-His-tag monoclonal antibody. All of the *Pfu* clones, except *Pfu8* demonstrated a clearly up-regulated band at ~80 kDa (Figure 4.23a). Similarly, all except *Pfu8* contained an ~80 kDa protein recognised by anti-His-tag monoclonal antibody (Figure 4.23b). The only *Taq* clone that failed to generate a visible ~80 kDa protein in SDS PAGE, was *Taq2* (Figure 4.24a). This was also the only *Taq* clone that failed to be recognised by the anti-His-tag monoclonal antibody (Figure 4.24b). On the basis of these results, four positive clones were randomly selected for further evaluation. These were '*Taq1*', '*Taq5*', '*Pfu2*' and '*Pfu9*'. When probed with mAb2B3 monoclonal antibody, *Taq5*, *Pfu2* and *Pfu9* lysates demonstrated strong and specific reactivity (Figure 4.25). However, *Taq1* lysate was not recognised by mAb2B3. This was despite the fact that *Taq1* had been earlier confirmed to produce an ~80 kDa protein bearing a His-tag (Figure 4.24). Such a conflicting result highlights the weakness in relying solely on fusion-tag 'flagging' for determining expression of recombinant proteins. The clone *Pfu9* was selected for further analysis.



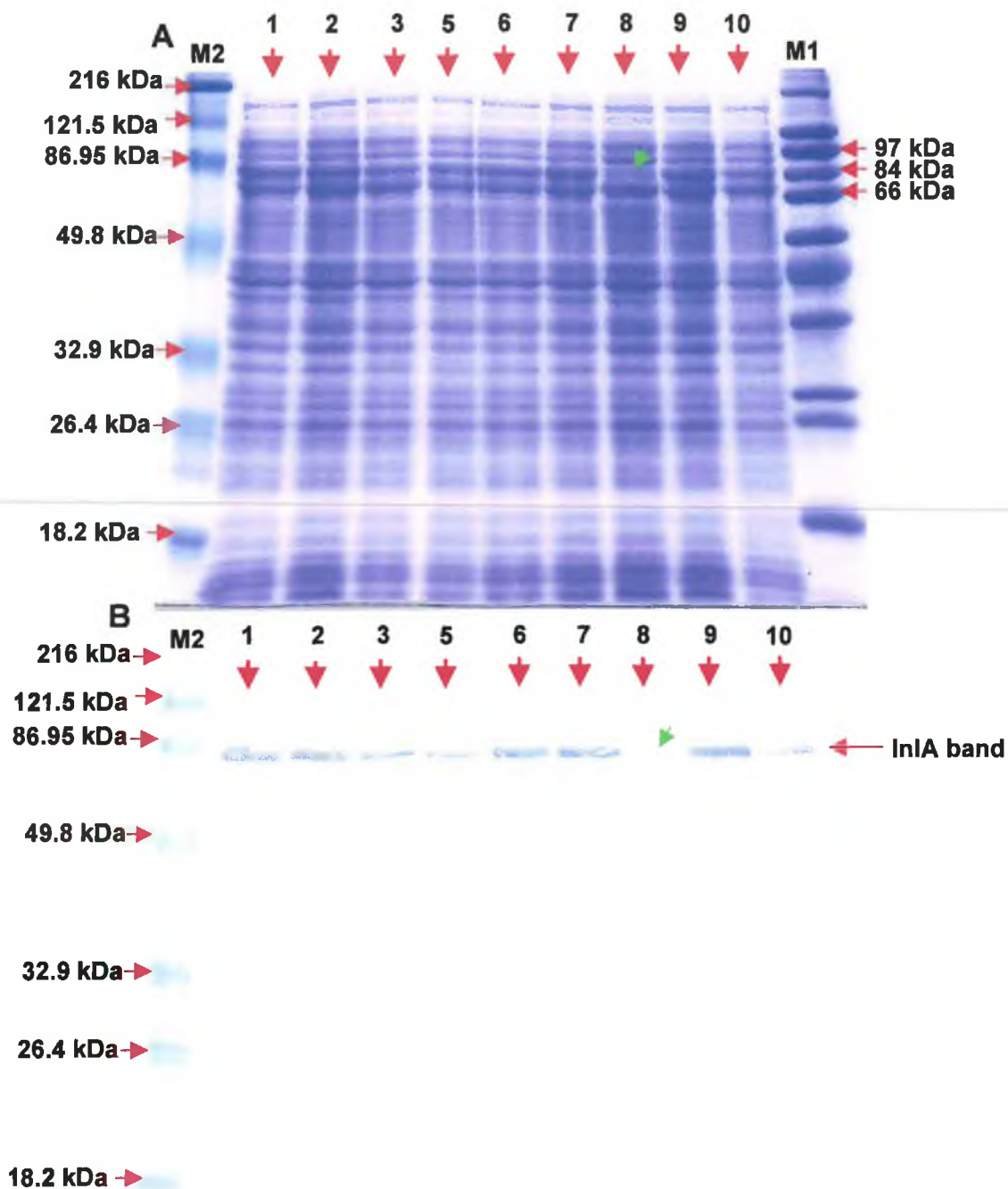


**Figure 4.23:** SDS PAGE (A) and Western blot (B) analysis of cell lysates from Pfu clones. Lysates from all clones, except Pfu8 (indicated by small arrow), demonstrated clearly up-regulated expression of an ~80 kDa protein that was specifically recognised with anti-His-tag monoclonal antibody. The loading volume was 20  $\mu$ l throughout. 'M1' and 'M2' refer to SigmaWide™ wide range and Pierce BlueRanger™ (prestained) molecular weight markers, respectfully.





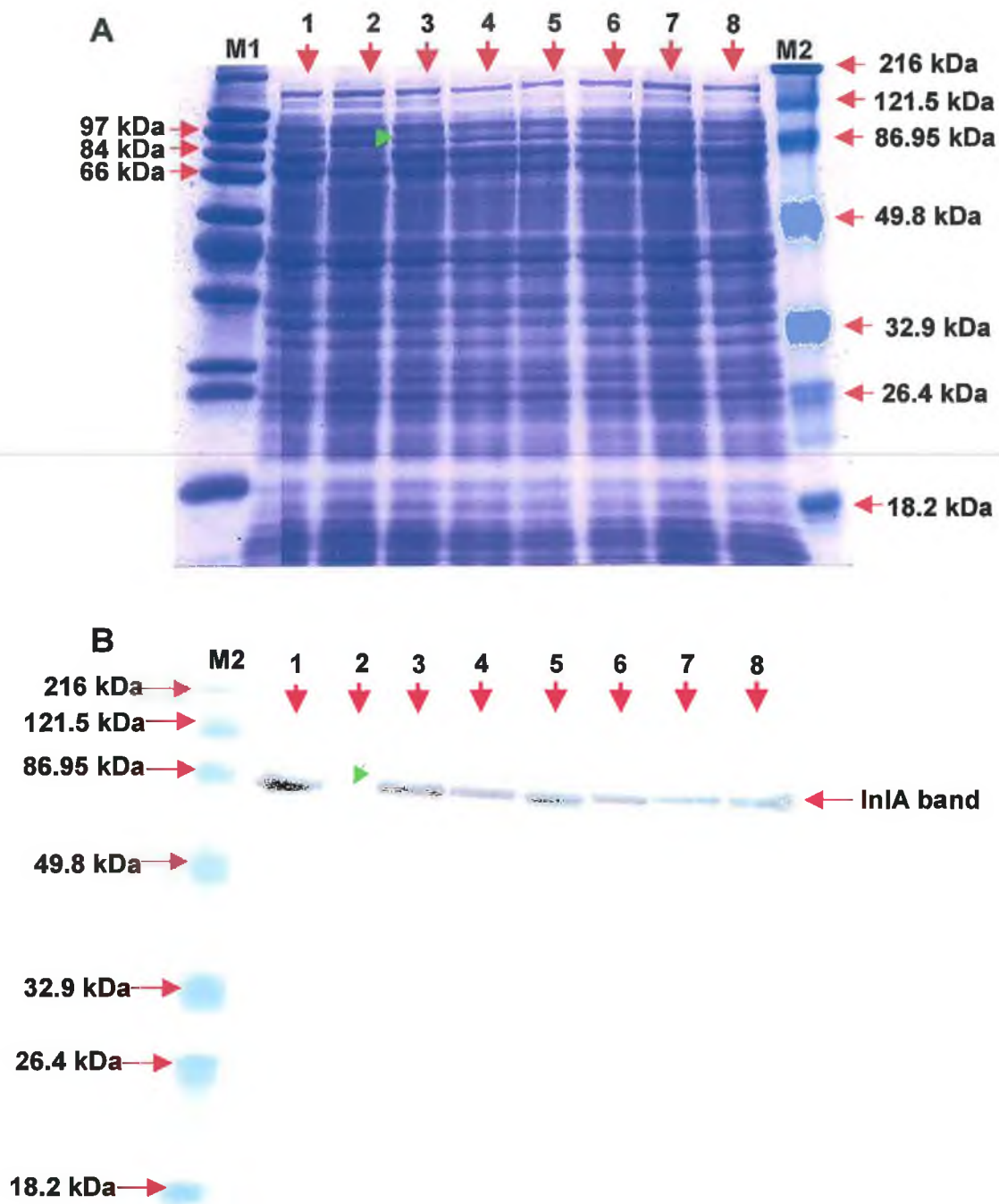


**Figure 4.24:** SDS PAGE, (A), and Western blot, (B), analysis of cell lysates from Taq clones. Lysates from all clones, except Taq2 (indicated by green arrow), demonstrated clearly up-regulated expression of an ~80 kDa protein that was specifically recognised with anti-His-tag monoclonal antibody. The loading volume was 20  $\mu$ l throughout. The Taq1 sample was accidentally loaded twice onto the SDS PAGE gel, hence, the extra lane 1. 'M1' and 'M2' refer to SigmaWide™ wide range and Pierce BlueRanger™ (prestained) molecular weight markers, respectively.



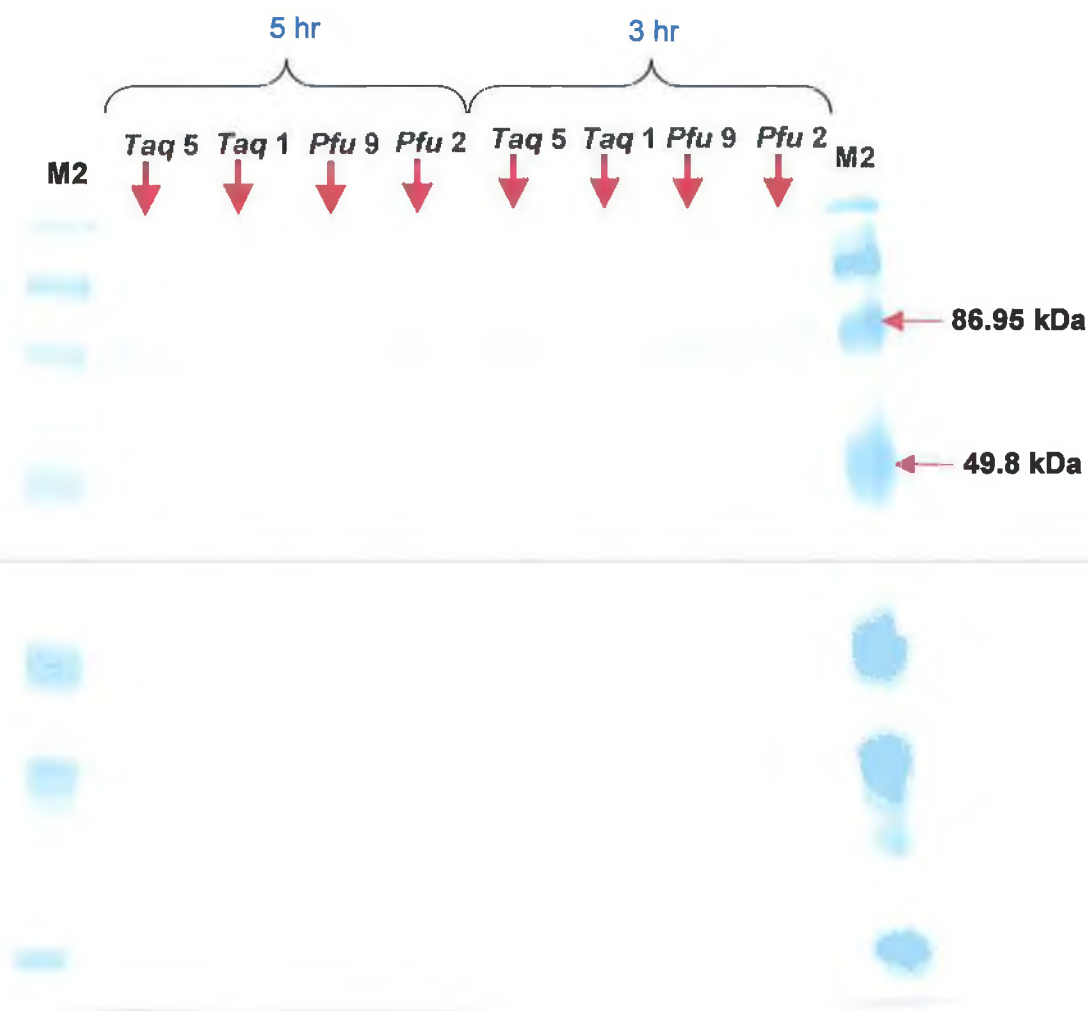


**Figure 4.25:** Immunoreactivity of recombinant InlA towards mAb2B3 monoclonal antibody. The set of results on the left hand side represent lysates from cultures induced for 5 hours with 1 mM IPTG and those on the right had been induced for just 3 hours. There was no apparent difference in the results for 5 and 3 hour induction periods. Lysate samples from clones Taq5, Pfu9 and Pfu2 exhibited strong activity when probed with monoclonal antibody 2B3. Taq1 lysate exhibited no significant activity. All lysates were prepared in 2x PBS and 20  $\mu$ l loading volumes were used throughout. 'M1' and 'M2' refer to SigmaWide™ wide range and Pierce BlueRanger™ (prestained) molecular weight markers, respectfully.

#### 4.2.4.2 Sequencing of the cloned truncated inlA gene sequence

In order to fully validate the apparent faithful expression of rInlA protein by Pfu9 it was necessary to confirm the fidelity of the pQE60-borne inlA gene sequence. Plasmid DNA derived from Pfu9 was sent to MWG-Biotech (UK) Ltd, for sequencing. The sequence data



was aligned (Figure 4.26), as previously described (Section 4.2.3.2). The cloned truncated *inlA* gene sequence demonstrated 100 % homology with the corresponding, respective sequences provided by Genedoc (reference AJ012346 ).

```

          *          20          *          40          *          6
COMPLETE_I : MRKKRYVWLKSILVAILVFGSGVWINTSNGTNAQAATITQDTFINQIFDTALAEKMT : 59
TRUNCATED_ : -----M-KT : 4
                                     KT

          0          *          80          *          100          *          1
COMPLETE_I : VLGKTNVTDIVSQTDLDQVTTLQADRLGIKSIDGVEYLNNLTQINFSSNNQLTBITPLKN : 118
TRUNCATED_ : VLGKTNVTDIVSQTDLDQVTTLQADRLGIKSIDGVEYLNNLTQINFSSNNQLTBITPLKN : 63
               VLGKTNVTDIVSQTDLDQVTTLQADRLGIKSIDGVEYLNNLTQINFSSNNQLTBITPLKN

          20          *          140          *          160          *
COMPLETE_I : LTKLVDIIMNNNQIADITPLANLTNLTGLTLFNNQITDIDPLKNLTNLRLELSSNTIS : 177
TRUNCATED_ : LTKLVDIIMNNNQIADITPLANLTNLTGLTLFNNQITDIDPLKNLTNLRLELSSNTIS : 122
               LTKLVDIIMNNNQIADITPLANLTNLTGLTLFNNQITDIDPLKNLTNLRLELSSNTIS

          180          *          200          *          220          *
COMPLETE_I : DISALSGLTSLQQLSFGNQVTDLKPLANLTTLERLDISSNKVSDISVLAKLTNLESIA : 236
TRUNCATED_ : DISALSGLTSLQQLSFGNQVTDLKPLANLTTLERLDISSNKVSDISVLAKLTNLESIA : 181
               DISALSGLTSLQQLSFGNQVTDLKPLANLTTLERLDISSNKVSDISVLAKLTNLESIA

          240          *          260          *          280          *
COMPLETE_I : TNNQISDITPLGILTNLDELSLNGNQLKDIGTLASLTNLTDLDLANNQISNLAPLSGLT : 295
TRUNCATED_ : TNNQISDITPLGILTNLDELSLNGNQLKDIGTLASLTNLTDLDLANNQISNLAPLSGLT : 240
               TNNQISDITPLGILTNLDELSLNGNQLKDIGTLASLTNLTDLDLANNQISNLAPLSGLT

          300          *          320          *          340          *
COMPLETE_I : KLTELKIGANQISNISPLAGLTALTNLLENQLEDISPISNLKNLTYLTLFYNNISDI : 354
TRUNCATED_ : KLTELKIGANQISNISPLAGLTALTNLLENQLEDISPISNLKNLTYLTLFYNNISDI : 299
               KLTELKIGANQISNISPLAGLTALTNLLENQLEDISPISNLKNLTYLTLFYNNISDI

          360          *          380          *          400          *
COMPLETE_I : SPVSSLTKLQRLFFYNNKVSVDVSSLANLTNINWLSAGHNQISDLTPLANLTRITQGLN : 413
TRUNCATED_ : SPVSSLTKLQRLFFYNNKVSVDVSSLANLTNINWLSAGHNQISDLTPLANLTRITQGLN : 358
               SPVSSLTKLQRLFFYNNKVSVDVSSLANLTNINWLSAGHNQISDLTPLANLTRITQGLN

          420          *          440          *          460          *
COMPLETE_I : DQAWTNAPVNYKANVSIPTVKNVTCALIAPATISDGGSYTEPDITWNLPSTNEVSYT : 472
TRUNCATED_ : DQAWTNAPVNYKANVSIPTVKNVTCALIAPATISDGGSYTEPDITWNLPSTNEVSYT : 417
               DQAWTNAPVNYKANVSIPTVKNVTCALIAPATISDGGSYTEPDITWNLPSTNEVSYT

          480          *          500          *          520          *
COMPLETE_I : FSQPVTIGKGTTFSGTVTQPLKAIENVKFHVIGKETTKEVEAGNLLTEPAKPVKEGHT : 531
TRUNCATED_ : FSQPVTIGKGTTFSGTVTQPLKAIENVKFHVIGKETTKEVEAGNLLTEPAKPVKEGHT : 476
               FSQPVTIGKGTTFSGTVTQPLKAIENVKFHVIGKETTKEVEAGNLLTEPAKPVKEGHT

          540          *          560          *          580          *
COMPLETE_I : FVGWFDATGCTKWNFSTDKMPTNDINLYAQFSINSYTATFDNDGVTTTSQTVDYQGLLQ : 590
TRUNCATED_ : FVGWFDATGCTKWNFSTDKMPTNDINLYAQFSINSYTATFDNDGVTTTSQTVDYQGLLQ : 535
               FVGWFDATGCTKWNFSTDKMPTNDINLYAQFSINSYTATFDNDGVTTTSQTVDYQGLLQ

```



```

      540          *          560          *          580          *
COMPLETE_I : FVGWFDQAQTGGTKWNFSTDKMPTNDINLYAQFSINSYTATFDNDGVTTSQTVDYQGLLQ : 590
TRUNCATED_ : FVGWFDQAQTGGTKWNFSTDKMPTNDINLYAQFSINSYTATFDNDGVTTSQTVDYQGLLQ : 535
      FVGWFDQAQTGGTKWNFSTDKMPTNDINLYAQFSINSYTATFDNDGVTTSQTVDYQGLLQ

      600          *          620          *          640
COMPLETE_I : EPTAPTKEGYTFKGYDAKTGGDKWDFATSKMPAKNITLYAQYSANSYTATFDVDGKST : 649
TRUNCATED_ : EPTAPTKEGYTFKGYDAKTGGDKWDFATSKMPAKNITLYAQYSANSYTATFDVDGKST : 594
      EPTAPTKEGYTFKGYDAKTGGDKWDFATSKMPAKNITLYAQYSANSYTATFDVDGKST

      *          660          *          680          *          700
COMPLETE_I : TQAVDYQGLLKEPKAPT KAGYTFKCYDEKTDGKKWDFATDKMPANDITLYAQFTKNPV : 708
TRUNCATED_ : TQAVDYQGLLKEPKAPT KAGYTFKGYDEKTDGKKWDFATDKMPANDITLYAQFTKNPV : 653
      TQAVDYQGLLKEPKAPT KAGYTFKGYDEKTDGKKWDFATDKMPANDITLYAQFTKNPV

      *          720          *          740          *          760
COMPLETE_I : APPTTGGNTPPITTNNGGNTTPPSANIPGSDTSNTSTGNSASTTSTMNAYDPYNSKEASL : 767
TRUNCATED_ : APPTTGGNTPPITTNNGGNTTPPSANIPGSDTSNTSTGNSASTTSTMNAYDPYNSKEASL : 712
      APPTTGGNTPPITTNNGGNTTPPSANIPGSDTSNTSTGNSASTTSTMNAYDPYNSKEAS

      *          780          *          800
COMPLETE_I : PTTGDS DNALYLLGLLAVGTAMALTKKARASK : 800
TRUNCATED_ : HHHHH----- : 717

```

**Figure 4.26:** Alignment of the cloned *inlA* gene sequence encoding truncated *rInlA*, with the *inlA* gene sequence (accession number AJ012346), derived from Genbank. The nucleotide sequences were translated into their respective constituent amino acid sequences and aligned using the online ClustalW program ([www.ebi.ac.uk/clustalw](http://www.ebi.ac.uk/clustalw)). The aligned sequences were imported into Genedoc and manipulated using Genedoc software. Sequences highlighted in black demonstrated 100 % homology. It was apparent from these results that the cloned protein was 100 % homologous with the native amino acid sequence from amino acid 58-776. The only areas of non-homology were the six histidine residues that had been purposely added to the C-terminal of the cloned protein and the additional glycine (G) residue at position '2' of the cloned protein. This was incorporated during the cloning stage to ensure that the gene sequence was 'in-frame' when ligated into the pQE60 plasmid.

#### 4.2.4.3 Time course experiments to optimise *rInlA* expression in *Pfu9*

*Pfu9* *rInlA* expression levels were analysed at 25 and 30 °C. Time point cell samples were resuspended in 2x PBS buffer and sonicated. The resulting cytoplasmic extracts were analysed by SDS-PAGE as shown in Figure 4.25. Lysates from the cultures induced at 30 °C exhibited significantly enhanced *rInlA* expression at significantly high levels within the 6 hour analysis window. Optimum expression levels were achieved between 4 and 6 hours of IPTG-induced expression at 30 °C.

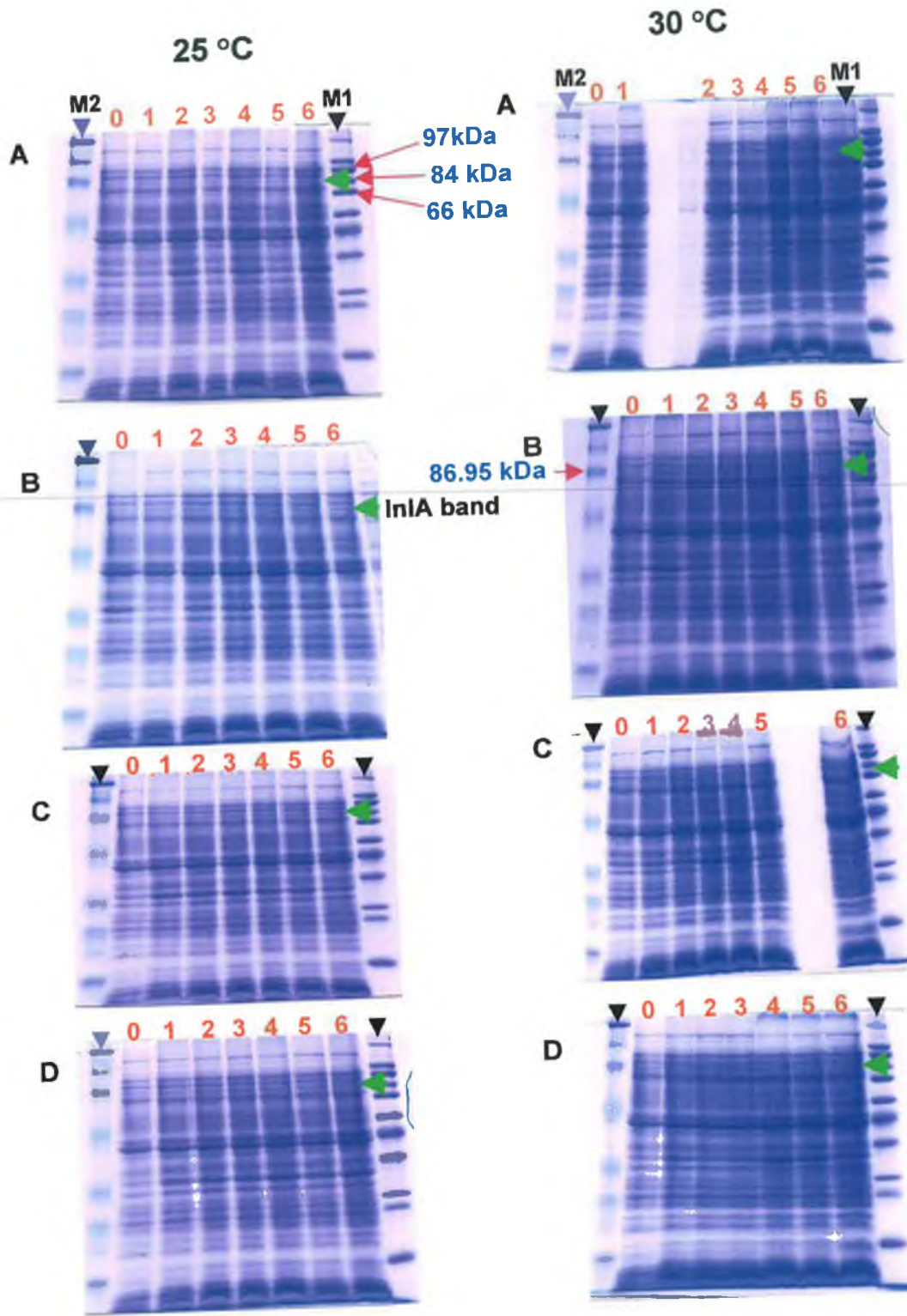




#### **4.2.4.4 Determination of the optimum IPTG concentration for induction**

Experiments to determine the optimum IPTG concentration for induction of recombinant InlA expression were carried as previously described in Section 4.2.3.1. Essentially the same set of time course experiments were conducted, however, the IPTG concentration was varied over the range 0, 0.05, 0.1, 0.5 and 1 mM IPTG. Figure 4.27 shows the corresponding SDS-PAGE time course gels obtained over this induction range. No significant levels of expressed rInlA protein bands were observed in the absence of IPTG induction, indicating that *E. coli* strains, such as XL10 Gold, harbouring the *laqI<sup>+</sup>* gene, produce sufficient quantities of the *lac* repressor protein to prevent undesired levels of basal expression rInlA. There was no pronounced difference in the level of expression between 0.05 and 1 mM IPTG induction. Slight variations in the sonication of each sample can result in the observation of unevenly expressed bands on the same gel. Due to the type of sonicator used, exact replication of sonication conditions (e.g. exact position and dept of the probe) were difficult to reproduce.







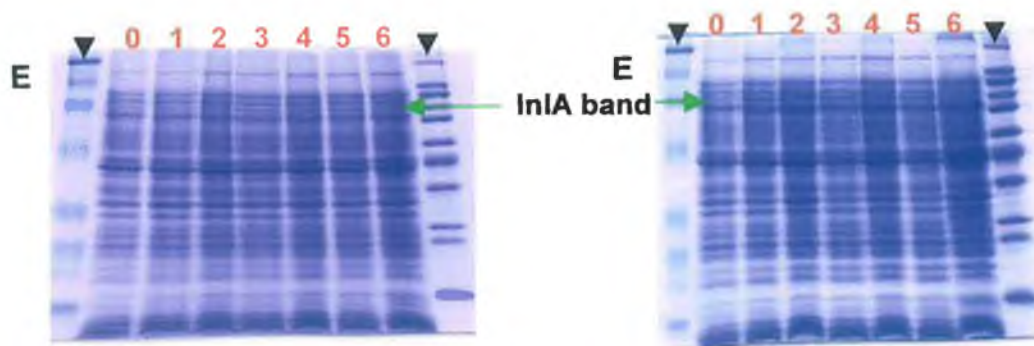


**Figure 4.27:** Effect of IPTG concentration and induction temperature on the expression of *rInlA* protein over time. The left-hand column represents Pfu9 clone induction at 25 °C and the right-hand column represents Pfu9 clone induction at 30 °C. Gels A-E represent *inlA* gene products induced with 0 mM, 0.05 mM, 0.1mM, 0.5mM and 1.0 mM IPTG, respectively. The red number headings refer to the duration of induction before sampling, (i.e. 0, 1, 2, 3, 4, 5 and 6 hours, respectively). 'M1' and 'M2' refer to SigmaWide™ (wide range) and BlueRanger® (prestained) molecular weight markers, respectively. The expected, *rInlA* band, is indicated by a green arrow. At 25 °C no significant levels of *InlA* protein expression were evident. This indicated that *rInlA* expression at this induction temperature was slow. It may well have been that allowing the induction period to run for longer than just 6 hours would have generated a more quantifiable level of *rInlA*. At 30 °C a significant increase in *rInlA* expression was evident, even at the lowest IPTG concentration, when compared to the 0 mM IPTG samples. Moreover, there seemed to be no discernable difference between the level of expression between the 0.05 and 1 mM IPTG samples. Thus, 1.0 mM IPTG was used for all further inductions of clone Pfu9 at an induction/expression temperature of 30 °C.



#### 4.2.5 Purification of the *inlA* gene product by IMAC

Having selected clone *Pfu9* on the basis of its stable production and activity of recombinant InlA, it was necessary to optimise the purification process and maximise the yield of pure and active product.

Immobilised metal chelate affinity chromatography (IMAC) is a technique by which proteins or other molecules can be separated based on their ability to form coordination complexes with immobilised metal ions (Porath *et al.*, 1975; Hermanson *et al.*, 1992). The majority of chelating groups used in IMAC are multidentate chelating compounds formed by the protein, metal ion and chelating group (Ueda *et al.*, 2003). Generally, Histidine residues are infrequent, amounting to approximately only 2 % of the amino acid content of globular proteins. In addition, only half of these residues are normally exposed on the protein surface (Ueda *et al.*, 2003). However, certain proteins from *E. coli*, namely superoxide dismutase (8 histidines, 195 amino acids), chloramphenicol acetyltransferase (12 histidines, 219 amino acids) and heat-shock protein (14 histidines, 624 amino acids), have been identified, which might bind to IMAC columns depending on the conditions used (Müller *et al.*, 1998b). Histidine is also the amino acid that exhibits the strongest interaction with immobilised metal ion matrices, as electron donor groups on the histidine imidazole ring readily form coordination bonds with the immobilised transition metal (Terpe, 2003). Hochuli and co-workers, (1987) reported the first practical application of histidine-targeted purification. This resulted in the development of a nitrilotriacetic acid matrix (NTA resin) currently supplied by Qiagen Ltd. (as Ni-NTA coupled to Sepharose® CL-6B) and used widely for routine IMAC processes. The hexahistidine tag facilitates binding to Ni-NTA matrices. It is poorly immunogenic, and at pH 8.0 the tag is small, uncharged and, thus, does not generally affect secretion, compartmentalisation or folding of the fusion protein within the expression host (Qiagen, 2000). Purification using polyhistidine tags has been carried out successfully using a number of expression systems including bacteria (Wizemann and von Braun, 1999; Rank *et al.*, 2001; Brennan *et al.*, 2002), yeast (Kaslow and Shiloch, 1994), mammalian cells (Janknecht *et al.*, 1991; Janknecht and Nordheim, 1992), and baculovirus-infected insect cells (Kuusinen *et al.*, 1995; Schmidt *et al.*, 1998). Figure 4.28 shows that NTA is a tetradentate chelating adsorbent that occupies four, of the six ligand binding sites, within the coordination sphere of the nickel ion, leaving two valency sites free to interact with the His-tag.







**Figure 4.28:** Monomeric subunit of Nickel-charged NTA resin. The high affinity coordination complex formed by interaction of the resin-bound  $\text{Ni}^{2+}$  molecule with histidine residues is highlighted by the red coordinate bonds.

#### 4.2.5.1 Optimisation of IMAC purification process

Retention of activity was of paramount importance in the case of the recombinant InlA protein and, as such, it was decided to attempt to optimise purification under native conditions. This entailed using a PBS-based, rather than a urea-based lysis buffer. It may be argued that the expression level results outlined in the previous section indicate a universally low level of recombinant InlA expression. This in turn may be construed as evidence that the recombinant protein was being housed in inclusion bodies and that yields might have been improved under harsher, 'denaturing' lysis conditions. However, previous experience with similar proteins, using the same expression system did not support this generalisation. Essentially, in this case a lower yield was seen as an affordable payoff for a higher quality end product. Given the low expression levels evident it was also decided to use a batch purification method (Section 2.9.16) in order to maximise sample:column interaction time and maintain strong 6xHis-tag/Ni-NTA retention.

A major consideration when purifying under native conditions, particularly in batch purification processes, was the potential for high background contaminants. The first consideration was thus, the overall Ni-NTA resin:lysate ratio. Figure 4.27 demonstrates that, by reducing the resin volume and diluting the lysate (thereby increasing its volume) it was found that purity was improved only slightly. However, the InlA sample loss, evident in the



flow-through, was also slightly reduced, indicating a small improvement in the process efficiency. Nonetheless, the amount of non-specific, contaminating bands was still at an unacceptably high level.

Attention next switched to the buffer composition used in the binding and washing stages of the purification process. This was principally PBS buffer at pH 6.6 containing 15 mM  $\beta$ -mercaptoethanol. The latter was added to prevent co-purification of unrelated host proteins that may have become coupled to the recombinant protein of interest via disulphide bonding during cell lysis. In order to combat charge-related non-specific ionic interactions occurring, the effect of increasing the salt concentration was examined (Figure 4.30). Increasing the concentration of NaCl in the buffers from 0.15 (standard PBS), to 0.5 and even 1.0 M NaCl did not reduce the binding capacity for the 6xHis-tagged recombinant protein. This was not surprising, as Hochuli and co-workers, (1988) had previously demonstrated that the 6xHis-tag/Ni-NTA interaction was stable in salt concentrations as high as 6 M guanidine hydrochloride. Unfortunately, the highest concentration of NaCl employed in this experiment only slightly reduced the proportion of contaminating bands as ascertained in the SDS PAGE gel analysis.



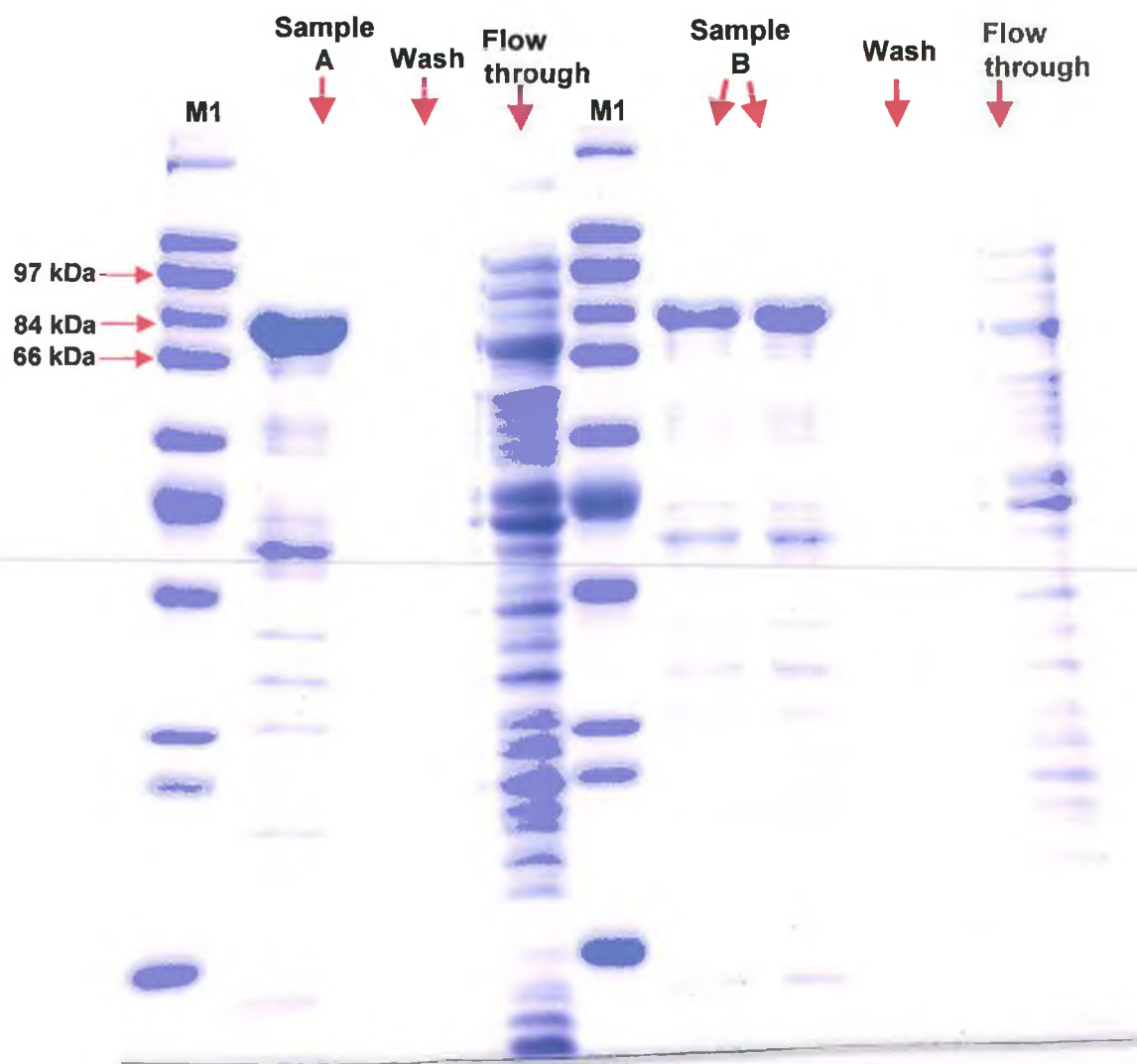


**Figure 4.29:** The effect of Ni-NTA resin volume and resin:lysate ratio on the yield and purity of IMAC-isolated recombinant InlA protein. Each lane was loaded with a 20  $\mu$ l sample volume. The binding/running/washing buffer used throughout was PBS supplemented with 15 mM  $\beta$ -mercaptoethanol. Lane 'A' represents the eluted fraction obtained from a 1/10 lysate (i.e. a 20 ml culture pellet resuspended in 2 mls lysis/binding/running buffer). The volume of Ni-NTA resin used was 1 ml (1:2, resin:lysate ratio). Lane 'B' represents a 1/20 lysate (i.e. a 20 ml culture pellet resuspended in 4 mls lysis/binding/running buffer). 'B1' demonstrates the result using a 1:4, resin:lysate ratio and 'B2' shows the purified components obtained using a 1:8 resin:lysate ratio. There was little apparent difference between the results for B1 and B2. Lane 'M1' contained SigmaWide™ wide range molecular weight marker. Overall, the results indicated that greater resin:lysate ratios resulted in slightly purer yields of recombinant His-tagged protein (probably due to competitive inhibition of non-specific binding). Moreover, when using the higher ratio, the flow through fraction contained significantly less recombinant protein, thereby reducing sample loss.



By far the most effective means of reducing the non-specific component was to supplement the binding and washing buffer with 20 mM imidazole and also to incorporate this during the pre-equilibration of the resin. In Figure 4.31 the results demonstrate that the presence of 10 mM imidazole gave rise to a significant reduction in the amount of co-purified contaminants. Increasing the concentration further, to 20 mM, removed almost all of the contaminants. This was due to the imidazole ring structure (which is a major component of the histidine molecule), 'mopping up' excess available nickel binding sites on the Ni-NTA column matrix and thus, inhibiting non-specific binding. On the basis of the results obtained, the optimum buffer composition for binding and washing was found to be PBS containing 15 mM  $\beta$ -mercaptoethanol, 1 M NaCl and 20 mM imidazole. In addition, as demonstrated in Figure 4.31, adding 1 % (v/v) of ionic detergent (Tween 20) did not have a deleterious effect on the 6xHis-tagged InlA/Ni-NTA column interaction and was, thus, also added to the running buffers as a precautionary additive, to prevent non-specific hydrophobic interactions.

The 'mopping up' effect of low imidazole concentrations referred to above could have been extrapolated to competitively elute the specifically bound 6xHis-tagged protein by simply increasing the concentration. Suggested concentrations for elution are reported to be between 20 and 250 mM (Janknecht *et al.*, 1991; Hefti *et al.*, 2001; Qiagen, 2002). However, reported disadvantages of using imidazole have indicated that it can have negative influences on NMR experiments, competition studies and crystallographic studies (Terpe, 2003). Significant residual imidazole can also result in protein aggregation (Hefti *et al.*, 2001). With this in mind, alternative elution methods were considered.

The highly efficient metal chelating compounds EDTA and EGTA could potentially have been employed to elute the recombinant protein as a metal-6xHis-tag-protein complex. This however, would have necessitated further processing to remove the 'stripped' Nickel ions from the eluant. Furthermore, this 'stripping' of Nickel from the NTA resin would have drastically reduced the lifetime of the column and required it to be recharged with Nickel ( $\text{NiCl}_2$ ) after every run. A useful feature of the histidine residues in the 6xHis-tag is that they have a  $\text{pK}_a$  of approximately 6.0 and thus become protonated if the pH is reduced to pH 4.5-4.3. In such conditions, the positively charged His-tag is no longer able to bind the Ni-NTA resin and is eluted. Sodium acetate buffer was chosen and the elution efficiency analysed over a broad range of buffer pH values from 5.76 to 4.5. The results indicated that for complete elution of bound His-tagged InlA, sodium acetate buffer at a pH of 4.5 was necessary (Figure 4.31). This pH was close to the isoelectric point (pI) of the native InlA protein (4.93) and the predicted pI of the recombinant version (4.92), calculated using online software ([www.ca.expasy.org/tools/pi\\_tool.html](http://www.ca.expasy.org/tools/pi_tool.html)). Hence, eluted fractions were immediately





neutralised with 1/10 the eluant volume of 1 M Tris-HCl (pH 8.5), to prevent denaturation of the recombinant InlA protein.

The full suite of optimised IMAC purification conditions were applied to the preparative, large-scale batch purification of rInlA protein for use in further studies involving the antibody 'mAb2B3'. Samples from each stage of the purification process were analysed by SDS PAGE to ensure no significant sample loss was occurring (Figure 4.32). Once purified and dialysed, the purified rInlA was probed separately with both anti-His-tag monoclonal antibody and the mAb2B3 monoclonal antibody (Figure 4.33). The results confirmed that the purification process had not adversely affected the rInlA protein and what was equally significant was that the ability of mAb2B3 to recognise its complementary, InlA-borne epitope and the anti-His-tag antibody to bind the C-terminal His-tag sequence had not been compromised.



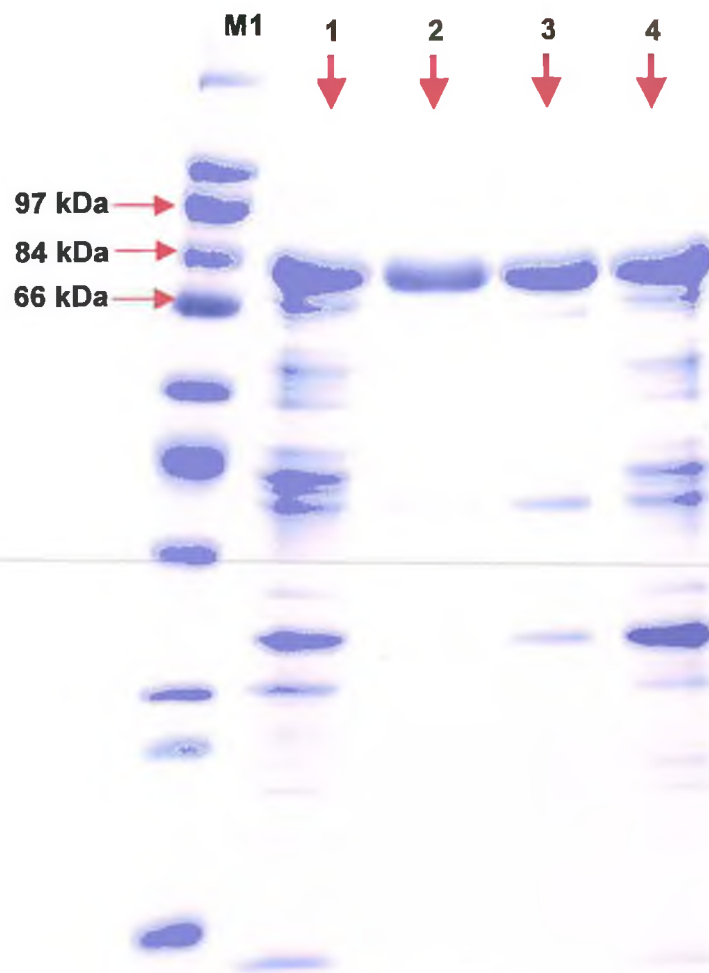


**Figure 4.30:** The effect of salt and imidazole concentration on the purity of IMAC-isolated recombinant InIA protein. Each lane was loaded with a 20  $\mu$ l sample volume. The binding/running/washing buffer used throughout was PBS supplemented with 15 mM  $\beta$ -mercaptoethanol. All samples originated from the same lysate (1/20 original culture volume) and were purified using a 1:4 (Ni-NTA:lysate ratio). In lanes 1 and 4 the buffer salt concentration had been increased to 0.5 and 1 M NaCl, respectively. In lanes 2 and 3 the buffer contained 1 M NaCl supplemented with 20 and 10 mM imidazole, respectively. The results indicated that increasing the salt concentration from 0.5 to 1 M NaCl only very slightly reduced the amount of non-specific components in the eluant. However, when 10 mM imidazole was present a significant reduction in the overall concentration of non-specific components became evident. Supplementing the buffer with 20 mM imidazole reduced the non-specific content even further. It was decided not to increase the imidazole concentration further as this could have competitively inhibited binding of the recombinant InIA protein to the Ni-NTA resin. Lane 'M1' contained SigmaWide™ wide range molecular weight marker.



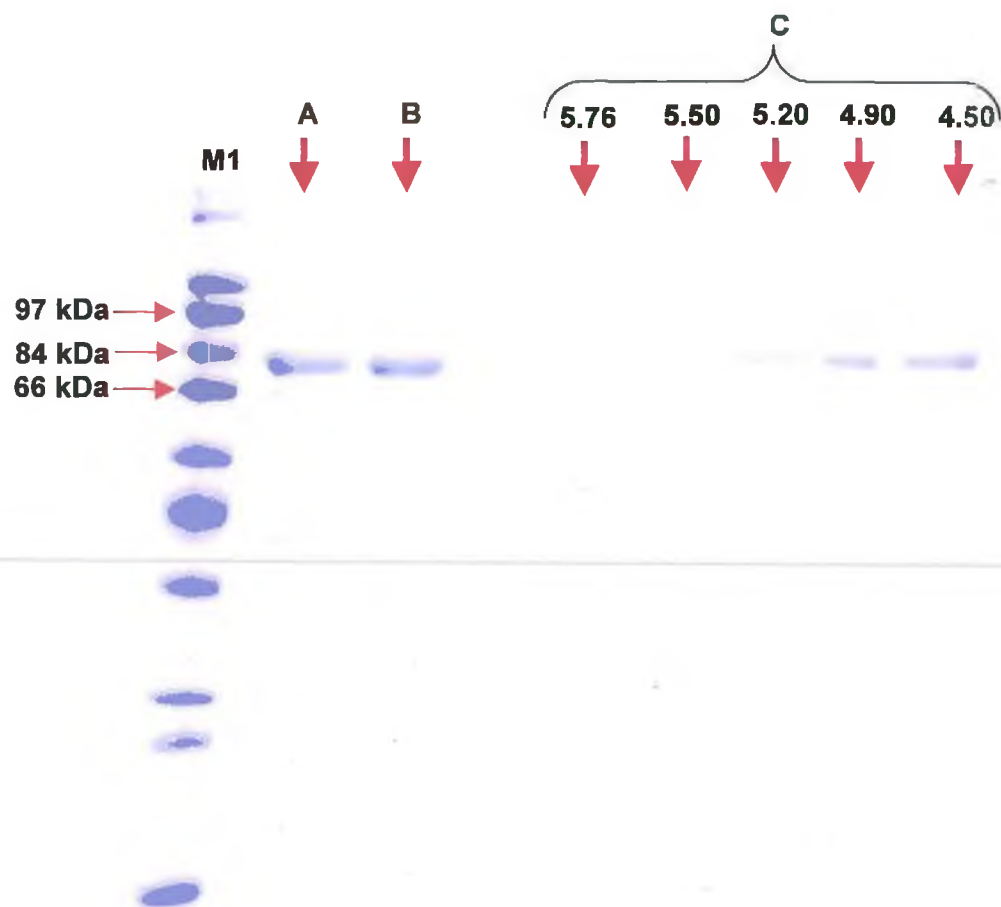


**Figure 4.31:** The effect of detergent concentration and elution pH on the purity of IMAC-isolated recombinant InlA protein. Lane 'M1' contained SigmaWide™ wide range molecular weight marker. The binding/running/washing buffer used throughout was PBS containing 15 mM  $\beta$ -mercaptoethanol and 1 M NaCl. Each lane was loaded with a 20  $\mu$ l sample volume. All samples originated from the same lysate (1/20 original culture volume) and were purified using a 1:4 (Ni-NTA:lysate) ratio. In lanes A and B the buffers used contained 0.5 and 1.0 % (v/v) Tween 20, respectively. There appeared to be no significant difference between the degree of apparent purity between samples A and B. The set of samples grouped under 'C' represent a sequential gradient elution using 100 mM sodium acetate buffer at pH 5.76 to 4.5. The running buffer in this case, was similar to that used for sample 'B' (i.e. containing 1 % v/v Tween20). These results indicated that for complete elution of the recombinant InlA protein, a pH of 4.5 was required.



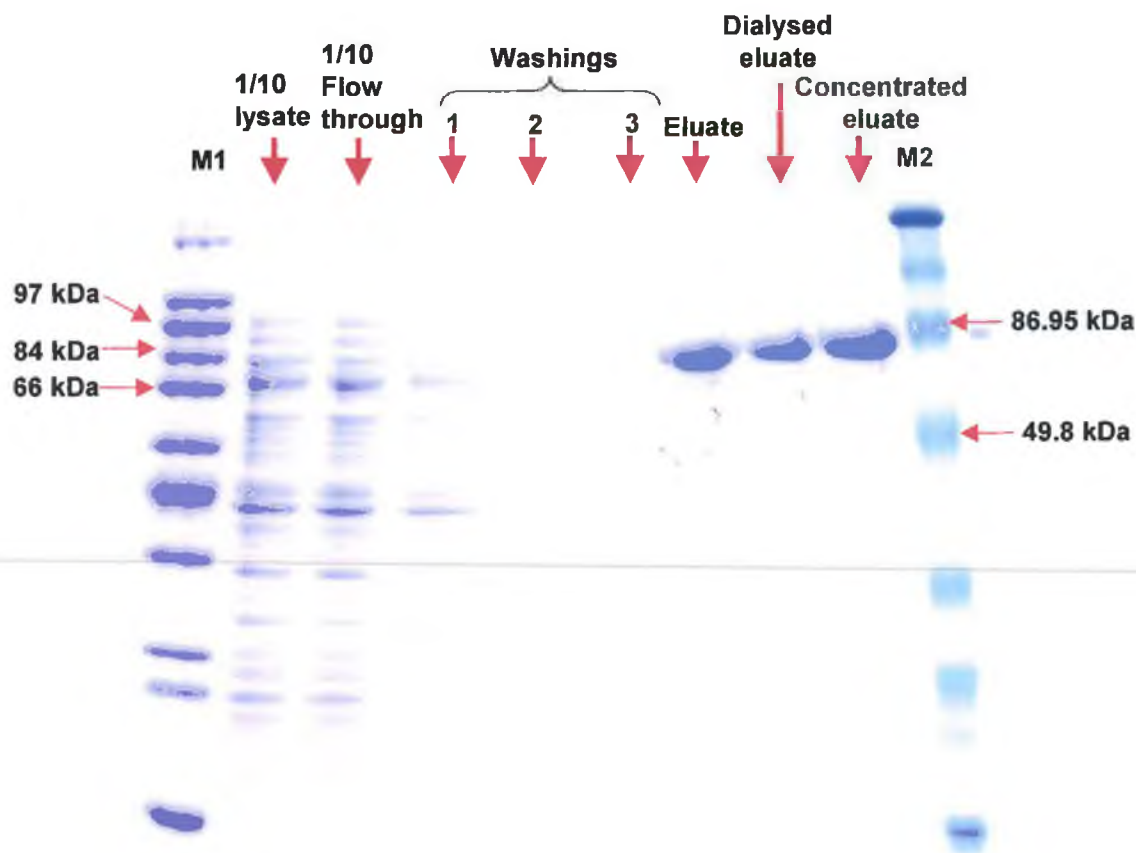


**Figure 4.32:** Purification of the recombinant InlA protein by immobilised metal affinity chromatography (IMAC). The Pfu9 clone was subcultured from an overnight culture at 1/20 into fresh LBB (containing ampicillin, tetracycline and 1 % (v/v) glucose), grown to an  $O.D_{600nm}$  of 0.6 and induced with 1.0 mM IPTG for 5 hours at 30°C. After 5 hours the cells were centrifuged for 20 minutes at 4000 rpm and the pellets resuspended in binding buffer (PBS containing 0.5 M NaCl, 20 mM imidazole, 15 mM  $\beta$ -mercaptoethanol) to a volume of 1/20 the original culture volume and sonicated. Cell lysates were incubated with Ni-NTA resin (1/4 the lysate volume, pre-equilibrated with binding buffer) for 1 hour 30 minutes at room temperature with constant mixing. The mixture was then centrifuged at 4000 rpm at 6 °C for 5 minutes and the supernatant decanted into a fresh tube (flow through). The Ni-NTA pellet with bound His-tagged protein was washed 3 times with PBS/T containing 0.5 M salt and 10 mM  $\beta$ -mercaptoethanol. Bound His-tagged proteins were eluted by incubation with 5 mls 100 mM sodium acetate buffer (pH 4.5) and neutralised with a 1/10 volume 1M Tris-HCl, pH 8.5. The resultant eluate was dialysed extensively against PBS and concentrated using a Centricon<sup>TM</sup> ultra-filtration tube with a 10 kDa cut-off. Purified proteins were stored at -20°C until required. Samples from each stage of the purification process (labelled on gel) were analysed by SDS PAGE to estimate the degree of purity and efficiency of the overall process.





'M1' and 'M2' refer to SigmaWide™ wide range and Pierce BlueRanger™ (prestained) molecular weight markers, respectively.

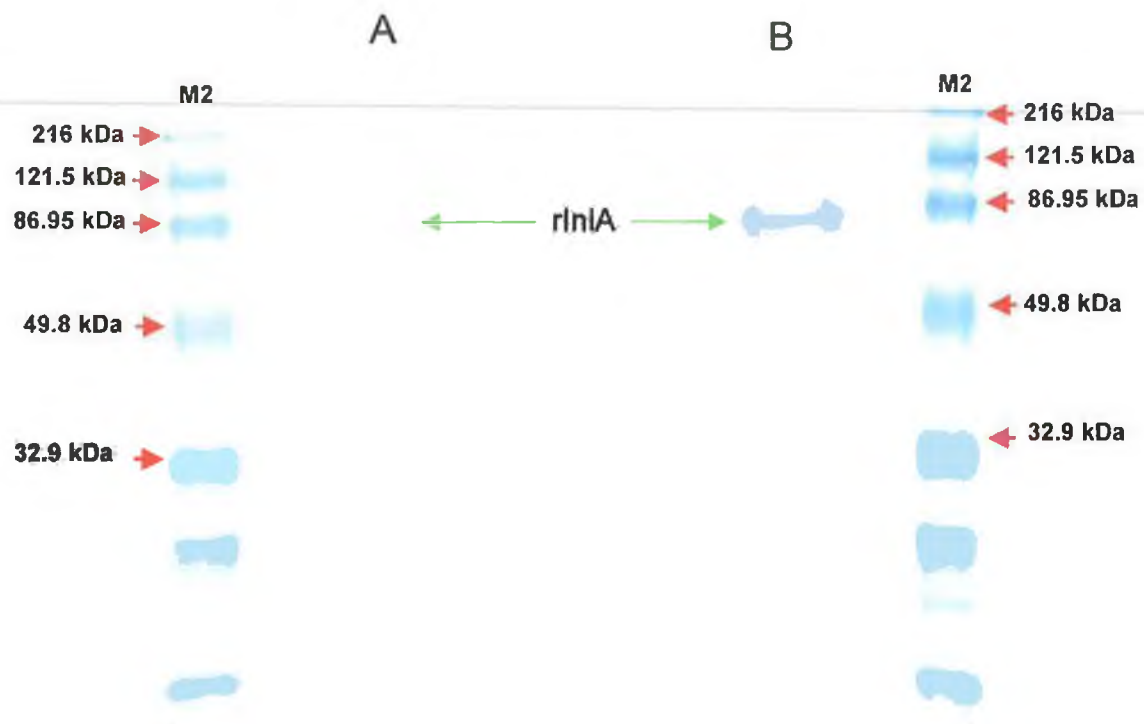


**Figure 4.33:** Immunoreactivity of purified recombinant InlA. Lanes designated 'M2', contained BlueRanger™ molecular weight marker. Panel 'A' represents the purified rInlA protein following immuno-probing with mAb2B3 monoclonal IgG2a antibody and secondary, AP-labelled caprine anti-IgG2a antibody. Panel 'B' demonstrates the same band following immunoprobings with murine HRP-labelled anti-His-tag monoclonal antibody.



### 4.3 Summary and conclusions

The previous chapter outlined the production of three panels of monoclonal antibodies to intact *L. monocytogenes* cells and *L. monocytogenes*-derived proteins. It also concluded that the most promising monoclonal antibody, in terms of specificity towards *L. monocytogenes* cells, was that which had been designated 'mAb2B3'. Analysis of the specific reactivity of this antibody towards a single, cell surface-derived protein (~80 kDa), led to the postulation that the antigen being recognised was possibly Internalin A (InlA). In order to confirm this, it was essential to derive a pure source of InlA protein and demonstrate specific reactivity of mAb2B3 towards it. In the absence of any published protocol for extraction of native InlA from *L. monocytogenes* cells, it was necessary to produce a recombinant version of the protein.

Genomic DNA was extracted from *L. monocytogenes* serotype 1/2a cells, using guanidium thiocyanate, and this was then used as the source material for PCR-based amplification of the *inlA* gene sequence. Initially the gene sequence encoding the full-length protein (minus the N-terminal signal sequence) was cloned into a pCR2.1 vector using a TA cloning kit and transformed into *E. coli* XL10-Gold® cells. Transformants containing the desired pCR2.1-*inlA* construct were selected using blue-white screening on LB agar plates containing X-gal reagent and were confirmed to contain the *inlA* insert by a combination of site-specific restriction and *inlA* gene-specific PCR. A pCR2.1-*inlA* plasmid construct was purified from a selected clone and digested with *Bam*HI and *Nco*I enzymes, before being directionally cloned into a pQE60 expression plasmid and transformed into competent *E. coli* XL10-Gold® cells. Successful transformants were again identified by *inlA* gene-specific PCR and *Eco*RI-restriction. The latter was made possible by virtue of a single *Eco*RI site being present on the native pQE60 plasmid several bps before the 5' *Nco*I insert ligation site and a second *Eco*RI site being introduced into the construct several bps before the 3' *Bam*HI insert ligation site when the insert was in the desired orientation. This construct positioned a 6xHis sequence at the C-terminal end of the rInlA protein.

Sequence analysis of the selected *E. coli*-borne pQE60-*inlA* plasmid construct indicated a 100 % homology with the known published sequence. However, when the selected clone was tested for specific InlA expression by SDS PAGE analysis of lysed cell cytoplasmic extract and subsequent immunoprobings with an anti-His-tag monoclonal antibody, results were somewhat inconclusive. Only very faint bands were evident upon immunoprobings samples that had been lysed under both native and denaturing conditions. A reassessment of the



strategy employed led to the conclusion that the most probable cause of this apparent lack of expression lay within the structure of the recombinant protein being expressed. More specifically, the presence of the hydrophobic cell wall anchoring domain was likely rendering the expression inefficient. Recombinant proteins with appreciable localised hydrophobic regions can have a toxic effect on host cells, most likely due to the association of the protein with or incorporation into vital membrane systems (Qiagen, 2002). The effect can be acute or chronic, whereby the toxic protein primarily reduces the growth rate of the host cells. The highly efficient transcription rates afforded by the optimised promoter regions on the expression plasmid exacerbate the negative effect on growth rates. This is even further compounded by metabolic demands imposed by translation of the recombinant protein. Even if only mildly toxic, as indicated by an initial poor level of expression for a given host cell culture this would, however, undoubtedly place a selective pressure on the host cells in favour cells bearing mutated, non-expressing plasmids. This would also explain why it was not possible to propagate *inlA*-transformed cells that did not harbour the *lacI<sup>f</sup>* genotype and were, thus, inherently subject to 'leaky' basal expression.

Therefore, the *inlA* gene sequence was cloned a second time. However, in addition to the sequence encoding the N-terminal signal peptide, the sequence encoding the 34 amino acid long C-terminal hydrophobic region was also excluded. At all times the overriding objective remained clear; that the recombinant product should retain activity towards the monoclonal antibody 'mAb2B3' (if this was in fact an InlA-specific antibody). The antibody had been raised against intact *L. monocytogenes* cells and thus, the removal of the signal sequence was not expected to affect the recognition process, since this would not have been present on the cell-bound version presented during immunisation and primary B-cell development. Likewise, the C-terminal region, being located principally in the sub cell wall, transmembrane region would not have been exposed on the intact cell. The truncated version was, therefore, expected to contain all the amino acid sequences necessary for correct functional folding and consequently for recognition by an InlA-specific antibody. The truncated *inlA* gene was 'directionally' cloned, into pQE60, thus, bypassing the TA cloning step and the associated complications earlier encountered with this method. This was made possible by employing primers that contained suitable 'clamp' sequences flanking the *Bam*HI and *Nco*I restriction termini. In addition, high fidelity *Pfu* polymerase was used in the *inlA* PCR amplification, thereby, obviating the need to perform confirmatory sequence analysis during the preliminary cloning stages.

Expression of the rInlA protein was investigated by SDS PAGE analysis of sonicated cell lysates in 2x PBS buffer, following optimised IPTG induction. Specific expression of an 80



kDa protein band was demonstrated only in cells containing the complete pQE60-*inlA* construct. No 80 kDa band was detectable in cells harbouring pQE60 alone. The 80 kDa protein also reacted specifically with an anti-His-tag monoclonal antibody in Western blot analysis, thus, confirming that the His-tag fusion had been faithfully translated, was accessible and had not been adversely affected during cell lysis.

Finally, purification of the His-tagged rInlA protein was optimised using Ni-NTA resin and the purified rInlA was shown to specifically react with the monoclonal antibody 'mAb2B3'. The latter was thus, confirmed to be an anti-InlA antibody.

To the best of my knowledge, this represents the first reported heterologous expression, in *E. coli*, of the complete extracellular domain of InlA with a 6xHis fusion tag suitable for rapid and efficient purification.





---

***Chapter 5***  
***Biosensor-Based Detection of *L.****  
***monocytogenes***



## **5.1 Introduction**

The use of biosensors for detection of pathogenic bacteria (Ivnitski *et al.*, 1999) and in particular, for the detection of foodborne pathogens (Haines and Patel, 1995; Rand *et al.*, 2002; Leonard *et al.*, 2003; Deisingh and Thompson, 2004a; Leonard *et al.*, 2004 and Leonard *et al.*, 2005) is gathering increasing prominence in the vast food-pathogen detection market (Alocilja and Radke, 2003). This is undoubtedly a direct result of the increasing industry-driven demand for rapid 'sample-to-result' analyses that can be automated and integrated 'on-line'.

### **5.1.1 Definition of biosensors**

A biosensor is best described as 'a compact analytical device incorporating a biological or biologically-derived sensing element that is either integrated within, or intimately associated with a physico-chemical transducer' (Turner *et al.*, 1997). The main transduction technologies employed in biosensor formats measure analyte-induced changes in optical, electrochemical or piezoelectric properties and are comparatively reviewed by Diamond, (1998) and Quinn and O'Kennedy, (1999).

The relative merits of each of the biosensor formats/categories, with specific reference to their capacity to mediate detection of bacterial entities, have been comprehensively reviewed elsewhere (Ivnitski *et al.*, 1999; Patel, 2002; Deisingh, 2003; Leonard *et al.*, 2003; Deisingh and Thompson, 2004b). Optical transducers are particularly attractive for application to direct (label-free) detection of bacteria (Ivnitski *et al.*, 1999). The research described in this chapter is restricted to the use of an optical biosensor that exploits the surface plasmon resonance (SPR) phenomenon, which, according to current market and research trends (Homola *et al.*, 1999a; Baird and Myszka, 2001; Rich and Myszka, 2001) is predicted to become one of the most widely used immunosensor platforms over the next 10 years.

### **5.1.2 History of surface plasmon resonance sensing**

Optical SPR was first demonstrated in 1968 by Otto. The technique found its first practical application as a tool for characterising solid phase media, such as thin films (Raether, 1977; Pockrand *et al.*, 1978) and monitoring processes at electrochemical interfaces (Gordon II and



Ernst, 1980). It was first employed in a sensing format for gas detection (Nylander *et al.*, 1982) and subsequently, was adapted for 'immuno-biosensing' of a specific antibody-antigen interaction (Liedberg *et al.*, 1983). These developments employed the 'Kretschman configuration' (Kretschman and Raether, 1968; Kretschman, 1971), which is more appropriate than the 'Otto configuration' for solution-phase sensing, typically required in clinical, food and environmental diagnostics. This technology was refined and optimised for biosensing applications and led to the commercialisation of the Biacore™ SPR biosensor in 1990 (Löfås *et al.*, 1991; Liedberg *et al.*, 1995) for generic biospecific/biomolecular interaction analysis (BIA) (Malmqvist, 1999).

### 5.1.3 Theory of surface plasmon resonance biosensing

An appreciation of the physico- and electro-chemical basis of SPR sensing (Salamon *et al.*, 1999; Liedberg and Johansen, 1998) requires a basic understanding of total internal reflection, evanescent wave and surface plasmon theory.

*Total internal reflection* (TIR) occurs at the interface between two non-absorbing materials when light impinges on the interface at or above an angle, specified as the critical angle ( $\theta_c$ ). Although no refraction occurs and the intensity of the reflected light is equal to the incident light intensity, a weak electrical field intensity component (*evanescent wave*) leaches perpendicularly into the lower refractive index medium and penetrates to a depth of approximately one wavelength, its amplitude decaying exponentially with increasing distance from the interface. If the interface is coated with a non-magnetic, noble-metal film that is much thinner ( $d=50$  nm) than the wavelength of the incoming visible light ( $\lambda=400$ - $800$  nm,  $760$  nm in Biacore™), a p-polarised charge density oscillation manifests at the metal/ambient dielectric interface. This is referred to as a *surface plasmon wave*. Gold thin films are preferred due to their demonstrated chemical resistance and tendency to produce strong plasmons and consequently, sharp reflectance minima (De Bruijn *et al.*, 1992).

Under conditions of TIR and when the energy and momentum of the incident light exactly matches that of the surface plasmon wave (i.e. when the vector component of the p-polarised incident light parallel to the interface, ' $K_x$ ', is equal to the surface plasmon wave vector, ' $K_{sp}$ '), a resonance condition is achieved. Resonance results in an increase in energy 'coupling' from the incident light, culminating in an enhanced evanescent wave field that is concomitantly reported as a decrease in the intensity of the reflected light. This can be 'tuned'



by varying the wavelength or angle of the incident light. The main disadvantage of the latter method is the requirement for complex, bulky and slow optical angle scanning components. However, this is overcome by employing a wedge-shaped incident beam (Matsubara *et al.*, 1988a; Matsubara *et al.*, 1988b) that comprises a continuum of pre-defined incident angles and a photodiode detector array that can accurately extrapolate the angle at which the reflected light intensity is minimal ( $\theta_{\text{SPR}}$ ). Thus, when the prism, incident wavelength, metal properties and temperature are kept constant,  $\theta_{\text{SPR}}$  varies only in response to changes in the refractive index of the ambient medium ( $n_2$ ), which is directly influenced by bio-specific binding events at the metal surface that occur within the approximate 300nm range of the enhanced evanescent field. The refractive index change can be directly related to the progress of the binding event (Stenberg *et al.*, 1991) by:

$$\Delta C = \Delta n_1 (\delta C / \delta n_1) \quad (\text{Equation 5.1})$$

Where	$\delta C / \delta n_1 =$	5-7g/cm <sup>3</sup>
	$\Delta n_1 =$	refractive index of sample.
and	$\Delta C =$	protein concentration.

The change in position of  $\theta_{\text{SPR}}$  is quantified in response units (RUs) and is monitored in 'real-time' as a function of time in a sensorgram.

There are a variety of Biacore™ sensor chips available (<http://www.biacore.com>) for general or specific applications. The majority incorporate a carboxymethylated (CM) dextran surface. This functions as an extended 3D-coupling matrix or 'hydrogel' (Löfås and Johnsson, 1990) and increases both the binding capacity and dynamic range of the biosensor. The most commonly used sensor chip is the 'CM5' chip, which possesses a hydrogel ~100 nm thick. For such a surface, a 1000 RU change corresponds to a 0.1° shift in  $\theta_{\text{SPR}}$  and a change in surface concentration of ~1 ng/mm<sup>2</sup> (Stenberg *et al.*, 1991). Assuming a 100 nm thick hydrogel, this corresponds to an effective surface concentration of 10 mg/ml. Generally the measured change in surface refractive index is independent of the protein/peptide type, although it can vary for more complex molecules, such as glycoproteins, lipids and nucleic acids (Stenberg *et al.*, 1991; Hashimoto, 2000; Hahnefeld *et al.*, 2004). The hydrogel also serves to create a hydrophilic environment with a low propensity for non-specific binding. The extensive carboxylation provides convenient sites for covalent attachment of amine containing molecules.





SPR biosensors have a number of advantages over traditional immunoassays and these were highlighted by Canziani *et al.*, (2004), as follows:

1. SPR technology can be used to measure complex formation without labelling of the reactants.
2. Complex formation can be monitored in real-time, providing detailed information about the kinetics and equilibrium dissociation constants.
3. Samples from crude preparations may be analysed.

In addition, the Biacore™ system is fully automatic, incorporates a reliable microfluidic system that facilitates accurate and precise sample delivery and flow-rate manipulation. Significantly, it also permits multi-channel analysis and thus, reference-subtraction (Ober and Ward, 1999), which is useful for comparative analyses and is a quintessential prerequisite for kinetic and affinity estimations. A significant advantage of SPR over optical detection techniques is that the incident light energy does not actually penetrate the bulk sample and thus, measurements can be made equally on coloured or turbid solutions and on clear clear samples (Markey, 2000). Typically Biacore™ and SPR/evanescent wave-based technologies have been routinely used for analysis of small molecules. With specific reference to foodstuffs, these include hormone (Gillis *et al.*, 2002), antibiotics (Haasnoot *et al.*, 2003) residues and small molecules that are indicative of microbial contamination such as microbial toxins (Homola *et al.*, 1999b; Daly *et al.*, 2000; Rasooly, 2001).

An overview of the Biacore™ system principles is provided in Figure 5.1. For a comprehensive treatment of the general principles and applications of Biacore™, the reader is directed to the dedicated text of Nagata and Handa, (2000). The technology and instrumentation underpinning SPR-based biosensors itself is well established. The most crucial determinant of assay performance undoubtedly surrounds the biospecificity component, more specifically, the choice of ligand and the immobilisation strategy. This is limited by the availability of suitably specific and stable receptor ligands. The role of ligand can be filled by molecules such as, antibodies, natural biological receptors or nucleic acids (McCormack *et al.*, 1998; Rogers, 1998). Most commonly, antibodies are used as current technologies allow for the production, selection and engineering of antibodies with the desired degree of specificity, affinity and physicochemical robustness for optimal performance as the biospecific component of biosensors (Alfthan, 1998; Fitzpatrick *et al.*, 2000; Benhar *et al.*, 2001; Hock *et al.*, 2002).



### P-polarised incident light

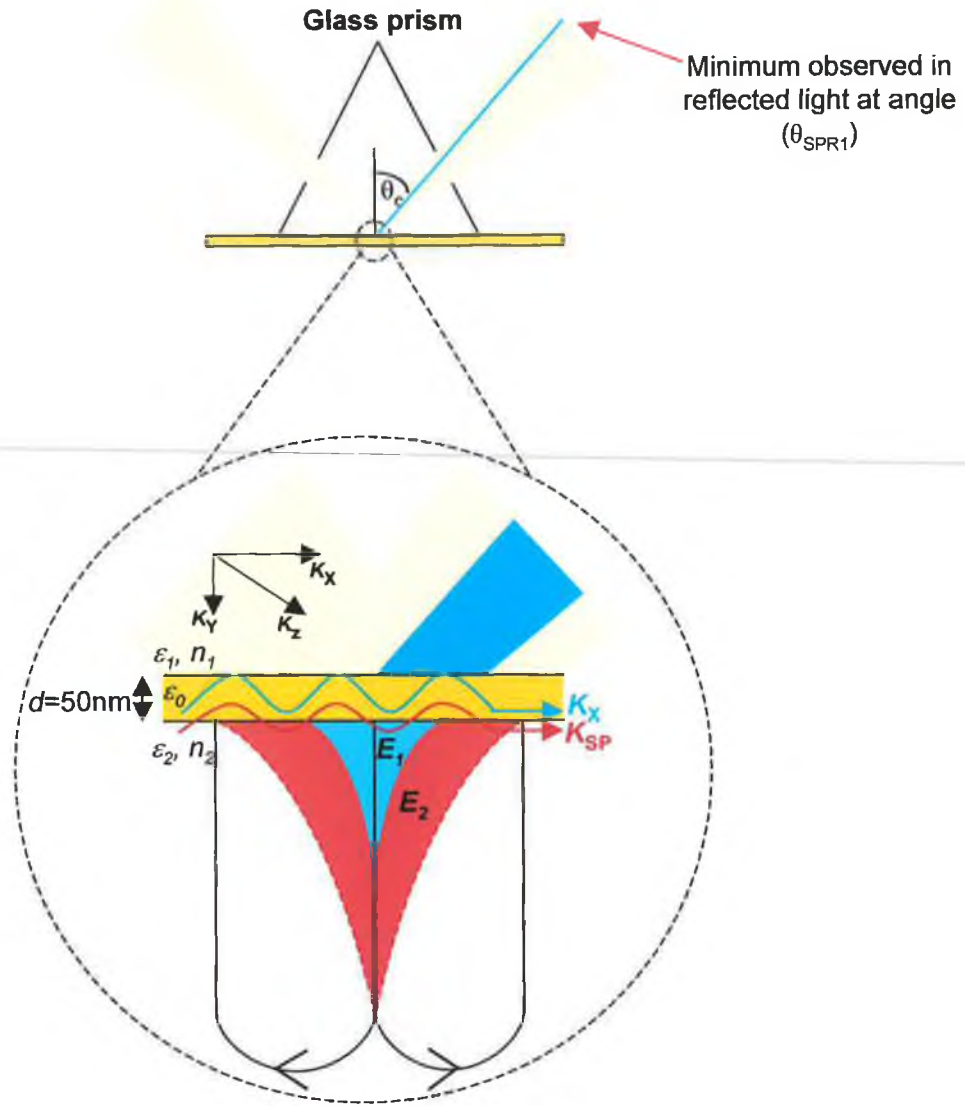


**Figure 5.1:** Evanescent wave theory and surface plasmon resonance at a metal-dielectric interface.  $\epsilon_1$  and  $\epsilon_2$  refer to the dielectric constants of the prism and ambient media, respectively. These constants determine the complex indices of refraction of each media ( $N$ ; where  $N = n - ik$ ;  $i = \sqrt{-1}$ ;  $k$  = the extinction coefficient and  $n$  = refractive index), according to  $\epsilon = N^2$ . Total internal reflection occurs at  $\theta \geq \theta_c = \arcsin(\sqrt{\epsilon_2/\epsilon_1})$ , where  $\sqrt{\epsilon_1} > \sqrt{\epsilon_2}$  and thus,  $n_1 > n_2$  and an evanescent wave ( $E_1$ ) extends across the metal film, decaying exponentially into the ambient medium. When the p-polarised incident light vector ( $K_x$ ), parallel to the incident plane, matches exactly the surface plasmon wave propagation vector ( $K_{SP}$ ), energy from the incident light is coupled into the surface plasmon wave and leads to an enhancement



of the net evanescent field ( $E_z$ ) and reduction in the intensity of the reflected light. That is, surface plasmon resonance occurs when  $K_x = K_{SP}$ , where;  $K_x = (\omega/c) \cdot \epsilon_1^{1/2} \sin\theta_{SPR}$  and  $K_{SP} = (\omega/c) \cdot \{\sqrt{(\epsilon_0)(\epsilon_2)/(\epsilon_0 + \epsilon_2)}\}$ .  $\omega$  = frequency of the incident light and surface plasmon wave ( $2\pi c/\lambda$ ),  $\epsilon_0$  = dielectric constant of the metal and  $c$  = speed of light in a vacuum. Thus, the resonance condition can be tuned by keeping the p-polarised incident wavelength ( $\lambda$ ) constant and varying the incident angle ( $\theta$ ), until  $K_x = K_{SP}$ , or vice versa. Furthermore, assuming  $\epsilon_0 \gg \epsilon_2$ , it follows that  $\sin\theta_{SPR} \propto \epsilon_2 \propto n_2$  and thus, when  $\epsilon_1$ ,  $\epsilon_0$  and  $\lambda$  are held constant,  $\Delta\theta_{SPR}$  is a function of mass changes caused by molecular binding events at the surface. (Adapted and amended from Liedberg and Johansen, 1998; Salamon et al., 1999).



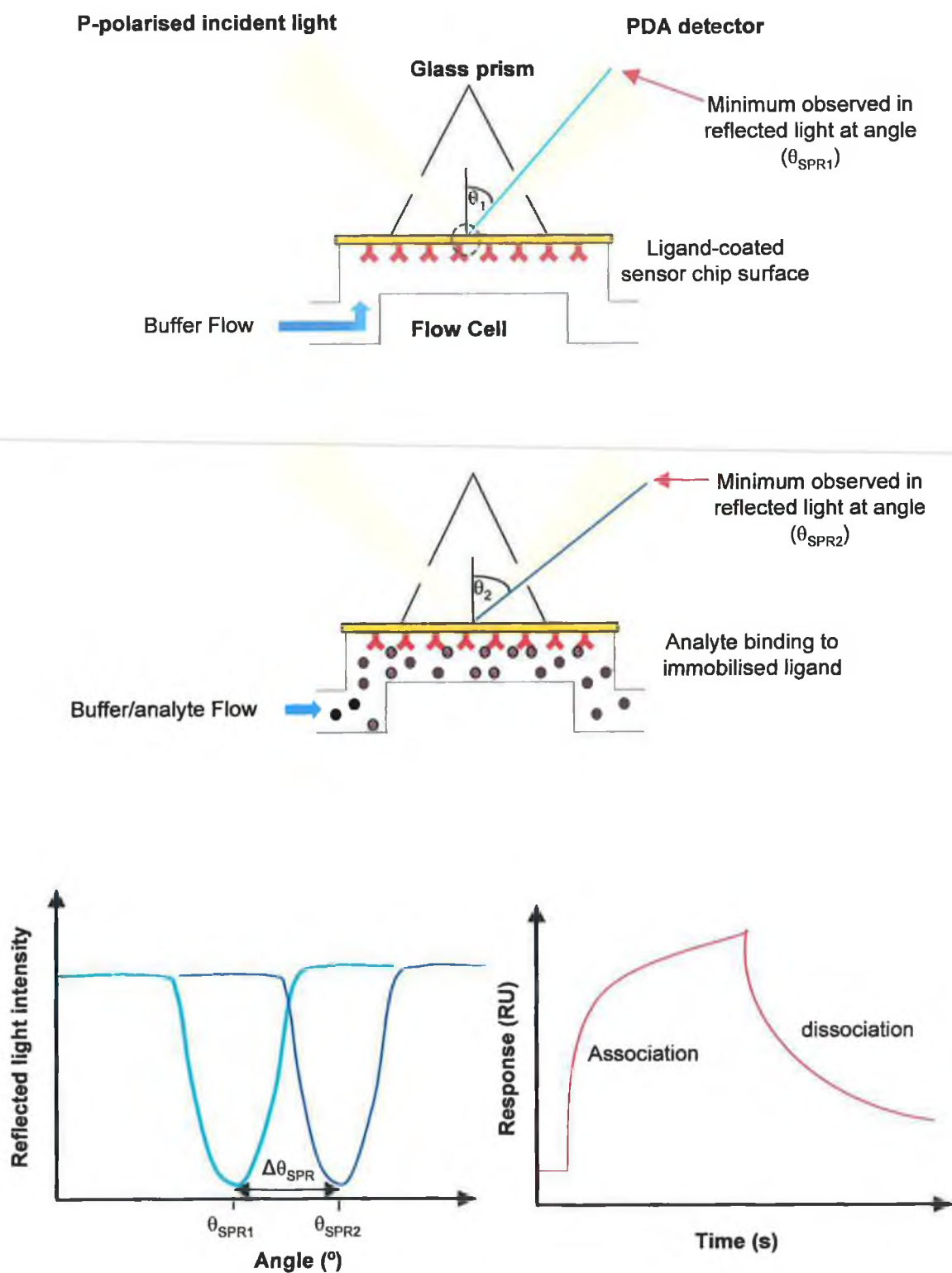


**Figure 5.2:** Schematic overview of BIA process using Biacore™ instrumentation. A light emitting diode (LED) emits light at 760 nm, which is then p-polarised and focused as a wedge-shaped beam (of multiple, defined angles) onto the sampling area. Under ambient





*conditions, with continual buffer flow over the sensor chip surface, a reflectance dip (the SPR minima) or 'shadow', is detected by a PDA detector, for  $\theta_{SPR1}$ . When analyte, (e.g. antigen) that is complementary to the immobilised ligand (e.g. antibody), is passed over the sensor chip surface it binds to the ligand and causes an increase in the mass concentration at the surface of the sensor chip and thus, an increase in the ambient refractive index close to the surface. This is detected as a shift in the angular position of the 'shadow' ( $\theta_{SPR2}$ ).  $\Delta\theta_{SPR}$  is measured in response units (RU) and it is monitored in real-time, with an adjustable data collection frequency of 1-10 Hz, on a sensorgram.*

The Biacore™ instrument is an extremely useful tool for rapidly evaluating antibody-antigen interactions, and throughout this chapter, it was employed as such, with respect to the monoclonal antibodies isolated in Chapter 3. The ELISA-based detection of *L. monocytogenes* cells (Section 3.2.7) was essentially, an indirect measurement, where solution-phase binding of mAb2B3 to cells was reported as an inversely proportional signal response. Moreover, the ELISA assay, by its very nature, incorporated multiple incubation stages, in addition to intermittent washing steps.

The key objective of this chapter was to assess the potential of using the SPR-based approach to monitor direct, real-time binding of *L. monocytogenes* cells to immobilised *L. monocytogenes*-specific antibody (mAb2B3).



## **5.2 Results and discussion**

### **5.2.1 Direct detection of *L. monocytogenes* cells using surface plasmon resonance**

The monoclonal antibody (mAb2B3) was chosen based on its demonstrated capacity to bind whole *L. monocytogenes* cells (Section 3.2.6.4) specifically via the InlA protein (Sections 4.2.4 and 4.2.5). In order to facilitate cell binding at the sensor chip surface, it was necessary to stably attach the antibody to the surface. Thus, a sequence of exploratory experiments was conducted, to find the optimal immobilisation strategy and sensor chip substrate-matrix compatibility.

#### **5.2.1.1 Pre-concentration of mAb2B3 monoclonal antibody onto the CM5 sensor chip surface**

Pre-concentration was assessed empirically, on a single flow cell of a freshly primed CM5 sensor chip surface (Section 2.10.1). The first consideration when designing the assay was to achieve efficient immobilisation of the monoclonal antibody. Efficient pre-concentration serves to concentrate the antibody to very high levels within the immediate vicinity of the dextran hydrogel and thus improve coupling yield to the activated carboxyl branches. Optimal pre-concentration is mediated by maximising the electrostatic interaction between the negatively-charged carboxymethylated dextran and the antibody. The antibody was prepared in a low ionic strength buffer, 10 mM sodium acetate (to minimise charge screening) at a range of pH values below the anticipated pI of immunoglobulin proteins (to confer a positive charge on the antibody molecule). Amine coupling, mediated by EDC/NHS surface-activation (Johnsson *et al.*, 1991; O'Shannessey *et al.*, 1992; Barié and Rapp, 2001) was employed throughout these studies and since activated carboxyl groups react best with uncharged amino groups, the highest buffer pH generating appreciable pre-concentration was chosen as the carrier buffer for immobilisation. In the case of mAb2B3, this was determined to be pH 4.0 (Figure 5.3a).

#### **5.2.1.2 Pre-concentration of IgG2a control antibody onto the CM5 sensor chip surface**

In order to facilitate reference-subtraction of bulk refractive index, systematic deviations, temperature drift and matrix effects, it was decided to conduct sample analysis in parallel, by simultaneous sample exposure to *L. monocytogenes*-specific (mAb2B3)- and a control (IgG2a)-immobilised surface (Sections 2.10.3). Blank dextran or dextran that had been subject to EDC/NHS activation and capping in the absence of a coupling ligand have been



frequently employed in this capacity. However, as mAb2B3 is an IgG2a monoclonal antibody, it was felt that an unrelated murine IgG2a antibody would serve as the most suitable control, since it would be expected to most closely replicate the ligand topography exhibited by the mAb2B3 test surface. Thus, a commercial, affinity-purified murine IgG2a standard was sourced (*Sigma, M-9144*) and it was subjected to the same pre-concentration evaluation as mAb2B3 (Section 2.10.1). For this particular antibody, optimal pre-concentration was achieved at pH 4.4 (Figure 5.3b).



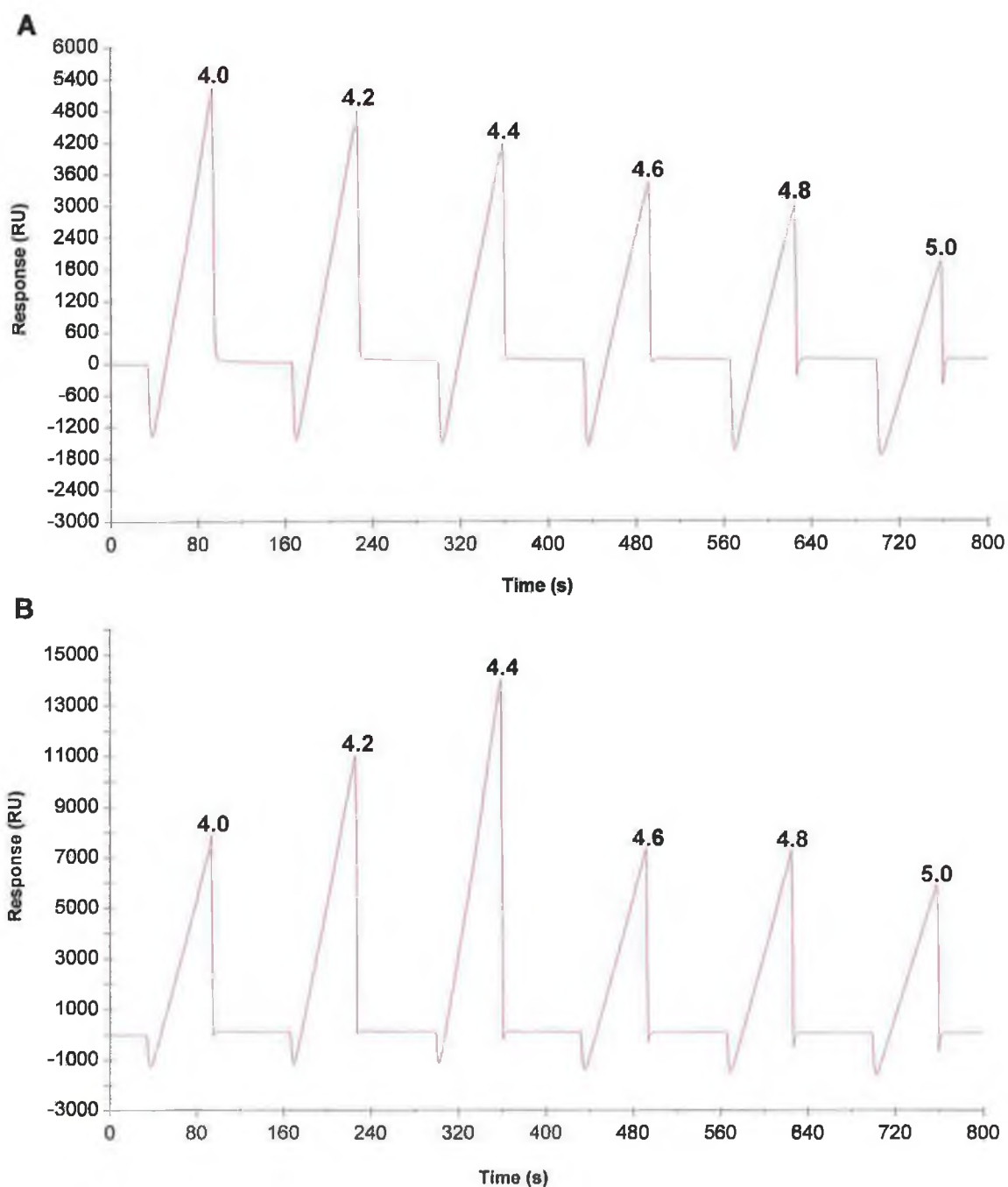


**Figure 5.3:** Antibody pre-concentration analyses. (A): pre-concentration of mAb2B3 onto the CM5 sensor chip surface. Maximum pre-concentration was observed at pH 4.0. (B): pre-concentration of IgG2a standard onto the CM5 sensor chip surface. Maximum pre-concentration was observed at pH 4.4. Thus 10 mM sodium acetate buffer at pH 4.0 and 4.4 were chosen as the immobilisation buffers for mAb2B3 and the standard IgG2a antibodies, respectively.





### 5.2.1.3 Immobilisation of mAb2B3 onto CM5 sensor chip

Protein A affinity-purified mAb2B3 was diluted to 100 µg/ml in 10 mM sodium acetate buffer at pH 4.0 and passed over a freshly EDC/NHS-activated CM5 surface in flowcell position 4 (Section 2.10.2). This was followed with a 'capping' step, mediated by exposure to 1 M ethanolamine for 11 minutes and a brief acid/base purge to remove loosely bound material. A final immobilised level of ~30000 RUs was achieved (Figure 5.4).

For the purposes of reference subtraction, the flowcell surface immediately downstream of the mAb2B3 active surface (flowcell surface 3) was immobilised with an equivalent level of the IgG2a control antibody (Section 2.10.3). The degree of non-specific binding to the control surface was challenged by simultaneously passing *L. monocytogenes* cells at  $1.07 \times 10^9$  cells/ml in HBS buffer over the mAb2B3 and control IgG2a surfaces. While a response in excess of 1200 RUs was achieved on the mAb2B3 surface, negligible binding was apparent on the control surface (Figure 5.5). This can be attributed to the high degree of immunospecificity of mAb2B3 with respect to *L. monocytogenes* cells and also to the NaCl and detergent content (150 mM and 0.05 % (v/v), respectively) in the sample and running buffer.

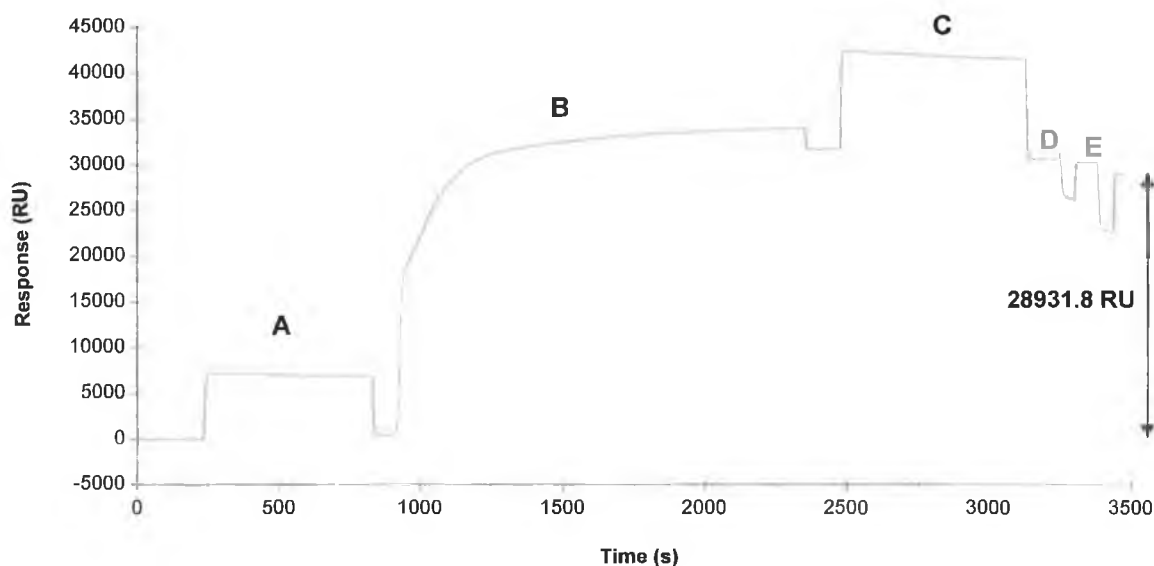


**Figure 5.4:** Immobilisation of mAb2B3, anti-InlA monoclonal antibody onto the CM5 sensor chip surface. (A) EDC/NHS activation, (B) binding of mAb2B3, (C) capping of unreacted groups, (D and E) regeneration pulse of 5 mM NaOH and 5 mM HCl, respectively. A final level of 28931.8 RUs covalently attached mAb2B3 was achieved.



#### 5.2.1.4 Assessment of specific cell-binding potential of mAb2B3-CM5 sensor surface:

It was clear that the amine coupling method resulted in a large amount of mAb2B3 efficiently coupled to the CM5 surface (Section 5.2.1.3). However, since this coupling procedure results in randomly cross-linked ligand, it was necessary to establish whether the intrinsic, *L. monocytogenes* cell-binding capacity of mAb2B3 had deteriorated significantly, following immobilisation. Fresh, LEB-cultured *L. monocytogenes* cells were washed, resuspended in PBS buffer at approximately  $1.07 \times 10^9$  cells/ml and simultaneously passed over both the mAb2B3-CM5 and IgG2a-CM5 surfaces at a flow rate of 1  $\mu$ l/min. While the response at the control surface remained essentially at the baseline level throughout, a clear kinetic association was observed for the mAb2B3 surface (Figure 5.5). The interaction was allowed to proceed for 15 minutes, to approach equilibrium. It was clear that the immobilised mAb2B3 retained sufficient activity to mediate binding of *L. monocytogenes* cells at the sensor surface. Binding of rInlA to the mAb2B3-cm5 surface was also clearly demonstrated (Figure 5.6).

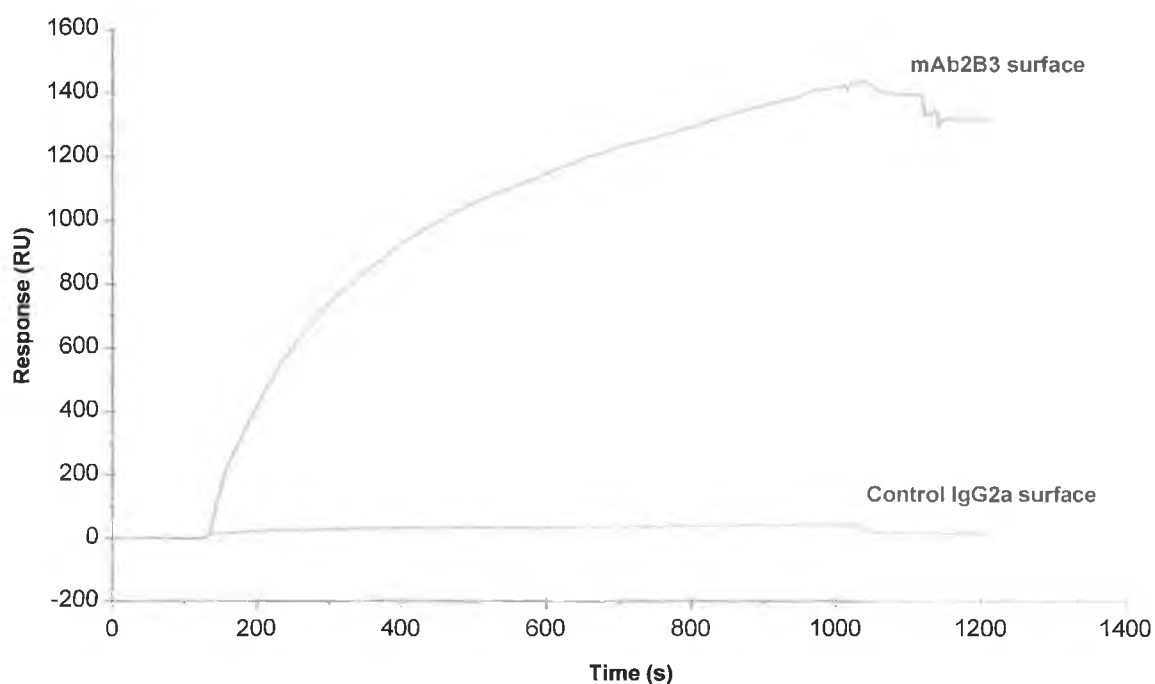


**Figure 5.5:** Real-time comparison of the mAb2B3-CM5 and control IgG2a surface binding-responses to *L. monocytogenes*. Approximately  $1.07 \times 10^9$  cells/ml *L. monocytogenes* cells in PBS were simultaneously passed over both surfaces at a flow rate of 1  $\mu$ l/min. The sensorgram clearly shows that there was substantial binding of *L. monocytogenes* cells to the



*mAb2B3* surface (red) at the concentration employed. Conversely, there was no apparent binding to the reference surface (blue). As the *L. monocytogenes* cell concentration used here was equivalent to the highest cell concentration used in all subsequent experiments, it was assumed that the chosen control surface was sufficient and underlined the cell-specificity of the *mAb2B3* monoclonal antibody.

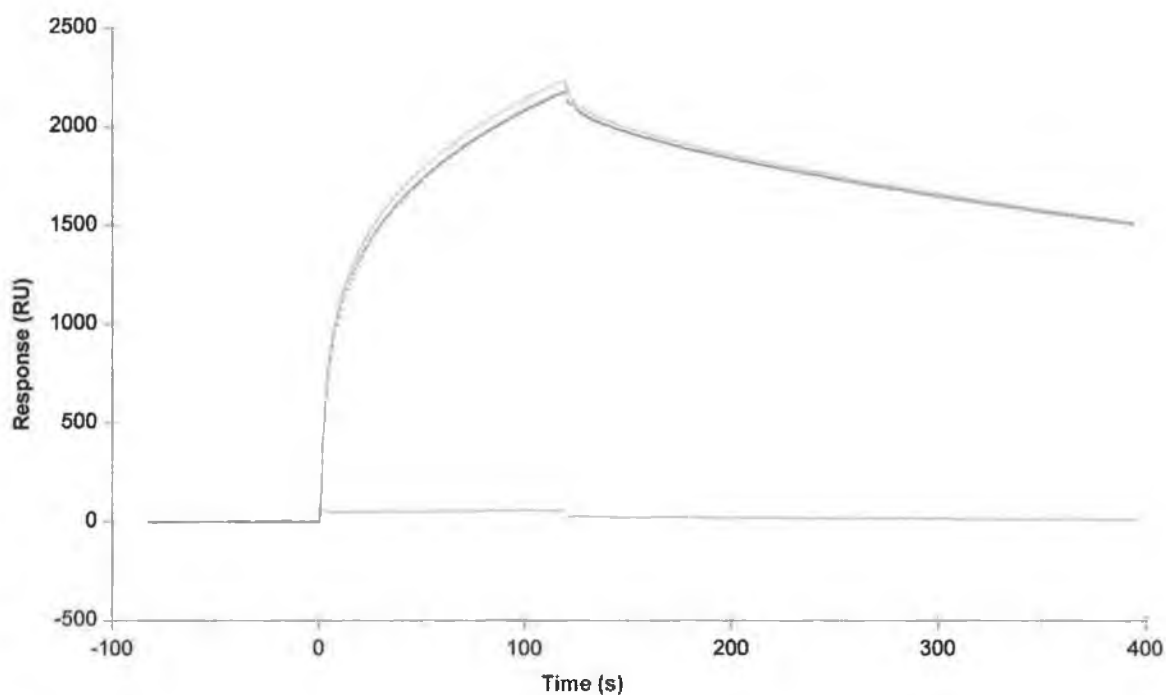


**Figure 5.6:** Real-time comparison of the *mAb2B3*-CM5 (red) and control-IgG2a (green) surface binding-responses to rInlA protein. Neat, freshly purified rInlA (Section 4.2.5) was simultaneously passed over both surfaces at a flow rate of 10  $\mu$ l/min. The appreciable reference-subtracted response (red) re-affirmed that the immobilised *mAb2B3* antibody was specifically binding to InlA protein.



#### 5.2.1.5 SEM and AFM image analysis of mAb2B3-captured *L. monocytogenes* cells on mAb2B3-immobilised sensor chip surface

In order to visualise the bound *L. monocytogenes* cells on the sensor chip surface SEM and AFM image analysis (Section 2.12) was performed (Figure 5.7).

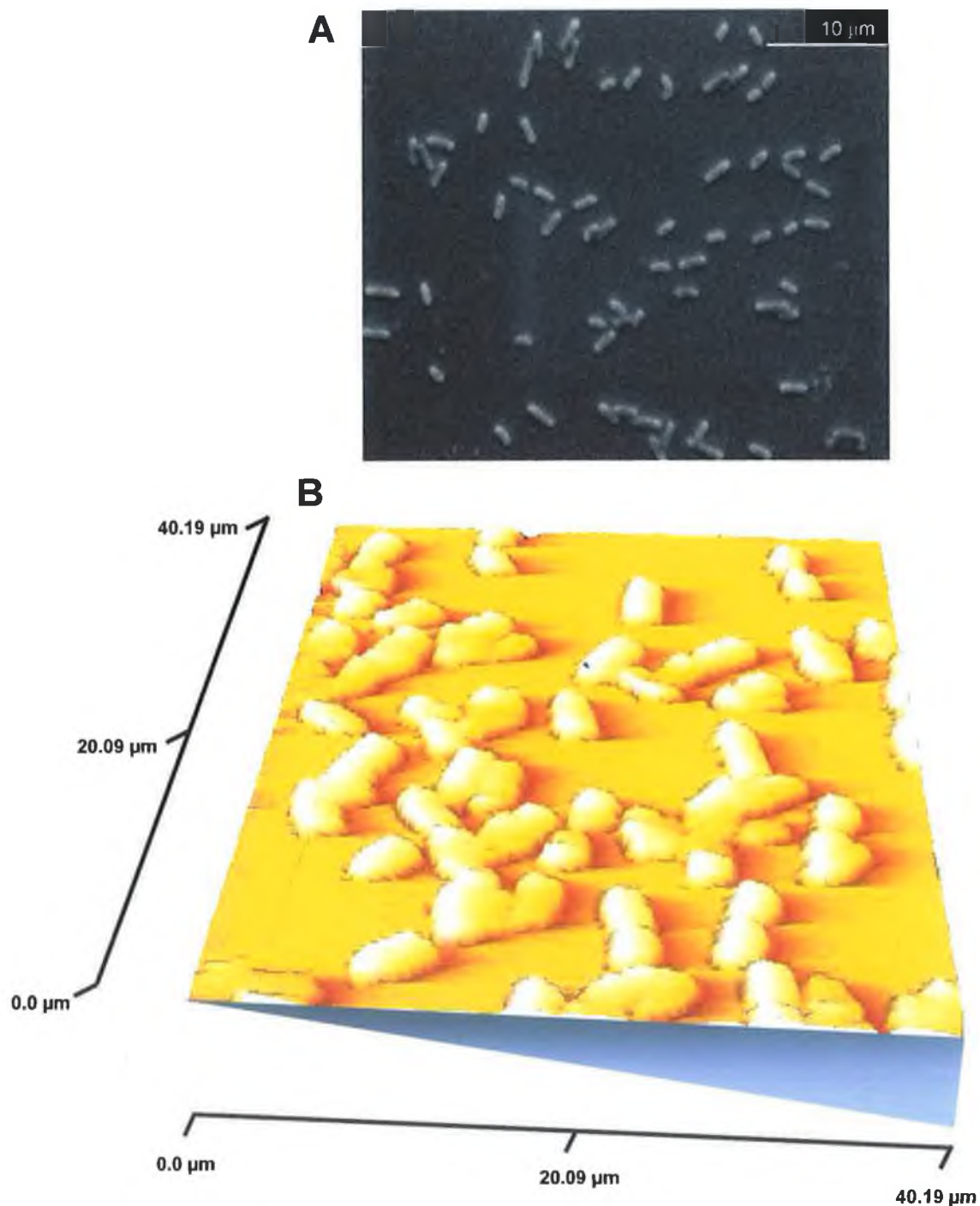


**Figure 5.7:** SEM (A) and AFM (B) analysis of surface topography of the sensor chip surface with mAb2B3-captured *L. monocytogenes* cells. The injected cell concentration corresponded to  $\sim 4.74 \times 10^8$  cells/ml.





#### **5.2.1.6 Immobilisation of mAb2B3 onto C1 sensor chip**

It has been suggested that the use of planar surfaces can eliminate certain problems relating to diffusion of ligates through a dextran matrix (Schuck, 1996), particularly if measuring whole cell binding (Leatherbarrow and Edwards, 1999). The main reasoning behind this theory is that the distance between the effective evanescent sensing region and bound cells is reduced, since there is no hydrogel barrier, thus, favouring an improved response-to-cell concentration ratio. This strategy was investigated for the mAb2B3-*L. monocytogenes* capture interaction, by coupling mAb2B3 to a C1 sensor chip surface. This possesses a planar, carboxylated surface that supports the same immobilisation chemistry as CM dextran surfaces, but lacks a dextran matrix. The mAb2B3 antibody was coupled to the C1 surface using ostensibly the same conditions as for the CM5 surface (Section 5.2.1.3). However, the coupling concentration was increased to 200 µg/ml of antibody and an extended activation time was incorporated to maximise ligand immobilisation potential and compensate for the expected reduction in net immobilisation due to absence of hydrogel matrix. Even with these precautionary amendments to the immobilisation procedure, the mAb2B3 level achieved was only 1709 RU (Figure 5.8).

#### **5.2.1.7 Assessment of specific cell-binding potential of mAb2B3-C1 sensor surface**

Fresh, LEB-cultured *L. monocytogenes* cells were washed, resuspended in HBS buffer at approximately  $1.07 \times 10^9$  cells/ml and simultaneously passed over both the mAb2B3-C1 and control-C1 surfaces at a flow rate of 1 µl/min. In this case the control consisted of a blank C1 surface that had been activated and capped in the absence of ligand. It was clear from the resulting binding profile that, even after 10 minutes exposure to the *L. monocytogenes* sample, that there was no significant binding to either the mAb2B3-C1 or control-C1 surfaces and consequently, no net binding response (Figure 5.9).



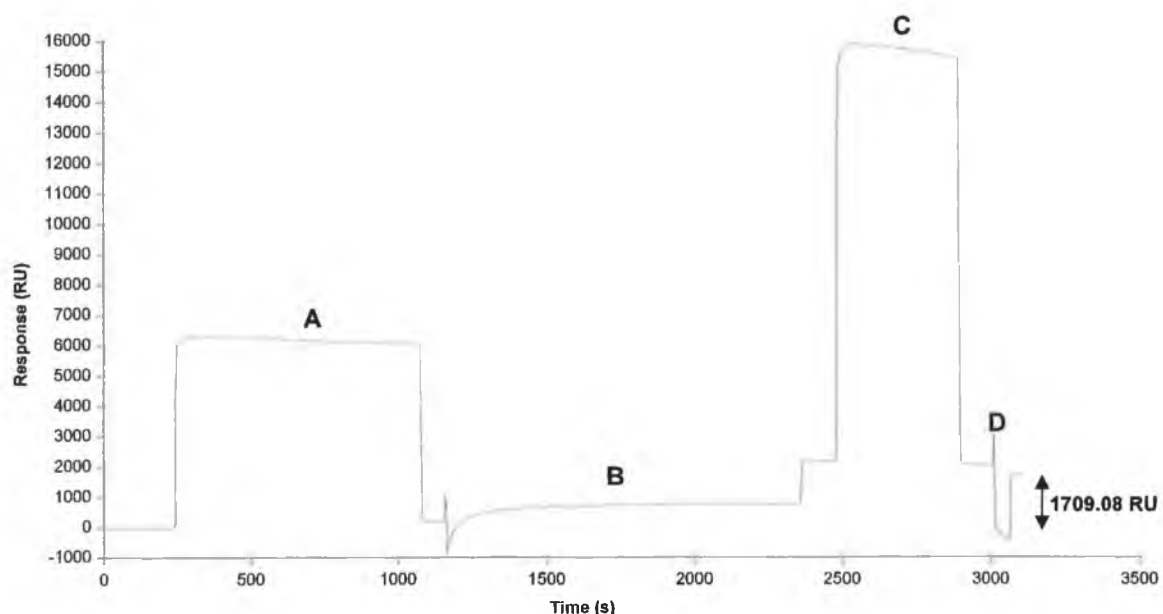


**Figure 5.8:** Immobilisation of mAb2B3, anti-InlA monoclonal antibody onto the C1 sensor chip surface. (A) EDC/NHS activation, (B) binding of mAb2B3, (C) capping of unreacted groups and (D), regeneration pulse of 5 mM HCl. A final level of 1709.08 RUs covalently attached mAb2B3 was achieved.

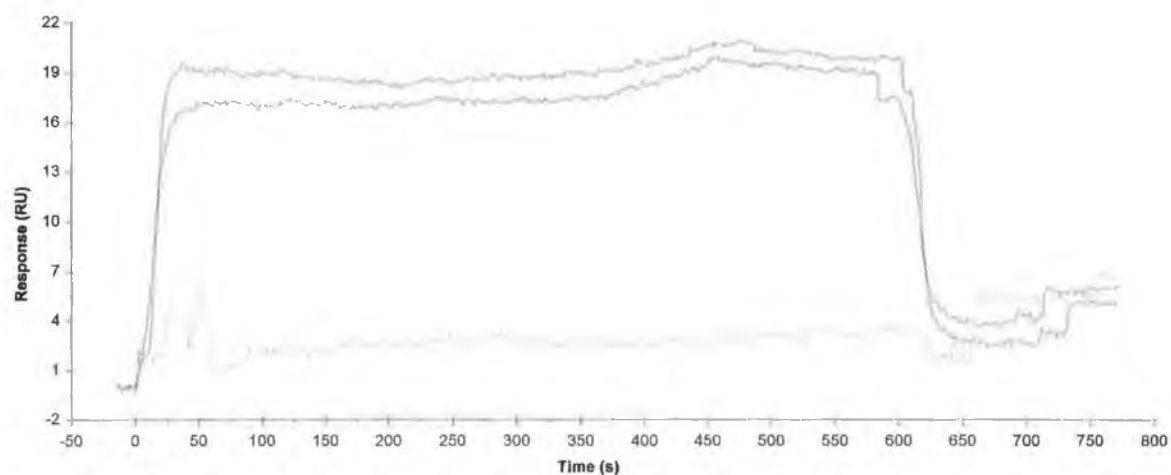


**Figure 5.9:** Real-time comparison of the mAb2B3-C1 (red) and control-C1 (blue) surface binding-responses to *L. monocytogenes*. Approximately  $1.07 \times 10^9$  cells/ml *L. monocytogenes* cells in HBS were simultaneously passed over both surfaces at a flow rate of  $1 \mu\text{l}/\text{min}$ . The negligible reference-subtracted response (green) indicated a clear failure of the planar biointerfacial assembly to capture *L. monocytogenes* cells under the operating conditions employed.



#### 5.2.1.8 Critical explanation of factors contributing to *L. monocytogenes* cell capture

It was initially, somewhat surprising to discover that the planar surface failed to perform better, or even on a par with the dextranated surface.

The feasibility and reliability of direct, covalent attachment of antibodies to carboxymethylated dextran surfaces has been widely validated (Buckle *et al.*, 1993; Johnsson *et al.*, 1995; Brynda *et al.*, 1999; Howell *et al.*, 1999). The benefit of using such hydrogel surfaces, with regard to the majority of molecular analytes, is the enhanced ligand immobilisation capacity and consequently, improved response-to-analyte concentration ratio.

Although models explaining the principal aspects of multivalent binding to immobilised ligands (Müller *et al.*, 1998c) are currently well established, similarly convincing models of whole cell binding to fixed ligands are not widely available and no general consensus prevails. The difficulty in explaining such binding is undoubtedly due to the extreme 'bulk' and non-ideal viscoelastic properties, exhibited by cellular structures. The frequently reported disproportionately low signals for whole cells (with an approximate dry cell weight of  $10^{-13}$ - $10^{-12}$  g), obtained relative to those from proteins (Perkins and Squirrel, 2000), is most likely due to the a major portion of the cell being outside the range of the evanescent field. This shortcoming is compounded by the fact that the refractive index of a typical bacterial cell ranges from 1.37 to 1.42 for the cytoplasmic and cell wall components, respectively, in comparison to that of protein solutions, which normally exhibit refractive indices approaching 1.51 (Watts and Lowe, 1994).

One of the most intuitive and rigorous insights into SPR-based whole cell-ligand interactions, was provided by Quinn *et al.*, (2000). The analysis was conducted on a CM5 chip similar to that used in the experiments described herein. It cannot be entirely extrapolated to describe the immobilised mAb2B3-*L. monocytogenes* cell interaction however, since, mammalian whole red blood cells were employed, the particular viscoelastic characteristics of which, caused them to adopt a flat-concave morphology. This caused them to essentially 'collapse' toward the high-amplitude region of the evanescent sensing region and meant that the capture antibody could be optimally orientated on a covalently pre-immobilised protein A hydrogel, without fear of subsequently captured cells being held predominantly outside the sensing region. Nonetheless, the model is consistent with accepted opinion, particularly in relation to mass-transfer limited (MTL) components (Schuck, 1996; Schuck and Minton, 1996), particulate fluid dynamics (Stamatakis and Tien, 1993; Hwang *et al.*, 1996), including the effect of wall shear stress (Zydney and Coulton, 1984), and many of the key thermodynamic interpretations and hypotheses were expected to relate directly to the immobilised mAb2B3-*L.*



*monocytogenes* binding interaction, under investigation. Although MTL contributions have to be eliminated for accurate kinetic interpretation (generally by increasing the flow rate) they can be tolerated for concentration measurements and generate quantifiable response at, or approaching the equilibrium level (Req), when the interaction time is sufficiently lengthened. Hence, the fifteen minute interaction time employed in the immobilised mAb2B3-*L. monocytogenes* binding cycle and reduced flow rate of 1 µl/min. Surprisingly, Koubová and co-workers (2000) have reported that increasing the flow rate actually improved bacterial cell binding, speculatively attributing the result to the narrowing of the boundary solvent layer (Kurrat *et al.*, 1994) at the sensor surface. However, this would appear to contradict the basic thermodynamic model, in particular, the shear induced force determinant which increases linearly with respect to the fluid velocity and the square of the cell diameter (Quinn, 1999) and is anomalous with all other available citations on biointerfacial cell-ligand interactions. In fact, it could quite conceivably, be a matrix artefact effect, especially since no reference subtraction step was included.

$$F_s = 1.276\pi (\rho_f) \cdot (d_p^2) \cdot (f) \cdot (U_f) \quad \text{(Equation 5.2, Quinn, 1999)}$$

Where;  $F_s$  = Shear-induced force.  
 $\rho_f$  = Fluid (buffer) density.  
 $d_p$  = Particle (cell) diameter.  
 $f$  = Friction factor.  
and  $U_f$  = Fluid velocity.

The cell surface location of the InlA protein, recognised by mAb2B3, has earlier been defined (Sections 3.2.6.4, 4.2.4 and 4.2.5) and it is felt that the distribution and accessibility of this antigen on the *L. monocytogenes* cell surface is of paramount importance in mediating whole cell binding at the sensor biointerface. Clear advantages of targeting somatic (O) antigens and the influence of the associated topographical microenvironment, with specific reference to biosensor-based cell detection, have also been cited by Olsen *et al.* (2003). This importance derives from the fact that a minimum, threshold avidity is required to enable cell binding and retention at the biointerface. This minimum threshold is in turn, dictated by the accumulative resistive forces that comprise shear, ionic, gravitational and lateral-elevation forces.





The controlled orientation of antibodies on sensor surfaces using protein A/G and Fc-specific antibodies has previously been reviewed (Lu *et al.*, 1996) and experimentally investigated (Quinn *et al.*, 1999) and has found recent generic application in a hybridoma screening format (Canziani *et al.*, 2004). Given the dimensions of the bacterial cell in relation to the surface-localised evanescent field, it was felt that such an orientation, constructed upon the ~100 nm hydrogel, would potentially render the cell attachment to the distal Fab domain of the immobilised antibody, beyond the effective evanescent sensing range. This postulation is supported by the findings of Lathrop and co-workers, (2003), who investigated a similar sensing platform using an anti-*Listeria* antibody in conjunction with a resonant mirror biosensor. The Biacore-based detection of *E. coli* O157:H7 reported by Frattamico and co-workers, (1998) yielded a similar observation, with a directly immobilised antibody surface exhibiting vastly superior performance than the protein A-anchored antibody surface. A further concern when using such a configuration was the associated requirement to constantly replenish the detector antibody between analyses leading to high consumption of valuable purified monoclonal antibody.

It might be suggested that oriented immobilisation of antibody on the planar C1 chip surface would ensure that subsequently bound cells were not rendered prohibitively distant from sensing region. However, while such a homogenous monolayer arrangement would undoubtedly be capable of high avidity binding to multiple sites on a planar, macromolecular structure, it is less certain that the non-planar nature of a typical bacterial cell would achieve the avidity threshold required for binding. In contrast, specific dynamic events within the hydrogel that contravene its restrictive classification as a classical 'brush-border' may aid cell binding. These include a significant degree of elasticity within the polymeric dextran (Rief *et al.*, 1997; Piehler *et al.*, 1999) that allows polymer-tethered antibodies to extend beyond the average, ambient equilibrium configuration (dependent on running buffer) and bind to complementary, surface-exposed antigen. Bonds formed by these 'rare extended conformations' are further aided by the increased intrinsic translational and rotational mobility exhibited by the tethered ligand when compared to the polymer itself (Jeppesen *et al.*, 2001). Thus, notwithstanding the random nature of the amine-coupling method employed and the associated risk to binding site integrity (Vaughan *et al.*, 2001; Vaughan *et al.*, 2003), a significant population of rare extended conformations bearing active antigen-binding domains can mediate attainment of the avidity threshold required for cell binding (Figure 5.10).

In summary, the successful binding of *L. monocytogenes* cells to the immobilised mAb2B3 antibody was attributed to the intrinsic antibody affinity and specificity towards somatically-



expressed InlA protein, selection of suitable thermodynamic operating conditions (i.e. low flow rate and extended contact time), and favourable contributions from the dextran hydrogel.

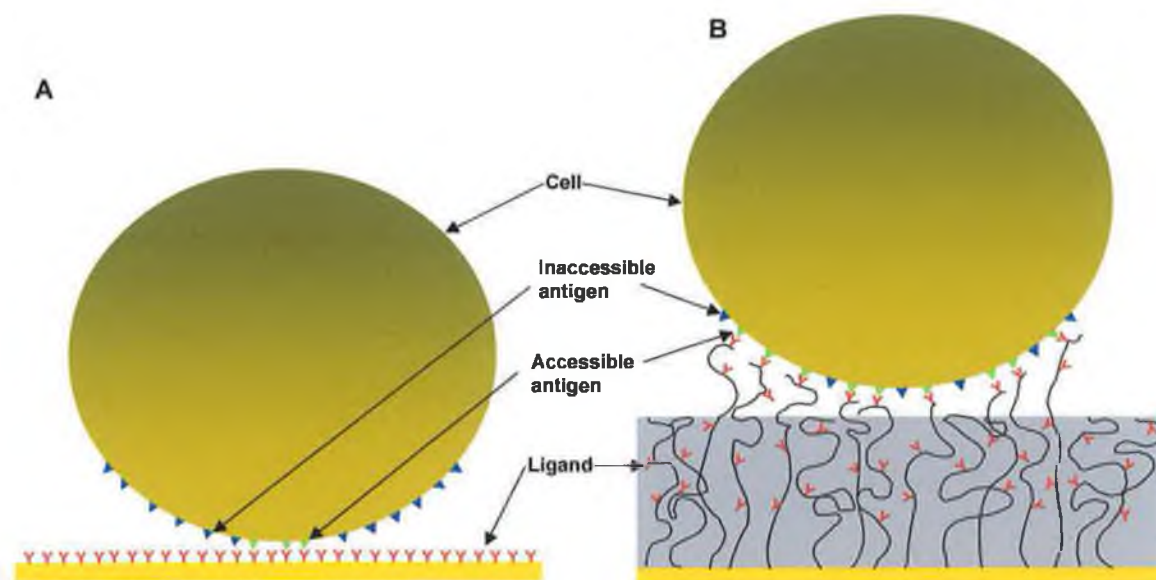


**Figure 5.10:** Schematic representation of whole cell binding to planar (A) and hydrogel-immobilised (B) ligand (antibody). Surface displayed ligand-complementary antigens are indicated as green (if accessible) and blue (if inaccessible). The binding of the macromolecular (cell) structure to the homogenously oriented, planar ligand is inherently less stable. This is due to the fact that the maximum number of accessible antigens is constrained by the non-planar complementarity of the cell morphology and thus, the threshold avidity is not achieved. Conversely, although the polymer-tethered ligand is randomly oriented within the hydrogel matrix, which itself adopts an apparent composite 'brush-border', dictated by the buffer ambience (grey), a significant number of 'rare extended conformations' are accommodated. These extend beyond the composite hydrogel matrix and thus, can probe a wider cell surface area and form multiple bonds with compatible surface antigen. The antigen binding is further perpetuated by the increased rotational and translational freedom exhibited by the polymer-tethered ligand over the rigidly immobilised planar arrangement. These key facets allow the minimum threshold avidity determinant to be more reliably achieved by the hydrogel-immobilised sensor chip surface.



#### **5.2.1.9 Development of a model SPR-based, cell-binding assay for direct detection of *L. monocytogenes***

*L. monocytogenes* serotype 1/2a cells, that had been actively growing at 37 °C in LEB broth, were harvested and washed twice in cold, sterile-filtered phosphate buffered saline (PBS) buffer before being adjusted to the desired cell concentration in fresh HBS buffer. The aims of the primary analysis were two-fold. Firstly, to establish whether real-time monitoring of the mAb2B3-*L. monocytogenes* cells was possible using the configuration employed and secondly, to estimate an approximate lower limit of quantitation (LLOQ). A flow rate of 1 µl/min was employed for all sample analyses in order to maximise the mAb2B3-*L. monocytogenes* interaction exposure and a nominal interaction time of 15 min was chosen, so as to allow the cell-antibody binding interaction to approach equilibrium.

Following a series of exploratory experiments, the concentrations of *L. monocytogenes* cells selected for testing ranged from  $1.07 \times 10^9$  to  $1.23 \times 10^7$  cells/ml (Figure 5.11). The upper cut-off concentration was defined to reduce the risk of the instruments intricate microfluidic valve assembly becoming clogged with cellular material. As a further precaution, each sample was mixed manually by pipette aspiration immediately prior to injection and a portion of each sample examined using an optical microscope to ensure there was no clumping of cells.

It was clear that the relationship between  $R_{eq}$  and cell concentration did not exhibit a direct, linear proportionality, this was particularly evident at the higher cell concentrations where  $R_{eq}$  values seemed disproportionately exaggerated. This is remarked upon in more detail in Section 5.2.1.13. Despite postulations to the contrary by Watts and Lowe (1994), it may be that the presence of previously bound *L. monocytogenes* cells at the surface actually result in cooperative binding of free cells, by reducing the frequency of free cell collisions with bound cells and thereby optimising spatial interaction with localised unoccupied ligand regions (Stamatakis and Tien, 1993; Quinn *et al.*, 2000). Such a distribution would be further stabilised by the pervading intra-cellular zeta-potential.



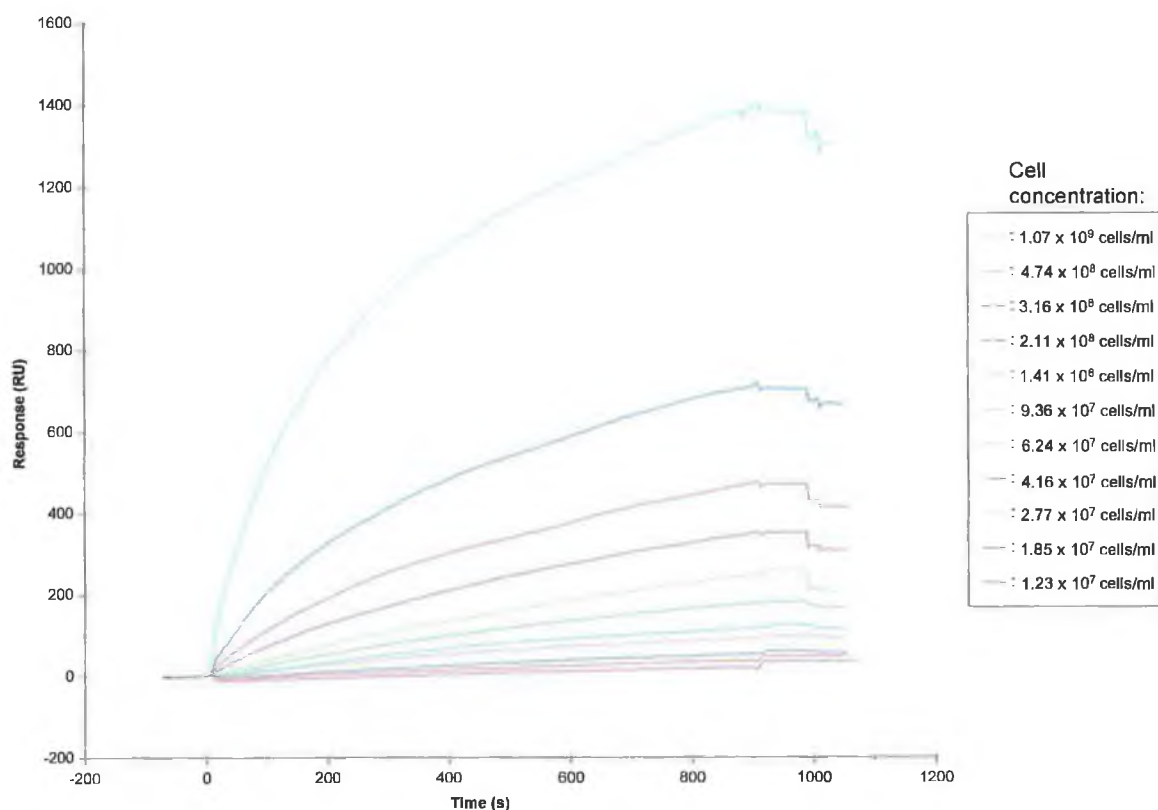


**Figure 5.11:** Overlaid binding profile for increasing concentrations of *L. monocytogenes* serotype 1/2a cells. The cells were passed over the mAb2B3-CM5 chip surface at a flow rate of 1  $\mu$ l/min for 15 minutes.

#### 5.2.1.10 Assessment of signal amplification using a sandwich-assay approach

In an effort to elicit signal enhancement following direct binding of bacteria to the immobilised capture antibody several authors have suggested merit in adopting a sandwich approach whereby a secondary, genus-specific polyclonal antibody is applied (Fratamico *et al.*, 1998; Bokken *et al.*, 2003). Typically, polyclonal antibody concentrations of at least 50  $\mu$ g/ml were required to achieve significant enhancement. With such a large consumption of polyclonal reagent the cost factor and batch-to-batch heterogeneity may hinder the routine testing potential. The effect of sandwich-enhancement using two anti-*Listeria* polyclonal antibodies was investigated. However, as Figure 5.12 clearly shows, no enhancement was achieved. This was not an entirely surprising result given the similar findings of Lathrop and co-workers, (2003).





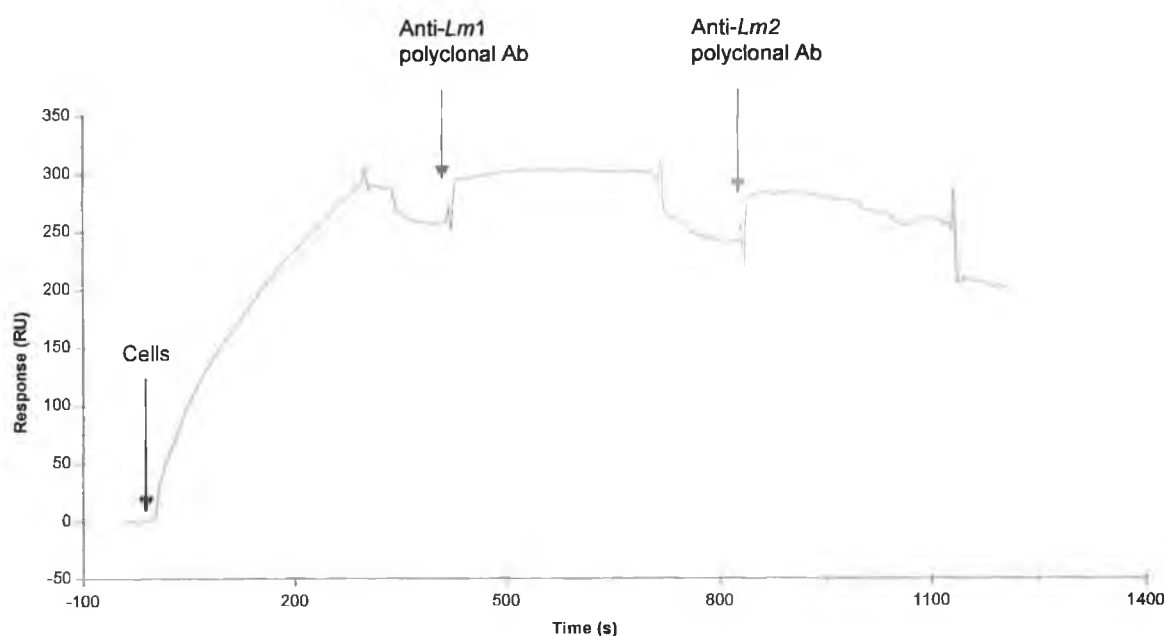


**Figure 5.12:** Sandwich approach to signal enhancement using polyclonal antibodies. Approximately 270 RUs of fresh *L. monocytogenes* 1/2a cells were captured on the mAb2B3 at a flow rate of 1  $\mu\text{l}/\text{min}$ . A 50  $\mu\text{l}$  aliquot of each of the anti-*L. monocytogenes* (Anti-Lm1 and Anti-Lm2) polyclonal antibodies were sequentially passed over the captured cells at 100  $\mu\text{g}/\text{ml}$  and 10  $\mu\text{l}/\text{min}$ .

Although these results clearly indicated the ineffectiveness of the sandwich-based approach to the direct enhancement of SPR response signals, it has proved useful as the basis for an alternative evanescent-wave-based biosensor platform, that has been successfully used for the detection of *E. coli* O157:H7 (DeMarco *et al.*, 1999; DeMarco and Lim, 2002). It operated on the principle of ‘reporter molecule fluorescence’. A biotinylated capture antibody was immobilised onto a streptavidin-coated fibre-optic waveguide. This was then incubated with a cell sample from an enrichment culture and followed by the addition of a secondary, Cy5-labelled ‘sandwich’ antibody. Fluorescent excitation of the Cy5-labelled antibody was induced by the propagating evanescent wave. When used to detect *L. monocytogenes*, an appropriate detection limit of approximately  $4 \times 10^8$  cells/ml was reported, following a twenty hour sample enrichment (Tims *et al.*, 2001). It has been a major tenet throughout this thesis that enrichment is an essential component of any immuno-based detection system for *L. monocytogenes*. Although the sensitivity and specificity of the ‘reporter-based-fluorescence’ format could undoubtedly be improved upon by incorporating more suitable antibodies it has



several weaknesses when compared to the direct SPR-based system described herein. The key limitations include a requirement for labelling (of both capture and sandwich antibodies), larger sample volumes, multiple washing steps and the need to prepare freshly derivatised waveguides between analyses.

#### ***5.2.1.11 Assessment of non-specific binding of non-*L. monocytogenes* cells to mAb2B3-CM5 sensor chip surface***

The monoclonal antibody mAb2B3 has been shown to specifically bind to the InlA protein (Sections 3.2.6.6 and 4.2.5), which itself, is exclusively present on the surface of pathogenic *L. monocytogenes* cells (Lebrun *et al.*, 1996) and no significant inter-species cross-reactivity in ELISA has been demonstrated (Section 3.2.6.5). Nonetheless, given the extensive heterogeneity between ELISA and SPR-based analysis platforms, the system was challenged with a panel of related *Listeria* spp. and representative non-*Listeria* spp., of both the gram-negative and gram-positive varieties. Given that environmental and food samples contaminated with *L. monocytogenes* would be predicted to be colonised with related *Listeria* spp. or at the very least, associated normal microflora, the ability to differentiate *L. monocytogenes* from these non-pathogenic species is critical.

When challenged individually with the selected panel of potential cross-reacting species at a similar concentration to that of the highest *L. monocytogenes* concentration tested ( $\sim 1.1 \times 10^9$  cells/ml), binding response levels were negligible in all cases (Figure 5.13). In fact none of the test strains generated a response above 8 RUs, which can be considered background.



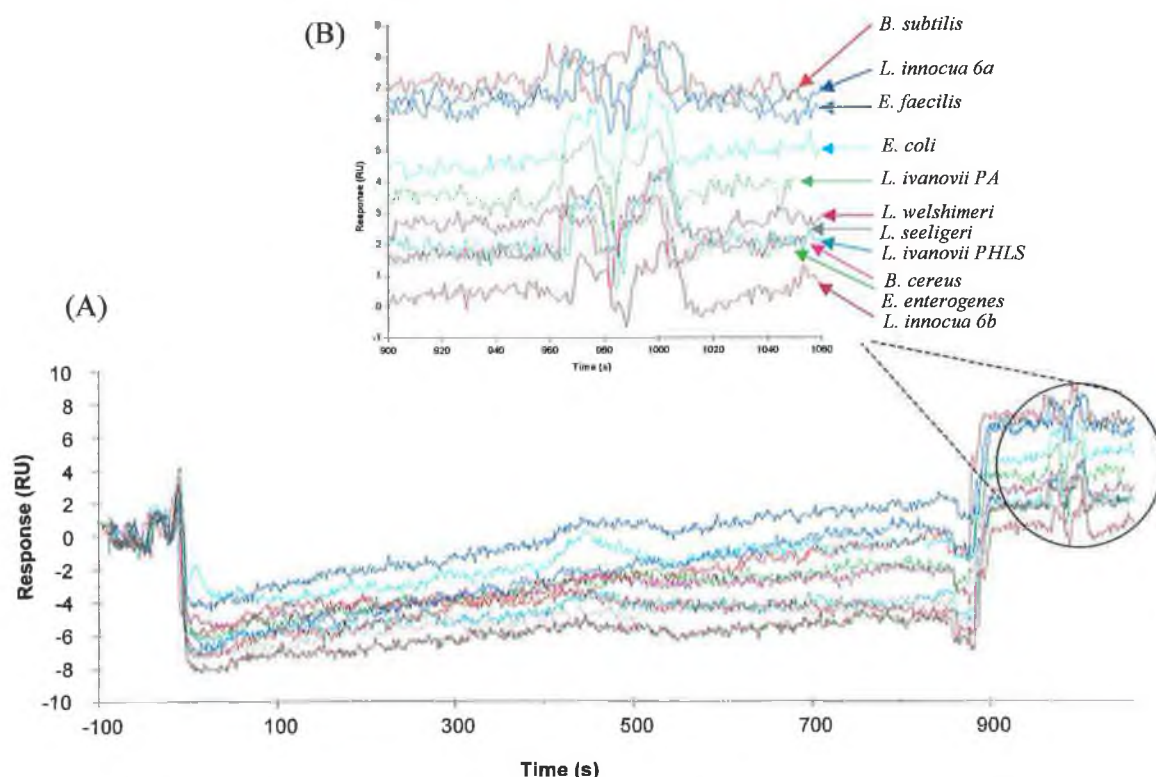


**Figure 5.13:** Binding response of a representative sample of non-*L. monocytogenes* cells. Cell concentrations were adjusted to  $1 \times 10^9$  cells/ml in PBS buffer prior to analysis. The overlaid, complete binding profile for each test strain is demonstrated (A), with the region corresponding to the final response values magnified and labelled (B). None of the strains tested generated a response value above 8 RUs.

#### 5.2.1.12 Assessment of non-specific binding of heat-inactivated *L. monocytogenes* cells to mAb2B3-CM5 sensor chip surface

A sample of *L. monocytogenes* cells was prepared in PBS at a concentration of  $3.16 \times 10^8$  cells/ml and passed over the mAb2B3-CM5 surface at  $1 \mu\text{l}/\text{min}$  for 15 minutes, replicating a typical assay cycle. Samples from the same cell suspension, after having been held at  $80^\circ\text{C}$  for 10 and 15 minutes, respectively, were also passed over the same test surface. Cells that had been heat-treated for 10 minutes demonstrated  $>80\%$  reduction in response generation, while 15 minute heat treatment resulted in total abrogation of a response level distinguishable above background (Figure 5.14). These results correspond with the ELISA profile for mAb2B3 outlined earlier (Section 3.2.6.4) and re-affirm that the *L. monocytogenes*-binding potential of mAb2B3 is dependent on favourable surface topography, facilitating InlA accessibility.



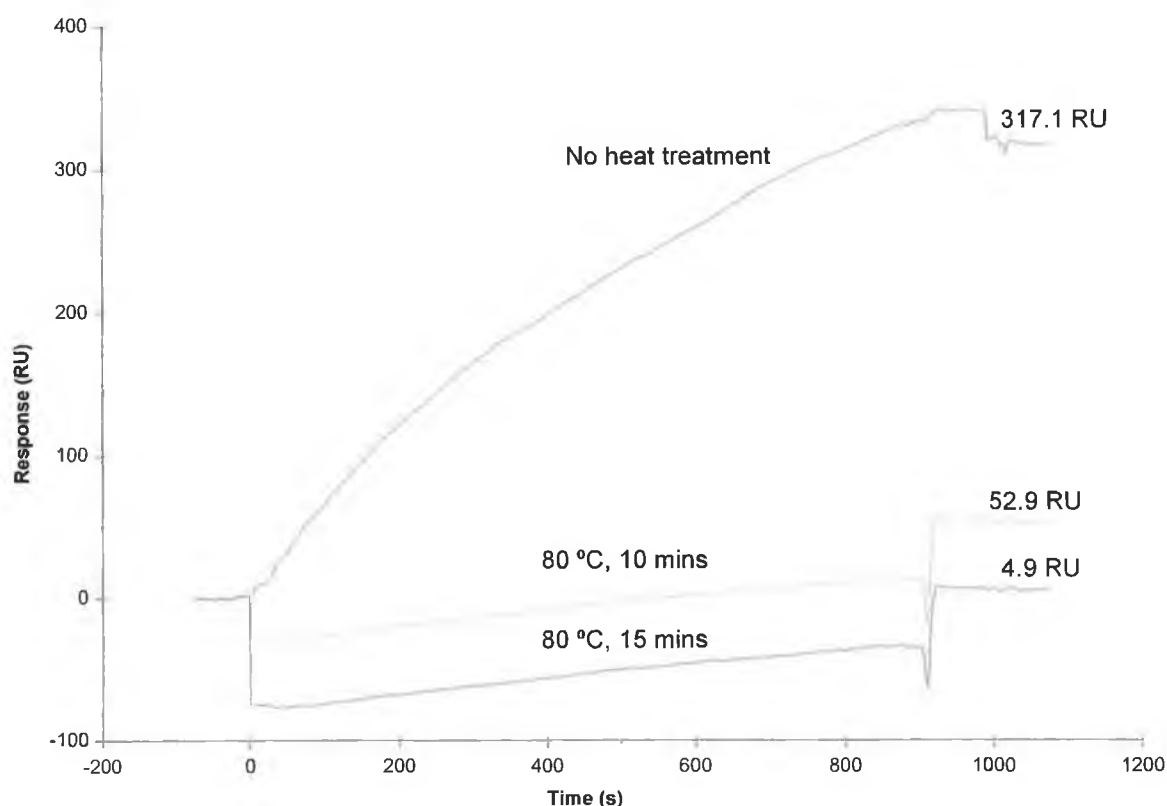


**Figure 5.14:** Binding response profile of *L. monocytogenes* cells following heat inactivation. Following treatment at 80 °C for 10 and 15 minutes, the response decreased from 317.1 RU (red) to 52.9 (green) and 4.9 (blue), respectively. This indicated a clear, inverse proportional relationship between degree of heat inactivation and absolute binding response levels.

It is noteworthy that, whereas the ELISA results demonstrated significant and substantial reduction in mAb2B3 binding-capacity following heat treatment of the *L. monocytogenes* cells at 80 °C for 10 minutes, the biosensor response was totally abrogated following just 15 minutes heat-treatment. This reflects a key difference in the ELISA and biosensor assay formats. In ELISA, the antibodies are free to individually interact with any available and accessible, InlA proteins. The resulting colourmetric response is the net of multiple independent mAb2B3-InlA interactions on the *L. monocytogenes* cell. Using the Biacore, direct cell-binding assay, antibodies are not free to independently ‘seek-out’ and individually bind to any available InlA proteins. They are restricted to such an extent that a binding event is only reported if the proportion of accessible, surface-displayed InlA proteins (which itself is directly proportional to the clinical significance of the strain (Jacquet *et al.*, 2004) is sufficient to generate the minimum cumulative threshold-avidity (Section 5.1) for whole-cell capture. This is an inherent advantage of the biosensor-based direct cell-binding strategy.





#### 5.2.1.13 Construction of a calibration curve for estimation of *L. monocytogenes* cell concentration

A key objective of this Chapter was to demonstrate that specific and direct binding of *L. monocytogenes* cells to an immobilised ligand, in this case mAb2B3 antibody, could be monitored using SPR. In order to further substantiate this principle it was deemed necessary to demonstrate a clear dose-response relationship. Thus, a standard calibration curve of response in RUs versus *L. monocytogenes* cell concentration (cells/ml) was constructed across the range of cell concentrations defined in Section 5.2.1.9. It must be acknowledged that although the SPR-binding event was a true 'real-time' event, the actual sample analysis was quite tedious. Due to the requirement for pre-injection sample mixing, coupled with the 15 minute injection time, meant that it took over 1 hour to obtain a single set of triplicate binding data for a given cell concentration. Thus, in order to obtain a set of binding results across the cell concentration range, it took over 14 hours of continual manning of the instrument. However, this probably reflects the fact that the instrument, in particular its sample handling and microfluidics components, were designed principally for smaller analytes.

In Section 5.2.1.9, it had been noted that the initial observations on cell-binding induced/cell concentration-dependent  $R_{eq}$  values indicated that higher cell concentrations were generating disproportionately higher responses. However, when the calibration curve data was fitted with a four-parameter equation, using BIAevaluation™ 3.1 software, it became clear that the relationship between the mean, absolute response and *L. monocytogenes* cell concentration was non-linear (Figure 5.15). The LOQD was estimated to be  $1.85 \times 10^7$  cells/ml (Table 5.1), where, acceptability was defined as predicted values falling within 20 % of the true value (i.e.  $100 \pm 20$  % recovery). However, when plotted with double-logarithmic scaling, a curve-linear relationship was resolved (Figure 5.16). This is consistent with the findings of several independent researchers investigating similar, electrochemical-based biosensor approaches to detection of bacterial cells (O'Sullivan *et al.*, 1999; Park *et al.*, 2000; Kim and Park 2003). Using this typical calibration, cell concentrations could reliably be determined down to 'at least'  $1.23 \times 10^7$  cells/ml (Table 5.1). However, reliable quantification may be an overly restrictive criterion on which to assess the assay performance. Furthermore, quantification may not be an absolute prerequisite since, as already emphasised (Section 1.6), current legislation dictates that a specific 'presence-or-absence' test is required. Following optimised enrichment of suspected contaminated samples, it would be reasonably expected that the enriched test sample would contain cell concentrations in excess of  $1 \times 10^7$  cells/ml. The cell-binding assay, as described, is capable of differentiating *L. monocytogenes* at this concentration from background noise and non-specific responses.



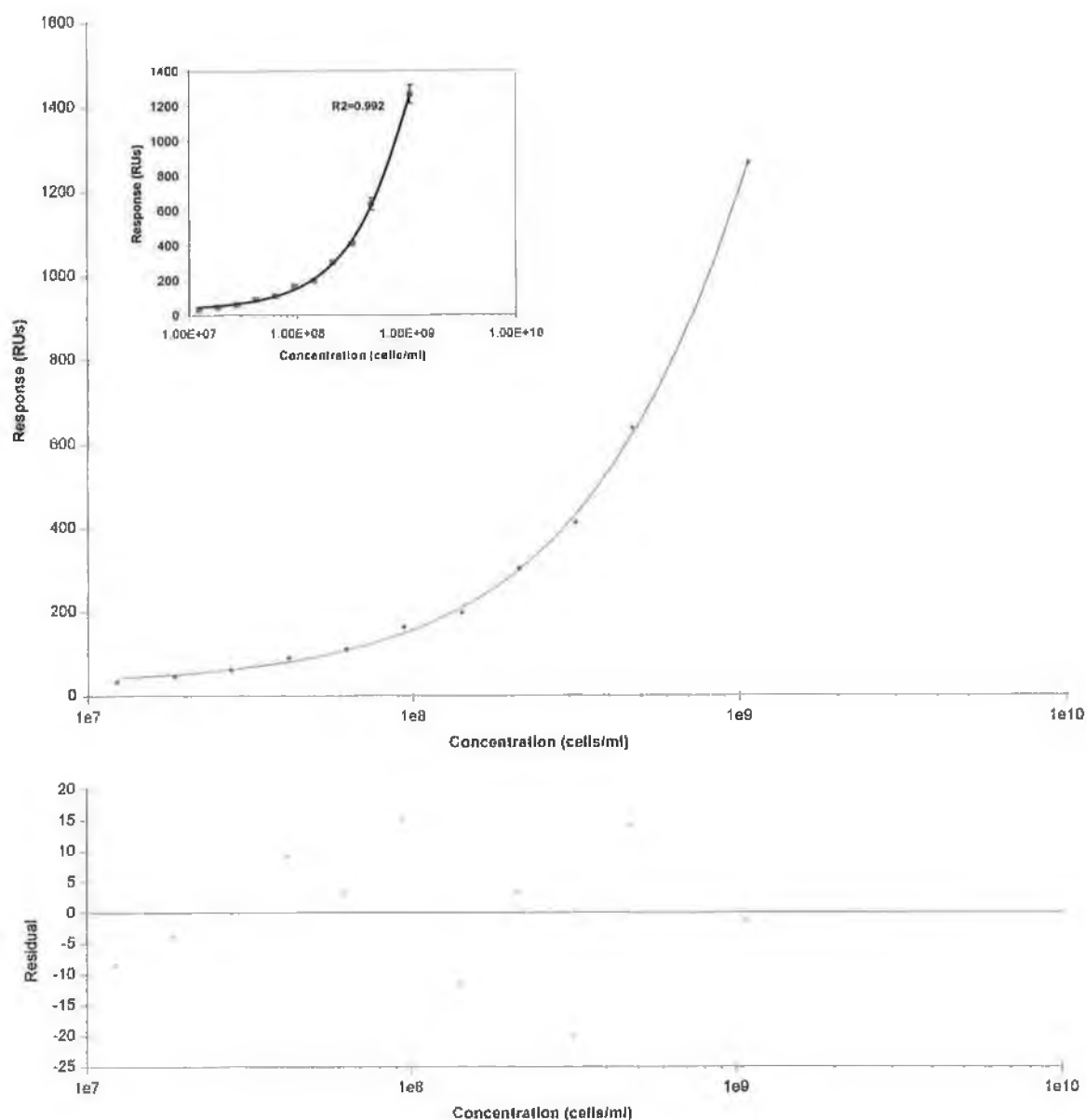


**Figure 5.15:** Semi-logarithmic calibration curve for estimation of cell concentration. The mean binding responses were plotted against the corresponding *L. monocytogenes* cell concentrations. Each data point in the representative curve corresponds to the mean of a single set of triplicate sample analyses. The data was fitted equally well with a four-parameter equation and a 3<sup>rd</sup> order polynomial function (insert), according to  $Y = -2 \times 10^{-25}(X)^3 + 2 \times 10^{-16}(X)^2 + 1 \times 10^6(X) + 30.61$ .



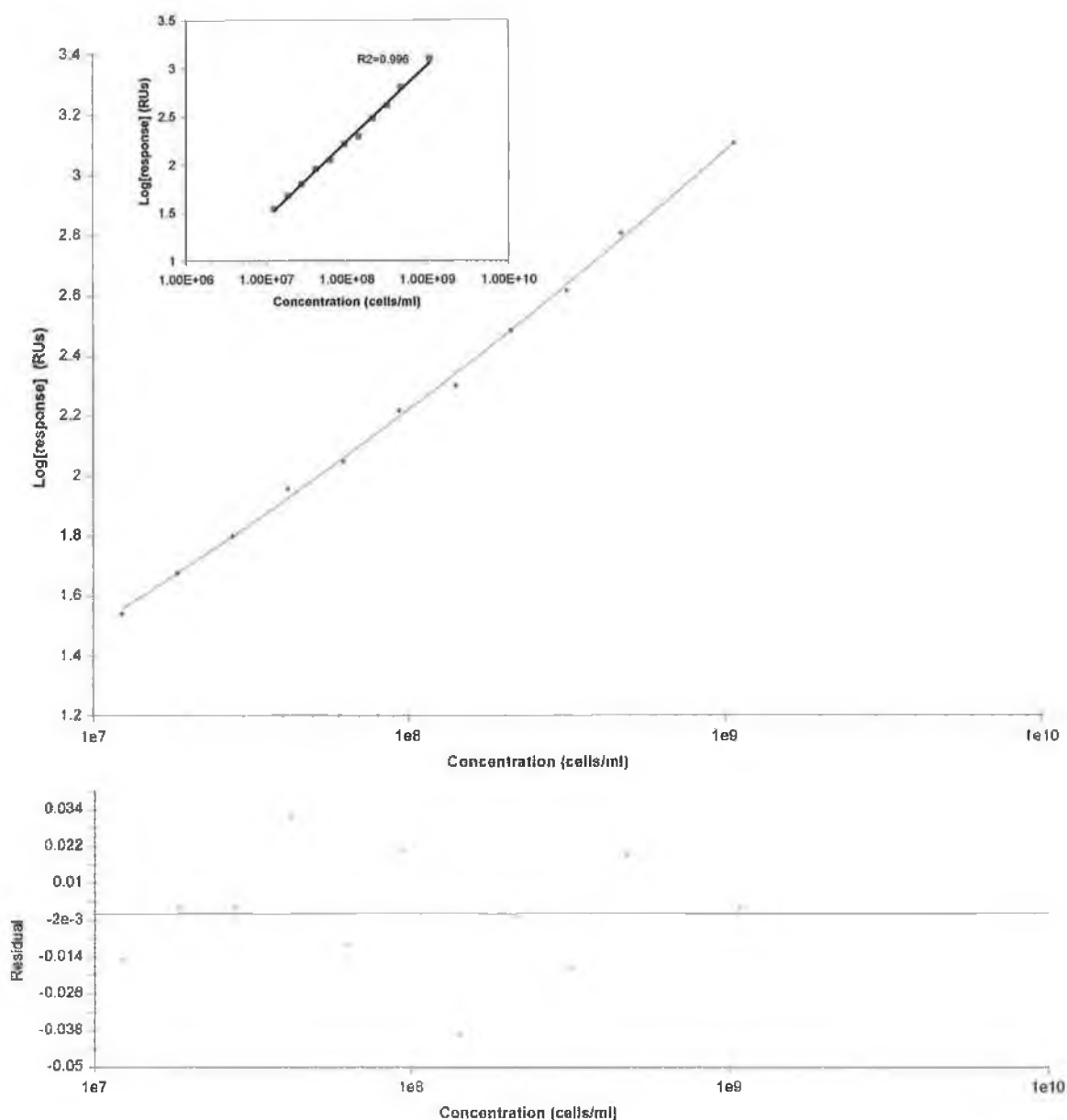


**Figure 5.16:** Double-logarithmic calibration curve for estimation of cell concentration. The log (mean binding responses) were plotted against the corresponding *L. monocytogenes* cell concentrations. Each data point in the representative curve corresponds to the mean of a single set of triplicate sample analyses. The data was fitted equally well with a four-parameter equation and a log-linear function (insert), according to  $Y = 0.345 \ln(X) - 4.117$ . The 'goodness-of fit' is indicated by the narrow residual plot and low  $\chi^2$  value ( $5.71 \times 10^{-4}$ ).



**Table 5.1:** Typical calibration curve data.

Concentration (cells/ml)	Mean response ± SD (RU)	% CV	A		B	
			Back- calculated value	%RE	Back- calculated value	%RE
$1.23 \times 10^7$	34.80 ± 0.954	2.74	$5.680 \times 10^6$	46.19	$1.166 \times 10^7$	94.80
$1.85 \times 10^7$	47.47 ± 2.51	5.30	$1.562 \times 10^7$	84.46	$1.863 \times 10^7$	100.68
$2.77 \times 10^7$	62.87 ± 6.59	10.47	$2.757 \times 10^7$	99.52	$2.790 \times 10^7$	100.73
$4.16 \times 10^7$	90.30 ± 7.58	8.40	$4.870 \times 10^7$	117.05	$4.589 \times 10^7$	110.31
$6.24 \times 10^7$	111.27 ± 3.02	2.71	$6.480 \times 10^7$	103.84	$6.050 \times 10^7$	96.96
$9.36 \times 10^7$	163.55 ± 5.88	3.59	$1.053 \times 10^8$	112.54	$9.943 \times 10^7$	106.23
$1.41 \times 10^8$	198.55 ± 6.04	3.04	$1.320 \times 10^8$	93.65	$1.261 \times 10^8$	89.46
$2.11 \times 10^8$	303.00 ± 6.98	2.30	$2.140 \times 10^8$	101.23	$2.104 \times 10^8$	99.72
$3.16 \times 10^8$	411.13 ± 11.77	2.86	$2.998 \times 10^8$	94.86	$3.013 \times 10^8$	95.37
$4.74 \times 10^8$	636.30 ± 35.36	5.56	$4.861 \times 10^8$	102.56	$4.980 \times 10^8$	105.07
$1.07 \times 10^9$	1265.44 ± 52.30	4.13	$1.069 \times 10^9$	99.88	$1.075 \times 10^9$	100.48

'A' denotes data extrapolated from the calibration curve in Figure 5.15. 'B' denotes data extrapolated from the calibration curve in Figure 5.16. The data represents the mean of a single set of triplicate sample analyses.

In a further test of the robustness of the assay, sensor baseline responses were monitored over a typical 30 sample assay run (Figure 5.17). An average downward baseline drift of  $3.09 \times 10^{-4}$  RU per assay replicate was noted. This was very small and was taken to indicate that the mAb2B3 surface was stable even over an extended range of sample analysis, with incorporated regeneration measures. This would obviously be an important consideration in terms of both commercial and routine analysis applications where the associated costs, necessitated by reagents, time and expertise involved in repeated pre-analysis surface preparation may otherwise be construed as prohibitive.





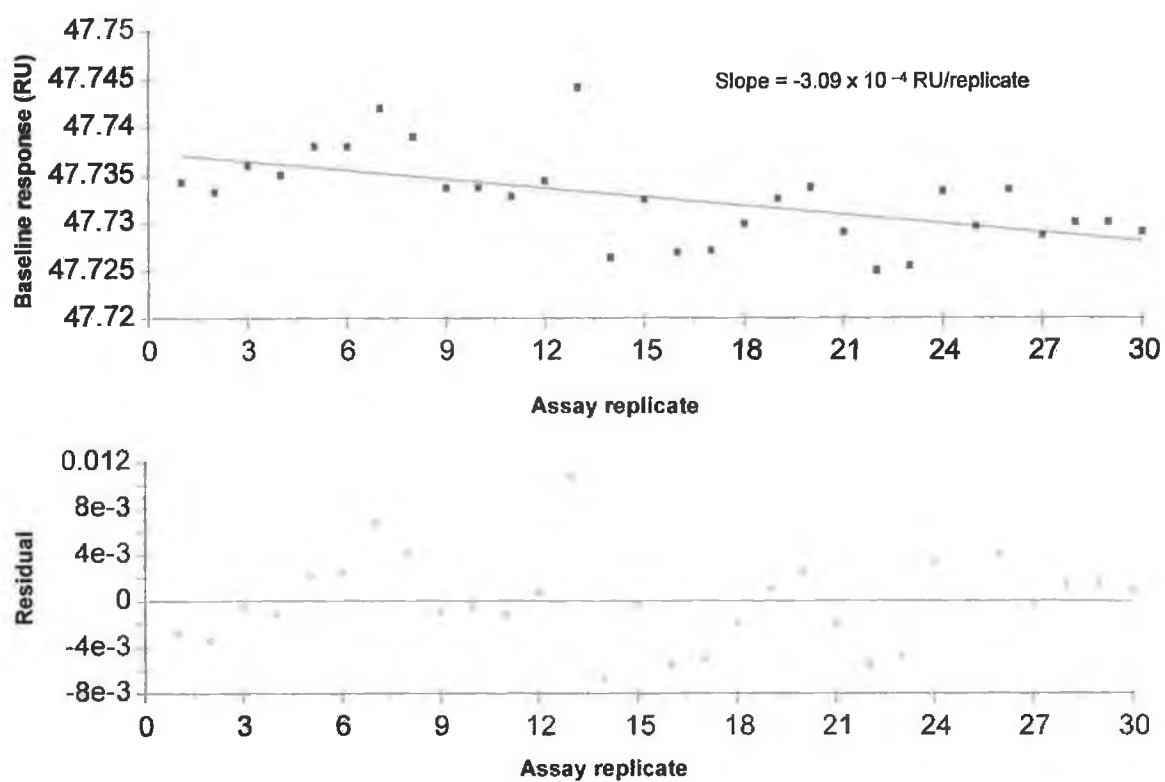


*Figure 5.17: Baseline-stability over a typical 30-sample assay. The small negative slope indicated a stable baseline with an average surface degeneration of  $3.09 \times 10^{-4} \text{ RU/replicate}$ , following surface regeneration with 5 mM NaOH.*



### **5.2.2 Biacore-based characterisation of the mAb2B3-InlA interaction**

Biacore was investigated in terms of its suitability for examining the binding characteristics of the mAb2B3-InlA interaction. It is universally agreed for such measurements to be considered reliable, the following should be observed:

1. Analyte and ligand must be pure and the concentration of analyte at least, must be known.
2. The smaller of the interacting molecules should be immobilised.
3. Analyte should preferentially be monovalent. When constrained to using bivalent analyte, an appropriate correction factor can be introduced, otherwise kinetic data is difficult to interpret and affinity measurements actually refer to avidity.
4. The immobilised ligand should be optimally oriented to ensure minimal steric hindrance of analyte.

#### **5.2.2.1 Characterisation of the mAb2B3-InlA interaction using a covalently-immobilised rInlA-CM5 surface**

##### **5.2.2.1.1 Pre-concentration of rInlA onto the CM5 sensor chip surface**

The purity of the monoclonal antibody 'mAb2B3' had been confirmed by SDS-PAGE Western blotting and SEC-HPLC (Section 3.2.6.3) and its concentration was known, specifically. In addition, it was anticipated that eventually, the rInlA-mAb2B3 interaction could potentially be exploited in an inhibition assay for *L. monocytogenes* cells, with improved sensitivity. Thus, despite the fact that mAb2B3 is, quite obviously, a bivalent molecule it was selected as the analyte and rInlA was chosen as the candidate ligand for immobilisation.

IMAC-purified rInlA protein in PBS was diluted 1/10 in 10 mM sodium acetate buffer across the pH range 3.6-5.5. Although the amine coupling reaction is known to proceed best at pH >4.0, pre-concentration at the lower pH values (3.6-3.8) was also assessed, bearing in mind the low predicted pI (4.9) of the rInlA molecule. Optimal pre-concentration was achieved at pH 4.5 (Figure 5.18).

##### **5.2.2.1.2 Preparation of rInlA-CM5 sensor chip surface**

IMAC-purified rInlA protein in PBS was diluted 1/10 in 10 mM sodium acetate buffer, pH 4.5 and passed over a freshly EDC/NHS-activated CM5 chip surface. Unreacted active groups



were 'capped' with 1 M ethanolamine (pH 8.5) and this was followed with a brief (30 second) pulse of 5 mM NaOH, to remove loosely (non-covalently) bound ligand and stabilise the baseline response. Approximately 8000 RU of rInIA was efficiently immobilised onto the CM5 matrix (Figure 5.19). An equivalent level of a control protein (commercial IgG2a) was immobilised on an adjacent surface located in the flow cell immediately downstream of the rInIA surface, to act as an on-line reference surface. Specific, reference-subtracted binding of mAb2B3 to the rInIA-CM5 sensor chip surface was then confirmed (Figure 5.20).

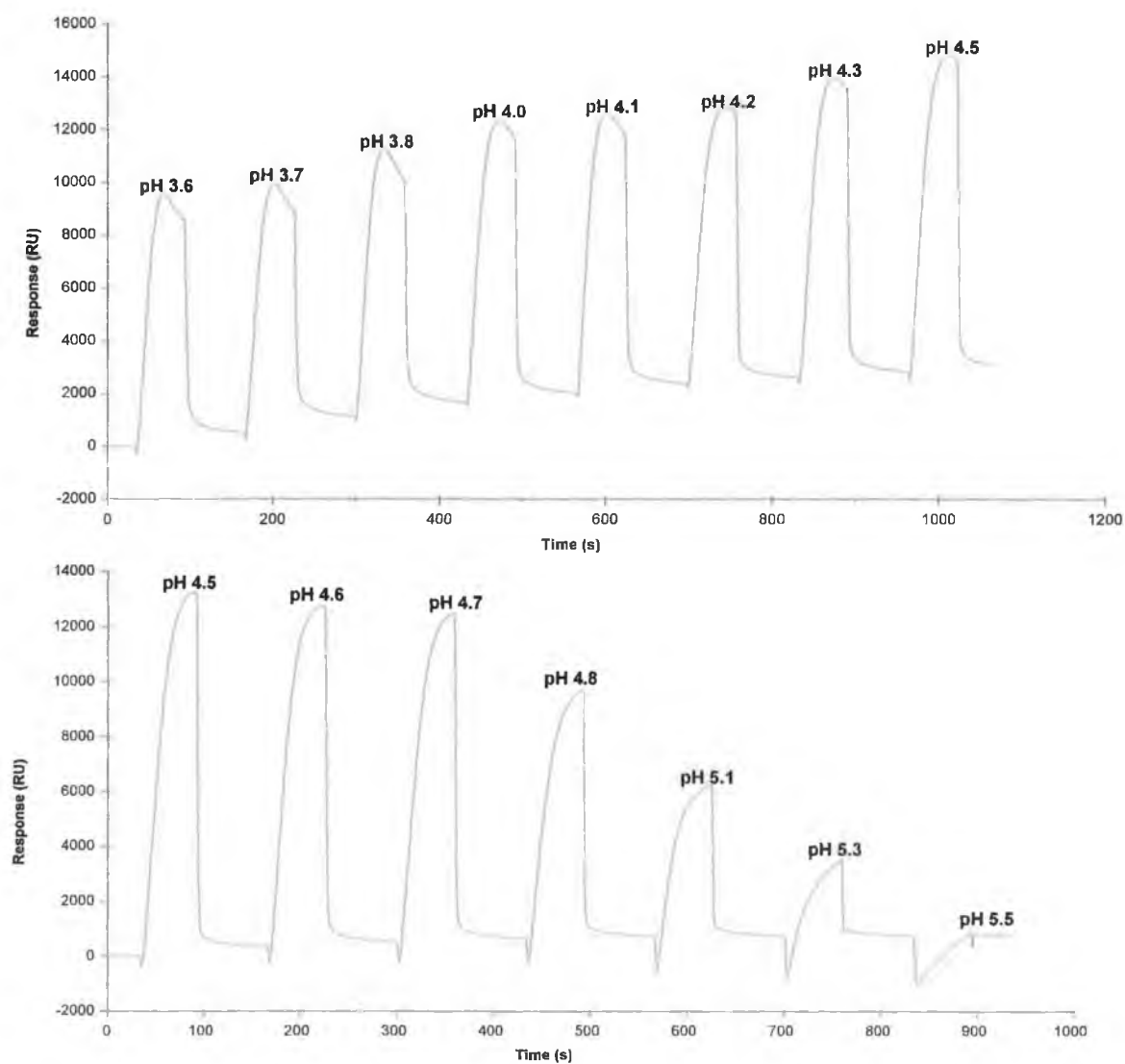


**Figure 5.18:** *rInIA* pre-concentration analyses. Top; pre-concentration of *rInIA* onto the CM5 sensor chip surface across the pH range 3.6-4.5. Bottom; pre-concentration of *rInIA* onto the CM5 sensor chip surface across the pH range 4.5-5.5. Maximum pre-concentration was observed at pH 4.5. Thus, 10 mM sodium acetate buffer at pH 4.5 was chosen as the immobilisation buffer for *rInIA* onto the CM5 surface.



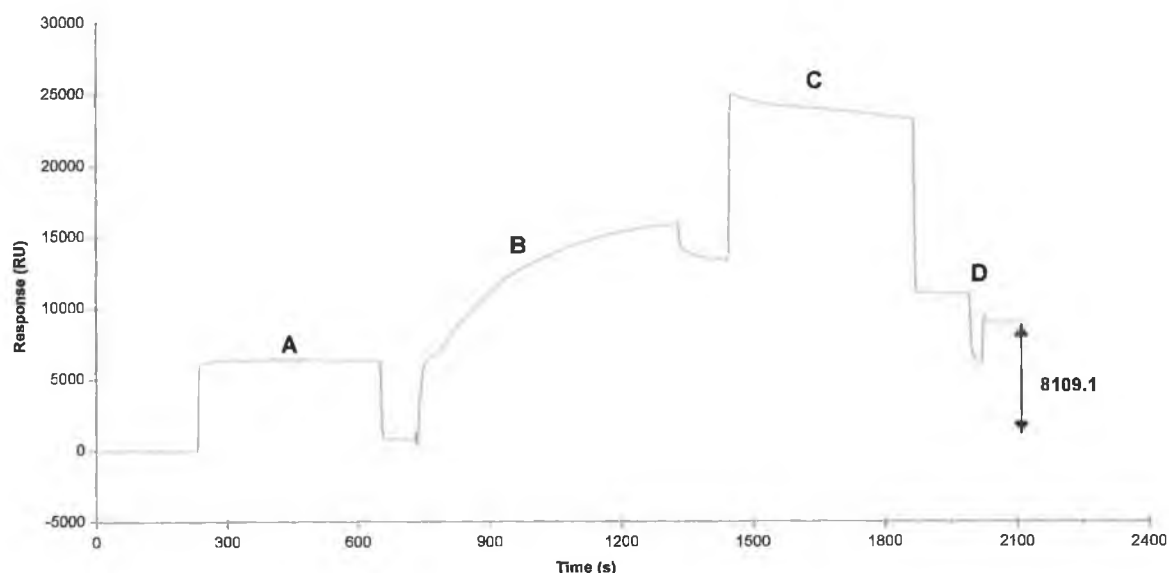


**Figure 5.19:** Immobilisation IMAC-purified rInA onto the CM5 sensor chip surface. (A) EDC/NHS activation, (B) binding of mAb2B3, (C) capping of unreacted groups and (D), regeneration pulse of 5 mM NaOH. A final level of 8109.1 RUs covalently attached rInA was achieved.

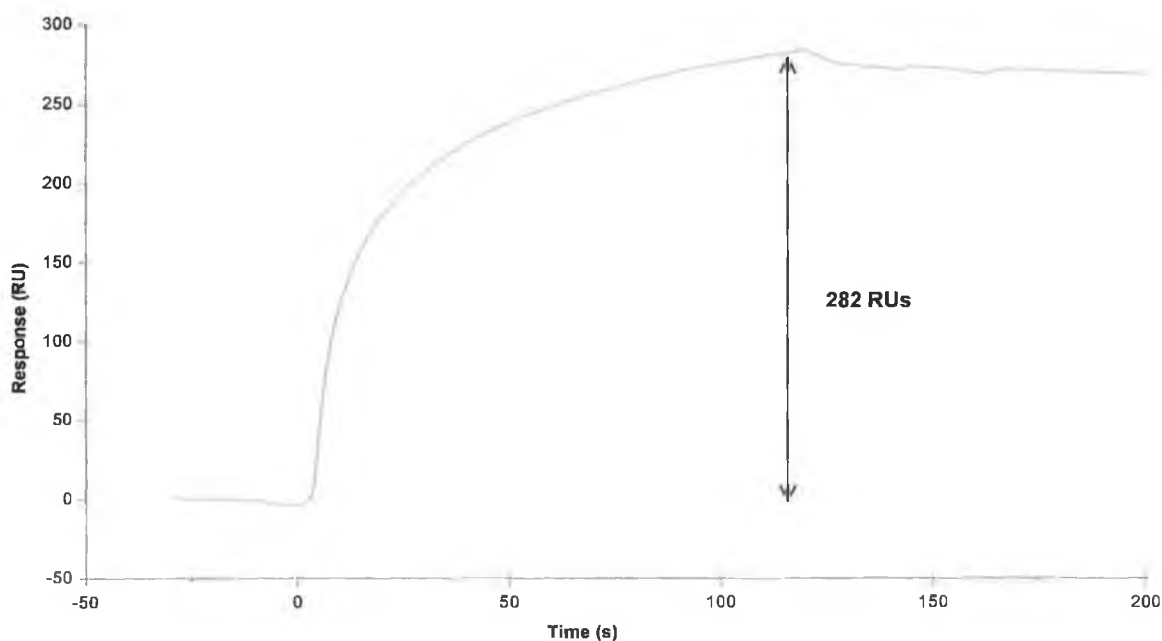


**Figure 5.20:** Surface saturation sensorgram (reference-subtracted) for the rInA-CM5 chip surface. Protein A-purified mAb2B3, at a 1/50 dilution in HBS, was passed over the surface at 10  $\mu$ l/min for 2 minutes. The saturated equilibrium response ( $R_{eq}$ ) was estimated at approximately 282 RUs. This was significantly lower than the predicted  $R_{eq}$  value and indicated sub-optimal surface activity.





### 5.2.2.1.3 Equilibrium steady-state affinity of mAb2B3 for amine-coupled rInIA

The amount of rInIA immobilised was quite high (8000 RUs) and would undoubtedly have prevented accurate kinetic determination of affinity data, ostensibly due to mass-transport limitation. However, because equilibrium measurements are unaffected by mass-transport or re-binding artefacts, high levels of immobilisation could be used to increase the binding response to appreciable/discernable levels for reliable estimation of steady-state affinity. Samples consisting of 200 µl of serial doubling dilutions of mAb2B3 ranging from  $3.3 \times 10^{-6}$  to  $1.29 \times 10^{-8}$  M were individually passed over the rInIA surface. To conserve antibody, samples of mAb2B3 were passed over the rInIA surface at a reduced flow rate of 2 µl/min. After the 40 min exposure equilibrium was approached and the equilibrium response (Req) was noted. Regeneration was achieved by stripping the rInIA from the anti-His surface with two 30 second pulses of freshly prepared 5 mM NaOH. All sensorgrams were reference subtracted from a murine IgG-immobilised reference surface. To remove systematic anomalies a blank run consisting of HBS, that contained no mAb2B3, was subtracted from each of the test sensorgrams. The relationship between the steady state equilibrium binding response (Req) and the corresponding affinity Results were plotted as Req versus mAb2B3 concentration and the data analysed using the BIAevaluation™ steady-state affinity model (Figure 5.21). The steady-state dissociation constant ( $K_D$ ) value was thus, calculated to be  $2.23 \times 10^{-7}$  M. This represents the reciprocal of the association constant ( $K_A$ ).

$$Req = \frac{K_A(C_A) i R_{max}}{K_A n (C_A) i + 1} \quad \text{(Equation 5.2)}$$

Where;	$Req$	=	Response value at equilibrium.
	$K_A$	=	Steady-state equilibrium affinity association constant ( $M^{-1}$ ).
	$n$	=	Steric hinderence factor and represents the average number of ligand sites occupied per analyte molecule.
	$(C_A)i$	=	Injected analyte concentration.
and	$R_{max}$	=	Maximal response.



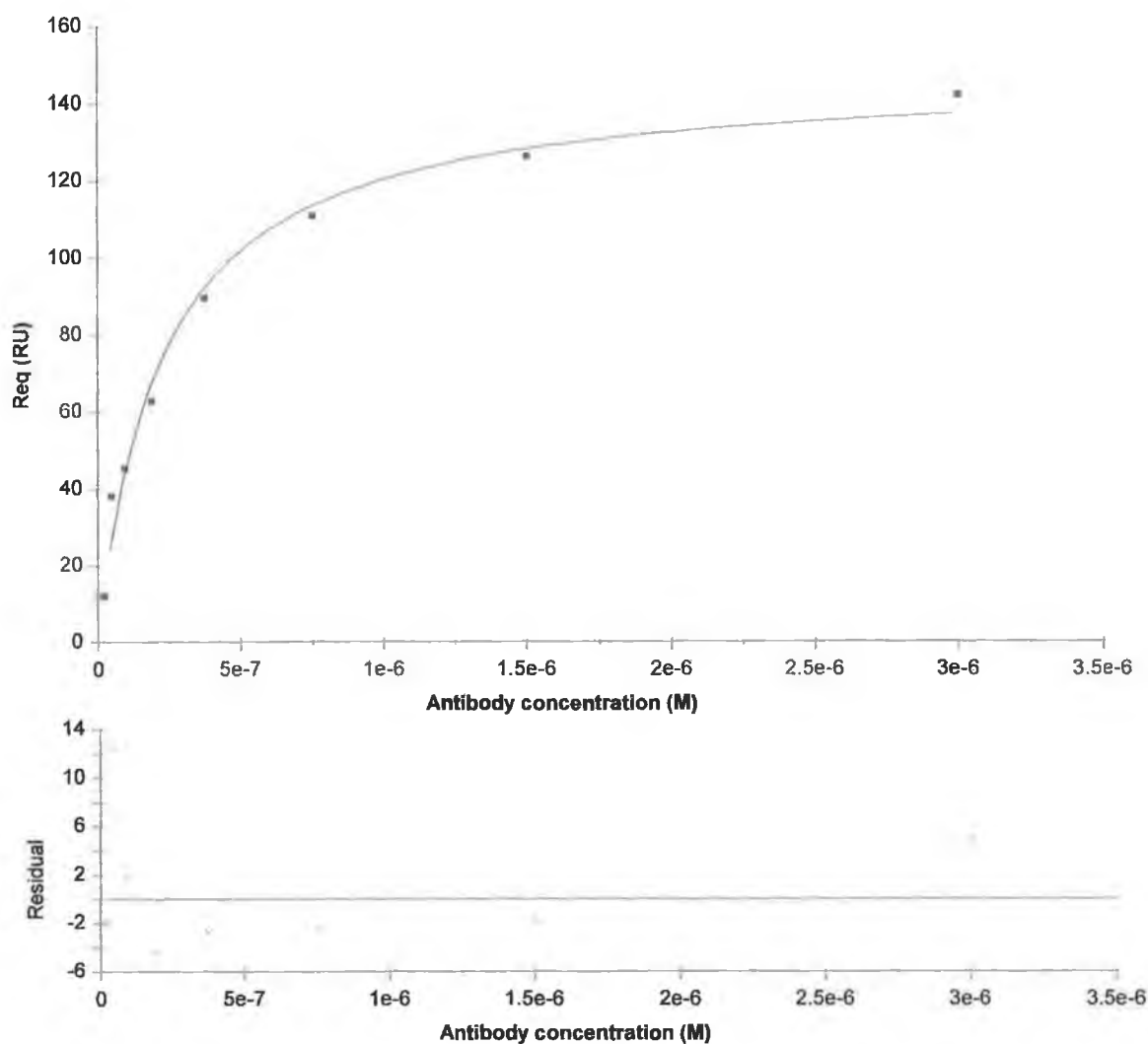


**Figure 5.21:** Steady-state affinity model of mAb2B3 binding to rInIA-CM5 surface. The Req values obtained following a 40 minute interaction period were plotted against their corresponding affinity-purified, mAb2B3 antibody concentrations. The  $K_D$  value was calculated by non-linear curve analysis, using a predefined steady-state affinity function provided in BIAevaluation<sup>TM</sup> software. Assuming  $n=1$ , the apparent  $K_D$  was estimated to be approximately  $2.23 \times 10^{-7}$  M.



The estimated  $K_a$  value was lower than expected, given the demonstrated capacity to efficiently bind and retain cells at the sensor chip surface (Sections 5.2.1.5 and 5.2.1.9) and it prompted a closer inspection of the immobilised ligand activity.

It was possible to approximate the theoretical maximum binding response ( $R_{max}$ ) according to the following equation (Equation 5.3) and thus, estimate the relative surface activity.

$$R_{max} = \frac{\text{Ligand level} \times \text{MW analyte} \times \text{binding stoichiometry}}{\text{MW ligand}} \quad (\text{Equation 5.3})$$

The immobilised ligand level was 8000 RUs (Figure 5.19). Thus, knowing that the molecular weights of mAb2B3 and rInlA were 150 kDa and 80 kDa, respectively and assuming a saturated binding response of 280 RUs (Figure 5.20), surface activity was interpreted to be 3.6 %. This is just an estimate and it is acknowledged that had the mAb2B3 antibody been used at a higher concentration, lower flow rate and the interaction time extended, the experimental  $R_{max}$  would have been greater, but not, however, to the extent that it would approach the theoretical maximum level.

It is possible that the sub-optimal immobilised ligand activity was a direct result of the random covalent nature of the amine coupling method leading to steric hindrance and abrogation of the intrinsic binding activity in mAb2B3 antibody that was cross-linked about the Fab region. In addition, on the basis of the pre-concentration observations (Figure 5.18), mAb2B3 immobilisation had been conducted at pH 4.5. This would be considered an average-to-high pH for typical amine coupling to a CM5 chip. Considering that the predicted pI of rInlA is 4.92, it is entirely possible that impurities in the IMAC-purified rInlA preparation were actually preferentially cross-linked at this pH. Thus, even if the impurities were present at very low levels and consequently, not apparent in SDS-PAGE analysis (Section 4.2.5.1), the low pH used could effectively pre-concentrate the impurity to a significant degree on the activated CM5 surface.

On the basis of the sub-optimal performance of the rInlA-CM5 chip surface, it was decided to investigate alternative means of directional non-covalent attachment of the rInlA ligand to the



sensor surface. In particular, exploiting the His-tag component was investigated for concomitant selective and oriented immobilisation of the rInIA ligand at the sensor surface.

#### **5.2.2.2 Analysis of the of the mAb2B3-InIA interaction using NTA chip technology**

The benefits of NTA for specific binding of oligohistidine-containing molecules has earlier been highlighted (Section 4.2.5). This specific affinity chelation has been harnessed for Biacore-based analysis of His-tagged proteins (Nieba *et al.*, 1997; Jisa and Jungbauer, 2003), using an NTA-coated sensor chip (Gershon and Khilko, 1995).

The NTA chip was considered particularly suitable, since the rInIA protein had been engineered to contain a C-terminal Hexa-Histidine tag (Sections 4.2.4 and 4.2.5). Thus, it should allow homogenous, oriented and regenerable immobilisation of rInIA. While undesirable preferential immobilisation of ligand impurities has been cited as a shortcoming with random, covalent coupling (Section 5.2.2.1.3), even if the ligand preparation is not 100 % pure, NTA preferentially specifically chelates only the oligohistidine-containing molecule.

##### **5.2.2.2.1 Optimisation of the NTA-linked rInIA surface operating conditions**

The NTA chip operating conditions are generic and have been validated with respect to NTA surface activation and regeneration conditions (Nieba *et al.*, 1997; Anon., Biacore, 2002). A typical binding cycle is depicted in (Figure 5.22). Firstly, the chelating capacity of the NTA was activated or 'charged', using a 500  $\mu\text{M}$  solution of  $\text{NiCl}_2$  (Section 2.10.5). IMAC-purified rInIA was then passed over the  $\text{Ni}^{2+}$ -charged NTA and anchored to the surface via its C-terminal His-tag. This was predicted to render the rInIA in the optimal orientation for exposure and steric accessibility of its epitope-bearing sequence, complementary to mAb2B3. Finally, mAb2B3 was passed over the chelated rInIA surface, and the degree of specific binding observed.





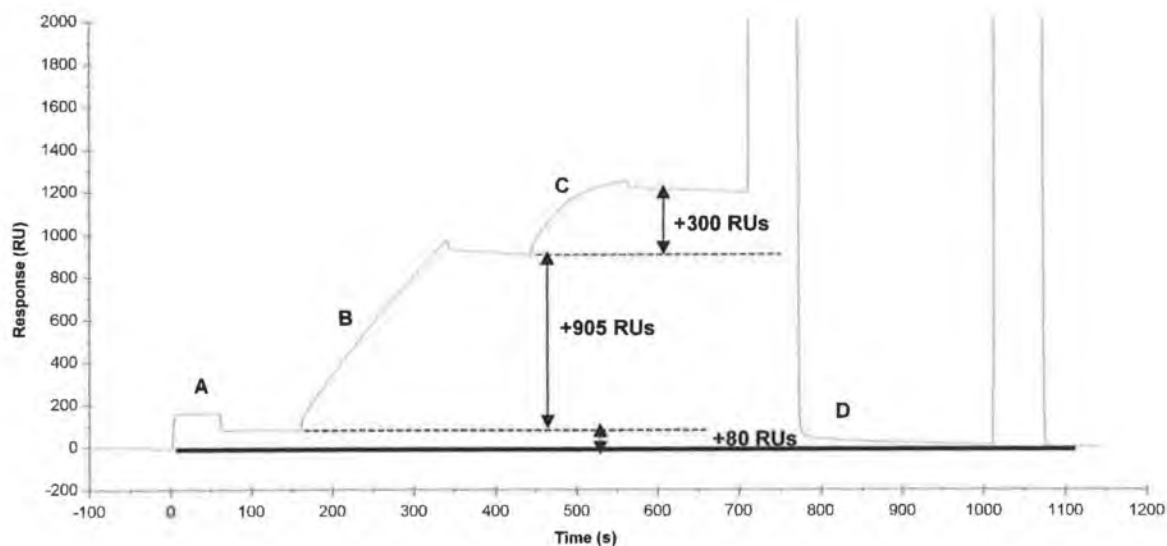


**Figure 5.22:** Complete binding cycle for the mAb2B3-rInlA interaction using NTA sensor chip technology. (A)  $\text{NiCl}_2$  activation of NTA surface, (B) capture of His-tagged rInlA, (C) binding of mAb2B3 to rInlA and (D), regeneration using a 1 minute pulse of  $400 \mu\text{M}$  EDTA (pH 8.3). A flow rate of  $20 \mu\text{l/min}$  was maintained throughout. Approximately 300 RUs of mAb2B3 was observed to bind 'apparently' to the captured rInlA surface. The sensorgram represents raw, non-reference subtracted binding data.

#### 5.2.2.2.2 Non-specific binding profile of NTA chip surface

The binding profile outlined in Figure 5.22 was as expected. However, unlike the CM-dextranated CM5 chip surface, where suitable reference material can be immobilised onto adjacent, downstream flow cells prior to sample analysis, when using the NTA chip, the active ligand surface preparation is integrated into each sample analysis and it is not possible to incorporate a stable, control surface that is independent of the test surface. Thus, on-line reference subtraction was not possible and no information on the non-specific binding contributions was garnered from the sensorgram in Figure 5.22. In order to further resolve any non-specific binding processes, a series of exploratory experiments were undertaken.

Firstly, the non-specific binding potential of the unactivated NTA was assessed. This was conducted by sequentially injecting a 1/100 dilution of mAb2B3, and a 1/10 dilution of IMAC-purified rInlA (in HBS), over the unactivated NTA and monitoring the respective



binding responses (Figure 5.23). It was clear that both mAb2B3 and rInlA exhibited negligible binding to the NTA matrix.

It was also necessary to check for non-specific binding of mAb2B3 to  $\text{Ni}^{2+}$ -charged NTA. This was determined by comparing the response levels for a 40  $\mu\text{l}$  injection of mAb2B3, diluted 1/100 in HBS and a blank injection, consisting of HBS buffer only (Figure 5.24). As expected, HBS did not elicit any apparent binding response. However, approximately 70 RUs of mAb2B3 were observed to bind the  $\text{Ni}^{2+}$ -charged NTA. In view of the lack of suitable on-line referencing function/facility, it was imperative that the degree of apparent non-specific binding be reduced, prior to further analysis or characterisation studies.

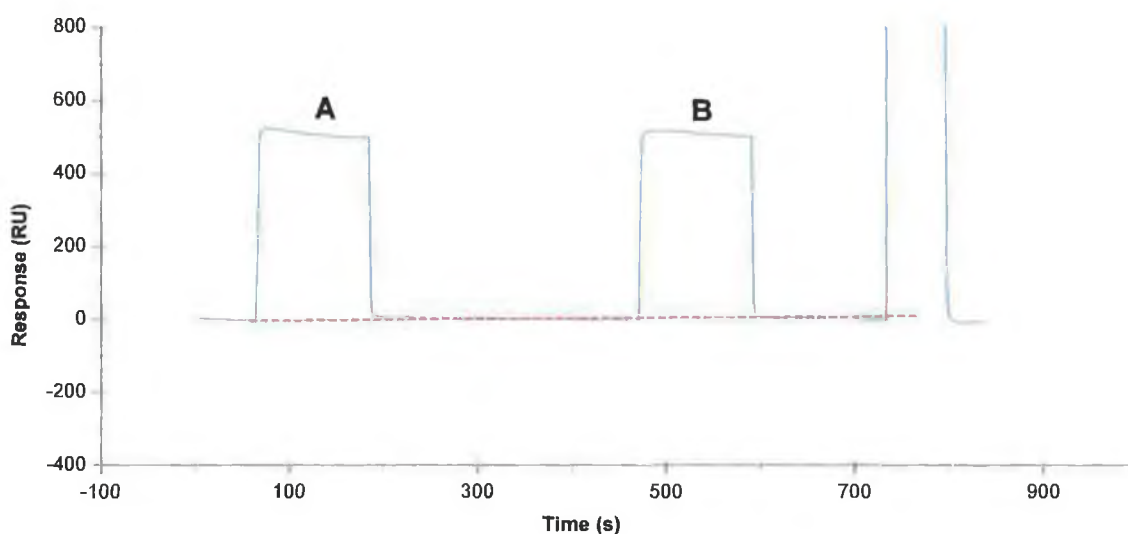


**Figure 5.23:** Non-specific binding profile of rInlA and mAb2B3 to NTA. A 1/10 dilution of IMAC-purified His-tagged rInlA (A) and a 1/100 dilution of affinity-purified mAb2B3 (B), in HBS buffer, were sequentially passed over a fresh, unactivated NTA chip surface, for two minutes at 10  $\mu\text{l}/\text{min}$ . The binding response was negligible in both instances.



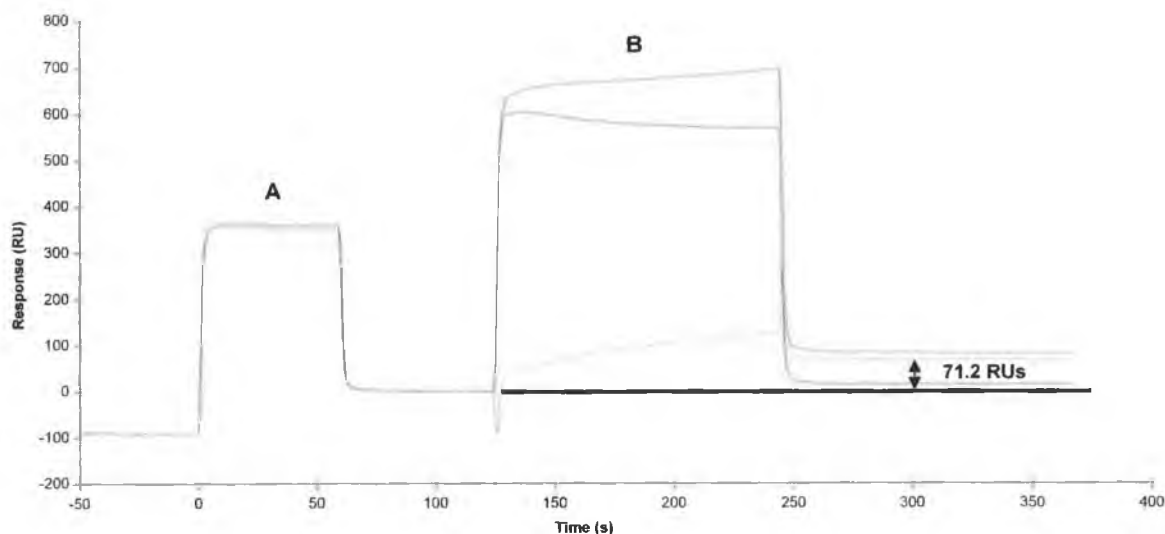


**Figure 5.24:** Non-specific binding profile of mAb2B3 to  $\text{Ni}^{2+}$ -charged NTA. The 'red' sensorgram corresponds to the NTA surface activated with  $\text{NiCl}_2$  (A) and exposed to a 1/100 dilution of mAb2B3 in HBS for two minutes, at 10  $\mu\text{l}/\text{min}$  (B). The 'blue' sensorgram represents the equivalent control response following a blank injection of HBS buffer containing no mAb2B3. The difference between the test and control interactions was plotted (green) and revealed 71.2 RUs of non-specific binding of mAb2B3 to  $\text{Ni}^{2+}$ -charged NTA.

It was possible that mAb2B3 was actually binding to the  $\text{Ni}^{2+}$ -activated NTA through histidine residues within its intrinsic amino acid composition, although this has not been frequently reported as an inherent complication. Moreover, the running buffer had been supplemented with 50  $\mu\text{M}$  EDTA, as recommended by Nieba *et al.*, 1997, to counteract non-specific monovalent histidine interactions. It was assumed more likely, that the non-specific binding forces were ostensibly ionic in nature. In order to overcome these ionic contributions, the salt concentration was increased from 150 mM to 500 mM and the binding response of mAb2B3 with  $\text{Ni}^{2+}$ -activated NTA was assessed across a range of pH values (Figure 5.25). The most pronounced non-specific responses were observed at the higher pH values tested, generated. This was not surprising, given that at higher pH values the protein would be expected to be less positively charged and thus interact to a greater degree with the  $\text{Ni}^{2+}$ -charged NTA. It was concluded that a combination of 500 mM NaCl and a pH value of 6.25 was most effective in combating non-specific binding.



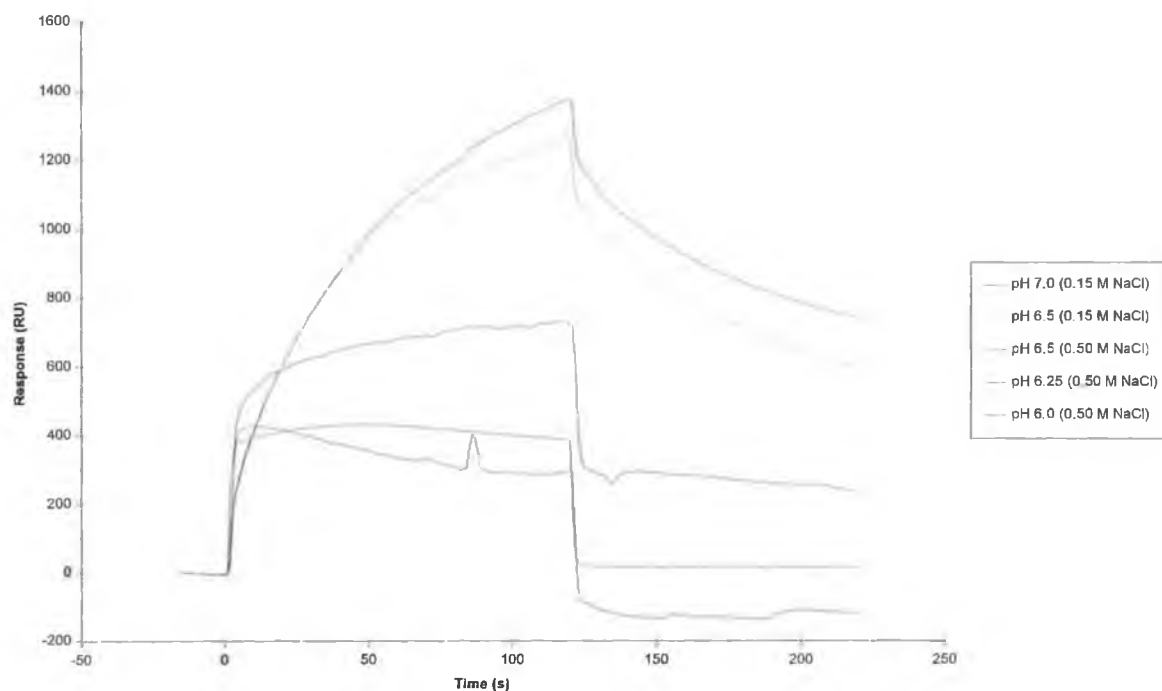


**Figure 5.25:** The effect of pH and salt concentration on non-specific binding of mAb2B3 to  $\text{Ni}^{2+}$ -charged NTA. A 1/2 dilution of mAb2B3 in HBS buffer of varying pH and NaCl concentrations were passed over the  $\text{Ni}^{2+}$ -activated NTA surface at 5  $\mu\text{l}/\text{min}$ , for two minutes. HBS buffer at pH 6.25 and containing 500 mM NaCl substantially reduced the degree of non-specific binding to  $\text{Ni}^{2+}$ -charged NTA.

The specific interaction of mAb2B3 with  $\text{Ni}^{2+}$ -NTA-anchored rInIA in the optimised buffer, was ultimately confirmed by comparing the mAb2B3 binding response levels with those on a  $\text{Ni}^{2+}$ -NTA surface to which, an unrelated His-tagged protein, designated rp18 (Figure 5.26). This was a *Brucella abortus*-derived protein that had been recombinantly expressed with a C-terminal His-tag, using the pQE60 vector cassette (provided by Lyndsey Dunne, DCU). There was no binding apparent on the  $\text{Ni}^{2+}$ -NTA-anchored rp18 surface. In fact there was a reduction in the baseline response level of approximately 100 RUs. This was due to dissociation of rp18 from the  $\text{Ni}^{2+}$ -charged NTA surface, which was undoubtedly exacerbated under the low pH and high salt composition of the sample buffer. Thus, when this reference response was subtracted from the mAb2B3 response at the  $\text{Ni}^{2+}$ -NTA-anchored rInIA surface ( $\sim 200$  RUs), the effective specific response was approximately 300 RUs. Given, that the rInIA capture level was approximately 900 RUs, this constitutes a specific surface activity of approximately 40 %. This was significantly greater than that achieved using direct covalent attachment of rInIA (Section 5.2.2.1.2), however, it was still lower than anticipated, given that





the rInlA ligand was optimally oriented. This was perhaps a result of the low pH/high salt combination needed to combat non-specific elements. Thus, although this series of experiments demonstrated clearly specific binding of mAb2B3 to rInlA, its usefulness was compromised by three significant weaknesses in the approach:

1. The somewhat harsh buffer conditions, necessary to elicit a verifiably specific response.
2. The associated low apparent surface activity.
3. The inability to incorporate an on-line reference subtraction component.

These are inherent weaknesses in the NTA chip technology and may explain the lack of published experimentation directly incorporating it. On the basis of these findings, it was concluded that the NTA chip was not the ideal surface for investigating the mAb2B3-rInlA interaction.



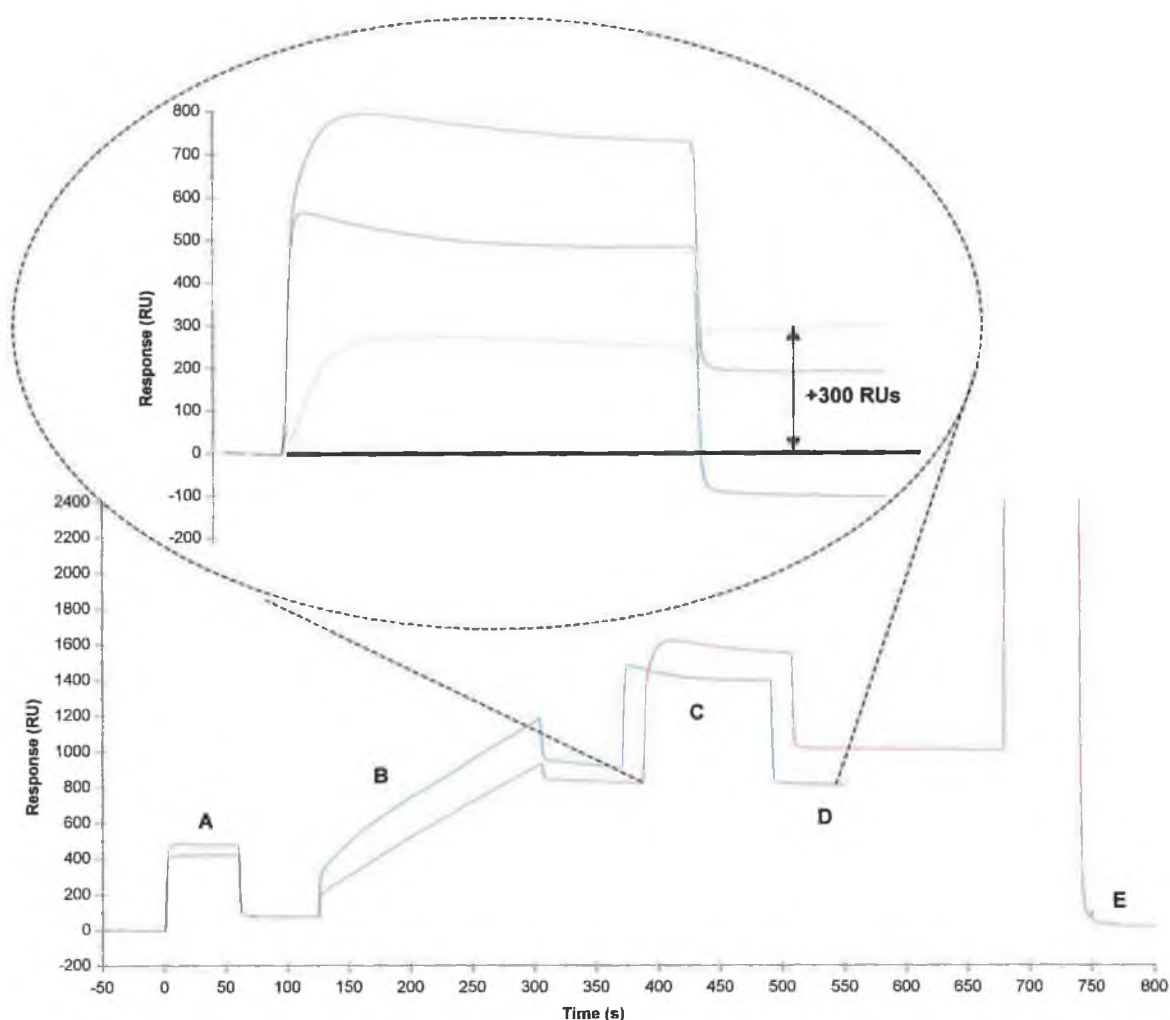


**Figure 5.26:** Optimised, specific binding of mAb2B3 to  $\text{Ni}^{2+}$ -activated NTA-anchored rInLA surface. A 1/2 dilution of mAb2B3 in HBS buffer (pH 6.25, 500 mM NaCl) was passed over rInLA (red)- and rp18 (blue)-captured surfaces. (A)  $\text{NiCl}_2$  activation, (B) binding of His-tagged ligand (rInLA or rp18) at a flow rate of 10  $\mu\text{l}/\text{min}$  for two minutes, (C) binding of mAb2B3, (D) bound level of mAb2B3 and (E) NTA surface regeneration using EDTA. The insert shows a magnified overview of the mAb2B3 binding interaction regions of the respective sensorgrams. The interaction regions were overlayed and aligned using BLAevaluation<sup>TM</sup> software and the reference-subtracted 'effective' response was superimposed (green). The data clearly demonstrate successful and specific binding of mAb2B3 to rInLA, anchored to  $\text{Ni}^{2+}$ -activated NTA via its C-terminal His-tag.



### **5.2.2.3 Characterisation of the mAb2B3-rInlA interaction using an anti-His-tag antibody ligand-capture approach**

#### **5.2.2.3.1 Pre-concentration of anti-His-tag antibody onto the CM5 sensor chip surface**

As a result of the inadequacies, revealed as inherent, when using the NTA methodology to controllably orient the rInlA protein, it was decided to investigate the potential of using an anti-His-tag antibody to capture the rInlA, via its C-terminal His-tag.

A recent survey of available anti-His-tag monoclonal antibodies has revealed a universally more specific propensity to bind oligohistidine tags, with a demonstrated lower tendency to non-specifically bind, isolated or clustered Histidine residues, occurring in the amino acid sequence of His-tagged proteins (Anon., Biacore, 2002). A BSA-free, anti-His-tag monoclonal antibody was sourced from Novagen (N70796), hereon referred to as 'Nova-His'. It was essential that the antibody was free from BSA and other carrier or stabilising proteins so as to prevent more favourable coupling of the undesired contaminating protein over the antibody itself, leading to lower apparent coupling efficiency, concomitantly interpreted as sub-optimal specific surface ligand activity.

The Nova-His antibody was adjusted to 50 µg/ml in 10 mM sodium acetate across the pH range 4.0-5.0 and the degree of pre-concentration was assessed as before (Section 2.10.1). Maximum pre-concentration was achieved in 10 mM sodium acetate buffer at pH 4.2 (Figure 5.27).



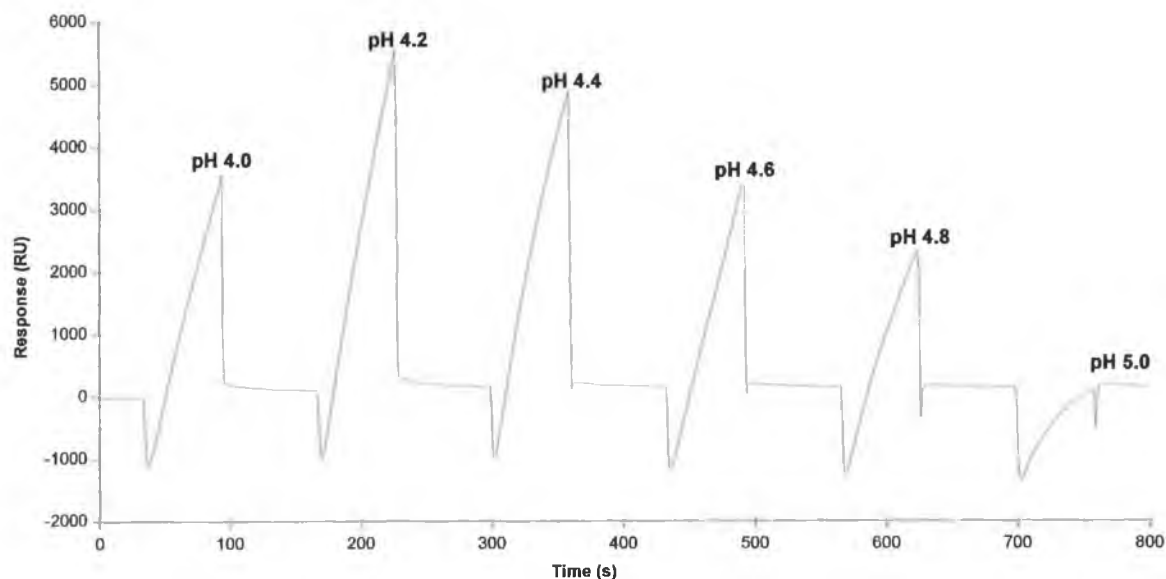


**Figure 5.27:** Pre-concentration of 'Nova-His' onto the CM5 sensor chip surface across the pH range 4.0-5.0. Maximum pre-concentration was observed at pH 4.5. Thus, 10 mM sodium acetate buffer at pH 4.5 was chosen as the immobilisation buffer for the Nova-His antibody onto the CM5 chip surface.

#### 5.2.2.3.2 Immobilisation of anti-His-tag antibody onto the CM5 sensor chip surface

It was important that maximum ligand coupling efficiency was achieved, to prevent the binding capacity of the Nova-His surface limiting the subsequent mAb2B3-rInIA interaction and also to reduce the net contribution of partial rInIA dissociation from the observed mAb2B3-rInIA interaction. The immobilisation (Figure 5.28) was controlled manually and incorporated an extra EDC/NHS activation pulse, to maximise the % reactive ester formation. In addition, following an initial exposure to Nova-His antibody in immobilisation buffer (10 mM sodium acetate, pH 4.2), a second ligand-binding pulse was incorporated to ensure the CM5 coupling capacity was fully exhausted. Coupling saturation was reached at approximately 8000 RUs. A control surface was prepared by immobilising a similar level of IgG2a control antibody in the flowcell immediately downstream of the Nova-His surface to facilitate on-line reference subtraction (Sections 2.10.3, 5.2.1.2 and 5.2.1.3).





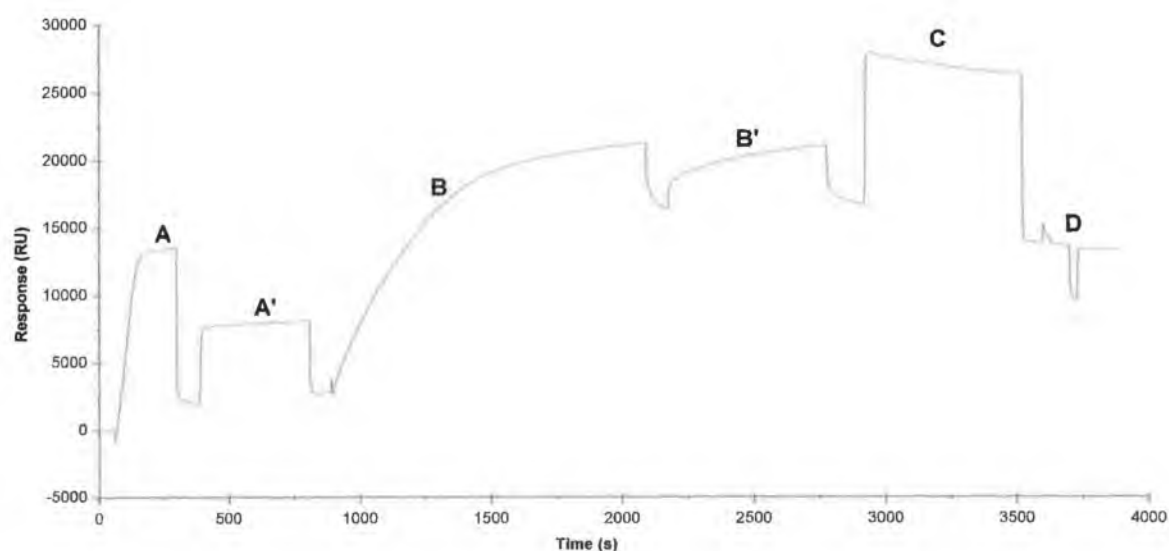


**Figure 5.28:** Immobilisation of 'Nova-His' antibody onto the CM5 sensor chip surface. The immobilisation was controlled manually, so as to ensure that the injected solution of 'Nova-His' antibody fully saturated the coupling capacity of the activated CM dextran. This included an extra surface activation pulse and a secondary immobilisation pulse to achieve saturation. (A) Preliminary EDC/NHS activation pulse, (A') secondary, complete EDC/NHS activation, (B) primary binding of 'Nova-His' antibody, (B') secondary binding of 'Nova-His' antibody (C) capping of unreacted groups and (D), regeneration pulse of 5 mM HCl. The difference in 'bound mAb2B3' levels achieved following the primary (B) and secondary (B') ligand injections was minimal, indicating maximum coupling. A final level of 8109.1 RUs covalently attached 'Nova-His' antibody was achieved.



When mAb2B3 was passed sequentially over the Nova-His and IgG2a reference surface, negligible binding was revealed (Figure 5.29), thus confirming the absence of significant non-specific binding.

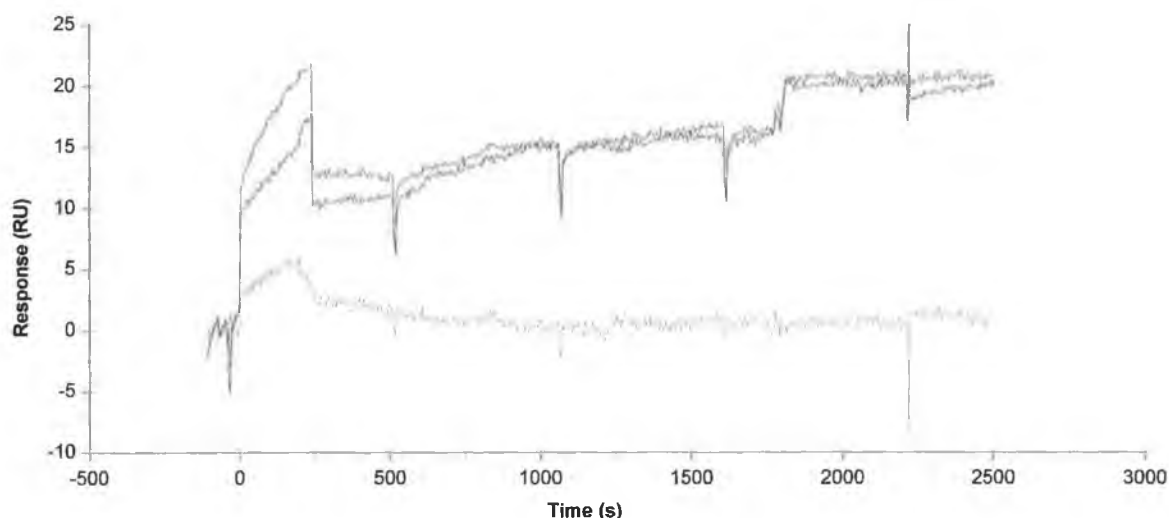
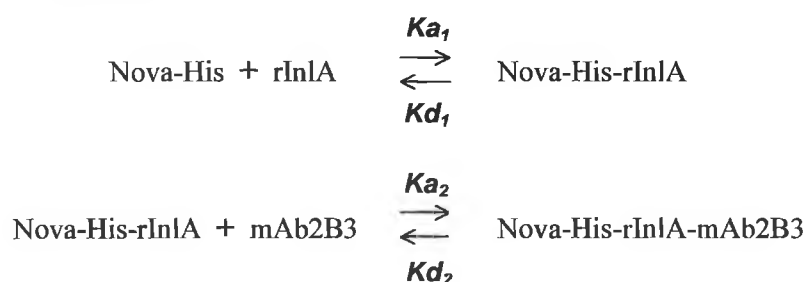


**Figure 5.29:** Non-specific binding profile of mAb2B3 on the Nova-His surface. A 1/10 dilution of mAb2B3 in HBS was serially passed over both the Nova-His (red) and control IgG2a (blue) surfaces. Negligible non-specific binding was demonstrated, as clearly demonstrated by the reference-subtracted plot (green).

Following capture of rInlA (~450 RUs), subsequent, specific binding of mAb2B3 was successfully demonstrated (Figure 5.30). Although the positive binding interaction was clearly visible over the early part of the sensorgram, immediately following injection of the mAb2B3 sample, the response began to decrease after approximately five minutes. This can be attributed to the more rapid dissociation of rInlA from the Nova-His surface. Although the on-line reference subtraction successfully prevented systematic deviations and peculiarities, the mAb2B3 binding region of the sensorgram actually represented a cumulative, non-resolved plot of two steady-state interactions:





In the interaction under investigation it was apparent that  $K_{d1} > K_{d2}$  and thus, the more rapid dissociation of rInlA from the Nova-His surface effectively masked the mAb2B3-rInlA binding response over an extended interaction period. The actual binding of mAb2B3 to rInlA was resolved by subtracting a blank injection cycle (i.e. HBS containing zero mAb2B3). This second referencing step efficiently compensated for the negative contribution of  $K_{d1}$  and revealed the surface-saturation response to be approximately 225 RUs. This reflected a specific surface activity of approximately 53 %, which was higher than that achieved using either direct covalent attachment (Section 5.2.2.1) or NTA capture (Section 5.2.2.2).

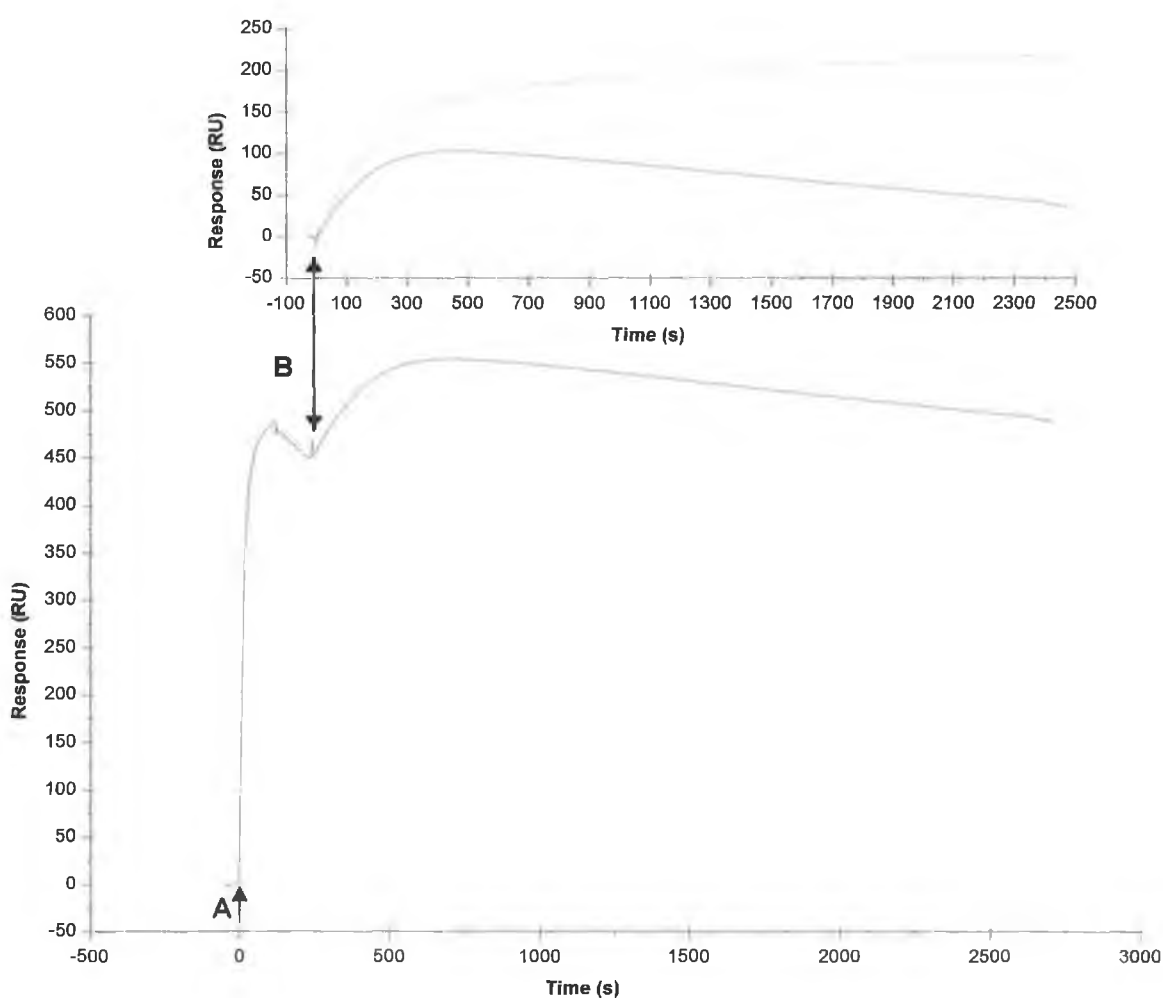


**Figure 5.30:** Complete binding cycle sensorgram for the mAb2B3-rInlA interaction on the Nova-His, anti-polyhistidine-derivatised CM5 surface. (A) Injection of 10  $\mu$ l of rInlA, diluted 1/10 in HBS. (B) After two minutes of buffer-flow, mAb2B3 was injected at  $1.5 \times 10^{-6}$  M across the surface, in HBS. The flow rate used throughout was 5  $\mu$ l/min. The inset shows the normalised, single online-referenced mAb2B3-rInlA binding response (red), with the true, double-referenced response data, superimposed (green).



#### 5.2.2.3.3 *Steady-state affinity of mAb2B3 on Nova-His-captured rInlA surface*

The steady-state affinity profile for mAb2B3, binding to Nova-His-captured rInlA, was investigated, using the optimised Nova-His capture approach and from the resultant binding data (Figure 5.31), a steady-state affinity model was plotted (Figure 5.32) and used to estimate the affinity constant ( $K_a$ ), as previously described (Sections 2.10.6 and 5.2.2.1.3). The calculated equilibrium steady-state dissociation constant  $K_D$  value ( $1.93 \times 10^{-7}$  M) was quite similar to that obtained using the covalently immobilised rInlA approach (Section 5.2.2.1.3). It was expected that since, in theory, the capture method facilitated homogenous, oriented immobilisation of rInlA, with demonstrated improved surface activity, the observed  $K_D$  value would be, accordingly, enhanced. The fact that this was not realised, along with the pervading non-ideal surface activity across all three rInlA immobilisation formats investigated, indicated that the IMAC-purified rInlA may have been compromised by intrinsic heterogeneities.

In addition, although the data is not shown, numerous attempts to characterise the mAb2B3-rInlA interaction by modelling the kinetic parameters were undertaken, yet they failed to yield data that could be adequately modelled. It is acknowledged that the universal applicability of ligand-capture immobilisation as a platform for kinetic interpretation of binding interactions is questionable (Quinn *et al.*, 1999). Nonetheless, it was felt that, given the careful referencing steps incorporated, the data would at least facilitate modelling, even if the extrapolations derived from resultant models was not ideal. The total failure of the data obtained to fit the kinetic models, further reinforced suspicion of rInlA heterogeneity at the chip surface.





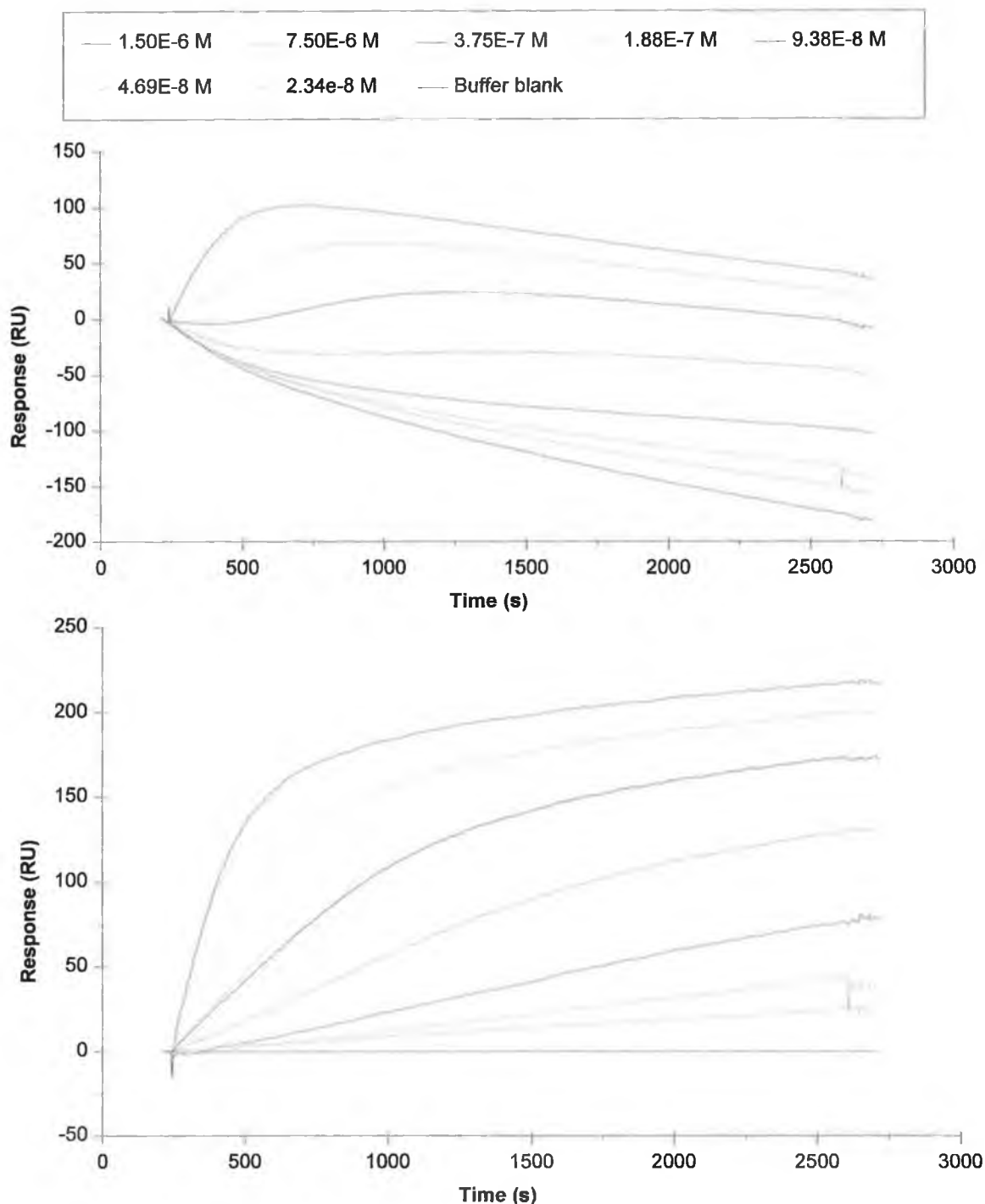


**Figure 5.31:** Overlaid steady-state sensorgrams depicting the binding profiles for mAb2B3 to His-tag-affinity-captured rInlA on an anti-His-tag-immobilised CM5 surface (Nova-His). The top sensorgram represents the data following on-line reference subtraction. The bottom sensorgram represents the same binding data, 'double-referenced' by subtracting the blank or 'buffer only' data, in order to compensate for rInlA dissociation (from anti-His-tag antibody) during the 40 minute binding interaction.



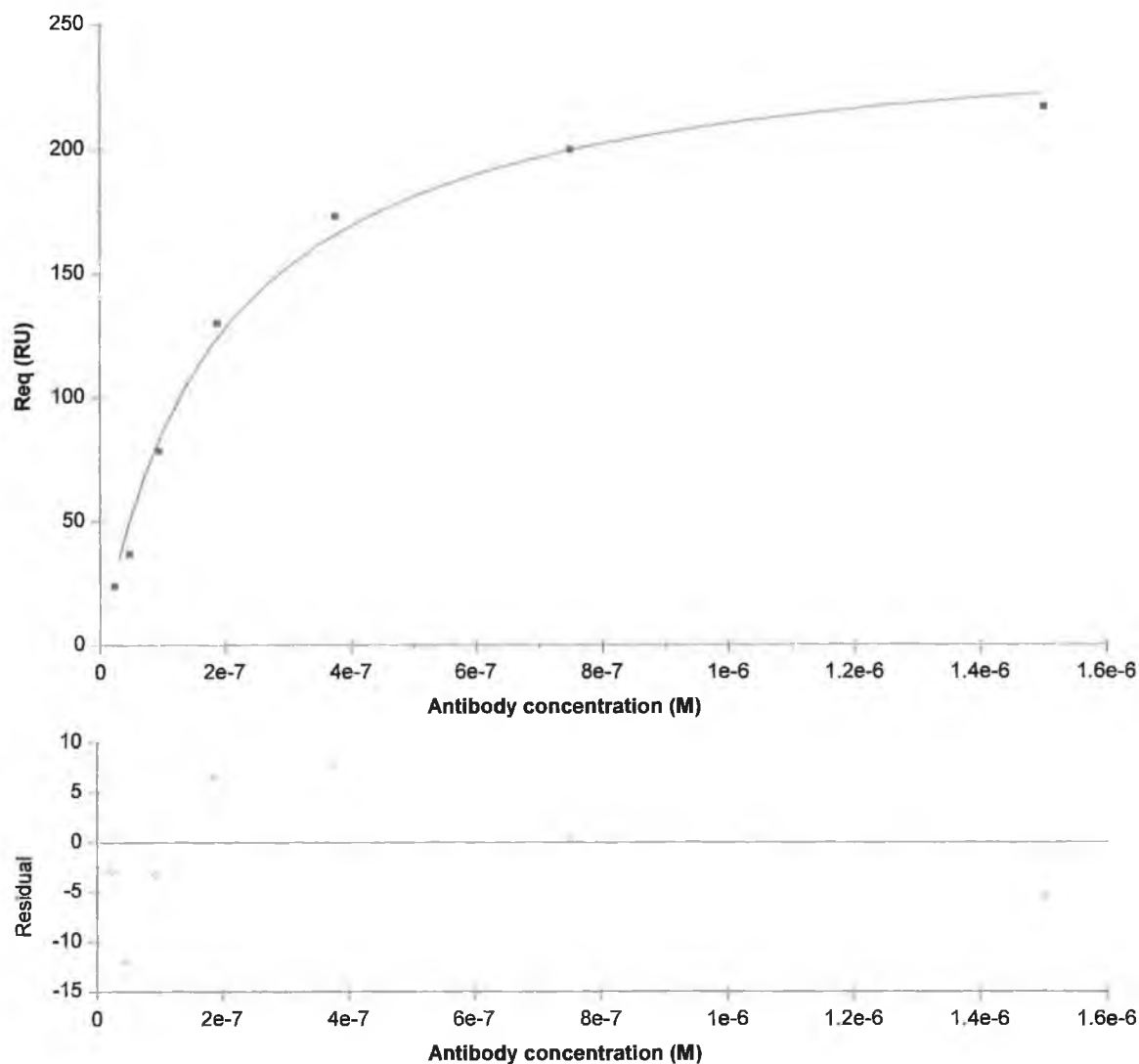


**Figure 5.32:** Steady-state affinity model of mAb2B3 binding to His-tag-affinity-captured rInlA on an anti-His-tag-immobilised CM5 surface (Nova-His). Req values were interpreted after a 40 minute interaction period and following double-reference subtraction, were plotted against their corresponding affinity-purified, mAb2B3 antibody concentrations. The  $K_D$  value was calculated by non-linear curve analysis, using a predefined steady-state affinity function provided in BIAevaluation<sup>TM</sup> software. Assuming  $n=1$ , the apparent  $K_D$  was estimated to be approximately  $1.93 \times 10^{-7}$  M.



#### **5.2.2.4 Non-denaturing PAGE analysis of IMAC-purified rInIA**

The deviations from ideal predictions, exhibited by the immobilised rInIA surfaces prompted a closer investigation into the disposition of the purified rInIA protein preparation. Preliminary characterisation of IMAC-purified rInIA by SDS-PAGE and Western blotting (Sections 4.2.5) had revealed it to be predominantly pure and immunoreactive towards mAb2B3. A neat sample of the IMAC-purified rInIA used in the Biacore experiments (Sections 5.2.1-5.2.3) was analysed by native, or non-denaturing PAGE (Section 2.3.3) across a range of gel acrylamide concentrations (7, 8, 9 and 10 % (w/v)), alongside molecular weight markers that 'bracketed' the known molecular weight of the His-tagged rInIA protein. However, even without referring to a standard curve, it was clear from the electrophoretic mobility that the apparent molecular weight was in fact, substantially greater than that confirmed by sequence analysis (Section 4.2.4.2) and SDS-PAGE (Section 4.2.5.1). The gel depicted in Figure 5.33 is typically representative of the electrophoretic resolution pattern obtained across the four gel acrylamide concentrations investigated. This strongly suggested that the rInIA protein was present, under the buffer conditions employed, as a multimeric compound. It has been demonstrated that even proteins that have been purified as monomeric, can, subsequently, multimerise over time and complicate SPR-based binding analysis (Van der Merwe *et al.*, 1993; Myszka, 1997).

#### **5.2.2.5 HPLC analysis of IMAC-purified rInIA**

In order to further resolve the apparent multimeric nature of the IMAC-purified rInIA, a neat sample in PBS was subjected to SEC-HPLC (Section 2.11.3). One major peak was observed and exhibited a retention time of 7.0 minutes (Figure 5.33). A series of molecular weight standards was also analysed under the same operating conditions. The retention time ( $T_r$ ) of each standard was recorded, and divided by the time taken for a sample to elute in the column void volume ( $v_o$ ). A constant flow rate was maintained (0.5 ml/min) and this rendered  $T_r$  to be equal to  $v_e$ . Thus, when the  $v_e/v_o$  values (Section 2.11.2) were plotted against the log of the molecular weight of the respective standard, a linear calibration curve was obtained. When the rInIA sample retention time was substituted into the standard curve (Figure 5.34), the peak molecular weight was calculated to be approximately 308 kDa. This corresponded to approximately four times the confirmed molecular weight of monomeric rInIA and thus, indicated that the IMAC-purified rInIA was actually present as a tetramer. It is thus postulated that steric complications, elicited by the tetrameric configuration were responsible for the non-ideal behaviour of the rInIA, when immobilised on the various sensor chip formats, notwithstanding the steps taken to ensure homogenous and oriented ligand immobilisation.



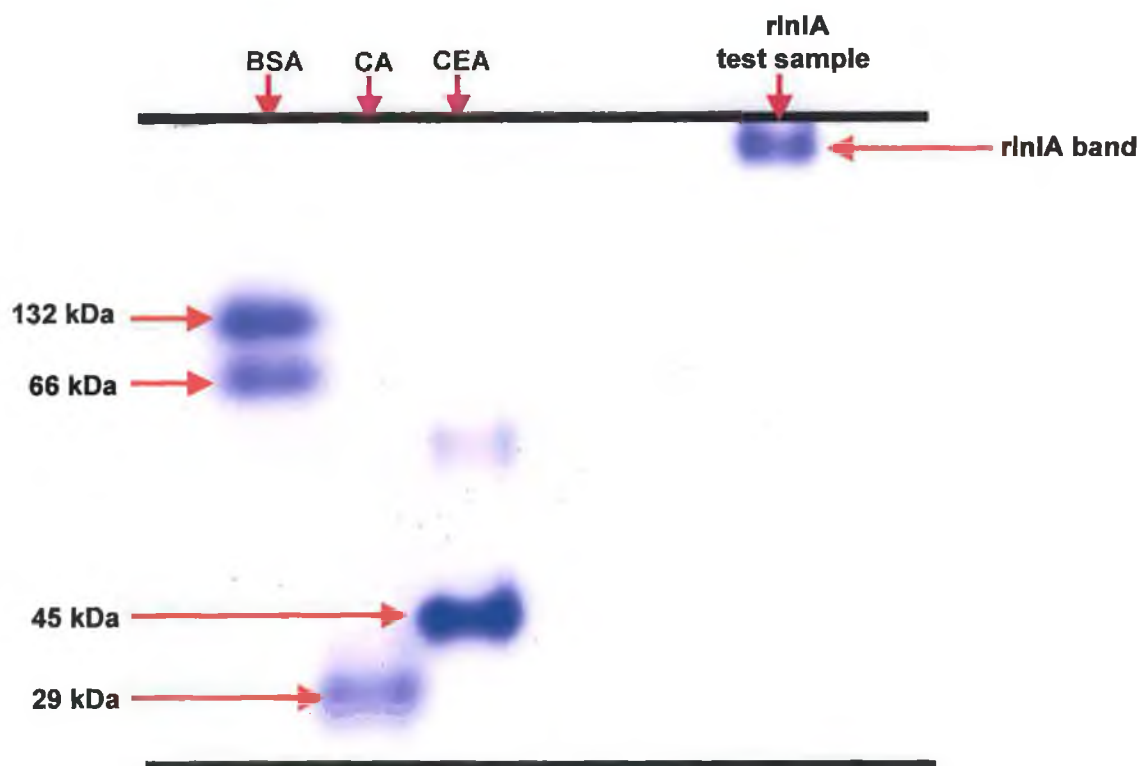


**Figure 5.33:** Non-denaturing PAGE analysis of IMAC-purified rInIA. The purified protein in PBS buffer was diluted 1/10 in non-denaturing sample buffer and loaded onto the gel. The molecular weight standard samples (bovine serum albumin (BSA), carbonic anhydrase (CA) and chicken egg albumin (CEA)) were chosen to bracket the predicted molecular weight of rInIA. The gel shown, consisted of the lowest acrylamide concentration investigated (i.e. 7 % (w/v)). Despite this, it was clear that the rInIA sample did not electrophoretically migrate significantly from the loading front. This was interpreted to indicate multimeric compound formation.





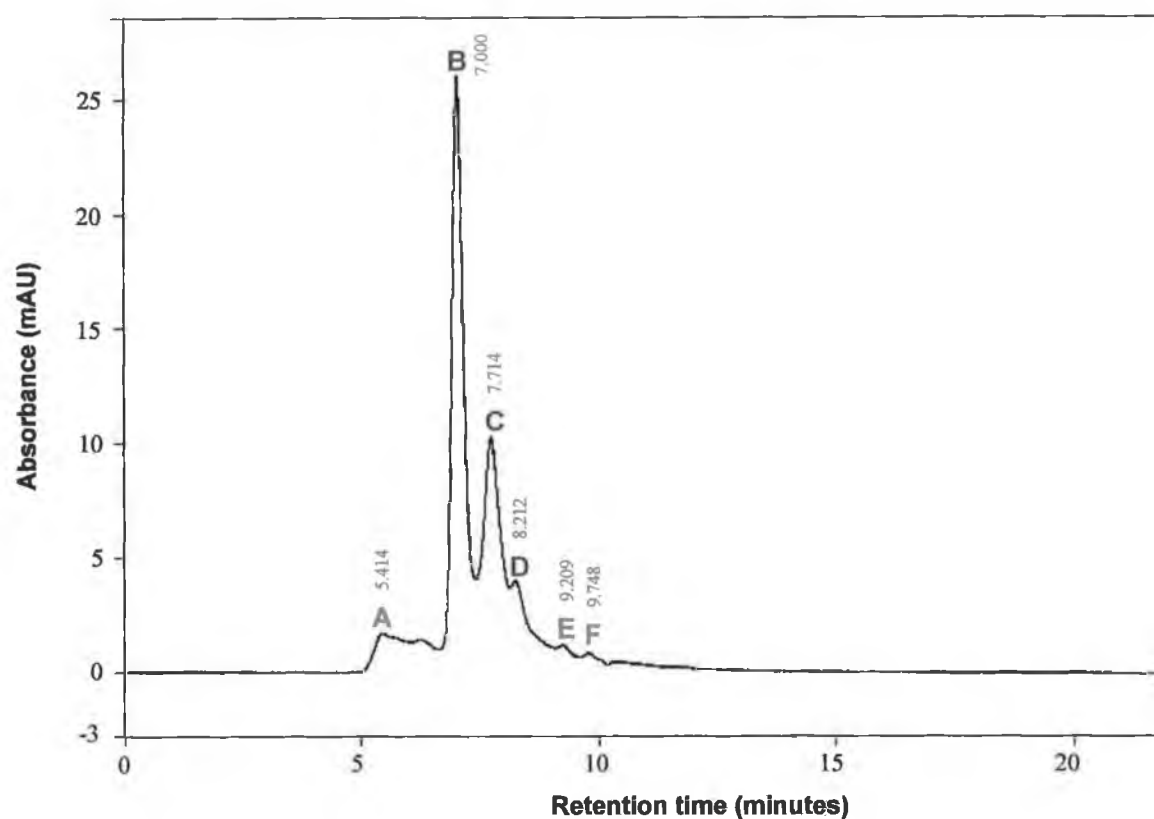


**Figure 5.34:** SEC-HPLC analysis of IMAC-purified rInIA. A neat sample of the purified rInIA, in PBS was applied to the HPLC column. A Phenomenex 3000 SEC column was used with PBS mobile phase at a flow rate of 0.5 ml/min and monitored by UV absorbance at 280 nm. One dominant peak was observed (B) at 7.0 minutes retention. A number of smaller, shoulder peaks were evident (A, C, D, E, and F).



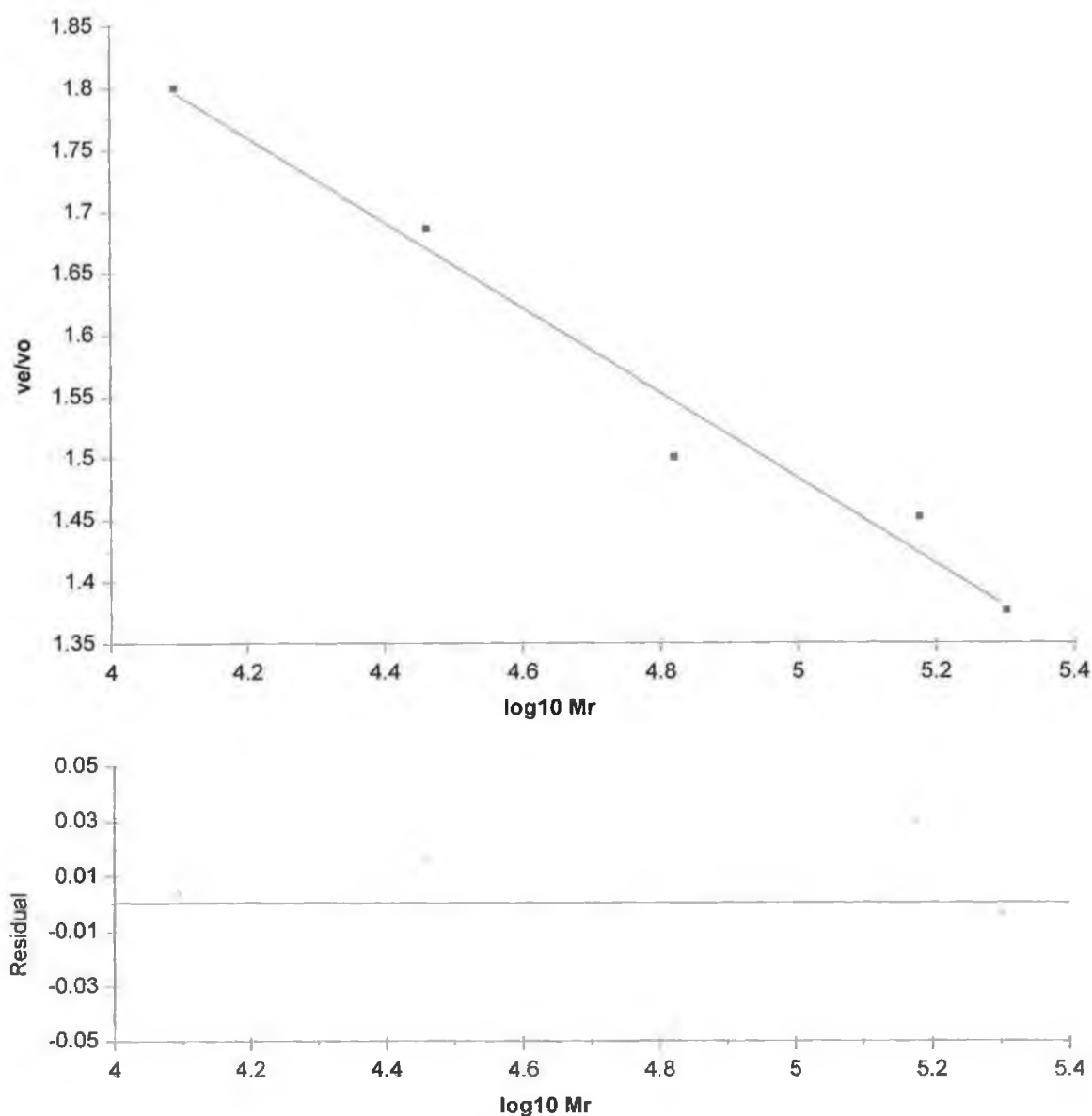


**Figure 5.35:** SEC-HPLC standard curve of  $ve/vo$  versus  $\log_{10}(Mr)$  for estimation of rlnA molecular weight. The  $vo$  value was calculated using blue dextran and the data points obtained for the molecular weight standards ( $\beta$ -amylase ( $\beta$ -A), 200 kDa; alcohol dehydrogenase (AD), 150 kDa; bovine serum albumin (BSA), 66 kDa; carbonic anhydrase (CA), 29 kDa and cytochrome C (CC), 12.4 kDa). The data was linearly resolved using a four-parameter equation.



### **5.2.3 Characterisation of the mAbG94F8-p60 interaction using Biacore**

The evidence garnered by ELISA and Western blot analyses in Section 3.2.2.3 had suggested that mAbG94F8 was specific for p60. However, this was subject to further confirmation. The Biacore system facilitated a more controllable analysis of the various parameters affecting binding, in a range of formats.

#### **5.2.3.1 Confirmation of p60-specificity of mAbG94F8 using Biacore**

The monoclonal antibody mAbG94F8 had been putatively designated ‘anti-p60’, based on preliminary inhibition-ELISA and Western blot analysis using *L. monocytogenes* culture supernatant-derived proteins (Sections 3.2.2.2 to 3.2.2.4). In addition, although a strong immunoreactivity was observed when rp60 was probed by Western blotting (Section 3.2.2.3), it was not possible to correspondingly confirm ‘non-reactivity’ towards LLO, due ostensibly to lack of availability of suitably pure native or recombinant LLO protein. Confirmation of this distinction in reactivity was necessary due to the fact that both p60 and LLO were present in *L. monocytogenes* culture supernatant (Section 3.2.1.2) and were of equivalent, indistinguishable molecular weights.

Subsequent to this particular set of experiments, a small quantity of recombinant LLO (rLLO) was sourced and a sample was kindly donated by Prof. Mauro Magnani (Centro di Biotecnologie, University of Urbino, Italy). The rLLO had been prepared as previously described (Giammarini *et al.*, 2003). Due to the limited amount of rLLO available, it was felt that immobilising it onto a sensor chip surface would enable the most judicious exploitation of the protein for analysis.

##### **5.2.3.1.1 Preparation of rLLO-CM5 sensor chip surface**

Pre-concentration was not performed, as a means of rationing the limited supply of rLLO protein. However, since the predicted theoretical pI of LLO was 6.7 (based on the Genbank accession number AF253320, UniProt reference number Q9L5B9, using the ProtParam function at <http://us.expasy.org/cgi-bin/protparam>) and the protein was known to be stable in acidic environments, it was felt that pH 4.5 would be adequate for pre-concentration and immobilisation. In order to ensure maximal covalent immobilisation capacity was achieved, a ‘double-activation’ step was incorporated. This entailed exposing the CM dextran to EDC/NHS for twice the normal activation time (i.e. 14, rather than 7 minutes). Approximately 2047 RUs of rLLO was covalently immobilised (Figure 5.36).



#### 5.2.3.1.2 Assessment of mAbG94F8 binding to immobilised rLLO

The binding response of mAbG94F8 against immobilised rLLO, was compared with that of polyclonal anti-LLO. The latter was affinity-purified (Section 2.6.3) from rabbit polyclonal antiserum, kindly donated by Prof. Chakraborty and Dr. Darji, University of Giessen, Germany. Affinity-purified mAbG94F8, in PBS, was diluted 1/10 in HBS buffer and fresh mAbG94F8 hybridoma supernatant was diluted 1/2 in HBS containing 1 M NaCl, to yield a final salt concentration of 0.5 M. The high salt was incorporated to minimise non-specific binding of heterogenous material from within the complex matrix of the cell culture medium. Both mAbG94F8 samples were individually, sequentially injected over the immobilised rLLO-CM5 surface and in both cases, binding responses were negligible (Figure 5.37). However, when the polyclonal anti-LLO antibody was passed over the surface, over 2000 RUs of antibody bound. This confirmed that the activity of the immobilised rLLO protein had not been substantially compromised by the immobilisation procedure. Cumulatively, these results confirmed that mAbG94F8 was not active against rLLO, and when considered alongside the results in Section 3.2.2.4, confirmed that mAbG94F8 was indeed specific for p60 and not LLO.

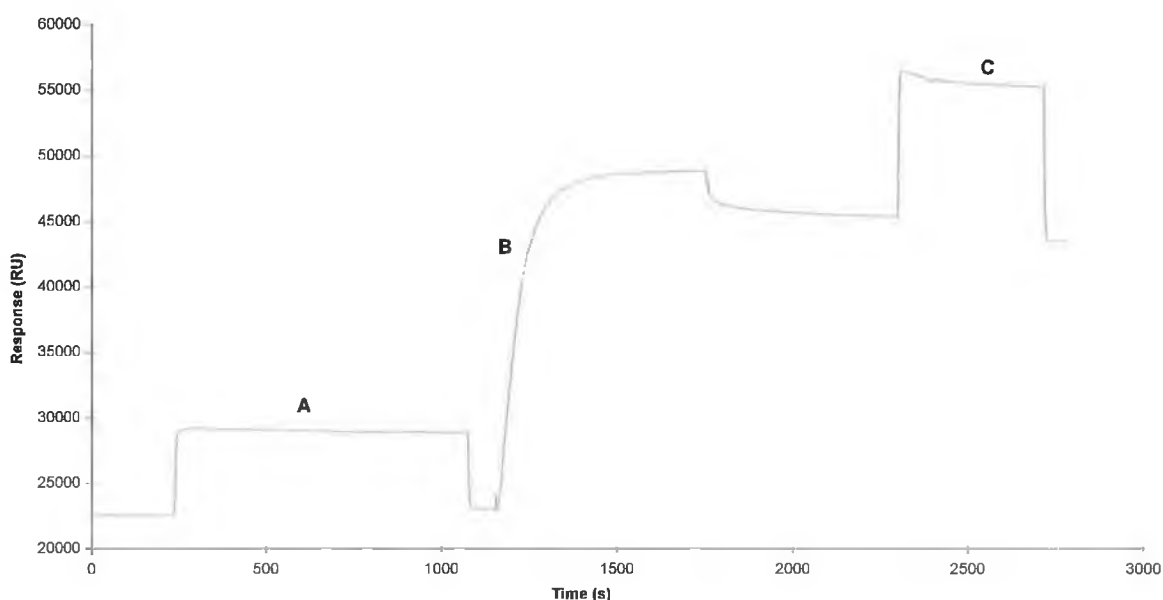


**Figure 5.36:** Immobilisation rLLO onto the CM5 sensor chip surface. (A) EDC/NHS 'double-activation', (B) covalent binding of rLLO and (C), capping of unreacted groups. A final level of 20447.0 RUs covalently attached rLLO was achieved.





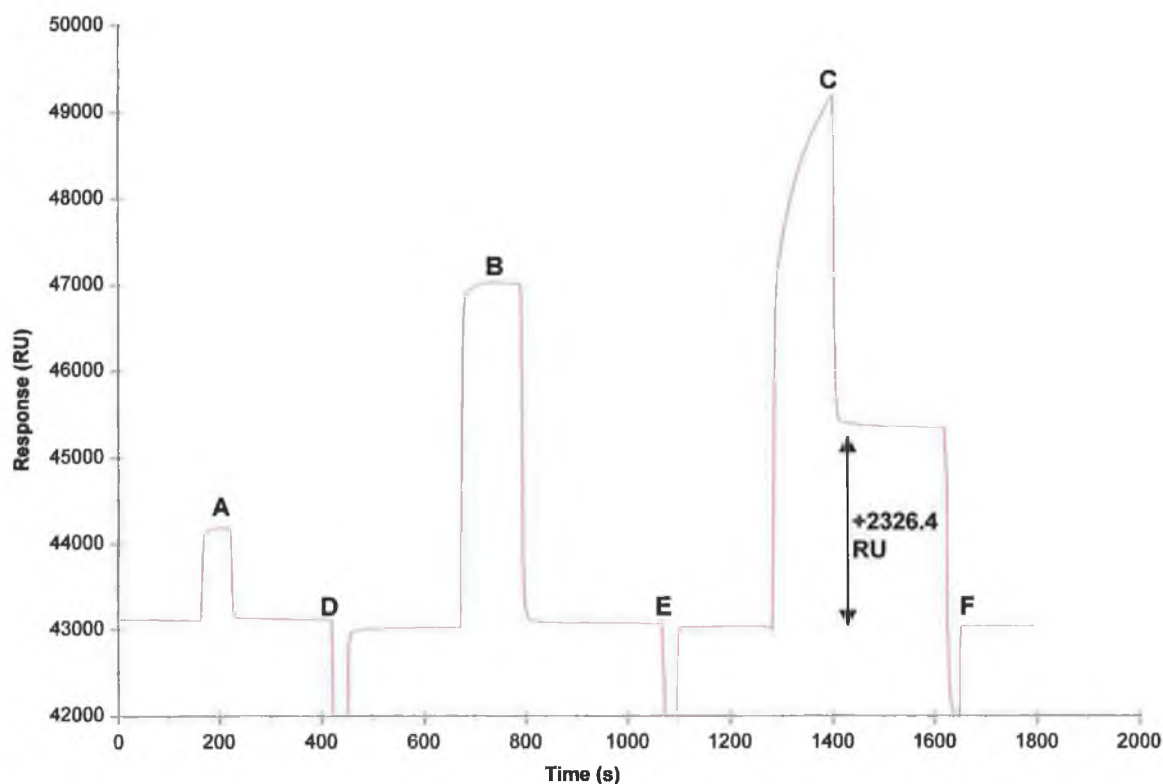


**Figure 5.37:** Binding analysis of putative anti-p60 mAbG94F8 and anti-LLO to rLLO-CM5 surface. The sensorgram depicts the raw, non-reference-subtracted binding responses obtained following sequential injection of (A) affinity-purified mAbG94F8, at a 1/10 dilution (~20 µg/ml) in HBS, (B) fresh mAbG94F8 hybridoma supernatant, at a 1/2 dilution in HBS (containing 0.5 M NaCl) and (C), anti-LLO polyclonal antibody, at a 1/100 dilution in HBS, across the rLLO-CM5 surface. The flow rate employed throughout was 10 µl/min and surface regenerations (D, E and F) were elicited with 5 µl pulses of 10 mM NaOH. Significant binding, was only demonstrated by the anti-LLO polyclonal antibody (2326.4 RUs).

### 5.2.3.2 Preparation of mAbG94F8-CM5 sensor chip surface

To facilitate the demonstration of specific binding of rp60 by mAbG94F8, the reverse configuration, with mAbG94F8 immobilised on the CM5 surface, was also investigated. Pre-concentration was conducted, as routinely described (Section 2.10.1), across the pH range 4.0-5.0 (Figure 5.38). Preliminary, exploratory experiments had indicated rp60 to be prone to non-specific binding (Paul Leonard, personal communication) and thus, to minimise the possibility of residual activated carboxyl groups, a 'double-capping' step was incorporated, whereby the period of exposure to capping reagent was doubled. Approximately 15800 RUs



of mAbG94F8 was efficiently immobilised (Figure 5.39). A blank reference surface was prepared, for the purposes of on-line reference subtraction, by subjecting a downstream flowcell surface to an identical activation and capping procedure, with the ligand-immobilisation step omitted.

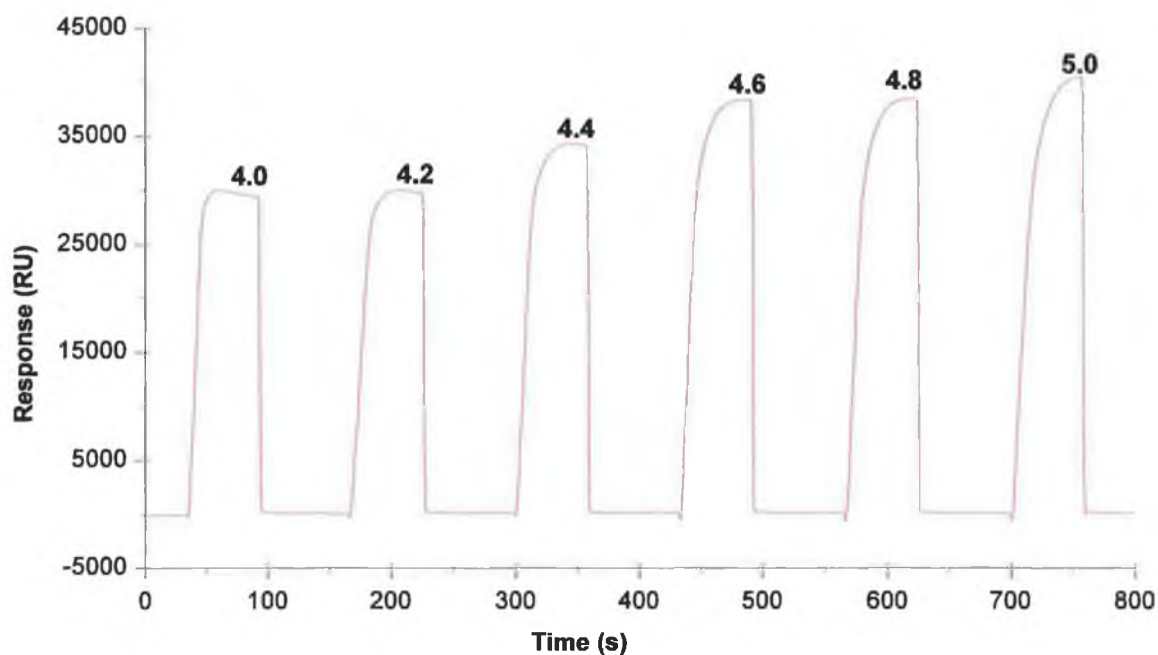


**Figure 5.38:** Pre-concentration of mAbG94F8 onto the CM5 sensor chip surface across the pH range 4.0-5.0. There was no substantial improvement in pre-concentration from pH 4.6 to 5.0 and, thus, 10 mM sodium acetate buffer at pH 4.7 was chosen as the immobilisation buffer for the mAbG94F8 antibody onto the CM5 chip surface.



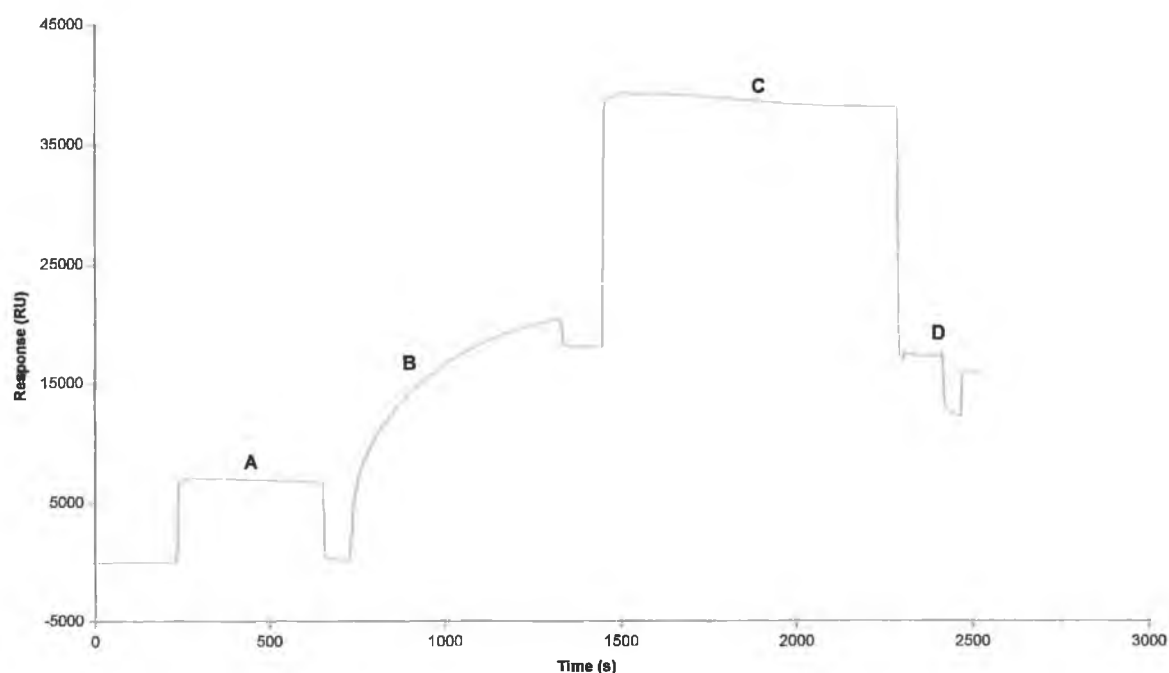


**Figure 5.39:** Immobilisation of mAbG94F8 onto the CM5 sensor chip surface. The immobilisation included an extended, 'double-capping' step, to minimise non-specific binding. (A) EDC/NHS activation, (B) covalent binding of mAb2B3 (125 µg/ml in 10 mM sodium acetate, pH 4.7) (C) capping of unreacted groups and (D), regeneration pulse of 5 mM HCl. The final level amounted to 15793.6 RUs of covalently attached mAbG94F8 was achieved.

### 5.2.3.3 Assessment of p60 protein binding to immobilised mAbG94F8

The specific activity of the mAbG94F8-CM5 surface, with respect to p60 protein was demonstrated by injecting fresh supernatant sample, from a *L. monocytogenes* culture at exponential growth in BHI broth, across the sensor surface. The supernatant was filtered using a 0.2 µm cut-off syringe filter to remove cells/particulate debris, before being injected. In addition, a neat sample of IMAC-purified rp60 was also injected across the surface. Following on-line reference subtraction, the overlaid binding interaction curves indicated response levels of approximately 64 and 634 RUs, respectively (Figure 5.40).



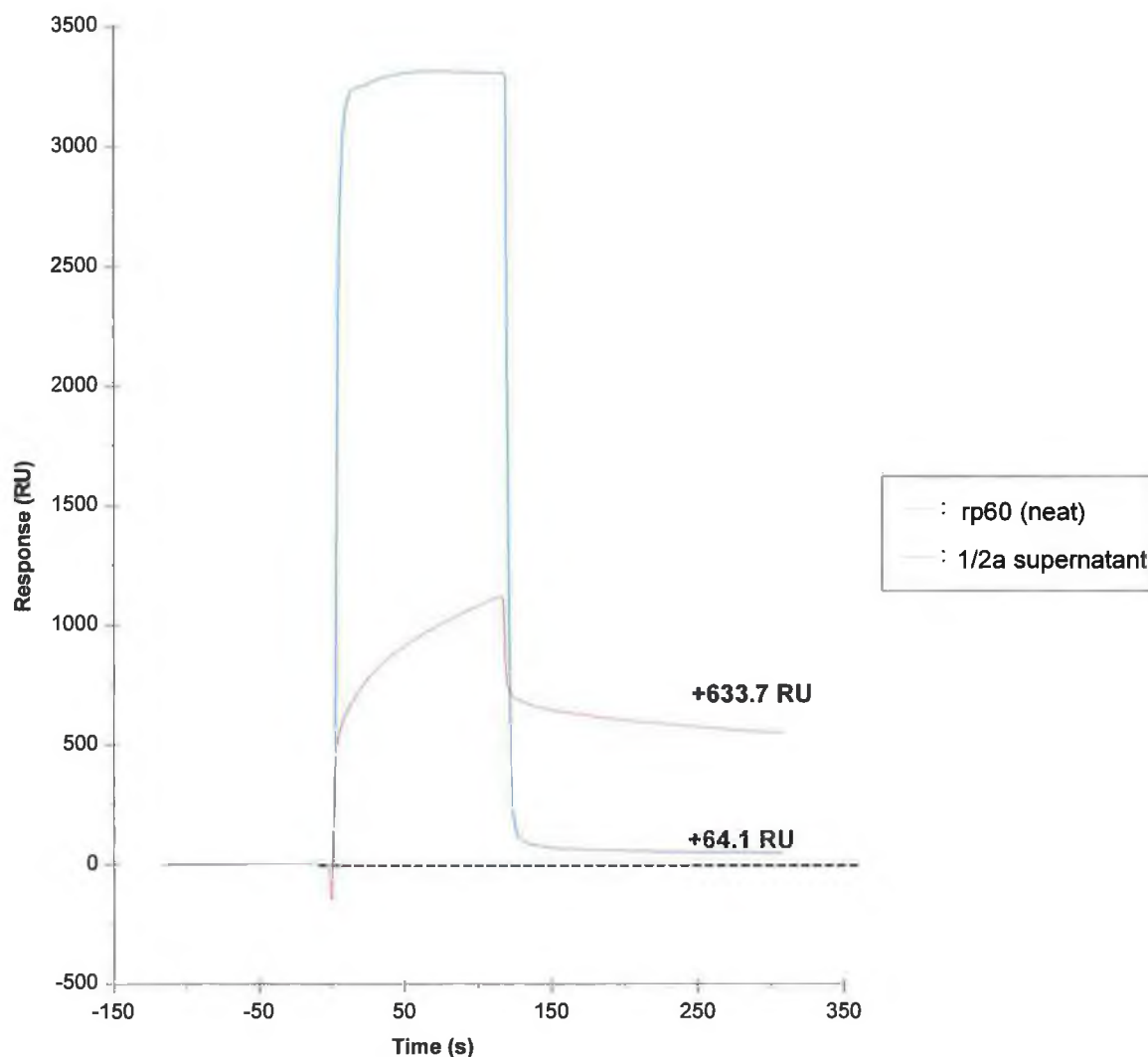


**Figure 5.40:** Sensorgram depicting binding of p60 to immobilised mAbG94F8. A 20  $\mu$ l sample of neat, IMAC-purified rp60 (red) and sterile filtered culture supernatant from a *L. monocytogenes* 1/2a culture in BHI broth was injected over the mAbG94F8-CM5 surface at a flow rate of 10  $\mu$ l/min. The broken line indicates the baseline response. Binding responses of 633.7 and 64.1 were recorded for the rp60 and culture supernatant samples, respectively.

#### 5.2.3.4 Immobilisation of rp60 onto the CM5 sensor chip surface

The findings of Sections 5.2.3.1-5.2.3.3, above, which confirmed that mAbG94F8 was reacting with p60 and not LLO, were in agreement with cross-reactivity results outlined in Section 3.2.2.4. The latter indicated that mAbG94F8 reacted specifically with a 60 kDa protein, present in the supernatant of each of the representative *L. innocua* and *L. ivanovii* species' tested. Although *L. ivanovii* produces a variant haemolysin, termed 'ivanolysin', *L. innocua* is a known non-haemolytic species.





Thus, in terms of the principle objective of this thesis (i.e. the specific detection of *L. monocytogenes*), the mAbG94F8 antibody was not ideal, due to the lack of species specificity and the fact that it is predominantly secreted into the culture medium. Nonetheless, the ability to specifically detect p60 protein in enrichment media may have potential implications for the development of a 'presumptive' test platform as a reliable indicator of listerial contamination. With this in mind, it was deemed a useful exercise to investigate the possibility of employing the SPR-based biosensor to specifically detect listerial p60 protein. This was assessed in a series of exploratory, empirically optimised experiments.

Immobilisation was performed using the standard EDC/NHS covalent attachment process (Sections 2.10.2, 5.2.1.1 and 5.2.1.2). Due to the extreme basicity of rp60, with a predicted pI of ~9.3, pre-concentration was not performed. Instead, immobilisation was conducted at the highest pI that is recommended as acceptable for EDC/NHS-mediated coupling. As this was significantly lower than 9.5, it was predicted to effectively preconcentrate the rp60 onto the CM-dextran matrix. An immobilised level of approximately 7500 RUs was achieved (Figure 5.41).

#### **5.2.3.5 Preliminary assessment of binding to the rp60-CM5 sensor chip surface**

Given the high intrinsic pI of rp60 (~9.3), it was anticipated that it would exhibit a significantly positive charge in HBS running buffer (pH 7.4). Experimentally, this manifested as a strong, non-specific ionic preconcentration (~2297 RUs) onto the negatively charged, unmodified CM-dextran matrix, following a two minute injection of rp60 at 25 µg/ml (Figure 5.42). When the same sample was passed over the rp60-immobilised surface, there was also substantial, yet significantly less binding (~1080 RUs) apparent. The net reduction in overall non-specific binding was attributed to the rp60 immobilisation step which effectively blocked, or 'capped' most of the charged or reactive carboxyl moieties. The incorporation of a 'double-capping' step (Figure 5.41) rendered it unlikely that substantial residual uncapped carboxyl groups were the main source of the non-specific pre-concentration of p60. It was felt most probable that rp60 was actually non-specifically 'binding to itself'. Thus, when an inhibition test was attempted, the antibody control (i.e. mAbG94F8 in HBS buffer, with no free rp60 antigen), generated a lower apparent binding response (105 RUs), than when incubated with excess rp60 protein (1080.1 RUs) (Figure 5.42). This could be interpreted as a combined response of individual non-specific binding of rp60 and specific binding of mAbG94F8 to available rp60 ligand on the chip surface. This would suggest that the mAbG94F8-rp60 interaction was not competitive in solution and re-affirm the suspicion of non-specific rp60-rp60 interaction. However, this assumption was in clear contradiction of the inhibition-ELISA outlined in Section 3.2.2.3, which clearly demonstrated that mAbG94F8



was capable of binding p60, albeit, the non-recombinant, crude extract version, in solution. It is plausible that the exaggerated binding response was actually a cumulative response for successfully bound mAbG94F8-rp60 complex, binding to the immobilised rp60, predominantly via the non-specific rp60-rp60 interaction. It was difficult to definitively resolve the binding pattern demonstrated in Figure 5.42. However, what was clearly apparent was, that these non-specific contributions rendered the sensor format unreliable for detection of free p60.

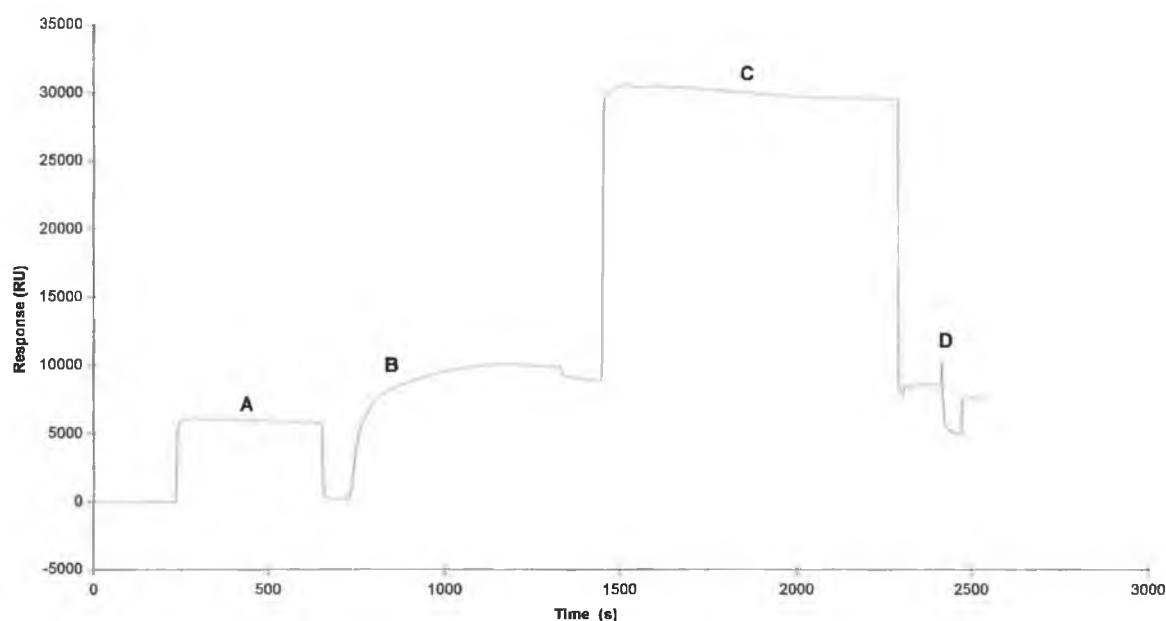


**Figure 5.41:** Immobilisation of rp60 onto the CM5 sensor chip surface. The immobilisation included a 'double-capping' step, to minimise non-specific binding. (A) EDC/NHS activation, (B) covalent binding of rp60 (100 µg/ml in 10 mM sodium acetate, pH 6.0) (C) capping of unreacted groups and (D), regeneration pulse of 5 mM HCl. A final level of 7543.8 RUs of covalently attached mAbG94F8 was achieved.



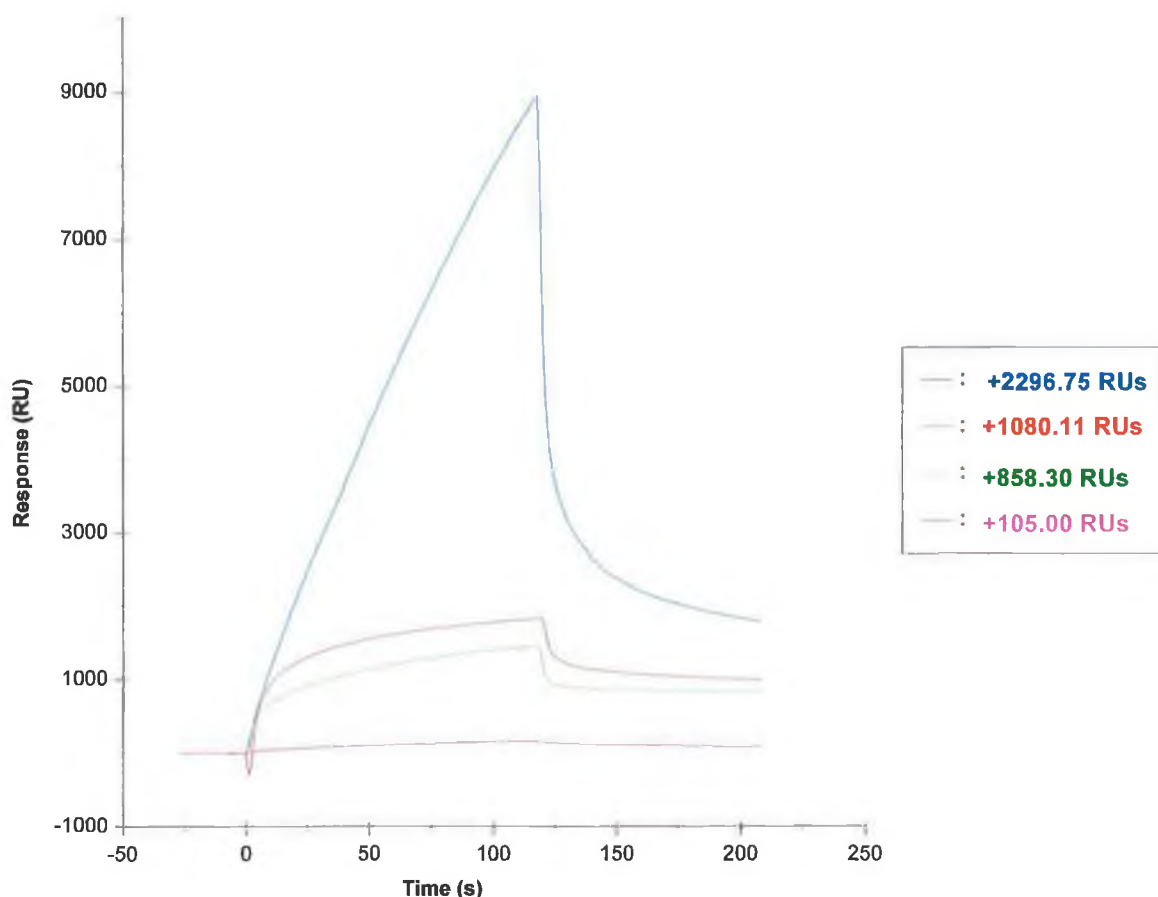


**Figure 5.42:** Preliminary binding profile of mAbG94F8 to rp60-CM5 surface. The colour-coded binding curves represent as follows: (blue), a 1:1 mixture of rp60 diluted 1/5 in HBS and HBS buffer alone (effective rp60 dilution of 1/10) injected across a blank, unmodified CM-dextran surface; (green), the same effective 1/10 rp60 solution injected across the rp60-immobilised CM5 surface; (pink), a 1/1000 dilution of mAbG94F8 in HBS injected across the rp60-immobilised CM5 surface and (red), a 1:1 mixture of rp60 diluted 1/5 in HBS and a 1/500 dilution of mAbG94F8 in HBS injected across the rp60-immobilised CM5 surface. The flow rate used throughout was 10  $\mu\text{l}/\text{min}$  and 20  $\mu\text{l}$  of each sample was injected. All curves were subjected to on-line reference subtraction and were overlayed, aligned and normalised using BIAevaluation<sup>TM</sup> software. Comparative binding response levels were taken 30 seconds after the end of each sample injection and the values are indicated in the inset box. Cumulatively, the data suggests strong non-specific binding of rp60 to CM-dextran and possibly rp60 itself, also.



### 5.2.3.6 The effect of salt concentration on binding to the rp60-CM5 surface

In an effort to reduce the contribution to non-specific binding, of the ionic interactions, a salt titration was conducted. NaCl concentrations of up to 0.5 M have been reported to reduce non-specific binding contributions in complex matrices such as urine and serum (Johansson and Hellenäs, 2004). mAbG94F8 at a 1/200 dilution and rp60 at a 1/500 dilution were empirically selected for analysis, since at these respective dilutions, both analytes generated comparative net binding responses of between 200 and 250 RUs. Across the range of NaCl concentrations assayed, the degree of non-specific binding of free rp60 to the immobilised rp60-CM5 surface decreased gradually from ~250 to ~50 RUs (Figure 5.43). However, across the same salt concentration range, the specific mAbG94F8 binding response remained constant and was essentially, unaffected.

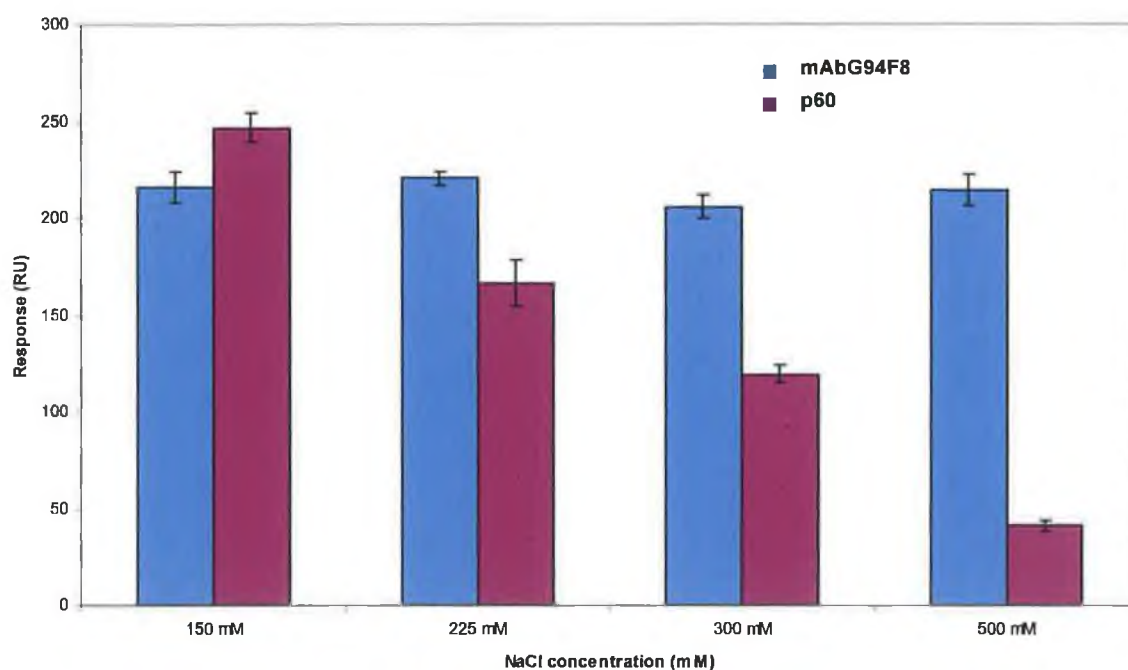


**Figure 5.43:** Effect of buffer NaCl concentration on binding to the rp60-CM5 surface. mAbG94F8 at a 1/200 dilution (blue) and rp60 at a 1/500 dilution (purple), were passed over the rp60-CM5 surface at 5  $\mu$ l/min for two minutes and the mean binding response level plotted. The data is the average of triplicate measurements. The response levels were measured in HBS buffer containing 0.150, 0.225, 0.300 and 0.500 M NaCl.





### 5.2.3.7 Immobilisation of rp60 onto the B1 sensor chip surface

The B1 sensor chip is equivalent to the generic CM5 sensor chip in terms of its hydrogel content, yet it contains 70 % less carboxyl groups. Therefore, it was postulated that the lower overall level of carboxylation would reduce the propensity for non-specific, cationic surface effects. Due to the reduced availability of available carboxyl groups and concomitant lower ligand immobilisation capacity, it was essential that the activation step of the immobilisation process was maximised. Thus, a 'double-activation' was employed and in addition, rp60 was used at twice the concentration (i.e. 200 µg/ml) and twice the volume that was used with the CM5 surface, to ensure the surface immobilisation capacity was fully saturated. Ethylenediamine was used as a capping agent instead of ethanolamine as a final precaution against non-specific binding. The final level of immobilised rp60 was, as expected, low (2163 RUs), yet it was sufficient for binding analysis (Figure 5.44). A comparable negative control surface was prepared by double-activation and diethylamine-capping of a downstream flow cell surface.

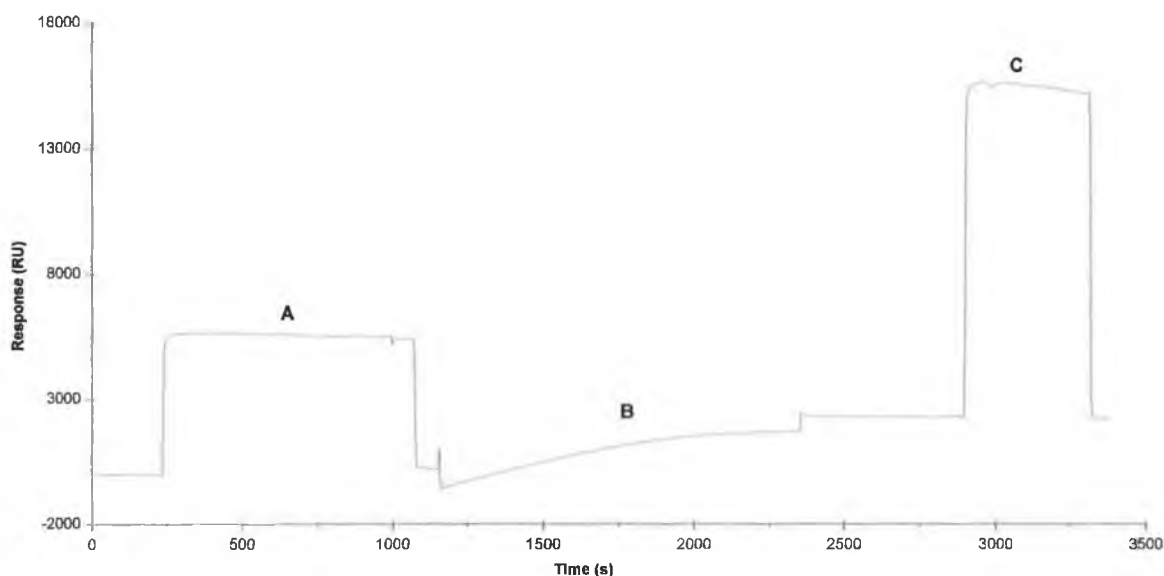


**Figure 5.44:** Immobilisation of rp60 onto the B1 sensor chip surface. The immobilisation included a 'double-capping' step, to minimise non-specific binding. (A) EDC/NHS activation, (B) covalent binding of rp60 (200 µg/ml in 10 mM sodium acetate, pH 6.0) and (C), capping of unreacted groups with ethylenediamine instead of ethanolamine. A final level of 2162.5 RUs of covalently attached rp60 was achieved.



### 5.2.3.8 Optimisation of binding to the rp60-B1 sensor chip surface

The individual binding responses of mAbG94F8 and rp60 were compared (Figure 5.45) on the rp60-B1 chip, using HBS running buffer containing 0.5 M NaCl. When the raw response curves were compared with the responses on the blank, 'capped' B1 reference surface, there was a net binding response of 192.75 RUs generated by specific mAbG94F8 binding. Conversely, a negligible response of ~2.5 RUs was demonstrated when free rp60 was injected. This indicated that the rp60-B1 chip was indeed less susceptible to non-specific binding.

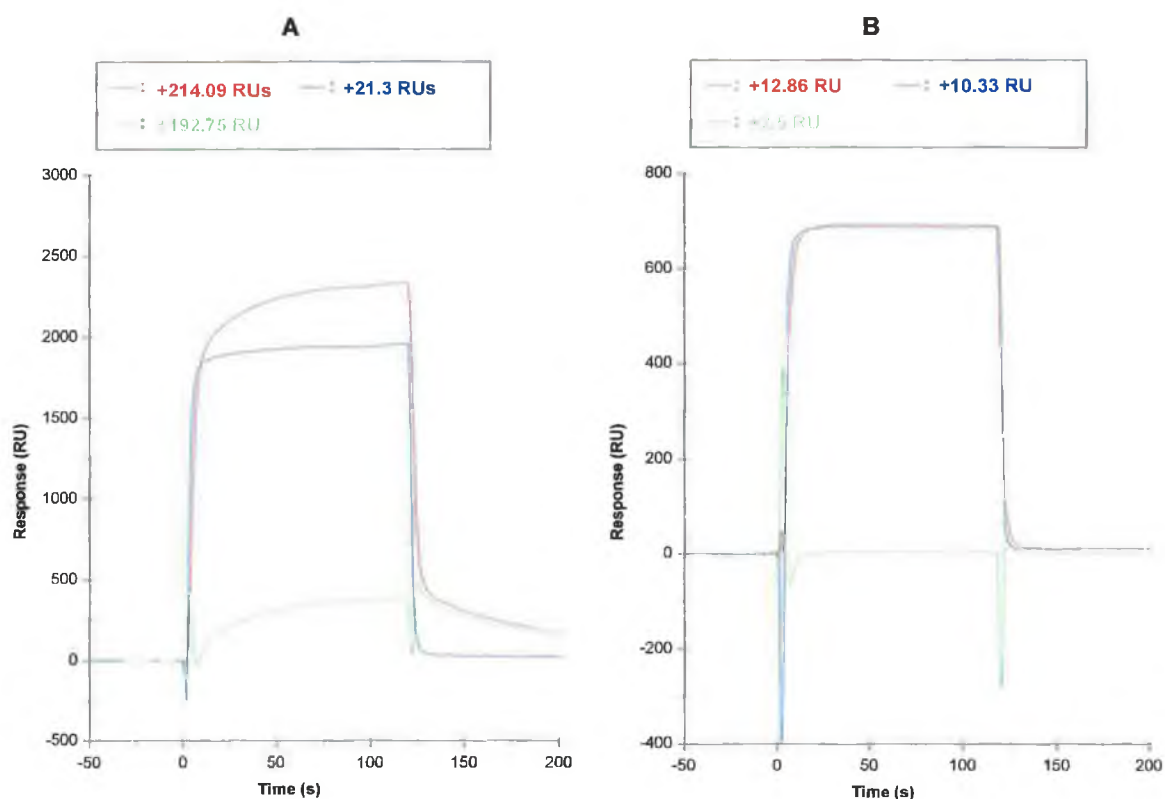


**Figure 5.45:** Comparison of mAbG94F8 (A) and free rp60 (B) binding to the rp60-B1 chip surface. The specific binding responses of mAbG94F8 (left) at a 1/50 dilution in HBS containing 0.5 M NaCl and rp60 (right), at a 1/100 dilution were compared following a two minute injection at 10  $\mu$ l/min. The red, blue and green colour-coding refers to the rp60-B1 surface response, control surface response and the reference-subtracted response, respectively. The sensorgrams were overlayed, aligned and normalised using BIAevaluation™ software. The net binding response elicited by mAbG94F8 was 192.7 RUs, while that elicited by free rp60 was negligible.



In order to conclusively demonstrate the specificity of the mAbG94F8-rp60 interaction using the rp60-immobilised B1 sensor chip, the reference subtracted responses of mAbG94F8 following pre-incubation at 37 °C in a 1:1 ratio with HBS alone and rp60, respectively, were compared (Figure 5.46). The clear reduction in net binding of mAbG94F8 was indicative of successful solution-phase inhibition and thus, confirmed that the complicated non-specific binding anomalies could be overcome by judicious buffer and surface optimisation.

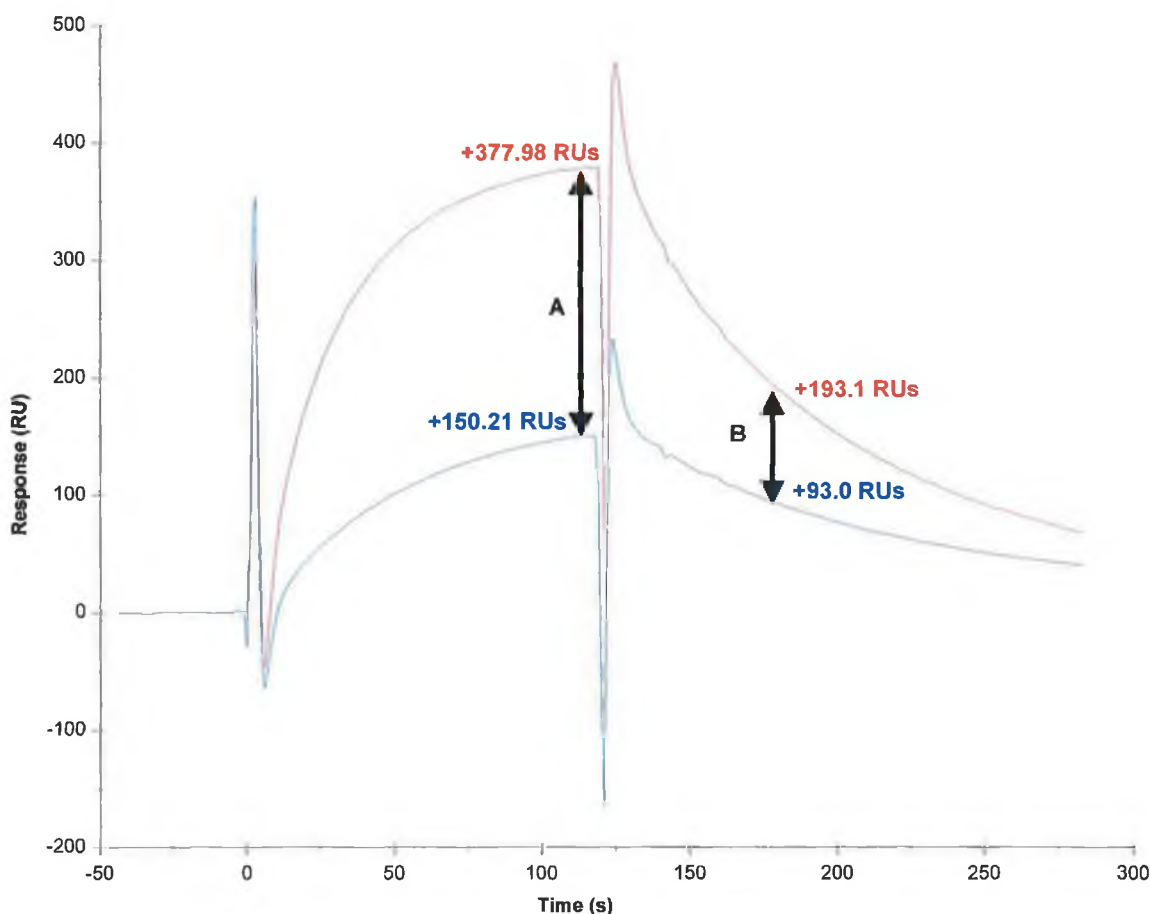


**Figure 5.46:** Solution-phase inhibition of mAbG94F8 binding to the rp60-B1 chip. The curves represent reference-subtracted binding response of a 1/25 dilution of mAbG94F8 following pre-incubation at 30 °C in a 1:1 ratio with HBS buffer alone (red) and a 1/50 dilution of rp60 (blue), respectively. Samples were injected for two minutes at a constant flow rate of 5 µl/min. The sensorgrams were overlaid, aligned and normalised using BIAevaluation™ software. The difference in Req response values (A) was approximately 277.77 RUs, and one minute after the end of the injection the response difference was approximately 100 RUs (B). The reduction in binding response clearly indicates significant specific, solution-phase binding of mAbG94F8 to rp60.



### 5.3 *Summary and conclusions*

The principle aim of this chapter was to evaluate the potential of employing a SPR biosensor-based, approach to facilitate direct and label-free detection of *L. monocytogenes*. This incorporated further characterisation of the *L. monocytogenes*-specific reagents described in Chapters 3 and 4.

The core achievement encompassed the demonstration of ‘real-time’ monitoring of direct binding of *L. monocytogenes* cells to the species-specific monoclonal antibody ‘mAb2B3’. It was found that optimal cell binding was achieved when mAb2B3 antibody was covalently attached, through amine-coupling, to a fully dextranated CM5 sensor chip hydrogel surface. Comparative analysis of these findings with recent reports in the literature revealed similar observations. Conversely, cells failed to bind efficiently to mAb2B3 antibody that was covalently linked to the equivalent non-dextranated, planar C1 sensor chip surface, despite the fact that this particular chip is actually marketed specifically for the detection of cells and other macromolecular entities. The binding levels achieved were comparable with those recently reported by Clyne and co-workers (2004), for specific capture of *Helicobacter pylori* cells with a compatible receptor ligand, covalently attached to a CM5 sensor chip surface. However, no attempts had previously been made to explain the improved cell binding at the hydrogel surface. A critical explanation was thus postulated, that accommodated consensus thermodynamic and fluid dynamic perspectives. A central tenet was the substantial elasticity exhibited by the dextran polymer and intrinsic translational and rotational mobility, which it conferred upon the covalently attached ligand. This facilitated multiple bond formation between the ubiquitously distributed InlA protein, on the cell surface, and the immobilised antibodies, which was sufficient to overcome the avidity-threshold required for stable cell binding at the hydrogel surface. Correspondingly, the accessibility and constitutive expression of InlA on the *L. monocytogenes* cell surface, was viewed as a quintessential factor in the success of the direct cell binding strategy.

Subsequently, it was demonstrated that a number of representative *Listeria* spp., other than *L. monocytogenes*, and a selection of non-*Listeria* genus bacteria failed to elicit a binding signal. Similarly, binding of *L. monocytogenes* cells was totally abrogated following treatment of the cells at 80 °C for an extended period. The results mirrored those observed in the ELISA-based characterisation of the mAb2B3-*L. monocytogenes* cell binding interaction, outlined in Chapter 3. These observations were interpreted as extremely significant, as they contribute to the possibility of reducing the false positive detection of non-pathogenic *Listeria* spp. and





heat-killed, non-viable/non-virulent *L. monocytogenes* cells, which are limitations associated with many of the currently available immuno- and DNA-based detection methods. They also, further reinforce the significance of the exclusivity of InlA to *L. monocytogenes*, and the associated cell topography.

Using the direct binding assay it was possible to detect *L. monocytogenes* cells at concentrations approaching  $1 \times 10^7$  cells/ml. In light of several reports that binding of a secondary antibody to captured cells resulted in enhanced response signals, a sandwich-type strategy was investigated, as a means of improving the sensitivity. However, two polyclonal antibodies, known to react with *Listeria* cells, failed to elicit any discernable signal improvement when passed over captured *L. monocytogenes* cells. This particular observation mirrored the findings of Lathrop and co-workers, (2003). Furthermore, as already alluded to, the threshold avidity was the principle limit to the assay sensitivity. More specifically, effective capture of cells at the sensor surface was only possible when then the cell concentration was sufficiently high to satisfy the combined thermodynamic, fluid dynamic and intracellular charge determinants that defined the avidity-treshold. Thus, it was unlikely that even substantial binding of secondary antibody would enhance detection limits to significantly below  $1 \times 10^7$  cells/ml.

The specific binding of mAb2B3 to rInlA was also confirmed through SPR-based characterisation of the interaction. Various immobilisation strategies were investigated with respect to rInlA. This was viewed as necessary, since the projected development of a standardised SPR-based competitive or inhibition assay format, pursuant to this research, was envisaged as a means of achieving greater sensitivity. Optimised immobilisation of rInlA was also required to facilitate estimation of the steady-state equilibrium affinity of mAb2B3 to rInlA. Initially, direct covalent attachment of rInlA to a CM5 sensor chip surface by amine-coupling, was favoured because of the stable and robust covalent linkage it conferred and the 're-usability' offered under conditions of optimised sample buffer and regeneration conditions.

Surprisingly, the estimated steady-state affinity, as represented by the apparent  $K_D$ , was quite low ( $2.23 \times 10^{-7}$  M). However, this estimate was interpreted tentatively, due to the fact that the apparent surface activity of the immobilised rInlA was calculated to be much lower than the theoretical prediction. This was attributed to the random nature of the immobilisation strategy. To overcome this limitation, a ligand capture approach was investigated. The initial capture strategy took advantage of the His-tag that had been incorporated at the rInlA C-terminal and available NTA-based chelating sensor chip technology. Unfortunately, with the NTA sensor



chip arrangement there was pervading non-specific binding of mAb2B3 to the  $\text{Ni}^{2+}$ -charged NTA matrix. Most of the non-specific binding was efficiently abrogated using sample buffer, at pH 6.25, in the presence of a high salt concentration (0.5 M). However, since the NTA chip arrangement did not facilitate 'on-line' reference subtraction, it was regarded as unreliable for the determination of affinity data. Such complications are probably the reason why the use of NTA sensor chips is infrequently reported in the literature.

In order to overcome the limitations of the NTA-based capture approach, an alternative strategy was investigated. This entailed the use of an anti-His-tag monoclonal antibody, which was immobilised to a CM5 surface through amine-coupling. This was not subject to non-specific binding artefacts and also, facilitated 'on-line' referencing of sensorgram data. However, the format was complicated by the fact that rInlA rapidly dissociated from the anti-His-tag surface. Thus, 'double-referencing' had to be incorporated in order to resolve the complex steady-state equilibrium binding profile represented by the cumulative raw sensorgram data. The association constant was estimated to be  $1.93 \times 10^{-7}$  M, which was comparable with the estimate obtained using the covalently immobilised rInlA surface. In addition, despite careful attention to ensure optimal orientation of the rInlA molecule, the concomitant improvement in apparent activity of the captured ligand was still substantially less than the predicted level.

It was concluded that the sub-optimal activity was caused by inherent anomalies within the rInlA molecule. Subsequent analysis indicated that the rInlA had assumed a multimeric disposition in solution, specifically a tetrameric conformation. This is an issue that will need to be addressed prior to incorporation of the rInlA molecule into any solution-phase assay format.

Although it had not been possible to confirm the specificity of mAbG94F8 for p60 protein using ELISA, it was possible to do this using Biacore. It was clearly demonstrated that mAbG94F8 bound specifically to a sensor chip surface with rp60 attached and not to one with rLLO attached. Furthermore, pursuant to the suggestion that the mAbG94F8 antibody could potentially be used in a presumptive or indicator test for listerial presence (Section 3.2.2.4), the possibility of performing such a test using the Biacore sensor was investigated. Despite the very high pI exhibited by p60 and its inherent 'stickiness', conditions were optimised that facilitated specific binding of p60 to be monitored in real-time.



***Chapter 6***  
***Overall Summary and Conclusions***



## 6.1 Overall summary and conclusions

The overall aim of this work was to develop a monoclonal antibody suitable for use in assays for the specific detection of *L. monocytogenes* cells, as detailed in Chapters 3, 4 and 5.

In Chapter 3, preliminary studies focussed on the production of antibodies to enriched protein fractions that had been derived from active cultures of pathogenic *L. monocytogenes*. The first monoclonal antibody was isolated following immunisation of mice with an enriched *L. monocytogenes* culture supernatant that had been crudely fractionated. This antibody reacted specifically with a 60 kDa protein present in the culture supernatant. It was initially unclear whether this protein was p60 or LLO. Following a comparative analysis of the antibody reactivity to extracellular proteins derived from various, representative *Listeria* spp., it was demonstrated that the antibody bound to a 60 kDa protein present in the supernatant of *L. monocytogenes*, *L. ivanovii* and *L. innocua*. Although *L. ivanovii* is known to produce a LLO homologue, *L. innocua* does not. Moreover, p60 homologous proteins are prevalent throughout the genus and thus, binding of the antibody to *L. innocua*-derived 60 kDa extracellular protein, was taken to indicate that the protein being recognised was indeed p60. This assumption was later verified by comparative SPR-based analysis of antibody binding to recombinant p60- and recombinant LLO-immobilised sensor chip surfaces. Despite the clear cross-reactivity with *L. innocua*- and *L. ivanovii*-derived proteins, it was suggested that the antibody could, potentially, be used for the presumptive detection of listerial contamination.

A second monoclonal antibody was produced using a more rational and targeted approach. This entailed immunising mice with a known *L. monocytogenes* pathogenicity marker protein, in this case, 'InlB'. The cell-membrane-anchored InlB protein was isolated using a crude, yet, highly efficient extraction protocol. Subsequently, a monoclonal antibody was raised against the InlB-enriched extract. The antibody bound to the extract in both inhibition-ELISA and Western blot formats. The specificity of the antibody for InlB was further confirmed by demonstrating binding to a recombinant version of the full-length mature InlB protein. Unfortunately, the antibody failed to bind strongly to whole *L. monocytogenes* cells. Interestingly, the antibody seemed to bind slightly better to heat-treated *L. monocytogenes* cells. It was thus, postulated that, perhaps the antibody bound to a region of the free InlB protein that was not freely accessible in the cell-bound form. This was a reasonable assumption, given the common assertion that InlB remains partially buried within the major cell wall structure. However, it was subsequently revealed, through epitope-profiling, that the antibody specifically bound to a sequence in the outermost and, thus, most exposed InlB





domain. This emphasised the role of the overall cell surface topography, in dictating the accessibility of the surface antigen.

Based on the inability of the anti-InlB antibody to bind whole *L. monocytogenes* cells, and the significant cross-reactivity of the anti-p60 antibody with *L. innocua*, it was necessary to adopt an alternative strategy. Mice were immunised with whole *L. monocytogenes* cells, rather than isolated cell-surface or extracellular proteins. Due to the complex nature of the whole cell immunogen, it was anticipated that a correspondingly, heterogeneous population of antibodies would result. This necessitated the implementation of a negative screening format, whereby hybridoma supernatants were screened in parallel, against both *L. monocytogenes* cells, and a representative, pooled selection of non-pathogenic *Listeria* spp. (*L. welshimeri*, *L. seeligeri* and *L. innocua*). This facilitated efficient isolation of an antibody that demonstrated a clear specificity for *L. monocytogenes* cells.

Further analysis of this antibody revealed that it bound to an ~80 kDa protein, specifically present in the solubilised cell wall protein fraction of *L. monocytogenes* cells. This 80 kDa protein was putatively postulated to be InlA. However, confirmation of this assumption required further characterisation. In the absence of an available method for reliable purification of native InlA, a recombinant version was heterologously expressed in *E. coli* (Chapter 4). The protein was efficiently purified via an incorporated His-tag, using IMAC with optimised buffer components. Specific binding of the antibody to this purified recombinant protein, confirmed its classification as an anti-InlA antibody.

It was also noted that the antibody demonstrated significantly greater binding to *L. monocytogenes* cells that had been cultured in LEB media, rather than in BHI media. Furthermore, following heat inactivation of the *L. monocytogenes* cells, the ability of the anti-InlA antibody to bind cells was significantly reduced. Thus, even though InlA is expressed constitutively, at a basal level in virulent *L. monocytogenes*, extrinsic factors affect the cellular topography, which in turn dictates the accessibility of surface-localised epitopes. The lack of cross-reactivity of this antibody with non-pathogenic *Listeria* spp. and heat-inactivated *L. monocytogenes* cells was exploited in an inhibition ELISA format for specific detection of *L. monocytogenes*.

In Chapter 5 the anti-InlA antibody was evaluated in terms of its potential application in the development of a SPR-based biosensor assay format (Biacore) for specific detection of *L. monocytogenes* cells. This format was successfully demonstrated to facilitate direct, label-free



detection of *L. monocytogenes* cell binding, in real-time. It was also possible to visualise the retention of cells at the sensor surface by means of SEM and AFM image analysis. Avidity effects were crucial to the cell binding process and it was proposed that a minimum threshold avidity determinant represented the main limiting factor to efficient cell binding. Initially, it was somewhat surprising that direct covalent attachment of the monoclonal antibody yielded the most efficient cell binding activity. The possible advantages afforded by this immobilisation strategy were critically assessed in conjunction with comparable citations in the literature. Notably, the significant contributory effect of the dextran hydrogel on cell retention at the sensor surface was emphasised. In particular, the enhanced rotational and translational freedom of the hydrogel-tethered antibody was defined as a highly advantageous factor for binding of cells and macromolecular structures in general.

The SPR-based cell binding experiments reflected those obtained using ELISA (Chapter 3), insofar as, negligible binding to non-*L. monocytogenes* cells and heat-inactivated *L. monocytogenes* cells, was observed. A representative calibration curve was constructed for direct binding analysis of *L. monocytogenes* cells from which, a limit of detection approaching  $1.23 \times 10^7$  cells/ml was estimated. Despite the fact that the antibody affinity, as determined by equilibrium steady-state measurements, was not exceptionally strong ( $K_D = 1.93 \times 10^{-7}$  M) the detection limit was actually slightly lower than the limit determined using ELISA ( $1.85 \times 10^7$  cells/ml).

It is acknowledged that neither of the assay formats demonstrated remarkable sensitivity in comparison with available citations in the literature. For example, similar ELISA-based cell-binding assays report limits of detection approaching of  $1 \times 10^5$  cells/ml (Eriksson *et al.*, 1995; Leonard *et al.*, 2004). Comparable biosensor-based assays vary wildly in their reported detection limits. However, attempts to improve the sensitivity of the *L. monocytogenes* direct cell binding assay, by using a sandwich format the sensor chip surface were unsuccessful, and it is unlikely that the sensitivity can be enhanced, based on direct, evanescent field-limited interrogation. Nonetheless, it is asserted that the assays described in this research are intended for the specific detection of *L. monocytogenes* cells from pre-enriched sample cultures. Thus, it is the antibody specificity that is the quintessential defining criteria of the assay performance. The limited sensitivity achievable using SPR with respect to low concentrations of whole microorganisms (Pourshafie *et al.*, 2004) is acknowledged. However, it has been suggested that all 'rapid methods' will likely require pre-enrichment to allow cells reach detectable numbers (Karamonová *et al.*, 2003) and this is a pervading tenet in the methodologies and opinions expressed throughout this thesis.



Consequently, the key merit of the work described herein rests in the demonstrated specificity of the anti-InlA monoclonal antibody for *L. monocytogenes* cells and the successful integration of this antibody with SPR-based biosensing instrumentation to facilitate reliable detection of *L. monocytogenes* cells. These results clearly emphasised the suitability of InlA as a marker for the specific immunodetection of *L. monocytogenes*. The major advantage of the SPR-based assay was, that it exhibited a rapid sample-to-result time and obviated the need for intermittent washing and sample manipulation steps, such as are required in traditional immunoassay platforms (e.g. ELISA).

Finally, as a closing caveat, it is important to emphasise that the method described herein, although referred to as a 'real-time' detection system, does not purport to obviate the need for a period of enrichment incubation. On the contrary, it is felt that the natural follow-on to this work should focus on developing an enrichment protocol that would optimise *L. monocytogenes* selectivity, InlA expression and cultivation time, as a logical complement to the SPR-based detection method. The main virtues of the system outlined arise from the culmination of the specificity afforded by the monoclonal antibody and the rapid, one-step, label-free, 'sample-to-result' confirmation, made possible using SPR technology.

Finally, it is concluded that the most likely way to achieve the requisite sensitivity and rapid sample analysis with respect to *L. monocytogenes* detection, will be a cumulative approach using classic microbiological, immunological and biosensor-based techniques.

In terms of future work arising from this body of research, associate researchers have already begun attempts to genetically modify the anti-InlB antibody for improved cell binding ability. In addition, novel labelling techniques are being investigated, with respect to the anti-InlA antibody, in order to facilitate a more sensitive ELISA- and fluorescence-based detection formats.



***Chapter 7***  
***References***





**Aguado, V., Vitas, A.I. and García-Jalón, I. (2004).** "Characterisation of *Listeria monocytogenes* and *Listeria innocua* from a vegetable processing plant by RAPD and REA." *Int. J. Food Microbiol.*, **90**, 341-347.

**Aldus, C.F., Van Amerongen, A., Ariëns, R.M.C., Peck, M.W., Wichers, J.H. and Wyatt, G.M. (2003).** "Principles of some novel rapid dipstick methods for detection and characterisation of verotoxigenic *Escherichia coli*." *J. Appl. Microbiol.*, **95**, 380-389.

**Alexander, A.V., Walker, R.L., Johnson, B.J., Charlton, B.R. and Woods, L.W. (1992).** "Bovine abortions attributable to *Listeria ivanovii*: four cases (1988-1990)." *J. Am. Vet. Med. Assoc.*, **200**, 711-714.

**Alfthan, K. (1998).** "Surface plasmon resonance biosensors as a tool in antibody engineering." *Biosens. Bioelectron.*, **13**, 653-663.

**Allerberger, F. and Guggenbichler, J.P. (1989).** "Listeriosis in Austria: report of an outbreak in 1986." *Acta Microbiologica Hungarica*, **36**, 149-152.

**Allerberger, F., (2002).** "*Listeria*: growth, phenotypic differentiation and molecular microbiology." *FEMS Immunol. Med. Microbiol.*, **1469**, 1-7.

**Almeida, P.F. and Almeida, R.C.C. (2000).** "A PCR protocol using *inl* gene as a target for specific detection of *Listeria monocytogenes*." *Food Control*, **11**, 97-101.

**Alocilja, E.C. and Radke, S.M. (2003).** "Market analysis of biosensors for food safety." *Biosens. Bioelectron.*, **18**, 841-846.

**Alvarez-Domínguez, C., Vázquez-Boland, J.A., Carrasco-Marín, E., López-Mato, P., Leyva-Cobián, F. (1997).** "Host cell heperan sulphate proteoglycans mediate attachment and entry of *Listeria monocytogenes*, and the listerial surface protein ActA is involved in heparan sulphate receptor recognition." *Infect. Immun.*, **65**, 78-88.

**Anonymous, (2002).** "Capture of Histidine-tagged proteins using NTA or anti-histidine antibodies." BIAcore Application Note 12, BR9002-84.



**Anonymous**, Centres for Disease Control and Prevention (CDC), (2003a). Quantitative assessment of relative risk to public health from foodborne *Listeria monocytogenes* among selected categories of ready-to-eat foods. *FDA/Centre for Food Safety and Applied Nutrition, USDA/Food Safety and Inspection Service, Centres for Disease Control and Prevention, USA*, Executive summary, viii-xv.

**Anonymous**, Centres for Disease Control and Prevention (CDC), (2003b). Quantitative assessment of relative risk to public health from foodborne *Listeria monocytogenes* among selected categories of ready-to-eat foods, II-Hazard identification. *FDA/Centre for Food Safety and Applied Nutrition, USDA/Food Safety and Inspection Service, Centres for Disease Control and Prevention, USA*, Interpretive summary, 9-23.

**Anonymous**, Centres for Disease Control and Prevention (CDC). (2000b). "Multistate outbreak of listeriosis-United States." *Morbidity and Mortality Weekly Report*, **49(50)**, 1129-1130.

**Anonymous**, Centres for Disease Control and Prevention (CDC). (2001). "Outbreak of listeriosis associated with Mexican-style cheese-North Carolina, October 2000-January 2001." *Morbidity and Mortality Weekly Report*, **50**, 560-562.

**Anonymous**, Centres for Disease Control and Prevention (CDC). (2002b). "Outbreak of listeriosis-Northeastern United States, 2002." *Morbidity and Mortality Weekly Report*, **51**, 950-951.

**Anonymous, FVO**. (2002a). "Health risks from *Listeria*." Swiss Federal Vet. Office-working group on zoonoses, *FVO-magazine*, June 2002, 14-15.

**Anonymous**, World Health Organisation/Food and Agriculture Organisation of the United Nations (WHO/FAO) working group. (1988). "Foodborne listeriosis." *Bull., W.H.O.*, **66**, 421-428.

**Anonymous**, World Health Organisation/Food and Agriculture Organisation of the United Nations (WHO/FAO). (2002). "Risk assessment of *Listeria monocytogenes* in ready-to-eat foods." Interpretative Summary.

**Arizcun, C., Vasseur, C. and Labadie, J.C.** (1997). "Effect of several decontamination procedures on *Listeria monocytogenes* growing in biofilms." *J. Food Protect.*, **61**, 731-734.



**Aureli, P.,** Fioruci, G.C., Caroli, D., Marchiaro, G., Novara, O., Leone, L and Salmaso, S. (2000). "An outbreak of febrile gastroenteritis associated with corn contaminated by *L. monocytogenes*." *N. Engl. J. Med.*, 342, 1236-1241.

**Axelsson, F.** and Sorin, M.-L. (1998). "Transia Listeria-Technical handbook." Diffchamb AB, Backa Bergögata 5, S-422 46 Hisings Backa, Sweden, Publication number: THLI01-9803.

**Azadian, B.,** Finnerty, G. and Pearson, A. (1989). "Cheese-borne *Listeria* meningitis in an immunocompetent patient." *Lancet*, 1, 322-323.

**Aznar, R.** and Alarcón, B. (2003). "PCR detection of *Listeria monocytogenes*: a study of multiple factors affecting sensitivity." *J. Appl. Microbiol.*, 95, 958-966.

**Babu, Y.S.,** Bugg, C.E. and Cook, W.J. (1988). "Structure of calmodulin refined at 2.2 Å resolution." *J. Mol. Biol.*, 204, 191-204.

**Badovinac, V.P.,** Nordyke Messingham, K.A., Hamilton, S.E. and Harty, J.T. (2003). "Regulation of CD8<sup>+</sup> T cells undergoing primary and secondary responses to infection in the same host." *J. Immunol.*, 170(10), 4933-4942.

**Badovinac, V.P.,** Porter, B.B. and Harty, J.T. (2002). "Programmed contraction of CD8(+) T cells after infection." *Nat. Immunol.*, 3(7), 619-626.

**Baird, C.L.** and Myszka, D.G. (2001). "Current and emerging commercial optical biosensors." *J. Mol. Recognit.*, 14, 261-268.

**Barié, N.** and Rapp, M. (2001). "Covalent bound sensing layers on surface acoustic wave (SAW) biosensors." *Biosens. Bioelectron.*, 16, 979-987.

**Beauregard, K.E.,** Lee, K.-D, Collier, R.J. (1997). "pH-dependent perforation of macrophage phagosomes by Listeriolysin O from *Listeria monocytogenes*." *J. Exp. Med.*, 186(7), 1159-1163.

**Benedict, C.L.,** Gilfillan, S., Thai, T.H. and Kearney, J.F. (2000). "Terminal deoxynucleotidyl transferase and repertoire development." *Immunol. Rev.*, 175, 150-157.



- Benhar, I., Eshkenazi, I., Neufeld, T., Opatowsky, J., Shaky, S. and Rishpon, J. (2001).** "Recombinant single chain antibodies in bioelectrochemical sensors." *Talanta*, **55**, 899-907.
- Berche, P., Gaillard, J.-L., Geoffroy, C and Alouf, J.E. (1987).** "T cell recognition of listeriolysin O during infection with *Listeria monocytogenes*." *J. Immunol.*, **139**(11), 3813-3821.
- Bergmann, B., Rafflesbauer, D., Kuhn, M., Goetz, M., Hom, S. and Goebel, W. (2002).** "InlA- but not InlB-mediated internalisation of *Listeria monocytogenes* by non-phagocytic mammalian cells needs the support of other internalins." *Mol. Microbiol.*, **43**(3), 557-570.
- Beuchat, L.R. and Brackett, R.E. (1990).** "Survival and growth of *Listeria monocytogenes* on lettuce as influenced by shredding, chlorine treatment, modified atmosphere packaging and temperature." *J. Food Sci.*, **55**(3), 755-758.
- Beumer, R.R. and Hazeleger, W.C. (2003).** "*Listeria monocytogenes*: diagnostic problems." *FEMS Immunol. Med. Microbiol.*, **35**, 191-197.
- Beumer, R.R., Te Giffel, M.C., Anthonie, S.V.R. and Cox, L.J. (1996).** "The effect of acriflavine and nalidixic acid on the growth of *Listeria* spp. in enrichment media." *Food Microbiol.*, **13**, 137-148.
- Bhunia, A.K. (1997).** "Antibodies to *Listeria monocytogenes*." *Crit. Rev. Microbiol.*, **23**(2), 77-107.
- Bhunia, A.K., Ball, P.H., Faud, B.W., Kurz, J.W., Emerson, J.W. and Johnson, M.G. (1991).** "Development and characterisation of a monoclonal antibody specific for *Listeria monocytogenes* and *Listeria innocua*." *Infect. Immun.*, **59**, 3176-3184.
- Bierne, H. and Cossart, P. (2002).** "InlB, a surface protein of *Listeria monocytogenes* that behaves as an invasin and a growth factor." *J. Cell Sci.*, **115**, 3357-3367.
- Bierne, H., Mazmanian, S.K., Trost, M., Pucciarelli, M.G., Liu, G, Dehoux, P., Jansch, L., Carcia-del-Portillo, F., Schneewind, O., and Cossart, P. (2002).** "Inactivation of the *srtA* gene in *Listeria monocytogenes* inhibits anchoring of surface proteins and affects virulence." *Mol. Microbiol.*, **43**(4), 871-884.





**Bille, J.**, (1990). "Epidemiology of human listeriosis in Europe with special reference to the Swiss outbreak." In: *Foodborne Listeriosis*. (Miller, A.J., Smith, J.L. and Somkuti, G.A., eds.), 71-74, Elsevier, Amsterdam, Netherlands.

**Bille, J.**, Catimel, B., Bannerman, E., Jacquet, C., Yershin, M.N., Caniaux, I., Monget, D. and Rocourt, J. (1992). "API *Listeria*, a new and promising one-day system to identify *Listeria* isolates." *Appl. Environ. Microbiol.*, **58**(6), 1857-1860.

**Bille, J.**, Rocourt, J. and Swaminathan, B. (1999). "*Listeria*, *Erysipelothrix*, and *Kurthia*." In: *Manual of Clinical Microbiology*, 7<sup>th</sup> edn. (Murray, P.R., Baron, E.J., Tenover, F.C. and Tenover, R.H., eds.), 346-356. ASM Press, Washington, DC, USA.

**Birchmeir, C.** and Gerardi, E. (1998). "Developmental roles of HGF/SF and its receptor, the c-Met tyrosine kinase." *Trends Cell Biol.*, **8**, 404-410.

**Boerlin, P.** and Piffaretti, J.-C. (1991). "Typing of human, animal, food and environmental isolates of *Listeria monocytogenes* by multilocus enzyme electrophoresis." *Appl. Environ. Microbiol.*, **57**, 1624-1629.

**Boerlin, P.**, Rocourt, J., Grimont, P.A.D., Jacquet, C. and Piffaretti, J.C. (1992). "*Listeria ivanovii* subspecies *londoniensis*." *Int. J. Syst. Bacteriol.*, **15**, 42-46.

**Bohne, J.**, Kestler, H., Uebele, C., Sokolovic, Z. and Goebel, W. (1996). "Differential regulation of the virulence genes of *Listeria monocytogenes*." *Mol. Microbiol.*, **20**, 1189-1198.

**Bokken, G.C.A.M.**, Corbee, R.J., van Knapen, F. and Bergwerff, A.A. (2003). "Immunochemical detection of *Salmonella* group B, D and E using optical surface plasmon resonance biosensor." *FEMS Microbiology Letts.*, **222**, 75-82.

**Bossi, G.** and Griffiths, G.M. (1999). "Degranulation plays an essential part in regulating cell surface expression of Fas ligand in T cells and natural killer cells." *Nat. Med.*, **5**, 90-96.

**Bouwer, H.G.**, Nelson, C.S., Gibbins, B.L., Portnoy, D.A. and Hinrichs, D.J. (1992). "Listeriolysin O is a target of the immune response to *Listeria monocytogenes*." *J. Exp. Med.*, **175**(6), 1467-1471.



**Braun, L., Dramsi, S., Dedoux, P., Bierne, H., Lindahl, G. and Cossart, P. (1997).** "InlB: an invasion protein of *Listeria monocytogenes* with a novel type of surface adhesion." *Mol. Microbiol.*, **25**(2), 285-294.

**Braun, L., Ghebrehiwet, B. and Cossart, P. (2000).** "gC1q-R/p32, a C1q-binding protein, is a receptor for the InlB invasion protein of *Listeria monocytogenes*." *EMBO J.*, **19**(7), 1458-1466.

**Braun, L., Nato, F., Payrastre, B., Mazie, J.C. and Cossart, P. (1999).** "The 213-amino-acid leucine-rich repeat region of the *Listeria monocytogenes* InlB protein is sufficient for entry into mammalian cells, stimulation of the PI 3-kinase and membrane ruffling." *Mol. Microbiol.*, **34**, 10-23.

**Braun, L., Ohayon, H. and Cossart, P. (1998).** "The InlB protein of *Listeria monocytogenes* is sufficient to promote entry into mammalian cells." *Mol. Microbiol.*, **27**, 1077-1087.

**Brehm, K., Haas, A., Goebel, W. and Kreft, J. (1992).** "A gene encoding a superoxide dismutase of the facultative intracellular bacterium *Listeria monocytogenes*." *Gene*, **118**, 121-125.

**Brehm, K., Kreft, J., Ripio, M.-T. and Vázquez-Boland, J.A. (1996).** "Regulation of virulence gene expression in pathogenic *Listeria*." *Microbiología SEM*, **12**, 219-236.

**Brehm, K., Ripio, M.-T., Kreft, J., and Vázquez-Boland, J.A. (1999).** "The *bvr* locus of *Listeria monocytogenes* mediates virulence gene repression by  $\beta$ -glucosides." *J. Bacteriol.*, **181**, 5024-5032.

**Brett, M. S. Y., Short, P. and McLaughlin, J. (1998).** "A small outbreak of listeriosis associated with smoked mussels." *Int. J. Food Microbiol.*, **43**, 223-229.

**Broer, J., Wehland, J. and Chakraborty, T. (1998).** "*L. monocytogenes* metalloprotease Mpl." In: *Handbook of proteolytic enzymes*, 1<sup>st</sup> edn, (Barrett, A.J., Rawlings, N.D. and Woessner, J.F., eds.), 1050-1051, Academic Press, London, UK.

**Brown, G. and Ling, N.R. (1988).** "Murine monoclonal antibodies." In: *Antibodies, Volume 1: a practical approach*, (Catty, D., ed.), 82.



- Brunt, L.M.,** Portnoy, D.A. and Unanue, E.R. (1990). "Presentation of *Listeria monocytogenes* to CD8<sup>+</sup> T cells requires secretion of hemolysin and intracellular bacterial growth." *J. Immunol.*, **145**, 3540-3546.
- Brynda, E.,** Homola, J., Houska, M., Pfeifer, P. and Škvor, J. (1999). "Antibody networks for surface plasmon resonance immunosensors." *Sens. Actuat. B*, **54**, 132-136.
- Bubert, A.,** Kestler, H., Götz, M., Böckmann, R. and Goebel, W. (1997a). "The *Listeria monocytogenes iap* gene as an indicator gene for the study of PrfA-dependent regulation." *Mol. Gen. Genet.*, **25**, 625-654.
- Bubert, A.,** Köhler, S. and Goebel, W. (1992b). "The homologous and heterologous regions within the *iap* gene allow genus- and species-specific identification of *Listeria* spp. by polymerase chain reaction." *Appl. Environ. Microbiol.*, **58**, 2625-2632.
- Bubert, A.,** Köhler, S., Frank, R. and Goebel, W. (1994). "Synthetic peptides derived from the *Listeria monocytogenes* p60 protein as antigens for the generation of polyclonal antibodies specific for secreted cell-free *L. monocytogenes* p60 proteins." *Appl. Environ. Microbiol.*, **60**(9), 3120-3127.
- Bubert, A.,** Kuhn, M., Goebel, W. and Köhler, S. (1992a). "Structural and functional properties of the p60 proteins from different *Listeria* species." *J. Bacteriol.*, **174**, 8166-8171.
- Bubert, A.,** Riebe, J., Schnitzler, N., Schönberg, A., Goebel, W. and Schubert, P. (1997b). "Isolation of catalase-negative *Listeria monocytogenes* strains from listeriosis patients and their rapid identification by anti-p60 antibodies and/or PCR." *J. Clin. Microbiol.*, **35**(1), 179-183.
- Bubert, A.,** Sokolovic, Z., Chun, S.K., Papatheodorou, L., Simm and Goebel, W. (1999). "Differential expression of *Listeria monocytogenes* virulence genes in mammalian host cells." *Mol. Gen. Genet.*, **261**, 232-336.
- Buchanan, R.L.,** Damert, W.G., Whiting, R.C. and van Schothorst, M. (1997). "Use of epidemiological and food survey data to estimate a purposefully conservative dose-response relationship for *Listeria monocytogenes* levels and incidence of listeriosis." *J. Food Protect.*, **68**(8), 918-922.



- Buchrieser, C.,** Rusniok, C., The *Listeria* Consortium, Kunst, F., Cossart, P. and Glaser, P. (2003). "Comparison of the genome sequences of *Listeria monocytogenes* and *Listeria innocua*: clues for evolution and pathogenicity." *FEMS Immunol. Med. Microbiol.*, **35**, 207-213.
- Buckle, P.E.,** Davies, R.J., Kinning, T., Yeung, D., Edwards, P.R., Pollard-night, D. and Lowe, C.R. (1993). "The resonant mirror: a novel optical sensor for direct sensing of biomolecular interactions-Part II: Applications." *Biosens. Bioelectron.*, **8**, 355-363.
- Bula, C.J.,** Bille, J. and Glauser, M.P. (1995). "An epidemic of food-borne listeriosis in western Switzerland: description of 57 cases involving adults." *Clin. Infect. Dis.*, **20**(1), 66-72.
- Buncic, S.,** Avery, S.M., Rocourt, J. and Dimitrijevic, M. (2001). "Can food-related environmental factors induce different behaviour in two key serovars, 4b and 1/2a, of *Listeria monocytogenes*?" *Int. J. Food Microbiol.*, **65**, 201-212.
- Burton, D.R.,** Pyati, J., Koduri, R., Sharp, S.J., Thornton, G.B., Parren, P.W.H.I., Sawyer, L.S.W., Hendry, R.M., Dunlop, N., Nara, P.L., Lamacchia, M., Garratty, E., Stiehm, E.R., Bryson, Y.J., Cao, Y., Moore, J.P., Ho, D.D. and Barbas, C.A. III. (1994). "Efficient neutralization of primary isolates of HIV-1 by a recombinant human monoclonal antibody." *Science*, **266**, 1024-1027.
- Butler, J.E.,** Ni, L., Nessler, R., Joshi, K.S., Suter, M., Rosenberg, B., Chang, J., Brown, W.R. and Canterero, L.A. (1992). "The physical and functional behaviour of capture antibodies adsorbed onto polystyrene." *J. Immunol. Meth.*, **150**, 77-90.
- Butman, B.T.,** Plank, M.C., Durham, R.J. and Mattingly, J.A. (1988). "Monoclonal antibodies which identify a genus-specific *Listeria* antigen." *Appl. Environ. Microbiol.*, **54**, 1564-1569.
- Cabanes, D.,** Dehoux, P., Dussurget, O., and Cossart, P. (2004). "Auto, a surface protein of *Listeria monocytogenes* required for entry into eukaryotic cells and virulence." *Mol. Microbiol.*, **51**(6), 1601-1614.





**Cabanes, D.**, Dehoux, P., Dussurget, O., Frangeul, L. and Cossart, P. (2002). "Surface proteins and the pathogenic potential of *Listeria monocytogenes*." *Trends Microbiol.*, **10**(5), 238-245.

**Camilli, A.**, Tilney, L.G. and Portnoy, D.A. (1993). "Dual roles of *plcA* in *Listeria monocytogenes* pathogenesis." *Mol. Microbiol.*, **8**, 143-157.

**Canterero, L.A.**, Butler, J.E. and Osborne, J.W. (1980). "The adsorptive characteristics of proteins for polystyrene and their significance in solid-phase immunoassays." *Anal. Biochem.*, **105**, 375.

**Canziani, G.**, Klakamp, S. and Myszka, D.G. (2004). "Kinetic screening of antibodies from crude hybridoma samples using BIAcore." *Anal. Biochem.*, **325**, 301-307.

**Capps, K.L.**, McLaughlin, E.M., Murray, A.W., Aldus, C.F., Wyatt, G.M., Peck, M.W, Van Amerongen, A., Ariens, R.M., Wichers, J.H., Baylis, C.L., Waering, D.R. and Bolton, F.J. (2004). "Validation of three rapid screening methods for detection of verotoxin-producing *Escherichia coli*: interlaboratory study." *J. AOAC Int.*, **87**(1), 68-77.

**Carrero, J.A.**, Calderon, B. and Unanue, E.R. (2004). "Listeriolysin O from *Listeria monocytogenes* is a lymphocyte apoptogenic molecule." *J. Immunol.*, **172**(8), 4866-4874.

**Chakraborty, T.**, Hain, T. and Domann, E. (2000). "Genome organisation and the evolution of the virulence gene locus in *Listeria* species." *Int. J. Med. Microbiol.*, **290**, 167-174.

**Chakraborty, T.**, Leimeister-Wächter, M., Domann, E., Hartl, M., Goebel, W., Nichterlein, T. and Notermans, S. (1992). "Coordinate regulation of virulence genes in *L. monocytogenes* requires the product of the *prfA* gene." *J. Bacteriol.*, **174**, 568-574.

**Chico-Calero, I.**, Suárez, M., González-Zorn, B., Scotti, M., Slaghuis, J. and Goebel, W. (2002). "Hpt, a bacterial homolog of the microsomal glucose-6-phosphate translocase, mediates rapid intracellular proliferation in *Listeria*." *Proc. Natl. Acad. Sci. USA*, **99**, 431-436.

**Chothia, C.** and Lesk, A.M (1987). "Canonical structures for the hypervariable regions of immunoglobulins." *J. Mol. Biol.*, **196**, 901-917.



**Ciclitira, P.J.**, Ellis, H.J., Richards, D. and Kemeny, D.M. (1986). "Gliadin-specific IgG subclass antibodies in patients with celiac disease." *Int. Arch. Allergy Appl. Immunol.*, **80**, 258-261.

**Cline, J.**, Braman J.C. and Hogrefe, H.H. (1996) "PCR fidelity of *Pfu* DNA polymerase and other thermostable DNA polymerases." *Nucleic Acids Res.*, **24(18)**, 3546-3551.

**Clyne, M.**, Dillon, P., Daly, S., O'Kennedy, R., May, F.E.B., Westley, B.R. and Drumm, B. (2004). "*Helicobacter pylori* interacts with the human single-domain trefoil protein TFF1." *Proc. Natl. Acad. Sci. USA*, **101(19)**, 7409-7414.

**Cocolin, L.**, Rantsiou, K., Iacumin, L., Catoni, C. and Comi, G. (2002). "Direct identification of *Listeria* spp. and *Listeria monocytogenes* by molecular methods." *Appl. Environ. Microbiol.*, **68(12)**, 6273-6282.

**Coconnier, M.H.**, Dlissi, E., Robard, M., Laboissee, C.L., Gaillard, J.L. and Servin, A.L. (1998). "*Listeria monocytogenes* stimulates mucin exocytosis in polarized non-secreting intestinal cells through action of listeriolysin O." *Infect. Immun.*, **66**, 3673-3681.

**Coconnier, M.H.**, Lorrot, M., Barbat, A., Laboissee, C.L. and Servin, A.L. (2000). "Listeriolysin O-induced stimulation of mucin exocytosis in polarized non-secreting intestinal cells: evidence for toxin recognition of membrane-associated lipids and subsequent toxin internalization through caveolae." *Cell. Microbiol.*, **2(6)**, 487-504.

**Coffey, A.**, Van Den Burg, B., Veltman, R. and Abee, T. (2000). "Characteristics of the biologically active 35-kDa metalloprotease virulence factor from *L. monocytogenes*." *J. Appl. Microbiol.*, **88(1)**, 132-141.

**Collins, A.M.**, Sewell, W.A. and Edwards, M.R. (2003). "Immunoglobulin gene rearrangement, repertoire diversity, and the allergic response." *Pharmacology and Therapeutics*, **100**, 157-170.

**Collins, M.D.**, Wallbanks, S., Lane, D.J., Shah, J., Nietupski, R., Smida, J., Dorsch, M. and Stackebrandt, E. (1991). "Phylogenetic analysis of the genus *Listeria* based on reverse transcriptase sequencing of 16S rRNA." *Int. J. Syst. Bacteriol.*, **41**, 240-246.



**Cornu, M.**, Kalmokoff, M. and Flandrois, J.-P. (2002). "Modelling the competitive growth of *Listeria monocytogenes* and *L. innocua* in enrichment broths." *Int. J. Food Microbiol.*, **73**, 261-274.

**Cossart, P.** and Lecuit, M. (1998). "Interactions of *Listeria monocytogenes* with mammalian cells during entry and actin-based movement: bacterial factors, cellular ligands and signalling." *EMBO J.*, **17**(14), 3797-3806.

**Cossart, P.** and Mengaud, J. (1989). "*Listeria monocytogenes*: a model system for the molecular study of intracellular parasitism." *Mol. Biol. Med.*, **6**, 463-474.

**Cossart, P.**, (2001). "Met, the HGF-SF receptor: another receptor for *Listeria monocytogenes*." *Trends in Microbiology.*, **9**(3), 105-107.

**Cossart, P.**, Pizarro-Cerdá, J. and Lecuit, M. (2003). "Invasion of mammalian cells by *Listeria monocytogenes*: functional mimicry to subvert cellular function." *Trends in Cell Biol.*, **13**(1), 23-31.

**Cossart, P.**, Vicente, M.F., Mengaud, J., Baquero, F., Perez-Diaz, J.C. and Berche, P. (1989). "Listeriolysin O is essential for virulence of *Listeria monocytogenes*: direct evidence obtained by gene complementation." *Infect. Immun.*, **57**, 3629-3636.

**Cummins, A.J.**, Fielding, A.J. and McLaughlin, J. (1993). "*Listeria ivanovii* infection in a patient with AIDS." *J. Infect.*, **28**, 89-91.

**Curiale, M.S.** and Lewis, C. (1994). "Detection of *Listeria monocytogenes* in samples containing *Listeria innocua*." *J. Food Protect.*, **57**, 1048-1051.

**da Silva, M.C.D.**, Destro, M.T., Hofer, E. and Tibana, A. (2001). "Characterisation and evaluation of some virulence markers of *Listeria monocytogenes* strains isolated from Brazilian cheeses using molecular, biochemical and serotyping techniques." *Int. J. Food Microbiol.*, **63**, 275-280.

**Dalton, C.B.**, Austin, C.C., Sobel, J., Hayes, P.S., Bibb, W.F., Graves, L.M., Swaminathan, B., Proctor, M.E. and Griffin, P.M. (1997). "An outbreak of gastroenteritis and fever due to *Listeria monocytogenes* in milk." *N. Engl. J. Med.*, **336**, 100-105.



- Daly, S., Keating, G.J., Dillon, P.P., Manning, B.M. and O’Kennedy, R. (2000).** “Development of surface plasmon resonance immunoassay for aflatoxin B1.” *J. Agric. Food Chem.*, **48**, 5097-5104.
- Danilova, N.P. (1994).** “ELISA screening of monoclonal antibodies to haptens- influence of the chemical structure of hapten-protein conjugates.” *J. Immunol. Meth.*, **173(1)**, 111-117.
- Darji, A., Bruder, D., Zur Lage, S., Gerstel, B., Chakraborty, T., Wehland, J. and Weiss, S. (1998).** “The role of the bacterial membrane protein ActA in immunity and protection against *Listeria monocytogenes*.” *J. Immunol.*, **161**, 2414-2420.
- Darji, A., Chakraborty, T., Niebuhr, K., Tsonis, N., Wehland, J. and Weiss, S. (1995a).** “Hyperexpression of listeriolysin in the non-pathogenic species *Listeria innocua* and high yield purification.” *J. Biotechnol.*, **43**, 205-212.
- Darji, A., Chakraborty, T., Wehland, J. and Weiss, S. (1995b).** “Listeriolysin generates a route for the presentation of exogenous antigens by major histocompatibility complex class I.” *Eur. J. Immunol.*, **25**, 2967-2971.
- De Bruijn, H.E., Kooyman, R.P.H. and Greve, J. (1992).** “Choice of metal and wavelength for SPR sensors: some considerations.” *Appl. Optics*, **31**, 440-442.
- De Chastellier, C. and Berche, P., (1994).** “Fate of *Listeria monocytogenes* in murine macrophages: evidence for simultaneous killing and survival of intracellular bacteria.” *Infect. Immun.*, **62**, 543-553.
- de Valk, H., Vaillant, V., Jacquet, C., Rocourt, J., Le Querrec, F., Stainer, F., Quelquejeu, N., Pierre, O., Pierre, V., Descenclos, J.C. and Goulet, V. (2001).** “Two consecutive nationwide outbreaks of listeriosis in France, October 1999-February 2000.” *Am. J. Epidemiol.*, **154**, 944-950.
- Decatur, A.L. and Portnoy, D.A. (2000).** “A PEST-like sequence in listeriolysin O essential for *Listeria monocytogenes* pathogenicity.” *Science*, **290(5493)**, 992-995.
- Deisingh, A.K. (2003).** “Biosensors for microbial detection.” *Microbiologist*, **4(2)**, 30-33.





**Deisingh, A.K.** and Thompson, M. (2004a). "Strategies for the detection of *Escherichia coli* O157:H7." *J. Appl. Microbiol.*, **96**, 419-429.

**Deisingh, A.K.** and Thompson, M. (2004b). "Biosensors for the detection of bacteria." *Can. J. Microbiol.*, **50**(2), 69-77.

**DeMarco, D.R.** and Lim, D.V. (2002). "Detection of *Escherichia coli* O157:H7 in 10- and 20-gram ground beef samples with an evanescent-wave biosensor with silica and polystyrene waveguides." *J. Food Protect.*, **65**(4), 596-602.

**DeMarco, D.R.**, Saaski, E.W., McCrae, D.A. and Lim, D.V. (1999). "Rapid detection of *Escherichia coli* O157:H7 in ground beef using a fibre-optic biosensor." *J. Food Protect.*, **62**, 711-716.

**Deneer, H.G.** and Boychuk, I. (1991). "Species-specific detection of *Listeria monocytogenes* by DNA amplification." *Appl. Environ. Microbiol.*, **57**(2), 606-609.

**Dhar, G.**, Faull, K.F. and Schneewind, O. (2000). "Anchor structure of cell wall proteins in *Listeria monocytogenes*." *Biochem.*, **39**, 3725-3733.

**Diamond, D.** (1998). "*Principles of Chemical and Biological Sensors*." (Diamond, D., ed.), Wiley, N.Y., *Chem. Anal.*, **150**.

**Diaz, M.** and Casali, P. (2002). "Somatic immunoglobulin hypermutation." *Curr. Opin. Immunol.*, **14**, 235-240.

**Dickneite, C.**, Böckmann, R., Spory, A., Goebel, W. and Sokolovic, Z. (1998). "Differential interaction of the transcription factor PrfA and the PrfA-activating factor (Paf) of *Listeria monocytogenes* with target sequences." *Mol. Microbiol.*, **27**, 915-928.

**DiMaio, H.** (2000). "*Listeria* infection in women." *Prim. Care Update Ob/Gyns.*, **7**, 40-45.

**Directive 92/95/EEC** (1992). European Parliament and Council Official Journal of the European Communities 1992, L 268/1, 14<sup>th</sup> September, 1992.

**Directive 93/43/EEC** (1993). European Parliament and Council Official Journal of the European Communities 1993, L 175/1, 19<sup>th</sup> July, 1993.



**Domann E.,** Wehland, J., Rohde, M., Pistor, S., Hartl, M., Goebel, W., Leimeister-Wächter, M., Wünscher, M. and Chakraborty, T. (1992). "A novel bacterial virulence gene in *Listeria monocytogenes* required for host cell microfilament interaction with homology to the proline-rich region of vinculin." *EMBO J.*, **11**, 1981-1990.

**Domann, E.,** Leimeister-Wächter, M., Goebel, W. and Chakraborty, T. (1991). "Molecular cloning, sequencing, and identification of a metalloprotease gene from *Listeria monocytogenes* that is species specific and physically linked to the listeriolysin gene." *Infect. Immun.*, **59**, 65-72.

**Donnelly, C.W.** (2001). "*Listeria monocytogenes*: a continuing challenge." *Nut. Revs.*, **59**(6), 183-194.

**Dorner, T.** Foster, S.J., Farner, N.L. and Lipsky, P.E. (1998). "Somatic hypermutation of human immunoglobulin heavy chain genes: targeting of RGYW motifs on both DNA strands." *Eur. J. Immunol.*, **28**, 3384-3396.

**Dorozynski, A.** (2000). "Seven die in French *Listeria* outbreak." *Brit. Med. J.*, **320**, 601.

**Doumith, M.,** Cazalet, C., Simoes, N., Frangeul, L., Jacquet, C., Kunst, F., Martin, P., Cossart, P., Glaser, P. and Buchrieser, C. (2004). "New aspects regarding evolution and virulence of *Listeria monocytogenes* revealed by comparative genomics and DNA arrays." *Infect. Immun.*, **72**, 1072-1083.

**Doyle, M.E.** (2001). "Virulence characteristics of *Listeria monocytogenes*." University of Wisconsin, *Food Research Institute Briefings*, October 2001, 1-13.

**Doyle, M.P.,** and Schoeni, J.L. (1997). "Comparison of procedures for isolating *Listeria monocytogenes* in soft, surface-ripened cheese." *J. Food Protect.*, **48**, 4-6.

**Dramsi, S.** and Cossart, P. (2002). "Listeriolysin O: a genuine cytolysin optimised for an intracellular parasite." *J. Cell Biol.*, **156**, 943-946.

**Dramsi, S.** and Cossart, P. (2003). "Listeriolysin O-mediated calcium influx potentiates entry of *Listeria monocytogenes* into human Hep-2 epithelial cells." *Infect. Immun.*, **71**, 3614-3618.



- Dramsi, S., Biswas, I., Maguin, E., Braun, L., Mastroeni, P. and Cossart, P. (1995).** "Entry of *Listeria monocytogenes* into hepatocytes requires expression of InlB, a surface protein of the internalin multigene family." *Mol. Microbiol.*, **16**, 251-261.
- Dramsi, S., Dehoux, P., Lebrun, M., Goosens, P.L. and Cossart, P. (1997).** "Identification of four new members of the internalin multigene family of *Listeria monocytogenes* EGD." *Infect. Immun.*, **65**, 1615-1625.
- Dramsi, S., Kocks, .C, Forestier, C. and Cossart, P. (1993).** "Internalin-mediated invasion of epithelial cells by *Listeria monocytogenes* is regulated by the bacterial growth state, temperature, and the pleiotropic activator prfA." *Mol. Miocrobiol.*, **9(5)**, 931-941.
- Drevets, D.A. (1999).** "Dissemination of *Listeria monocytogenes* by infected phagocytes." *Infect. Immun.*, **67**, 3512-3517.
- Drevets, D.A., Sawyer, R.T., Potter, T.A. and Campbell, P.A. (1995).** "*Listeria monocytogenes* infects human endothelial cells by two distinct mechanisms." *Infect. Immun.*, **63**, 4268-4276.
- Duggan, J. and Philips, C.A. (1998).** "*Listeria* in the domestic environment." *Nut. Food Sci.*, **2**, 73-79.
- Dumont, J. and Cotoni, L. (1921).** "Bacille semblable à celui du rouget du porc rencontré dans le L.C.R. d'un méningitique." *Ann. Inst. Pasteur*, **35**, 625-633.
- Dussurget, O., Cabanes, D., Dehoux, P., Lecuit, M., Buchrieser, C., The European *Listeria* Consortium, Glaser, C., and Cossart, P. (2002).** "*Listeria monocytogenes* bile salt hydrolase is a PrfA-regulated virulence factor involved in the intestinal and hepatic phases of listeriosis." *Mol. Microbiol.*, **45(4)**, 1095-1106.
- Dussurget, O., Pizarro-Cerdá, J. and Cossart, P. (2004).** "Molecular determinants of *Listeria monocytogenes* virulence." *Annu. Rev. Microbiol.*, **58**, 587-610.
- Dykes, G.A. and Moorhead, S.M. (2000).** "Survival of osmotic and acid stress by *Listeria monocytogenes* strains of clinical or meat origin." *Int. J. Food Microbiol.*, **56**, 161-166.



**Ebe, Y., Hasegawa, G., Takatsuka, H., Umez, H., Mitsuyama, M., Arakawa, M., Mukaida, N. and Naito, M. (1999).** "The role of Kupffer cells and regulation of neutrophil migration into the liver by macrophage inflammatory protein-2 in primary listeriosis in mice." *Pathol. Int.*, **49**, 519-532.

**Edelson, B.T. and Unanue, E.R. (2001).** "Intracellular antibody neutralises *Listeria* growth." *Immunity*, **14**, 503-512.

**Elgert, K.D. (1996)** "Antibody structure and function." In: *Immunology: understanding the immune system*. John Wiley and Sons Inc., New York, USA, 58-103.

**Engelbrecht, F., Dickneite, C., Lampidis, R., Gotz, M., DasGupta, U. and Goebel, W. (1998a).** "Sequence comparison of the chromosomal regions encompassing the internalin C genes (*inlC*) of *Listeria monocytogenes* and *L. ivanovii*." *Mol. Gen. Genet.*, **257**(2), 186-197.

**Engelbrecht, F., Domínguez-Bernal, G., Hess, J., Dickneite, C., Greiffenberg, L., Lampidis, R., Raffelsbauer, D., Daniels, J.J., Kreft, J., Kaufmann, S.H., Vázquez-Boland, J.A. and Goebel, W. (1998b).** "A novel PrfA-regulated chromosomal locus, which is specific for *L. ivanovii*, encodes two small, secreted internalins and contributes to virulence in mice." *Mol. Microbiol.*, **30**(2), 405-417.

**Ericsson, H., Eklöw, A., Danielson-Tham, M.-L., Loncarevic, S., Mentzing, L.-O, Persson, I., Unnerstad, H. and Tham, W. (1997).** "An outbreak of listeriosis suspected to have been caused by rainbow trout." *J. Clin. Microbiol.*, **35**, 2904-2907.

**Ericsson, H., Stålhandske, P., Danielson-Tham, M.-L., Bannerman, E., Bille, J., Jacquet, C., Rocourt, J., Ursing, J. and Tham, W. (1996).** "Division into five groups by REA of the most frequently isolated phagovar of *Listeria monocytogenes* in Sweden 1976-1985." *Med. Microbiol. Letts.*, **5**, 3872-3874.

**Eriksson, P.V., Di Paola, G.N., Pasetti, M.F. and Manghi, M.A. (1995).** "Inhibition enzyme-linked immunosorbent assay for detection of *Pseudomonas fluorescens* on meat surfaces." *Appl. Environ. Microbiol.*, **61**(1), 397-398.

**Ermolaeva, S., Novella, S., Vega, Y., Ripio, M.-T., Scotti, M. and Vázquez-Boland, J.A. (2004).** "Negative control of *Listeria monocytogenes* virulence genes by a diffusible autorepressor." *Mol. Microbiol.*, **52**(2), 601-611.





**Eshhar, Z.** (1985). "Monoclonal antibody strategy and techniques." (Springer, T.A., ed.), Plenum Press, New York, 3-41.

**Esvan, H., Minet, J., Lacie, C. and Cormier, M.** (2000). "Protein variations in *Listeria monocytogenes* exposed to high salinities." *Int. J. Food Microbiol.*, **55**, 151-155.

**Farber, J.M.** (1991). "Health risk assessment of *Listeria monocytogenes* in Canada." *Int. J. Food Microbiol.*, **30**, 145-156.

**Farber, J.M. and Hartwig, J.** (1996). "The Canadian position on *Listeria monocytogenes* in ready-to-eat foods." *Int. J. Food Microbiol.*, **30**, 145-156.

**Farber, J.M. and Peterkin, P.I.** (1991). "*Listeria monocytogenes*, a foodborne pathogen." *Microbiol. Rev.*, **55**, 476-511.

**Feeney, A.J., Victor, K.D., Vu, K., Nadel, B. and Chukwuocha, R.U.** (1994). "Influence of the V(D)J recombination mechanism on the formation of the primary T and B cell repertoires." *Semin. Immunol.*, **6**, 155-163.

**Fernandez-Garayzabal, J.F., Suarez, G., Blanco, M.M., Gibello, A. and Domínguez, L.** (1996). "Taxonomic note: a proposal for reviewing the interpretation of the CAMP reaction between *Listeria monocytogenes* and *Rhodococcus equi*." *Int. J. Syst. Bacteriol.*, **46**, 832-834.

**Fiala, G. and Stetter, K.D.** (1986). "*Pyrococcus furiosus* sp. Nov. represents a novel genus of marine heterotrophic archaeobacteria growing optimally at 100 °C." *Arch. Microbiology*, **145**, 56.

**Findlay, J.W.A., Smith, W.C., Lee, J.W., Nordblom, G.D., Das, I., DeSilva, B.S., Khan, M.N. and Bowsher, R.R.** (2000). "Validation of immunoassays for bioanalysis: a pharmaceutical industry perspective." *J. Pharma. Biomed. Anal.*, **21**, 1249-1273.

**Finlay, B.B. and Ruschkowski, S.** (1991). "Cytoskeletal rearrangements accompanying *Salmonella* entry into epithelial cells." *J. Cell. Sci.*, **99**, 283-296.

**Fitzpatrick, J., Fanning, L., Hearty, S., Leonard, P., Manning, B.M. Quinn, J.G. and O'Kennedy, R.** (2000). "Applications and recent developments in the use of antibodies for analysis." *Anal. Letts.*, **33**, 2563-2609.



**Flaherty, K.M.,** Zozulya, S., Stryer, L. and McKay, D.B. (1993). "Three-dimensional structure of recoverin, a calcium sensor in vision." *Cell*, **75**, 709-716.

**Fleming, D.W.,** Cochi, S.L., MacDonald, K.L., Brondum, J., Hayes, P.S., Plikaytis, B.D., Holmes, M.B., Audurier, A., Broome, C.V. and Reingold, A.L. (1985). "Pasteurised milk as a vehicle of infection in an outbreak of listeriosis." *New Engl. J. Med.*, **312**(7), 404-407.

**Fluit, A.C.,** Torensma, R., Klapwijk, P. and Verhoef, J., (1993). "Detection of *Listeria monocytogenes* in cheese with the magnetic immuno-polymerase chain reaction assay." *Appl. Environ. Microbiol.*, **59**, 1289-1293.

**Foote, J. and** Eisen, H.N. (1995). "Kinetic and affinity limits on antibodies produced during immune responses." *Proc. Natl. Acad. Sci. USA*, **92**, 1254-1256.

**Fratamico, P.M.,** Strobaugh, T.P., Medina, M.B. and Gehring, A.G. (1998). "Detection of *Escherichia coli* O157:H7 using a surface plasmon resonance biosensor." *Biotechnology Techniques*, **12**(7), 571-576.

**Freitag, N.E.,** Rong, L. and Portnoy, D.A. (1993). "Regulation of the *prfA* transcriptional activator of *Listeria monocytogenes*: multiple promoter elements contribute to intracellular growth and cell-to-cell spread." *Infect. Immun.*, **61**, 2537-2544.

**Frischknecht, F. and** Way, M. (2001). "Surfing pathogens and the lessons learned for actin polymerisation." *Trends in Cell Biology*, **11**(1), 30-38.

**Frye, D.M.,** Zweig, R., Sturgeon, J., Tormey, M., Le Cavalier, M., Lee, I., Lawani, L. and Mascola, L. (2002). "An outbreak of febrile gastroenteritis associated with *Listeria monocytogenes*." *Clin. Infect. Dis.*, **35**, 943-949.

**Gaillard, J.L.,** Berche, P., Frehel, C., Gouin, E. and Cossart, P. (1991). "Entry of *Listeria monocytogenes* is mediated by internalin, a repeat protein reminiscent of surface antigens from Gram-positive cocci." *Cell*, **65**, 1127-1141.

**Galán, J.E.** (2000). "Alternative strategies for becoming an insider: lessons from the bacterial world." *Cell*, **103**, 363-366.



**Garrec, N.,** Dilasser, F., Pourcher, A.M., Perelle, S. and Fach, P. (2003). "Comparison of a cultural method with ListerScreen plus Rapid'L.mono or PCR-ELISA methods for the enumeration of *L. monocytogenes* in naturally contaminated sewage sludge." *J. Microbiol. Meth.*, **55**, 763-773.

**Gauss, G.H.** and Lieber, M.R. (1996). "Mechanistic constraints on diversity in human V(D)J recombination." *Mol. Cell. Biol.*, **16**, 258-269.

**Gavalchin, J.,** Tortorello, M.L., Malek, R., Landers, M. and Batt, C.A. (1991). "Isolation of monoclonal antibodies that react preferentially with *Listeria monocytogenes*." *Food Microbiol.*, **8**, 325-330.

**Geignat, G.,** Nichterlein, T., Kretschmar, M., Schenk, S., Hof, H., Lalic-Multhaler, M., Goebel, W. and Bubert, A. (1999). "Enhancement of the *Listeria monocytogenes* p60-specific CD4 and CD8+ T cell memory by non-pathogenic *Listeria innocua*." *J. Immunol.*, **162**, 4781-4789.

**Geignat, G.,** Schenk, S., Skoberne, M., Goebel, W. and Hof, H. (2001). "A novel approach of direct ex vivo epitope mapping identifies dominant and subdominant CD4 and CD8 T cell epitopes from *Listeria monocytogenes*." *J. Immunol.*, **166**, 1877-1884.

**Gekara, N.O.** and Weiss, S. (2004). "Lipid rafts clustering and signalling by listeriolysin O." *Biochem. Soc. Trans.*, **32**, 712-714.

**Gentschev, I.,** Sokolovic, Z., Köhler, S., Krohne, G.F., Hof, H., Wagner, J. and Goebel, W. (1992). "Identification of p60 antibodies in human sera and presentation of this listerial antigen on the surface of attenuated *Salmonellae* by the HlyB-HlyD secretion system." *Infect. Immun.*, **60**, 5091-5098.

**Geoffroy, C.,** Gaillard, J.-L., Alouf, J.E. and Berche, P. (1989). "Production of thiol-dependent haemolysins by *Listeria monocytogenes* and related species." *J. Gen. Microbiol.*, **135**, 481-487.

**Geoffroy, C.,** Gaillard, J.-L.L., Alouf, J.E. and Berche, P. (1987). "Purification, characterisation and toxicity of the sulphhydryl-activated hemolysin listeriolysin O from *L. monocytogenes*." *Infect. Immun.*, **55**, 1641-1646.



**Geoffroy, C.,** Raveneau, J., Beretti, J., Lecroisey, A., Vázquez-Boland, J., Alouf, J.E. and Berche, P. (1991). "Purification and characterisation of an extracellular 29-kilodalton phospholipase C from *Listeria monocytogenes*." *Infect. Immun.*, **59**, 2382-2388.

**Gerner-Smidt, P.,** Weischer, M., Jensen, A. and Fredriksen, W. (1995). "Listeriosis in Denmark- results of a 10 year survey." In: *XIII Int. Symp. Problems of Listeriosis*, Perth, Western Australia, Promaco Coventions Pty Ltd., 472.

**Gershon, P.D.** and Khilko, S. (1995). "Stable chelating linkage for reversible immobilization of oligohistidine tagged proteins in the BIAcore surface plasmon resonance detector." *J. Immunol. Meth.*, **183**, 65-76.

**Giammarini, C.,** Andreoni, F., Amagliani, G., Casiere, A., Barocci, S. and Magnani, M. (2003). "High-level expression of the *Listeria monocytogenes* Listeriolysin O in *Escherischia coli* and preliminary characterization of the purified protein." *Protein expression and production*, **28**, 78-85.

**Gillis, E.H.,** Gosling, J.P., Sreenan, J.M. and Kane, M. (2002). "Development and validation of a biosensor-based immunoassay for progesterone in bovine milk." *J. Immunol. Meth.*, **267**, 131-138.

**Girard, K.F.,** Sbarra, A.J. and Bardawil, W.A. (1963). "Serology of *Listeria monocytogenes*. I. Characteristics of the soluble hemolysin." *J. Bacteriol.*, **85**, 349-355.

**Glaser, P.,** Frangeul, L., Buchrieser, C., Rusniok, C., Amend, A., Baquero, F., Berche, P., Bloecker, H., Brandt, P., Chakraborty, T., Charbit, A., Chetouani, F., Couve, E., de Daruvar, A., Dehoux, P., Domann, E., Domínguez-Bernal, G., Duchaud, E., Durant, L., Dussurget, O., Entian, K.-D., Fsihi, H., Portillo, F.G.-D., Garrido, P., Gautier, L., Goebel, W., Gómez-López, N., Hain, T., Hauf, J., Jackson, D., Jones, L.M., Kaerst, U., Kreft, J., Kuhn, M., Kunst, F., Kurapkat, G., Madueño, E., Maitournam, A., Vicente, J.M., Ng, E., Nedjari, H., Nordsiek, G., Novella, S., de Pablos, B., Pérez-Díaz, J.C., Purcell, R., Remmel, B., Rose, M., Schlueter, T., Simoes, N., Tierrez, A., Vázquez-Boland, J.A., Voss, H., Wehland, J. and Cossart, P. (2001). "Comparative genomics of *Listeria* species." *Science*, **294**, 849-852.

**Glass, A.,** Walsh, C.M., Lynch, D.H. and Clark, W.R. (1996). "Regulation of the Fas lytic pathway in cloned CTL." *J. Immunol.*, **156**, 3638-3644.





**Gledel, J.** (1987). "Epidemiology and significance of listeriosis in France." In: *Joint HHO/ROI consultation on prevention and control* (Schönberg, A, Ed.), 9-20.

**Glomski, I.J.,** Gedde, M.M., Tsang, A.W., Swanson, J.A. and Portnoy, D.A. (2002). "The *Listeria monocytogenes* hemolysin has an acidic pH optimum to compartmentalize activity and prevent damage to infected host cells." *J. Cell Biol.*, **156**(6), 1029-1038.

**Goldfine, H.** and Knob, C. (1992). "Purification and characterisation of *Listeria monocytogenes* phosphatidylinositol-specific phospholipase C." *Infect. Immun.*, **60**, 4059-4067.

**Goldfine, H.** Wadsworth, S.J. and Johnston, N.C. (2000). "Activation of host phospholipases C and D in macrophages after infection with *Listeria monocytogenes*." *Infect. Immun.*, **68**, 5735-5741.

**Golnazarian,, C.A.,** Donnelly, C.W., Pintauro, S.J. and Howard, D.B. (1989). "Comparison of infectious dose of *Listeria monocytogenes* F5817 as determined for normal versus compromised C57B1/6J mice." *J. Food Protect.*, **52**, 696-701.

**Golsteyn Thomas, E.J.,** King, R.K., Burchak, J. and Gannon, V.P. (1991). "Sensitive and specific detection of *Listeria monocytogenes* in milk and ground beef with the polymerase chain reaction." *Appl. Environ. Microbiol.*, **57**(9), 2576-2580.

**Gordon II, J.G.** and Ernst, S. (1980). "Surface plasmons as a probe of the electrochemical interface." *Surface Sci.*, **101**, 499-506.

**Gouin, E.,** Dehoux, P., Mengaud, J., Kocks, C. and Cossart, P. (1995). "*iactA* of *Listeria ivanovii*, althoughdistantly related to *Listeria monocytogenes actA*, restores actin tail formation in a *L. monocytogenes actA* mutant." *Infect. Immun.*, **63**, 2729-2737.

**Gouin, E.,** Mengaud, J. and Cossart, P. (1994). "The virulence gene cluster of *Listeria monocytogenes* is also present in *Listeria ivanovii*, an animal pathogen, and *Listeria seeligeri*, a nonpathogenic species." *Infect. Immun.*, **62**, 3550-3553.

**Goulet, V.,** Jacquet, C., Vaillant, V., Rebiere, I., Mouret, E., Lorente, C., Maillot, E., Stainer, F. and Rocourt, J. (1995). "Listeriosis from consumption of raw-milk cheese." *Lancet*, **345**, 1581-1582.



**Goulet, V.,** Rocourt, J., Rebiere, I., Jacquet, C., Moyse, C., Dehaumont, P., Salvat, G. and Veit, P. (1998). "Listeriosis outbreak associated with the consumption of rillettes in France in 1993." *J. Infect. Dis.*, **177**, 155-160.

**Gray, M.L.** and Killinger, A.H. (1966). "*Listeria monocytogenes* and listeric infections." *Bacteriol. Revs.*, **30(2)**, 309-340.

**Gray, M.L.,** Stafseth, H.J., Thorp, F., Sholl, L.B. and Riley, W.F. (1948). "A new technique for isolating listerellae from the bovine brain." *J. Bacteriol.*, **55**, 471-476.

**Gregory, S.H.,** Sagnimeni, A.J. and Wing, E.J. (1997). "Internalin B promotes the replication of *Listeria monocytogenes* in mouse hepatocytes." *Infect. Immun.*, **65(12)**, 5137-5141.

**Greiffenberg, L.,** Goebel, W., Kim, K.S., Weiglein, I., Bubert, A., Engelbrecht, F. (1998). "Interaction of *Listeria monocytogenes* with human brain microvascular endothelial cells: InlB-dependent invasion, long-term intracellular growth and spread from macrophages to endothelial cells." *Infect. Immun.*, **66**, 5620-5267.

**Grenklo, S.,** Geese, M., Lindberg, U., Wehland, J., Karlsson, R. and Sechi, A.S. (2003). "A crucial role for profilin-actin in the intracellular motility of *Listeria monocytogenes*. *EMBO Reports*, **4(5)**, 523-529.

**Grif, K.,** Hein, I., Wagner, M., Brandl, E., Mpamuga, O., McLaughlin, J., Dierich, M.P. and Allerberger, F. (2001). "Prevalence and characterisation of *Listeria monocytogenes* in faeces of healthy Austrians." *Wien. Klin. Wochenschr.*, **113**, 737-742.

**Grundling, A.,** Gonzalez, M.D. and Higgins, D.E. (2003). "Requirement of the *Listeria monocytogenes* broad-range phospholipase PC-PLC during infection of human epithelial cells." *J. Bacteriol.*, **185**, 6295-6307.

**Gunasinghe, C.P.G.L.,** Henderson, C. and Rutter, M.A. (1994). "Comparison study of two plating media (PALCAM and Oxford) for detection of meat products following a variety of enrichment procedures." *Lett. Appl. Microbiol.*, **18**, 156-158.



**Guzman, C.A.**, Domann, E., Rhode, M., Bruder, D., Darji, A., Weiss, S., Wehland, J., Chakraborty, T. and Timmis, K.N. (1996). "Apoptosis of mouse dendritic cells is triggered by listeriolysin, the major virulence determinant of *Listeria monocytogenes*." *Mol. Microbiol.*, **20**, 119-126.

**Haas, A.** and Goebel, W. (1992). "Microbial strategies to prevent oxygen-dependent killing by phagocytes." *Free Rad. Res. Commun.*, **16**, 137-157.

**Haas, C.N.**, Thayyar-Madabusi, A., Rose, J.B. and Gerba, C.P. (1999). "Development and validation of dose-response relationship for *Listeria monocytogenes*." *Quantitative Microbiol.*, **1**, 89-102.

**Haasnoot, W.**, Cazemier, G., Koets, M. and Van Amerongen, A. (2003). "Single biosensor immunoassay for the detection of five aminoglycosides in reconstituted skimmed milk." *Anal. Chim. Acta*, **488**(1), 53-60.

**Hahne, M.**, Renno, T., Schroeter, M., Irmeler, M., French, L., Bornard, T., MacDonald, H.R. and Tschoop, J. (1996). "Activated B cells express functional Fas ligand." *Eur. J. Immunol.*, **26**, 721-724.

**Hahnefeld, C.**, Drewianka, S. and Herberg, F.W. (2004). "Determination of kinetic data using surface plasmon resonance biosensors." In: *Methods in Molecular Medicine*, (vol. 94), 2<sup>nd</sup> edn. (Decker, J. and Reischl, U., eds.), chapter 19, 299-320. Humana Press Inc., Totowa, NJ, USA.

**Haines, J.** and Patel, P.D. (1995). "Detection of food borne pathogens using BIA." *BIAcore AB Biotechnology note*, 31.

**Hakanson, K.**, Broder, D., Wang, A.H. and Miller, C.G. (2000). "Crystallization of peptidase T from *Salmonella typhimurium*." *Acta Crystallogr. D Biol. Crystallogr.*, **56**, 924-926.

**Hannig, G.** and Makrides, S. C. (1998). "Strategies for optimising heterologous protein expression in *Escherichia coli*." *Trends Biotechnol.*, **16**, 54-60.

**Harpaz, Y.** and Chothia, C. (1994). "Many of the immunoglobulin superfamily domains in cell adhesion molecules and surface receptors belong to a new structural set which is close to that containing variable domains." *J. Mol. Biol.*, **238**, 528-539.



- Harty, J.T.**, and Bevan, M.J. (1992). "CD8<sup>+</sup> T cells specific for a single nonamer epitope of *Listeria monocytogenes* are protective *in vivo*." *J. Exp. Med.*, **175**(6), 1531-1540.
- Harty, J.T.**, and Pamer, E.G. (1995). "CD8 T lymphocytes specific for the secreted p60 antigen protect against of *Listeria monocytogenes*." *J. Immunol.*, **154**(9), 4642-4650.
- Hashimoto, S.** (2000). "Principles of BIACORE." In: *Real-time analysis of biomolecular interactions-applications of BLAcore*." Springer-Verlag, Tokyo, Japan.
- Hayes, P.S.**, Graves, L.M., Ajello, G.W. Swaminathan, B., Weaver, R.E., Wenger, J.D., Schuchat, A., Broome, C.V. and The *Listeria* Study Group. (1991). "Comparison of cold enrichment and U.S. Department of Agriculture methods for isolating *L. monocytogenes*." *Appl. Environ. Microbiol.*, **57**, 2109-2113.
- Heffron, S.E.**, Moe, G.R., Sieber, V., Mengaud, J., Cossart, P., Vitali, J. and Jurnak, F. (1998). "Sequence profile of the parallel beta helix in the pectate lyase superfamily." *J. Struct. Biol.*, **122**(1-2), 223-235.
- Hefti, M.H.**, Caroline, J.G., der Troon, V.V., Dixon, R. and Vervoot, J. (2001). "A novel purification method for histidine-tagged proteins containing a thrombin cleavage site." *Anal. Biochem.*, **295**, 180-185.
- Hein, I.**, Klein, D., Lehner, A., Bubert A., Brandl, E. and Wagner, M. (2001). "Detection and quantification of the *iap* gene of *Listeria monocytogenes* and *Listeria innocua* by a new real-time quantitative PCR." *Res. Microbiol.*, **152**, 37-46.
- Heitmann, M.**, Gerner-Smidt, P. and Heltberg, O. (1997). "Gastroenteritis caused by *Listeria monocytogenes* in a private day-care facility." *The Pediatric Infect. Dis. J.*, **16**, 827-828.
- Henry, B.S.** (1933). "Dissociation in the genus *Brucella*." *J. Infect. Dis.*, **52**, 374-402.
- Herald, P.J.** and Zootola, E.A. (1988). "Attachment of *Listeria monocytogenes* to stainless steel surfaces at various temperatures and pH values." *J. Food Sci.*, **53**, 1549-1562.
- Hermanson, G.T.**, Krishna Mallia, A. and Smith, P.K. (1992). "Immobilisation of ligands." In: *Immobilised affinity ligand techniques*, Academic Press Ltd., London, 137-279.





**Herron, S.R.**, Benen, J.A.E., Scavetta, R.D., Visser, J. and Jurnak, F. (2000). "Structure and function of pectic enzymes: virulence factors of plant pathogens." *Proc. Natl. Acad. Sci. USA*, **97**(16), 8762-8769.

**Hitbold, E.M.**, Safley, S.A. and Ziegler, H.K. (1996). "The presentation of class I and class II epitopes of listeriolysin O is regulated by intracellular localization and by intercellular spread of *Listeria monocytogenes*." *J. Immunol.*, **157**(3), 1163-1175.

**Ho, J.L.**, Shands, K.N., Friedland, G., Eckind, P. and Fraser, D.W. (1986). "An outbreak of type 4b *Listeria monocytogenes* infection involving patients from eight Boston hospitals." *Arch. Internal Med.*, **146**, 520-524.

**Hochuli, E.**, Döbeli, H. and Schacher, A. (1987). "New metal chelate adsorbent selective for proteins and peptide containing neighbouring histidine residues." *J. Chromatography* **411**, 177-184.

**Hock, B.** Steifert, M. and Kramer, K. (2002). "Engineering receptors and antibodies for biosensors." *Biosens. Bioelect.*, **17**, 239-249.

**Hofman, A.D.** and Wiedmann, M. (2001). "Comparative evaluation of culture- and BAX polymerase chain reaction-based detection methods for *Listeria* spp. and *Listeria monocytogenes* in environmental and raw fish samples." *J. Food Protect.*, **64**, 1521-1526.

**Holt, M.R.** and Koffer, A. (2001). "Cell motility: proline-rich proteins promote protrusions." *Trends in Cell Biology*, **110**, 38-46.

**Homola, J.**, Yee, S.S. and Gauglitz, G. (1999a). "Surface plasmon resonance sensors: review." *Sens. Actuat. B*, **54**, 3-15.

**Homola, J.**, Dostálek, J., Chen, S., Rasooly, A., Jiang, S. and Yee, S.S. (1999b). "Spectral surface plasmon biosensor for detection of staphylococcal enterotoxin B in milk." *Int. J. Food Microbiol.*, **75**, 61-69.

**Howell, S.**, Kenmore, M., Kirkland, M. and Badley, A. (1999). "High-density immobilization of an antibody fragment to a carboxymethylated dextran-linked biosensor surface." *J. Mol. Recognit.*, **11**, 200-203.



**Hsih, H.Y.** and Tsen, H.Y. (2001). "Combination of immunomagnetic separation and polymerase chain reaction for the simultaneous detection of *Listeria monocytogenes* and *Salmonella* spp. in food samples." *J. Food Protect.*, **64**(11), 1744-1750.

**Hudson, J.A.**, Lake, R.J., Savill, M.G., Scholes, P. and McCoermick, R.E. (2001). "Rapid detection of *Listeria monocytogenes* in ham samples using immunomagnetic separation followed by polymerase chain reaction." *J. Appl. Microbiol.*, **90**, 614-621.

**Hudson, L.** and Hay, F.C. (1980). "The lymphocyte: its role and function." In: *Practical Immunology*, 2<sup>nd</sup> edn, (Hudson, L. and Hay, F.C., eds.), Blackwell Scientific Publications, Oxford, UK, 24-50.

**Hwang, S.**, Chang, D.J. and Chen, C. (1996). "Steady state permeate flux for particle cross-flow filtration." *Chem. Eng. J.*, **61**, 171-178.

**Ingianni, A.**, Floris, M., Palomba, P., Madeddu, M.A., Quartuccio, M. and Pompei, R. (2001). "Rapid detection of *Listeria monocytogenes* in foods, by a combination of PCR and DNA probe." *Mol. Cellular Probes*, **15**(5), 275-280.

**Inhoue, H.**, Nojima, H. and Okayama, H. (1990). "High efficiency transformation of *Escherichia coli* with plasmids." *Gene*, **96**, 23-28.

**Ireton, K.** and Cossart, P. (1996). "A role for phosphoinositide 3-kinase in bacterial invasion." *Science*, **274**(5288), 780-782.

**Ireton, K.** and Cossart, P. (1998). "Interaction of invasive bacteria with host signalling pathways." *Curr. Opin. Cell. Biol.*, **10**(2), 276-283.

**Ireton, K.**, Payrastre, B and Cossart, P. (1999). "*Listeria monocytogenes* protein InlB is an agonist of mammalian phosphoinositide 3-kinase." *J. Biol. Chem.*, **274**(24), 17025-17032.

**ISO 10 560:1999** "Milk & milk products- detection of *Listeria monocytogenes*." International Organisation for Standardisation, Geneva, Switzerland.

**ISO 11 290-1:1996** "Microbiology of food & animal feeding stuffs- Horizontal method for the detection and enumeration of *Listeria monocytogenes*, Part 1: detection method." International Organisation for Standardisation, Geneva, Switzerland.



**ISO 11 290-1:1996** "Microbiology of food & animal feeding stuffs- Horizontal method for the detection and enumeration of *Listeria monocytogenes*, Part 2: enumeration method." International Organisation for Standardisation, Geneva, Switzerland.

**Ivanov, I.** (1962). "Untersuchungen über die Listeriose der schaffe in Bulgarian Monatsh." *Vet. Med.*, **17**, 729-736.

**Ivnitski, D.**, Abel-Hamid, I, Atanasov, P. and Wilkins, E. (1999). "Biosensors for detection of pathogenic bacteria." *Biosens. Bioelectron.*, **14**, 599-624.

**Jacob, J.**, Przylepa, J., Miller, C. and Kelsoe, G. (1993). "In situ studies of the primary immune response to (4-hydroxy-3-nitrophenyl)acetyl:III. The kinetics of V region mutation and selection in germinal centre B cells." *J. Exp. Med.*, **178**, 1293-1307.

**Jacquet, C.**, Catimel, B., Brosch, R., Buchrieser, C., Dehaumont, P., Goulet, V., Lepoutre, A., Veit, P. and Rocourt, J. (1995). "Investigations related to the epidemic strain involved in the French listeriosis outbreak in 1992." *Appl. Environ. Microbiol.*, **61**, 2242-2246.

**Jacquet, C.**, Doumith, M., Gordon, J.I., Martin, P.M.V., Cossart, P. and Lecuit, M. (2004). "A molecular marker for evaluating the pathogenic potential of *Listeria monocytogenes*." *J. Infect. Dis.*, **189**, 2094-2100.

**Janeway, C.A., Jr.**, Travers, P., Walport, M. and Capra, J.D. (1999). "The recognition of antigen." In: *Immunobiology: The immune system in health and disease*, 4<sup>th</sup> edn. Garland Publishing New York, USA, 79-113.

**Janknecht, R.** and Nordheim, A. (1992). "Affinity purification of histidine-tagged proteins transiently produced in HeLa cells." *Gene*, **121**, 321-324.

**Janknecht, R.**, de Martynoff, G., Hipskind, R., Nordheim, A. and Stunnenberg, H.G. (1991). "Rapid and efficient purification of native histidine-tagged protein expressed by recombinant vaccina virus." *Proc. Natl. Acad. Sci. USA*, **88**, 8972-8976.

**Jay, J.M.** (1996). "Prevalence of *Listeria* spp. in meat and poultry products." *Food Control*, **7(4-5)**, 209-214.



- Jenkins, E.M.**, Njoku-Obi, A.N. and Adams, E.W. (1964). "Purification of the soluble hemolysin of *Listeria monocytogenes*." *J. Bacteriol.*, **88**, 418-424.
- Jensen, A.**, Frederiksen, W. and Gerner-Smidt, P. (1994). "Risk factors for Listeriosis in Denmark, 1989-1990." *Scand. J. Infect. Dis.*, **26**, 171-178.
- Jeppesen, C.**, Wong, J.Y., Kuhl, T.L., Israelachivili, J.N., Mullah, N., Zalipsky, S. and Marques, C.M. (2001). "Impact of polymer tether length on multiple ligand-receptor bond formation." *Science*, **293**, 465-468.
- Jerpseth, B.**, Callahan, M. and Greener, A. (1997). *Strategies*, **10(2)**, 37-39.
- Jiang, J.**, Zhang, Y., Krainer, A.R. and Xu, R.M. (1999). "Crystal structure of human p32, a doughnut-shaped acidic mitochondrial matrix protein." *Proc. Natl. Acad. Sci. USA.*, **96**, 3572-3577.
- Jisa, E.** and Jungbauer, A. (2003). "Kinetic analysis of estrogen receptor homo- and heterodimerisation *in vitro*." *J. Steroid Biochem. Mol. Biol.*, **84**, 141-148.
- Johanson, J.**, Mandin, P., Renzoni, A., Chiaruttini, C., Springer, M. and Cossart, P. (2002). "An RNA thermosensor controls expression of virulence genes in *Listeria monocytogenes*." *Cell*, **110(5)**, 551-561.
- Johansson, M.A.** and Hellenäs, K.-E. (2004). "Matrix effects in immunobiosensor determination of clenbuterol in urine and serum." *Analyst*, **129**, 438-442.
- Johnsson, B.**, Löfås, S. and Lindquist, G. (1991). "Immobilisation of proteins to a carboxymethyl-dextran-modified gold surface for biospecific interaction analysis in surface plasmon resonance sensors." *Anal. Biochem.*, **198**, 268-277.
- Johnsson, B.**, Löfås, S., Lindquist, G., Edstrom, A., Muller-Hillgren, R.M. and Hansson, A. (1995). "Comparison of methods for immobilization to carboxymethyl dextran sensor surfaces by analysis of the specific activity of monoclonal antibodies." *J. Mol. Recognit.*, **8**, 125-131.





**Jonquières, R.,** Bierne, H. and Cossart, P. (1998). "The *inlA* gene of *Listeria monocytogenes* LO28 harbours a nonsense mutation resulting in release of internalin." *Infect. Immun.*, **66**, 3420-3422.

**Jonquières, R.,** Bierne, H., Fiedler, F., Gounon, P. and Cossart, P. (1999). "Interaction between the protein InlB of *Listeria monocytogenes* and lipotechoic acid: a novel mechanism of protein association at the surface of Gram-positive bacteria." *Mol. Microbiol.*, **34**(5), 902-914.

**Jung, S.,** Unutmaz, D., Wong, P., Sano, G., De los Santos, K., Sparwasser, T., Wu, S., Vuthoori, S., Ko, K., Zavala, F., Pamer, E.G., Littman, D.R. and Lang, R.A. (2002). "In vivo depletion of CD11c(+) dendritic cells abrogates priming of CD8(+) T cells by exogenous cell-associated antigens." *Immunity*, **17**(2), 211-220.

**Jung, Y.S.,** Frank, J.F., Brackett, R.E. and Chen, J. (2003). "Polymerase chain reaction detection of *Listeria monocytogenes* on frankfurters using oligonucleotide primers targeting the genes encoding internalin AB." *J. Food Protect.*, **66**(2), 237-241.

**Juntilla, J.** and Brander, M. (1989). "*Listeria monocytogenes* septicaemia associated with consumption of salted mushrooms." *Scand. J. Infect.*, **21**, 339-342.

**Kaclíková, E.,** Kuchta, T., Kay, H. and Gray, D. (2001). "Separation of *Listeria* from cheese and enrichment media using antibody-coated microbeads and centrifugation." *J. Microbiol. Meth.*, **46**, 63-67.

**Kaclíková, E.,** Pangallo, D., Drahovská, H., Oravcová, K. and Kuchta, T. (2003). "Detection of *Listeria monocytogenes* in food, equivalent to EN ISO 11290-1 or ISO 10560, by a three-days polymerase chain reaction-based method." *Food Control*, **14**(3), 175-179.

**Kajava, A.V.** (1998). "Structural diversity of leucine-rich repeat proteins." *J. Mol. Biol.*, **277**, 519-527.

**Kamei, T.,** Matozaki, T., Sakisaka, T., Kodama, A., Yokoyama, S., Peng, Y.-F., Nakano, K., Takaishi, K. and Takai, Y. (1999). "Coendocytosis of cadherin and c-Met coupled to disruption of cell-cell adhesion in MDCK cells: regulation by Rho, Rac and small G proteins." *Oncogene*, **18**(48), 6776-6784.



**Kampelmacher, E.H.** and van Noorle Jansen, L.M. (1980). "Listeriosis in humans and animals in the Netherlands, 1958-1977." *Zentralblatt Bakteriol. Microbiol. Hyg. A*, **246**, 211-217.

**Karamonova, L., Blažka, M., Fukal, L., Rauch, P., Greifova, M., Horáková, K., Tomáška, M., Roubal, P., Brett, G.M. and Wyatt, G.M.** (2003). "Development of an ELISA specific for *Listeria monocytogenes* using a polyclonal antibody raised against a cell extract containing internalin B." *Food and Agricult. Immunol.*, **15(3-4)**, 167-182.

**Karlin, S.** and Mrazek, J. (2000). "Predicted highly expressed genes of diverse prokaryotic genomes." *J. Bacteriol.*, **182**, 5238-5250.

**Karunasagar, I., Lampidis, R., Goebel, W. and Kreft, J.** (1997). "Complementation of *Listeria seeligeri* with the *plcA-prfA* genes from *L. monocytogenes* activates transcription of seeligerolysin and leads to bacterial escape from the phagosome of infected mammalian cells." *FEMS Microbiol. Letts.*, **146**, 303-310.

**Kasibhatala, S., Brunner, T., Genestier, L., Echeverri, F., Mahboubi, A. and Green, D.R.** (1998). "DNA damaging agents induce expression of Fas ligand and subsequent apoptosis in T lymphocytes via the activation of NF-Kb and AP-1." *Mol. Cell*, **1**, 543-551.

**Kasibhatla, S., Genestier, L. and Green, D.R.** (1999). "Regulation of Fas-ligand expression during activation-induced cell death in T lymphocytes via nuclear factor  $\kappa$ B." *J. Biol. Chem.*, **274**, 987-992.

**Kaslow, D.C. and Shiloach, J.** (1994). "Production, purification and immunogenicity of a malarian transmission-blocking vaccine candidate: TBV25H expressed in yeast and purified using nickel-NTA agarose." *BioTechnology*, **12**, 494-499.

**Kathariou, S.** (2002). "*Listeria monocytogenes* virulence and pathogenicity, a food safety perspective." *J. Food Protect.*, **65**, 1811-1829.

**Kathariou, S., Mizumoto, C., Allen, R.D., Fok, A.K. and Benedict, A.A.** (1994). "Monoclonal antibodies with a high degree of specificity for *Listeria monocytogenes* serotype 4b." *Appl. Environ. Microbiol.*, **60(10)**, 3548-3552.



**Kayal, S., Lilienbaum, A., Join-Lambert, O., Li, X., Israel, A. and Berche, P. (2002).** "Listeriolysin O secreted by *Listeria monocytogenes* induces NF-kappaB signalling by activating the IkappaB kinase complex." *Mol. Microbiol.*, **44**(5), 1407-1419.

**Kayal, S., Lilienbaum, A., Poyart, C., Memet, S., Israel, A. and Berche, P. (1999).** "Listeriolysin O-dependent activation of endothelial cells during infection with *Listeria monocytogenes*: activation of NF-kappa B and upregulation of adhesion molecules and chemokines." *Mol. Microbiol.*, **31**(6), 1709-1722.

**Kemeny, D.M. (1992).** "Quantitation." In: *A practical guide to ELISA*. (Kemeny, D.M., ed.), Pergamon Press, Oxford, UK, 57-67.

**Kemeny, D.M. (1992).** "Titration of antibodies." *J. Immunol. Meth.*, **150**(1-2), 57-76.

**Kerksiek, K.M., Busch, D.H., Pilip, I.M., Allen, S.E. and Pamer, E.G. (1999).** "H2-M3-restricted T cells in bacterial infection: rapid primary but diminished memory responses." *J. Exp. Med.*, **190**, 195-204.

**Kerksiek, K.M., Ploss, A., Leiner, I., Busch, D.H. and Pamer, E.G. (2003).** "H2-M3-restricted memory T cells: persistence and activation without expansion." *J. Immunol.*, **170**, 1862-1869.

**Kibler, D. and Hampson, S. (2002).** "Characterising the *E. coli* Shine-Dalgarno site: probability matrices and weight matrices." International Conference on Mathematical and Engineering Techniques in Medicine and Biological Science (METMBS-2002), (<http://www.ics.uci.edu/~kibler/pubs/Metmbs02.pdf>), 358-364.

**Kiener, P.A., Davis, P.M., Rankin, B.M., Klebanoff, S.J., Ledbetter, J.A., Starling, G.C. and Liles, W.C. (1997).** "Human monocytic cells contain high levels of intracellular Fas ligand: rapid release following cellular activation." *Cell*, **68**, 521-531.

**Kim, N. and Park, I.-S. (2003).** "Application of a flow type antibody sensor to the detection of *Escherichia coli* in various foods." *Biosens. Bioelectron.*, **18**, 1101-1107.

**King, D.J. (1998)** "Preparation, structure and function of monoclonal antibodies". In: *Applications and engineering of monoclonal antibodies*. Taylor and Francis Ltd., London, UK, 1-21.



**Kobe, B.** and Kajava, A.V. (2001). "The leucine-rich repeat as a protein recognition motif." *Curr. Opin. Struct. Biol.*, **11**, 725-732.

**Kocks, C. E.**, Hellio, R., Gounon, P., Ohayn, H. and Cossart, P. (1993). "Polarised distribution of *Listeria monocytogenes* surface protein ActA at the site of directional actin assembly." *J. Cell Sci.*, **105**, 699-710.

**Kocks, C.E.**, Gonin, E., Tabouret, Berche, P., Ohayon, H. and Cossart, P. (1992). "*L. monocytogenes*-induced actin assembly requires the *actA* gene product, a surface protein." *Cell*, **68**, 521-531.

**Kohda, C.**, Kawamura, I., Baba, H., Nomura, Ito, Y., Kimoto, T., Watanabe, I. and Mitsuyama, M. (2002). "Dissociated linkage of cytokine-inducing activity and cytotoxicity to different domains of listeriolysin O from *Listeria monocytogenes*." *Infect. Immun.*, **70**(3), 1334-1341.

**Köhler, S.**, Bubert, A., Vogel, M. and Goebel, W. (1991) "Expression of the *iap* gene coding for protein p60 of *Listeria monocytogenes* is controlled on the posttranscriptional level." *J. Bact.*, **173**(15), 4668-4674.

**Köhler, S.**, Bubert, A., Vogel, M. and Goebel, W. (1991). "Expression of the *iap* gene coding for protein p60 is controlled at the post transcriptional level." *J. Bacteriol.*, **173**, 4668-4674.

**Kolb-Mäurer, A.**, Pilgrim, S., Kämpgen, E., McLellan, A.D., Bröcker, E.-B., Goebel, W. and Gentschev. (2001). "Antibodies against listerial protein 60 act as an opsonin for phagocytosis of *Listeria monocytogenes* by human dendritic cells." *Infect. Immun.*, **69**(5), 3100-3109.

**Koubová, V.**, Brynda, E., Karasová, L., Škvor, J., Homola, J., Dostálek, J., Tobiška, P. and Rošický, J. (2000). "Detection of foodborne pathogens using surface plasmon resonance biosensors." *Sens. Actuat. B*, **74**, 100-105.

**Kreft, J.**, Dumbsky, M. and Theiss, S. (1995). "The actin-polymerisation protein from *Listeria ivanovii* is a large repeat protein which shows only limited amino acid sequence homology to ActA from *Listeria monocytogenes*." *FEMS Microbiol Letts.*, **126**, 113-122.





**Kreft, J., Vázquez-Boland, J.A., Altrock, S., Domínguez-Bernal, G. and Goebel, W. (2002).** "Pathogenicity islands and other virulence elements in *Listeria*." *Curr. Top. Microbiol. Immunol.*, **264(2)**, 109-125.

**Kretschmann, E. (1971).** "The determination of the optical constants of metals by excitation of surface plasmon resonance." *Z. Phys.*, **241**, 313-324.

**Kretschmann, E. and Raether, H. (1968).** "Radiative decay of non-radiative surface plasmons excited by light." *Z. Naturforsch.*, **23(A)**, 2135-2136.

**Krüll, M., Nost, Hippenstiel, S., Domann, E., Chakraborty, T. and Suttorp, N. (1997).** "*Listeria monocytogenes* potently induces up-regulation of endothelial adhesion molecules and neutrophil adhesion to cultured human endothelial cells." *J. Immunol.*, **159(4)**, 1970-1976.

**Kuhn, M. and Goebel, W. (1989).** "Identification of an extracellular protein of *Listeria monocytogenes* possibly involved in intracellular uptake by mammals." *Infect. Immun.*, **57(1)**, 55-61.

**Kuhn, M. and Goebel, W. (1994).** "Induction of cytokines in phagocytic mammalian cells infected with virulent and avirulent *Listeria* strains." *Infect. Immun.*, **62**, 348-356.

**Kuhn, M. and Goebel, W. (1995).** "Molecular studies on the virulence of *Listeria monocytogenes*." *Gen. Eng.*, **17**, 31-51.

**Kurrat, R.G., Ramsden, J.J. and Prenosil, J.E. (1994).** "Kinetic model for serum albumin adsorption: experimental verification." *J. Chem. Soc. Faraday Trans.*, **90**, 587-590.

**Kuusinen, A., Arvola, M., Oker-Blom, C. and Keinänen, K. (1995).** "Purification of recombinant GLUR-D glutamate receptor produced in Sf21 insect cells." *Eur. J. Biochem.*, **233**, 720-726.

**Kwong, P.D., Wyatt, R., Robinson, J., Sweet, R.W., Sodroski, J. and Hendrickson, W.A. (1998).** "Structure of an HIV gp120 envelope glycoprotein in complex with the CD4 receptor and a neutralising antibody." *Nature*, (London), **393**, 648-659.



**Kyte, J.** and Doolittle, R.F. (1982). "A simple method for displaying the hydropathic character of a protein." *J. Mol. Biol.*, **157**(1), 105-132.

**Lalic-Mülthaler, M.**, Bohne, J. and Goebel, W. (2001). "In vitro transcription of PrfA-dependent and -independent genes of *Listeria monocytogenes*." *Mol. Microbiol.*, **42**(1), 111-120.

**Lammerding, A.M.**, Glass, K.A., Gendron-Fitzpatrick, A. and Doyle, M.P. (1992). "Determination of virulence of different strains of *Listeria monocytogenes* and *L. innocua* by oral inoculation of pregnant mice." *Appl. Environ. Microbiol.*, **58**, 3991-4000.

**Lampidis, R.**, Gross, R., Sokolovic, Z., Goebel, W. and Kreft, J. (1994). "The virulence regulator protein of *Listeria ivanovii* is highly homologous to PrfA from *Listeria monocytogenes* and both belong to the Crp-Fnr family of transcription regulators." *Mol. Microbiol.*, **13**, 141-151.

**Lantz, P.G.**, Tjerneld, F., Borch, E., Hahn-Hagerdal, B. and Radstrom, P. (1994). "Enhanced sensitivity in PCR detection of *Listeria monocytogenes* in soft cheese through use of an aqueous two-phase system as a sample preparation method." *Appl. Environ. Microbiol.*, **60**, 3416-3418.

**Lara-Tejero, M.** and Pamer, E.G. (2004). "T cell responses to *Listeria monocytogenes*." *Curr. Opin. Microbiol.*, **7**, 45-50.

**Lathrop, A.A.**, Jaradat, Z.W., Haley, T. and Bhunia, A.K. (2003). "Characterisation and application of a *Listeria monocytogenes* reactive antibody C11E9 in a resonant mirror biosensor." *J. Immunol. Meth.*, **281**, 119-128.

**Le Souëf, P.N.** and Walters, B.N.E. (1981). "Neonatal listeriosis. A summer outbreak." *Med. J. Australia*, **2**, 188-191.

**Leatherbarrow, R.J.** and Edwards, P.R. (1999). "Analysis of molecular recognition using optical biosensors." *Curr. Opin. Chem. Biol.*, **3**, 544-547.

**Leblond-Francillard, M.**, Gaillard, J.-L. and Berche, P. (1989). "Loss of catalase activity in Tn1545-induced mutants does not reduce growth of *Listeria monocytogenes* in vivo." *Infect. Immun.*, **57**, 2569-2573.



**Lebrun, M., Audurier, A. and Cossart, P. (1994).** "Plasmid-borne cadmium resistance genes in *Listeria monocytogenes* are similar to *cadA* and *cadC* of *Staphylococcus aureus* and are induced by cadmium." *J. Bacteriol.*, **176**, 3040-3048.

**Lebrun, M., Mengaud, J., Ohayon, H., Nato, F. and Cossart, P. (1996).** "Internalin must be on the bacterial surface to mediate entry of *Listeria monocytogenes* into epithelial cells." *Mol. Microbiol.*, **21(3)**, 579-592.

**Leclerc, V., Dufour, B., Lombard, B., Gauchard, F., Garin-Bastuji, B., Salvat, G., Brisabois, A., Poumeyrol, M., De Buyser, M.-L., Gnanou-Besse, N. and Lahellec, C. (2002).** "Pathogens in meat and milk products: surveillance and impact on human health in France." *Livestock Production Sci.*, **76**, 195-202.

**Leclercq, A. (2004).** "Atypical colony morphology and low recoveries of *Listeria monocytogenes* Strains on Oxford, PALCAM, Rapid'L.mono and ALOA solid media." *J. Microbiol. Meth.*, **57**, 251-258.

**Lecuit, M., Dramsi, S., Gottardi, C., Chaiken, M.F., Gumbiner, B and Cossart, P. (1999).** "A single amino acid in the E-cadherin molecule was responsible for host specificity towards the human pathogen *Listeria monocytogenes*." *EMBO J.*, **18(14)**, 3956-3963.

**Lecuit, M., Ohayon, H., Braun, L., Mengaud, J. and Cossart, P. (1997).** "Internalin of *Listeria monocytogenes* with an intact leucine-rich repeat region is sufficient to promote internalisation." *Infect. Immun.*, **65(12)**, 5309-5319.

**Lecuit, M., Vandormael-Pournin, S., Lefort, J., Huerre, M., Gounon, P., Dupuy, C., Babinet, C. and Cossart, P. (2001).** "A transgenic model for listeriosis: role of internalin in crossing the intestinal barrier." *Science*, **292(5522)**, 1722-1725.

**Lefkovitz, I. (1979).** "Limiting dilution analysis." In: *Immunological Methods*, Vol. 1 (Lefkovitz, I. and Pernis, P., eds.), Academic Press, New York, 355-370.

**Leimeister-Wächter, M., and Chakraborty, T. (1992).** "Detection of listeriolysin, the thiol-dependent haemolysin in *Listeria monocytogenes*, *Listeria ivanovii* and *Listeria seeligeri*." *Infect. Immun.*, **57**, 2350-2357.



**Leimeister-Wächter, M.**, Domann, E. and Chakraborty, T. (1991). "Detection of a gene encoding a phosphatidylinositol-specific phospholipase C that is co-ordinately expressed with listeriolysin in *Listeria monocytogenes*." *Mol. Microbiol.*, **5**, 361-366.

**Leimeister-Wächter, M.**, Haffner, C., Domann, E., Goebel, W., and Chakraborty, T. (1990). "Identification of a gene that positively regulates expression of listeriolysin, the major virulence factor of *Listeria monocytogenes*." *Proc. Natl. Acad. Sci. (USA)*, **87**, 8336-8340.

**Lennon, D.**, Lewis, B., Mantell, C., Becroft, D., Dove, B., Farmer, K., Tonkin, S., Yates, N., Stamp, R. and Mickleston, K. (1984). "Epidemic perinatal listeriosis." *Pediatric Infect. Dis.*, **3**, 30-34.

**Lenz, L.L.** and Bevan, M.J. (1997). "CTL responses to H2-M3-restricted *Listeria* epitopes." *Immunol. Rev.*, **158**, 115-121.

**Leonard, P.**, Hearty, S., Brennan, J., Dunne, L., Quinn, J., Chakraborty, T. and O'Kennedy, R. (2003). "Advances in biosensors for detection of pathogens in food and water." *Enz. Microbial Technol.*, **32**, 3-13.

**Leonard, P.**, Hearty, S., Quinn, J. and O'Kennedy, R. (2004). "A generic approach for the detection of whole *Listeria monocytogenes* cells in contaminated samples using surface plasmon resonance." *Biosens. Bioelectron.*, **19**, 1331-1335.

**Leonard, P.**, Hearty, S., Wyatt, G., Quinn, J. and O'Kennedy, R. (2005). "Development of a surface plasmon resonance-based immunoassay for *Listeria monocytogenes*." *J. Food. Protect.*, **68**(4), 728-735.

**Lie' vin-Le Moal, V.**, Huet, G., Aubert, J.-P, Bara, J., Forgue-Lafitte, M.-E., Servin, A.L. and Coconnier, M.-H. (2002). "Activation of mucin exocytosis and upregulation of *MUC* genes in polarized human intestinal mucin-secreting cells by the thiol-activated exotoxin listeriolysin O." *Cell. Microbiol.*, **4**(8), 515-529.

**Lieber, M.** (2000) "Antibody diversity: A link between switching and hypermutation." *Curr. Biol.*, **10**, 798-800.





**Liedberg, B.** and Johansen, K. (1998). "Affinity biosensing based on surface plasmon resonance detection." In: *Biosensors: Techniques and protocols*. (Rogers, K. and Mulchandani, A., eds) Humana Press Inc., Totowa, NJ, USA., *Meth. Biotechnol.*, **7**, 31-54.

**Liedberg, B.**, Lundström, I. and Stenberg, E. (1993). "Principles of biosensing with an extended coupling matrix and surface plasmon resonance." *Sens. Actuat. B*, **11**, 63-72.

**Liedberg, B.**, Nylander, C. and Lundström, I. (1983). "Surface plasmon resonance for gas detection and biosensing." *Sens. Actuat.*, **4**, 299-304.

**Liedberg, B.**, Nylander, C. and Lundström, I. (1995). "Biosensing with surface plasmon resonance- how it all started." *Biosens. Bioelectron.*, **10**, i-ix.

**Lietske, R.** and Unsicker, K. (1985). "A statistical approach to determine monoclonality after limiting cell plating of a hybridoma clone." *J. Immunol. Meth.*, **76**, 223-228.

**Lindqvist, R.** and Westöö, A. (2000). "Quantitative risk assessment for *Listeria monocytogenes* in smoked or gravid salmon and rainbow trout in Sweden." *Int. J. Food Microbiol.*, **58**, 181-196.

**Lingnau, A.**, Domann, E., Hudel, M., Bock, M., Nichterlein, T., Wehland, J. and Chakraborty, T. (1995). "Expression of the *Listeria monocytogenes* EGD *inlA* and *inlB* genes, whose products mediate bacterial entry into tissue culture cell lines, by PrfA-dependent and – independent mechanisms." *Infect. Immun.*, **63**(10), 3896-3903.

**Lingnau, A.**, Domann, E., Hudel, M., Bock, M., Nichterlein, T., Wehland, J. and Chakraborty, T. (1995). "Expression of the *L. monocytogenes* EGD *inlA* and *inlB* genes, whose products mediate bacterial entry into tissue culture cell lines, by prfA-dependent and -independent mechanisms." *Infect. Immun.*, **63**(10), 3896-3903.

**Linnan, M.J.**, Mascola, L., Lou, X.D., Goulet, V., May, S., Salminen, C., Hird, D.W., Yonekura, M.L., Hayes, P., Weaver, R., Audurier, A., Pilkaytis, B.D., Fannin, S.L., Kleks, A. and Broome, C.V. (1988). "Epidemic listeriosis associated with Mexican-style cheese." *New Engl. J. Med.*, **319**(13), 823-828.

**Littlefield, J.W.** (1964). "Selection of hybrids from mating fibroblasts *in vitro* and their presumed recombinants." *Science*, **145**, 709.



**Löfås, S.**, and Johnsson, B. (1990). "A novel hydrogel matrix on gold surfaces in surface plasmon resonance sensor for fast and efficient covalent immobilisation of ligands." *J. Chem. Soc. Chem. Commun.*, **21**, 1526-1528.

**Löfås, S.**, Malmqvist, M., Rönnerberg, I., Stenberg, E., Liedberg, B. and Lundström, I. (1991). "Bioanalysis with surface plasmon resonance." *Sens. Actuat. B*, **5**, 79-84.

**Loiseau, O.**, Cottin, J., Robert, R., Tronchin, G., Mahaza, C. and Senet, J.M. (1995). "Development and characterisation of monoclonal antibodies specific for the genus *Listeria*." *FEMS Immunol. Med. Microbiol.*, **11**, 219-230.

**Loncarevic, S.**, Tham, W. and Danielson-Tham, M.-L. (1996). "Prevalence of *Listeria monocytogenes* and *Listeria* spp. in smoked and gravid fish." *Acta Vet. Scand.*, **37**, 13-18.

**Longhi, C.**, Maffeo, A., Penta, M., Petrone, G., Seganti, L. and Conte, M.P. (2003). "Detection of *Listeria monocytogenes* in Italian-style soft cheeses." *J. Appl. Microbiol.*, **94**(5), 879-885.

**Lorber, B.** (1997). "Listeriosis." *Clin. Infect. Dis.*, **24**, 1-11.

**Low, J.C.**, Wright, F., McLaughlin, J. and Donachie, W. (1993). "Serotyping and distribution of *Listeria* isolates from causes of ovine listeriosis." *Vet. Rec.*, **133**, 165-166.

**Lu, B.**, Smyth, M.R. and O'Kennedy, R. (1996). "Oriented immobilization of antibodies and its applications in immunoassays and immunosensors." *Analyst*, **121**, 29R-32R.

**Lundberg, K.S.**, Shoemaker, D.D., Adams, M.W.W., Short, J.M., Sorge, J.A. and Mathur, E.J. (1991). "High-fidelity amplification using a thermostable DNA polymerase isolated from *Pyrococcus furiosus*." *Gene*, **108**(1), 1-6.

**Lyytikäinen, O.**, Autio, T., Majjala, R., Ruutu, P., Hokanen-Buzalski, T., Miettinen, M., Hatakka, M., Mikkola, J., Anttila, V.-J., Johansson, T. and Rantala, L. (2000). "An outbreak of *Listeria* from raw milk." *J. Food Protect.*, **58**, 1139-1141.

**MacDonald, F.** and Sutherland, A.D. (1994). "Important differences between the generation times of *L. monocytogenes* and *L. innocua* in two *Listeria* enrichment broths." *J. Dairy Res.*, **61**, 433-436.



**Machesky, L.M.**, and Insall, R.H. (1998). "Scar1 and the related Wiskott-Aldrich syndrome protein, WASP, regulate the actin cytoskeleton through the Arp2/3 complex." *Curr. Biol.*, **8**, 1347-1356.

**Machesky, L.M.**, Mullins, R.D., Higgs, H.N., Kaiser, D.A., Blanchoin, L., May, R.C., Hall, M.E. and Pollard, T.D. (1999). "Scar, a WASp-related protein, activates nucleation of actin filaments by the Arp2/3 complex." *Proc. Natl. Acad. Sci. USA*, **96**, 3739-3744.

**Makino, S.**, Okada, Y. and Maruyama, T. (1995). "A new method for direct detection of *Listeria monocytogenes* from foods by PCR." *Appl. Environ. Microbiol.*, **61**, 3745-3747.

**Malmqvist, M.** (1999). "BIACORE: an affinity biosensor system for characterisation of biomolecular interactions." *Biochem. Soc. Trans.*, **27**, 335-340.

**Mansell, A.**, Braun, L., Cossart, P. and O'Neil, L.A. (2000). "A novel function of InlB from *Listeria monocytogenes*: activation of Nf-kappaB in J774 macrophages." *Cell Microbiol.*, **2(2)**, 127-136.

**Manzano, M.**, Cocolin, L., Ferroni, P., Cantoni, C. and Comi, G. (1997). "A simple and fast PCR protocol to detect *Listeria monocytogenes*." *J. Sci. Food Agric.*, **74**, 25-30.

**Marino, M.**, Braun, L., Cossart, P. and Ghosh, P. (1999). "Structure of the InlB Leucine-rich repeats, a domain that triggers host cell invasion by the bacterial pathogen *L. monocytogenes*." *Mol. Cell*, **4(6)**, 1063-1072.

**Marino, M.**, Braun, L., Cossart, P. and Ghosh, P. (2000). "A framework for interpreting the leucine-rich repeats of *Listeria internalins*." *Proc. Natl. Acad. Sci. USA*, **97(16)**, 8784-8788.

**Markey, F.** (2000). "Principles of surface plasmon resonance." In: *Real-time analysis of biomolecular interactions-applications of BIAcore*." Springer-Verlag, Tokyo, Japan.

**Marquis, H.**, Doshi, V. and Portnoy, D.A. (1995). "The broad-range phospholipase C and a metalloprotease mediate listeriolysin O-independent escape of *Listeria monocytogenes* from a primary vacuole in human epithelial cells." *Infect. Immun.*, **63**, 4531-4534.



**Marquis, H.**, Goldfine, H. and Portnoy, D.A. (1997). "Proteolytic pathways of activation and degradation of bacterial phospholipase C during intracellular infection by *Listeria monocytogenes*." *J. Cell. Biol.*, **137**, 1381-1392.

**Marth, E.H.** (1993) Growth and survival of *Listeria monocytogenes*, *Salmonella* species, and *Staphylococcus aureus* in the presence of sodium chloride: a review. *Dairy Food Env. Sanit.*, **13**, 14-8.

**Matsubara, K.**, Kawata, S. and Minami, S. (1988a). "Optical chemical sensor based on surface plasmon resonance." *Appl. Optics*, **27**(6), 1160-1163.

**Matsubara, K.**, Kawata, S. and Minami, S. (1988b). "A compact surface plasmon resonance sensor for water in process." *Appl. Spect.*, **42**, 229-240.

**Mattingly, J.A.**, Butman, B.T., Plank, M.C., Durham, R.J. and Robison, B.J. (1988). "Rapid monoclonal antibody-based enzyme-linked immunosorbent assay for detection of *Listeria* in food products." *J. AOAC Int.*, **71**, 679-681.

**May, R.C.**, Hall, M.E., Higgs, H.N., Pollard, T.D., Chakraborty, T., Wehland, J., Machesky, L.M. and Sechi, A.S. (1999). "The Arp2/3 complex is essential for the actin-based motility of *Listeria monocytogenes*." *Curr. Biol.*, **9**, 759-762.

**McBlane, J.F.**, Van Gent, D.C., Ramsden, D.A., Romeo, C., Cuomo, C.A., Gellert, M. and Oettinger, M.A. (1995). "Cleavage at a V(D)J recombination signal requires only RAG1 and RAG2 proteins and occurs in two steps." *Cell*, **83**, 387-395.

**McCormack, T.**, Keating, G., Killard, A., Manning, B.M. and O'Kennedy, R. (1998). "Biomaterials for biosensors." In: *Principles of Chemical and Biological Sensors*. (Ed. Diamond, D.), Wiley, N.Y., *Chem. Anal.*, **150**, 133-194.

**McCullough, K.C.** and Spier, R.E. (1990). "Monoclonal antibodies in biotechnology: theoretical and practical aspects." Cambridge University Press.

**McHeyzer-Williams, L.J.**, Driver, D.J. and McHeyzer-Williams, M.G. (2001). "Germinal centre reaction." *Curr. Opin. Hematol.*, **8**, 52-59.





- McKeller, R.C.** (1994). "Identification of the *Listeria monocytogenes* virulence factors involved with the CAMP reaction." *Lett. Appl. Microbiol.*, **18**, 79-81.
- McLaughlan, A.M.** and Foster, S.J. (1998). "Molecular chatacterization of an autolytic amidase of *Listeria monocytogenes* EGD." *Microbiol.*, **144**, 1359-1367.
- McLaughlin, J.** (1996). "The relationship between *Listeria* and listeriosis." *Food Control*, **7**, 187-193.
- McLaughlin, J.** (1997a). "The discovery of *Listeria*." *PHLS Microbiol. Digest*, **14**, 76-78.
- McLaughlin, J.** (1997b). "The identification of *Listeria*." *Int. J. Food Microbiol.*, **38**, 77-81.
- McLaughlin, J.** (1997c). "The pathogenicity of *Listeria monocytogenes*: a public helth perspective." *Rev. Med. Microbiol.*, **8**, 1-14.
- McLaughlin, J.,** Hall, S.M., Velani, S.K. and Gilbert, R.J. (1991). "Human listeriosis and pâté: A possible association." *Brit. Med J.*, **303**, 773-775.
- McLaughlin, J.,** Mitchel, R.T., Smerdon, W.J. and Jewell, K. (2004). "*Listeria monocytogenes* and listeriosis: a review of hazard characterisation for use in microbiological risk assessment of foods." *Int. J. Food Microbiol.*, **92**, 15-33.
- Mead, P.S.,** Slutsker, L., Dietz, McCaig, L.F., Bresee, J.S., Shapiro, C., Griffin, P.M. and Tauxe, R.V. (1999). "Food-related illness and death in the United States." *Emerg. Infect. Dis.*, **5**, 607-625.
- Medina, M.B.,** Van Houten, L., Cooke, P.H. and Tu, S.I. (1997). "Real-time analysis of antibody binding interactions with immobilized *E. coli* O157:H7 cells using the BIAcore." *Biotechnol. Tech.*, **11(3)**, 173-176.
- Mengaud, J.,** Braun-Breton, C. and Cossart, P. (1991b). "Identification of a new operon involved in *Listeria monocytogenes* virulence: its first gene encodes a protein homologous to bacterial metalloproteases." *Infect. Immun.*, **59**, 1043-1049.



**Mengaud, J., Dramsi, S., Gouin, E., Vázquez-Boland, J.A., Milon, G. and Cossart, P.** (1991c). "Pleiotropic control of *Listeria monocytogenes* virulence factors by a gene that is autoregulated." *Mol. Microbiol.*, **5**, 2273-2283.

**Mengaud, J., Geoffroy, C. and Cossart, P.** (1991a). "Identification of phosphatidylinositol-specific phospholipase C activity in *Listeria monocytogenes*: a novel type of virulence factor?" *Mol. Microbiol.*, **5**, 367-372.

**Mengaud, J., Ohayon, H., Gounon, P., Mège, R.M. and Cossart, P.** (1996). "E-cadherin is the receptor for internalin, a surface protein required for entry of *Listeria monocytogenes* into epithelial cells." *Cell*, **84**, 923-932.

**Merrick, J.C., Edelson, B.T., Bhardwaj, V., Swanson, P.E. and Unanue, E.R.** (1997). "Lymphocyte apoptosis during early phase of *Listeria* infection in mice." *Am. J. Pathol.*, **151**, 785-792.

**Meyer-Broseta, S., Diot, A., Bastian, S., Rivière, J. and Cerf, O.** (2002). "Estimation of low bacterial concentration: *Listeria monocytogenes* in raw milk." *Int. J. Food Microbiol.*, **80**, 1-15.

**Miettinen, M.K., Siitonen, A., Heiskanen, P., Haajanen, H., Björkroth, K.J. and Korkaela, H.J.** (1999). "Molecular epidemiology of an outbreak of febrile gastroenteritis caused by *L. monocytogenes* in cold-smoked rainbow trout." *J. Clin. Microbiol.*, **37**, 2358-2360.

**Milenbachs Lukowiak, A., Mueller, K.J., Freitag, N.E. and Youngman, P.** (2004). "Deregulation of *Listeria monocytogenes* virulence gene expression by two distinct and semi-independent pathways." *Microbiol.*, **150**, 321-333.

**Milenbachs, A.A., Brown, D.P., Moors, M. and Youngman, P.** (1997). "Carbon source regulation of virulence gene expression in *Listeria monocytogenes*." *Mol. Microbiol.*, **23**(5), 1075-1085.

**Miller, R. and Britigan, B.E.** (1997). "Role of oxidants in microbial pathophysiology." *Clin. Microbiol. Rev.*, **10**, 1-18.



**Milohanic, E.,** Glaser, P., Coppée, J.Y., Frangeul, L., Vega, Y., Vázquez-Boland, J.A., Kunst, F., Cossart, P. and Buchrieser, C. (2003). "Transcriptome analysis of *Listeria monocytogenes* identifies three groups of genes differently regulated by PrfA." *Mol. Microbiol.*, **47**(6), 1613-1625.

**Milohanic, E.,** Jonquières, R., Berche, P., Cossart, P. and Caillard, J.-L. (2001). "The autolysin Ami contributes to the adhesion of *Listeria monocytogenes* to eukaryotic cells via its cell wall anchor." *Mol. Microbiol.*, **39**(5), 1212-1224.

**Milohanic, E.,** Jonquières, R., Glaser, P., Dehoux, P., Jacquet, C., Berche, P., Cossart, P. and Caillard, J.-L. (2004). "Sequence and binding activity of the autolysin-adhesion Ami from epidemic *L. monocytogenes* 4b." *Infect. Immun.*, **72**(8), 4401-4409.

**Misrachi, A.,** Watson, A.J. and Coleman, D. (1991). "*Listeria* in smoked mussels in Tasmania." *Comm. Dis. Intel.*, **15**, 427.

**Mitchell, D.L.** (1991). "A case cluster of listeriosis in Tasmania." *Communicable Dis. Intelligence*, **15**, 427.

**Moors, M.A.,** Levitt, B., Youngman, P. and Portnoy, D.A. (1999). "Expression of listeriolysin O and ActA by intracellular and extracellular *Listeria monocytogenes*." *Infect. Immun.*, **67**, 131-139.

**Müller, K.M.,** Arndt, K.M., Bauer, K. and Plückthun, A. (1998b). "Tandem Immobilised Metal-Ion Affinity Chromatography/Immunoaffinity purification of His-tagged Proteins; evaluation of two anti-His tag monoclonal antibodies." *Anal. Biochem.*, **259**, 54-61.

**Müller, K.M.,** Arndt, K.M. and Plückthun, A. (1998c). "Model and simulation of multivalent binding to fixed ligands." *Anal. Biochem.*, **261**(2), 149-158.

**Müller, S.,** Hain, T., Pashalidis, P., Lingnau, A., Domann, E., Chakraborty, T. and Wehland, J. (1998a). "Purification of the *inlB* gene product of *Listeria monocytogenes* and demonstration of its biological activity." *Infect. Immun.*, **66**(7), 3128-3133.

**Muramatsu, M.,** Kinoshita, K., Fagarasan, S., Yamada, S., Shinkai, Y. and Honjo, T. (2000). "Class switch recombination and hypermutation require activation-induced cytidine deaminase (AID), a potential RNA editing enzyme." *Cell*, **102**, 553-563.



**Murray, E.G.D., Webb, R.A. and Swann, M.B.R. (1926).** "A disease of rabbits characterised by large mononuclear leucocytosis, caused by a hitherto undescribed bacillus *Bacterium monocytogenes*." *J. Pathol. Bacteriol.*, **29**, 407-439.

**Muyldermans, S., Cambillau, C. and Wyns, L. (2001).** "Recognition of antigens by single-domain antibody fragments: the superfluous luxury of paired domains." *Trends Biochem. Sci.*, **26(4)**, 230-235.

**Myszka, D.G. (1997).** "Kinetic analysis of macromolecular interactions using surface plasmon resonance biosensors." *Curr. Opin. Biotechnol.*, **8**, 50-57.

**Nagata, K. and Handa, H. (eds.), (2000).** "Real-time analysis of biomolecular interactions-applications of BIAcore." Springer-Verlag, Tokyo, Japan.

**Navarre, W.W. and Schneewind, O. (1999).** "Surface proteins of Gram-positive bacteria and mechanisms of their targeting to the cell wall envelope." *Microbiology and Mol. Biol. Rev.*, **63(1)**, 174-229.

**Nelson, K.E., Fouts, D.E., Mongodin, E.F., Ravel, J., DeBoy, R.T., Kolonay, J.F., Rasko, D.A., Angiuoli, S.V., Gill, S.R., Paulsen, I.T., Peterson, J., White, O., Nelson, W.C., Nierman, W., Beanan, M.J., Brinkac, L.M., Daugherty, S.C, Dodson, R.J., Durkin, A.S., Madupu, R., Haft, D.H., Selengut, J., Van Aken, S., Khouri, H., Fedorova, N., Forberger, H., Tran, B., Kathariou, S., Wonderling, L.D., Uhlich, G.A., Bayles, D.O., Luchansky, J.B. and Fraser, C.M. (2004).** "Whole genome comparisons of serotype 4b and 1/2a strains of the food-borne pathogen *Listeria monocytogenes* reveal new insights into the core genome components of this species." *Nuc. Acids Res.*, **32(8)**, 2386-2395.

**Nieba, L., Nieba-Axmann, S.E., Persson, A., Hämäläinen, M., Edebratt, F., Hansson, A., Lidholm, J., Magnusson, K., Karlsson, A.F. and Plückthun, A. (1997).** "BIAcore analysis of histidine-tagged proteins using a chelating NTA sensor chip." *Anal. Biochem.*, **252**:217-228.

**Niebuhr, K., Ebel, F., Reinhard, M., Domann, E., Carl, U.D., Walter, U., Gertler, F.B., Wehland, J. and Chakraborty, T. (1997).** "A novel proline-rich motif present in ActA of *Listeria monocytogenes* and cytoskeletal proteins is the ligand for the EVH1 domain, a protein module present in the Ena/VASP family." *EMBO J.*, **16(17)**, 5433-5444.





**Nishibori, T.**, Xiong, H., Kawamura, I., Arakawa, M. and Mitsuyama, M. (1996). "Induction of cytokine gene expression by listeriolysin O and roles of macrophages and NK cells." *Infect. Immun.*, **64**, 3188-3195.

**Nørrung, B.**, Anderson, J.K. and Schlundt, J. (1999). "Incidence and control of *Listeria monocytogenes* in foods in Denmark." *Int. J. Food Microbiol.*, **53**, 195-203.

**Norton, D.M.** (2002). "Polymerase chain reaction-based methods for detection of *Listeria monocytogenes*: towards real time screening for food and environmental samples." *J. AOAC Int.*, **77**, 602-617.

**Norton, D.-M.**, and Batt, C.A. (1999). "Detection of viable *Listeria monocytogenes* with a 5' nuclease PCR assay." *Appl. Environ. Microbiol.*, **65**(5), 2122-2127.

**Norton, D.M.**, McCamey, M., Boor, K.J. and Wiedman, M. (2000). "Application of the BAX for screening/genus *Listeria* polymerase chain reaction system for monitoring *Listeria* species in cold-smoked fish and in the smoked fish processing environment." *J. Food Protect.*, **63**, 343-346.

**Notermans, S.H.W.**, Dufrenne, J., Leimeister-Wächter, M., Domann, E. and Chakraborty, T. (1991). "Phosphatidylinositol-specific phospholipase C activity as a marker to distinguish between pathogenic and nonpathogenic *Listeria* species." *Appl. Environ. Microbiol.*, **57**(9), 2666-2670.

**Notermans, S.H.W.**, Dufrenne, J., Teunis, P. and Chakraborty, T. (1998). "Studies on the risk assessment of *Listeria monocytogenes*." *J. Food Protect.*, **61**, 244-248.

**Novy, R.** and Morris, B. (2001). "Use of glucose to control basal expression in the pET System." In: *inNovations: advanced products and protocols for molecular biology research*, newsletter of Novagen, no 13, Novagen Inc., a brand of CN Biosciences Ltd, Nottingham, UK.

**Nyfelt, A.** (1929). "Étiologie de la mononucléose infectieuse." *C.R. Soc. Biol.*, **101**, 590-591.

**Nylander, C.**, Leidberg, B. and Lind, T. (1982). "Gas detection by means of surface plasmon resonance." *Sens. Actuat.*, **3**, 79-88.



- O'Shannessey, D.J.**, Bringham-Burke, M. and Peck, K. (1992). "Immobilisation chemistries suitable for use in the BIAcore surface plasmon resonance detector." *Anal. Biochem.*, **205**, 132-136.
- O'Sullivan, C.K.**, Vaughan, R. and Guilbault, G.G. (1999). "Piezoelectric immunosensors-theory and applications." *Anal. Letts.*, **32**, 2353-2377.
- Ober, R.J.** and Ward, E.S. (1999). "The choice of reference cell in the analysis of kinetic data using BIAcore." *Anal. Biochem.*, **271**, 70-80.
- Oettinger, M.A.**, Schatz, D.G., Gorka, C. and Baltimore, D. (1990). "RAG-1 and RAG-2, adjacent genes that synergistically activate V(D)J recombination." *Science*, **248**, 1517-1523.
- Ohlin, M.** and Zouali, M. (2003). "The human antibody repertoire to infectious agents: implications for disease pathogenesis." *Molecular Immunology*, **40**, 1-11.
- Ohya, S.**, Tanabe, Y., Makino, M., Nomura, T., Xiong, H., Arakawa, M. and Mitsuyama, M. (1998a). "The contributions of reactive oxygen intermediates and reactive nitrogen intermediates to listericidal mechanisms differ in macrophages activated pre- and post-infection." *Infect. Immun.*, **66**, 4043-4049.
- Ohya, S.**, Xiong, H., Tanabe, Y., Arakawa, M. and Mitsuyama, M. (1998b). "Killing mechanisms of *Listeria monocytogenes* in activated macrophage by an improved assay system." *J. Med. Microbiol.*, **47**, 211-215.
- Okutani, A.**, Okada, Y., Yamamoto, S. and Igimi, S. (2004). "Overview of *Listeria monocytogenes* contamination in Japan." *Int. J. Food Microbiol.*, **2(1)**, 131-140.
- Old, R.W.**, and Primrose, S.B. (1989). "Expression in *E. coli* of cloned DNA molecules." In: *Principles of gene manipulation- an introduction to genetic engineering*, 4<sup>th</sup> edn., Oxford, UK, (Old, R.W., and Primrose, S.B., eds.). Blackwell Scientific Publications, 143-168.
- Olier, M.**, Pierre, F., Rousseaux, S., Lemaître, J-P, Rousset, A., Piveteau, P. and Guzzo, J. (2003). "Expression of truncated internalin A is involved in impaired internalization of some *Listeria monocytogenes* isolates carried asymptotically by humans." *Infect. Immun.*, **71(3)**, 1217-1224.



**Olsen, E.V.**, Pathirana, S.T., Samoylov, A.M., Barbaree, J.M., Chin, B.A., Neely, W.C. and Vodanyoy, V. (2003). "Specific and selective biosensor for Salmonella and its detection in the environment." *J. Immunol. Meth.*, **53**, 273-285.

**Olsen, J.E.** (2000). "DNA-based methods for detection of foodborne pathogens." *Food Res. Int.*, **33**, 257-266.

**Otto, A.** (1968a). "Excitation of nonradiative surface plasma waves in silver by the method of frustrated total internal reflection." *Z. Phys.*, **216**, 398-410.

**Otto, A.** (1968b). "A new method for exciting nonradiative surface plasma oscillations." *Phys. Stat. Sol.*, **26**, K99-K101.

**Ouadrhiri, Y.**, Scorneaux, B., Sibille, Y. and Tulkens, P.M. (1999). "Mechanisms of the intracellular killing and modulation of antibiotic susceptibility of *Listeria monocytogenes* in THP-1 macrophages activated by gamma interferon." *Antimicrob. Agents Chemother.*, **43**, 1242-1251.

**Pak, S.-L.**, Spahr, U., Jemmi and Salman, M.D. (2002). "Risk factors for *L. monocytogenes* contamination of dairy products in Switzerland, 1990-1999." *Prev. Vet. Med.*, **53**, 55-65.

**Pamer, E.G.**, Harty, J.T. and Bevan, M. (1991). "Precise prediction of a dominant class I MHC-restricted epitope of *L. monocytogenes*." *Nature*, (London), **353**, 852-855.

**Pandripally, V.K.**, Westbrook, D.G., Sunki, G.R. and Bhunia, A.K. (1999). "Surface protein p104 is involved in adhesion of *Listeria monocytogenes* to human epithelial cell line Caco-2." *J. Med. Microbiol.*, **48**, 117-124.

**Pangallo, D.**, Kacálíková, E., Kuchta, T. and Drahovská. (2001). "Detection of *Listeria monocytogenes* by polymerase chain reaction oriented to the *inlB* gene." *Microbiologica*, **24**, 333-339.

**Parekh, R.B.**, Dwek, R.A., Rudd, P.M. and Rademacher, T.W. (1989). "N-glycosylation and in vitro enzymatic activity of human recombinant tissue plasminogen activator expressed in Chinese hamster ovary cells and a murine cell line." *Biochemistry*, **28**(19), 7670-7679.



**Parida, S.K.**, Domann, E., Rohde, M., Müller, S., Darji, A., Hain, T., Wehland, J. and Chakraborty, T. (1998). "Internalin B is essential for adhesion and mediates the invasion of *Listeria monocytogenes* into human endothelial cells." *Mol. Microbiol.*, **28**, 81-93.

**Park, I.-S.**, Kim, W.-Y and Kim, N. (2000). "Operational characteristics of an antibody-immobilized QCM system detecting *Salmonella* spp." *Biosens. Bioelectron.*, **15**, 167-172.

**Patel, P.D.** (2002). "(Bio)sensors for measurement of analytes implicated in food safety: a review." *Trends Anal. Chem.*, **21**(2), 96-115.

**Paul, M.L.**, Dwyer, D.E., Chow, C., Robson, J., Chambers, Eagles, G. and Ackerman, V. (1994). "Listeriosis-a review of eighty-four cases." *Med. J. Aust.*, **160**, 489-493.

**Pavlov, Y.I.**, Rogozin, I.B., Galkin, A.P., Aksenova, A.Y., Hanaoka, F., Rada, C. and Kunkel, T.A. (2002). "Correlation of somatic hypermutation specificity and A-T base pair substitution errors by DNA polymerase  $\eta$  during copying of a mouse immunoglobulin  $\kappa$  light chain transgene." *Proc. Natl. Acad. Sci. USA*, **99**, 9954-9959.

**Perkins, E.A.** and Squirrel, D.J. (2000). "Development of instrumentation to allow the detection of microorganisms using light scattering in combination with surface plasmon resonance." *Biosens. Bioelectron.*, **14**, 853-859.

**Pesce, A.J.**, Ford, D.J., Gaizutis, M. and Pollak, V.E. (1977). "Binding of proteins to polystyrene in solid-phase immunoassays." *Biochem. Biophys. Acta*, **492**, 399.

**Piehler, J.**, Brecht, A., Hehl, K. and Gauglitz, G. (1999). "Protein interactions in covalently attached dextran layers." *Colloids Surfaces B: Biointerfaces*, **13**, 325-336.

**Pilgrim, S.**, Kolb-Mauer, A., Gentshev, I., Goebel, W. and Kuhn, M. (2003). "Deletion of the gene encoding the p60 in *Listeria monocytogenes* leads to abnormal cell division and loss of actin-based motility." *Infect. Immun.*, **71**, 3473-3484.

**Pirie, J.H.** (1940). "The genus *Listerella* Pirie." *Science*, **91**, 383.

**Pistor, S.**, Chakraborty, T., Walter, U. and Wehland, J. (1995). "The bacterial actin nucleator protein ActA of *Listeria monocytogenes* contains multiple binding sites for host microfilament proteins." *Curr. Biol.*, **5**, 517-525.





- Pistor, S., Grobe, L., Sechi, A.S., Domann, E., Gerstel, B., Machesky, L.M., Chakraborty, T. and Wehland, J. (2000).** "Mutations of arginine residues within the 146-KKRRK-150 motif of the ActA protein of *Listeria monocytogenes* abolish intracellular motility by interfering with the recruitment of the Arp2/3 complex." *J. Cell. Sci.*, **113**, 3277-3287.
- Pitcher, D.G., Saunders, N. A. and Owen, R. J. (1989).** "Rapid extraction of bacterial genomic DNA with guanidium thiocyanate." *Letts. Appl. Microbiol.*, **8**, 151-156.
- Pockrand, I., Swalen, J.D., Gordon, J.G. and Philpott, M.R. (1978).** "Surface plasmon spectroscopy of organic monolayer assemblies." *Surface Sci.*, **74**, 237-244.
- Porath, J., Carlson, J., Olsson, I. And Belfrage, G. (1975)** "Metal chelate affinity chromatography, a new approach to protein fractionation." *Nature*, (London), **258**, 598-599.
- Portnoy, D.A., Jacks, P.S. and Hinrichs, D.J. (1988).** "Role of hemolysin for the intracellular growth of *Listeria monocytogenes*." *J. Exp. Med.*, **167**, 1459-1471.
- Pourshafie, M.R., Marlund, B.I. and Ohlson, S. (2004).** "Binding interactions of *Escherichia coli* with globo-tetraosylceramide (globoside) using a surface plasmon resonance biosensor." *J. Microbiol. Methods*, **58**, 313-320.
- Poyart, C., Abachin, E., Razafimantsoa, I., Gaillard, J.-L, Alouf, J.E. and Berche, P. (1993).** "The zinc metalloprotease of *Listeria monocytogenes* is required for maturation of phosphatidylcholine phospholipase C: direct evidence obtained by gene complementation." *Infect. Immun.*, **61**, 1576-1580.
- Poyart-Salermont, C., Carlier, C., Trieu-Cuot, P., Courtieu, A.-L. and Courvalin, P. (1990).** "Transferable plasmid-mediated antibiotic resistance in *Listeria monocytogenes*." *Lancet*, **335**, 1422-1426.
- Pron, B., Boumaila, C., Jaubert, F., Sarnacki, S., Monnet, J.P., Berche, P. and Gaillard, J.L. (1998).** "Comprehensive study of intestinal stage of listeriosis in a rat ligated ileal loop system." *Infect. Immun.*, **66**, 747-755.
- QIAGEN Ltd. (2000).** The QIA Expressionist: A handbook for the high-level expression and purification of 6 HIS-tagged proteins, QIAGEN Ltd., West Sussex, UK.



**Quinn, J.G.** (1999). "Real-time biomolecular interaction analysis: novel applications and developments." Ph. D. Thesis, Dublin City University, Ireland.

**Quinn, J.G.** and O'Kennedy, R. (1999). "Transduction platforms and biointerfacial design of biosensors for real-time biomolecular interaction analysis." *Anal. Letts.*, **32(8)**, 1475-1417.

**Quinn, J.G.**, O'Neil, S., Doyle, S., McAtamney, C., Diamond, D., McCraith, B.D. and O'Kennedy, R. (2000). "Development and application of surface plasmon resonance-based biosensors for the detection of cell-ligand interactions." *Anal. Biochem.*, **281**, 135-143.

**Quinn, J.G.**, Patel, P., Fitzpatrick, B., Manning, B., Dillon, P., Daly, S., O'Kennedy, R., Alcocer, M., Lee, H., Morgan, M. and Lang, K. (1999). "The use of regenerable, affinity ligand-based surfaces for immunosensor applications." *Biosens. Bioelectron.*, **14**, 587-595.

**Rada, C.** and Milstein, C. (2001). "The intrinsic hypermutability of antibody heavy and light chain genes decays exponentially." *EMBO J.*, **20**, 4570-4576.

**Raether, H.** (1977). "Surface plasma oscillations and their applications." *Phys. Thin Films*, **9**, 145.

**Rafflelsbauer, D.**, Bubert, A., Engelbrecht, F., Scheinpflug, J., Simm, A., Hess, J., Kaufmann, S.H.E. and Goebel, W. (1998). "The gene cluster *inlC2DE* of *Listeria monocytogenes* contains additional internalin genes and is important for virulence in mice." *Mol. Gen. Genet.* **260**, 144-158.

**Raggatt, P.** (1991). "Data processing." In: *Principles and practice of immunoassay*. (Price, C.P. and Newman, D.J., eds.), Stockton Press, New York, USA, 190-218.

**Raju, T.S.** (2003) "Glycosylation variations with expression systems and their impact on biological activity of therapeutic immunoglobulins." *Bioprocess Int.*, **1(4)**, 44-53.

**Raju, T.S.**, Briggs, J.B., Borge, S.M. and Jones, A.J.S. (2000). "Species-specific variation in glycosylation of IgG: evidence for the species-specific sialylation and branch-specific galactosylation and importance for engineering recombinant glycoprotein therapeutics." *Glycobiology*, **10(5)**, 477-486.



**Ramage, C.P.**, Low, J.C., McLaughlin, J. and Donachie, W. (1999). "Characterisation of *Listeria ivanovii* isolates from the UK using pulsed-field gel electrophoresis." *FEMS Microbiol. Letts.*, **15**, 349-353.

**Rand, G.A.**, Ye, J., Brown, C.W. and Letcher, S.V. (2002). "Optical biosensors for food pathogen detection." *Food Technol.*, **56(3)**, 32-37.

**Rank, K.B.**, Mildner, A.M., Leone, J.W., Koeplinger, K.A., Chou, K.C., Tomasselli, A.G., Heinrikson, R.L. and Sharma, S.K. (2001). "[W206R]-procaspase 3: an inactivateable substrate for caspase 8." *Protein Expr. Purif.*, **22**, 258-266.

**Rasooly, A.** (2001). "Surface plasmon resonance analysis of Staphylococcal Enterotoxin B in food." *J. Food Protect.*, **64**, 37-43.

**Regulation (EC) No. 178/2002** (2002). "European Parliament and Council of 28<sup>th</sup> January 2002 laying down the general principles and requirements of food law, establishing the European Food Safety Authority and laying down procedures in matters of food safety." *Official J. Europ. Communities*, 2002, L 31/1, 1<sup>st</sup> February 2002.

**Renzone, A.**, Cossart, P., and Dramsi, S. (1999). "PrfA, the transcriptional activator of virulence genes, is upregulated during interaction of *Listeria monocytogenes* with mammalian cells and in eukaryotic cell extracts." *Mol. Microbiol.*, **34**, 552-561.

**Renzone, A.**, Klarsfeld, A., Dramsi, S. and Cossart, P. (1997). "Evidence that PrfA, the pleiotropic activator of virulence genes in *Listeria monocytogenes*, can be present but inactive." *Infect. Immun.*, **65**, 1515-1518.

**Repp, H.**, Pamukci, Z., Koschinski, A., Domann, E., Darji, A., Birringer, J., Brockmeier, D., Chakraborty, T. and Dreyer, F. (2002). "Listeriolysin of *Listeria monocytogenes* forms Ca<sup>2+</sup>-permeable pores leading to intracellular Ca<sup>2+</sup> oscillations." *Cell Microbiol.*, **4(8)**, 483-491.

**Revy, P.**, Muto, T., Levy, Y., Geissmann, F., Plebani, A., Sanal, O., Catalan, N., Forveille, M., Dufourcq-Labelouse, R., Gennery, A., Tezcan, I., Ersoy, F., Kayserili, H., Ugazio, A.G., Brousse, N., Muramatsu, M., Notarangelo, L.D., Kinoshita, K., Honjo, T., Fischer, A. and Durandy, A. (2000) "Activation-induced cytidine deaminase (AID) deficiency causes the autosomal recessive form of the hyper-IgM syndrome (HIGM2)." *Cell*, **102**, 565-575.



**Rich, R.L.** and Myszka, D.G. (2001). "Survey of the year 2000 commercial optical biosensor literature." *J. Mol. Recognit.*, **14**, 273-294.

**Riedo, F.X.**, Pinner, R.W., De Lourdes Tosca, M., Cartter, M.L., Graves, L.M., Reeves, M.W., Weaver, R.E., Plikaytis, B.D. and Broome, C.V. (1994). "A point-source foodborne outbreak: documented incubation period and possible mild illness." *J. Infect. Dis.*, **170**(3), 693-696.

**Rief, M.**, Oesterhelt, F., Heymann, B. and Gaub, H.E. (1997). "Single molecule force spectroscopy on polysaccharides by atomic force microscopy." *Science*, **275**, 1295-1297.

**Rijpens, N.** and Herman, L. (2004). "Comparison of selective and nonselective primary enrichments for the detection of *Listeria monocytogenes* in cheese." *Int. J. Food Microbiol.*, **94**, 15-22.

**Ripio, M.T.**, Brehm, K., Lara, M., Suárez, M. and Vázquez-Boland, J.A. (1997b). "Glucose-1-phosphate utilization by *Listeria monocytogenes* is PrfA dependent and co-ordinately expressed with virulence factors." *J. Bacteriol.*, **179**, 7174-7180.

**Ripio, M.-T.**, Domínguez-Bernal, G., Brehm, K., Berche, P., Suárez, M. and Vázquez-Boland, J.A. (1996). "Transcriptional activation of virulence genes in wild-type strains of *Listeria monocytogenes* in response to a change in the extracellular medium composition." *Res. Microbiol.*, **147**, 311-384.

**Ripio, M.T.**, Domínguez-Bernal, G., Lara, M., Suárez, M. and Vázquez-Boland, J.A. (1997a). "A Gly145Ser substitution in the transcriptional activator PrfA causes constitutive overexpression of virulence factors in *Listeria monocytogenes*." *J. Bacteriol.*, **179**, 1533-1540.

**Ripio, M.T.**, Dominguez-Bernal, G., Suárez, G., Brehm, K., Berche, P. and Vázquez-Boland, J.A. (1996). "Transcriptional activation of virulence genes in wild-type strains of *Listeria monocytogenes* in response to a change in the extracellular medium composition." *Res. Microbiol.*, **147**, 371-384.

**Rocourt, J.** (1994). "*Listeria monocytogenes*: the state of the art." *Dairy Food Environ. Sanitation*, **14**, 70-82.





**Rocourt, J.** (1999). "The genus *Listeria* and *Listeria monocytogenes*: phylogenetic position, taxonomy and identification." In: *Listeria, Listeriosis and Food Safety*, 2<sup>nd</sup> edn. (Ryser, E.T. and Marth, E.H., eds.), 1-20, Marcel Dekker Inc., New York, USA.

**Rocourt, J., Boerlin, P., Grimont, P.A.D., Jacquest, C. and Piffaretti, J.C.** (1992). "Assignment of *Listeria grayi* and *Listeria murrayi* to a single species, *Listeria grayi*, with a revised description of *Listeria grayi*." *Int. J. Syst. Bacteriol.*, **42**, 69-73.

**Rocourt, J., Hof, H., Schrettenbrunner, A., Malinverni, R. and Bille, J.** (1986). "Acute purulent *Listeria seeligeri* meningitis in an immunocompetent adult." *Schweiz. Med. Wochenschr.*, **116**, 248-251.

**Rogers, H.W., Callery, M.P., Deck, B. and Unanue, E.R.** (1996). "*Listeria monocytogenes* induces apoptosis of infected hepatocytes." *J. Immunol.*, **156**, 679-684.

**Rogers, K.R.** (1998). "Principles of affinity-based biosensors." In: *Biosensors: Techniques and protocols*. (Rogers, K. and Mulchandani, A., eds.) Humana Press Inc., Totowa, N.J., USA., *Meth. Biotechnol.*, **7**, 3-18.

**Rogozin, I.B., Pavlov, Y.I., Bebenek, K., Matsuda, T. and Kunkel, T.A.** (2001) "Somatic mutation hotspots correlate with DNA polymerase  $\eta$  error spectrum." *Nat. Immunol.*, **2**, 530-536.

**Rossen, L., Norskov, P., Holmstrom, K. and Rasmussen, O.F.** (1992). "Inhibition of PCR by components of food samples, microbial diagnostic assays and DNA extraction solutions." *Int. J. Food Microbiol.*, **17**, 37-45.

**Rubin, R.L., Hardtke, M.A. and Carr, R.I.** (1980). "The effect of high antigen density on solid-phase radioimmunoassays for antibody regardless of immunoglobulin class." *J. Immunol. Meth.*, **33**, 287.

**Ruhland, G.J., Hellwig, M., Wanner, S., Frank, R. and Goebel, W.** (1993). "Cell-surface location of *Listeria*-specific protein p60-detection of *Listeria* cells by indirect immunofluorescence." *J. Gen. Microbiol.*, **139**, 609-616.

**Ryser, E.T.** (1999). "Foodborne listeriosis." In: *Listeria, Listeriosis and Food Safety*, 2<sup>nd</sup> edn. (Ryser, E.T. and Marth, E.H., eds.), 299-358, Marcel Dekker Inc., New York, USA.



**Salamina, G.E.**, Dalle Donne, E., Nicolini, A., Poda, G., Cesarone, D., Bucci, M., Fini, R., Maldini, M., Schuchat, A., Swaminathan, B., Bibb, W., Rocourt, J., Binkin, N. and Salmaso, S. (1996). "A foodborne outbreak of gastroenteritis involving *Listeria monocytogenes*." *Epidemiol. Infect.*, **117**, 429-436.

**Salamon, Z.**, Brown, M.F. and Tollin, G. (1999). "Plasmon resonance spectroscopy: probing molecular interactions within membranes." *Trends Biochem.*, **4**, 213-219.

**Sallen, B.A.**, Rajoharison, S., Desverenne, S., Quinn, F. and Mabilat, C. (1996). "Comparative analysis of 16S and 23S rRNA sequences of *Listeria* species." *Int. J. Syst. Bacteriol.*, **46**, 669-674.

**Salonen, E.M.** and Vaheri, A. (1979). "Immobilisation of viral and mycoplasmal antigens and of immunoglobulins on polystyrene surface for immunoassays." *J. Immunol. Meth.*, **30**, 209.

**Saphire, E.O.**, Parren, P.W.H.I., Pantophlet, R., Zwick, M.B., Morris, G.M., Rudd, P.M., Dwek, R.A., Stanfield, R.L., Burton, D.R. and Wilson, I.A. (2001) "Crystal structure of a neutralising human IgG against HIV-1: a template for vaccine design." *Science*, **293**, 1155-1159.

**Saphire, E.O.**, Stanfield, R.L., Max-Crispin, M.D., Parren, P.W.H.I., Rudd, P.M., Dwek, R.A., Burton, D.R. and Wilson, I.A. (2002). "Contrasting IgG structures reveal extreme asymmetry and flexibility." *J. Mol. Biol.*, **319**, 9-18.

**Sawchuk, D.J.**, Weis-Garcia, F., Malik, S., Besmer, E., Bustin, M., Nusenzweig, M.C. and Cortes, P. (1997). "V(D)J recombination: modulation of RAG1 and RAG2 cleavage activity on 12/23 substrates by whole cell extract and DNA-binding proteins." *J. Exp. Med.*, **185**(11), 2025-2032.

**Scheu, P.**, Gasch, A. and Berghof, K. (1999). "Rapid detection of *Listeria monocytogenes* by PCR-ELISA." *Letts. Appl. Microbiol.*, **29**, 416-420.

**Schlech, W.F III.** (2000). "Foodborne listeriosis." *Clin. Infect. Dis.*, **31**, 770-775.



**Schlech, W.F III**, Lavigne, P.M., Bortolussi, R.A., Allen, A.C., Haldane, E.V., Wort, A.J., Hightower, A.W., Johnson, S.E., King, S.H., Nicholls, E.S. and Broome, C.V. (1983). "Epidemic listeriosis: Evidence for transmission by food." *Med. Intelligence.*, **308**, 203-206.

**Schluter, D.**, Domann, E., Buck, C., Hain, T., Hof, H., Chakraborty, T. and Deckert-Schluter, M. (1998). "Phosphatidylcholine-specific phospholipase C from *Listeria monocytogenes* is an important virulence factor in murine cerebral listeriosis." *Infect. Immun.*, 5930-5938.

**Schmid, M.**, Walcher, M., Bubert, A., Wagner, M., Wagner, M. and Schleifer, K.H. (2003). "Nucleic acid-based, cultivation-independent detection of *Listeria* spp. and genotypes of *L. monocytogenes*." *FEMS Immunol. Med. Microbiol.*, **35(3)**, 215-225.

**Schmid, M.W.**, Ng, E.Y.W., Lampidis, R., Emmerth, M., Walcher, M., Kreft, J., Goebel, W., Wagner, M. and Schleifer, K.-H. (2005). "Evolutionary history of the genus *Listeria* and its virulence genes." *Sys. Appl. Microbiol.*, **28**, 1-18.

**Schmidt, M.**, Tuominen, N., Johansson, T., Weiss, S.A., Keinänen, K. and Oker-Blom, C. (1998). "Baculovirus-mediated large scale expression and purification of a poly-histidine-tagged *Rubella* virus capsid protein." *Protein Expr. Purif.*, **12**, 323-330.

**Schönberg, A.**, Bannerman, E., Courtieu, A.L., Kiss, R., McLaughlin, J., Shah, S. and Wilhelms, D. (1996). "Serotyping of 80 strains from the WHO multicentre international typing study of *L. monocytogenes*." *Int. J. Food Microbiol.*, **32(3)**, 279-287.

**Schubert, W.-D.** and Heinz, D.W. (2003). "Structural aspects of adhesion to and invasion of host cells by the human pathogen *Listeria monocytogenes*." *ChemBioChem*, **4**, 1285-1291.

**Schubert, W.D.**, Göbel, G., Diepholz, M., Darji, A., Kloer, D., Hain, T., Chakraborty, T., Wehland, J., Domann, E. and Heinz, D.W. (2001). "Internalins from the human pathogen *Listeria monocytogenes* combine three distinct folds into a contiguous internalin domain." *J. Mol. Biol.*, **312(4)**, 783-794.

**Schuchat, A.**, Swaminathan, B. and Broome, C.V. (1991a). "Epidemiology of human listeriosis." *Clin. Microbiol. Rev.*, **4(3)**, 169-183.

**Schuchat, A.**, Swaminathan, B. and Broome, C.V. (1991b). "*Listeria monocytogenes* CAMP reaction." *Clin. Microbiol. Rev.*, **4(3)**, 396.



**Schuck, P.** (1996). "Kinetics of ligand binding to receptor immobilised in a polymer matrix, as detected with an evanescent wave biosensor 1: a computer simulation of the influence of mass transport." *Biophys. J.*, **70**, 1230-1249.

**Schuck, P.** and Minton, P. (1996). "Analysis of mass transport-limited binding kinetics in evanescent wave biosensors." *Anal. Biochem.*, **240**, 262-272.

**Schüller, S., Kügler, S.** and Goebel, W. (1998). "Suppression of major histocompatibility complex class I and class II gene expression in *Listeria monocytogenes*-infected murine macrophages." *FEMS Immunol. Med. Microbiol.*, **20**, 289-299.

**Schwan, W.R., Demuth, A., Kuhn, M.** and Goebel, W. (1994). "Phosphatidylinositol-specific phospholipase C from *Listeria monocytogenes* contributes to intracellular survival and growth of *Listeria innocua*." *Infect. Immun.*, **62**, 4795-4803.

**Schwartz, B., Ciesielski, C.A., Broome, C.V., Gaventa, S., Brown, G.R., Gellin, A., Hightower, W., Mascola, L.** and Listeriosis Study Group. (1988). "Association of sporadic listeriosis with consumption of uncooked hot dogs and undercooked chicken." *Lancet*, **2(8614)**, 779-782.

**Schwartz, B., Hexter, D., Broome, C.V., Hightower, W., Hirschhorn, R.B., Porter, J.D., Hayes, P.S., Bibb, W.F., Lorber, B.** and Faris, D.G. (1989). "Investigation of an outbreak of listeriosis: New hypotheses for the etiology of epidemic *Listeria monocytogenes* infections." *J. Infect. Dis.*, **159(4)**, 680-685.

**Scott Merrel, D.** and Camili, A. (2002). "Acid tolerance of gastrointestinal pathogens." *Curr. Opin. Microbiol.*, **5(1)**, 51-55.

**Scotter, S.L., Langton, S., Lombard, B., Schulten, S., Nagelkerke, N., In't Veld, P.H., Rollier, P.** and Lahellec, C. (2001a). "Validation of ISO method 11290 Part 1-Detection of *Listeria monocytogenes* in foods." *Int. J. Food Microbiol.*, **64**, 295-306.

**Scotter, S.L., Langton, S., Lombard, Lahellec, C., B., Schulten, S., Nagelkerke, N., In't Veld, P.H.** and Rollier, P. (2001b). Validation of ISO method 11290 Part 2-Enumeration of *Listeria monocytogenes* in foods." *Int. J. Food Microbiol.*, **70**, 121-129.





**Sedgwick, J.D.** and Czerkinsky, C. (1992). "Detection of cell-surface molecules, secreted products of single cells and cellular proliferation by enzyme immunoassay." *J. Immunol. Meth.*, **30**, 159-175.

**Seeliger, H.P.R.** (1988). "Listeriosis-history and actual developments." *Infection*, **16**, S80-S84.

**Seeliger, H.P.R.** and Hühne, K. (1979). "Serotyping of *Listeria monocytogenes* and related species." In: *Methods in Microbiology*, (Bergan, T. and Norris, J., eds.), **13**, 31-49, Academic Press, New York, USA.

**Seeliger, H.P.R.** and Jones, D. (1986). "Genus *Listeria*." In: *Bergey's Manual of Systematic Bacteriology*, (Sneath, P.H.A., Mair, N.S., Sharpe, M.E. and Holt, J.G., eds.), 1235-1245, Williams and Wilkins, Baltimore, Md., USA.

**Sewell, A.M.**, Warburton, D.W., Boville, A., Daley, E.F. and Mullen, K. (2003). "The development of an efficient and rapid enzyme-linked fluorescent assay method for the detection of *Listeria* spp. from foods." *Int. J. Food Microbiol.*, **81**, 123-129.

**Sheehan, B.**, Klarsfeld, A., Msadek, T. and Cossart, P. (1995). "Differential activation of virulence gene expression by PrfA, the *Listeria monocytogenes* virulence regulator." *J. Bacteriol.*, **177**, 6469-6476.

**Shen, H.**, Miller, J.F., Fan, X., Kolwyck, D., Ahmed, R. and Harty, J.T. (1998). "Compartmentalization of bacterial antigens: differential effects on priming of CD8 T cells and protective immunity." *Cell*, **92**(4), 535-545.

**Shen, Y.**, Naujokas, M., Park, M. and Ireton K. (2000). "InlB mediated-dependent internalisation of *Listeria monocytogenes* is mediated by the Met receptor tyrosine kinase." *Cell*, **103**, 501-510.

**Shetron-Rama, L.M.**, Marquis, H., Bouwer, H.G.A. and Freitag, N.E. (2002). "Intracellular induction of *Listeria monocytogenes actA* expression." *Infect. Immune.*, **70**, 1087-1096.

**Shine, J.** and Dalgarno, L. (1975). "Determinant of cistron specificity in bacterial ribosomes." *Nature*, (London), **254**, 34-38.



**Shulman, M., Wilde, C.D. and Köhler, G. (1978).** "A better cell line for making hybridomas secreting specific antibodies." *Nature*, (London.), **276**, 269-270.

**Sibeliuss, U., Rose, F., Chakraborty, T., Darji, A., Wehland, J., Weiss, S., Seeger, W. and Grimminger, F. (1996).** "Listeriolysin is a potent inducer of the phosphatidylinositol response and lipid mediator generation in human endothelial cells." *Infect. Immun.*, **64(2)**, 674-676.

**Sibeliuss, U., Schulz, E.C., Rose, F., Hatter, K., Jacobs, T., Weiss, S., Chakraborty, T., Seeger, W. and Grimminger, F. (1999).** "Role of *Listeria monocytogenes* exotoxins listeriolysin and phosphatidylinositol-specific phospholipase C in activation of human neutrophils." *Infect. Immun.*, **67(3)**, 1125-1130.

**Siddique, I.H., I-Fong Lin, S. and Chung, R.A. (1974).** "Purification and characterisation of hemolysin produced by *Listeria monocytogenes*." *Am. J. Vet. Res.*, **35**, 289-296.

**Siegman-Igra, Y., Levin, R., Weinberger, M., Golan, Y., Schwartz, D., Samra, Z., Konigsberger, H., Yinnon, A., Rahav, G., Keller, N., Bishara, N., Karpuch, J., Finkelstein, R., Alkan, M., Landau, Z., Novikov, J., Hassin, D., Rudnicki, C., Kitzes, R., Ovadia, S., Shimoni, Z., Lang, R. and Shohat, T. (2002).** "*Listeria monocytogenes* infection in Israel and review of cases worldwide." *Emerg. Infect. Dis.*, **8(3)**, 305-310.

**Silva, I.M.M., Almeida, R.C.C., Alves, M.A.O. and Almeida, P.F. (2003).** "Occurrence of *Listeria* spp. in critical control points and the environment of Minas Frescal cheese processing." *Int. J. Food. Microbiol.*, **81(3)**, 241-248.

**Sim, J., Hood, D., Finnie, L., Wilson, M., Graham, C., Brett, M. and Hudson, J.A. (2002).** "Series of incidents of *Listeria monocytogenes* non-invasive febrile gastroenteritis involving ready-to-eat meats." *Letts. Appl. Microbiol.*, **35**, 409-413.

**Singleton, P. (1995)** "Molecular biology I: genes and gene expression" In: *Bacteria in biology, biotechnology and medicine*, (3<sup>rd</sup> edition, Wiley publishing) 83-113.

**Siragusa, G.R. and Johnson, M.G. (1990).** "Monoclonal antibody specific for *Listeria monocytogenes*, *Listeria innocua* and *Listeria welshimeri*." *Appl. Environ. Microbiol.*, **56**, 1897-1904.



**Skoble, J., Portnoy, D.A. and Welch, M.D. (2000).** "Three regions within ActA promote Arp2/3 complex-mediated actin nucleation and *Listeria monocytogenes* motility." *J. Cell Biol.*, **150**, 527-538.

**Slaghuis, J., Goetz, M., Engelbrecht, F. and Goebel, W. (2004).** "Inefficient replication of *Listeria innocua* in the cytosol of mammalian cells." *J. Infect. Dis.*, **189**(3), 393-401.

**Slutsker, L. and Schuchat, A. (1999).** "Listeriosis in humans." In: *Listeria, Listeriosis and Food Safety*, 2<sup>nd</sup> edn. (Ryser, E.T. and Marth, E.H., eds.), 75-95, Marcel Dekker Inc., New York.

**Smeardon, W.J., Roberts, I.S., Jones, D. and Andrew, P.W. (2001).** "Surveillance of listeriosis in England and Wales, 1995-1999." *Commun. Dis. Pub. Health*, **4**, 188-193.

**Smith, G.A., Marquis, H., Jones, S., Johnston, N.C., Portnoy, D.A. and Goldfine H. (1995).** "Two distinct phospholipases C of *Listeria monocytogenes* have overlapping roles in escape from vacuole and cell-to-cell spread." *Infect. Immun.*, **63**, 4231-4237.

**Solve, M., Boel, J. and Nørrung, B. (2000).** "Evaluation of a monoclonal antibody able to detect live *Listeria monocytogenes* and *Listeria innocua*." *Int. J. Food Microbiol.*, **57**, 219-224.

**Spreng, S., Dietrich, G., Goebel, W and Gentschev, I. (2003).** "Protection against murine listeriosis by oral vaccination with recombinant *Salmonella* expressing protective listerial epitopes within a surface-exposed loop of the TolC-protein." *Vaccine*, **21**, 746-752.

**Stamatakis, K. and Tien, C. (1993).** "A simple model of cross-flow filtration based on particle adhesion." *AIChE J.*, **39**(8), 1292-1302.

**Stenberg, E., Persson, B., Roos, H. and Urbaniczky, C. (1991).** "Quantitative determination of protein with surface plasmon resonance by using radiolabelled proteins." *J. Colloid Interfac Sci.*, **143**, 513-526.

**Stuart, S.E. and Welshimer, H.J. (1974).** "Taxonomic re-examination of *Listeria pirie* and transfer of *Listeria grayi* and *Listeria murrayi* to a new genus, *Murraya*." *Int. J. Syst. Bacteriol.*, **24**(2), 177-185.



**Suárez, M.,** Gonzalez-Zorn, B., Vega, Y., Chico-Calero, I. and Vázquez-Boland, J.A. (2001). "A role for ActA in epithelial cell invasion by *Listeria monocytogenes*." *Cell Microbiol.*, **3**(12), 853-864.

**Suda, T.,** and Nagata, S. (1994). "Purification and characterization of the Fas-ligand that induces apoptosis." *J. Exp Med.*, **179**(3), 873-879.

**Suda, T.,** Okazaki, T., Naito, Y., Yokota, T., Arai, N., Ozaki, S., Nakao, N and Nagata, S. (1995). "Expression of the Fas ligand in cells of T cell lineage." *J. Immunol.*, **154**, 3806-3813.

**Sutton, J.M.** and Richardson, D.R. (1998). "*E. coli* expression vectors" In: *Vectors: expression system*, (Jones, P., ed.) (Essential Techniques Series, Wiley Publishing), London, Eds. 3-20.

**Swanson, J.A.** and Baer, S.C. (1995). "Phagocytosis by zippers and triggers." *Trends in Cell Biol.*, **5**, 89-93.

**Tabouret, M.C.,** De Rycke, J. and Dubray, G. (1992). "Analysis of surface proteins of *Listeria* in relation to species, serovar and pathogenicity." *J. Gen. Microbiol.*, **138**, 743-753.

**Tang, P.,** Rosenshine, I., Cossart, P. and Finlay, B.B. (1996). "Listeriolysin O activates mitogen-activated protein kinase in eukaryotic cells." *Infect. Immun.*, **64**, 2359-2361.

**Tang, P.,** Rosenshine, I., Tang, P. and Finlay, B.B. (1994). "*Listeria monocytogenes*, an invasive bacterium, stimulates MAP kinase upon attachment to epithelial cells." *Mol. Biol. Cell*, **5**, 455-464.

**Taylor, C.M.,** Beresford, M., Epton, H.A.S., Sigee, D.C., Shama, G., Andrew, P.W. and Roberts, I.S. (2002). "*Listeria monocytogenes relA* and *hpt* mutants are impaired in surface-attached growth and virulence." *J. Bact.*, **184**(3), 621-628.

**Terpe, K.** (2003). "Overview of tag protein fusions: from molecular and biochemical fundamentals to commercial systems." *Appl. Microbiol. Biotechnol.*, **60**, 523-533.

**Tims, B.T.,** Dickey, S.S., DeMarco, D.R. and Lim, D.V. (2001). "Detection of low levels of *Listeria monocytogenes* within 24 hours using an evanescent wave biosensor." *Am. Clin. Lab.*, **20**(8), 28-29.





- Ton-That, H.,** Liu, G., Mazmanian, S.K., Faull, K.Y. and Schneewind, O. (1999). "Purification and characterisation of sortase, the transpeptidase that cleaves surface proteins of *Staphylococcus aureus* at the LPXTG motif." *Proc. Natl. Acad. Sci. USA*, **96(22)**, 12424-12429.
- Torensma, R.,** Visser, M.J.C., Aarsman, C.J.M., Poppelier, M.J.J.G., Fluit, A.C. and Verhoef, J. (1993). "Monoclonal antibodies that react with live *Listeria* spp." *Appl. Environ. Microbiol.*, **59**, 2713-2716.
- Trusolino, L. et al.,** (1998). "Interactions between scatter factors and their receptors: hints for therapeutic applications." *FASEB J.*, **12**, 1267-1280.
- Turner, A.P.F.,** Karube, I. and Wilson, G. (1987). "Biosensors: fundamentals and applications." Oxford University Press, Oxford, UK.
- Ueda, E.K.M.,** Gout, P.W. and Morganti, L. (2003). "Current and prospective applications of metal ion-protein binding." *J. Chromatography A*, **988**, 1-23.
- Unanue, E.R.** (1997a). "Studies in listeriosis show the strong symbiosis between the innate cellular and T-cell response." *Immunol. Rev.*, **158**, 11-25.
- Unanue, E.R.** (1997b). "Inter-relationship among macrophages, natural killer cells and neutrophils in early stages of *Listeria* resistance." *Curr. Opin. Immunol.*, **9**, 35-43.
- Unnerstad, H.** (2001). "*Listeria monocytogenes* - strain diversity demonstrated by genotyping." Doctoral thesis, Dept. Food Hygiene, Swedish University of Agricultural Sciences, Uppsala, Sweden.
- Unnerstad, H.,** Bannerman, E., Bille, J., Danielson-Tham, M.-L., Waak, E. and Tham, W. (1996). "Prolonged contamination of a dairy with *Listeria monocytogenes*." *Neth. Milk Dairy J.*, **50**, 493-499.
- Urdahl, K.B.,** Sun, J.C. and Bevan, M.J. (2002) "Positive selection of MHC class Ib-restricted CD8(+) T cells in hematopoietic cells." *Nat. Immunol.*, **3**, 772-779.



- Uyttendale, M., Van Hoorde, I. and Debevere, J. (2000).** "The use of immuno-magnetic separation as a tool in a sample preparation for direct detection of *L. monocytogenes* in cheese." *Int. J. Food Microbiol.*, **54**, 205-212.
- Van der Merwe, P.A., Brown, M.H., Davis, S.J. and Barclay, A.N. (1993).** "Affinity and kinetic analysis of the interaction of the cell adhesion molecules rat CD2 and CD48." *EMBO. J.*, **12**, 4945-4954.
- Vaughan, R.D., Carter, R.M., O'Sullivan, C.K. and Guilbault, G.G. (2003).** "A quartz crystal microbalance (QCM) sensor for the detection of *Bacillus cereus*." *Anal. Letts.*, **36**(4), 731-747.
- Vaughan, R.D., O'Sullivan, C.K. and Guilbault, G.G. (2001).** "Development of a quartz crystal microbalance (QCM) immunosensor for the detection of *Listeria monocytogenes*." *Enz. Microbial Technol.*, **29**, 635-638.
- Vázquez-Boland, J.A., Domínguez, L., Fernández-Gagayzábal, J.F. and Suárez, G. (1992).** "*Listeria monocytogene* CAMP reaction." *Clin. Microbiol. Rev.*, **5**, 343.
- Vázquez-Boland, J.A., Dominguez, L., Roderiguez-Ferri and Suárez, G. (1989).** "Purification and characterisation of two *Listeria ivanovii* cytolysins, a sphingomyelinase C and a thiol-activated toxin (ivanolysin O)." *Infect. Immun.*, **57**, 3928-3935.
- Vázquez-Boland, J.A., Domínguez-Bernal, G., González-Zorn, B., Kreft, J. and Goebel, W. (2001a).** "Pathogenicity islands and virulence evolution in *Listeria monocytogenes*." *Microb. Infect.*, **3**, 571-584.
- Vázquez-Boland, J.A., Kuhn, M., Berche, P., Chakraborty, T., Domínguez-Bernal, G., Goebel, W., González-Zorn, B., Wehland, J. and Kreft, J. (2001b).** "*Listeria* pathogenesis and molecular virulence determinants." *Clin. Microbiol. Rev.*, **14**(3), 584-640.
- Vega, Y., Rauch, M., Banfield, M.J., Ermolaeva, S., Scortti, .M, Goebel, W. and Vázquez-Boland, J.A. (2004).** "New *Listeria monocytogenes* *prfA*\* mutants, ranscriptional properties of PrfA\* proteins and structure-function of the virulence regulator PrfA." *Mol. Microbiol.*, **52**(6), 1553-1565.



**Verma, N.K.,** Ziegler, H.K., Stocker, B.A. and Schoolnik, G.K. (1995). "Induction of a cellular immune response to a defined T cell epitope as an insert in the flagellin of a live vaccine strain of *Salmonella*." *Vaccine*, **13**, 235-244.

**Villanueva, M.S.,** Sijts, A.J.A.M. and Pamer, E.G. (1995). "Listeriolysin is processed efficiently into an MHC class I-associated epitope in *Listeria monocytogenes*-infected cells." *J. Immunol.*, **155**(11), 5227-5233.

**Vlaemynck, G.,** Lafarge, V. and Scotter, S. (2000). "Improvement of the detection of *Listeria monocytogenes* by the application of ALOA, a diagnostic, chromogenic medium." *J. Appl. Microbiol.*, **88**, 430-441.

**Wadsworth, S.J. and** Goldfine, H. (2002). "Mobilization of protein kinase C in macrophages induced by *Listeria monocytogenes* affects its internalization and escape from the phagosome." *Infect. Immun.*, **70**, 4650-4660.

**Wagner, M. and** Allerberger, F. (2002). "Characterisation of *Listeria monocytogenes* recovered from 41 cases of sporadic listeriosis in Austria by serotyping and pulsed-field gel electrophoresis." *FEMS Immunol. Med. Microbiol.*, **1467**, 1-8.

**Walker, S.J.,** Archer, P. and Banks, J.G., (1990). "Growth of *Listeria monocytogenes* at refrigeration temperatures." *J. Appl. Bacteriol.*, **68**, 157-162.

**Wampler, J.L.,** Kim, K.P., Jaradat, Z.W. and Bhunia, A.K. (2004). "Heat-shock protein 60 acts as a receptor for the *Listeria* adhesion protein in Caco-2 cells." *Infect. Immun.*, **72**(2), 931-936.

**Watanabe-Fukunaga, R.,** Brannan, C.I., Itoh, N., Yonehara, S., Copeland, N.G., Jenkins, N.A. and Nagata, S. (2002). "The cDNA structure, expression and chromosomal assignment of the mouse Fas antigen." *J. Immunol.*, **148**, 1284-1279.

**Watts, H.J. and** Lowe, C.R. (1994). "Optical biosensor for monitoring microbial cells." *Anal. Chem.*, **66**, 2465-2470.

**Webster D.M.,** Henry, A.H. and Rees, A.R. (1994). "Antibody-antigen interactions." *Curr. Opin. Struct. Biol.*, **4**, 123-129.



**Weiglein, L.,** Goebel, W., Troppmair, J., Rapp, U.R., Demuth, A. and Kuhn, M. (1997). "*Listeria monocytogenes* infection of HeLa cells results in listeriolysin O-mediated transient activation of the Raf-MEK-MAP kinase pathway." *FEMS Microbiol. Letts.*, **148**, 189-195.

**Weir, D.M.** (1988). "Immunity." In: *Immunology-(Student notes)*, (Weir, D.M., ed.), 6<sup>th</sup> edn, Churchill Livingstone, Edinburgh, UK, 3-12.

**Wentworth Jr., P.,** McDunn, J.E., Wentworth, A.D., Takeuchi, C., Nieva, J., Jones, T., Bautista, C., Ruedi, J.M., Gutierrez, A., Janda, K.D., Babior, B.M., Eschenmoser, A. and Lerner, R.A. (2002). "Evidence for antibody-catalyzed ozone formation in bacterial killing and inflammation." *Science*, **298**, 2195-2199.

**Wentworth, A.D.,** Jones, L.H., Wentworth Jr., P., Janda, K.D. and Lerner, R.A. (2000). "Antibodies have the intrinsic capacity to destroy antigens." *Proc. Natl. Acad. Sci. USA*, **97**, 10930-10935.

**Wernars, K.,** Heuvelman, C.J., Chakraborty, T. and Notermans, S.H.W. (1991). "Use of the polymerase chain reaction for direct detection of *Listeria monocytogenes* in soft cheese." *J. Appl. Bacteriol.*, **70**, 121-126.

**Wewetzer, K.** and Seilheimer, B. (1995). "Establishment of a single-step hybridoma cloning protocol using an automated cell transfer system: comparison with limiting dilution." *J. Immunol. Meth.*, **179**, 71-76.

**Wieckowska-Szakiel, M.,** Bubert, A., Rozalski, M., Krajewska, U., Rudnica, W. and Rozalska, B. (2002). "Colony-blot assay with anti-p60 antibodies as a method for quick identification of *Listeria* in food." *Int. J. Food Microbiol.*, **72(1-2)**, 63-71.

**Wiedman, M.,** Bruce, J.L., Keating, C., Johnson, A.E., McDonough, P.L. and Batt, C.A. (1997). "Ribotypes and virulence gene polymorphisms suggest three distinct *Listeria monocytogenes* lineages with differences in pathogenic potential." *Infect. Immun.*, **65**, 2707-2716.

**Williams, J.R.,** Thayyullathil, C. and Freitag, N.E. (2000). "Sequence variations within PrfA DNA binding sites and effects on *Listeria monocytogenes* virulence gene expression." *J. Bacteriol.*, **182(3)**, 837-841.





**Wilson, I.G.** (1997). "Inhibition and facilitation of nucleic acid amplification." *Appl. Environ. Microbiol.*, **63**, 3741-3751.

**Wizemann, H.** and von Braun, A. (1999). "Purification of *E. coli*-expressed HIS-tagged hepatitis B core antigen by Ni<sup>2+</sup>-chelate affinity chromatography." *J. Virol. Meth.*, **77**, 189-197.

**Wong, A.C.** (1998). "Biofilms in food processing environments." *J. Dairy Sci.*, **81**, 2765-2770.

**Wong, P.** and Pamer, E.G. (2001). "Cutting edge: antigen-independent CD8 T cell proliferation." *J. Immunol.*, **165**, 6833-6839.

**Wong, P.** and Pamer, E.G. (2003). "Feedback regulation of pathogen-specific T cell priming." *Immunity*, **18**, 499-511.

**Wu, L.** and Filutowicz, M. (1999). "Hexahistidine (His6)-tag dependent protein dimerization: a cautionary tale." *Acta Biochim. Pol.*, **46**, 591-599.

**Wuenschel, M.D., Köhler, S., Bubert, A., Gerike, U. and Goebel, W.** (1993). "The *iap* gene of *Listeria monocytogenes* is essential for cell viability, and its gene product, p60, has bacteriolytic activity." *J. Bacteriol.*, **175**, 3491-3501.

**Yoder, M.D., Keen, N.T. and Jurnak, F.** (1993). "New domain motif: the structure of the pectate lyase C, a secreted plant virulence factor." *Science*, **260**, 1503-1507.

**Yokoyama, E., Maruyama, S. and Katsube, Y.** (1998). "Production of bacteriocin-like-substance by *Listeria innocua* against *Listeria monocytogenes*." *Int. J. Food Microbiol.*, **40**, 133-137.

**Zenewicz, L.A., Foulds, K.E., Jiang, J., Fan, X. and Shen, H.** (2002). "Nonsecreted bacterial proteins induce recall CD8<sup>+</sup> T cell responses but do not serve as protective antigens." *J. Immunol.*, **169**, 5805-5812.

**Zenewicz, L.A., Skinner, J.A., Goldfine, H. and Shen, H.** (2004). "*Listeria monocytogenes* virulence proteins induce surface expression of Fas ligand on T lymphocytes." *Mol. Microbiol.*, **51**(5), 1483-1492.



**Zola, H. and Brooks, (1985).** "Techniques for the production and characterisation of monoclonal hybridoma antibodies." In: *Monoclonal Hybridoma Antibodies: techniques and application*, (Hurrel, J.G.R., ed.), CRC Press, Inc. Boca Raton, Florida, 1-59.

**Zydney, A.L. and Coulton, C.K. (1984).** "A red cell deformation model for hemolysis in cross flow membrane plasmapheresis." *Chem. Eng. Commun.*, **30**, 191-207.

